



Exploiting Synthetic Lethality in Ovarian Cancer

Thesis submitted for the degree of Doctor of Philosophy

Northern Institute for Cancer Research

Rachel Louise O'Donnell

Clinical Research Fellow

Northern Gynaecological Cancer Centre, Queen Elizabeth Hospital, Gateshead

Supervisors

Professor Richard J Edmondson

Professor of Gynaecological Oncology, Faculty Institute for Cancer Sciences,
University of Manchester

Professor Nicola J Curtin

Professor of Cancer Therapeutics, Northern Institute for Cancer Research,
University of Newcastle upon Tyne

2016

Statement of Originality

The work described in the thesis was carried out between December 2011 and February 2015 at the Northern Institute for Cancer Research, Newcastle University and the Northern Gynaecological Oncology Centre, Gateshead. The work is original except where acknowledged in the references and has not been, or will not be, submitted for a degree, diploma or any other qualification at any other university.

Abstract

The term ovarian cancer describes a set of distinct and heterogeneous diseases with an overall poor prognosis. Standard treatment strategies are limited and new novel therapies targeting the molecular pathways dysregulated in ovarian cancer are being explored with a goal of personalising provision of treatment, based upon accurate biomarker testing.

There are two major challenges if progress is to continue with a measureable clinical impact. Firstly, the mechanism of action of emerging therapies must be understood with reliable biomarkers capable of accurately predicting response to therapy. Secondly, for biomarkers to be useful in their accurate prediction of response, a thorough understanding of how to test a patient is needed. As our understanding of inter- and intra-tumour heterogeneity grows, the ability to test a single sample of tumour that is representative becomes more challenging and it is likely that new clinical strategies for testing multiple areas of the same tumour, at multiple time points, are required if our understanding of tumour biology is to translate into survival benefit for patients. Detection and subsequent testing of circulating tumour cells may offer the ability to test cells representative of the entire tumour without the need for invasive testing but a clear understanding of the consequences of intra-tumoural heterogeneity is needed.

This PhD aimed to address these challenges by firstly exploring the potential role of sapacitabine, a novel oral nucleoside analogue, for the treatment of ovarian cancer alongside the poly (ADP-ribose) polymerase (PARP) inhibitor rucaparib and platinum. Homologous recombination DNA repair functional status has been explored as a biomarker for their stratified use. Additionally, this project aimed to explore the feasibility of detecting circulating tumour cells in ovarian cancer using ImageStream technology, which combines flow cytometry with high resolution immunofluorescent microscopy.

Acknowledgments

Throughout my undergraduate and postgraduate medical training, I have been privileged to work under the supervision and mentorship of so many incredible people and I have always felt inspired to push myself to be able to contribute to my field. This PhD has pushed me to my absolute limits academically, physically and emotionally but it has also rewarded me in so many ways.

This work has created a lifetime of further questions but it has only been possible because of the unbelievable support from friends and colleagues at the NICR and NGOC and my family and friends. Perhaps the most important people to thank are those women, alongside their families, who have battled ovarian cancer. I have been honoured to care for them and take pride in using their donated samples in order to contribute to forwarding the understanding and treatment of this devastating disease. Each 'PCO' sample represents a woman who selflessly considered others as she fought for her own health. This work is dedicated to all of these women and their families for their strength, determination and inspiration.

I thank Richard and Nicola for their continuous support and guidance and apologise for the length of my acknowledgements - I still have not learnt to write concisely!

I thank James, Mum, Dad and Becky as well as friends who have tirelessly supported me, encouraged me during busy times and forgiven my absence.

I am grateful to all of my colleagues, in particular Aiste, Angelika, Peter, Barry, Laura and Fiona for their help and expertise in the lab and the North Terrace. Colleagues who have been actively involved in various parts of this project have been acknowledged separately within relevant chapters and publications.

Thank you also to Emilia, who arrived just in time to become a helpful distraction!

Finally, I thank the NGOC, Clovis and Cyclacel for funding this project.

Contents

Statement of Originality	i
Abstract	ii
Acknowledgments	iii
Contents	iv
List of Abbreviations	ix
List of Figures and Tables	xi
Chapter 1: Introduction	1
1.1. Ovarian Cancer	2
1.1.1. Epidemiology	2
1.1.2. Risk Factors	3
1.1.3. Pathogenesis	5
1.2. Current Classification System of Ovarian Cancer	8
1.3. The Reclassification of Ovarian Cancer?	11
1.3.1. Why Should the Current Classification System be Updated?	11
1.3.2. How Should Ovarian Cancer be Classified?	12
1.4. DNA Damage Repair (DDR) Pathways	13
1.4.1. Direct Repair by O ⁶ -methylguanine-DNA Methyltransferase (MGMT)	14
1.4.2. Base Excision Repair (BER)	15
1.4.3. Nucleotide excision repair (NER)	17
1.4.4. Mismatch Repair (MMR)	19
1.4.5. Double Strand Break Repair (DSB)	22
1.4.6. Non-Homologous End Joining (NHEJ)	22
1.4.7. Homologous Recombination repair (HR)	23
1.5. Other Pathways Important in Ovarian Cancer	28
1.6. Current Treatment Strategies in Ovarian Cancer	31
1.6.1. Ovarian Cancer Surgery	31
1.6.2. Tumour Sampling for Histological and Molecular Subtyping	32
1.6.3. Chemotherapy	33
1.6.4. Platinum	34
1.6.5. Second Line Agents	36
1.7. Targeted Therapies for Ovarian Cancer?	38
1.7.1. Angiogenesis Inhibitor: Bevacizumab	38
1.7.2. PARP Inhibitors	39
1.8. Rationale for this Project	48
Chapter 2. Hypothesis and Aims	49
2.1. Primary Cultures	50
2.2. Solid Tumour Culture and Heterogeneity	51
2.3. Sapacitabine	52
2.4. Circulating Tumour Cells	53

Chapter 3. Materials and Methods	49
3.1. General Equipment.....	49
3.2. Chemicals and Reagents.....	50
3.3. General Laboratory Practice.....	53
3.4. Cell Culture.....	53
3.4.1. Cell lines.....	53
3.4.2. Primary Ovarian Ascitic Cancer Cells (PCO).....	56
3.5. Cytotoxicity and Proliferation Assays.....	59
3.5.1. Colony Formation Assays.....	59
3.5.2. Growth Assay (Sulforhodamine B [SRB]).....	60
3.5.3. Growth Inhibition Assays.....	61
3.6. Homologous Recombination Repair Functional Assay.....	63
3.6.1. Principles of the Assay.....	63
3.6.2. Assay Protocol.....	65
3.6.3. Immunofluorescence Microscopy: Focus Counting.....	66
3.7. 8-hydroxy-2'-deoxyguanosine: A functional BER assay.....	67
3.8. RNA Genome Expression Arrays.....	69
3.9. PARP Assay.....	72
3.10. Western Blotting.....	74
3.11. Clinical Definitions.....	76
3.12. Statistical Analysis.....	76
Chapter 4. Assessment of the Primary Ovarian Cancer (PCO) Culture Model and	
Exploration of Biological Markers of Clinical Survival	78
4.1. Introduction: Primary Culture.....	78
4.2. Aims.....	79
4.3. Methods.....	80
4.3.1. Characterisation.....	80
4.3.2. Morphology.....	80
4.3.3. Immunofluorescence Characterisation Panel.....	81
4.3.4. Formal Histopathology.....	84
4.3.5. Surface Antigen Characterisation Timeline.....	84
4.3.6. Reducing Analysis Time of PCO cultures (Characterisation and HR Assay).....	84
4.3.7. Cytocentrifugation.....	84
4.3.8. Coverslip Cultures.....	85
4.3.9. PCO culture, HR Functional Assay, Cell Proliferation, PARP Assays and Gene Expression Methods.....	85
4.4. Results.....	86
4.5. PCO Collection.....	86
4.6. Clinical Characteristics.....	86
4.7. Characterisation.....	87
4.7.1. Original Characterisation Protocol and its Limitations.....	87
4.7.2. Expanded Characterisation Panel.....	88
4.7.3. CA125 Expression: Immunofluorescence vs. Immunohistochemistry.....	90
4.7.4. Epithelial Mesenchymal Transition (EMT) and PCO Phenotype.....	92
4.7.5. Stability of Characterisation Phenotype with Time and Passage.....	93
4.7.6. Morphology.....	95
4.8. PCO Culture Growth.....	96
4.8.1. Growth and HR Status.....	97
4.9. PCO-2 Cultures.....	98
4.9.1. PCO vs PCO-2 Antigen Characterisation.....	98
4.9.2. PCO vs PCO-2 Growth.....	100
4.9.3. PCO vs. PCO-2 HR Status.....	101
4.10. Homologous Recombination DNA Repair Status of PCO Cultures.....	102

4.11. Sensitivity to Cytotoxic Agents.....	103
4.11.1. Selection of Methodology: SRB vs. WST-1 vs. Colony Formation vs. Cell Counting	104
4.11.2. SRB Assay to evaluate effect of cytotoxic agents on PCO cultures.....	105
4.11.3. Sensitivity to Rucaparib and Cisplatin by HR Status	108
4.11.4. Sensitivity Rucaparib vs. Cisplatin	109
4.12. Clinical Application of HR Assay.....	111
4.12.1. Cytoentrifugation and Coverslip Culture	111
4.12.2. PARP Activity as a Surrogate Assay for HR Function.....	113
4.12.3. HR Gene Expression as a Surrogate for HR Function	116
4.13. Alternative HR analysis.....	121
4.13.1. Correlation of Focus Count With Rucaparib Sensitivity	122
4.13.2. Correlation of Focus Count With Cisplatin Sensitivity	122
4.13.3. Rad51 Alone as a Predictor of HR Function.....	127
4.14. Clinical correlations.....	128
4.14.1. HR Status as a Predictor of Survival	128
4.14.2. Clinical vs. <i>Ex Vivo</i> Sensitivity to Platinum	130
4.14.3. Growth as a Predictor of Time to Relapse (PFS)	132
4.15. Summary.....	134
4.16. Discussion.....	135
Chapter 5. Inter- and Intra-tumoural Heterogeneity.....	142
5.1. Introduction	142
5.1.1. Heterogeneity in Ovarian Cancer: What is Already Known?	143
5.1.2. Reported Solid Culture Methodologies	146
5.2. Aims	147
5.3. Methods	148
5.4. Results	148
5.5. PCO Solid Culture Case Series	150
5.5.1. Culture Success.....	150
5.5.2. Patient Demographics.....	151
5.6. Heterogeneity as a Prognostic Marker	160
5.7. HR of Ascites as a Prognostic Marker	164
5.8. Histology as a Prognostic Marker	167
5.9. Surgical Cytoreduction as a Prognostic Marker	167
5.10. Longitudinal Sequential Samples	168
5.11. Discussion.....	173
5.12. Conclusions	181
Chapter 6. Sapacitabine as a Therapeutic Agent in the Treatment of	
Ovarian Cancer	182
6.1. Introduction	182
6.2. Sapacitabine	183
6.2.1. Structure	183
6.2.2. Function and Mechanism of Action.....	183
6.2.3. Sapacitabine and DNA Repair Pathways	186
6.3. Aims	192
6.4. Methods	192
6.4.1. Cell lines	193
6.4.2. Growth Inhibition of BER Proficient and Deficient Cells by CNDAC With and Without Nucleoside Transport Inhibitors.....	193
6.4.3. Development of an Assay of BER Function.....	194
6.4.4. Western Blotting.....	195

6.5.	Results	196
6.5.1.	Cell Lines	196
6.5.2.	Assessing Cytotoxicity in PCO Samples	200
6.5.3.	Sensitivity of PCO to CNDAC, Cisplatin and Rucaparib in Relation to HR Status	200
6.5.4.	HR and the Prediction of CNDAC Sensitivity.....	208
6.5.5.	CNDAC in Sequential or Combination Drug Regimes.....	209
6.5.6.	Investigation of Alternative DNA Repair Mechanisms as Possible Determinants of Sensitivity to CNDAC	210
6.5.7.	Base Excision Repair	214
6.5.8.	Interaction of HR and BER Functional Status	221
6.5.9.	Investigation of Uptake of CNDAC by Nucleoside Transporters Using Inhibitors	222
6.5.10.	Expression of Proteins Implicated in CNDAC Sensitivity: ENT, dCK, CDA ..	224
6.5.11.	BER Gene Expression as a Surrogate for BER Function.....	227
6.6.	Discussion.....	229
6.6.1.	Sapacitabine in the Treatment of Ovarian Cancer	229
6.6.2.	HR as a Biomarker of Sensitivity to CNDAC	230
6.6.3.	Interaction of Other Cellular Pathways in the Sensitivity to CNDAC	232
6.6.4.	Cellular Uptake and Metabolism of CNDAC	235
6.7.	Conclusions	235
Chapter 7. Circulating Tumour Cells in Ovarian Cancer		236
7.1.	Introduction	236
7.1.1.	The Origin of CTCs	236
7.1.2.	Pharmacodynamic Biomarkers Using CTCs	238
7.1.3.	CTCs vs Circulating DNA.....	238
7.1.4.	CTCs in Ovarian Cancer.....	240
7.1.5.	CTC Challenges.....	242
7.1.6.	CTC Detection Techniques.....	243
7.1.7.	ImageStream	245
7.2.	Aims	246
7.3.	Method Development.....	247
7.3.1.	Antibody Selection	247
7.3.2.	ImageStream Settings	247
7.3.3.	Characterisation of OVCAR3 Cell Line and PCO Cultures	249
7.3.4.	Retrieval of Spiked 'CTC'	251
7.3.5.	ImageStream Data Analysis Algorithm	252
7.3.6.	Retrieval Results Without Enrichment	255
7.3.7.	Enrichment	256
7.3.8.	Enrichment Results.....	259
7.3.9.	Retrieval Results with Enrichment	259
7.4.	Results: Ovarian Cancer Patient Sample Results	262
7.4.1.	Enumeration.....	262
7.4.3.	CTC Enumeration and Survival	269
7.4.4.	Objects of Interest.....	270
7.4.5.	Healthy Volunteer Blood without spiked 'CTC'	274
7.4.6.	ImageStream HR Assay	274
7.4.7.	HR Assay in CTCs	277
7.4.8.	Imagestream for the characterisation of Ascites	278
7.4.9.	Ascitic Fluid	280
7.5.	Summary.....	284
7.6.	Discussion.....	285
7.6.1.	Why are there so few CTCs in Ovarian Cancer?	288
7.6.2.	Can ImageStream Assessment of Ascites make Real Time HR Assessment Possible?	290
7.7.	Conclusions	291

Chapter 8: Discussion	292
8.1. Summary of Results	293
8.2. A New Treatment Strategy for Ovarian Cancer	297
8.3. Redefining Ovarian Cancer	299
8.4. Ovarian Cancer Heterogeneity: Implications for Academia	300
8.5. Strengths and Weaknesses	300
8.6. Future Work	302
Appendices	304
Appendix 1: PhD Publications	304
Appendix 2: Published Abstracts	305
Appendix 3: Oral Presentations	306
Appendix 4: Poster Presentations	307
Appendix 5: Consent Form for Tissue Collection	310
References	324

List of Abbreviations

Abbreviation	Full Terminology	Abbreviation	Full Terminology
3AB	3-Aminobenzamide	ECL	Enhanced chemiluminescence
8-OHdG	8-oxo-7,8-dihydro-2'-deoxyguanosine	ED	Effective dose
8-oxoG	8-oxoguanine	EDTA	Ethylenediaminetetraacetic acid
Ab	Antibody	ELISA	Enzyme-linked immunoabsorbent assay
ADP	Adenosine diphosphate ribose	EMT	Epithelial mesenchymal transition
AKT	Serine/threonine protein kinase	ENT	Equilibrative nucleoside transporter
AML	Acute myeloid leukaemia	EOC	Epithelial ovarian cancer
ATCC	American Tissue Culture Collection	EORTC	European Organisation for Research and Treatment of Cancer
ATM	Ataxia-telangiectasia-mutated kinase	EpCAM	Epithelial cell adhesion molecule
ATP	Adenosine 5'-triphosphate	FACS	Fluorescence-activated cell sorting
ATR	Human Ataxia telangiectasia-related	FBS	FBS Foetal bovine serum
AUC	Area under curve	FCS	Fetal bovine serum
BER	Base excision repair	FDA	Food and drug association
BRAF	Serine/threonine-protein kinase B-Raf	FEN	Flap structure-specific endonuclease
BRCA 1	Breast cancer susceptibility protein 1	FFPE	Formalin-fixed paraffin-embedded
BRCA 2	Breast cancer susceptibility protein 2	FIGO	International Federation of Gynaecology and Obstetrics
BSA	Bovine serum albumin	FISH	Fluorescent in situ hybridisation
BSO	Bilateral salpingo oophorectomy	FITC	Fluorescein isothiocyanate
CA125	Cancer antigen 125	GI50	Growth inhibition (50%)
CCD	Charge coupled device	GOG	Gynaecological Oncology Group
CDA	Cytidine deaminase	Gy	Gray (irradiation unit)
CI	Confidence interval / Combination index	H&E	Haematoxylin and eosin
CK	Cytokeratin	H2AX	H2A histone family, member X
CLL	Chronic lymphocytic lymphoma	HCl	Hydrochloric acid
CML	Chronic myeloid leukaemia	HE4	Human epididymis protein 4
CNDAC	2-C-cyano-2-Deoxy-1-D-arabino-pentofuranosylcytosine	HEPES	4-(2-hydroxyethyl)-1-piperazineethanesulfoni acid
CNddc	2'-C-cyano-2',3'-didehydro-2',3'-dideoxycytidine	HGSC	High grade serous cancer
CTC	Circulating tumour cell	HK10	human Kallikrein 10
DAPI	4',6-diamidino-2-phenylindole	HNPCC	Hereditary non-polyposis colorectal cancer
dCK	Deoxycytidine kinase	HR	Homologous recombination
DDR	DNA damage response	HRC	Homologous recombination competent
DMSO	Dimethyl sulphoxide	HRD	Homologous recombination deficient
DNA	Deoxyribonucleic acid	HRP	Horseradish peroxidase
DNA-PK	DNA-dependent protein kinase	HRT	Hormone replacement therapy
DP	Dipyridamole	HU	Hydroxyurea
DSB	Double strand break	IC	Inclusion cyst
DT	Doubling time	IDS	Interval debulking surgery

IP	Intra-peritoneal	PCO	Primary culture ovary
IR	Ionising radiation	PCR	Polymerase chain reaction
ITH	Intra-tumour heterogeneity	PE	Phycocerythrin
IV	Intra-venous	PFS	Progression free survival
KRAS	Ki-ras2 Kirsten rat sarcoma viral oncogene homolog	pH	Potential of hydrogen
LC50	Lethal dose (50%)	Pol	DNA polymerase
LD	Limiting dose	PPV	Positive predictive value
LOH	Loss of heterozygosity	PTEN	Gene encoding phosphatase and tensin homolog
MAPK	Mitogen-activated protein kinase	RAD51	Rad 51 homolog
MGMT	O6-methylguanine-DNA methyltransferase	RBC	Red blood cell
miRNA	MicroRNAs	RCLB	Red cell lysis buffer
MMR	Mismatch repair	RCT	Randomised controlled trial
MOC31	Antibody to an epithelial glycoprotein	RECIST	Response Evaluation Criteria in Solid Tumours
MRN	MRE11, Rad51, NBS1 complex	RNA	Ribonucleic acid
MSI	Microsatellite instability	ROC	Receiver operating characteristic
MUC16	Mucin 16	ROS	Reactive oxygen species
MX	Methoxyamine	RPM	Revolutions per minute
NACT	Neoadjuvant chemotherapy	RPMI	Roswell Park Memorial Institute developed medium
NAD+	Nicotinamide adenine dinucleotide	SD	Standard deviation
NADH	Reduced form of NAD+	SEM	Standard error of the mean
NBMPR	Nitrobenzylmercaptapurine ribonucleoside	SLL	Small lymphocytic lymphoma
NER	Nucleotide excision repair	SNP	Single nucleotide polymorphism
NGOC	Northern Gynaecological Oncology Centre	SRB	Sulforhodamine B
NHEJ	Non-homologous end joining	SSB	Single strand break
NHS	National Health Service	TAM	Tumour-associated macrophage
NICE	National Institute for Clinical Excellence	TCA	Trichloroacetic acid
NPV	Negative predictive value	TCGA	The Cancer Genome Atlas
NSCLC	Non-small cell lung cancer	TMA	Tissue microarray
NT	Nucleoside transporter	TP53	Gene encoding tumour suppressor protein (p53)
OCP	Oral contraceptive pill	TZ	Temozolomide
OD	Optical density	UV	Ultraviolet
OS	Overall survival	v/v	by volume
OSE	Ovarian surface epithelium	VEGF	Vascular endothelial growth factor
OVCAR	Ovarian cancer	w/v	by weight
p53	Tumour suppressor protein encoded by TP53 gene	WBC	White blood cell
PAR	Poly(ADP-ribose) polymer	WST-1	Water soluble tetrazolium salts
PARP	Poly(ADP-ribose) polymerase	WT	Wild type
PARPi	Poly(ADP-ribose) polymerase inhibitor	XRCC	X-ray cross complementing
PBS	Phosphate buffered saline	γH2AX	Histone H2A variant X

List of Figures and Tables

- Figure 1.1 - 1: Ovarian Cancer, age-standardised five-year relative survival rates, England and Wales 1971-1995, England 1996-2009; Cancer Research UK.
- Figure 1.4 - 1: Base excision repair pathway.
- Figure 1.4 - 2: Nucleotide excision repair pathway.
- Figure 1.4 - 3: Mismatch repair pathway.
- Figure 1.4 - 4: Non-homologous end joining pathway.
- Figure 1.4 - 5: Homologous recombination pathway.
- Figure 1.6 - 1: Platinum-resistance definition by the Gynaecologic Oncology Group (GOG).
- Figure 1.7 - 1: Synthetic lethality in HR defective tumours with PARP inhibition.
- Figure 3.4 - 1: PCO collection flow chart for sample analysis.
- Figure 4.3 - 1: PCO culture morphology reference Images.
- Figure 4.7 - 1: PCO immunofluorescent characterisation panel.
- Figure 4.7 - 2: Concordant CA125 expression in PCO 158.
- Figure 4.7 - 3: Relationship between serum CA125 and CA125 protein expression detected by immunohistochemistry and immunofluorescence.
- Figure 4.7 - 4: Cytokeratin and vimentin co-expression in PCO 163.
- Figure 4.8 - 1: PCO growth.
- Figure 4.8 - 2: Growth rate PCO cultures by HR status results.
- Figure 4.9 - 1: Doubling time for PCO vs. PCO-2 cultures.
- Figure 4.10 - 1: HR assay. Immunofluorescence detection of nuclear γ H2AX (A) and Rad51 (B) in PCO 164.
- Figure 4.11 - 1: Comparison of growth inhibition by rucaparib using SRB, WST-1 proliferation assays and cell counting in PCO 170.
- Figure 4.11 - 2: Rad51 foci count and growth inhibition by rucaparib and cisplatin.
- Figure 4.11 - 3: Sensitivity to cisplatin and rucaparib stratified by HR Status.
- Figure 4.11 - 4: Growth inhibition by rucaparib (A) and cisplatin (B) in PCO cultures by HR functional status.
- Figure 4.11 - 5: Resistance to rucaparib and cisplatin.
- Figure 4.12 - 1: PCO HR status: comparison of HR results following traditional culture technique vs. direct culture onto coverslips.
- Figure 4.12 - 2: Stimulated PARP activity in PCO. A: Immunoblot; B: Standard curve; C: Stimulated PAR activity expressed as mean (SD) PAR pmol/ 10^6 cells.
- Figure 4.12 - 3: Correlation of PAR level and % survival 10 μ M cisplatin (A) and 100 μ M rucaparib (B).
- Figure 4.12 - 4: RNA expression of key components of the HR DNA repair pathway for 24 PCO samples.
- Figure 4.12 - 5: RNA expression of key components of the HR DNA repair pathway in PCO grouped by HR status, n=24.
- Figure 4.12 - 6: Correlation between PARP-1 RNA expression and sensitivity to rucaparib (% survival at 100 μ M).
- Figure 4.13 - 1: Fold increase in Rad51 focus formation from control with subsequent HR classification.
- Figure 4.13 - 2: Correlation of γ H2AX and Rad51 foci counts with % survival at 100 μ M rucaparib.
- Figure 4.13 - 3: Correlation of γ H2AX and Rad51 foci counts with % survival at 10 μ M cisplatin.
- Figure 4.13 - 4: ROC curve of ability of Rad51 foci count to predict HR function.

- Figure 4.14 - 6: Kaplan-meier survival curves for patients stratified by HR function of ascitic PCO cultures.
- Figure 4.14 - 7: Ex vivo PCO culture sensitivity to cisplatin as a predictor of clinical sensitivity to platinum based chemotherapy.
- Figure 4.14 - 8: Correlation of PCO culture doubling time with PFS and OS.
- Figure 5.1 -1: Somatic evolution .
- Figure 5.4 - 1: Fibroblast exclusion using selective seeding.
- Figure 5.5 - 1: Solid PCO cultures.
- Figure 5.5 - 2: Summary of characterisation antigen detection.
- Figure 5.5 - 3: PCO 179. Solid tumour biopsies taken from five intra-abdominal sites cultured, alongside ascites culture (A). (B) Intra-tumoural heterogeneity of antigen detection of EpCAM and CA125 using immunofluorescent microscopy. (C) Variable proliferation following 10-day exposure to rucaparib, assess using SRB assay.
- Figure 5.5 - 4: PCO subculture doubling time.
- Figure 5.5 - 5: Growth comparison. A: HRC vs HRD; B: Ascites vs solid cultures.
- Figure 5.5 - 6: Growth inhibition.
- Figure 5.6 - 1: Kaplan-meier survival curves: heterogeneous HR cultures vs homogeneous HR cultures.
- Figure 5.6 - 2: Cytoreductive surgical outcome by homogenous and heterogeneous functional groupings.
- Figure 5.7 - 1: Kaplan-meier survival curves for PFS/OS by HR status (A), histological subtype (B) and outcome of cytoreductive surgery (C).
- Figure 5.10 - 1: Longitudinal sampling.
- Figure 5.12 - 1: Tumour evolution and intra-tumour heterogeneity.
- Figure 6.2 - 1: Structure of sapacitabine, CNDAC, gemcitabine and ara-C.
- Figure 6.2 - 2: Incorporation of CNDAC into DNA, β -elimination resulting in CNddC.
- Figure 6.2 - 3: S-Phase stalled replication forks.
- Figure 6.2 - 4: CNDAC metabolism.
- Figure 6.5 - 1: Cytotoxicity of CNDAC and cisplatin in cell lines matched for BRCA1/2 mutations.
- Figure 6.5 - 2: Sensitivity of each PCO culture to CNDAC (A), cisplatin (B), and rucaparib (C).
- Figure 6.5 - 3: Sensitivity to CNDAC, rucaparib and cisplatin stratified by HR status.
- Figure 6.5 - 4: Correlation studies between percentage survival at given concentrations of CNDAC, cisplatin and rucaparib.
- Figure 6.5 - 5: Correlation of sensitivity of PCO cultures to cisplatin and CNDAC.
- Figure 6.5 - 6: Resistance (A) and sensitivity (B) to CNDAC, cisplatin and rucaparib b.
- Figure 6.5 - 7: ROC analysis for HR status and CNDAC sensitivity.
- Figure 6.5 - 8: Cell proliferation by CNDAC (SRB assay) with matched cell lines for NHEJ, BER, and NER DNA repair.
- Figure 6.5 - 9: Inhibition of BER using methoxyamine.
- Figure 6.5 - 10: 8-OHdG baseline levels in PCO samples.
- Figure 6.5 - 11: Correlation of 8-OHdG with CNDAC sensitivity.
- Figure 6.5 - 12: ROC 8-OHdG of 1.5 to predict CNDAC sensitivity.
- Figure 6.5 - 13: Incidence of BER and HR dysfunction in PCO cultures with corresponding grouped sensitivity to CNDAC.
- Figure 6.5 - 14: CNDAC cell proliferation assays using AA8 and EM9 cell lines with addition of DP or NBMPR.
- Figure 6.5 - 15: Western blot for protein expression of ENT1, CDA, dCK in PCO cultures.

- Figure 6.5 - 16: RNA expression of key components of the BER DNA repair pathway in PCO grouped by BER status, n=24.
- Figure 7.3 - 1: Scatterplot showing the area and aspect ratio of OVCAR3 cell line sample (incubated with EpCAM, CK, CA125 and DRAQ5) based upon brightfield image (MO1).
- Figure 7.3 - 2: ImageStream cell line characterisation results.
- Figure 7.3 - 3: CTC analysis algorithm.
- Figure 7.3 - 4: CTC retrieval without WBC enrichment.
- Figure 7.3 - 5: EasySep™ CD45 depletion of WBC (STEMCELL Technologies, 2013).
- Figure 7.3 - 6: Comparison of depletion methods.
- Figure 7.3 - 7: Retrieval of malignant cells from whole blood.
- Figure 7.4 - 1: CTC frequency and relation to stage of disease and extra-peritoneal disease.
- Figure 7.4 - 1: Cell plot of ovarian cancer CTC with nucleated cells (DRAQ5 nuclear stain) with variable expression of EpCAM, CK and CA125.
- Figure 7.4 - 2: CTC characterisation.
- Figure 7.4 - 3: Three representatives CTC from PCO 202.
- Figure 7.4 - 4: CTC area.
- Figure 7.4 - 5: Correlation of CTC frequency/ml with survival.
- Figure 7.4 - 6: Objects of interest from healthy volunteer sample.
- Figure 7.4 - 7: CTC from PCO 173, 180 and 213 showing CTC surrounded by WBC.
- Figure 7.4 - 8: ImageStream assessment of HR function in a panel of cell lines.
- Figure 7.4 - 9: γ H2AX and Rad51 nuclear foci.
- Figure 7.4 - 10: Mean γ H2AX foci count in PCO cultures using ImageStream.
- Figure 7.4 - 11: ImageStream antigen characterisation of PCO ascites.
- Figure 7.4 - 12: ImageStream characterisation of ascitic PCO samples.
- Figure 7.4 - 13: ImageStream cell plot of the major sub-populations of cells identified within the ascitic fluid of PCO209. A: EpCAM only. B: CK only. C: CA125 only. D: All. E: EpCAM and CK. F: EpCAM and CA125. G: CK and C A-125.
- Figure 7.4 - 14: γ H2AX Foci in fresh ascites.
- Figure 8.2 - 1: Schematic for the sequential Provision of Targeted Agents following Interim Tumour Sampling and Biomarker Testing
- Figure 9.1 - 1: CA125 conjugation validation.
- Figure 9.2 - 1: HR assay optimisation of nuclear, γ H2AX and Rad51 foci masks.
- Figure 9.3 - 1: γ H2AX focus dose response comparing three ImageStream masks with traditional immunofluorescent microscopy and manual counting.
- Figure 9.4 - 1: γ H2AX foci following irradiation at different doses. Assessment of count using ImageStream.
- Figure 9.5 - 1: HR method optimisation in PCO cultures.

Table 1.1 - 1:	<i>FIGO (International Federation of Gynaecology and Obstetrics) surgical staging of ovarian cancer with five-year stage-specific relative survival rates, Cancer Research UK.</i>
Table 1.1 - 2:	<i>Risk factors for ovarian cancer development.</i>
Table 1.1 - 3:	<i>Ovarian cancer classification with frequencies and common genetic mutations.</i>
Table 1.6 - 1:	<i>Randomised Controlled Trials (RCT) for chemotherapy treatment for ovarian cancer</i>
Table 1.6 - 2:	<i>Second line chemotherapy agents in the treatment of ovarian cancer</i>
Table 1.7 – 1:	<i>Clinical trials of olaparib and rucaparib PARPi.</i>
Table 3.4 - 1:	<i>Cell lines.</i>
Table 3.6 - 1:	<i>Microscope settings for immunofluorescent HR assay.</i>
Table 3.8 – 1:	<i>HR genes analysed in RNA genome analysis.</i>
Table 3.8 – 2:	<i>BER genes analysed in RNA genome analysis.</i>
Table 4.3 – 1:	<i>Antibodies for the PCO immunofluorescent characterisation panel.</i>
Table 4.3 - 2:	<i>Immunofluorescence microscope settings for PCO culture characterisation.</i>
Table 4.6 - 1:	<i>Summary of PCO patient demographics.</i>
Table 4.7 - 1:	<i>Immunofluorescent characterisation timeline.</i>
Table 4.7 - 2:	<i>Histological subtype, characterisation antigen expression, HR DNA repair status in PCO cultures (n=61) stratified by morphological subtype.</i>
Table 4.9 - 1:	<i>Immunofluorescent antigen characterisation of matched PCO and PCO-2 cultures.</i>
Table 4.9 - 2:	<i>Summary of antigen expression of PCO and PCO-2 cultures.</i>
Table 4.9 - 3:	<i>Functional HR status of paired PCO and PCO-2 cultures.</i>
Table 4.10 - 1:	<i>Functional HR status of PCO cultures by histological subtype.</i>
Table 4.11 - 1:	<i>Comparing cytotoxicity to rucaparib in a cell line panel by colony formation assay and proliferation assays.</i>
Table 4.11 - 2:	<i>Comparison of growth inhibition, determined by SRB assay, by rucaparib and cisplatin stratified by HR functional status.</i>
Table 4.12 - 1:	<i>PCO culture antigen characterisation.</i>
Table 4.14 - 1:	<i>Patient demographic data stratified by HR status.</i>
Table 5.4 - 1:	<i>Optimisation of solid culture methodology.</i>
Table 5.5 - 1:	<i>Solid tumour patient demographics.</i>
Table 5.5 – 2:	<i>Solid tumour morphological classification by histological subtype.</i>
Table 5.5 – 3:	<i>PCO solid tumour samples with HR status and corresponding sensitivities to rucaparib and cisplatin, determined using SRB cell proliferation assay.</i>
Table 5.6 - 1:	<i>Intra-tumoural heterogeneity of HR status and survival (PFS and OS).</i>
Table 5.6 – 2:	<i>PCO patient demographics with heterogeneity of HR function ordered by progression free and overall survival.</i>
Table 5.8 – 1:	<i>Incidence of HRC and HRD by histological subtype.</i>
Table 5.9 – 1:	<i>The distribution of surgical outcome within the homogeneous and heterogeneous tumour groups.</i>
Table 6.2 - 1:	<i>CNDAC in clinical trials.</i>
Table 6.4 – 1:	<i>Agents for the inhibition of BER or transporter protein, their mode of action and hypothesis for effect with simultaneous treatment with sapacitabine.</i>
Table 6.4 - 2:	<i>Antibodies for western blot.</i>
Table 6.5 - 1:	<i>Cell line panel: growth characteristics and cytotoxicity by CNDAC, rucaparib and cisplatin.</i>
Table 6.5 - 2:	<i>Comparison of SRB with colony formation in cell lines matched for BRCA 1/2.</i>
Table 6.5 - 3:	<i>CNDAC in combination with PARPi.</i>

Table 6.5 - 4:	<i>Cell line panel used to explore the contribution of NHEJ, BER, NER, p53 and MMR in the sensitivity to CNDAC.</i>
Table 6.5 - 5:	<i>Sensitivity to CNDAC and cisplatin assessed by proliferation assay in cell line panels matched for functional/defective DNA repair pathways.</i>
Table 6.5 - 6:	<i>Cytotoxic effect of methoxyamine (MX): Percentage survival AA8 and EM9 cells with addition of MX.</i>
Table 6.5 - 7:	<i>ROC analysis of predictability of 8-OHdG values to predict sensitivity to CNDAC.</i>
Table 6.5 - 8:	<i>Mean GI₅₀ of paired cell lines following exposure to CNDAC with NBMPR or DP.</i>
Table 7.1 - 1	<i>Differences between CTC and ctDNA analyses.</i>
Table 7.1 - 2:	<i>CTC detection technologies.</i>
Table 7.3 - 1:	<i>ImageStream laser and channel settings for flouorochrome conjugated antibodies.</i>
Table 7.3 - 2:	<i>Characterisation of OVCAR3 cell line using traditional fixed immunofluorescent microscopy and ImageStream.</i>
Table 7.3 – 3:	<i>Depletion methods.</i>
Table 7.4 - 1:	<i>Patient demographics and numbers of circulating tumour cells in blood from patients with ovarian cancers.</i>
Table 7.4 – 2:	<i>ImageStream setting HR assay.</i>
Table 8.1 - 1:	<i>Summary of objectives and project outcomes</i>
Table 8.3 - 1:	<i>Ovarian Cancer Clinical and Radiological Definitions of Disease Response</i>
Table 9.1 - 1:	<i>Optimisation of cell suspension fixation.</i>
Table 9.2 - 1:	<i>Imagestream settings fro Rad51 foci HR assay.</i>

Chapter 1: Introduction

Cancer is a disease that is known to many but understood by few. We define cancer as an uncontrolled division of abnormal cells and with the understanding that there are more than 100 distinct types of cancer, each with multiple subtypes found within specific organs, the problem we face in treating this disease is overwhelming. There are now several lines of evidence which indicate that tumorigenesis is a multistep process and that these steps reflect genetic alterations that drive the progressive transformation of normal human cells into highly malignant derivatives (Hanahan 2000). This thesis aims to further develop our understanding of ovarian cancer and some of its unique molecular derangements aiming to exploit them with the use of targeted cytotoxic agents.

The present chapter focuses on a literature review exploring the biology of epithelial ovarian cancer and how this may be exploited with the use of biomarkers of response to cytotoxic agents. The current classification system and current management strategies are described and this is presented alongside a proposed new classification system whereby groupings are based upon actual tumour biology rather than mere morphological appearance.

1.1. Ovarian Cancer

1.1.1. Epidemiology

Ovarian Cancer poses a significant challenge to both clinicians and researchers. Worldwide, there are more than 200,000 new cases each year, which accounts for around 4% of all cancers diagnosed in women. The risk of developing ovarian cancer by age 75 years varies, ranging from 0.5% to 1.6% (National Cancer Institute 2014 Lawrenson 2009). Although standard treatment with a combination of debulking surgery and platinum based chemotherapy produces a good rate of response initially, almost all disease relapses and develops resistance to standard platinum chemotherapy treatments. Despite much research and the introduction of new chemotherapy agents such as taxanes, the overall mortality has changed little over the past 20 years with the 5-year overall survival remaining low at 40%, Figure 1.1 - 1.

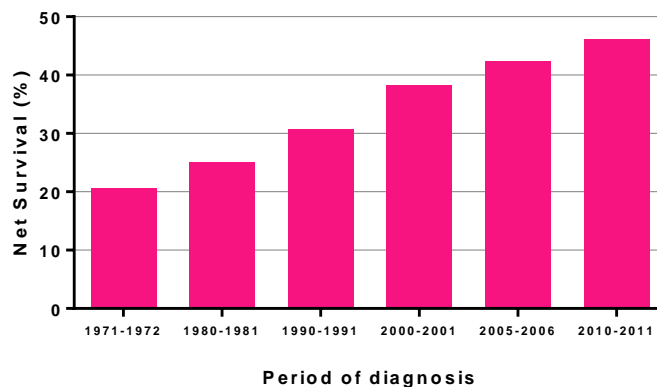


Figure 1.1 - 1: Ovarian cancer, age-standardised five-year relative survival rates, England and Wales 1971-1995, England 1996-2009; Cancer Research UK.

The poor prognosis in ovarian cancer is complex and thought to be multifactorial. The insidious onset of non-specific symptoms, coupled with a lack of a reliable detection method for early stage disease, results in a late stage at presentation at which time there are widespread metastases throughout the peritoneal cavity (Jemal 2009), Table 1.1 - 1. Aggressive surgical and medical treatment and a greater determination to treat recurrent disease is thought to be responsible for the small improvement in survival since the 1980s (Kitchener 2008) but the high rate of recurrence and the frequent development of chemoresistance has prevented further improvements.

FIGO Stage	Description	% of Cases	% 5-yr Survival
Stage I Limited to ovaries/fallopian tubes	IA: Limited to one ovary/fallopian tube IB: Both ovaries/fallopian tubes IC: Stage IA/IB with capsule rupture, malignant ascites/peritoneal washings	29	92
Stage II Involves ovaries/tubes extending to pelvic organs or primary peritoneal cancer	IIA: Extension onto the uterus and/or fallopian tubes and/or ovaries. IIB: Extension to other pelvic intraperitoneal tissues	4	55
Stage III Abdominal and/or lymph node disease	IIIA: Positive lymph nodes or microscopic extrapelvic peritoneal involvement IIIB: Peritoneal metastasis <2 cm IIIC: IIIB with extension to liver/spleen surface	45	22
Stage IV Distant metastasis	IVA: Pleural effusion with positive cytology IVB: Parenchymal metastases	15	6

Table 1.1 - 1: FIGO (International Federation of Gynaecology and Obstetrics) surgical staging of ovarian cancer (Prat 2013) with five-year stage-specific relative survival rates, Cancer Research UK.

1.1.2. Risk Factors

Although ovarian cancer aetiology remains unclear, several risk factors have been identified, which can be broadly classified as hereditary or sporadic cancer.

A hereditary predisposition occurs in 10 - 15% of cases and is caused by germline mutations in the tumour suppressor genes *BRCA1* and *BRCA2* or mutations in DNA mismatch repair (MMR) as seen in hereditary non-polyposis colorectal cancer (HNPCC) (Risch 2001, Gayther 2010). The lifetime risk of developing epithelial ovarian cancer (EOC) in women with a germline *BRCA1/2* mutation can be up to 66% and 27% respectively (Robles-Diaz 2004). Many different germline mutations in *BRCA1* and *BRCA2* genes have been described and tumorigenesis in individuals with germline *BRCA* mutations requires somatic inactivation of the remaining wild-type allele, suggesting that the *BRCA* genes are tumour suppressors (Smith, Easton et al. 1992, Collins, McManus et al. 1995). Biochemical, genetic and cytological studies have revealed multiple functions for *BRCA1* and *BRCA2*. They have been shown to be involved in DNA damage repair, specifically homologous recombination (reviewed in (Scully and

Livingston 2000)), to function as transcriptional co-regulators through direct interaction with sequence-specific transcription factors and with components of the transcriptional machinery (reviewed in (Monteiro 2000)) and they may also regulate transcription of genes involved in other cellular functions (Harkin, Bean et al. 1999). It has been proposed that chromosomal instability, as a result of *BRCA1/2* deficiency, may be the pathogenic basis for breast and ovarian cancer tumour formation (Welch and King 2001) and the influence of oestrogen may paradoxically facilitate cell growth rather than the expected apoptosis with loss of the wild-type allele in women with inherited *BRCA* mutations (Welch and King 2001). The expression of *BRCA1/2* is upregulated during puberty and pregnancy, when oestrogen levels are dramatically increased, suggesting that oestrogen might stimulate expression of *BRCA1* and/or *BRCA2* (Welch and King 2001). Ovarian cancers with *BRCA1/2* mutations have classical features in terms of histology, survival and chemosensitivity.

Much remains unknown about sporadic ovarian cancer but advancing age confers the greatest risk with more than 85% of patients aged 50 years or older at diagnosis. Additional risk factors have been identified and are summarised in Table 1.1 - 2. Epidemiological studies have identified that factors that reduce ovulation (combined oral contraceptive pill use, breastfeeding and term pregnancies, hysterectomy and sterilisation) are protective against the development of ovarian cancer.

Risk Factors for Ovarian Cancer Development	Protective Factors
Increasing age White ethnicity Polycystic ovarian syndrome Family history Nulliparity Early menarche/Late menopause Hormone replacement therapy and Fertility drugs No contraceptive use Talcum powder Obesity (endometrioid, mucinous and low grade serous subtypes (Olsen, Nagle et al. 2013)) Smoking (mucinous subtype (Jordan, Whiteman et al. 2006))	Parity Combined oral contraceptive pill Breastfeeding Hysterectomy

Table 1.1 - 2: Risk factors for ovarian cancer development (Fathalla 1971, Huncharek 2003, Kurian 2005, Salehi 2008, Sueblinvong 2009, Lahmann 2010).

1.1.3. Pathogenesis

Ovarian cancer can develop from epithelium, stroma or germ cells. Epithelial ovarian cancer (EOC) is by far the commonest type in the adult population and this thesis will focus upon this subtype.

Progress in the understanding of the biology and treatment of ovarian cancer is complicated by a lack of understanding of its origin. There are several theories for the site of origin and pathogenesis of ovarian cancer.

Ovarian Surface Epithelium (OSE)

Sir Spencer Wells proposed that ovarian cancer arises from OSE in 1872. OSE are mesothelial-like cells that share embryological origin with the Mullerian tract epithelium, which eventually gives rise to the tubal, endometrial and endocervical epithelium (Ahmed 2012). It has been hypothesised that EOC arise from the less differentiated OSE cells and subsequently differentiate into histological subtypes according to specific molecular perturbations (Ahmed 2012). Fathalla proposed repeated ovulation, associated with inflammation, induces surface epithelial dysplasia (Fathalla 1971). Ovarian biopsies from women receiving ovulation stimulating fertility treatment have revealed a higher rate of dysplasia (Fathalla 1971). This theory is further supported by the finding

that pregnancy and oral contraceptive pill use, which prevent ovulation, protect against ovarian cancer development.

Inclusion Cysts

With age, invaginations develop in the OSE that may be incorporated into the ovarian stroma, forming inclusion cysts (IC) (Folkins 2009). The formation of ICs lined by OSE cells was suggested as the origin of EOC but this was later refuted (Dubeau 1999) and it was suggested that these cancers arise from secondary Mullerian tract structures. Dubeau's argument was based on the fact that cells within ICs are indistinguishable from adjacent mesothelial cells lining the peritoneum, yet EOCs do not resemble mesothelial tumours (Ahmed 2012).

Fallopian Tube

Piek *et al.* first proposed the fallopian tube, with subsequent implantation on the peritoneum and ovary, as the origin of EOC in 2001 (Piek 2001, Piek 2007). Since then, evidence has accumulated to support this theory (Lee 2006, Medeiros 2006, Kindelberger 2007, Lee 2007, Herrington 2010, Przybycin 2010). Initial evidence came from prophylactic salpingo oophorectomy specimens from *BRCA* patients, which showed occasional high grade serous carcinomas (HGSC) in the ovary but more commonly in the fimbrial tube (serous tubal intraepithelial carcinomas (TIC) (McCluggage 2011). Further studies systematically examined the tubes in patients with sporadic HGSC and found similar lesions in up to 60% of cases (Kindelberger 2007, Przybycin 2010).

A study examining fallopian tubes in a consecutive series of ovarian carcinomas, identified serous TIC in nearly 60% of HGSC but not in other morphological subtypes (Przybycin 2010). At the time of surgery, the fallopian tube often appears macroscopically normal even in the presence of extensive disseminated disease throughout the pelvis and abdomen. It is possible therefore that in these cases, the fallopian tubes are not involved in the disease process or that the abnormal cells are shed from the tube and there is something within the tube, which prevents implantation in that site.

Whilst these various theories account for many of the recognised risk factors for development of ovarian cancer, it is appreciated that tumorigenesis is a multifactorial process and a better understanding may be achieved through a combination of the above. It may also be possible that the heterogeneous nature of ovarian cancer with its distinct morphological subtypes have distinct and different pathogenic processes (Shih and Kurman 2004). For instance, HGSC may originate in the fallopian tube mucosa with cancer cells being shed into the peritoneal cavity. They may implant into inclusion cysts causing development of cancerous ovarian masses or they may implant onto peritoneal surfaces, resulting in primary peritoneal cancer. Endometrioid and clear cell ovarian cancers may in fact originate within the endometrial cavity as there have been links to retrograde menstruation (Kurman 2011) and endometriosis (Worley 2013). Mucinous histological subtype may originate from the OSE and develop through a stepwise process. This theory of multiple aetiologies and sites of origin may explain the heterogeneous behaviour of ovarian cancer and the variable patterns of dissemination.

1.2. Current Classification System of Ovarian Cancer

The WHO first categorized ovarian cancers in 1973 into distinct morphological categories based upon the cells from which they were derived; surface epithelial, germ and mesenchymal cells (Scully 1975). Ninety per cent of adult ovarian cancers epithelial in origin and sub classification of EOC into distinct histological types (high grade serous [68%], endometrioid [9%], clear [13%], mucinous [3%] and low grade serous [7%]) is well established (Kaku 2003). The clinical characteristics and natural behaviour of ovarian tumours vary according to histology and grade (Silverberg 2000, Itamochi 2002, Stany 2008) with poorer overall prognosis seen in higher grade tumours of all subtypes (Omura 1991, Stany 2008). Surgical stage, extent of residual disease, patient performance status, grade and histological subtype have known prognostic significance. However, prognostication remains inaccurate (Agarwal and Kaye 2005). Although differences in response to chemotherapy and survival are recognised between different histological subtypes, no reliable predictors are available to indicate which patients will respond to chemotherapy and, therefore, in view of the obvious lack of any reliable selection criteria, currently all patients receive postoperative chemotherapy. In the provision of standard platinum based chemotherapy to all subtypes, it has been recognised that certain histological subtypes are not chemosensitive and alternative treatment strategies have been explored. Perhaps the best example of this is low grade serous ovarian cancer with 6% reported as being platinum sensitive (Gershenson, Sun et al. 2009). Alternative treatments including hormonal therapies (Gershenson, Sun et al. 2012) and MEK inhibitors (Farley, Brady et al. 2013) have therefore been explored with ongoing clinical trials in these areas. Detailed understanding of the individual challenges within each histological subtype is however required if the introduction of new agents is to translate into better response and overall survival.

More recently, following an understanding that ovarian cancer subtypes develop through disruption of distinct genetic and biological pathways, a new classification system categorising EOC into type I or II groups has been proposed, Table 1.1 – 3 (Shih and Kurman 2004). This simple reproducible

system is based upon clinicopathological behaviour and genetic mutations and indicates that the two tumour subtypes develop via different pathways (Shih 2004, Vang 2009).

Type I tumours are indolent and are thought to evolve in a stepwise manner from borderline tumours (Russell 2004). They are associated with distinct molecular changes that are rarely found in type II tumours and commonly involve KRAS, BRAF and p53 mutations (Singer, Oldt et al. 2003, Russell 2004, Singer, Stohr et al. 2005, Heinzelmann-Schwarz 2006). Endometrioid and clear cell ovarian carcinomas have been shown to be associated with micro-satellite instability (MSI) (Gras 2001) with hMLH1 promoter hypermethylation and loss of expression of hMSH2 (Geisler 2001). Mutations in the PI3K and Wnt signalling pathway have also been found in endometrioid and clear cell EOCs (Willner 2007). Conversely, type II tumours are aggressive and rapidly progress to advanced disease. They have no recognisable precursor lesions and are chromosomally unstable with distinctly different mutational patterns compared to type I tumours. Mutations in p53 are present in more than 90% (Ahmed 2010, Kurman 2010) and mutations in KRAS/BRAF are rare (Singer, Oldt et al. 2003). Other features include Akt2 overexpression, p16 promoter methylation/mutation and mutation of the PI3K pathway (Wang 2005, Nakayama 2006).

	Description	Typical Morphological Subtypes (frequency)	Common Genetic Mutations
Type I (25%)	Slow growing, diagnosed at lower grades Identifiable precursor lesions Resistant to platinum chemotherapy	Low grade serous and mucinous borderline (7%) Serous borderline (6%) Mucinous (3%) Low grade endometrioid (9-11%) Clear cell (12-13%) Malignant Brenner tumours	KRAS / BRAF (4-67%) p53 (0-9%) MMR pathway (13-50%) PI3K pathway PTEN / PIK3CA(20%) ERBB2
Type II (75%)	Rapid growth with early metastasis. No defined precursor lesions. Sensitive to platinum chemo	High grade serous carcinomas (68 - 71%) Undifferentiated carcinomas (1%) Malignant mixed mesodermal tumours High grade endometrioid (9-11%)	BRCA 1/2 p53 (50-98%) Akt2 (12-18%) p16 (10-17%) PIK3CA CCNE1

Table 1.1 - 3: Ovarian cancer classification (Shih 2004) with frequencies (McCluggage 2011) and common genetic mutations.

Histological classification is used in clinical practice to define an individual's cancer but neither histology nor classification into type I or II groupings has clinical use in terms of provision of prognostic information or guidance for provision of treatments. In the search for a clinically meaningful classification, recent work has subdivided HGSC using genomic (TCGA 2011), gene expression (Tothill 2008) and functional (TCGA 2011, Mukhopadhyay 2012) techniques. This has generated at least four distinct gene expression subgroups (Tothill 2008, Tan 2013) and at least two functional subgroups (Mukhopadhyay 2012). The subgroups defined have distinct prognostic behaviour as well as differences in their sensitivity to conventional and novel chemotherapy agents.

1.3. The Reclassification of Ovarian Cancer?

1.3.1. *Why Should the Current Classification System be Updated?*

The current classification system based upon morphological features is of little clinical use as the histological subtype does not accurately predict disease behaviour, tumour spread, response to standard or novel therapies or reliably correlate with overall survival (Pieretti 2002, Bamias 2011). The observed clinical differences among ovarian tumour subtypes are likely to reflect different underlying molecular mechanisms associated with a variety of genetic mutations. Visible morphological differences may be accompanied by differences in the protein expression, which orchestrate cellular function and behaviour (Faratian 2011). However, there may be further genetic heterogeneity, which is responsible for changes in cell function, and therefore dictates tumour behaviour and response to therapy, which may not necessarily be reflected in changed morphology. In addition, poor tumour differentiation and non-uniformity can mean that it is not always possible to accurately assign a single histological subtype to a tumour. There is also significant inter-observer variability and a lack of reproducibility of subtype reporting (Cramer 1987, Shimizu 1998).

Despite the heterogeneity, ovarian cancer is treated as a single disease using a combination of debulking surgery and platinum-based chemotherapy. The observed heterogeneity of the clinical behaviour of ovarian cancer and its response to standard treatment, alongside the growing data reporting molecular heterogeneity and the accompanying sensitivity to novel therapies, suggests that the reclassification of ovarian cancer is long overdue (Hennessy 2008). A classification system reflecting the tumour biology may also assist in the identification and development of biomarkers used for the prediction of response to therapy.

1.3.2. How Should Ovarian Cancer be Classified?

There is much data describing gene expression in ovarian cancer (Fekete 2011). The genes most commonly mutated in ovarian cancer include *p53*, *KRAS*, *CTNNB1*, *CDKN2A*, *PTEN*, *PIK3CA* and *BRAF*. Common mutations seen in tumour suppressor genes include *BRCA1/2*, *RB1*, *ARH1*, *GATA1*, *RNASET2*, *LOT1*, *DCC* and *FHIT*. Amplification or overexpression of the oncogenes *CMYC*, *ERBB2*, *HRAS*, *CSF1R*, *ECCF1*, *EGFR*, *P13K/AKT2*, *PTEN/MMAC1*, *FGF3*, *MDM2*, *BCL2* and *EGFR* are also commonly reported (Bast 2009, Lawrenson 2009). Gene expression studies have been shown to be useful for distinguishing ovarian tumour subtypes (Vang 2009). However, gene expression does not always correlate with protein translation and cellular function (Gustafsson 2011) and meta-analysis of all available ovarian cancer gene profiling signatures has, to date, failed to identify clinically relevant gene sets (Fekete 2011) that have been reproducible in second data sets. It is therefore perhaps more meaningful to analyse disease-related molecular pathways, which have been shown to, or are hypothesised to, directly correlate with clinical sensitivity or prognosis.

1.4. DNA Damage Repair (DDR) Pathways

Under physiological conditions, cells are constantly exposed to DNA damage caused by both endogenous and exogenous sources. In healthy cells, the DNA damage response (DDR) comprises of a number of cell cycle checkpoints and DNA repair pathways designed to signal DNA damage to repair and cell cycle arrest to allow time for repair and prevent damage being passed on to daughter cells. The repair pathway activated depends upon the type of damage and these pathways form a highly complex interacting mechanism for repair. There are six major pathways responsible for the repair of endogenous and exogenous DNA lesions: direct repair, mismatch repair (MMR), base excision repair (BER), nucleotide excision repair (NER) and double strand break (DSB) repair comprising homologous recombination (HR) and non-homologous end joining (NHEJ) (Hoeijmakers 2001, Bernstein 2002). Dysregulation of the DDR can lead to genomic instability that itself promotes cancer development but the exact disruptions, which in combination result in the development of cancer is not yet clear. Hanahan *et al* (2000) suggest that the huge number of cancer cell genotypes is a manifestation of six essential alterations in cell physiology that collectively dictate malignant growth: self-sufficiency in growth signals, insensitivity to growth-inhibitory (antigrowth) signals, evasion of programmed cell death (apoptosis), limitless replicative potential, sustained angiogenesis, and tissue invasion and metastasis. Each of these acquired capabilities represents the successful overriding of an anticancer defence mechanism (Hanahan 2000).

In cancer, dysregulation of the DDR is common presenting both challenges and opportunities for tumour-specific cancer treatment. Upregulated DNA repair pathways can cause resistance to DNA-damaging chemotherapy and radiotherapy and so inhibitors of these pathways have the potential to sensitize cells to these therapies (Curtin 2012). Loss of a DDR pathway can also lead to dependence on a compensatory pathway, which can then be targeted rendering subsequent DNA damage by cytotoxic agents irreparable and resulting in cell death. For this reason, dysfunctional DNA repair pathways have been shown to be important in many cancers, including ovarian cancer, and categorizing

tumours according to functional DDR pathways may result in clinically relevant groupings or provide biomarkers capable of predicting response and thereby enabling stratification of appropriate therapies.

1.4.1. Direct Repair by O⁶-methylguanine-DNA Methyltransferase (MGMT)

The simplest form of DNA repair is the direct reversal of the lesion. Use of cancer agents such as temozolomide, dacarbazine and nitrosoureas, alongside erroneous methylation, causes alkylation of the O₆ position of guanine. Unrepaired O₆-methylguanine is mutagenic as it results in mismatch of alkylated guanine with thymine instead of cytosine during replication (Saffhill 1985). Direct repair by O₆-methylguanine-DNA methyltransferase (MGMT) removes the alkyl group. However, if this pathway is deficient, O₆-methylguanine remains, resulting in persistent mismatching of bases during replication. The MMR pathway attempts to correct this but as the alkylated base is permanently bound with template DNA, repair is unsuccessful, triggering repeated cycles of excision and attempted repair and ultimately resulting in apoptosis. MGMT-deficient cells are highly sensitive to alkylating agents.

1.4.2. Base Excision Repair (BER)

BER is the main guardian against damage due to reactive oxygen species (ROS) including that resulting from cellular metabolism, methylation, deamination and hydroxylation (Hoeijmakers 2001). Dysregulation of ROS metabolism, leading to accumulation of DNA damaging agents, coupled with polymorphisms/ mutations that compromise BER function, is commonly seen in cancer (Curtin 2012). The most common base oxidations produced by ROS are 8-oxoguanine (8-oxoG) and 5-hydroxycytosine, which mispair with adenine and thymine, respectively (Lindahl 1993, Van Loon 2010, Curtin 2012). 8-oxo-7,8-dihydro-2'-deoxyguanosine (8-OHdG) is repaired by the DNA glycosylase and BER enzyme OGG1 (Almeida 2007). If left unrepaired 8-OHdG, bound to adenine, is highly mutagenic and leads to G to T transversion mutations (David 2007). The 8-OHdG – A mispair can be corrected by BER that involves DNA synthesis and preferential insertion of the correct C base mediated by DNA polymerase β (Pol β) (Krahn 2003).

The BER pathway is subdivided into short patch (single nucleotide replacement) and long patch BER (two to 13 nucleotides are replaced), depending on the nature of the 5' and 3' ends and, possibly, ATP availability (De Vos 2012), and is the process that removes damaged DNA bases and repairs single-strand breaks that arise following removal of the break.

In both pathways, the damaged base is removed by specific glycosylases forming an abasic site (or apurinic or apyrimidinic [AP] site), which is then hydrolysed by an AP endonuclease, such as APE1. The 'nick' is then repaired by short patch (the predominant mode) or long patch BER, Figure 1.4 - 1. In short patch repair, PARP-1 activation, resulting in production of PAR, leads to relaxation of the chromatin fibre and facilitates recruitment of proteins necessary for repair. PARP-1 mediated recruitment of XRCC1 is followed by nucleotide replacement by DNA polymerase- β (Pol β) and the gap is rejoined by ligase 3 (LIGIII). In long patch repair, XRCC1 recruits polynucleotide kinase (PNK), which converts the damaged DNA ends into 5'-phosphate and 3'-hydroxyl moieties. Proliferating cell nuclear antigen (PCNA) and Pol δ or Pol ϵ

extend and fill the nucleotide gap. FEN1 cleaves the resulting flap and re-joining is completed by LIGI (Baute 2008, Kummar 2012).

BER and Ovarian Cancer

Oxidative damage is generally increased in tumours: increased metabolism, oncogenic signalling and mitochondrial dysfunction result in 100-fold more 8-OxoG in cancer tissues than in normal tissues (Wiseman 1996).

Chemotherapeutic agents achieve cellular cytotoxicity by inducing DNA damage. However, proficient BER in cancer cells results in therapeutic resistance and adversely impact patient outcomes. BER factors, therefore, are emerging as important prognostic factors as well as predictors of response to cytotoxic therapy in patients.

Inhibition of BER (using methoxyamine) has been shown to sensitise cells to the alkylating agent temozolamide in ovarian cancer cell lines (Fishel 2007) and it has recently been shown that APE1 is overexpressed in 71.9% of ovarian cancers. Expression in this series has been shown to correlate with tumour type, optimal debulking, and overall survival (Al-Attar, Gossage et al. 2010).

Additional studies have also demonstrated altered APE1 expression or cytoplasmic localisation of APE1 to be associated with platinum resistance or overall prognosis (Zhang, Wang et al. 2009, Sheng, Zhang et al. 2012).

In a prospective cohort study of 310 ovarian cancer patients treated with platinum-based chemotherapy a lower survival rate and significant increased risk of death was observed in patients with XRCC1 399 Arg/Arg genotype (Cheng 2012).

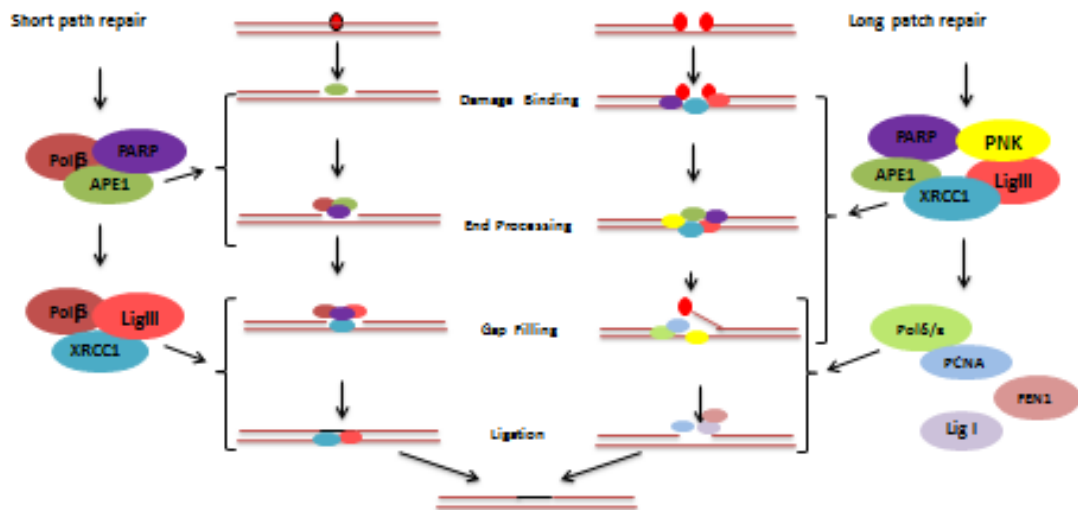


Figure 1.4 - 1: Base excision repair pathway. Short-patch repair takes place after the excision of a damaged base. It involves PAR mediated recruitment of XRCC1 (scaffold protein), followed by DNA pol β and DNA ligase III which conducts the ligation of the DNA. Long-patch repair occurs after direct DNA breaks and involves recruitment of XRCC1 followed by polynucleotide kinase (PNK), which converts the damaged ends to 5'-phosphate and 3'-hydroxyl moieties. Proliferating cell nuclear antigen (PCNA) and DNA polymerase δ/ϵ extend and fill the gap by 2–15 nucleotides, and FEN1 cleaves the resulting flap. The nick is then ligated by DNA ligase I.

1.4.3. Nucleotide Excision Repair (NER)

NER deals with the wide class of helix-distorting lesions that interfere with base pairing and generally obstruct transcription and normal replication (Hoeijmakers 2001), for example, UV radiation induced thymidine dimers (T-T), and intra-strand cross links, such as platinum-DNA adducts. There are two NER subpathways: global genome NER (GG-NER), which surveys the entire genome (both coding and non-coding genes) for distorting injury (Le Page 2000, Tang 2000) and transcription-coupled repair (TC-NER), Figure 1.4 - 2.

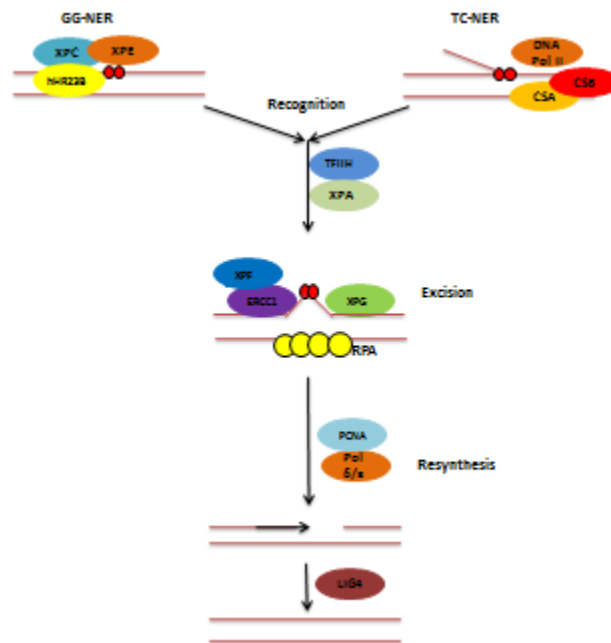


Figure 1.4 - 2: Nucleotide excision repair pathway. In GG-NER the protein complex XPC-hHR23B screens the genome (both coding and non-coding genes) for irregularities in the DNA structure such as bulky adducts (Le Page 2000, Tang 2000). TC-NER, exclusive to transcription, focuses on damage that blocks DNA polymerase II before CSA and CSB displace the stalled polymerase making DNA accessible for repair (Tornaletti 1999, Christmann 2003). Upon recognition of the DNA lesion, (either by binding of XPC-hHR23B or DNA polymerase II stalling) a cascade of proteins are recruited. These proteins are the same for both TC-NER and GG-NER. XPB and XPD helicases (which are both components of the multi-unit transcription factor TFIIH) open the region incorporating the lesion (Le Page 2000). The single-stranded-binding protein replication protein A (RPA) binds to the corresponding undamaged strand and stabilises it. In the rate-limiting step, the endonucleases XPG and ERCC1-XRF complex then cleave the open DNA strands and excise the damaged site. Resynthesis of the removed region is carried out by DNA polymerase δ/ϵ , ligase 3 and ERCC3 (Hoeijmakers 2001).

NER and Ovarian Cancer

NER is a key pathway involved in mediating resistance to platinum. Multiple studies have shown high mRNA levels of some of the NER components in cisplatin-resistant ovarian cancer cells, mouse models and human tissue (Dabholkar 1994, Damia 1998, Dabholkar 2000), with greatest correlation seen between ERCC1 mRNA levels with cisplatin resistance (Ferry 2000, Li 2000). *In vitro* studies have demonstrated sensitivity to platinum in NER defective human ovarian cell lines, in particular those with reduced levels of ERCC1 and xeroderma pigmentosum complementation group F proteins. Cell lines with intrinsic cisplatin resistance have been shown to have increased sensitivity to

cisplatin after antisense RNA inhibition of ERCC1 (Selvakumaran 2003). In addition, cell lines that developed resistance in vitro after exposure to cisplatin chemotherapy were found to have increased expression of ERCC1 (Ferry 2000).

1.4.4. Mismatch Repair (MMR)

Mismatch repair (MMR) is a highly conserved, strand-specific repair pathway, which follows a stepwise process. MMR is responsible for the recognition and repair of DNA damage caused by deamination, oxidation and replication errors and also targets DNA cross-links, dimers and alkylated bases. External agents, such as cisplatin, can cause such damage by inducing cross-links between adjacent guanine residues or nucleoside analogues.

MMR is subdivided into two pathways according to the protein complexes that bind to the DNA lesion, Figure 1.4 - 3. The products of six genes (MLH1, MSH2, PMS1, PMS2, MSH6 and MSH3), originally identified for their involvement in Hereditary Non Polyposis Colorectal Cancer (HNPCC) syndrome, participate in MMR (Scartozzi 2003). When a mismatch is detected, MSH2 associates with either MSH6 or MSH3 to form MutS α and MutS β complexes respectively (Acharya 1996). These complexes assemble at the DNA mismatch site and recruit a third heterodimer, which comprises of MLH1 partnered with PMS2. The two protein complexes have overlapping specificities and functions, which ensure the majority of common replication errors are recognised and efficiently processed. Excision of the mismatch is performed by exonuclease 1 and proliferating cell nuclear antigen (PCNA) and it is followed by resynthesis DNA polymerase δ and religation of the DNA strand (Wu 2008, Boland 2010).

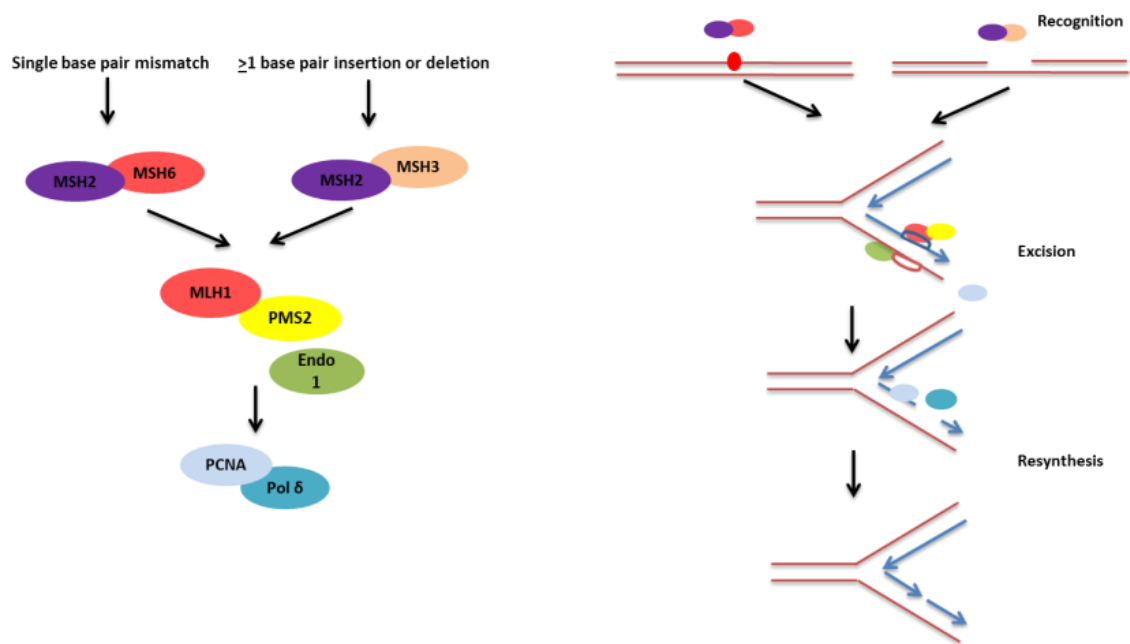


Figure 1.4 - 3: Mismatch repair pathway. The MutS α (MSH2/MSH6) heterodimer recognizes base-base mismatches and small insertion deletion loops (IDL). The MutS β (MSH2/MSH3) heterodimer recognizes single nucleotide mismatches as well as longer IDLs (10-nucleotide loops). In association with the MutL heterodimer, MutH is activated which nicks the unmethylated strand containing the incorrect base. The cleaved strand then undergoes exonuclease activity, DNA resynthesis and ligation.

MMR and Ovarian Cancer

A significant proportion of carcinomas, including endometrial, ovarian, oesophageal, colorectal and head and neck cancers, develop through defective MMR (Gurin 1999, Hayashi 2003, Demokan 2006, Sinicrope 2012). Defects in MMR may be inherited, as in HNPCC (Watson 2001, Lynch 2009), or may occur through epigenetic silencing of an essential MMR gene (Suzuki 1999, Esteller 2000, Peltomaki 2003). HNPCC leads to increased risk of colon cancer (80% life time), endometrial cancer (40 - 69%) and ovarian cancer (12%) (Watson 2001). Mutations in *MLH1* (50%), *MSH2* (39%) and *MSH6* (7%) account for the majority of reported germline variants (Peltomaki and Vasen 2004, Anacleto 2005).

When MMR is deficient, which has been reported in around 15% (0 - 39%) of ovarian tumours (Buller 2001, Helleman 2006), the cells bypass the intra-strand crosslinks and continue to proliferate in spite of the DNA damage and are therefore resistant to platinum agents as well as DNA methylating agents and thiopurines (Brown 1997, Vaisman 1998, Strathdee 1999, Helleman 2006).

Defects in the MMR pathway have been demonstrated to be significantly higher in tumours post-chemotherapy compared to untreated controls. These findings suggest resistance development by chemotherapy selection for subpopulations of intrinsically resistant cancer cells (Brown 1997, Scartozzi 2003, Cooke 2011). The presence of microsatellite instability (MSI) has been confirmed as a marker of MMR deficiency and takes into account mutations and epigenetic silencing of the functional pathway. Mutations in *MLH/MSH* account for 2% of all ovarian cancers. However, MSI has been reported in around 15% (0 - 39%) of ovarian tumours, mostly in endometrioid types (Buller 2001, Gras 2001, Zhang 2008). Two separate studies have raised the possibility that defective MMR may have prognostic significance (Fujita 1995, King 1995) and it is reasonable to hypothesise that MSI, indicating MMR deficiency in ovarian cancer, is a potential biomarker of platinum sensitivity.

Cisplatin-resistant ovarian cell lines have been shown to be defective in MMR (Drummond 1996) and acquire an MSI phenotype when resistance develops (Anthony 1996). Cell lines deficient in hMLH1 have previously been shown to be tolerant to DNA damage induced by alkylating agents (Koi 1994) and restoration of MMR in such cell lines can increase their sensitivity to cisplatin (Aebi 1996). In a study by Scartozzi *et al* (Scartozzi 2003), loss of hMLH1 was observed in over 50% of 34 stage III/IV ovarian cancers. Loss of hMLH1 has been shown to be significantly higher in ovarian tumours post chemotherapy compared to untreated tumours, suggesting that exposure to chemotherapy induces positive selection for MMR deficient tumour cells *in vivo* (Brown 1997). In a study by Watanabe *et al.* (Watanabe 2001), a change in microsatellite stability was seen after five to six cycles of cisplatin; post treatment biopsies showing MSI and down regulation of *hMLH 1* expression. Similar results were seen in a study by Fink *et al.* (Fink 1998). Gifford *et al* (Gifford 2004) reported that 25% of the plasma DNA samples collected at relapse in advanced ovarian cancer patients enrolled in the SCOTROC1 study, were newly diagnosed to be positive for *hMLH1* methylation, which correlated with poor overall survival.

1.4.5. Double Strand Break Repair (DSB)

One of two pathways with overlapping components repairs DSB. HR involves alignment of a homologous chromatid to provide a template for error free repair and is limited to the S/G2 phase of the cell cycle when a sister chromatid is present (Lieber 2010). Non-homologous end joining (NHEJ) is the predominant method of repair in G0/G1 but functions in all stages of the cell cycle. NHEJ does not require a complementary template as it repairs the defect by direct ligation and is therefore error prone (Lieber 2008, Helleday 2010). Central to the DNA damage and repair responses are sensors, particularly the phosphatidylinositol 3-kinase-related protein kinase family, including DNA-dependent protein kinase (DNA-PK), ataxia telangiectasia mutated (ATM) and ATM- and Rad3-related protein (ATR). ATM, ATR and DNA-PK orchestrate the initiation of cell cycle checkpoints and DSB repair. These three proteins have many common substrates. However, they are generally thought to be involved in unique signalling pathways.

Additionally, 53BP1 and BRCA1 directly influence DSB repair pathway choice by regulating 5' end resection. In G1 the resection of the 5' end is halted by the 53BP1/Rif1 proteins allowing Ku to bind and NHEJ to predominate (Chapman 2012, Chapman 2013). Synthesis of BRCA1 in S and G2 phases inhibits Rif1 and allows 5' end resection with subsequent inhibition of NHEJ and repair by HR (Chapman 2012, Chapman 2013).

1.4.6. Non-Homologous End Joining (NHEJ)

NHEJ repairs double strand breaks without the need for a homologous copy of the broken region of DNA, so is not restricted to a certain cell cycle phase. DNA sensors; DNA dependent protein kinase catalytic subunit (DNA-PKcs) and ATM play important roles in NHEJ by detecting DNA damage and signalling for repair responses (Drouet 2006). After DNA DSBs occur, NHEJ is initiated and the phosphorylated Ku70/Ku80/DNA-PK_{CS} complex (DNA-PK) allows the alignment of the DNA strands, which are subsequently joined by the ligase IV/XRCC4 complex (Martensson 2002), Figure 1.4 - 4.

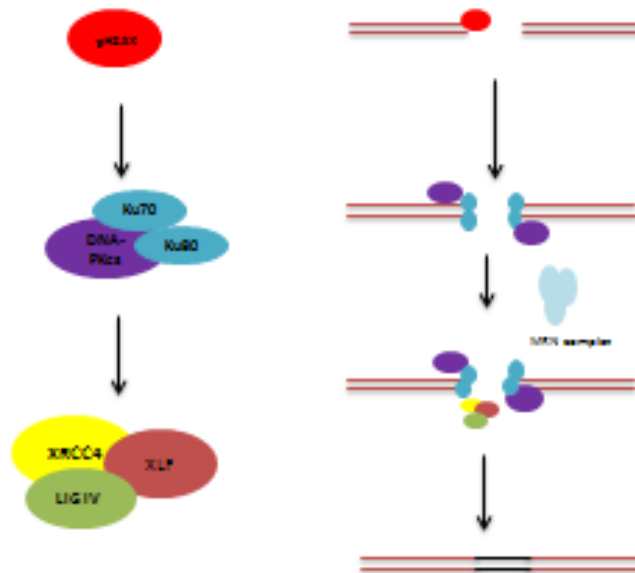


Figure 1.4 - 4: Non-homologous end joining pathway. After phosphorylation of H2AX at DNA DSB sites, NHEJ is initiated by the binding of the Ku heterodimer (composed of Ku70 and Ku80). DNA-PKcs is then recruited and binds to the DNA end, activating its serine/threonine kinase activity. The Ku70/Ku80/DNA-PKcs complex, referred to as DNA-PK, holds the two DNA strands together in a synapse (Martensson 2002). Activation of DNA-PK by phosphorylation allows the alignment of the DNA strands, which are subsequently joined by the ligase IV/XRCC4 complex. This reaction is stimulated by XLF protein, which interacts with XRCC4 (Van Gent 2007) to catalyse the final end-joining reaction.

The NHEJ Pathway and Ovarian Cancer

NHEJ has been shown to be defective in 45% of EOC (McCormick 2015). The relationship between its functional status and that of HR appears to be complex and there are emerging theories, based upon *ex vivo* cultures of ovarian cancer, that NHEJ is in fact the predominant pathway of DNA DSB repair in ovarian cancer.

1.4.7. Homologous Recombination Repair (HR)

HR is an error free template-dependent repair pathway of complex DNA damage principally DNA DSB, stalled replication forks or collapsed forks (Doe 2002, Michel 2004, Shrivastav 2008). It is a process by which breaks are repaired through the use of homologous sequences of DNA in sister chromatid as a template for repair, occurring primarily during the

M phase of the cell cycle (Kennedy 2006). A DSB is recognised by the MRN complex (formed from MRE11, Rad50 and NSB1) before phosphorylation of H2AX, NBS1, *BRCA1* and FANCD2. RPA then binds and unwinds the DNA structure and Rad51 binds allowing invasion of the homologous sequence on the sister chromatid. This is used as a template for repair,

Figure 1.4 - 5.

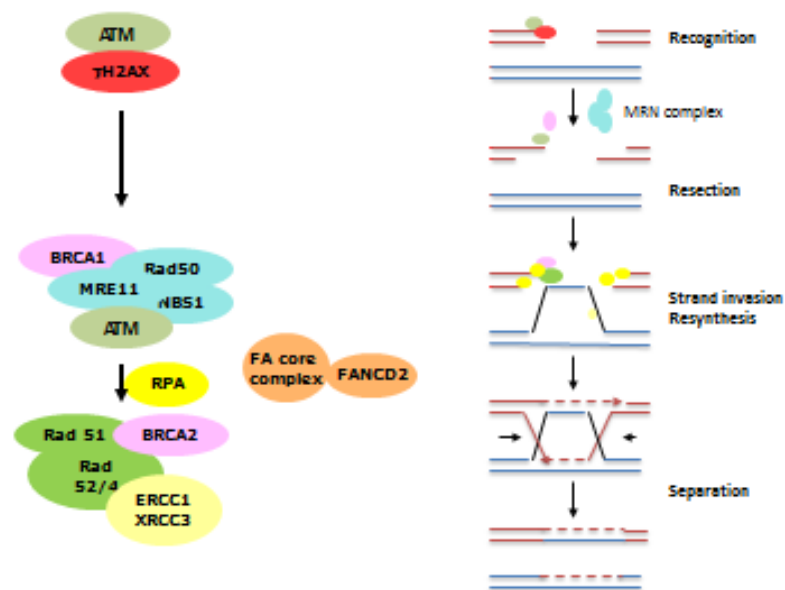


Figure 1.4 - 5: Homologous recombination pathway (Cerbinskaite 2012). The MRN complex undergoes a series of conformational changes to attract, activate and increase affinity of ATM at the DSB site (Paull 2005, You 2005, Chistiakov 2008). ATM-dependent phosphorylation of H2AX, NBS1, *BRCA1* and FANCD2 occurs before replication protein A (RPA) binds to facilitate unwinding of the DNA secondary structure allowing access for the substrates of DNA repair (Sung 2006, Jacquemont 2007, Xing 2008, Hartlerode 2009). *BRCA2* mediates the loading of Rad51 onto the RPA coated single strand ends (Valerie 2003, Sy 2009, Zhang, Ma et al. 2009). After identification of the homologous sequence on the sister chromatid, Rad51 forms a nucleoprotein filament on the ssDNA and catalyses the invasion of the homologous sequence on the sister chromatid, which is then used as a template for accurately repairing the broken ends by DNA synthesis (Hoeijmakers 2001, Gudmundsdottir 2006). After replication

has extended past the region of the DSB, strand replication continues to the end of the chromosome (Hoeijmakers 2001, Khanna 2001, Bast 2010).

HR and Ovarian Cancer

The tumour suppressor genes *BRCA1* and *BRCA2* are currently the only genes to be identified as highly penetrant ovarian cancer susceptibility genes (Gayther 1999). *BRCA1* and *BRCA2* tumour suppressor genes have crucial functions in the HR pathway by promoting efficient and precise repair of DSB. Inactivation of *BRCA1* or *BRCA2* results in genetic instability. Homozygous *BRCA1* mutation is lethal in mice (Gowen 1996) and down regulation of *BRCA1* leads to cell cycle arrest or apoptotic cell death (Bouwman 2010). *BRCA2* functions are largely limited to DNA repair (Chistiakov 2008) controlling localisation and DNA binding of Rad51 (Davies 2001).

The vast majority of tumours from women with germline *BRCA1/2* mutations show loss of heterozygosity of the wild type allele at the *BRCA1/2* loci (Ramus 2003) and are considered HR deficient (Venkitaraman 2004). Carriers of mutations in *BRCA1* or *BRCA2* have up to a 66% lifetime risk of ovarian cancer, section 1.1.2 (Robles-Diaz 2004). Ovarian cancers with germline or somatic *BRCA1/2* mutation genes have unique features in terms of histology, survival and chemo sensitivity.

Tumours with *BRCA1* or *BRCA2* mutations have been shown to be defective in HR (Moynahan 1999, Moynahan 2001) and this has fuelled the interest in the HR pathway in both breast and ovarian cancer.

PolyADP-ribose polymerase 1 and 2 (PARP-1/2) enzymes have important roles in signalling single-strand DNA breaks as part of the base excision repair (BER) pathway (Dantzer 1999, Dantzer 2000) and represent a novel target in cancer therapy. Inhibition of PARP leads to an accumulation of unrepaired SSB that will convert to DSB and, unless repaired by HR, will lead to cell death (Schultz 2003). Understanding of this phenomenon has led to the development of PARP inhibitors (PARPi) and HR defective cell lines (*BRCA1/2* defective) have been shown to be 100 - 1000 fold more sensitive to PARPi than heterozygote or wild type cell lines (Bryant 2005, Farmer 2005). Additionally, PARP inhibitors have shown to be highly effective in the treatment of *BRCA1/2* mutated solid tumours (Plummer, Jones et al. 2008, Fong 2009, Audeh 2010, Tutt 2010).

The function of the entire repair HR pathway can be affected if one or more genes are defective and a number of mutations, other than *BRCA 1/2*, in a variety of genes within the HR pathway have been reported (Cerbinskaite 2012). Some of these mutations have also been shown to result in sensitivity to PARP inhibitors (McCabe, Turner et al. 2006). Mukhopadhyay *et al* describe a functional assay to identify HR deficient ovarian cancers based upon quantification of immunofluorescent Rad51 nuclear foci formation following induction of DNA damage (Mukhopadhyay 2010). Failure to induce Rad51 foci formation following DNA damage has been shown to be a reliable indicator of HR deficient ovarian cancers and correlates with *ex vivo* sensitivity to PARPi as well as clinical sensitivity to platinum chemotherapy (Mukhopadhyay 2010, Mukhopadhyay 2012).

Proteins involved in DSB repair pathways have also been implicated in chemoresponse to platinum (Martin et al. 2008). It is known that *BRCA* deficient ovarian cancers are platinum sensitive (Cass et al. 2003). *In vitro*, it has been seen that defects in the Fanconi-anaemia/*BRCA* pathway (FANCF inactivation by methylation) can enhance sensitivity to cisplatin in cell lines and that demethylation can induce platinum resistance (Taniguchi et al. 2003). *BRCA1* deficient mammary tumours have been shown to be highly sensitive to PARPi alone and in combination with platinum drugs (Rottenberg et al. 2008).

1.5. Other Pathways Important in Ovarian Cancer

Dysregulation of proliferative signalling pathways is a characteristic of cancer cells. “Gain of function” mutations in the MAPK or PI3K/Akt/mTOR pathways are well described and known to be important in endometrioid and clear cell EOCs.

The mitogen-activated protein kinase (MAPK) pathway is key to the transduction of external mitogenic signals to the nucleus after a mitogen binds to a cell membrane receptor kinase (Dong 2002). Oncogenic mutations in the pathway lead to activation of the pathway in the absence of a mitogenic signal leading to carcinogenesis (Smalley 2003). *KRAS*, *BRAF* and *ERBB2* mutations are well documented in ovarian cancer and result in constitutive activation of the MAPK pathway. These are mutually exclusive mutations and are not specific to morphological subtypes with 66% of mucinous, 33% of low grade/borderline serous and 17% of endometrioid cancers having *KRAS* mutations, the majority being a single amino acid substitution (V12G) (Nakayama 2008). The *KRAS* variant has been shown to be a statistically significant predictor for platinum resistance (Ratner 2011). *BRAF* mutation (a single nucleotide substitution) leading to elevated kinase activity (Davies 2002) is seen in 33% of the low grade serous tumours (Shih 2004, Nakayama 2008, Geyer 2009).

Overexpression of *CMYC* and *ERBB2* is seen in 36 - 76% and 10 - 20% of advanced stage EOCs and is also associated with poor prognoses (Dimova 2006, Nakayama 2006, Vang 2009).

The PI3K/Akt/mTOR pathway transduces extra cellular signals associated with cellular growth, proliferation and apoptosis. Binding of extracellular signals, e.g. EGF to the receptor tyrosine kinases, results in translocation and activation of PI3K heterodimers (Chen and Guan 1994, Vanhaesebroeck 1999) resulting in phosphorylation of phosphatidylinositol-containing lipids (PIP). PIPs mediate recruitment of signalling proteins (Toker 1997) including Akt (a serine/threonine protein kinase) (Jiang 1999) which translocates to the nucleus and mediates the activation/ inhibition of various targets resulting in cellular survival and cell growth and proliferation. Amplification of the PI3K catalytic subunit and the lost function of PTEN are frequently detected in ovarian cancer cells (Yokomizo

1998, Meng 2006) with *PIK3CA* being increased in copy number in 40% of ovarian cancer cell lines and patient tumour samples, particularly endometrioid and clear cell subtypes (Shayesteh 1999).

The tumour suppressor gene *PTEN* (phosphatase and tensin homologue deleted from chromosome 10) is known to inhibit the PI3K/Akt pathway and therefore *PTEN* mutations result in activation of PI3K/Akt pathway and subsequent increased cell survival (Nagata 2004). Decreased *PTEN* expression has been shown to play a role in progression of ovarian disease (Schondorf 2003).

The most well described tumour suppressor gene *TP53* is implicated in the development of several cancer types. It is involved in controlling cell cycle, apoptosis and maintaining the genome integrity. The *TP53* gene located on the short arm of chromosome 17 (17p13.1) encodes p53 (Isobe 1986). If the *TP53* gene is damaged, tumour suppression is severely reduced and the cells will continue to divide uncontrollably.

Following DNA damage, levels of the transcription factor p53 rapidly increase. p53 binds to the DNA, inducing expression of either p21 (Waf1/Cip1) or expression of bax, PIGs, IGF-BP3, Fas, FasL and DR5. The binding of p21 to CDK/cyclin complexes induces G1 arrest (Smith 2003) until the DNA damage is repaired. If the damage is irreparable, p53 induces the expression of apoptotic genes. Unsurprisingly, missense mutations resulting in overexpression of mutated p53 protein is seen in almost half of all cancers (Levine 1997). *TP53* mutation is almost invariably present in HGSC and p53 has been implicated in the regulation of *BRCA1* function (Bouwman 2010) and in the transcriptional regulation of Rad51 (Arias-Lopez 2006). Because of its almost universal expression, it is not of substantial prognostic or predictive significance (Ahmed 2010).

Mutant *TP53* has been shown to directly decrease tumour cell sensitivity to chemotherapeutic agents and promote the emergence of drug resistance in both *in vivo* and *ex vivo* studies (Lowe 1994, Righetti 1996, Blandino 1999, Knappskog 2012, Lai 2012). Examination of the p53 pathway and the

association of *TP53* mutation with HGSC have singled out the p53 gene as a molecular target for novel cancer therapeutics. p53 gene replacement therapy within the cancer cells is one such approach that has not only become feasible but may also show benefit (Roth 1996, Nielsen 1997, Nielsen 1998, Buller, Runnebaum et al. 2002). Vaccine-induced p53-specific immune responses were previously reported to be associated with improved response to secondary chemotherapy in patients with small cell lung cancer (Antonia 2006). The effect of p53 vaccination is now being explored in ovarian cancer patients (Leffers 2012).

1.6. Current Treatment Strategies in Ovarian Cancer

1.6.1. Ovarian Cancer Surgery

Surgery plays a pivotal role in the management of ovarian cancer and has evolved since the first report of an inverse relationship between survival and the size of residual disease following surgery in 1975 (Griffiths 1975). The significance of optimal resection (to less than one cm residual tumour) is well established in both retrospective and prospective randomised controlled trials (RCTs) and maximal cytoreduction has been shown to be one of the most powerful determinants of survival among patients with stage III/IV EOC (Griffiths 1975, Hoskins 1994, Bristow 2002) with an improvement in survival of 5.5% with every 10% increment in cytoreduction (Bristow 2002).

Two management strategies with variable orders of treatment are used for advanced stage disease: primary debulking surgery followed by six cycles of adjuvant chemotherapy (platinum +/- taxol) or three cycles of neoadjuvant chemotherapy (NACT), at which time response to treatment is assessed and, if appropriate, interval debulking surgery (IDS) is followed by a further three cycles. Surgery is undertaken at a time when optimal cytoreduction is thought to be achievable. Two major clinical trials, the European Organisation for Research and Treatment of Cancer (EORTC) 55971 (Vergote 2010) and Chemotherapy or Upfront Surgery (CHORUS) (Kehoe 2015) aimed to compare the clinical outcomes of these two management options. EORTC has not shown any difference in survival between the two groups but subgroup analysis showed survival was significantly associated with optimal resection of the tumour whether undertaken as primary or interval surgery (Vergote 2010). Two recent Cochrane Reviews reported similar survival benefit from optimal cytoreduction (Elattar 2011, Al Rawahi 2013).

The Biological Benefits of Surgery

Many theoretical explanations for the benefits of cytoreductive surgery have been proposed including; 1) excision of poorly vascularised tumour; 2) enhancement of the immune system; 3) improved cell kill with residual tumour being better perfused and in the growth phase; 4) small volume of tumour leading to better efficacy of chemotherapy and 5) reduced resistance to chemotherapy due to the reduced bulk of tumour and removal of chemo-resistant clonogenic cells (Covens 2000).

Surgical 'Resectability' and Tumour Biology

The ability to completely resect EOC may not necessarily be merely a reflection of the ability of the surgeon but may, in part, be a reflection of the biological aggressiveness of the disease. A retrospective review of the Gynaecologic Oncology Group (GOG) data showed that survival in women who had their large volume extra-pelvic disease cytoreduced to optimal (less than one cm) was poorer compared to women presenting with de novo optimal volume (less than one cm) extra-pelvic disease (Hoskins 1992). Similarly, Hacker *et al.* reported poorer prognosis in women with >10 cm metastatic disease compared to women with small volume initial tumour load (<10 cm), despite both groups being optimally cytoreduced (Hacker 1983).

1.6.2. Tumour Sampling for Histological and Molecular Subtyping

Tumour sampling is infrequent during standard treatment strategies and currently limited to histological review at initial diagnosis. Therefore, treatment strategies are often largely independent of the actual tumour biology and cellular characteristics.

Tumour sampling prior to surgery is commonly only done when there is diagnostic doubt or when disease is extensive, suggesting that NACT with IDS may be preferred. In these circumstances, typically a single biopsy is taken from one region, most commonly the omentum, which may or may not be representative of the primary tumour in the pelvis. Even at relapse, biopsies are infrequent but if taken, would again typically be limited to a single image guided

biopsy. Laparoscopy is being used in some units as an aid to pre-operative diagnosis and staging but does not form part of routine practice and its ability to predict optimal cytoreduction is not yet clear (Fagotti 2008).

It is not yet clear if solid tumour biopsy is superior to ascitic cell sampling in terms of biomarker assessment. Both sampling techniques are however invasive procedures and alternative less invasive sampling techniques should be considered if we are to move towards biomarker stratification of therapy.

1.6.3. Chemotherapy

Ovarian cancer, irrespective of histological subtype, stage or surgical outcome, is currently treated with a combination of cytoreductive surgery and platinum chemotherapy, with or without taxanes.

There has been much research to investigate which patients should receive chemotherapy, the optimum regimen and optimum order of treatment, Table 1.6 - 1. Attempts to improve the standard two drug chemotherapy by adding a third agent failed to affect PFS or OS but did result in increased side-effects (Du Bois 2006, Pfisterer 2006, Bookman 2009, Hoskins 2010).

Trial	Description	Reference
GOG 111	Paclitaxel and cisplatin combined produced a higher response rate and a longer PFS in comparison to the standard cyclophosphamide and cisplatin regimen	(McGuire 1996)
OV10		(Piccart 2000)
GOG132	Single agent cisplatin vs. paclitaxel/cisplatin combination with no benefit to the paclitaxel/cisplatin regimen	(Muggia 2000)
GOG158	14% reduction in risk of disease progression following paclitaxel and carboplatin	(Bookman 2003)
ICON3	Paclitaxel/carboplatin vs. a control arm of single-agent carboplatin or the three drug combination (cyclophosphamide, doxorubicin and cisplatin) with no survival benefit seen with the addition of taxol.	(ICON Collaborators 2002)

Table 1.6 - 1: Randomised Controlled Trials (RCT) for chemotherapy treatment for ovarian cancer.

1.6.4. Platinum

Mechanism of Action

Cisplatin and carboplatin are transported into the cell by a copper transporter (CTR1). Once inside the cell, it is activated through a series of aquation reactions, whereby one of the chloride ligands is displaced by water. Aquated platinum readily binds DNA, with a preference for purine bases, (Jamieson 1999) forming monoadducts. Intra- and inter-strand DNA crosslinks are subsequently formed, causing conformational DNA changes, impairing replication and DNA synthesis (Siddik 2003). Platinum-induced DNA lesions attract DNA binding proteins that either signal for apoptosis or initiate DNA MMR, which can lead to continued cell viability and result in platinum resistance (Tapia 2012).

Platinum Resistance

Approximately 80% of ovarian cancers are sensitive to platinum therapy at presentation but the vast majority of patients will develop resistance and ultimately succumb to their disease as a result of ineffective second line therapies in the presence of chemo resistance (Thigpen 1993). Intrinsic and acquired resistance results from the numerous genetic and epigenetic changes occurring in cancer cells, which may include alterations in proliferation signalling pathways, for example P13K/Akt/mTOR or MAPK pathways, section 1.5.1, suppression of tumour suppressor genes, for example PTEN, section 1.5.3, changes to drug import/export, for example CTR1/ATP7 copper transporters in platinum resistance; and changes in DNA damage response.

Definitions

GOG adopted the definition of chemosensitivity based upon clinical criteria from a retrospective case series. Following initial treatment when patients were re-challenged with platinum, those with a longer interval from the last dose of platinum had better response and overall outcome (Ledermann 2010). This clinical observation set the basis for the current classification of platinum resistance, Figure 1.6 - 1, (Tapia 2012) and allowed the commonly used stratification criteria in clinical trials of recurrent EOC. Platinum resistant disease

is defined as disease that recurs within 6 months of completion of chemotherapy, with platinum sensitive disease defined as recurrence beyond 12 months, although there is variability in this definition. Refractory disease demonstrates no response to chemotherapy with either static or progressive disease seen up to the date of their post chemotherapy treatment evaluation.

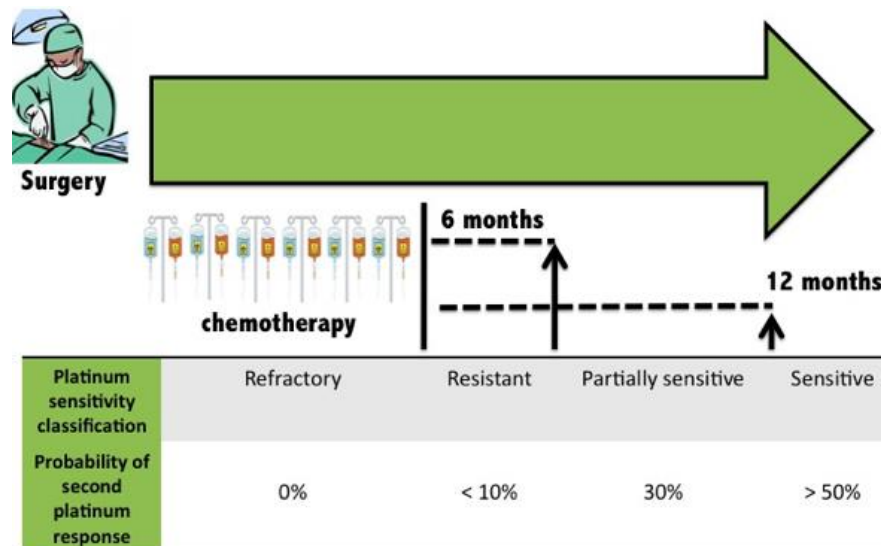


Figure 1.6 - 1: Platinum-resistance definition by the Gynaecologic Oncology Group (GOG). Platinum sensitivity is classified as resistant, partially sensitive or sensitive, according to the time elapsed since finishing first-line treatment. Probability of re-treatment response is shown for each group of patients (Tapia 2012).

Treatment options are limited at relapse and the toxicities of conventional first and second line chemotherapies and the frequent development of chemo-resistance limits their use (Guppy 2005, Markman 2009). The current treatment for platinum-resistant EOC consists of chemotherapy agents whose mechanism of action is different from that of platinum (Harter 2006). Selection of second line agent is currently largely based upon likely tolerance by patients rather than tailored according to the biology of the disease.

1.6.5. Second Line Agents

Treatment of recurrent disease is considered palliative and is initiated with the goals of controlling disease-related symptoms, limiting treatment-related toxicity, maintaining or improving quality of life, delaying time to progression and prolonging survival (Herzog 2004). Numerous second line agents are available, Table 1.6 - 2. Typically, one, or a maximum of two, agents are given at one time due to potent side effects and the typical frailty of patients. There is little guidance available to assist in the appropriate selection of an effective second line agent and the decision is frequently based upon the likely patient tolerability as well as evidence from limited clinical trials.

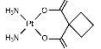
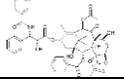
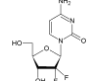
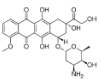
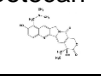
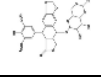
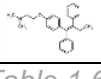
Cytotoxic Agent	Mechanism of Action	Licensed Indication	Common / Significant Side-effects
Platinum 	Alkylating agents which irreversibly bind to DNA bases, resulting in DNA fragmentation as well as formation of DNA cross-links preventing DNA synthesis or transcription.	<ul style="list-style-type: none"> • First line • Recurrent platinum sensitive disease 	<ul style="list-style-type: none"> • Myelosuppression • Renal impairment • Peripheral neuropathy
Paclitaxel 	Binds to the β subunit of tubulin arresting microtubule function, preventing intracellular transportation. Additionally induces apoptosis by binding to Bcl-2 arresting its anti-apoptotic function (Gaitanis 2010).	<ul style="list-style-type: none"> • First line with platinum • Recurrent disease 	<ul style="list-style-type: none"> • Myelosuppression • Peripheral neurotoxicity • Fatigue/Myalgia
Gemcitabine 	A nucleoside analogue activated intracellularly to dFdCTP by deoxycytidine kinase. Incorporation of dFdCTP into DNA results in inhibition of DNA synthesis and induction of apoptosis.	<ul style="list-style-type: none"> • Monotherapy in pre-treated patients. 	<ul style="list-style-type: none"> • Myelosuppression • Hepatic impairment
Doxorubicin 	Antineoplastic anthracycline antibiotic with antimetabolic and cytotoxic activity. Doxorubicin forms complexes with DNA by intercalation between base pairs. It inhibits topoisomerase II activity preventing DNA religation (Weiss 1992).	<ul style="list-style-type: none"> • Paclitaxel and platinum refractory disease 	<ul style="list-style-type: none"> • Fatigue • Mucositis/stomatitis •
Bevacizumab 	A recombinant monoclonal antibody that binds to VEGF preventing interaction with Flt-1 and KDR receptors. This prevents blood vessel proliferation and tumour metastasis (Velcheti 2006).	<ul style="list-style-type: none"> • Suboptimal cytoreduction and recurrent disease 	<ul style="list-style-type: none"> • Hypertension • Fatigue • GI perforation / fistula
Topotecan 	A synthetic camptothecin derivative that binds to the topoisomerase I-DNA complex interfering with the replication fork at SSB, leading to replication arrest and DNA DSB (Dennis 1997, Kollmannsberger 1999).	<ul style="list-style-type: none"> • Paclitaxel and platinum refractory disease 	<ul style="list-style-type: none"> • Myelosuppression
Etoposide 	A semisynthetic derivative of podophyllotoxin. Inhibits DNA topoisomerase II, thereby inhibiting DNA re-ligation causing critical errors in DNA synthesis and subsequent apoptosis.	<ul style="list-style-type: none"> • Recurrent ovarian cancer 	<ul style="list-style-type: none"> • Myelosuppression • Fatigue
Tamoxifen 	Tamoxifen selectively binds to oestrogen receptors (ER) resulting in up/down regulation of oestrogen dependent genes resulting in reduced DNA polymerase activity and impaired thymidine utilization (Jordan 2006).	<ul style="list-style-type: none"> • Oestrogen receptor positive cancers 	<ul style="list-style-type: none"> • Headaches • Hot flushes • Fatigue

Table 1.6 - 2: Second line chemotherapy agents in the treatment of ovarian cancer.

1.7. Targeted Therapies for Ovarian Cancer?

Despite the growing understanding of the molecular complexity and heterogeneous nature of ovarian cancer, the disease continues to be treated as a single entity. The majority of patients are treated with surgery and chemotherapy but the timing of this, alongside the highly variable treatment of recurrent disease makes incorporation of disease biology into clinical decision making highly complex. Additionally, in spite of the availability of multiple second line therapies, their effect upon overall survival is relatively modest. The inability to predict their effect for each individual, coupled with their side-effects, limits their use.

Novel biological agents, aim to target tumour cells and /or the tumour microenvironment by exploiting specific molecular abnormalities within tumour-specific oncogenic pathways. A number of agents are currently being investigated including PARP, mTOR, MEK, EGFR and HER2 inhibitors (Mazzoletti 2010, Gui 2012, Vergote 2012, Anglesio 2013, Farley 2013, Naumann 2013). These agents aim to cause selective cancer cell cytotoxicity by inhibiting key cellular pathways making them more susceptible to chemotherapy agents. Adverse systemic effects are hence reduced. When used in combination, these novel agents provide an opportunity to potentiate action and counteract resistance of current cytotoxic therapies (Drew 2009). However, of more importance to this project is their use as monotherapies in tumours with defective DNA repair pathways.

1.7.1. *Angiogenesis Inhibitor: Bevacizumab*

Angiogenesis, the process of new blood vessel growth, has an essential role in tumour formation, growth, metastasises and repair (Hollingsworth 1995) and is under the control of a complex interaction between angiogenic factors, including vascular endothelial growth factor (VEGF) and inhibitors. In ovarian cancer, increased levels of VEGF are associated with poor prognosis and have been confirmed in multivariate analysis as an independent prognostic indicator of

survival (Hollingsworth 1995, Hartenbach 1997, Alvarez 1999, Shen 2000, Xu 2000, Sonmezer 2004, Duncan 2008).

Bevacizumab, a recombinant humanised monoclonal antibody to the VEGF ligand, has shown single-agent activity in phase 2 EOC trials (Burger 2007, Cannistra 2007) and two phase 3 trials (GOG 0218 and ICON7) have demonstrated extended PFS of up to 4 months following standard chemotherapy for stage III/IV disease (Burger 2011, Perren 2011). Furthermore, addition of bevacizumab to chemotherapy in platinum sensitive (OCEANS study) (Aghajanian 2012) and platinum resistant (AURELIA study) (Pujade-Lauraine 2012) recurrent disease has been shown to improve PFS. Bevacizumab is currently licensed in combination with carboplatin and paclitaxel for first line treatment of suboptimally cytoreduced FIGO stage 3/4 EOC and in combination with carboplatin and gemcitabine for the treatment of first recurrence platinum-sensitive cancer (Aghajanian 2012). Benefit in the treatment of platinum resistant disease has not been seen in a phase 3 trial but this may be due to the limitations of the trial design. Several markers that have been explored, include the measurement of angiogenesis, the measurement of secreted factors and/or cytokines such as VEGF, interleukin (IL)-8 and IK-6 and circulating endothelial cells (Campos 2009).

1.7.2. PARP Inhibitors

PARP and the Development of PARP Inhibitors

The PARP inhibitors represent one of the most exciting recent developments in cancer therapy. Poly (ADP-ribose) polymerase (PARP) is a family of 17 proteins involved in a number of cellular processes involving mainly DNA repair and programmed cell death. All members of the PARP family have different cellular functions with only PARP1, PARP2, VPARP (PARP4), Tankyrase-1 and -2, (PARP-5a, PARP-5b) having confirmed PARP activity. The other members of the family are mono ADP ribosylators or have unknown function. PARP-1 is however the founding member and has been the most extensively studied. The gene encoding PARP-1 protein is *ADPRT- 1* gene located on 1q41-q42 (Auer 1989). PARP is activated by binding to a DNA break (De Murcia 1994), resulting

in a cascade of intracellular signals and culminating in either DNA repair as part of the BER pathway or apoptosis (Dantzer 1999, Dantzer 2000). Inhibition of PARP leads to accumulation of SSB that convert to DSB during replication (Schultz 2003, Gottipati 2010), Figure 1.7 - 1. In isolation, this is insufficient to cause cell death as DSB can be repaired by the HR DNA repair pathway. However, if the HR pathway is defective, as in *BRCA1* or *BRCA2* deficient cancer cells, then cell death results (Bryant 2005, Farmer 2005). This phenomenon, whereby two non-lethal genetic mutations that are innocuous if present in isolation, but, result in cell death when present in combination, is termed synthetic lethality (Dobzhansky 1946, Helleday 2008). Cancer therapy aims to exploit this phenomenon by exposing tumour cells known to be deficient in one DNA repair pathway to an agent that targets its synthetically lethal partner pathway, thereby causing selective tumour cell death (Helleday 2008). As non-cancer cells are likely to be competent in both DNA repair pathways, non-cancer cells remain viable thereby reducing systemic side-effects.

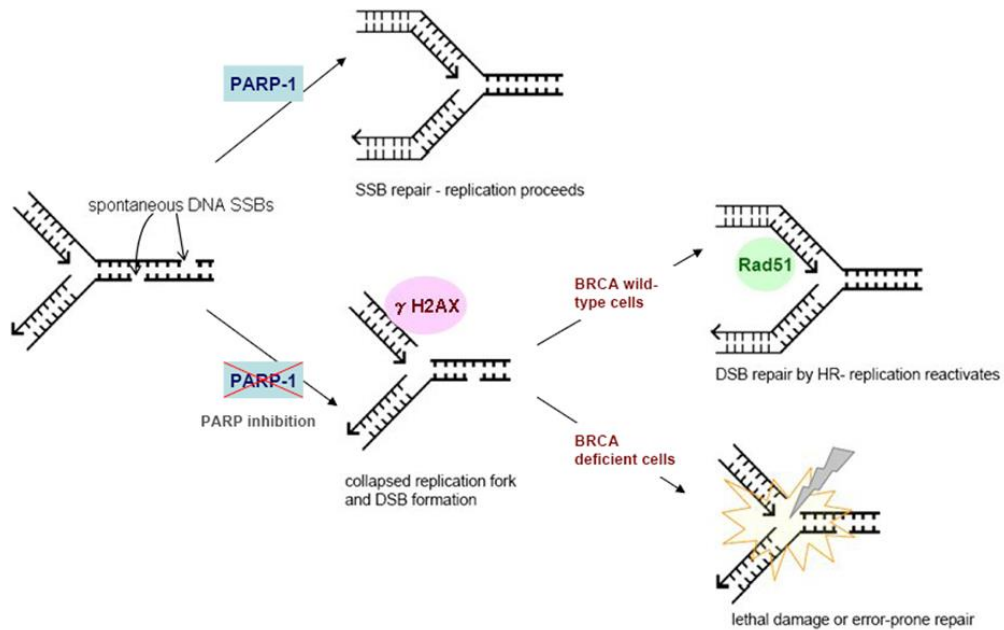


Figure 1.7 - 1: Synthetic lethality in HR defective tumours with PARP inhibition. The mechanism of PARP inhibitors is based on inhibition of PARP-1-dependent BER that leads to persistent DNA single strand breaks. Those breaks are subsequently converted into DSB due to collision of progressing replication fork with SSB. In normal cells, these DSBs would be repaired by HR thereby PARPi have no overall cytotoxic effect. However in cancer cells defective in BRCA1/2 and therefore defective in HR, DSBs cannot be repaired which leads to DNA fragmentation and cell death with the defect in HR and the inhibition of BER being synthetically lethal in combination.

The first generation of PARPi were the 3-substituted benzamides (Purnell 1980), which decreased DNA repair capacity, thereby enhancing the cytotoxic effect of DNA methylating agents in murine leukaemia cells (Durkacz 1980). Several generations of PARPi have since been developed and were designed to improve on the potency and specificity for PARP (Iwashita, Mihara et al. 2004, Curtin 2005, Jagtap, Baloglu et al. 2005, Loh 2005, Wells 2006, Ferraris 2010) Since the development of first generation PARP inhibitors, several compounds i.e., isoquinolines, methyl-quinazolin and phenanthridinones (Suto 1991, Banasik 1992, Griffin 1995) have been explored to develop PARPi which have been used as potent radio and chemosensitizers (Tentori, Leonetti et al. 2003, Veuger 2003, Calabrese 2004).

Interest in PARPi was initially concentrated to those breast and ovarian cancer patients with germline mutations in *BRCA1* and *BRCA2*, following

demonstration of sensitivity to PARPi in *BRCA* defective cell lines and xenograft models (Bryant 2005, Farmer 2005, Plummer 2007, Drew 2011). There was an observed 100-1000 fold increase in sensitivity to PARPi compared to heterozygous or *BRCA* wild-type in hamster cell lines (Bryant 2005, Farmer 2005) and a 5-7 fold increase in human cell lines (Drew 2011).

PARPi sensitivity has also been demonstrated in cell lines harbouring mutations in the genes encoding various other components of the HR pathway (namely *ATM*, *Rad51*, *Rad54*, *RPA1*, *NBS1*, *ATR*, *CHK1*, *CHK2* and *FANC* group), consistent with the hypothesis that these therapies, at least in part, work by exploiting the concept of synthetic lethality (McCabe, Turner et al. 2006). In 2011, the Cancer Genome Atlas Research Network reported defective HR DNA repair in up to 50% of HGSCs providing confidence that PARPi could be effectively utilised in this condition (Cancer Genome ResearchNetwork 2011). This hypothesis has been supported by the double-blind phase II trial in patients with platinum-sensitive relapsed EOC, which demonstrated a significant increase in PFS in individuals treated with olaparib monotherapy in comparison to placebo (Ledermann 2012).

Clinical Trials

Several generations of PARPi have been developed (Ferraris 2010). PARPi (rucaparib) first entered clinical trials in 2003. They were used to potentiate the effect of radio- and chemo-therapies and showed a beneficial effect in several cancers (Plummer 2005). Clinical trials initially concentrated on assessing the effect of PARP inhibition in hereditary breast and ovarian cancers but their use has since been explored in sporadic EOC and platinum resistant EOC. Ongoing and completed clinical trials for rucaparib and olaparib are summarised in Table 1.7 - 1. The situation is however not universally positive with negative studies reported in heavily pre-treated sporadic triple negative cancer (Gelmon 2010) and no evidence of activity in combination with temozolomide (Isakoff 2010). To understand why some studies have succeeded, and others failed, biomarkers capable of predicting sensitivity, or resistance, are required (Turner 2011).

PARP inhibitors only target HR-defective tumour cells, therefore, their associated side-effects, including myelosuppression and nausea, are relatively mild (Plummer 2007). Long-term effects of PARPi treatment are awaited from clinical trials.

Drug	Study Population	Drug Regimen	Phase	Outcome	Reference
Olaparib	<ul style="list-style-type: none"> • BRCA1/2 breast/ovarian ca • Triple negative breast ca • Sporadic ovarian cancer 	100 mg bd to 600 mg bd)	I	Dose escalation with Grade 1/2 toxicities: nausea (32%), fatigue (30%), vomiting (20%). 5% anaemia, 3% Grade 4 thrombocytopenia. 12/19 BRCA carriers had radiological/ biochemical response or disease stabilization.	(Fong 2009)
	<ul style="list-style-type: none"> • Advanced stage pre-treated EOC with BRCA1/2 mutations 	40 mg od to 600 mg bd. Dose expansion cohort: 200 mg bd	I	Dose- escalation and single-stage expansion of a phase I trial. 20/50 achieved complete/partial response (RECIST) or biochemical response and 3/50 achieved disease stabilisation. Overall clinical benefit in 46% of BRCA patients.	(Fong 2010)
	<ul style="list-style-type: none"> • BRCA1/2 ovarian cancer • Recurrent sporadic EOC 	400 mg bd or 100 mg bd	II	Objective tumour response rate was 33% (400 mg bd) with a median PFS of 5.8 months. Complete/partial response (RECIST) or stable disease in 57.6% of patients (400 mg) vs. 16.7% (100 mg).	(Audeh 2010)
	<ul style="list-style-type: none"> • Triple negative breast cancer • Sporadic ovarian cancer 	400 mg bd	II	25/63 ovarian cancer patients had clinical response (28 of which were BRCA1/2 mutant).	(Gelmon 2011)
	<ul style="list-style-type: none"> • Platinum sensitive relapsed HGSC pre-treated with 2+ platinum agents 	400 mg bd vs. placebo	II	Double-blind RCT with an increase in PFS with olaparib (median PFS 8.4 months) monotherapy in comparison to placebo (median PFS 4.8 months). No significant difference was seen for OS.	(Ledermann 2012).
	<ul style="list-style-type: none"> • BRCA1/2 relapsed ovarian cancer 	400 mg bd vs. doxorubicin 50 mg/m ²	II		(NCT00628251)
Rucaparib	<ul style="list-style-type: none"> • Advanced solid malignancies 	Dose escalation with (100 mg/m ²) temozolomide (TZ) and 12 mg/m ² PARPi with 200 mg/m ² TZ	I	PARP inhibition was seen in all 33 patients with advanced solid malignancies. No toxicity attributable to Rucaparib alone was observed.	(Plummer, Jones et al. 2008)
	<ul style="list-style-type: none"> • Chemo naïve metastatic melanoma 	12 mg/m ² PARPi with oral TZ 200 mg/m ²	II	46 patients with metastatic melanoma had a response rate of 17.4% with a median time to progression of 3.5 months and median OS of 9.9 months.	(Plummer 2013)
	<ul style="list-style-type: none"> • BRCA1/2 breast • BRCA1/2 ovarian cancer 		II	Ongoing. Dose escalation followed by open-label multicentre study	(NCT00664781)

Table 1.7– 1: Clinical trials of olaparib and rucaparib PARP inhibitors.

Rationale for HR Functional Assay

BRCA mutant ovarian cancers represent only 10 - 15% of all ovarian cancers and it is clear from molecular studies, as well as clinical trials, that the potential scope of PARPi should not be limited to familial cancers.

The tumour suppressor genes *BRCA1* and *BRCA2* are currently the only genes to be identified as highly penetrant ovarian cancer susceptibility genes (Gayther 1999). The vast majority of tumours from women with germline *BRCA1/2* mutations show loss of heterozygosity of the wild type allele at the *BRCA1/2* loci (Ramus 2003) and are considered HR deficient (Venkitaraman 2004).

Ovarian cancers with germline mutations in *BRCA1/2* genes represent 15% of all EOC and have classical features in terms of histology, survival and chemosensitivity. The term 'BRCAlike' is used to describe tumours without germline *BRCA* mutations, but which have a similar phenotype (Turner 2004). The loss of function of other components in the HR pathway, resulting in an overall pathway function defect, has been demonstrated to account for these similarities (Turner 2004). A number of mutations in a variety of genes within the HR pathway have been reported (Cerbinskaite 2012). Testing for each of these individual genetic mutations may be impractical and their cumulative effect on overall function of the pathway remains unknown. Pennington *et al* demonstrated that 31% of ovarian carcinomas had a deleterious germline (24%) and/or somatic (9%) mutation in one or more of the 13 homologous recombination genes: *BRCA1*, *BRCA2*, *ATM*, *BARD1*, *BRIP1*, *CHEK1*, *CHEK2*, *FAM175A*, *MRE11A*, *NBN*, *PALB2*, *Rad51C*, and *Rad51D* (Pennington 2014). An assay to test the end function of the pathway, irrespective of mutation of its individual components, has been developed and demonstrates that in actual fact up to 50% of sporadic EOC are HR defective (Mukhopadhyay 2010).

Therefore relying upon *BRCA* mutations in isolation, or even genomic sequencing of all HR genes, may underestimate patients with defective HR and who would therefore respond to PARPi by 20 - 35%. Additionally, the overall effect upon function of isolated mutations in single genes within the HR pathway is unknown and epigenetic silencing, endogenous repressors or mutations /

dysregulation of other components of HR may interact and change functional status.

The Development of the Rad51 Assay to Determine Functional Homologous Recombination Repair Status

The Rad51 assay was developed in Newcastle University and adapted by Mukhopadhyay *et al* for use in ovarian cancer primary cultures generated from malignant ascites (Mukhopadhyay 2010).

The assay aims to assess the ability of a live cell population to identify DNA damage, which is specifically repaired by homologous recombination (DSB, stalled/collapsed replication forks). There are a series of proteins and factors, which take part in the HR repair of the DNA and the assay combines an assessment of the cell's ability to recognise and quantify DNA damage with the cells ability to complete the cascade of complex protein interactions required for repair using HR.

A key component in DNA repair is the histone protein H2AX, which becomes rapidly phosphorylated to form large numbers of γ H2AX at DSB, creating a focus where proteins involved in DNA repair and chromatin remodelling accumulate (Mukhopadhyay 2010). This amplification makes it possible to detect DSBs with an antibody to γ H2AX, with the number of DSBs estimated from the number of foci (Bonner, Redon et al. 2008, {Paull, 2000 #698}). Rad51 is a crucial downstream protein involved in HR repair, which is relocalised within the nucleus in response to DNA damage to form distinct foci that can be visualized by immunofluorescent microscopy and are thought to represent assemblies of proteins at these sites of HR repair(Mukhopadhyay 2010).

Therefore, it was hypothesised that quantification of Rad51 could serve as a marker of HR function to distinguish between HR-competent and HR-defective cells (Lee, Roques et al. 2009).

The HR Rad51 assay protocol is described in detail in section 3.6. Briefly, primary cell cultures generated from malignant ascites, or solid tumour, growing exponentially in an adherent monolayer are seeded onto sterile coverslips and double strand (DSB) DNA damage induced. After assessment of several methodologies to induce DNA damage (irradiation, hydroxyurea, PARPi),

induction with 2 Gy irradiation and incubated with 10 μ M PARP inhibitor to maintain DSB was selected on account of its safety and consistency. Cells are fixed after 24 hours and following permeabilisation and washing and blocking steps, described in detail in Section 3.6, immunofluorescent labelled antibodies are used to identify nuclear foci of γ H2AX and Rad51.

Image-J technology, previously validated against manual foci counting by two independent reviewers, is used to calculate the mean foci count per cell and counts compared to untreated controls, without DNA DSB induction. Foci counting, not quantification of actual protein levels, is important as it indicates that the protein is functioning within the pathway and prevents high levels of non-functional protein resulting from genetic or epigenetic alterations resulting in false positive results. Further experiments demonstrated consistent co-localisation of γ H2AX and Rad51 within the nucleus.

In initial experiments the actual Rad51 counts obtained were highly variable indicating a range of baseline Rad51 foci activity and the comparison to untreated controls was introduced to control for this. Additionally, despite standardisation of induction of DNA DSB levels of γ H2AX were also variable and a standard of a two fold increase in γ H2AX foci was adopted as a measure of induction of sufficient DNA damage in order to enable assessment of pathway function.

Initial experiments included Rad51 assays alongside cytotoxicity to PARP inhibitors in paired cell lines (mutations in key proteins in the HR pathway with WT) as well as 25 primary cultures generated from ovarian cancer patients (Mukhopadhyay 2010). There was an increase in γ H2AX foci in all cultures confirming induction of DNA damage. Rad51 foci increased following treatment by \sim 2-fold compared with controls in 9 of 25 primary cultures, which were therefore deemed to be HR competent. In the remaining 16 cultures, there was no increase or even a decrease in Rad51 foci in response to DNA damage and therefore, they were deemed to be HR deficient. There was good correlation in Rad51 foci counting between two reviewers and good agreement in prediction of HR status. The cultures predicted to be HR competent on the basis of Rad51 focus formation remained viable in both cytotoxicity and cell proliferation assays

with PARP inhibitor, further supporting the utility of the assay. The definitions for competent HR function was therefore adopted as more than a twofold rise in the mean Rad51 foci count/cell following induction of DNA damage defined as at least a two fold increase in γ H2AX foci formation.

		γ H2AX	
		>2 fold	<2 fold
Rad 51	>2 fold	Competent	Invalid
	<2 fold	Defective	Invalid

1.8. Rationale for this Project

Despite a growing appreciation of the molecular differences between, and within, the histological subtypes of ovarian cancer, it is essential that we understand what effect these mutations have upon the biology of the tumour. Although some mutations have been shown to be associated with prognostic differences, no reliable biomarkers, capable of predicting actual response to therapy, have translated into clinical practice.

This project aims to further explore the potential of HR functional status in predicting disease response and gain an understanding of its clinical application in terms of tumour sampling and its ability to accurately predict disease behaviour.

Chapter 2. Hypothesis and Aims

This project seeks to develop and exploit the concept of synthetic lethality further. Firstly, by developing a greater understanding of HR function in ovarian cancer and by exploring more clinically relevant tests for HR status. Secondly, by exploring whether other cytotoxic agents can also be used in a synthetically lethal manner; and finally, by considering how to sample ovarian tumours so that the biological assessment of the chosen sample is representative and correlates with clinical outcome.

2.1. Primary Cultures

Hypotheses

- Epithelial cells can be cultured from malignant ascites obtained during surgery for ovarian cancer and the functional homologous recombination assay can be performed which predicts sensitivity to cytotoxic agents.
- *Ex vivo* culture has no effect upon cell phenotype in terms of antigen expression or EMT phenotype.

Aims

- To characterise PCO cultures derived from ascitic samples in terms of antigen expression, growth potential and morphology in order to further understand the strengths and weaknesses of this model.
- To understand the extent of epithelial mesenchymal transition (EMT) within ovarian cancer and the effect of *ex vivo* culture upon this.
- To explore the presence of subpopulations of cells within ascites, their antigen expression, growth and HR status.
- To determine the homologous recombination (HR) DNA repair status of PCO cultures with corresponding *ex vivo* sensitivity to rucaparib and cisplatin and to compare with *in vivo* platinum sensitivity and clinical outcome.
- To explore the ability to simplify the currently complex HR assay in order to transform it into a reliable, reproducible and clinically applicable process, enabling rapid, large volume turnover in clinical trials and routine practice and to explore alternative assays for HR function based on expression signatures at RNA level.
- Assess the utility of *ex vivo* proliferation assays in predicting clinical response to platinum chemotherapy.

2.2. Solid Tumour Culture and Heterogeneity

Hypotheses

- Epithelial cells can be cultured from solid tumour obtained during surgery for ovarian cancer and the functional homologous recombination assay can be performed, which can predict sensitivity to cytotoxic agents.
- Within ovarian cancer, subpopulations exist. Sampling tumour from different anatomical sites will demonstrate heterogeneity in morphology, antigen expression, DNA repair function and response to cytotoxic agents.

Aims

- Explore the feasibility of culturing ovarian cancer solid tumour from various metastatic sites within the abdomen.
- Explore spatial intra-tumoural heterogeneity (ITH) within an individual's cancer by characterising PCO subcultures in terms of antigen expression, growth potential and morphology alongside functional HR status and sensitivity to PARP inhibitors and platinum.
- Investigate intra-tumoural heterogeneity as a prognostic marker alongside other recognised prognostic markers (histological subtype and surgical cytoreduction).
- Investigate temporal changes in HR status using longitudinally collected samples of ovarian cancer.

2.3. Sapacitabine

Hypotheses

- CNDAC (the metabolically active component of sapacitabine) is cytotoxic in HR defective cell lines and PCO (primary culture ovary) cultures.
- Alternative DNA repair mechanisms also play important roles in the prediction of sensitivity to CNDAC in cell lines and PCO cultures.

Aims

- Assess the cytotoxic effect of CNDAC and its effect upon cell survival/proliferation of cell lines with mutations in the homologous recombination DNA repair pathway.
- Determine the HR status of PCO samples derived from ascitic cultures, with corresponding sensitivity to CNDAC, rucaparib and cisplatin.
- Establish if defects in other DNA repair pathways are determinants of sensitivity to CNDAC.
- Establish a functional assay to test base excision repair status and assess its potential use as a biomarker for stratification of CNDAC therapy.
- Explore the effect of variable CNDAC uptake (by ENT receptor), activation (by dCK) and deactivation (by CDA) upon *ex vivo* sensitivity to CNDAC.

2.4. Circulating Tumour Cells

Hypotheses

- CTCs can be reliably detected and quantified within whole blood from ovarian cancer patients.
- CTC number predicts PFS/OS with greater numbers seen in higher stage disease
- HR status can be performed using ImageStream on cell lines, PCO cultures and on CTC.
- Ascites can be processed using ImageStream to identify and characterise tumour cells and the HR assay can be applied to such cells

Aims

- Develop a method for sample preparation of whole blood to positively identify ovarian cancer cells from blood cells, using cell lines and healthy volunteer blood.
- Develop a method for data handling and analysis of such samples.
- Develop a method for the accurate identification, quantification and characterisation of CTCs from whole blood taken from ovarian cancer patients
- Correlate enumeration of CTCs with stage of disease/PFS/OS
- Develop a method for application of the HR functional assay based upon γ H2AX and Rad51 foci formation to cell lines, PCO cultures, and CTC using ImageStream.
- Explore the alternative approach of using ImageStream technology to directly characterise and functionally assess the cellular component of malignant ascites.

Chapter 3. Materials and Methods

3.1. General Equipment

Equipment	Manufacturer
Agilent 2100 Bioanalyser	Agilent Technologies, USA
Agilent RNA Bioanalyser	Agilent Technologies, USA
Balance model Ohaus Discovery Balance DV215CD	Ohaus, UK
BD Falcon round bottom polystyrene 14 ml tubes	BD Biosciences, UK
ColCount™ colonies counter	Oxford Optronix Ltd., UK
Coulter Counter model Z1	Beckman Coulter Ltd., UK
Cytospin (Shandon)	Thermo Scientific, UK
Digital pH meter model pH302	Hanna Instruments, UK
EasySep™ big easy magnet	Stemcell Technologies, UK
Fuji LAS-3000 Luminescent Image Analyser	Raytek Ltd.
Haemocytometer (Improved Neubauer)	Weber Scientific, UK
ImageStream Mark-II	Amnis Corporation, USA
Immunoblot manifold	Department of engineering, Newcastle University, UK
Leica DMR Immunofluorescent microscope	Leica microscopes, Germany
Incubator MCO-20AIC	Sanyo E&E Europe BV, Medical Division, UK
Lambda 2 Spectrophotometer	Perkin Elmer, USA
Micro-balance	Mettler Toledo
NanoDrop ND-1000 UV spectrophotometer	Fisher Scientific, UK
Orbital shaker IKA-Vibrax-VKR	Sigma Aldrich
Platform shaker	IKA Vibrax, Germany
Qiagen RNA easy Mini kit	Qiagen, UK
Refrigerated centrifuge	MSE Falcon 6/300
Refrigerated microcentrifuge	Eppendorf centrifuge 5417R
Spectramax 250 microplate reader	Molecular Devices
Sterile cell culture flasks 25 cm ² , 75 cm ²	Corning Incorporated, USA
Stuart Vortex mixer	Scientific Laboratory Supplies, UK
Vacusaft Comfort IBS Integra aspiration system	BD Biosciences, UK
Water bath	Gallenkamp, UK
X-ray irradiator XSTRAHL RS320	Gulmay Medical Ltd., UK
VisCam® software	VWR International Ltd., UK

3.2. Chemicals and Reagents

Reagent	Order No.	Manufacturer
10H PAR antibody (1.5 mg/ml)		Dr Alex Burke
4-15% Mini-PROTEAN® TX™ gels	456-1085	Bio-Rad Laboratories, USA
Acetic acid	A6283-2.5L	Sigma Aldrich Company Ltd., UK
Albumin bovine serum (BSA)	A9647	Sigma Aldrich Company Ltd., UK
Amersham ECL detection fluid	RPN2232	GE Healthcare Life Sciences, UK
Amersham Hybond ECL nitrocellulose membrane	RPN303D	GE Healthcare Life Sciences, UK
Anti-CD56 V450 (clone H130) mouse monoclonal antibody	560367	BD Biosciences, USA
Anti-CDA rabbit polyclonal antibody	Ab82347	Abcam, UK
Anti-D2-40 mouse monoclonal antibody	IS072	Dako, France
Anti-dCK rabbit polyclonal antibody	Ab96599	Abcam, UK
Anti-ENT antibody (rabbit polyclonal anti-human ENT1)	Ab48607	Abcam, UK
Anti-EpCAM (CD326) Alexa Fluor® 488 mouse monoclonal antibody	324310	Biologend, UK
Anti-MOC-31 monoclonal mouse antibody	M3525 (01)	Dako, France
Anti-mouse Alexa Fluor®546 goat IgG (H+L) monoclonal antibody	A-11030	Life Technologies Ltd, UK
Anti-mouse goat monoclonal HRP antibody	P0447	Dako, France
Anti-MUC16 (CA125) [X75] mouse monoclonal antibody	AB1107	Abcam, UK
Anti-pancytokeratin (clone C-11) PE mouse monoclonal antibody	10478	Cayman Chemical, USA
Anti-pancytokeratin FITC (clone C11), mouse monoclonal antibody	CBL234F	Upstate Millipore Corp., USA
Anti-phospho-histone H2AX (Ser 139), mouse monoclonal antibody, clone JBW301	05-636	Upstate, Millipore Corp, USA
Anti-rabbit Alexa Fluor®488 goat IgG (H+L) monoclonal antibody	A-11034	Life Technologies Ltd, UK
Anti-rabbit goat monoclonal HRP antibody	A0545-1ml	Sigma Aldrich Company Ltd., UK
Anti-rabbit PE-Cy5.5 goat IgG (H+L) monoclonal antibody	L42018	Invitrogen, USA
Anti-Rad51 (Ab-1) rabbit polyclonal antibody	PC130	Calbiochem, USA
Anti-vimentin (clone EPR3776) rabbit monoclonal antibody	ab92547	Abcam, UK
APEX™ Alexa Fluor® 594 antibody labelling kit	A10474	Invitrogen, USA
AutoMACS rinsing solution	130-091-222	Miltenyi Biotec, Germany
Cal-lyse™ lysing solution	GAS-0105-100	Invitrogen, USA
Chromatography filter paper	3030917	Whatman
Cisplatin	400-040-M250	Enzo Life Sciences
CNDAC		Cyclacel, UK
Collagense/Dispase	11097113001	Roche Diagnostics, Ltd., UK

Crystal violet	C6158-50G	Sigma Aldrich Company Ltd., UK
Cyto-Chex® BCT blood collection tubes	213361	Streck, USA
DC™ Protein Assay	500-0111	Bio-Rad Laboratories, USA
Dextran	31390	Sigma Aldrich Company Ltd., UK
Digitonin	D141	Sigma Aldrich Company Ltd., UK
Dipyridamole D9766	D9766-1G	Sigma Aldrich Company Ltd., UK
DMSO	D8418-50ML	Sigma Aldrich Company Ltd., UK
DRAQ 5	DR50200	Biostatus, UK
Dried non-fat milk powder		Marvel Premier Int Foods Ltd., UK
Dynabeads® CD45	1153D	Invitrogen, USA
DynaMag	12321D	Invitrogen, USA
EasySep™ Human CD45 Depletion Kit	18259	Stemcell Technologies, UK
EDTA	E9884	Sigma Aldrich Company Ltd., UK
EGTA	E3889	Sigma Aldrich Company Ltd., UK
Ethanol	10107	BDH Ltd., UK
FACS Clean	340345	Beckman coulter
FACSFlow™	342003	BD Biosciences, USA
FcR Blocking Reagent, human	130-059-901	Miltenyi Biotec, Germany
Foetal bovine serum (FBS)	10106-169	Gibco, Scotland
Gen Elute Mammalian Genomic DNA Miniprep kit	G1N350	Sigma Aldrich Company Ltd., UK
Goat serum	X090710	Dako, France
HEPES	H3784	Sigma Aldrich Company Ltd., UK
HT 8-oxo-dG ELISA kit II	4380-096-K	Trevigen, USA
Hydrochloric acid	H1756	Sigma Aldrich Company Ltd., UK
Hygromycin B (50 mg/ml)	10687-010	Invitrogen, USA
Isopropanol	10224BQ	BDH Ltd., UK
Lysing Solution, Whole Blood Lysing Solution	010S-100	Invitrogen, USA
MACS BSA Stock Solution	130-091-376	Miltenyi Biotec, Germany
MACS CD45 microbeads	130-045-801	Miltenyi Biotec, Germany
MACS® CD45 Microbead	130-045-801	Miltenyi Biotec, Germany
MEGM BulletKit (CC-3151 & CC-4136)	CC-3150	Lonza, Switzerland
Methanol	M/4056/017	Fisher Scientific Int Ltd., UK
Methoxyamine	226904-1G	Sigma Aldrich Company Ltd., UK
MiniMACS™ separator	130-042-102	Miltenyi Biotec, Germany
Mini-PROTEAN Tetra cell System	165-8004	Bio-Rad Laboratories, USA
Mini-PROTEAN TGX Gel (4-15%)	456-1085	Bio-Rad Laboratories, USA
Nicotinamide adenine dinucleotide (NAD+)	N1511	Sigma Aldrich Company Ltd., UK
Nylon net filter (180 µm pore)	NY8H09000	Millipore, UK
Oligonucleotide (CGGAATTCCG)		Invitrogen, USA
PAR polymer	202-043-C001	Enzo Life Sciences
Parafilm	PM996	Pechiney plastic packaging, USA

Penicillin/Streptomycin (10,000 µg/ml)	P4333	Sigma Aldrich Company Ltd., UK
Phosflow Lyse/Fix buffer	558049	BD Biosciences, USA
Phosflow Perm/Wash I	557885	BD Biosciences, USA
Ponceau S solution	P7170-1L	Sigma Aldrich Company Ltd., UK
Propidium iodide (PI)	P4170	Sigma Aldrich Company Ltd., UK
RNA Bioanalyser 6000 Nano kit	5067-1511	Agilent technologies, USA
RNA easy Mini kit	74106	Qiagen
RNase	R5503-1G	Sigma Aldrich Company Ltd., UK
RoboSep buffer	20104	Stemcell Technologies, UK
RosetteSep™ Human CD45 Depletion Cocktail,	15122	Stemcell Technologies, UK
RPMI 1640 with L-glutamine	R8758	Sigma Aldrich Company Ltd., UK
Rucaparib, AG014699		Clovis, USA
S-(4-Nitrobenzyl)-6-thioinosine (NBMPR)	N2255-25MG	Sigma Aldrich Company Ltd., UK
Spectra™ multicolour broad range protein ladder	26634	Life Technologies Ltd, UK
Speed Beads	4000400	Amnis, USA
Sulforhodamine B (SRB)	230162-5G	Sigma Aldrich Company Ltd., UK
TransFix® vacuum collection tubes	TVT-10-50	Cytomark
Trichloroacetic acid (TCA)	T4885	Sigma Aldrich Company Ltd., UK
Tris	T6066	Sigma Aldrich Company Ltd., UK
Trypan blue 0.4%	T8154	Sigma Aldrich Company Ltd., UK
Trypsin-EDTA 2.5% (10x)	T4174	Sigma Aldrich Company Ltd., UK
Tween 20	P1379	Sigma Aldrich Company Ltd., UK
Vacutainer® collection tubes containing K3EDTA	366450	BD Biosciences, USA
Vectashield mounting medium with DAPI	H-1200	Vector, USA
Virkon®	1.3E+11	Antec International Ltd., UK
WST-1	5015944001	Roche Diagnostics, Ltd., UK
β-Mercaptoethanol	M6250-10ml	Sigma Aldrich Company Ltd., UK

Stock solutions of rucaparib (10 mM), CNDAC (10 mM), methoxyamine (1 M), NBMPR (10 mM), and dipyrindamole (10 mM) were dissolved in DMSO, aliquoted and stored at -80 °C. All experiments were corrected for 1% DMSO in final concentration. Cisplatin (2 mM) was dissolved in PBS and stored as above.

3.3. General Laboratory Practice

All experiments were performed to university standards, complying with the Control of Substances Hazardous to Health Regulations 2002 (COSHH) and Biological COSHH (BioCOSHH). Routinely used chemicals, reagents and equipment are detailed in the tables below. Preparations of specific reagents for investigations are described in the relevant sections below.

3.4. Cell Culture

3.4.1. Cell lines

Experiments were carried out using cells lines described in Table 3.4 - 1. All media were stored at 4 °C and warmed to 37 °C prior to use. All cells were handled separately with their own reagents and underwent regular mycoplasma testing (MycoAlert Mycoplasma detection kit; Lonza). Early passages (<35) of cell lines were grown in at 37 °C, 5% CO₂, 95% humidified air, maintained at exponential growth. Passage was performed using an aseptic technique in a containment level II laminar flow microbiological cabinet. Medium was aspirated and cells washed with PBS before incubation with 5 ml 0.25% trypsin-EDTA for at 37°C until detachment. The cell suspension was centrifuged at 50 g for 5 minutes, the supernatant discarded and the cell pellet re-suspended in 10 ml medium before 10 µl of the solution was loaded onto a Neubauer Haemocytometer. Cells were seeded into flasks / culture dishes as required.

Cell line	ATCC number	Description	Media	Doubling Time (hours)	Source
OVCAR3	ATCC® HTB-161	Human ovarian adenocarcinoma derived from ascites after combination chemotherapy with cyclophosphamide, adriamycin, and cisplatin (Hamilton 1983).	RPMI 1640 medium with 25 mM HEPES modification, mom L-glutamine, 10% heat inactivated fetal calf serum (FCS), penicillin (100 U/ml) and streptomycin (100 up/ml), referred to as 10% RPMI		ATTC©
A2780		Human ovarian adenocarcinoma derived from tumour from an untreated patient. p53 and MMR-proficient, (Anthoney 1996)	10% RPMI		ATTC©
CP70-B1 CP70-A2		A2780 derivatives. MMR-defective (<i>hMLH1</i> promoter hypermethylation) (Strathdee 1999). CP70-B1 cells have functional MMR (chromosome 3 transfer). CP70-A2 cells carry a transferred chromosome 3 with mutant <i>hMLH1</i> (Plumb 2006), both CP70 derivatives carry a dominant-negative p53 mutation (Brown 1993, Lu, Errington et al. 2001).	10% RPMI		R Brown (Beatson Laboratories, UK)
UWB1-289	ATCC®CRL-2945	Human ovarian serous carcinoma derived from a patient with breast cancer age 42 and ovarian cancer age 54. Germline <i>BRCA1</i> mutation within exon 11 and a deletion of the wild-type allele (DelloRusso 2007).	50% Mammary Epithelial Cell Growth Medium™ and 50% RPMI with 20 mM L-glutamine, 10% FCS, penicillin (100 U/ml) and streptomycin (100 µg/ml).	53	ATTC©
UWB1-289 BR-1	ATCC®CRL-2946	Derivative of UWB1-289 transfected with a pcDNA3 plasmid carrying wild-type <i>BRCA1</i> . Transfected cells were selected with addition of G418.	50% MEGM and 50% RPMI + 200 µg/ml G418	45	ATTC©
VC8		Chinese hamster lung fibroblasts derived from V79. Biallelic nonsense mutation in <i>BRCA2</i> (Wiegant 2006).	10% RPMI	39	M. Zdzienicka (University of Leiden, Netherlands)
VC8 BR-2		Derivative of VC8 transfected with bacterial artificial chromosome (BAC) containing wild type murine <i>BRCA 2</i> .	10% RPMI	25	
VC8 PIR clone 1c		PARPi-resistant derivative of VC8 derived by mutagenesis with ethyl methane sulphonate (EMS) followed by selection in 4-amino-1,8-naphthalimide (ANI, PARPi).	10% RPMI	23	T. Helleday (Oxford University, UK)

L1210	ATCC®CRL-219	Murine leukaemia lymphocyte cell line established from a tumour developed following skin paintings with 0.2% methylcholanthrene in ether. Internal control PAR assay	Dulbecco's Modified Eagle's Medium (DMEM) supplemented with 20 mM L-glutamine, 10% FCS, penicillin (100 U/ml) and streptomycin (100 µg/ml)		ATTC©
V3		DNA-PK _{CS} deficient Chinese hamster ovary cells defective in non-homologous end-joining (NHEJ) DNA repair (Whitmore 1989)	DMEM supplemented with 20 mM L-glutamine, 10% FCS, penicillin (100 U/ml) and streptomycin (100 µg/ml)	48	P Jeggo (University of Sussex, United Kingdom)
V3-YAC		Derived from V3 Chinese hamster ovary cells, transfected with a yeast artificial chromosome (YAC) carrying the human DNA-PK _{CS} gene, competent in NHEJ.	DMEM, as above, with addition of 200 µg/ml G418.	38	
AA8	ATCC® CRL-1859	Derivative of the CHO-K1 cell line. 21 chromosome line, heterozygous at the aprt locus (Thompson, Fong et al. 1980).	10% RPMI	16	ATTC©
EM9	ATCC® CRL-1861	BER deficient with XRCC1 mutation derived from AA8 (Thompson, Rubin et al. 1980, Thompson, Brookman et al. 1982). Defective in SSB repair with a 10-fold higher baseline frequency of sister chromatid exchange relative to AA8 and a 2-fold greater sensitivity to irradiation.	10% RPMI	18	ATTC©
UV5	ATCC® CRL-1865	AA8 derived UV sensitive cell line defective in NER. CXPB mutation resulting in an amino acid substitution within excision repair complementation group 2 (Thompson, Rubin et al. 1980, Thompson, Brookman et al. 1982, Weber 1994).	10% RPMI	53	ATTC©
MCF7	ATCC® HTB-22	Derived from a patient with breast adenoma and pleural effusion carry nonmutated BRCA1/2 (Elstrodt 2006).	10% RPMI	38	ATTC©
Capan-1	ATCC® HTB-79	Human pancreatic cancer cells with mutated BRCA2 (6174delT) in one allele and loss of the other allele (Goggins 1996).	DMEM:Hams F12 1:1 supplemented with 2 mM glutamine and 15% FCS	77	ATTC©
MX-1	ATCC®	Derived from a primary ductal breast carcinoma of a 40yr old patient with BRCA1 truncating mutation at codon 999 and 2 nonsynonymous SNPs in BRCA2 (BRCA2 16864A>C, Asn289His, and BRCA2 221847A>G, Asn991Asp) .	DMEM:Hams F12 1:1 supplemented with 2 mM glutamine and 10% FCS	27	ATTC©

Table 3.4 - 1: Cell lines.

3.4.2. Primary Ovarian Ascitic Cancer Cells (PCO)

Ethical approval was granted (12/NW/0202) and specimens were registered in accordance with the Human Tissue Act. Following written consent (see Appendix 5), ascitic fluid and solid tumour was collected from patients at the Northern Gynaecological Oncology Centre (NGOC), Gateshead, UK. Ascites was aspirated directly from the patient into a sterile suction bottle, either at the time of surgery for ovarian cancer or following a therapeutic ward paracentesis. Solid tumour, collected at the time of surgery, was placed into a sterile universal, containing culture medium (RPMI 1640 medium supplemented with 20% FCS, 20 mM L-Glutamine and 1% penicillin and streptomycin) pre-warmed to 37 °C. Samples were transported from the hospital to the lab immediately, in compliance with UK Category B regulations UN3373. Samples were given a unique identifier, 'PCO', followed by a serial number to maintain anonymity. Multiple derivative samples were generated from each PCO sample collected and used in multiple assays, *Figure 3.4 - 1*. For all patient samples collected detailed clinical data was recorded including treatments undertaken and where appropriate, PFS/OS, see Appendix 6 for a summary.

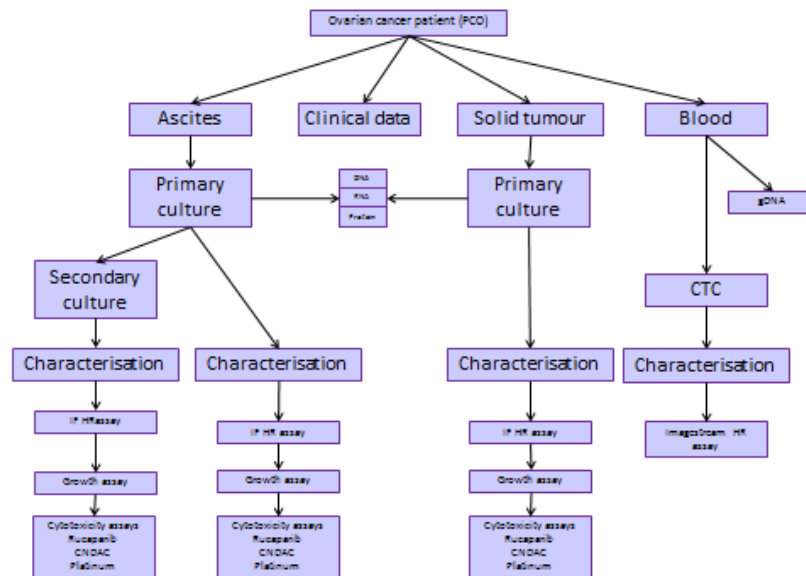


Figure 3.4 - 1: PCO collection flow chart for sample analysis.

Ascitic Culture

20 ml of ascites was added to 20 ml of medium (RPMI 1640 medium supplemented with 20% FCS, 20 mM L-glutamine and 1% penicillin and streptomycin) in T75 flasks. Medium was replaced on day 5 to 7. Ascites fluid is often contaminated with red blood cells, mucin or fatty tissue but these contaminants do not adhere and are therefore removed during media changes. Aspirated media/ascitic fluid from the PCO samples was collated from a number of matched samples and reseeded into a T175 flask. The resulting adherent monolayer cultures were labelled 'PCO x-2' to denote their secondary nature. Ascitic cultures were collected and maintained by Dr Angelika Kaufmann and me. Michelle Dixon and Aiste McCormick also contributed to maintenance. Cell lines and established PCO cultures were frozen at early passage by re-suspending cell pellets in 1 ml of freezing medium (RPMI medium, 10% FCS and 10% dimethyl sulphoxide [DMSO]) and slowly freezing to $-120\text{ }^{\circ}\text{C}$. Frozen samples were rapidly defrosted, centrifuged to remove freezing media and re-suspended in pre-warmed medium before transferring into 25 cm^3 culture flasks and incubated at $37\text{ }^{\circ}\text{C}$.

Ascites Cytocentrifugation and Coverslip Culture

Cytospinning is a form of cell centrifugation and was explored as a method of increasing the speed of analysis of PCO ascitic samples to enable more rapid characterisation and determination of HR status.

A 10% RCLB solution (Ammonium chloride, Stemcell, UK) was added to ascites (1:4, v/v) and incubated on a rocker at $37\text{ }^{\circ}\text{C}$ for 5 minutes. The lysate was centrifuged at 300 G for 5 minutes before washing the cell pellet with PBS and re-suspended in 10 ml of media. 200 μl of the ascitic /media solution was cytopun using the Shandon cytospin2 centrifuge at 450 RPM for 5 minutes before air drying, fixing with methanol and storing at $-20\text{ }^{\circ}\text{C}$ for later analysis.

Ascitic fluid samples were cultured directly onto sterilised coverslips to reduce the time taken to characterise and perform functional assays on culture cells. Two ml ascitic fluid was added to sterilised coverslips with media (1:1, v:v) in 6-well plates and incubated at $37\text{ }^{\circ}\text{C}$ for 48 hours to allow cell adherence. Cells

were then either fixed with methanol for characterisation studies or DNA DSB induced for the HR assay.

Solid Tumour Culture: Final Assay Protocol

Ascitic fluid and solid tumour were collected from each patient. A solid tumour sample from the bulk of the disease in the ovary was taken in every case with additional biopsies from multiple other intra-abdominal sites collected where possible, Appendix 7. Ascites was aspirated into sterile bottles and solid tumour (approximately 1 cm³) placed into sterile containers with warmed media.

Once in the laboratory, solid tumour was dissected into 3 mm³ pieces and collagenase/dispase solution (1 mg/1 ml in full medium) added to immerse the sample. The sample was incubated for 2 hours at 37°C on an orbital shaker at 2 g before centrifuging at 400 g for 5 minutes, PBS washing and re-suspending in full medium. Samples were transferred into T25 flasks for 30 minutes to allow fibroblast seeding. Fibroblasts were disposed of and the epithelial cell suspension transferred to a T25 flask for on-going culture.

3.5. Cytotoxicity and Proliferation Assays

3.5.1. Colony Formation Assays

Principles of the Assay

Colony formation assay is a technique for studying the effect of cytotoxic agents on the survival and proliferation of proliferating cells by assessing the ability of cells to form colonies. Colony formation assays were performed to study the effect of cisplatin, rucaparib and CNDAC on cell survival in cell lines.

Assay protocol

Each cell line was plated at low density estimated to give colony numbers between 30 and 200 into a 6 well plate for 24 hours to allow attachment. Media was replaced with media containing a cytotoxic agent at increasing drug concentrations in 1% DMSO with controls treated with 1% DMSO. After 24 hours, incubation media was replaced with drug-free media and incubated at 37 °C for 14 days. Media was aspirated, plates were PBS washed, then fixed with 2 ml of Carnoy's fixative (acetic acid: methanol 1:3 v/v) for 5 minutes at room temperature, followed by addition of 5 ml 1% crystal violet (in PBS w/v) to stain colonies before washing with water and drying. Colonies were manually counted and percentage survival calculated using the formula:

$$\text{Cloning efficiency (CE) \%} = \text{Colonies counted} / \text{cells seeded} \times 100$$

$$\text{Survival \%} = \text{CE treated cells} / \text{CE control} \times 100$$

3.5.2. Growth Assay (Sulforhodamine B [SRB])

Principles of the Assay

SRB assay is used to determine cell density of adherent cells based upon the measurement of cellular protein. SRB is an aminoxanthene water-soluble dye that binds to basic amino acids of cellular proteins under acidic conditions producing a colour change quantified using a spectrophotometer. The amount of dye extracted from the stained cells is directly proportional to the cell mass (Vichai 2006). The advantages of the SRB assay include practicality and flexibility. This method has limitations in that an increase in cell size in response to a drug could be interpreted as an increase in cell number, and therefore is only accurate as long as the cell size remains constant (Skehan 1990). SRB assays were used to determine the effect of cisplatin, rucaparib and CNDAC on cell proliferation in cell lines and PCO cultures.

Cell Growth and Doubling Times

Cells were seeded at concentrations of 500, 1000 and 2000 cells/well in 100 µl medium with six replicate wells for each cell concentration in 96 well plates. After 24 hours for attachment, cells were fixed at 24 hour intervals for 10 days with 20 µl of 50% trichloroacetic acid (TCA) per well, and stored at 4 °C. Plates were then washed three times with distilled water and dried. 100 µl of 0.4% SRB solution (in 1% acetic acid) was added to each well for 30 minutes at room temperature, after which the unbound SRB dye was removed by washing 4 times with 1% acetic acid. A blank control was created after adding SRB to a well containing full medium but no cells. The protein-bound dye was dissolved in 100 µl of 10 mM Tris (pH 10.5) solution for optical density determination at 570 nm using a Spectra Max 250 microplate reader. Doubling time was calculated using Graphpad PRISM (version 5) software.

3.5.3. Growth Inhibition Assays

SRB

Cells were seeded into 96 well plates at a concentration of 1000 cells/ well in 100 µl medium with 6 replicate wells per concentration. After 24 hours for adherence media was replaced with media containing increasing concentrations of cytotoxic agent with an untreated control, all corrected for 1% DMSO. Cells were incubated for 3 doubling times (cell lines) or 10 days (PCO cultures) before fixing and staining, using the protocol above.

The mean optical density for each drug treatment were obtained and expressed as a percentage of the related untreated or treated control. Growth inhibitory GI_{50} values (the concentration that results in 50% growth inhibition) and percentage survival at each drug concentration were calculated using a point to point curve on Graphpad Prism software. Final data represented the mean of three experimental repeats, each experiment containing six replicates, with SEM.

WST-1 Assay

Principles of the Assay

Viable cellular enzymes cleave tetrazolium salts to formazan resulting in a colour change (Berridge 2005). Increasing numbers of viable cells results in an increase in the overall activity of mitochondrial dehydrogenases in the sample leading to an increase in the amount of formazan dye formed which is quantified by a multi well spectrophotometer. The WST-1 assay was used to assess the effects of cytotoxic agents on cell proliferation in parallel to the SRB assay in cell lines and PCO cultures.

Assay Protocol

Cells were prepared as for an SRB assay. Following incubation with increasing doses of cytotoxic agent 10 µl of WST-1 cell proliferation reagent was added to each well. A blank control was created after adding WST-1 reagent to a well

containing full medium but no cells. The plates were returned to the incubator and the absorbance was read at 450 nm after 15 minutes. Data analysis was performed as in the SRB assay.

Cell Counting Assay

Assay Protocol

PCO cultures were seeded in triplicate into six well plates at a concentration of 2×10^5 /ml for 24 hours. Media was replaced with media containing increasing concentrations of cytotoxic agent, with an untreated control with equivalent 0.1% DMSO. After 10 days media was aspirated, cells were PBS washed and trypsinised. 100 μ l of the cell suspension was added to 990 μ l of FACS rinse and the cell concentration determined by Coulter counter. A mean of three measurements per sample was used and normalised to untreated controls.

3.6. Homologous Recombination Repair Functional Assay

3.6.1. Principles of the Assay

There are three principles of the immunofluorescent HR assay:

1. Induction of DNA DSB damage
2. Quantification of DNA damage by γ H2AX foci
3. Quantification of Rad51 foci as a marker of DNA repair by HR.

DSB as well as stalled/collapsed replication forks are the substrates for HR DNA repair and therefore induction and quantification of DNA damage and quantification of proteins used by the HR pathway provides the basis for this assay,

Figure 1.4 - 5. H2AX becomes phosphorylated to form foci of γ H2AX at the site of DNA DSB and the number of foci has been shown to correlate with the number of DSBs (Rogakou 1998, Sedelnikova 2002). There is a variable background γ H2AX signal expressed mostly in S-phase associated with DNA replication (Celeste 2003) and this is controlled for when quantifying DNA damage.

Rad51 is the central protein required for HR and is re-localised within the nucleus in response to DSB DNA damage to form distinct foci. Rad51 unwinds duplex DNA and forms helical nucleoprotein filaments at the site of a DNA break (Thacker, 2005). Rad51-coated nucleoprotein filament carries out the search for homology and strand invasion in HR (Sung 1994, Baumann 1996, Lundin 2003). Quantification of Rad51 in response to DNA damage serves as a marker of HR function allowing distinction between competent and defective cells,

Figure 1.4 - 5. Both γ H2AX and Rad51 were localised by binding of specific antibodies followed by fluorescently tagged secondary antibodies and immunofluorescence microscopy. DAPI, a fluorescent DNA stain was used to identify nuclei.

3.6.2. Assay Protocol

Cells were cultured on glass coverslips at a concentration of 5×10^5 cells/well. After adherence DNA DSB were induced with 2 Gy ionising irradiation (Irradiator XSTRAHL RS320, Gulmay Medical Ltd., UK) at a dose rate of 2.4 Gy/min, 310 kV, 10 mA. Standard operating procedure for using the irradiator in NICR (D3300 X-ray system) was followed. Incubation for 24 hours with media containing 10 μ M rucaparib (a potent inhibitor of PARP-1/2 Ki <5 nM/L) in 1% DMSO prevented repair of SSB and DSB induced by irradiation thereby creating stalled/collapsed replication forks.

All experiments were performed alongside untreated controls with equivalent 1% DMSO. Coverslips were washed with PBS and fixed with ice-cold methanol (-20 °C) for 20 minutes. Cells were rehydrated with two PBS washes and transferred to 90 mm petri dishes covered with parafilm. Cells were blocked for 1 hour at room temperature in KCM buffer (120 mM KCl, 20 mM NaCl, 10 mM Tris-HCl, 1 mM EDTA, pH 8.0), 0.1% Triton X-100, 2% bovine serum albumin, and 10% milk powder to reduce non-specific binding. Cells were incubated overnight at 4 °C with primary anti- γ H2AX histone IgG mouse monoclonal antibody or primary anti-Rad51 IgG rabbit polyclonal antibody at a concentration of 1:100 in blocking buffer. After three 15 minute washes with KCM buffer with 0.1% Triton, cells were incubated with the corresponding secondary antibody, Alexa Fluor® 546-conjugated goat anti-mouse IgG antibody or Alexa Fluor® 488-conjugated goat anti-rabbit antibody, for 1 hour at room temperature in the dark. After washing, coverslips were mounted on glass slides with 4 μ l Vectashield DAPI mounting media and foci images with the Leica DMR fluorescent microscope, Table 3.6 - 1.

Stain	Filter colour	Excitation (nm)	Emission (nm)	Gamma	Gain	Exposure (m seconds)
Rad51	Green	495	519	0.35	16	3500
γ H2AX	Red	556	573	0.35	16	3500
DAPI	Blue			0.35	4	300

Table 3.6 - 1: Microscope settings for immunofluorescent HR assay.

3.6.3. Immunofluorescence Microscopy: Focus Counting

Image J counting software (Abramoff 2004, Znojek 2011) was used to count γ H2AX and Rad51 foci in at least 50 cells across three microscope fields. Overlapping cells and cells with fragmented nuclear outline on DAPI staining were excluded to avoid over/under estimation of foci counts. The mean number of foci/cell in treated cells was normalised to untreated controls and results expressed as the fold increase from untreated controls. Image J software has previously been validated when compared to manual counting by several independent reviewers (Mukhopadhyay 2010). Cells were classed as HR competent if there was more than a 2-fold increase in Rad51 foci after DNA damage, confirmed by a 2-fold increases in γ H2AX, and HR defective if less than a 2-fold increase in Rad51 foci count was seen.

3.7. 8-hydroxy-2'-deoxyguanosine: A functional BER assay

Principles of the Assay

8-hydroxy-2'-deoxyguanosine (8-OHdG) is produced during oxidative DNA damage with the main attack site by oxidative radicals at the N7-C8 bond (Chiou 2003). Cells competent in BER remove the 8-oxo-dG and have low residual levels, whilst cell lines defective in BER fail to remove 8-oxo-dG and have high residual levels. Trevigen's competitive ELISA kit quantifies baseline, unstimulated, 8-OHdG in DNA using colorimetric detection. The assay uses an 8-OHdG pre-coated 96 strip well plate to which samples are added followed by an anti-8-OHdG monoclonal mouse antibody. The 8-OHdG monoclonal antibody binds competitively to 8-OHdG immobilized on pre-coated wells and in the sample. Antibody bound to 8-OHdG in the sample is washed away while antibody bound to 8-OHdG attached to the well is retained. The remaining 8-OHdG is quantified using colorimetric detection with HRP conjugate and colorimetric substrate. Colour formation is inversely proportional to 8-OHdG present in sample. High 8-OHdG levels indicate defective BER whilst low levels indicate competent repair.

Assay Protocol

Cell pellets were prepared from PCO cultures when 80% confluent and stored at -80 °C. DNA extraction was performed using the Sigma-Aldrich Gen Elute Mammalian Genomic DNA Miniprep kit as per manufacturer's instructions. DNA concentration and purity was checked by Nano drop 1000 UV Spectrophotometer. DNA with 260/280 OD ratio of 1.6 to 1.9 were considered adequate quality and stored at -20 °C until further use.

DNA at a concentration of more than 50 µg/ml was required for use in functional assays. DNA was concentrated by adding 300 µl 100% ethanol and 13 µl sodium acetate (pH 5.5) at -20°C for 30 minutes. Samples were centrifuged at 120 g for 15 minutes before washing with 70% ethanol and resuspending in elution buffer. DNA was re-quantified as above.

Equivalent DNA from PCO samples alongside positive and negative controls (AA8 and BER cell lines) were prepared to quantify baseline 8-OHdG. 1X cations were added to each sample followed by 2 µl DNase I per 50 µg DNA and incubated at 37 °C for 1 hour. 2 µl alkaline phosphatase per 50 µg DNA was added and incubated at 37 °C for 1 further hour. DNA samples were ready for the ELISA. Standards were prepared as per manufacturers instruction by adding 3 µl of 200 nM 8-OHdG solution to 297 µl of assay diluent. Serial dilutions were prepared from this. Samples and standards (25 µl) were added to the 96 well plate with 25 µl 1:250 8-OHdG monoclonal solution and incubated at 25°C for 1 hour. Plates were washed 4 times with 0.1% (v/v) Tween PBS before adding 50 µl of goat 1:500 anti-mouse IgG-HRP conjugate to each well and incubating for 1 hour at 25 °C. After washing 4 times with 0.1% Tween PBS 50 µl TACS-sapphire™ was added and the plate incubated in the dark for 5 minutes. 50 µl 0.2 M HCl was added to each well to stop the reaction and the plate read at 450 nm using Spectramax 250 microplate reader.

Data Interpretation

Data analysis was performed using the Trevigen online worksheet: http://www.trevigen.com/docs/1309882151.4380_096_k_8_ohdg_calculation_worksheet.xls. Briefly, the mean absorbance of each 8-OHdG standard and blank was calculated. Following subtraction of the blank reading, the log of 8-OHdG

standard concentrations (nM) was plotted against the relative absorbance. The standard curve is a second order polynomial function represented by the equation: $y = a + bx + cx^2$, where y is the relative absorbance, x is the log of 8-OHdG concentration in nM and a, b and c are coefficients. The 8-OHdG sample concentrations were calculated by interpolation from the standard curve.

3.8. RNA Genome Expression Arrays

Principles of the Assay

The relative expression of particular genes involved in DNA DSB repair was determined in selected PCO, stratified by HR or BER functional status.

RNA was extracted, quality checked then processed by the Oxford genomics centre (Oxford, UK) using Illumina Genome Studio and HumanHT 12v4.0 R1 15002873 array, as per manufacturer's instructions.

Assay Protocol

Reagents and RNA were kept on ice throughout the experiments and contamination minimized by using RNAPrep solution for cleaning all surfaces, and RNase/DNase-free pipette tips and tubes. RNA was extracted from frozen cell pellets using the Qiagen RNeasy Mini kit as per manufacturer's instructions. Briefly, cells were lysed and homogenised, then RNA was bound to an RNeasy silica gel membrane in spin-column format, after which contaminants were removed by washing in provided buffers. RNA was eluted in 30 μ l nuclease-free distilled water (dH₂O).

RNA concentration and purity was checked by Agilent RNA bioanalyser and RNA 6000 Nano Lab chip kit (Agilent technologies, USA) as per manufacturer's instructions. Briefly, 2 μ l samples of concentrated RNA extract are treated for 2 minutes at 70 °C before adding 1 μ l aliquots to the Agilent RNA chip. A 6-peak RNA nano ladder is included in the chip for control. Data analysis was done using the 2100 Expert software. Good quality RNA was verified by the presence of a sharp distinction at the small side of both the 18 S and 28 S ribosomal RNA bands and peaks. Any smearing or shouldering to the rRNA bands or peaks

was indicative of RNA degradation. A RNA integrity number (RIN) of >8.0 was considered satisfactory.

The HumanHT-12 v4 Expression BeadChip consist of oligonucleotides immobilised to beads held in microwells on the surface of an array substrate and provides genome-wide transcriptional coverage of well-characterized genes, gene candidates, and splice variants, with high-throughput processing of 12 samples per BeadChip. Each array on the HumanHT-12 v4 Expression BeadChip targets more than 47,000 probes derived from the National Centre for Biotechnology Information Reference Sequence (NCBI) RefSeq Release 38 (2009). Labelled cRNA are detected by hybridisation to 50-mer probes on the Beadchip. After washing and staining steps using the Direct Hybridization Assay, beadchips are scanned on the HiScan or iScan systems. Illumina Genome Studio Gene expression software is used to extract relative gene expression across samples, clustering them into differential groups. The comparative Ct ($\Delta\Delta\text{Ct}$) method was used to assess the expression level of components of each pathway relative to endogenous controls normalized to the reference panel. The fold change differences in expression of each gene between sample categories (HRC and HRD; BER competent and BER defective) was calculated. The HR genes analysed are describes in Table 3.8 - 1. The BER genes analysed are described in Table 3.8 – 2.

Gene	Description
APE1	The damaged base is removed by specific glycosylases forming an abasic site (or apurinic or apyrimidinic [AP] site), which is then hydrolysed by an AP endonuclease, such as APE1.
XRCC1	XRCC1, a scaffold protein, is recruited to the site of DNA damage followed by DNA pol β and DNA ligase III that conducts the ligation of the DNA.
Pol β	
LIGIII	
PNK	
PCNA	PNK converts damaged DNA ends to 5'-phosphate and 3'-hydroxyl moieties. PCNA and DNA polymerase δ/ϵ extend and fill the gap, and FEN1 cleaves the resulting flap. The nick is then ligated by DNA ligase I.
FEN1	
LIGI	
PARP	
PARP	Following DNA damage, activated PARP-1 binds to SSB releasing PAR. This leads to the relaxation of chromatin facilitating access and the recruitment of the proteins necessary for repair (Althaus 1993, Dantzer 2000, Schreiber 2006).

Table 3.8 – 2: BER genes analysed in RNA genome analysis.

Gene	Description
ATM	The phosphoinositide-3-kinase-like protein kinases, ATM and ATR signal in response to DNA damage by phosphorylating BRCA1 (Cortez 1999), NBS1 (Gatei 2000), Rad51 (Baskaran 1997), p53 (Siliciano 1997) and the checkpoint kinases Chk2 and Chk1 (Abraham 2001) resulting in cell cycle arrest, activation of DNA repair pathways or triggering apoptosis (Zhou 2000, McGowan 2004).
ATR	
Rad50	
NSB1	
BRCA1	The BRCA genes regulate the HR machinery by binding to Rad51 recombinase (Pellegrini 2002).
BRCA2	BRCA2 functions are largely limited to DNA repair and recombination. BRCA2 protein controls the availability, localization, DNA binding activity and nucleofilament stabilization of Rad51 (Yu 2003, Esashi 2007, Thorslund 2007, Ayoub 2009) (Carreira 2009, Shivji 2009). BRCA2 stimulates Rad51-dependent strand exchange (Pellegrini 2002). Jensen <i>et al.</i> (2010) described that BRCA2 acts by targeting Rad51 to the ssDNA, enabling displacement of the replication protein-
Rad51	Rad51 family consists of several proteins, which preferentially bind to single stranded DNA, and form complexes with each other. Rad51, Rad52, Rad54 are components of the Rad52 epistasis group (Petrini 1997, Baumann 1998, Takata 2000). Rad51 unwinds duplex DNA and forms helical nucleoprotein filaments at the site of a DNA break (Thacker 2005). Rad51-coated nucleoprotein filament carries out the search for homology and strand invasion in HR (Sung 1994, Baumann 1996, Lundin 2003).
Rad52	Rad52 can recruit Rad51 to ssDNA, perhaps loading Rad51 on to the DNA and facilitating nucleoprotein filament formation (Sung 1997, New 1998, Van Dyck 1999, Wray 2008).
Rad54	Rad54 is also important in HR repair promoting branch migration (Bugreev 2006); loss of Rad54 leads to recombinational deficiencies and DSB repair defects (Essers and de Wit 1997, Mazin 2003, Chi 2006).
XRCC2	XRCC2 and XRCC3, members of the Rad51 family, maintain chromosomal stability during homologous recombination (Liu 1998, Forget 2004, Liu 2005, Krupa 2009) (Tambini 2010) and have been implicated to maintain a balance between short and long tract gene conversions between the sister chromatids (Nagaraju 2009).
XRCC3	
FANCD2	ATM-dependent phosphorylation of H2AX, NBS1, BRCA1 and FANCD2 occurs before replication protein A (RPA) binds to facilitate unwinding of the DNA secondary structure allowing access for the substrates of DNA repair (Sung 2006, Jacquemont 2007, Xing 2008, Hartlerode 2009).
RPA	
PARP	Following DNA damage, activated PARP-1 binds to SSB releasing PAR. This leads to the relaxation of chromatin facilitating access and the recruitment of the proteins necessary for repair (Althaus 1993, Dantzer 2000, Schreiber 2006).

Table 3.8 – 1: HR genes analysed in RNA genome analysis.

3.9. PARP Assay

Principles of the Assay

Poly(ADP-ribose) (PAR) is quantified following maximal stimulation of a defined quantity of permeabilised cells during a 6-minute reaction. Excess NAD⁺, a substrate for the PARP enzyme, alongside oligonucleotides that mimic DSB thereby activating PARP are added. The reaction is stopped by adding rucaparib and placing the samples on ice. Cells are blotted on to a membrane that is treated with anti- PAR primary antibody followed by secondary antibody conjugated with HRP. A chemiluminescence agent is added and following image capture with a sensitive camera, PARP activity is expressed as 'luminescent arbitrary units'. This assay has been previously validated in our laboratory (Plummer 2005) to GCLP standard and used as a pharmacodynamic endpoint for clinical trials (Plummer, Jones et al. 2008).

Assay Protocol

PCO cell pellets and one 10⁶ cell aliquot of L1210 (quality control) were defrosted, washed twice in ice cold PBS and permeabilised with digitonin (0.15 mg/ml) at room temperature for 5 minutes. Nine volumes of ice-cold isotonic buffer (7 mM HEPES, 26 mM KCl₂, 0.1 mM Dextran, 0.4 mM EGTA, 0.5 mM MgCl₂, 45 mM sucrose dissolved in distilled water, pH 7.8) was added and the samples placed on ice. A 10 µl cell suspension was mixed 1:1 (v/v) with trypan blue and permeabilised cells counted. The cell suspension was diluted with isotonic buffer to a density of 6 x 10⁵ cells/ ml. Duplicate PCO samples (1000 cells) were exposed to oligonucleotide at 200 µg/mL in the presence of excess NAD⁺ (7 mM) in reaction buffer (100 mM Tris-HCl, 120 mM MgCl₂, pH 7.8) for 6 minutes at 27 °C alongside unreacted cells.

500 µl of the PARP reaction mixture was loaded in duplicate alongside corresponding unreacted samples and PAR standards (0 – 25 pmol) into a 48-well manifold containing a nitro cellulose Hybond-N membrane and drawn through using a vacuum pump. 400 µl 10% trichloroacetic acid / 2% sodium pyrophosphate followed by 800 µl 70% ethanol were drawn through the membrane as a fixative. The membrane was PBS washed 3 times and blocked

(5% milk powder in 0.0005% Tween-20 PBS) for 1 hour. Mouse monoclonal anti-PAR 10H antibody (1:1000) was added at for 1 hour, followed by polyclonal goat anti-mouse IgG anti-PAR horseradish peroxidase–conjugated antibody (1:1000). Secondary antibody was followed by Amersham ECL detection fluid and chemiluminescence recorded by Fujifilm LAS 3000 imager then analysed using Aida Image Analyser software (version 3.28.001,). Three blank areas were defined on the image and the relative luminescence of each sample in 'luminescent arbitrary units (LAU / mm²)' calculated.

Data Analysis

A standard curve was constructed by non-linear regression of the PAR standard values using Graph Pad Prism 6. The resulting equation relating PAR to chemiluminescence ($R^2 \geq 0.9$) was used to calculate the amount PAR present in each well. Results were expressed as picomoles of ADP-ribose monomer incorporated per 10^6 permeabilised cells. Results were normalised to PAR in internal controls (L1210 cell line) to account for inter-assay variability. PAR activity in stimulated cells was expressed as the percentage of the activity in untreated control cells.

3.10. Western Blotting

Principles of the Assay

Western blotting separates and identifies specific proteins extracted from cells by electrophoretically separating proteins by molecular weight. Protein samples are denatured using SDS (sodium dodecyl sulfate) and heating, as 3D structure may prevent antibody binding and slow transition through the gel. Denatured protein samples are then run through a polyacrylamide gel under electric current. Larger proteins migrate the least whilst smaller proteins move further in the same time period. Resulting protein bands are transferred onto nitrocellulose membranes by blotting using an electric current to move negatively charged proteins from the gel, to the membrane. The membrane is placed in blocking buffer to prevent non-specific binding of antibodies to the membrane and the target protein is then positively identifying using a specific primary antibody to the protein of interest followed by a secondary –HRP conjugated antibody directed at the primary antibody. Once primary and secondary antibodies are hybridised, antibodies can be visualised using ECL (enhanced chemiluminescence), which reacts with HRP to emit chemiluminescence that can be detected and visualised by CCD (charge coupled device) camera. Detected protein size can be estimated by the inclusion of and comparison with a predetermined molecular weight marker. The number of antibody molecules which can bind to each protein (and hence the amount of label detected) is proportional to the amount of protein present, therefore protein expression levels can be compared between samples.

Assay Protocol

Culture medium was removed and cells PBS washed. Cells were lysed with addition of 300 µl of SDS lysis buffer (SDS sample buffer with 10% β-Mercaptoethanol) and stored at -80 °C for later analysis. Protein concentration was quantified using a colorimetric Bio-Rad DC™ protein assay as per manufacturer's instructions. Briefly, alkaline copper tartrate solution is added to protein solution followed by Folin reagent. The reaction between protein and copper in an alkaline medium, and the subsequent reduction of Folin reagent by

the copper-treated protein results in colour formation (predominantly due to tyrosine and tryptophan residues) read at 405 - 750 nm absorbance. Protein concentration was estimated from the corrected mean absorbance values by the spectrophotometer software (SOFTmax Pro 3.0, molecular Devices Corporation), via comparison to a bovine serum albumin (BSA) standard curve which was also prepared each time the assay was performed. Samples were diluted to 20 mg/ml protein before lysates were denatured at 100 °C for 5 minutes. Gels were assembled and resolved in a Mini-PROTEAN Tetra cell. Lysates were loaded into 4-15% Mini-PROTEAN® TGX™ gels alongside multicolour broad range protein ladder (4 kDa to 250 kDa). Proteins were separated by electrophoresis at 200 mVolts for 1 hour in buffer (77.9% glycine, 16.6% tris-base, 5.48% SDS) before protein transfer to Hybond ECL membrane. Gels were placed in transfer cassettes with the membrane sandwiched between 3 mm Whatman chromatography papers and transfer sponges, all soaked in transfer buffer (78.7% glycine, 21.2% tris-base). Electrophoresis for transfer was undertaken in the tetra cell filled with transfer buffer at 100 mVolts and ice pack for 1 hour. Membranes were blocked in 5% non-fat milk powder solution for 1 hour at RT after which membranes were incubated in primary antibody in TBST with 1% milk at 4 °C overnight. Membranes were washed for 15 minutes with TBST (Tris-buffered-saline solution containing 0.05% tween) and horseradish peroxidase-conjugated secondary antibodies were applied in TBST with 1% milk for 60 min at RT. Membranes were washed with TBST before detection of bound antibodies using ECL detection solution. Chemiluminescence was imaged using the Fuji-imager (Lass3000). Membranes were washed with TBST and incubated with Ponceau S solution (0.1% Ponceau S [w/v] and 5.0% acetic Acid [w/v]) for 5 minutes before repeat imaging for total protein quantification using the Fuji-imager. All immune-blotting experiments were carried out in triplicate.

3.11. Clinical Definitions

Surgical staging was assessed in accordance with International Federation of Gynaecologists and Obstetricians (FIGO) classification. Complete debulking was defined as no visible disease; optimal debulking was defined as ≤ 1 cm (diameter) residual disease, and suboptimal debulking was > 1 cm (diameter) residual disease.

Disease progression was determined based on CA125 marker levels and imaging results according to Gynaecologic Cancer Inter Group (GCIg) modification of Response Evaluation Criteria in Solid Tumours (RECIST) guidelines modified for ovarian cancer (Therasse 2000, Rustin 2004, Rustin 2011), or on clinical examination. Progression-free survival (PFS) was defined as the interval between histological diagnosis and first progression, death due to disease or last follow-up. Death due to a non-disease related cause was not considered an event in the calculation of PFS. Overall survival (OS) was defined as the interval between histological diagnosis and the date of death due to disease, or last follow-up (active follow-up for 5 years, passive thereafter).

3.12. Statistical Analysis

Microsoft Excel 2010 and Graph Pad PRISM version 6 software were used for simple statistical analyses.

Cytotoxicity Assays

In the colony formation assays, each experimental point was set up in triplicate and each assay was repeated identically and independently three times. The final data were expressed as a percentage of the survival that took place in control wells where cells were not exposed to any drugs. IC_{50} values were determined for each experiment. To evaluate the differences across various experimental conditions students t-test was used to evaluate differences between individual pairs of experimental conditions.

Proliferation Assays

For cell proliferation assays, each experimental point was set up with six replicates and data expressed as the mean and standard error of the mean (SEM). GI₅₀ values were calculated using a point to point graph of percentage growth inhibition with increasing drug concentration. Differences in survival between treated cells were determined by One-Way ANOVA, Two-Way ANOVA or paired t-test as appropriate.

Survival

Progression free (PFS) and overall survival (OS) was evaluated with Kaplan-Meier survival analyses. Univariate analysis of differences between the various cohorts of each experiment was performed using the log rank test (Mantel Cox).

Correlation

The Spearman test was applied for analyses of correlations.

For all statistical analyses, significant differences were set as $p < 0.05$.

Receiver Operating Characteristic (ROC) Curve

A ROC curve, using the area under the curve (AUC), is used to assess the ability of a numerical score to accurately predict a binomial outcome. This is done by assessing the cut off value that discriminates the two groups by tabulating sensitivity and specificity of the test at various cut off values. A table of sensitivity and specificity for each value is created and is used to draw a graph of 100%-Specificity% vs. Sensitivity%. The area under a ROC curve quantifies the overall ability of the test to discriminate between the two outcomes. An area of 1 represents a perfect test; an area of 0.5 represents a worthless test. A p value tests the null hypothesis that the area under the curve really equals 0.05.

Chapter 4. Assessment of the Primary Ovarian Cancer (PCO) Culture Model and Exploration of Biological Markers of Clinical Survival

4.1. Introduction: Primary Culture

Established cell lines provide an invaluable tool for studying biological functions at the molecular and cellular level. Existing human ovarian cancer cell lines possess the advantage of high proliferative capacity, clonogenicity and extended life span in culture. However, most have acquired significant genetic alterations from their cells of origin, including deletion or upregulation of regulatory cell cycle genes supporting immortality. Additionally, there is evidence to suggest that many cell lines contain significant misidentification, duplication and loss of integrity (Korch 2012).

Primary cells isolated from patients are often considerably different from cell lines of similar origin. The ability to culture freshly isolated OSE (ovarian surface epithelium) and EOC (epithelial ovarian cancer) cells from patients provides an important experimental system that resembles the patient situation more closely (Dunfield 2002, Mukhopadhyay 2010).

Ascitic fluid is an abundant resource in ovarian cancer patients, is relatively easy to obtain and culturing the suspended cells is technically straightforward. Ascitic cultures have been shown to generate epithelial cell rich populations and have been used in this study to further explore the application of functional assays in the stratification of therapy in ovarian cancer. In this study, this method has been considered the benchmark technique for biological testing of primary material against which exploratory techniques are tested.

The use of cultures derived from patient ascites has arisen due to the ongoing search for cancer biomarkers, capable of predicting response to conventional and novel (e.g. PARPi) therapy. In ovarian cancer, a number of potential biomarkers have been tested including BRCA status. This alone has failed to be shown to be predictive. In one phase 2 trial of olaparib many ovarian cancer patients showed response to olaparib therapy despite no BRCA mutation and

there was also a low overall response in BRCA patients with response in only 7/17 patients (Gelmon 2011) . These difficulties in identifying a single biomarker have forced clinicians and academics to reassess the current approach. It appears that a functional assay, developed by Newcastle University, distinguishing ovarian cancer into groups based upon a competent or defective HR DNA repair pathway shows greatest promise (Mukhopadhyay 2010, TCGA 2011, Mukhopadhyay, Plummer et al. 2012).

Work in this Chapter aims to develop our understanding of the ascitic primary culture model as well as explore alternative approaches to the complex functional HR assay previously described, with the goal of incorporating HR function as a biomarker into large scale clinical trials.

4.2. Aims

- To characterise PCO cultures derived from ascitic samples in terms of antigen expression, growth potential and morphology in order to further understand the strengths and weaknesses of this model.
- To understand the extent of epithelial mesenchymal transition (EMT) within ovarian cancer and the effect of *ex vivo* culture upon this.
- To explore the presence of subpopulations of cells within ascites, their antigen expression, growth and HR status.
- To determine the homologous recombination (HR) DNA repair status of PCO cultures with corresponding *ex vivo* sensitivity to rucaparib and cisplatin and to compare with *in vivo* platinum sensitivity and clinical outcome.
- To explore the ability to simplify the currently complex HR assay in order to transform it into a reliable, reproducible and clinically applicable process, enabling rapid, large volume turnover in clinical trials and routine practice and to explore alternative assays for HR function based on expression signatures at RNA level.
- Assess the utility of *ex vivo* proliferation assays in predicting clinical response to platinum chemotherapy.

4.3. Methods

4.3.1. Characterisation

Ascitic fluid is composed of multiple cellular components. A characterisation panel consisting of culture morphology, immunofluorescent antigen detection, cross-referenced with standard pathological examination of matched tumour FFPE was developed to confirm exclusive growth of cancer cells.

4.3.2. Morphology

Brightfield microscopy images of cultures were captured using VisCam® software. Comparison to three reference images allowed classification into cobblestone, mesenchymal or spindle morphologies. A cobblestone monolayer is typical of epithelial-like cells and describes polygonal cells with regular dimensions, which grow attached to the culture substrate in discrete patches. Mesenchymal morphology describes bipolar or multipolar cells with elongated shapes. Spindle morphology is most typical of fibroblast-like cells, which are elongated regular shaped cells with indistinct cell boundaries typically growing in the same orientation. In controversial cases, final assignment to a morphological category was validated by two further reviewers, Figure 4.3 - 1.

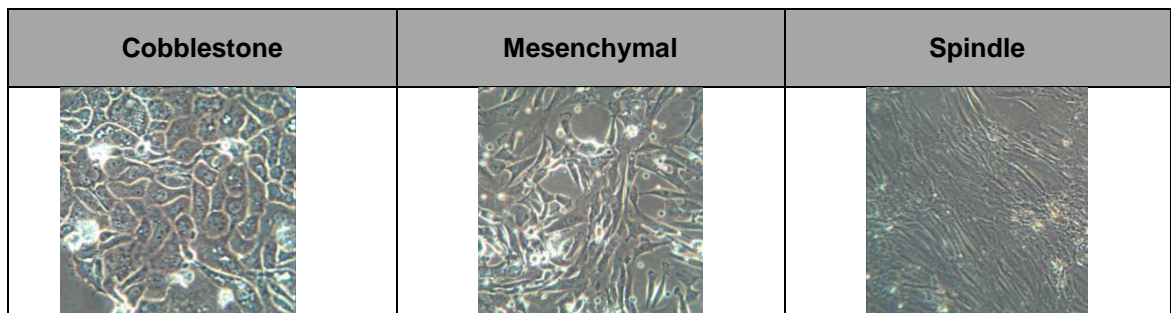


Figure 4.3 - 1: PCO culture morphology reference images. Brightfield microscopy (x10) demonstrating cobblestone, mesenchymal and spindle cell morphology.

4.3.3. Immunofluorescence Characterisation Panel

Standard techniques for immunofluorescence were used to detect epithelial, ovarian and mesenchymal antigens, Table 4.3 - 1. Briefly, cells were cultured on glass coverslips before methanol fixation. After PBS wash, coverslips were incubated with primary antibody solution for 1 hour followed by the appropriate secondary antibody. Coverslips were mounted onto glass slides with 4 µl DAPI mounting media and images captured using a Leica DMR fluorescent microscope and RT SE6 Slider Camera Spot advanced software version 3.408, Table 4.3 -2. Antigen expression was scored as absent, patchy or strong using reference images obtained from positive and negative cell line controls. In controversial cases, final assessment of antigen expression was validated by two further reviewers.

Antigen		Species	Conc	Secondary Antibody
CK	Cytokeratins are intermediate filaments, produced by epithelial cells, which make up the majority of the cytoskeleton. Epithelial in origin if > 95% of cells express	Mouse monoclonal FITC conjugated, Clone C11, (Upstate Millipore ,USA)	1:100	N/A
EpCAM	Cell surface glycosylated protein is expressed in normal epithelial cells as well as carcinomas. EpCAM functions as a calcium independent cell adhesion molecule and is believed to be involved in carcinogenesis by its ability to induce genes involved in cellular metabolism and proliferation (Strand 1989, Munz 2004, Rao 2005).	Mouse monoclonal Alexa Fluor® 488–conjugated, (Biolegend, UK)	1:100	NA
CA125	The ovarian tumour marker CA125 is expressed in approximately 80% of epithelial ovarian cancers (Rosen 2005), It is expressed on human MUC16, a cell surface bound mucin that is also shed by proteolytic cleavage. MUC16 facilitates the binding of ovarian tumour cells to mesothelial cells lining the peritoneal cavity.	Mouse monoclonal, (Abcam, USA)	1:100	1:1000 Alexa Fluor® 546 goat anti-mouse (Invitrogen, USA)
MOC-31	Epithelial transmembrane glycoprotein 2 (EGP-2, also known as ESA, GA733-2, KSA) is present on most normal and malignant epithelia (Souhami 1991, Hecht 2006) enabling discrimination from mesothelial derived tumours with a specificity of 87-100% and specificity of 89% (Ruitenbeek 1994, Morgan 1999, Hecht 2006, Kundu 2011)	Mouse monoclonal, (Dako, France)	1:100	1:1000 Alexa Fluor® 596 goat anti-mouse (Invitrogen, USA)
Vimentin	Marker commonly used to detect epithelial-mesenchymal transition (EMT). It is a protein that, in humans, is encoded by the VIM gene. Vimentin is a type III intermediate filament protein that is expressed in mesenchymal cells.	Rabbit monoclonal, clone EPR3776, (Abcam, USA)	1:100	1:1000 Alexa Fluor® 488 goat anti-rabbit (Invitrogen, USA)
D2-40	Anti-D2-40 identifies an O-linked sialoglycoprotein present on germ cell tumours but not epithelial cells (Marks 1999).	Mouse monoclonal, (Dako, France)	1:100	1:1000 Alexa Fluor® 596 goat anti-mouse (Invitrogen, USA)

Table 4.3 - 1: Antibodies for the PCO immunofluorescent characterisation panel.

Stain	Filter Colour	Excitation (nm)	Emission (nm)	Gamma	Gain	Exposure (m seconds)
DAPI	Blue	358	461	1.00	2	500
CK	Green	494	521	1.00	4/8	5000
EpCAM	Green	495	521	1.00	4/8	8000
CA125	Red	556	573	1.00	8	8000
MOC-31	Red	556	573	1.00	8	8000
Vimentin	Red	495	519	1.00	2	2000
D240	Red	556	573	1.00	8	8000

Table 4.3 - 2: Immunofluorescence microscope settings for PCO culture characterisation using antigen panel.

Morphology and the immunofluorescent characterisation panel aimed to assess the degree of epithelial mesenchymal transition (EMT) within the cultures and several subsequent experiments were designed to explore the effect of prolonged *ex vivo* culture upon morphology and antigen expression, Section 4.7.5. EMT, described in detail in Section 4.7.2, is a biological process that allows epithelial cells to undergo multiple biochemical changes, which ultimately lead to increased stability of the acquired mesenchymal phenotype. The completion of an EMT is signalled by the degradation of underlying basement membrane and the formation of a mesenchymal cell with enhanced migratory capacity, invasiveness, greater resistance to apoptosis and increased production of extracellular matrix components (Kalluri 2003, Polyak 2009). Sustained activation of EMT leads to progressive epigenetic alterations in cells, inducing heritable effects that maintain the mesenchymal state even after EMT-initiating signals are no longer present (Dumont, Wilson et al. 2008). The phenotype of each PCO culture was investigated as part of the characterisation assessment in order to explore the possible effect of *ex vivo* culture upon phenotype.

4.3.4. Formal Histopathology

Formal cytological and histological examination of ascites and solid tumour was used to further characterise cultures, assigning each specimen to an ovarian histological subtype according to universal World Health Organisation criteria (Tavassoli 2003). This was performed by NGOC pathologists blinded to the other characterisation studies.

When all characteristics were in keeping with epithelial ovarian origin, samples were used in subsequent experiments. Where results were inconsistent with epithelial origin, cultures were discarded.

4.3.5. Surface Antigen Characterisation Timeline

In order to assess the potential effects of time, *ex vivo* culture and passage on antigen expression, ascites was cultured directly onto glass coverslips and fixed at various time points, without passage. Immunofluorescent detection of antigen expression was assessed and compared to parallel PCO cultures following repeated passage. Ascitic samples were cytocentrifuged directly onto coverslips for immediate processing to assess antigen expression at time zero.

4.3.6. Reducing Analysis Time of PCO Cultures (Characterisation and HR Assay)

Ascitic cellular fluid was centrifuged directly onto glass slides or cultured onto coverslips and then used directly for immunofluorescent microscopy.

4.3.7. Cytocentrifugation

Ascitic samples were incubated with 10% ammonium chloride red cell lysis buffer (RCLB) solution (1:4 v/v) at 37 °C for 5 minutes. (For HR analysis, DSB were induced by incubation with 10 µM rucaparib for 24 hours, alongside untreated control). Following centrifugation (300 g for 5 minutes) and PBS washing, cells were re-suspended in 10 ml of media. 200 µl of the ascitic/media solution was centrifuged (Shandon Cytospin 2 centrifuge) at 45 g for 5 minutes before fixation with methanol.

4.3.8. Coverslip Cultures

Ascitic fluid was added to coverslips with media (1:1 v/v) in 6-well plates and incubated at 37 °C for 48 hours to allow adherence. Cells were then either fixed with methanol for characterisation or DNA DSB induced for the HR assay.

4.3.9. PCO culture, HR Functional Assay, Cell Proliferation, PARP Assays and Gene Expression Methods

The method for PCO ascitic culture, HR functional assay, proliferation assays (SRB, WST-1), cell counting assay, PARP activity assay and RNA analysis are described in detail in Chapter 3 Methods.

4.4. Results:

4.5. PCO Collection

Patients enrolled in this study belonged to a defined geographical area covered by the North of England Cancer Network and were registered with the NGOC at Queen Elizabeth Hospital, Gateshead. Demographic and surgicopathological data were collected from the hospital and pathology databases. The histological diagnosis of ovarian cancer was confirmed by independent pathologists and surgical stage, grade and cell type were classified according to WHO and FIGO standards (Prat 2013).

Between 2011 and 2014, 84 ascitic samples were collected at the time of surgery (n=69, 82%) or drainage of symptomatic ascites (n=15, 18%). Of the 69 samples collected intra-operatively, 55 (80%) were collected during primary surgery and 14 (20%) during interval surgery following chemotherapy.

Successful culture was achieved in 72 cases (86%). Three cultures were discarded due to failed epithelial characterisation, another three became infected and 5 samples excluded due to non-ovarian cancer pathology, leaving 61 cultures that were used in further experiments.

4.6. Clinical Characteristics

The mean age at diagnosis of the PCO patients was 63 years (41-85). The majority of patients were diagnosed at advanced stage (FIGO stage IIIC/IV n=55), with HGSC being the predominant subtype (n=47). A summary of patient characteristics is given in Table 4.6 – 1 with further detail in Appendix 6.

Demographic		Median (range) / n (%)
Age at presentation (years)		63 (41 – 85)
Serum CA125 at presentation (U/l)		1252 (6 – 10000)
Histology	High grade serous carcinoma (HGSC)	47 (77.0)
	Clear cell	2 (3.3)
	Endometrioid	1 (1.6)
	Other	11 (18.0)
Time of collection	Primary surgery (pre-chemotherapy)	43 (70.5)
	Interval surgery (post- chemotherapy)	18 (29.5)
Surgical outcome	Optimal/Complete	47 (77.0)
	Suboptimal	7 (11.5)
	No debulking surgery	7 (11.5)
FIGO Stage	Stage I	2 (3.3)
	Stage II	2 (3.3)
	Stage III	46 (75.4)
	Stage IV	9 (14.8)
	No staging	2 (3.3)

Table 4.6 - 1: Summary of PCO patient demographics. See Appendix 6 for detailed individual PCO patient data.

4.7. Characterisation

4.7.1. Original Characterisation Protocol and its Limitations

The original protocol for PCO culture characterisation was limited to cobblestone morphology and more than 95% expression of a single antigen, cytokeratin (CK). More than 20 cytokeratins have been identified, of which subtypes 8, 18, and 19 are the most abundant in simple epithelial cells (Barak 2004). However, ascitic mesothelial cells have also been reported to express cytokeratins (5, 7, 8, 14, 17, 18, and 19) and therefore CK should not be used in isolation. This was further confounded when PCO 160 was shown to express CK but formal histology confirmed an ovarian dysgerminoma.

4.7.2. Expanded Characterisation Panel

The characterisation panel was expanded to include further epithelial markers, an ovarian marker, mesenchymal markers and germ cell markers. Selection of antigens, alongside details of the antibodies used, is described in detail in Table 4.3 – 1. A summary of the characterisation profile from all PCO cultures is shown in Figure 4.7 - 1. All PCO included for further analysis expressed cytokeratins and the majority expressed an epithelial marker (EpCAM or MOC31) or the ovarian marker CA125. This work was conducted by myself with contributions by Michelle Dixon, Angelika Kaufmann and Aiste McCormick.

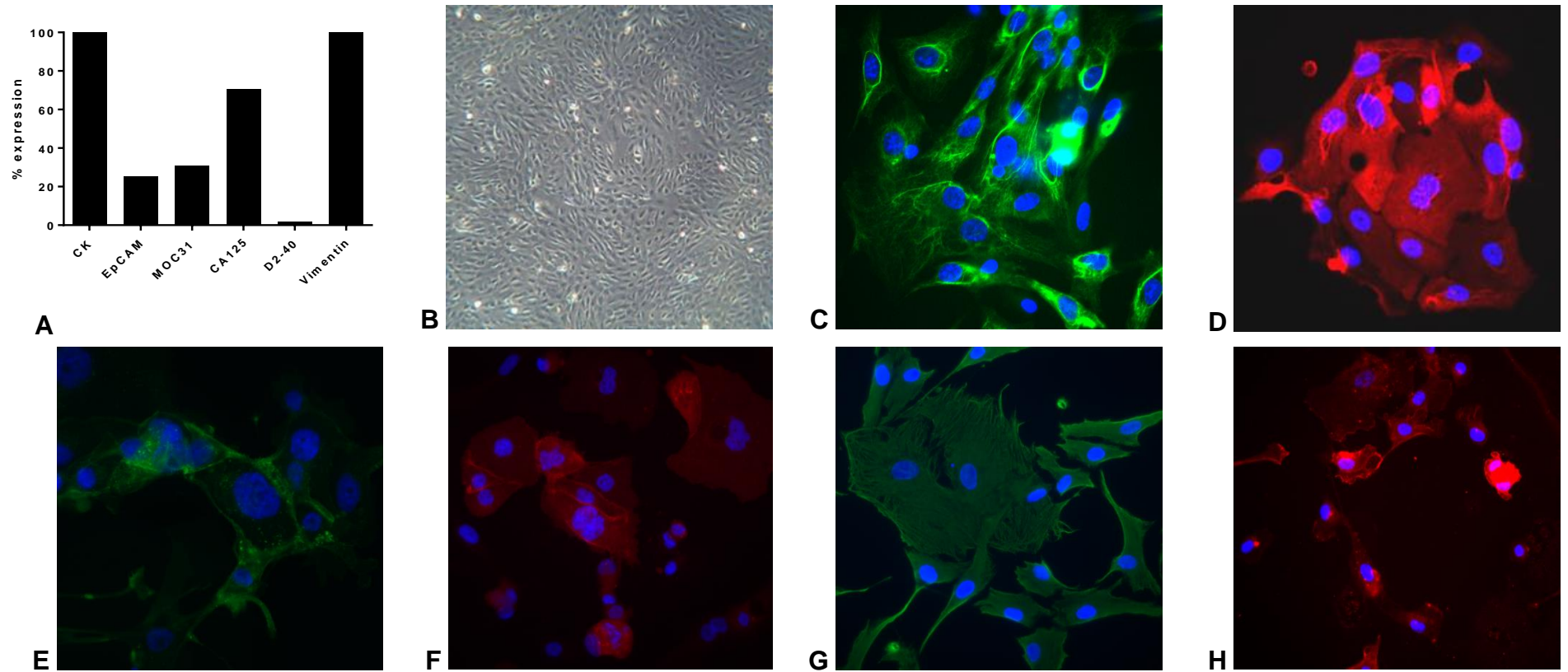


Figure 4.7 - 1: PCO immunofluorescent characterisation panel A: Summary of PCO antigen expression, n=61 shown as % expression of each antigen across all cultures; B: Brightfield - cobblestone monolayer. Immunofluorescent images; C: FITC-anti-CK; D: Alexa Fluor 596 anti-CA125; E: Alexa Fluor 488 anti-EpCAM; F: Alexa Fluor 596 anti-MOC 31; G: Alexa Fluor 488 anti-Vimentin; H: Alexa Fluor 596 anti-D240 (PCO 160 – dysgerminoma).

4.7.3. CA125 Expression: Immunofluorescence vs. Immunohistochemistry

In a subset of PCO samples (n=32), immunofluorescent (IF) assessment of CA125 expression using ascites cultures was compared with immunohistochemical (IHC) detection using matched FFPE tissue, Figure 4.7 - 2. Concordance of results from the two assessments was seen in 18 (56.3%) cases; 15 of which had positive expression of CA125 and 3 with no expression. Of the 14 (43.8%) discordant cases, CA125 expression was detected by IF but not IHC. Several CA125 antibodies had been tested, alongside positive cell line controls and discordance is therefore thought to represent true differences in expression between the samples tested. There was no relationship between serum CA125 level tested and CA125 detection using immunofluorescence of PCO cultured cells, (t-test, $p = 0.2701$) or IHC on FFPE ($p=0.2693$), Figure 4.7 - 3.

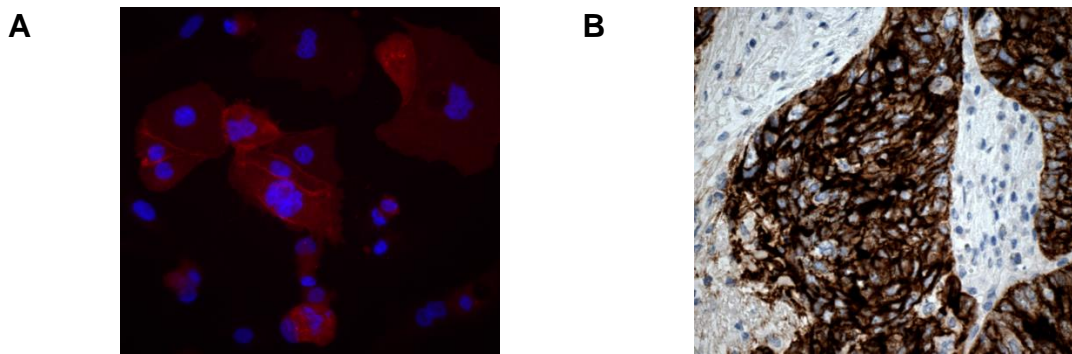


Figure 4.7 - 2: Concordant CA125 expression in PCO 158. A: Immunofluorescent detection of CA125. PCO 158 cells were seeded at 8×10^6 on sterile glass coverslips and following fixation/permeabilisation with methanol and PBS washing, incubated with 1:100 anti-CA125 antibody for 1 hour. After PBS washing, slides were incubated with an Alexafluor 596 secondary antibody and image captured with immunofluorescent microscopy. B: Immunohistochemical detection of CA125 using matched FFPE (performed by pathology Queen Elizabeth Hospital, Gateshead).

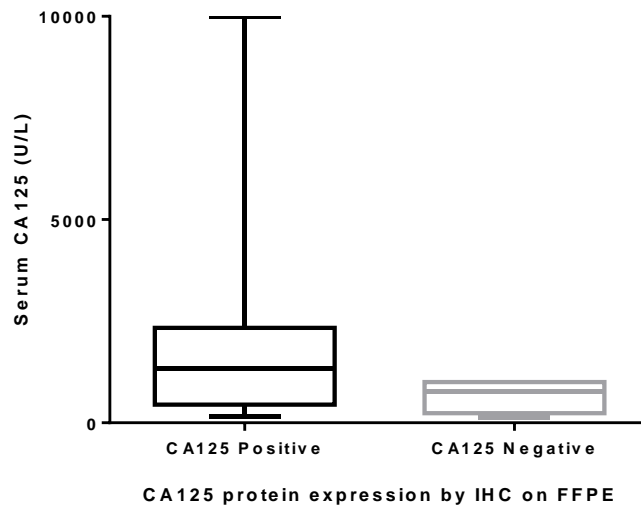
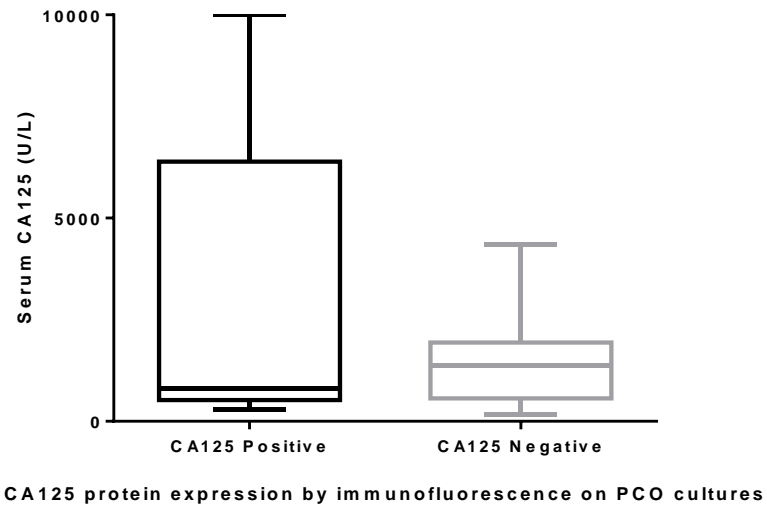
A**B**

Figure 4.7 – 3. Relationship between Serum CA125 (U/L) and CA125 protein expression, detected by immunohistochemistry (A) and serum CA125 with CA125 detected by immunofluorescence on corresponding PCO culture (B). Briefly, PCO cells were seeded at 8×10^6 on sterile glass coverslips and following fixation/permeabilisation with methanol and PBS washing, incubated with 1:100 anti-CA125 antibody for 1 hour. After PBS washing, slides were incubated with an Alexafluor 596 secondary antibody and image captured with immunofluorescent microscopy. Immunohistochemical detection of CA125 was performed by the pathology department at Queen Elizabeth Hospital, Gateshead.

4.7.4. Epithelial Mesenchymal Transition (EMT) and PCO Phenotype

EMT, first described in 1982 (Hay 1995), is a biological process that allows epithelial cells to undergo multiple biochemical changes enabling them to assume a mesenchymal phenotype with enhanced migratory capacity, invasiveness, greater resistance to apoptosis and increased production of extracellular matrix components (Kalluri 2003, Polyak 2009). Induction of EMT has been associated with poor clinical outcome in multiple tumour types (Sabbah 2008) and has also been implicated in two of the most important processes responsible for cancer-related mortality: progression to distant metastases and acquisition of cellular resistance (Polyak 2009). The phenotype of each PCO culture was investigated as part of the characterisation assessment in order to explore the possible effect of *ex vivo* culture upon phenotype.

All PCO cultures were shown to co-express vimentin and CK, Figure 4.7 - 4, suggesting a mixed epithelial-mesenchymal phenotype. Only 25% and 31% of cultures diffusely expressed the epithelial markers EpCAM and MOC31 respectively, Figure 4.7 - 1, and it was unclear if this lower than anticipated level of expression of cell surface epithelial markers reflected *in vivo* expression or whether a process of EMT was induced during *ex vivo* culture. A series of experiments were subsequently designed to explore the effect of prolonged culture upon antigen expression.

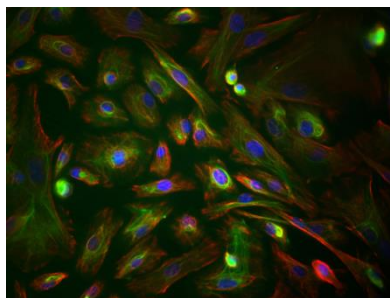


Figure 4.7 - 4: Cytokeratin and vimentin co-expression in PCO 163. PCO 163 cells were seeded at 8×10^6 on sterile glass coverslips and following fixation/permeabilisation with methanol and PBS washing, incubated with 1:100 primary antibody for 1 hour. After PBS washing, slides were incubated with a secondary antibody with fluorochrome and image captured with immunofluorescent microscopy. FITC-conjugated Cytokeratin (green), Alexaflour 596-vimentin (red), DAPI nuclear stain (blue).

4.7.5. Stability of Characterisation Phenotype with Time and Passage

Firstly, three separate ascitic cultures were plated directly onto sterilised coverslips and fixed at various timepoints as indicated in Table 4.7 – 1. An ascitic sample was also cytospun onto a coverslip and fixed immediately for a time 0 control. As the majority of PCO cultures are characterised at passage 1 or 2, a parallel sample was characterised following passage to assess the potential effect of harvesting by trypsin and re-plating upon expression of markers.

There appears to be little change with time in the expression of epithelial, mesenchymal and ovarian antigens, suggesting that *ex vivo* culture alone does not alter phenotype or induce EMT. However, when the same cultures were re-characterised after undergoing passage with trypsin and re-plating, there was reduced detection of surface antigens (* in Table 4.7 - 1). Loss of EpCAM, CA125 and MOC-31 expression suggests that cell surface antigens may be affected by the mechanical/biochemical stresses of passage or that the process of passage results in selection of sub-populations. When PCO cultures, following passage with trypsin, were re-characterised 7 days later, without further passage, they did not regain their epithelial phenotype. Seven days however may be insufficient time for cells to re-express cell surface markers

after 'stripping' with trypsin. The short life span of PCO cultures prevented further assessment of this.

PCO 226 Antigen	Time from Collection							Passage
	0 hrs	24 hrs	48 hrs	72 hrs	1 wk	2 wks	3 wks	P1
CK	+	+	+	+	+	+	+	+
EpCAM	+	+	+	+	+	+	+	- *
CA125	+	+	+	+	patchy	patchy	patchy	patchy
MOC31	+	+	+	+	+	+	+	patchy
D240	-	-	-	-	-	-	-	-
Vimentin	+	+	+	+	+	+	+	+
PCO 232 Antigen	Time from Collection							Passage
	0 hrs	24 hrs	48 hrs	72 hrs	1 wk	2 wks	3 wks	P1
CK	+	+	+	+	+	+	+	+
EpCAM	-	-	-	-	-	-	-	-
CA125	+	patchy	patchy	patchy	patchy	patchy	patchy	- *
MOC31	patchy	patchy	patchy	patchy	patchy	patchy	patchy	patchy
D240	-	-	-	-	-	-	-	-
Vimentin	+	+	+	+	+	+	+	+
PCO 233 Antigen	Time from Collection							Passage
	0 hrs	24 hrs	48 hrs	72 hrs	1 wk	2 wks	3 wks	P1
CK	+	+	+	+	+	+	+	+
EpCAM	patchy	patchy	patchy	patchy	patchy	patchy	patchy	- *
CA125	patchy	patchy	patchy	patchy	patchy	patchy	patchy	- *
MOC31	-	-	-	-	-	-	-	-
D240	-	-	-	-	-	-	-	-
Vimentin	+	+	+	+	+	+	+	+

Table 4.7 - 1: Immunofluorescent characterisation timeline. Antigen expression was assessed at time 0, 24, 48, 72 hrs, 1, 2, 3 wks by fixed immunofluorescence. Antigen detection was assessed as positive (+), negative (-), or patchy in comparison to positive and negative cell line reference images. Highlighted in grey: parallel results for immunofluorescent assessment of antigen detection following routine passage. * = loss of cell surface antigen following passage with trypsin.

4.7.6. Morphology

52 PCO cultures underwent formal morphological classification. 42 (80.8%) had a cobblestone morphology and 10 (19.2%) were mesenchymal. None of the cultures were classified as spindle cell. There was no relationship between histological subtype and morphological appearance with no significant difference seen in the proportion of cultures of cobblestone or mesenchymal morphology within each histological subtype, Table 4.7 - 2. A significantly greater proportion of PCO with cobblestone morphology were HRD but this may be a reflection of the higher proportion of unclassified PCO cultures within the mesenchymal morphological group.

Additionally, there was no significant difference in the expression of characterisation antigens between the morphological subgroups, with the exception of MOC31. This was expressed in 8/23 (34.7%) of cultures classified as cobblestone in comparison to 7/10 (70%) of mesenchymal cultures, (Chi², p<0.0001). Numbers within the mesenchymal group were however small (n=10).

		Cobblestone (n=43)	Mesenchymal (n=17)	Chi² p
PCO	PCO	2 (97.7)	10 (58.8)	0.0019 *
	PCO-2	1 (2.3)	7 (41.2)	0.0001 *
Histology	HGSC	35 (81.2)	14 (82.4)	0.8759
	Mucinous	1 (2.3)	0 (0)	-
	Clear cell	1 (2.3)	0 (0)	0.1573
	Endometrioid	1 (2.3)	1 (5.9)	0.8960
	Other	5 (11.6)	2 (11.8)	
HR status	Competent	22 (51.2)	7 (41.2)	0.2971
	Defective	18 (41.9)	4 (23.5)	0.0267 *
	Unclassified	3 (7.0)	6 (35.3)	0.0001 *
CK	n=60#	43 /43(100)	17/17 (100)	-
EpCAM	n=49#	7/35 (20)	4/14 (28.6)	0.1985
CA125	n=54#	25/40 (62.5)	9/14 (64.3)	0.9293
MOC31	n=39#	8/23 (34.7)	7/10 (70)	0.0006 *
D240	n=34#	1/27 (3.7)	0/7 (0)	-
Vimentin	n=49#	36/36 (100)	13/13 (100)	-

Table 4.7 - 2: Histological subtype, characterisation antigen expression, HR DNA Repair Status in PCO Cultures (n=61) stratified by Morphological Subtype. PCO-2 cultures are described in full in section 4.9. HR status of PCO and PCO-2 cultures are described in sections 4.10 and 4.9.3. # total number of cultures tested for selected antigen

4.8. PCO Culture Growth

The median PCO growth rate is markedly slower than many cell lines and is highly variable with a median doubling time (DT) of 133 hours, range of 35–487 hours, Figure 4.8 - 1. The typically prolonged doubling time may be a consequence of *ex vivo* culture itself. Malignant cells within ascites are held in suspension before they are deposited upon peritoneal surfaces, where they proliferate. Despite provision of fluid and heat with cell cultures being grown at 37 °C, 5% CO₂, 95% humidified air, an excess of L-glutamine and growth factors (fetal calf serum), the peri-tumoural microenvironment is lacking and this may result in the prolonged doubling time seen.

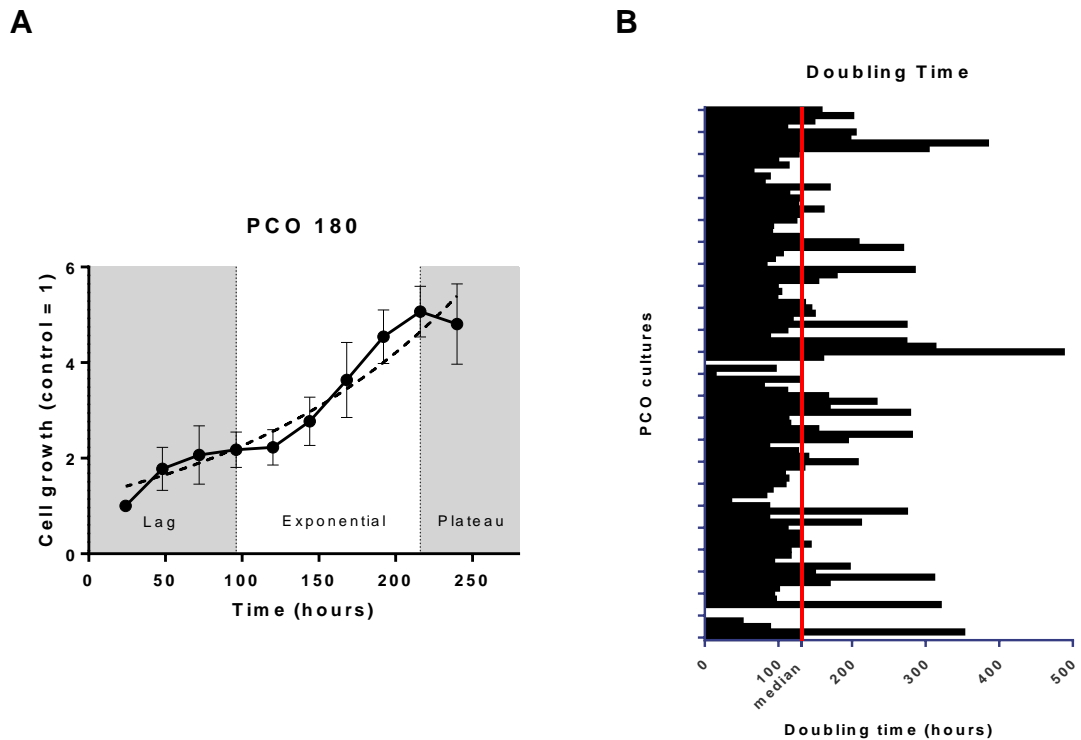


Figure 4.8 - 1: PCO growth. A: Growth curve for PCO 180 showing lag, exponential and plateau growth phases. B: Doubling time (hours) for all PCO cultures. Histogram of the doubling time for each PCO. Red line represents the median doubling time of all cultures. Briefly, cells were seeded at 500, 1000 and 2000 cells/well with six replicate wells for each cell concentration and were fixed at 24 hour intervals for 10 days with TCA. After washing cells were stained with 0.4% SRB solution. Protein-bound dye was dissolved in 10 mM Tris solution and optical density determination by spectrophotometry.

4.8.1. Growth and HR Status

The growth rate of PCO cultures, stratified according to homologous recombination (HR) status (see section 4.10 for full details on HR status), shows no significant difference in the mean DT of HR competent (HRC) and HR defective (HRD) cultures. The median DT of HRC cultures was 127.7 hours (range 35.0–486.7) $n=29$, in comparison to 135.0 hours (83.0–312.4), $n=21$, for HRD cultures, t test $p=0.7935$, Figure 4.8 - 2.

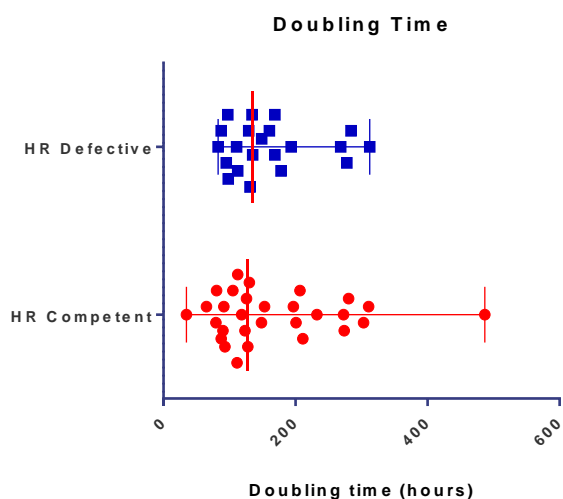


Figure 4.8 - 2: Growth rate PCO cultures by HR status results. Dot plot of doubling time (hours), determined by SRB proliferation assay, of PCO cultures stratified into HRC and HRD cultures. Median of group shown with red vertical line with corresponding range.

4.9. PCO-2 Cultures

PCO cultures are a limited resource. Most cultures senesce after five passages, indicating that the ovarian cancer stem cell population is unlikely to be present. 'PCO-2' is the monolayer cell culture formed from the aspirated media/ascites mix following initial seeding of the standard PCO culture. As the cells present in ascites are in suspension *in situ*, it was hypothesised that the stem cell population may in fact remain in suspension longer whilst other cellular populations attach to the plastic of the culture flasks. A subset of cultures with matched PCO and PCO-2 cultures (n=22) underwent antigen characterisation assessment and HR assessment to further explore this, Table 4.9 - 1, Table 4.9 - 2. PCO-2 experiments were conducted by myself and Aiste McCormick.

4.9.1. PCO vs. PCO-2 Antigen Characterisation

Concordance in the expression of markers between PCO and PCO-2 cultures was seen in 86.2% of cases, Table 4.9 - 1. Discordance in the remaining 13.8% was seen in the cell surface antigens (EpCAM, MOC31 and CA125). This may therefore represent loss of antigen detection due to the mechanical and biochemical effects of passage with trypsin, as discussed in Section 4.7.5.

Alternatively, the discrepancies may be a reflection of failed assays or genuine heterogeneity in expression between subpopulations of cells cultures.

When all PCO and all PCO-2 cultures were grouped together, no significant difference was seen in the detection of the epithelial or mesenchymal markers.

A statistically significant higher percentage of PCO cultures expressed CA125 in comparison to PCO-2 samples, $p=0.035$, Table 4.9 - 2.

PCO	CK		EpCAM		MOC31		CA125		D240		Vimentin	
	PCO	PCO-2	PCO	PCO-2	PCO-2	PCO-2	PCO	PCO-2	PCO	PCO-2	PCO	PCO-2
170	+	+	-		-		+	-	-		+	
171	+	+	-		-		+	+	-		+	
174	+	+	-		-		+	+	-		+	
175	+	+	-		+		+	P	-		+	
177	+	+	P	P	+		+	+	-		+	
180	+	+	-	-	-	+	+	+	-	-	+	+
182	+	+	+	P	+		+	+	-		+	
197	+	+	-	+	-		-	-	-	-	+	+
209	+	+	-	-	-	-	+	-	-	-	+	+
211	+	+	-	-	-	-	P	P	-	-	+	+
213	+	+	-	+	-	-	-	-	-	-	+	+
222	+	+	+	+	+	+	P	P	-	-	+	+
224	+	+	-	-	-	P	P	P	-	-	+	+
225	+	+	-	-	-	-	-	-	-	-	+	+
226	+	+	-	-	+	-	-	P	-	-	+	+
227	+	+	-	-	-	+	P	-	-	-	+	+
229	+	+	-	-	-	-	-	-	-	-	+	+
230	+	+	-	-	-	-	-	P	-	-	+	+
233	+	+	-	-	-	-	-	-	-	-	+	+
234	+	+	+	-	-	-	-	-	-	-	+	+
238	+	-	+	-	-	-	P	P	-	-	+	+
239	+	+	-	-	-	-	-	-	-	-	+	+

Table 4.9 - 1: Immunofluorescent antigen characterisation of matched PCO and PCO-2 cultures. Antigen detection was assessed using fixed immunofluorescence as positive (+), negative (-), or patchy in comparison to positive and negative cell line reference images.. Grey denotes discordance between matched samples.

Antigen			PCO Expression n (%)	PCO-2 Expression n (%)	Chi ² p
Epithelial	CK	n=83	61/61 (100)	22/22 (100)	-
	EpCAM	n=59	13/51 (25.5)	6/18 (33.3)	0.2935
	MOC31	n=60	14/45 (31.1)	5/15 (33.3)	0.8026
Ovarian	CA125	n=76	39/55 (70.9)	10/21 (47.6)	0.0350 *
Germ cell	D240	n=62	0/46 (0)	0/16 (0)	-
Mesenchymal	Vimentin	n=63	47/47 (100)	16/16 (100)	-

Table 4.9 - 2: Summary of antigen expression of PCO and PCO-2 cultures.

4.9.2. PCO vs. PCO-2 Growth

Although PCO-2 took longer to establish from time of collection in comparison to standard PCO cultures of ascites from the same patient, there was no significant difference in SRB determined doubling time (DT) between PCO and PCO-2 cultures, one-way ANOVA p=0.9812,

Figure 4.9 - 1.

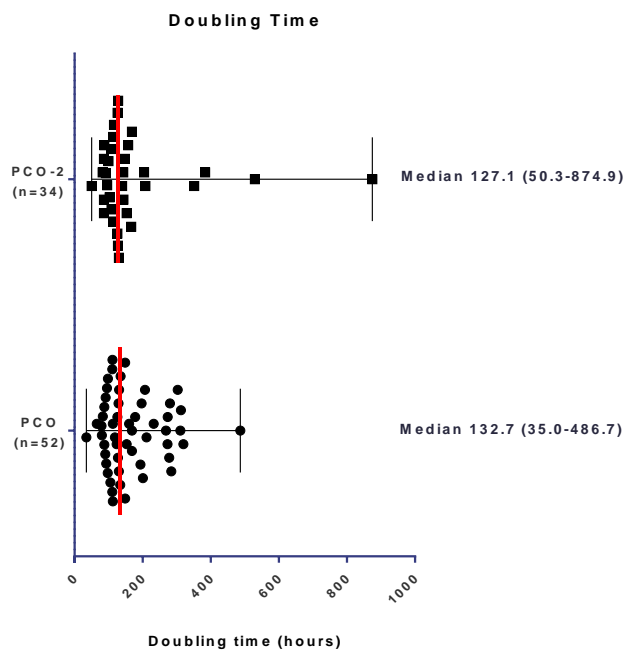


Figure 4.9 - 1: Doubling time for PCO vs. PCO-2 cultures. Cells were seeded at 1000 cells/well and fixed at 24 hour intervals for 10 days. Cell proliferation was determined by SRB assay and doubling time (DT) calculated. Median DT is shown with the red line, with corresponding range.

4.9.3. PCO vs. PCO-2 HR Status

No significant differences were detected in the phenotype of the PCO vs. PCO-2 populations. A number of PCO-2 samples were assessed for HR function alongside their paired PCO, Table 4.9 - 3.

PCO	HR Status PCO	HR Status PCO-2
229	HRC	HRD
230	HRC	HRD
233	HRC	HRD
234	HRC	HRD
238	HRD	HRD
239	HRC	HRD

Table 4.9 - 3: Functional HR status (determined by Rad51 foci assay) of paired PCO and PCO-2 cultures. Discordance between PCO and their corresponding PCO-2 cultures is seen in 5/6 patient samples.

Considerable discordance is seen between PCO and PCO-2 cultures with 5/6 patient samples showing HRC in their PCO culture but HRD being shown in the corresponding PCO-2 culture. This may reflect genuine heterogeneity between different cell populations. However, in this small cohort, all PCO-2 cultures were HRD. There are two possible explanations. Firstly, the group of cells that remain in suspension for longer (PCO-2) represent a genuine different subpopulation to PCO cells, which differ in their ability to repair DNA damage. Alternatively, as the PCO-2 cells remain in suspension for longer with fewer media changes, the cells may undergo senescence and therefore are unable to fully repair DSB, reflecting their dying status rather than a genuine pathway dysfunction.

4.10. Homologous Recombination DNA Repair Status of PCO Cultures

These studies were conducted by myself and Michelle Dixon. In total, 56 PCO cultures have been classified according to HR functional status. In all 56 cultures, DNA DSB damage was confirmed by a greater than 2 fold increase in γ H2AX. Of the 56 cultures, 34 (60.7%) had a greater than 2 fold increase in Rad51 foci formation and were therefore classified as HR competent (HRC) and 22 (39.3%) were HR defective (HRD), Figure 4.10 - 1. This predominance of HRC tumours may be a reflection of the cohort tested, with 22 (36.6%) being sampled following administration of chemotherapy (15/22 HRC, 7/22 HRD).

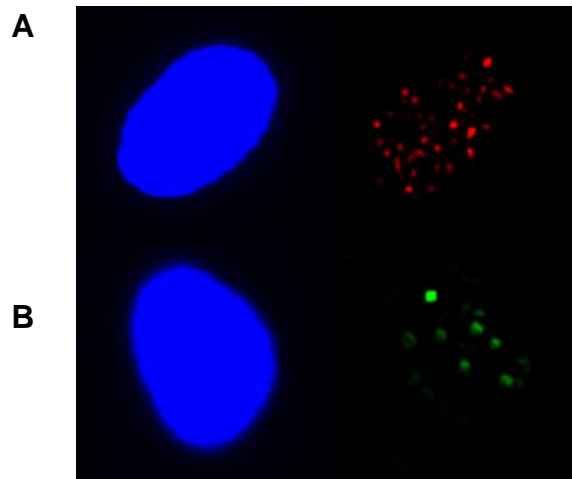


Figure 4.10 - 1: HR assay. Immunofluorescence detection of nuclear γ H2AX (A) and Rad51 (B) in PCO 164. DAPI nuclear stain is used to make a nuclear mask enabling quantification of intra-nuclear foci using ImageJ technology.

When subdivided according to histological subtype, there were in general, no significant differences in the proportion of each subtype being HRC, Table 4.10 - 1. The predominance of HRC tumours within the 'mixed/other' group should be interpreted with care, owing to the small number within this group and the mix of actual histologies included. This group included 3 mixed endometrioid/clear cell (2 HRC), 1 HGSC/clear cell (HRC), 2 low grade serous carcinomas (1 HRC), 1 ovarian carcinosarcoma (HRC) and 1 enteric type mucinous tumour arising from within a teratoma (HRC).

Histological Subtype		HRC n (%)	HRD n (%)
HGSC	n=43	24 (54.5)	20 (45.5)
Mucinous	n=2	1 (50.0)	1 (50.0)
Clear cell	n=2	2 (100)	0 (0)
Endometrioid	n=1	1 (100)	0 (0)
Mixed / Other ovarian	n=8	6 (75.0)	2 (25.0)
All	n=56	34 (60.7)	22 (39.3)

Table 4.10 - 1: Functional HR status of PCO cultures by histological subtype. HR status was determined by quantification of nuclear Rad51 foci following induction of DNA DSB with 2 Gy irradiation and incubation with 10 μ M rucaparib. HRC was defined as more than a 2 fold increase in Rad51 foci formation, in comparison to untreated controls.

4.11. Sensitivity to Cytotoxic Agents

Numerous established assays exist for sensitivity testing of cytotoxic agents. Colony formation studies are considered the gold standard but rely upon the ability of the culture to form discrete, quantifiable colonies. However, PCO cultures do not proliferate well at low density and fail to form countable colonies precluding this assay. Several assays were tested as alternatives, including the cell proliferation assays SRB and WST-1; as well as cell counting, using a panel of cell lines before adopting SRB as the preferred single method for PCO assessment.

Discrepancies in results from sensitivity assays using different techniques are well described. The Cancer Cell Line Encyclopaedia (CCLE) (Barretina 2012) and Cancer Genome Project (CGP) (Garnett 2012) provide gene-expression profiles and drug-sensitivity assays with 471 overlapping cell lines. Analysis shows low correlation between the two data sets (Weinstein 2013). The gene-expression profiles showed good concordance, whereas the sensitivity to agents did not, which is likely to reflect the two different readouts (cellular ATP vs. dehydrogenase activity) of cytotoxicity used.

4.11.1. Selection of Methodology: SRB vs. WST-1 vs. Colony Formation vs. Cell Counting

A series of experiments comparing the selected assays were conducted in two sets of cell lines (VC8, VC8 BRCA2, VC8 PIR; UWB1-289, UWB1-289 BRCA1), paired for BRCA mutation with WT, (see section 6.5.1 for full experimental details) and in PCO samples, Figure 4.11 - 1. SRB assay determines cell density based upon the measurement of cellular protein, with a directly proportional relationship between protein measurement and cell mass (Vichai 2006). WST-1 is a tetrazolium salt that is reduced to a coloured formazan by the action of mitochondrial dehydrogenase activity, which is proportional to cell number (Berridge 2005), see Chapter 3 for details of assay protocols.

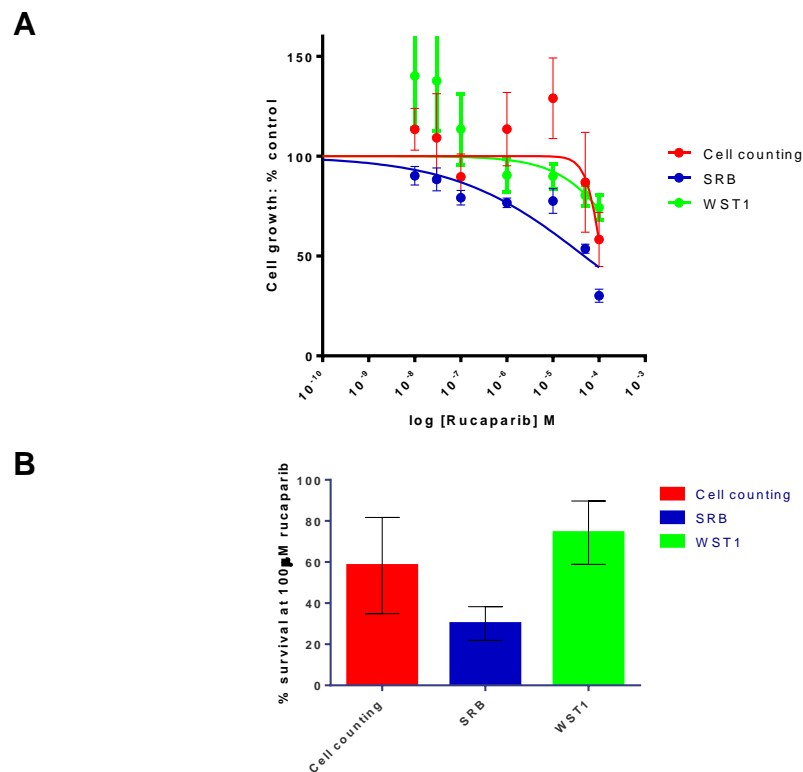


Figure 4.11 - 1: Comparison of growth inhibition by rucaparib using SRB, WST-1 proliferation assays and cell counting in PCO 170. PCO 170 cells were treated with rucaparib at various concentrations, as indicated, for 10 days and cell number estimated by SRB or WST-1 assays or cell counting. Data are the mean values if 6 repeats, error bars represent SD.

Review of the comparative assessments of the proliferation assays (SRB and WST-1) with cytotoxicity assays (colony formation), using cell lines paired for BRCA mutation with WT (VC8/VC8-BRCA2/VC8-PIR, UWB1-289/UWB1-289-BRCA1) and PCO samples, confirmed that a single methodology was essential in order to ensure results obtained from sequentially acquired PCO samples were directly comparable. SRB was selected as the methodology of choice due to its simplicity, reproducibility and concordance with colony formation assays, Table 4.11 - 1. Good correlation was observed between SRB and colony formation assays, $r = 0.9856$ ($p=0.0021$). Correlation between WST-1 and colony formation assay was poor, Pearsons correlation $r = -0.0729$ ($p = 0.9072$).

Cell Line	GI ₅₀ μ M SRB	GI ₅₀ μ M WST-1	LC ₅₀ μ M Colony formation
	Mean (SD)		
VC8	9.5 (1.7)	0.0003 (0.000006)	0.6 (0.3)
VC8 BR2	907.3 (150.1)	67.2 (77.2)	384.4 (143.5)
VC8 PIR	8.5 (1.5)	143.7 (246.3)	11.8 (4.9)
UWB1-289	0.2 (0.3)	0.4 (0.3)	0.5 (0.1)
UWB1-289 BR1	8.2 (0.7)	2429 (4194)	68.9 (9.5)

Table 4.11 - 1: Comparing cytotoxicity to rucaparib in a cell line panel by colony formation assay and proliferation assays. Colony formation: cells were treated with cytotoxic agent at various concentrations, as indicated, for 24 hours and survival was determined with colony formation assay. Data are the mean values (SD) from three independent experiments, with triplicate values for each concentration (colony formation) and six replicates for SRB and WST-1 assays.

4.11.2. SRB Assay to Evaluate Effect of Cytotoxic Agents on PCO Cultures

Having optimised the methodology for assessment of cytotoxicity, the sensitivity of each PCO culture to rucaparib and cisplatin was determined using SRB proliferation assays and correlated with HR functional status, Figure 4.11 - 2, Figure 4.11 - 3. It was not feasible to determine the doubling time (DT) of each PCO prior to SRB assay due to their limited life span. The median DT for PCO was 132 hours and a standard incubation time of 10 days was adopted. Concentration-response curves were generated but in many cases it was not possible to accurately calculate a GI₅₀ because of insufficient suppression of

growth at the highest concentrations used. For this reason, data are given as % control cell growth at a single drug concentration.

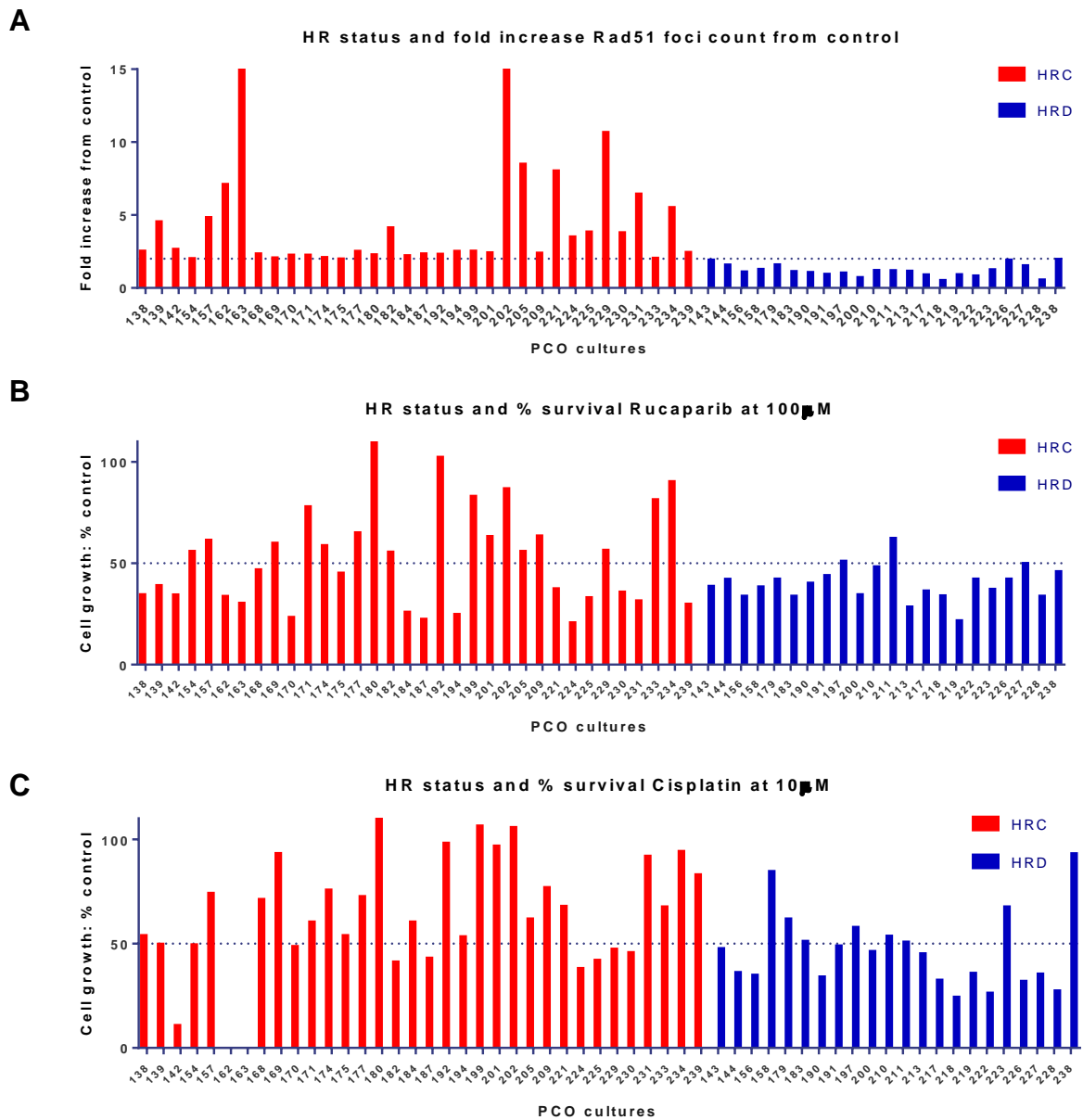
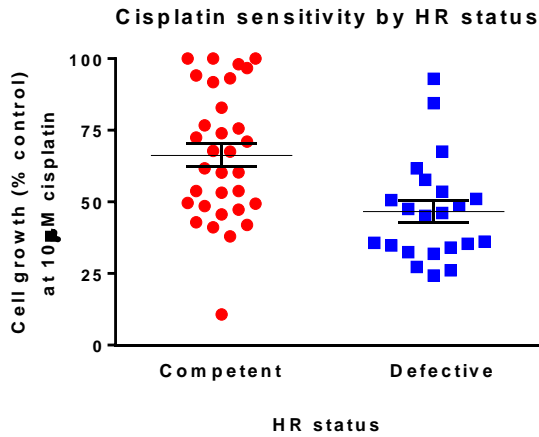
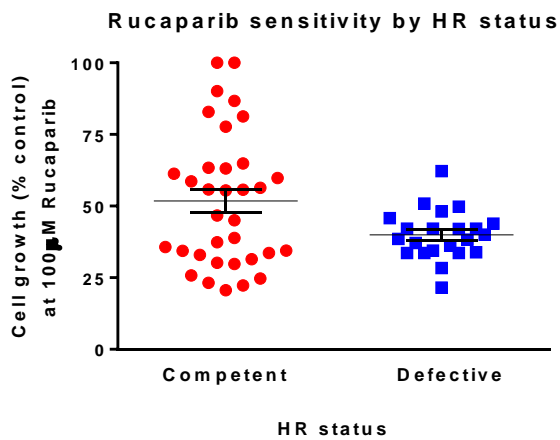


Figure 4.11 - 2: Rad51 foci count and growth inhibition by rucaparib and cisplatin. Each PCO underwent the HR Rad51 assay to characterise cultures into HRC (60.7%) and HRD (39.3%) categories. Briefly, cells were treated with 2 Gy irradiation and 10 μ M rucaparib before quantifying nuclear γ H2AX and Rad51. Results are expressed as fold change from equivalent counts in untreated controls. Each culture was also treated with rucaparib (B) or cisplatin (C) at various concentrations for 10 days before determining growth inhibition by SRB assay. Results are expressed as % survival at 100 μ M rucaparib or 10 μ M cisplatin, compared to untreated controls. Red bars = HR competent, Blue bars = HR defective cultures. See Appendix 6 for detailed patient demographics and assay outcomes.



HR	Mean % survival	SEM
HRC n=32	66.9	4.2
HRD n=22	46.6	3.8
p (t-test)	0.0014 *	



HR	Mean % survival	SEM
HRC n=32	52.3	4.2
HRD n=22	39.9	1.8
p (t-test)	0.0275 *	

Figure 4.11 - 3: Sensitivity to cisplatin and rucaparib stratified by HR status. Data from Figure 4.11 - 2 using SRB cell proliferation assay were grouped into HRC and HRD cultures and analysed for significance. T-test was used to compare the mean % survival at a given concentration of cytotoxic agent (see Y axis) between the HRD and HRC groupings.

4.11.3. Sensitivity to Rucaparib and Cisplatin by HR Status

When grouping all cultures into their functional HR groups, there are statistically significant differences between the mean GI₅₀ and percentage survival of drug of each group, Table 4.11 - 2, Figure 4.11 - 4, suggesting HR stratification to reliably predict sensitivity.

However, assessing the response in each individual patient reveals large overlap of responses within the two groups. HRD cultures can be resistant to both rucaparib and cisplatin, whilst HRC cultures can be sensitive to one or both agents. 2/22 (9.1%) HRD PCOs have more than 50% cell survival at 100 µM of rucaparib indicating resistance. 17/34 (50%) HRC PCOs are sensitive to rucaparib with less than 50% cell survival at 100 µM rucaparib. The PPV and NPV for HR function in the prediction of sensitivity to rucaparib was 91.7% and 36.4%. PPV and NPV for cisplatin sensitivity was 73.0% and 27.8%.

	HRC n=34	HRD n=22	t test p
Rucaparib			
Mean % survival at 100 µM rucaparib (SEM)	52.3 (4.2)	39.9 (1.8)	0.0275 *
Mean GI ₅₀ (SEM)	69.0 (6.8)	35.1 (7.4)	0.0017 *
Cisplatin			
Mean % survival at 10 µM cisplatin (SEM)	66.9 (4.2)	46.6 (3.8)	0.0014 *
Mean GI ₅₀ (SEM)	9.2 (0.3)	5.5 (0.8)	0.0001 *

Table 4.11 - 2: Comparison of growth inhibition, determined by SRB assay, by rucaparib and cisplatin stratified by HR functional status. Briefly, PCO cell cultures were seeded at density of 1000 cells/well, with six replicates per condition, and exposed to increasing concentrations of rucaparib or cisplatin for 10 days, corrected for 1% DMSO. After fixation with TCA, bound protein was quantified using 0.4% SRB solution by spectrophotometry.

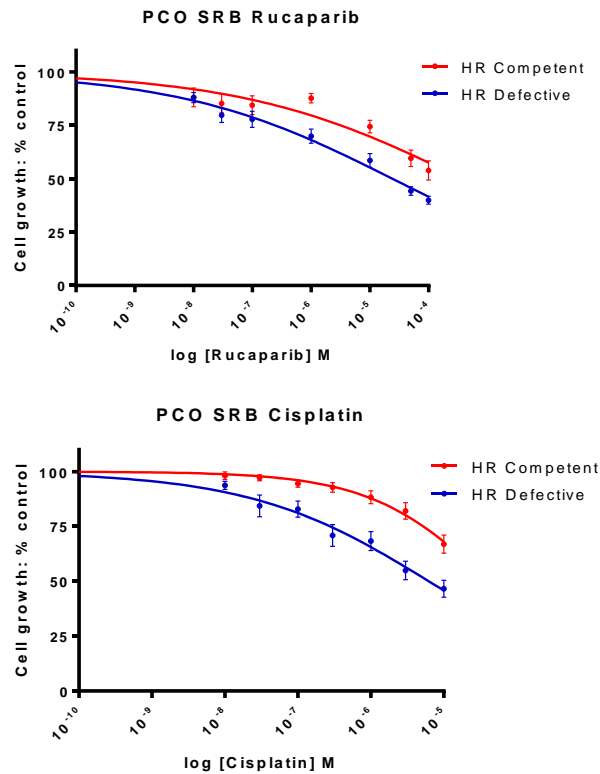


Figure 4.11 - 4: Growth inhibition by rucaparib (A) and cisplatin (B) in PCO cultures by HR functional status. Cells were treated with rucaparib or cisplatin at various concentrations, as indicated for 10 days and cell proliferation determined by SRB assay. Results are the mean of 6 repeats at each concentration. Error bars represent SD.

4.11.4. Sensitivity Rucaparib vs. Cisplatin

Work in this thesis adds to a small published dataset (Mukhopadhyay 2010, Mukhopadhyay 2012) demonstrating that HRD PCOs are more sensitive to rucaparib *ex vivo* in comparison to HRC cultures. This study confirms published data and additionally, has extended cytotoxic assessment to cisplatin *ex vivo*. In this dataset 16/54 (29.6%) PCOs were resistant to both rucaparib and cisplatin, Figure 4.11 - 5. 13/16 (81.3%) of these cultures were HRC. Of the 21 cultures sensitive to both agents, 18/21 (85.7%) were HRD, Fishers exact test, $p < 0.0001$.

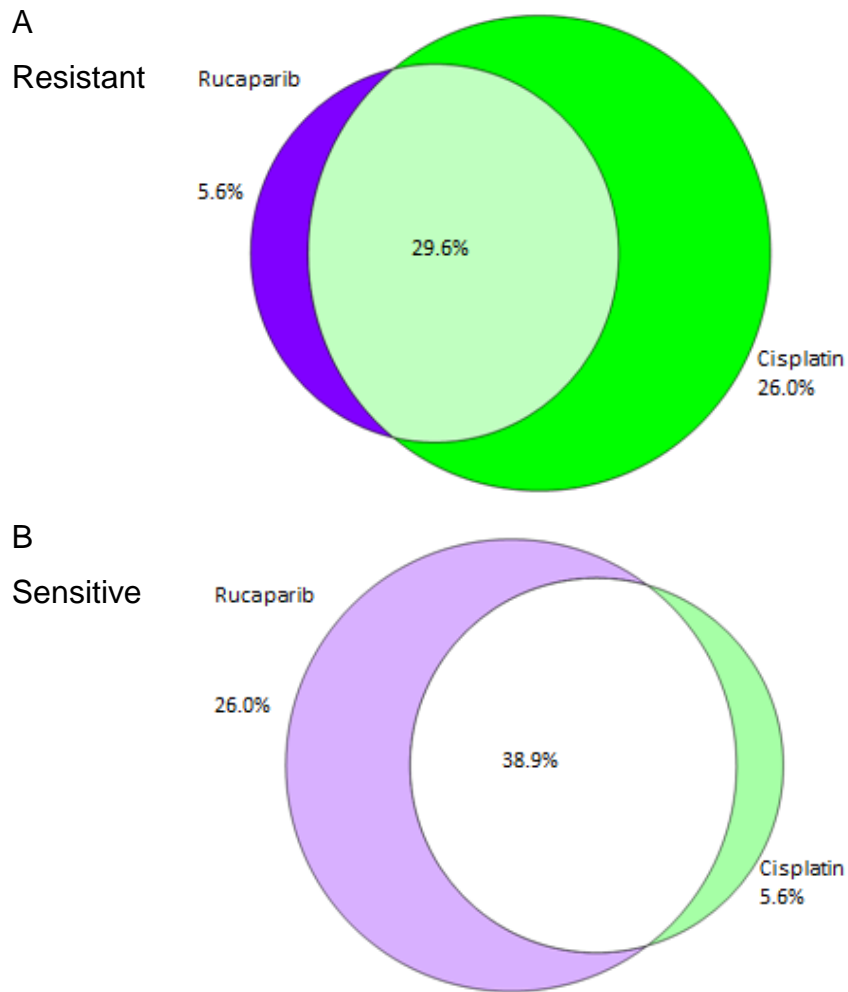


Figure 4.11 - 5: Resistance to rucaparib and cisplatin. The percentage of PCO cultures resistant to rucaparib and/or cisplatin is shown numerically within Venn diagram (A) and the percentage of PCO cultures sensitive to rucaparib and/or cisplatin are shown Venn diagram (B).

4.12. Clinical Application of HR Assay

The HR assay is currently complex, lengthy and user dependent. Simplification of the assay protocol may also facilitate its application into clinical trials and routine clinical practice. Additionally, although cultures are typically developed within 14 days from collection, further analysis for the Rad51 assay with concurrent testing for sensitivity to cytotoxic agents using SRB assays can take a further 14 days. This leaves a very small window for experiments before planning chemotherapy. Alternative methodologies were explored in an attempt to reduce the time taken from sample collection until assignment of HR status.

4.12.1. Cytocentrifugation and Coverslip Culture

These studies were conducted with Anna Grundy and Laura Woodhouse (MRes 2012).

In parallel to standard PCO culture, nine ascitic samples were 1) cytospun directly onto coverslips and 2) cultured directly onto coverslips. Each PCO culture, cytospun and coverslip culture sample underwent characterisation (morphology assessment and immunofluorescent assessment of CK and CA125), as well as assessment of the feasibility of performing HR assays, see section 3.4.2 for assay details.

Characterisation

Cytocentrifugation: Contamination of slides with cellular debris and frequent cellular damage prevented accurate assessment of characterisation antigens. Assessment was possible in only 5/9 of the PCO tested. Concordance with parallel conventional IF characterisation was poor, with discordance in 90% of cases.

Coverslip Culture: The morphological appearance of cells cultured on coverslips was similar to parallel flask cultures. Characterisation of coverslip cultures showed 100% staining for CK and CA125. Concordance with parallel conventional IF characterisation was high with agreement in 80%. Discordance was seen, with loss of CA125 membrane antigen expression, in 2 cultures at

passage 1 (following passage with trypsin), Table 4.12 - 1. It is possible this represents chemical/mechanical loss of the cell surface antigen, as previously described, section 4.7.5.

PCO		PCO Conventional Culture	Coverslip Culture	Cytospun
162	CK	+	+	-
	CA125	+	+	-
163	CK	+	+	-
	CA125	+	+	+
164	CK	+	+	-
	CA125	-	+	Patchy
167	CK	+	+	-
	CA125	-	+	Patchy
168	CK	+	+	-
	CA125	+	+	Patchy

Table 4.12 - 1: PCO culture antigen characterisation. Characterisation of cultures, using three culture techniques, from five PCO patients were compared for expression of CK and CA125. Conventional culture: a 50:50 (v:v) ascites: media mix was cultured in T75 flasks. Cells were trypsinised and replated prior for antigen characterisation at passage 1. Coverslip culture: a 50:50 ascites: media mix was cultured directly onto sterilised glass coverslips. Cytospinning: Fresh ascites was cytopun directly onto glass coverslips for immediate characterisation, without culture.

Homologous Recombination Repair Assay

Cyto centrifugation: Nuclear γ H2AX foci were visible but Rad51 detection was poor and fold increase in γ H2AX foci inadequate. HR status could not be determined.

Coverslip Cultures: The HR assay was successfully performed on 5/5 cultures with 100% concordance with parallel traditional HR assays, Figure 4.12 - 1. However, the γ H2AX and Rad51 fold increase was typically much lower. This may be a reflection of the earlier passage at which the HR assay was performed or that the cells had failed to replicate.

HR assay: Standard culture vs coverslip culture

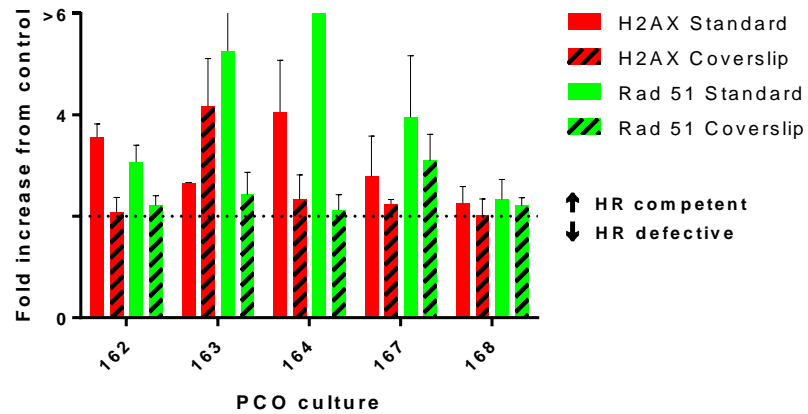


Figure 4.12 - 1: PCO HR status: comparison of HR results following traditional culture technique vs. direct culture onto coverslips. Rad51 fold increase in 5 PCOs comparing standard technique with and coverslip cultures (+/- SEM). 100% concordance between functional status was seen.

Time for Assay Result

Culturing directly onto coverslips reduced the time taken to determine the HR status from a mean of 11.6 days (SD 2.5) to 5.3 (1.6) days.

4.12.2. PARP Activity as a Surrogate Assay for HR Function

These assays were performed with Dr Miranda Patterson and James Murray. Although PCO cultures provide an exceptionally useful model for the study of cancer cell biology, it may be favourable to generate a more clinically applicable HR assay. A single surrogate marker for HR function would reduce the need for complex multistep assays requiring live cultured tissues.

Poly (ADP-ribose) (PAR) polymerase 1 (PARP1) is activated (forming PAR) by DNA SSB, DSB and stalled replication forks to facilitate DNA repair within several pathways including BER, NHEJ and HR. PARP is expressed variably in all nucleated human cells excluding neutrophils (Schreiber 2002) with variable expression between tissues. Pilot studies measuring PARP-1 activity in PBMCs from healthy volunteers and metastatic melanoma patients before and during temozolomide therapy and in tumour biopsies revealed large inter-individual

differences in PARP activity in both healthy volunteers and cancer patients (Plummer 2005).

PARP-1 has been shown to be hyperactivated in BRCA2-defective cells and additionally PARP activity has been shown to revert to near normal levels in PARPi-resistant BRCA2-defective cells (Gottipati 2010). On the basis of this and other clinical studies PARP activity assay has been proposed as a surrogate marker for HRD (Plummer 2005, Zaremba 2009). PARP activity was assessed in PCO cell pellets, already characterized by HR status with sensitivity data to both rucaparib and cisplatin. 24 cryofrozen PCO samples were assessed for stimulated PARP activity (9 HRD, 15 HRC).

HRD PCO cultures had significantly less PARP activity than HRC cultures, with a mean PAR formation of 24.0 (SEM 3.6) pmol/10⁶ cells and 41.9 (4.8) respectively, Mann Whitney test $p = 0.0248$, Figure 4.12 - 2. The ability of the PAR level detected to predict sensitivity to rucaparib and cisplatin was explored using correlation of PAR level with % survival at 10 μ M cisplatin and 100 μ M rucaparib, Figure 4.12 - 3, but no significant relationship was detected.

HR and PARP are both involved in the repair of DNA strand breaks and replication lesions and may act in a complementary fashion, so that if one pathway is lost, the other needs to be upregulated to compensate for the loss. However, in the study by Gottipati *et al.* (2010), increased PARP activity found in HR defective cells was not explained by accumulation of DNA lesions known to trigger PARP activity (i.e., DNA strand breaks or damaged replication forks). PARP is involved in multiple DNA repair pathways and the low PARP activity seen in the group of HRD tumours in this study may actually reflect alternative dysfunctional pathways. Interpretation of PARP activity in a larger group of samples characterised for other pathway function may clarify this relationship. PARP activity therefore serves as a poor biomarker for predicting sensitivity to cytotoxic agents. It is known that PARP-1 and PARP-2 expression varies widely across all nucleated human cells excluding neutrophils (Schreiber 2002, Csete 2009). Large inter-individual differences in PARP activity has also been reported in healthy volunteer and cancer patients before and during therapy. This may at least in part explain the variable levels in this study.

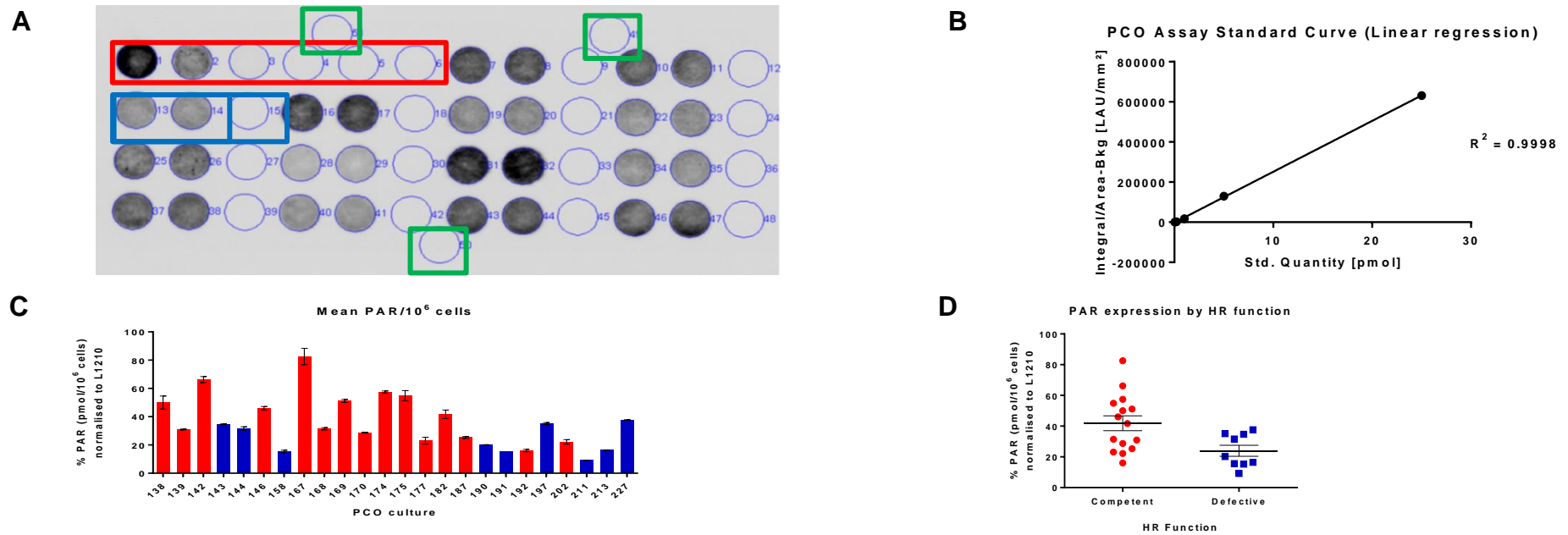


Figure 4.12 - 2: Stimulated PARP activity in PCO. PAR is quantified following maximal stimulation of permeabilised cells during a 6-minute reaction with excess NAD⁺ and oligonucleotides. Cells are blotted on to an immunoblot membrane and treated with anti-PAR primary antibody followed by secondary antibody conjugated with HRP. A chemiluminescence agent is added and PARP activity is expressed as 'luminescent arbitrary units'. A: Immunoblot; Dots 1-6 (red) show results for 25, 10, 5, 1, 0.2, 0 pmol PAR standards. PCO duplicates (blue), alongside corresponding unreacted samples. Dots 49, 50, 51 (green) show background blank measurements. B: A standard curve constructed by non-linear regression of PAR standard values and the resulting equation relating PAR to chemiluminescence ($R^2 \geq 0.9$) used to calculate the amount PAR present in each well.; C: Results expressed as picomoles of ADP-ribose monomer incorporated per 10⁶ permeabilised cells and PAR activity in stimulated cells expressed as the percentage mean (SD) PAR pmol/10⁶ cells of activity in untreated control cells. HRC (red), HRD (blue) D: PARP activity stratified by HR function demonstrating association between HRC and high PAR activity.

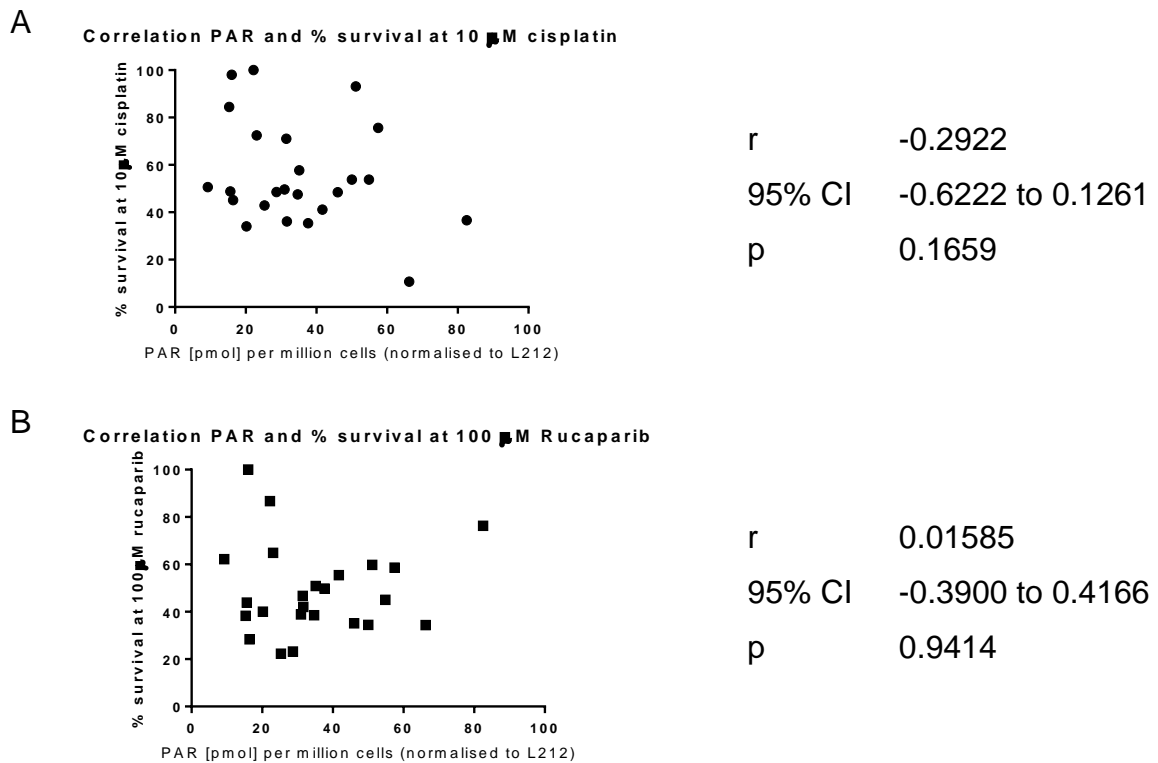


Figure 4.12 - 3: Correlation of PAR level and % survival 10 μ M cisplatin (A) and 100 μ M rucaparib (B).

4.12.3. HR Gene Expression as a Surrogate for HR Function

DNA micro-arrays have become an established tool to study gene expression patterns in ovarian cancers for both diagnostic and prognostic markers (Hibbs 2004, Spentzos 2004). This approach carries the advantage of high throughput analysis and also the use of RNA which can be extracted easily from clinical material including FFPE tissues.

Gene expression profiling using FFPE samples comparing (Jazaeri 2002) profiles from *BRCA1/2* mutated cancers with sporadic EOC showed a *BRCA*-like profile in many of the sporadic EOC (named *BRCA* linked). In another micro-array dataset which included 61 patients with EOCs (sporadic/ *BRCA* mutant) Konstantinopoulos *et al.* (2010) developed a *BRCA-like* profile. The *BRCAness* profile in sporadic EOC was shown to correlate with responsiveness to platinum and PARP inhibitors (in cell lines) and was predictive of a subset of sporadic EOCs with improved outcome. Additionally, Pennington *et al* (2014)

have demonstrated that 31% of 390 ovarian cancers tested had at least one loss-of-function germline or somatic homologous recombination mutation and that this correlated with *in vivo* platinum sensitivity and overall survival. The ongoing ARIEL 2, a phase 2 trial of rucaparib therapy for women with relapsed HGSC or endometrioid ovarian cancer, aims to identify a molecular signature of HRD and this will be evaluated further in ARIEL 2 (NCT01891344) and in ARIEL 3 (NCT01968213) which aims to assess rucaparib as maintenance therapy. Abkevich *et al* studied the association between HR defected and genomic patterns of loss of heterozygosity (LOH) and found that an HRD score (defined as the number of regions within HR pathway components where LOH had occurred) was capable of detecting HR defects regardless of aetiology or mechanism (Abkevich 2012).

In order to identify potential biomarkers of the HR pathway, which would be suitable for clinical use, RNA expression of key components of the pathway were examined and correlated with HR function. Using RNA extracted from the PCO ascitic cultures characterised for HR function (Rad51 assay) and assessed for sensitivity to rucaparib and cisplatin, the relative expression of genes involved in DNA DSB repair was determined by the Oxford genomics centre (Oxford, UK) using Illumina Genome Studio and HumanHT 12v4.0 R1 15002873 array, as per manufacturer's instructions, see Chapter 3. 24 PCO samples, 14 of which were HRC and 10 of which were HRD were tested. All patients had RNA extracted from the same ascitic fluid primary culture as used in the Rad51 assay and PARP inhibitor cytotoxicity assay. The relative expression of each component of the HR DNA repair pathway was calculated and differences between the HRD and HRC group expression calculated.

Stratification by HR function

The 10 HRD samples were compared as a group with 14 HRC samples to study whether a panel of genes could be identified to differentiate the two groups, Figure 4.12 - 4. More than 47000 probes were used to assess fold change in

expression and each PCO sample appeared to be dysregulated in some component of the HR pathway. 14 key components of the HR pathway were assessed and compared between the two functional groups with significance detected in three components with 2 components upregulated (ATM, MRE11) and one down regulated (Rad51) in the HRC group in comparison to HRD. Statistical significance was seen between the expression of ATM, MRE11 and Rad51 in HRC compared to HRD groups, Figure 4.12 - 5. ATM, which is involved in several DNA repair pathways and in the detection of DSB, is significantly upregulated in HRC in comparison to HRD. MRE11 forms part of the MRN complex, which is involved in the detection and binding of DSB and it may therefore be that cells are HRD because they cannot identify, bind and initiate the HR pathway as efficiently as HRC cultures. Interestingly, significantly higher Rad51 expression was seen in HRD cultures in comparison to HRC cultures although I had hypothesised that Rad51 may be higher in HRC cultures. The HR assay is not based upon absolute levels of Rad51 to determine functional status but a change in level in response to DNA damage. This higher baseline level in the RNA sampled may therefore represent dysfunctional Rad51 present in the nucleus but not the functional Rad51 needed for HR.

Although no correlation between RNA expression of these markers with sensitivity to rucaparib or cisplatin was seen, further evaluation of these components for use as a surrogate biomarker for HR status is required. BRCA2 was down regulated in 6/10 HRD samples and 6/14 HRC samples, but not to a statistically significant degree. BRCA1 was upregulated in 5/10 HRD and 6/14 HRC samples with copy fold changes in excess of 200 universally across the three probes used.

Future work will aim to explore unsupervised hierarchical clustering upon an expanded panel of samples.

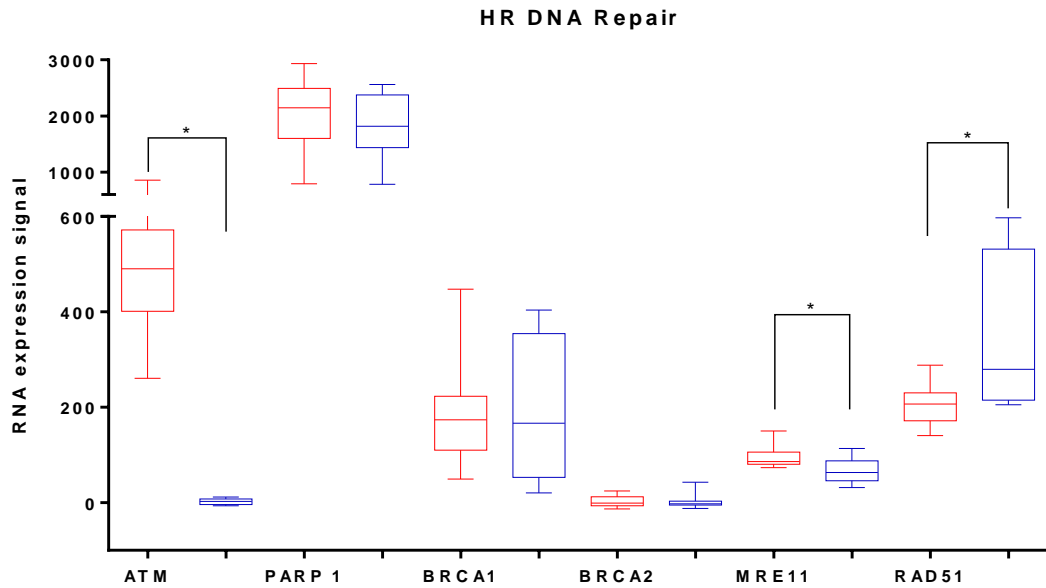


Figure 4.12 - 5: RNA expression of key components of the HR DNA repair pathway in PCO grouped by HR status, $n=24$. The mean and SD are plotted with HRC cultures shown in red and HRD shown in blue.

PARP1 mRNA as a Surrogate for HRD

There was no statistically significant difference in PARP1 mRNA levels between the HRC and HRD groups tested with only a modest increase in the HRC group. This trend was however consistent with the PARP activity, section 4.12.2. In this group of samples however, there was a significant correlation between PARP1 expression and sensitivity to rucaparib, $r^2=0.2213$, $p=0.0102$, Figure 4.12 - 6.

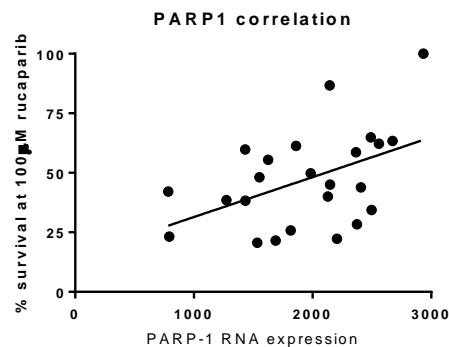


Figure 4.12 - 6: Correlation between PARP-1 RNA expression and sensitivity to rucaparib (% survival at 100 μ M).

4.13. Alternative HR analysis

A cut-off of a 2-fold increase in Rad51 foci in comparison to control was assigned during development of the HR assay based upon Rad51 counts in cell lines with known HR function (Mukhopadhyay 2010, Drew 2011). This cut off enabled reliable discrimination between PCOs that were sensitive or resistant to rucaparib. The actual focus count as well as the fold increase from control was highly variable, Figure 4.13 - 1, and in order to explore if simplification of the HR assay may be possible, the ability of isolated foci counts to predict HR function was assessed.

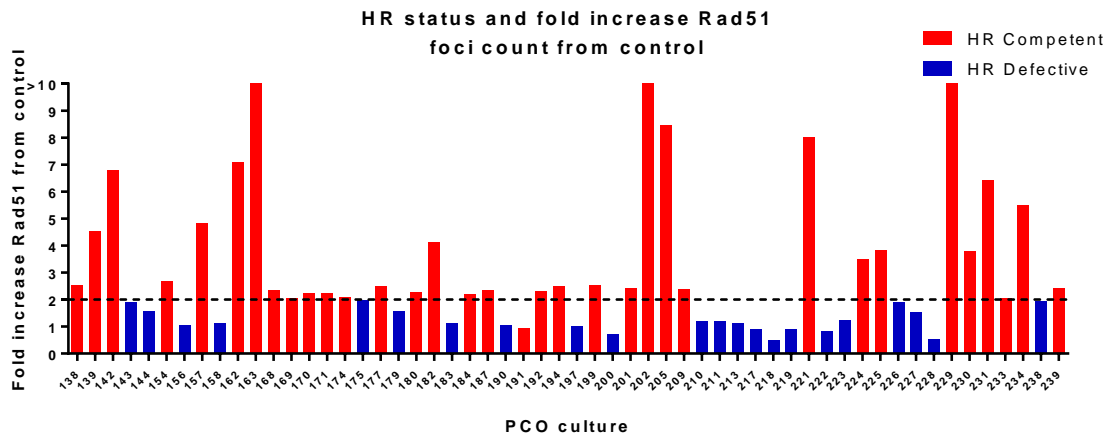


Figure 4.13 - 1: Fold increase in Rad51 focus formation from control with subsequent HR classification. DNA DSB induction and repair following 2 Gy IR and 24 hour exposure to rucaparib in PCO cultures. A 2-fold increase in γ H2AX foci from baseline (not shown) indicated induction of DNA DSB. A 2-fold or greater increase in quantification of Rad51 nuclear foci following DNA DSB compared to untreated controls indicated functional HR competence (red bars). Less than 2-fold increase indicated defective HR function (blue bars). Data are expressed as the percentage of untreated control.

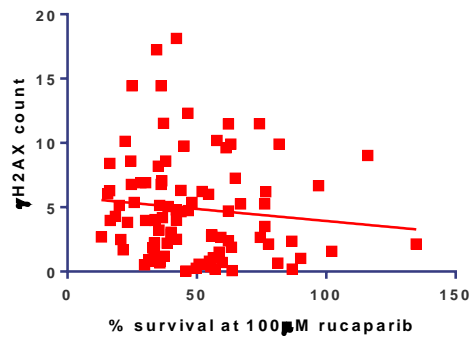
4.13.1. Correlation of Focus Count With Rucaparib Sensitivity

Although using HR status to stratify patients into two groups will enrich the population of patients who will respond to platinum or rucaparib, this approach may still result in a proportion of patients who will undergo treatment from which they will not benefit and a proportion of patients who may not be given treatment who would have responded. One possible reason for this may be incorrect assignment to the functional groups. It is unclear if there is a relationship between the actual foci count and sensitivity to cytotoxic agents and correlation between Rad51 foci counts with percentage survival at 100 μ M rucaparib/10 μ M cisplatin was assessed. The correlation between mean Rad51 focus count of control, after induction of DNA damage following IR and rucaparib, and fold increase with the % survival to rucaparib was calculated, Figure 4.13 – 2. There was a statistically significant positive correlation between the mean Rad51 focus count following induction of DNA damage (IR and rucaparib) and percentage survival at 100 μ M rucaparib. A positive correlation between higher fold increase in Rad51 foci formation with higher percentage survival at 100 μ M rucaparib. This reinforces the relationship between quantification of Rad51 foci indicating HR pathway function and its association with resistance to rucaparib.

4.13.2. Correlation of Focus Count With Cisplatin Sensitivity

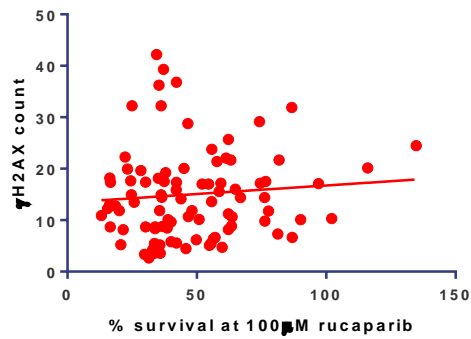
The same analysis was repeated with percentage survival at 10 μ M cisplatin, Figure 4.13 - 3. Similar results were obtained demonstrating that there is a positive correlation between Rad51 count, (following DSB and fold increase) with percentage survival at 10 μ M cisplatin. As above, there is a negative relationship between Rad51 focus count at baseline and percentage survival.

Rucaparib % survival at 100 μ M vs γ H2AX count (control)



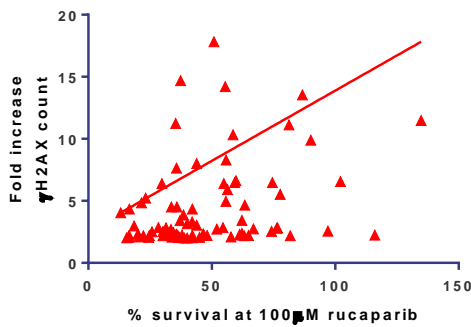
$r = -0.110$
 $95\% \text{ CI} = -0.307 \text{ to } 0.096$
 $p = 0.293$

Rucaparib % survival at 100 μ M vs γ H2AX count after IR and rucaparib



$r = 0.0822$
 $95\% \text{ CI} = -0.124 \text{ to } 0.281$
 $p = 0.433$

Rucaparib % survival at 100 μ M vs γ H2AX count (fold increase)



$r = 0.130$
 $95\% \text{ CI} = -0.076 \text{ to } 0.325$
 $p = 0.214$

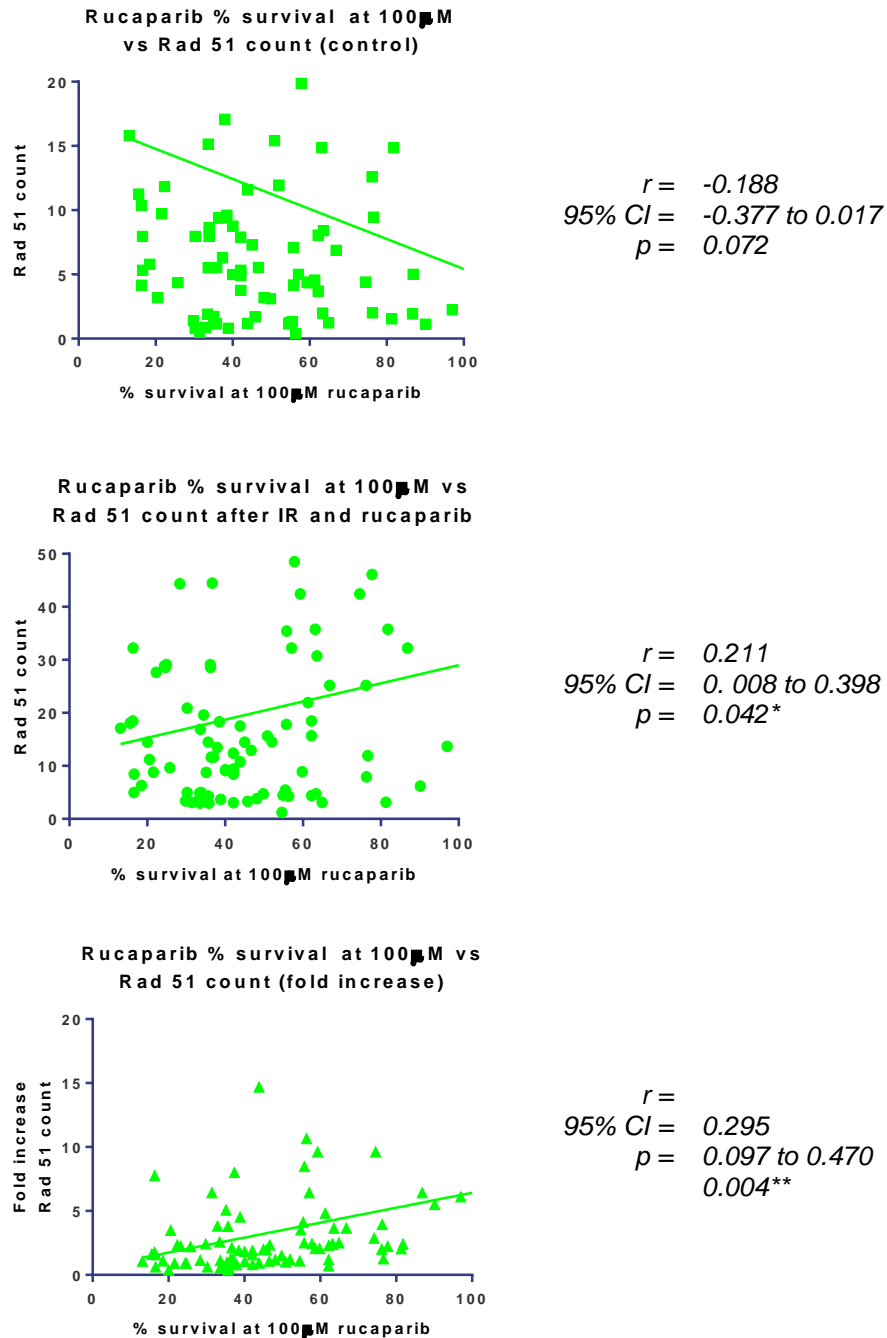
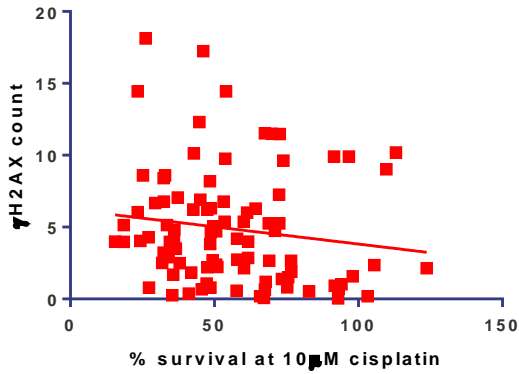


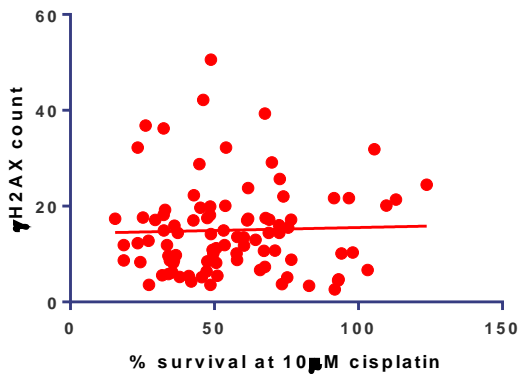
Figure 4.13 - 2: Correlation of γ H2AX and Rad51 foci counts with % survival at 100 μ M rucaparib. Following 2 Gy irradiation and incubation with 10 μ M rucaparib for 24 hours the nuclear foci of γ H2AX and Rad51 were counted using Image-J technology (described in section 3.6.3). Counts were expressed as mean foci count per cell and compared to untreated control cells. Each PCO culture was treated with rucaparib at various concentrations for 10 days before determining growth inhibition by SRB assay. Results are expressed as % survival at 100 μ M rucaparib compared to untreated controls.

Cisplatin % survival at 10 μ M vs γ H2AX count (control)



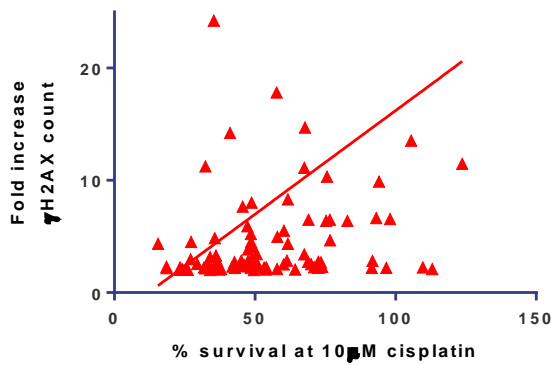
$r = -0.1443$
 95% $CI = -0.3391$ to 0.06236
 $p = 0.1699$

Cisplatin % survival at 10 μ M vs γ H2AX count after IR and rucaparib



$r = 0.03129$
 95% $CI = -0.1747$ to 0.2346
 $p = 0.7672$

Cisplatin % survival at 10 μ M vs γ H2AX count (fold increase)



$r = 0.2161$
 95% $CI = 0.01177$ to 0.0430
 $p = 0.0386^*$

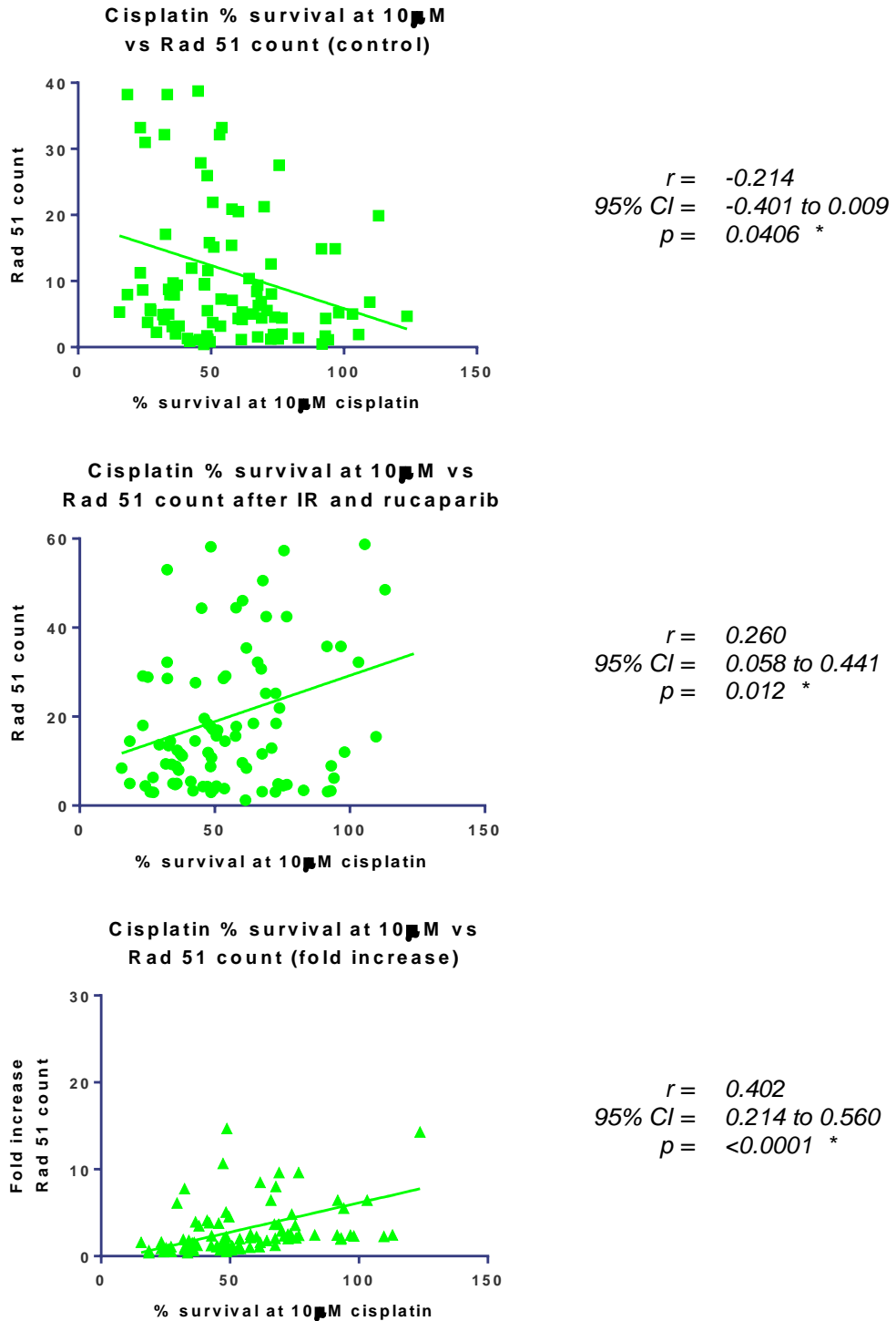
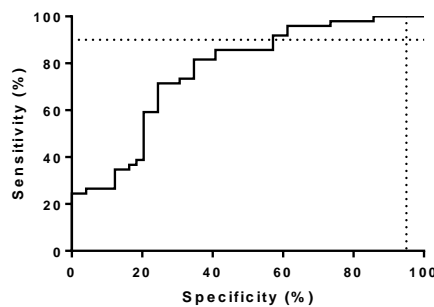


Figure 4.13 - 3: Correlation of γ H2AX and Rad51 foci counts with % survival at 10 μ M cisplatin. Following 2 Gy irradiation and incubation with 10 μ M rucaparib for 24 hours the nuclear foci of γ H2AX and Rad51 were counted using Image-J technology (described in section 3.6.3). Counts were expressed as mean foci count per cell and compared to untreated control cells. Each PCO culture was treated with cisplatin at various concentrations for 10 days before determining growth inhibition by SRB assay. Results are expressed as % survival at 10 μ M cisplatin compared to untreated controls.

4.13.3. Rad51 Alone as a Predictor of HR Function

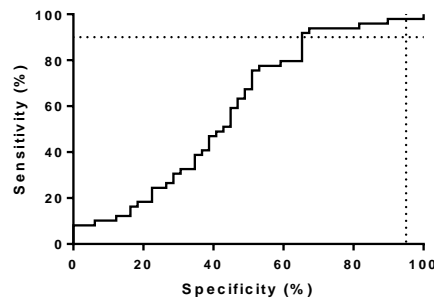
This alternative analysis utilising single measurements from the HR assay, thereby potentially enabling a simplified protocol, suggests that there is correlation between sensitivity to cytotoxic agents and the mean Rad51 foci count. To further assess this relationship and to determine if the Rad51 count in isolation could be used to reliably predict HR functional status, ROC analysis was performed to assess the predictability of HR status, Figure 4.13 - 4.

ROC curve: Rad 51 count (control) and HR function



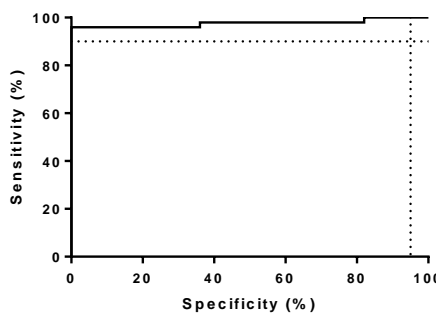
<i>AUC</i>	0.7688
<i>95% CI</i>	0.6731 - 0.8605
<i>p</i>	< 0.0001 *
<i>Sensitivity</i>	61.2%
<i>Specificity</i>	93.9%
<i>PPV</i>	62.0
<i>NPV</i>	38.3

ROC curve: Rad 51 count (DSB) and HR function



<i>AUC</i>	0.5898
<i>95% CI</i>	0.4750 - 0.7045
<i>p</i>	0.1258
<i>Sensitivity</i>	81.6%
<i>Specificity</i>	93.9%
<i>PPV</i>	93.0
<i>NPV</i>	83.6

ROC curve: Rad 51 count (fold increase) and HR function



<i>AUC</i>	0.9759
<i>95% CI</i>	0.9403 - 1.012
<i>p</i>	<0.0001 *
<i>Sensitivity</i>	82.0%
<i>Specificity</i>	98.0%
<i>PPV</i>	97.6
<i>NPV</i>	84.5

Figure 4.13 - 4: ROC curve of ability of Rad51 foci count to predict HR function.

The above analyses reinforces that fold increase, as currently used in the HR assay, is the most reliable way to ascertain HR functional status but also suggests that the baseline Rad51 foci count also shows a predictive relationship with HR function, Figure 4.13 - 4. This may offer one possible way in which the HR assay could be modified in order for it to be more easily incorporated into a research trial or the routine clinical setting.

4.14. Clinical Correlations

Survival data was calculated using the date of diagnosis, defined as the date of histological/cytological confirmation of EOC. For overall survival (OS), patients who died at follow-up (any cause) were uncensored, whereas patients alive at follow-up were censored (Bergmann 2007). For progression free survival (PFS) patients who died of cancer or who were alive with objective tumour progression were considered as uncensored, whereas patients who died of other reasons or alive without tumour progression at follow up were considered as censored.

4.14.1. HR Status as a Predictor of Survival

It is well known that BRCA deficient cancers have distinct clinicopathological features and patients typically have improved OS and PFS compared to non BRCA related sporadic EOCs (Pharoah 1999, Chetrit 2008). This is at least in part, likely to be due to increased sensitivity to platinum based chemotherapy (Foulkes 2006, Konstantinopoulos 2010). HR deficient tumours from our group have previously been shown to have better PFS than HRC tumours (Mukhopadhyay 2012) and assessment of PFS and OS has been repeated in this larger dataset.

Univariate analyses for OS and PFS were generated by Kaplan-Meier Survival curves and differences in survival experience between HR competent and HR deficient patients were assessed for statistical significance using log rank (Mantel- Cox) test, Figure 4.14 - 6. Patients with HRC cultures (n=35) had a median progression free survival (PFS) of 11 months (95% CI 0.4 – 1.6) in comparison to 13 months (0.6 – 2.3) for patients with HRD cultures (n=22), log-

rank (Mantel-Cox) test $p=0.0574$. Median OS of HRC cultures was 27 months (0.6 – 2.4) in comparison to 23 months (0.4 – 1.8) in HRD cultures, $p=0.3868$. These small none statistically significant differences were not explained by the differences in patient demographics, histology or surgical outcome, Table 4.14 - 1.

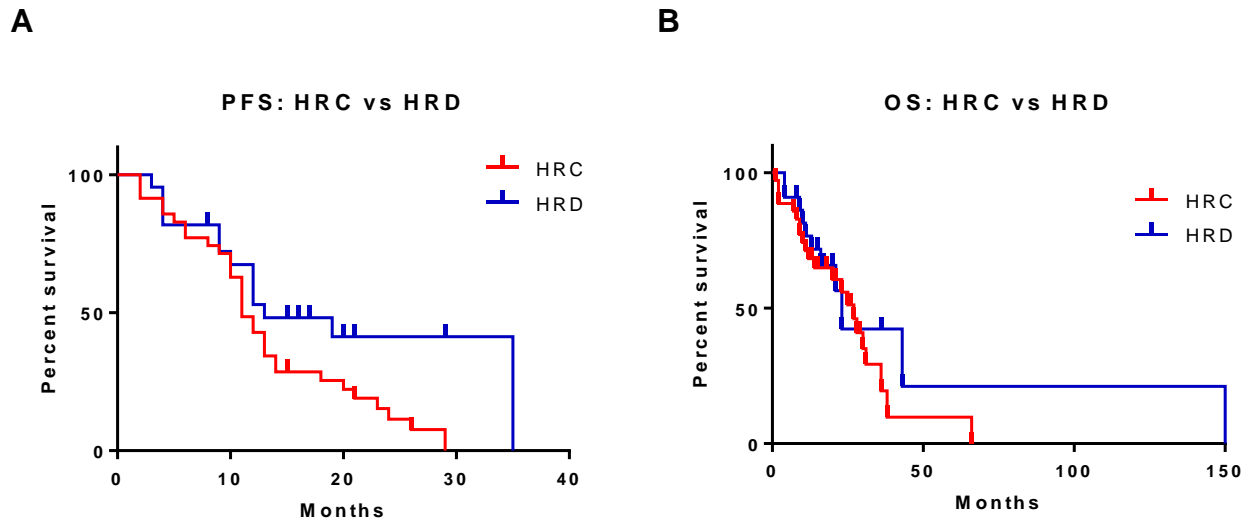


Figure 4.14 - 6: Kaplan-meier survival curves for patients stratified by HR function of ascitic PCO cultures. (A) Progression free survival (PFS) and (B) Overall survival (OS). Univariate analyses for OS and PFS were generated by Kaplan-Meier survival curves and log-rank (Mantel-Cox) tests used for statistical significance.

Demographic	HRC (35)	HRD (22)	p
	Median (range) / n (%)		
Age at presentation (years)	65 (41 – 85)	63 (41-85)	0.8291
Serum CA125 at presentation (U/l)	1252 (6-10000)	1000 (6-10000)	0.765
Histology			
HGSC	25 (71.4)	19 (86.4)	0.2313
Non-HGSC	10 (28.6)	3 (13.6)	
Time of ascitic sample collection			
Primary surgery / pre-chemotherapy	25 (71.4)	16 (72.7)	0.8676
Interval surgery / post- chemotherapy	10 (28.6)	6 (27.3)	
Surgical outcome			
Complete /	25 (71.4)	18 (81.8)	0.3788
Optimal	5 (14.3)	2 (9.1)	
Suboptimal	5 (14.3)	2 (9.1)	
No debulking surgery			
FIGO Stage			
Stage I	1 (4.5)	1 (4.5)	0.4233
Stage II	1 (4.5)	1 (4.5)	
Stage III	29 (82.9)	16 (72.7)	
Stage IV	4 (11.4)	4 (18.2)	

Table 4.14 - 1: Patient demographic data stratified by HR status. See appendix 6 for detailed raw data for individual patients.

4.14.2. Clinical vs. Ex Vivo Sensitivity to Platinum

Almost all of the patients from this study received platinum-based chemotherapy during their treatment. Response to chemotherapy was determined by serial clinical examinations, serum CA125 levels and computed tomography (CT) scans at predefined intervals and at completion of chemotherapy unless new onset symptoms warranted urgent evaluation. Comparison was made with pre- treatment imaging and tumour markers. Tumour response was defined as radiological evidence of complete/ partial response by RECIST criteria or a CA125 response defined as more than 50% decline sustained for at least 4 weeks (Therasse 2000). Tumour progression /recurrence were defined as presence of progressive disease on CT scan, rising CA125 levels or clinical evidence. Clinically, patients who have 6 months or more of disease free survival following treatment with platinum are defined as having platinum sensitive disease (PFS \leq 6 months). Platinum-refractory or resistant disease is defined by disease recurrence prior to cessation of therapy

(refractory) or within 6 months after cessation (resistant). By stratifying patients according to their clinical sensitivity to platinum, assessment of the ability of *ex vivo* culture proliferation assays as biomarkers of actual clinical outcome could be made. An ROC area of 0.5530 indicates poor ability of *ex vivo* culture sensitivity to predict clinical sensitivity to platinum, $p=0.4962$, Figure 4.14 - 7. Patients who had received NACT prior to ascitic sampling or who had residual tumour following surgery (suboptimal cytoreduction) were excluded from analysis as rapid progression is more likely with residual bulky disease.

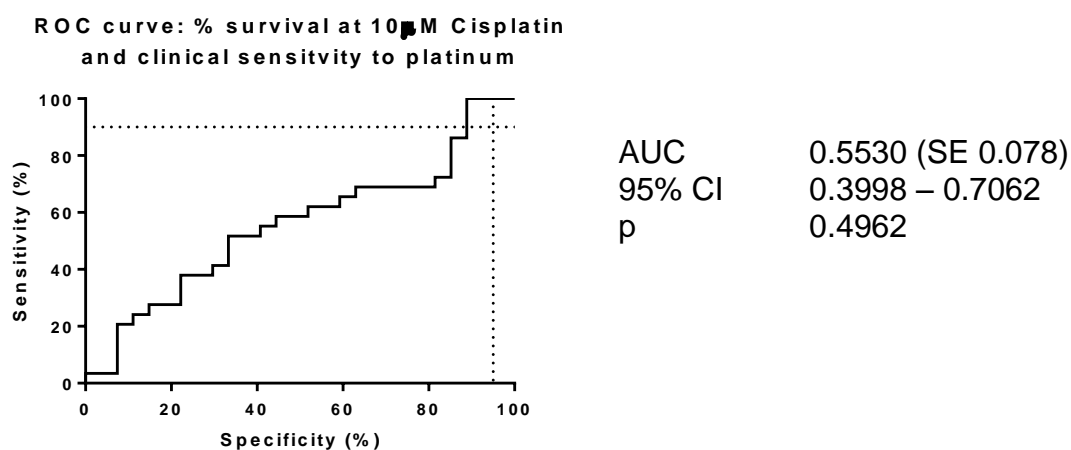


Figure 4.14 - 7: Ex vivo PCO culture sensitivity to cisplatin as a predictor of clinical sensitivity to platinum based chemotherapy. Analysis was limited to patients whose cultures were collected at primary surgery, with optimal / complete cytoreduction and who went on to receive 6 cycles of platinum based chemotherapy. Ex vivo sensitivity was determined by SRB proliferation assay and results expressed as % survival from control after 10 days incubation with 10 μ M cisplatin.

4.14.3. Growth as a Predictor of Time to Relapse (PFS)

The variability of clinical tumour progression, relapse and response to treatment is well recognised but there are currently no reliable pathological or clinical factors that are capable of predicting the disease course or time to next relapse. All PCO cultures were handled in the same way and the only explanation for the variable growth rates seen is a biological difference in the cells themselves. The ability of the *ex vivo* doubling time to predict PFS and OS was therefore explored.

Positive correlation is seen between the *ex vivo* growth rate of PCO cultures and time to relapse (progression free survival), $p=0.0459$, Figure 4.14 - 8. *Ex vivo* growth rate may be one indirect indicator of prognosis.

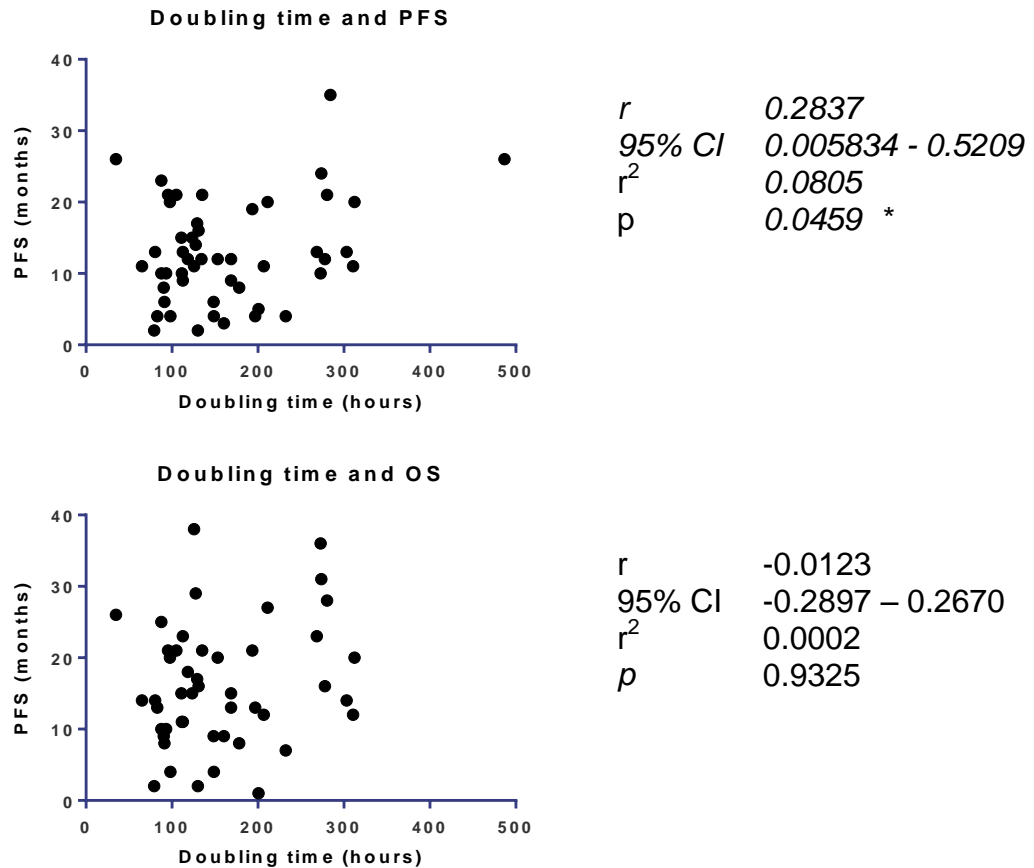


Figure 4.14 - 8: Correlation of PCO culture doubling time with PFS and OS. There is a statistically significant positive correlation between DT and PFS, $p=0.04$.

An arbitrary cut-off of a 2-fold increase in Rad51 foci in comparison to control was assigned during development of the HR assay (Mukhopadhyay 2010, Drew 2011). This cut off enabled reliable discrimination between PCOs that were sensitive or resistant to rucaparib in initial assays and therefore formed the basis of the definition for HRC and HRD cultures. The actual foci count as well as the fold increase from control is highly variable, Figure 4.11 - 2A.

4.15. Summary

- The antigen panel tested indicate that ovarian tumours undergo epithelial mesenchymal transition and that this is not exclusively a phenomenon seen during ex-vivo culture.
- *Ex vivo* PCO sensitivity to cisplatin and rucaparib is associated with HR function with greater association in rucaparib (likely owing to cisplatin's multiple modes of action and resistance).
- HRD PCO cultures had significantly less PARP activity than HRC cultures, but this failed to correlate with sensitivity to cisplatin or rucaparib.
- Differential gene signatures that correlate with HR functional are promising but require further investigation. Paradoxically Rad51 was downregulated in HRC cultures and gene signatures require further evaluation.
- HR function of primary ovarian cancer cultures determined by Rad51 foci quantification is reliable but fold change is the most reliable way to assess function.
- Application of the HR status to prediction of overall clinical outcome is complex and should be interpreted alongside other clinical variables including surgical outcome, treatment provided and other patient morbidity
- Use of HR status is likely to enrich a population of patients which are likely to respond to PARPi and should be incorporated into future clinical trials

4.16. Discussion

As the appreciation of the need for novel therapeutics in ovarian cancer grows with the recognition that stratification of therapy based upon tumour biomarkers is favourable, the need for a realistic *ex vivo* ovarian cancer cell model becomes paramount for the pre-clinical testing of cytotoxic agents.

Several methods for the culture of primary ovarian cancer cells isolated from ascites have been described (Hirte 1992). These methods however require complex multi-step procedures. Dunfield *et al* and Shepherd *et al* describe a more simple and reliable culture method involving mixing ascites directly with medium which results in epithelial cell culture (Dunfield 2002, Shepherd 2006). This technique has been adapted and used throughout this thesis and has been utilised and adapted by other groups for successful establishment of cultures from malignant ascites (Ince 2015).

This primary culture model has many advantages including the relative ease of obtaining primary material and a straightforward technique resulting in generation of an epithelial rich cell population. This project however has also highlighted some limitations and we must acknowledge the complexities of characterisation and the possible effects of *ex vivo* culture upon surface antigen detection, see section 4.7.4, 4.7.5. Some histological subtypes are underrepresented using this technique and the added appreciation of possible intra-tumoural heterogeneity with subpopulations of cells with different biological function also forces us to reassess the ability of PCO cultures from ascites to represent the entire tumour and therefore accurately predict disease behaviour. The increased morphological and antigen expression differences are likely to be accompanied by differences in other protein expression which orchestrate cellular function and behaviour, and therefore, the appearance of the cell (Faratian 2011). However, there may also be further genetic heterogeneity, not responsible for cellular appearance, which is responsible for cellular function, which therefore determines tumour behaviour and response to therapy. The relationship between morphological and molecular heterogeneity and prognosis is not yet known.

Although there are several possible explanations for the discrepancy seen between CA125 expression using IHC and IF microscopy of matched samples from PCO patients (section 4.7.3.), this may provide the first evidence of intra-tumoural heterogeneity. It is possible that the ascitic cell population cultured genuinely express CA125 whilst the solid tumour tissue examined by IHC represents a different subpopulation of cells with different underlying molecular mechanisms associated with a variety of genetic mutations. Other explanation for discordant CA125 expression may be sampling error, as not all FFPE samples are uniform tumour deposits and may include other non-tumour tissues such as stroma or vascular tissue. Alternatively, the fixation and antigen retrieval protocol for FFPE tissues may result in reduced exposure of the epitope and/or affinity of Ab for the antigen.

Although concordance in antigen expression was seen in 86.2% cases between PCO and PCO-2 cultures analysed a statistically significant higher percentage of PCO cultures expressed CA125 in comparison to PCO-2 samples. PCO-2 cultures result in monolayers with the same morphological and immunofluorescent features as the original PCO cultures and behave similarly in terms of their growth patterns. The small degree of discordance in antigen expression between PCO and the corresponding PCO-2 again, raising the possibility of two distinct subpopulations. PCO-2 cultures also senesced after several passages with little to indicate that they contain stem cells responsible for the continued exponential growth seen clinically in vitro. These cultures do however provide an additional resource for further experiments.

The series of expanded characterisation experiments for PCOs has increased our understanding of the effect of culture on primary cells. We can now appreciate that culture on plastic alone does not induce significant changes in antigen expression but the mechanical and chemical effects of passage are more likely to be responsible for loss of cell surface antigens, (Sections 4.7.4 and 4.7.5). As the majority of PCO cultures undergo characterisation assessment between passage 1 and 3, this may at least in part explain the lower than anticipated detection of surface epithelial and ovarian markers. The almost universal expression of vimentin in all subcultures, even at time zero,

suggests that EMT is a process that takes place *in vivo*. The extent of EMT within a tumour may be variable with a spectrum of phenotypes ranging from pure epithelial to pure mesenchymal with a population of cells with mixed phenotypes of varying degrees (Kalluri 2009). The universal expression of vimentin in ascites may be a reflection of the prolonged lag time thought to exist between the development of ovarian cancer and clinical presentation.

Characterisation of cultures should therefore ideally be performed at time 0, prior to passage. If the characterisation panel could be performed upon all cells simultaneously with a tumour specific marker, i.e. p53 in HGSC, this would enable more robust characterisation. Ideally, the actual cells that had undergone characterisation could then be cultured and used in subsequent experiments.

The data suggests that HR function remains important in determining sensitivity to PARPi and platinum agents irrespective of the underlying genetic mechanisms for dysfunction. Its PPV and NPV of 91.7 and 36.4 (Rucaparib); and PPV of 73.0 and NPV of 27.8 (cisplatin) although not ideal to provide robust guidance for the stratification of therapy are, as far as we are aware, the highest in the literature. Stratification of therapy based upon HR status of ascites would be likely however to enrich the population and result in higher levels of response in comparison to universal provision of therapy.

There is a pressing need to identify unifying biomarkers of HR deficiency that detect the resulting functional defect in HR irrespective of all of the diverse mechanisms involved in the pathway each with their own detectable variable mutations. Such a marker of 'BRCAness' may predict the benefit from PARPi in ovarian cancer and potentially multiple other cancer types, regardless of the underlying molecular mechanism (Turner 2011).

Despite several methodological approaches to the identification of HR defective tumours using mutational screening, gene expression profiling, loss of heterozygosity (LOH) assays, telomeric allelic imbalances and large scale transition scores, the limitations that result in a relatively low positive predictive value for these biomarkers remain (Watkins 2014). These gene signatures, however, have not yet achieved widespread use. This may be partly because of

concerns of reproducibility. Additionally, tumours whose genome has undergone one or more events that restore HR function are likely to be misclassified as HRD as a result of prior repair deficiency and its genomic scarring. In a way analogous to microsatellite instability in mismatch repair deficient cancers, there is likely to be a genomic mutational pattern that predicts for underlying HR deficiency (Turner 2011). Proposals have been made to integrate a genomic scar-based biomarker with a marker of resistance in an attempt to improve the performance of any companion diagnostic for PARP inhibitors but as yet this has not been tested in clinical samples (Watkins 2014). Several unsupervised multi-strategy approaches and statistical methods have been developed to identify informative genes from a high throughput genomic data and identify differentially expressed genes (Li 2008, Liu 2010) and may represent a superior method of analysis in future studies. Of particular interest is a DNA repair pathway–focused score developed by Kang *et al* (Kang 2012) using the TCGA dataset. This was analysed strategically assessing the repair pathways predominantly involved in repair of platinum-induced DNA damage they identified a high risk gene signature, reproducible in validation datasets, and correlated with survival (Kang 2012).

Gene expression arrays are the most appealing of the surrogate assays for HR function due to their high throughput analysis and ease of application to historical datasets. The differential expression of several genes in this small dataset between HRD and HRC cultures, with upregulation of ATM and MRE and down regulation of Rad51, is promising but should not be over interpreted. It is unlikely that one marker in isolation is capable of predicting function of the entire pathway and therefore expansion of this dataset combining regression analysis of all relevant components is required. Interestingly significantly higher Rad51 expression was seen in HRD cultures in comparison to HRC cultures, (section 4.11.3). Based upon the HR pathway, we had hypothesised that Rad51 may have been higher in HRC cultures. The HR assay is not based upon absolute levels of Rad51 to determine functional status, but a change in level in response to DNA damage. This higher baseline level in the RNA sampled may

therefore represent dysfunctional Rad51 present in the nucleus but not the functional Rad51 needed for HR which forms foci.

Assay	Advantages	Disadvantages
Rad51 functional assay	Identifies HRD irrespective of cause at time of treatment decision	Needs viable tissue, complex and lengthy
HR gene mutation	Rapid, can be done on FFPE material.	Does not identify epigenetic silencing and mutations in HR genes not yet identified
Gene expression profiling	Rapid, can be done on FFPE material.	Unreliable, conflicting data in literature
Loss of heterozygosity (LOH)	Identifies HRD irrespective of cause. Can be done on FFPE material	Genomic scarring, will not identify revertants or where HR has been restored by other means (e.g. loss of 53BP1)

The literature suggests a correlation between chemo sensitivity to platinum and PARP inhibitors. BRCA deficient EOCs have been shown to have increased platinum sensitivity (Taniguchi 2003). In clinical studies, response to the oral PARP inhibitor olaparib seems to correlate with platinum free interval, platinum sensitive cancers showing a greater clinical benefit rate (Fong 2010).

Interestingly 14/54 (26%) PCO cultures showed sensitivity to rucaparib *ex vivo* that were resistant to cisplatin *ex vivo* (see section 4.13.4). Similar complexities have been encountered in clinical studies where resistance to PARP inhibitor was seen in platinum sensitive patients or PARP sensitivity seen in platinum resistant patients (Fong 2010), and indicates that other mechanisms may be responsible as well.

In this data set *ex vivo* growth rate may serve as an indicator of prognosis with shorter PFS seen in patients with more rapid doubling times (see section 4.12.3). It is likely that growth rate is just one of many biological properties that may serve as a prognostic marker. As knowledge of these individual markers grows, it may be possible to combine them creating a scoring system that includes clinical, pathological and biological information that may guide response to treatment and prognosis facilitating clinical counselling and provision of adjuvant treatments.

The preclinical testing of rucaparib in PCO cultures in this study, with sensitivity seen in approximately 50% of cultures (section 4.11.2) creates optimism for its

use in the clinical setting in both platinum naïve and platinum resistant disease. This however will only translate into prolonged survival if *ex vivo* cultures are genuinely representative of *the* tumour. The inability of cisplatin sensitivity *ex vivo* to accurately predict clinical sensitivity to platinum chemotherapy is likely to be multifactorial. Perhaps the adherent monolayers of cells cultured represent just one subpopulation and are not representative of the residual microscopic tumour following surgery. Additionally, the standardised SRB protocol used, which did not take into account the doubling time of individual cultures, may have overestimated sensitivity in rapidly growing cultures and underestimated sensitivity in slow growing cultures. Finally, this analysis has not taken into account histological subtype, the residual volume of tumour at the end of surgery, and combination chemotherapy treatments actually given, which have previously been identified as being important in the prediction of overall clinical outcome (Von Heideman 2014).

Exploration of the use of more clinically applicable assays as surrogates for the functional HR assay is essential if HR functional status is to be used to guide therapy for patients in routine practice. The functional assay utilising cultures cells is not reproducible outside of the research setting. The finding of greater PARP activity in HRC cultures in comparison to HRD cultures (section 4.13.2) is promising that this rapid and resource-friendly assay may be used clinically. This PARP activity in HRC cultures may actually be a marker of a functional BER pathway and this may explain the lack of correlation seen between PAR level and % survival in sensitivity studies to cisplatin and rucaparib. The difference seen in PARP activity between the two experiments is likely to reflect simple inter-assay variability. Extreme culture conditions i.e., freeze and thaw can alter PARP activity as well, although it has been shown that there is no deterioration of PARP activity in frozen samples up to 15 weeks (Plummer 2005).

Irrespective of these points, the current cell culture model remains a valuable resource, which far exceeds cell line models in its ability to replicate *in vivo* tumour biology. It serves as a valuable resource for *ex vivo* testing and to survey tumour molecular aberrations, which may serve as druggable targets.

Future work may focus upon ongoing development of the culture model whereby characterisation and molecular analysis of HR function could be performed simultaneously in a rapid, reproducible and clinically relevant manner.

As we continue to evaluate various techniques during the search for accurate and reliable biomarkers, the importance of the actual sample taken to provide the biological information should not be forgotten. Gene mutation analysis undertaken by Pennington *et al* (2014) revealed improved survival in cases with somatic mutations in HR genes but this did not reach statistical significance. They hypothesised that somatic mutations would be less stable over time due to clonal selection and would have less impact on overall survival than germline mutations but they based their analysis upon single tumour biopsies only and may in fact not identified all of the mutations present in the bulk of the tumour.

Chapter 5. Inter- and Intra-tumoural Heterogeneity

5.1. Introduction

In many malignancies the extent of tumour heterogeneity is an emerging theme that is incompletely understood. How molecular heterogeneity affects tumour evolution and clinical progression is unknown and additionally the interaction with unique environmental factors that influence heterogeneity is also yet to be characterised.

Heterogeneity in cancer is driven by two principle factors: the introduction of genetic (or epigenetic) alterations mediated, for example, by genomic instability, and the evolutionary selection thereof (Alizadeh 2001). Not all of the somatic mutations that occur have a phenotypic or functional effect and are therefore termed passenger mutations, Figure 5.1 – 1. Furthermore selection pressure for particular phenotypic alterations can favour the outgrowth of cells with passenger genetic alterations associated with that phenotype. It may be more clinically relevant to examine the functional effects of heterogeneity rather than just relying on genomic variation.

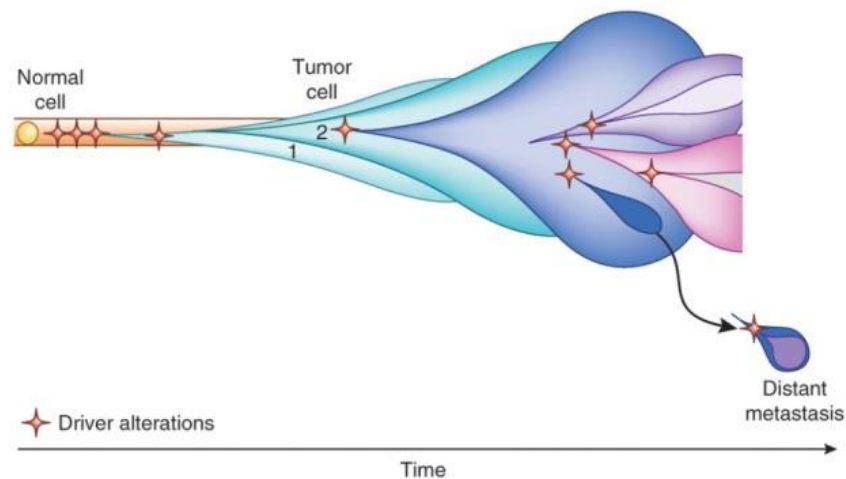


Figure 5.1 -1: Somatic evolution (Alizadeh 2001). In tumour evolution, driver alterations result in formation of the initial clone. As further driver alterations occur, clones branch off forming subclones.

A significant proportion of ovarian cancer patients present with large volume ascites. However, limiting sampling to ascites under represents the broad range of histological subtypes as the majority of patients with ascites have HGSC. Additionally, patients undergoing interval debulking surgery after chemotherapy often do not have ascites. Cultures derived from solid tumour, particularly in the absence of ascites, enables exploration of the broad range of histological subtypes ensuring that inter-tumoural functional heterogeneity between all histological subgroups is explored. Additionally, solid tumour culture from multiple anatomical sites allows investigation of the intra-tumoural heterogeneity (ITH) at a functional as well as morphological level.

Throughout this chapter, the term inter-tumour heterogeneity is used to describe differences seen in tumours from different patients and the term intra-tumour heterogeneity (ITH) is used to describe differences seen in tumours from different locations within the same patient.

5.1.1. *Heterogeneity in Ovarian Cancer: What is Already Known?*

Ovarian cancer is recognised as a heterogeneous disease and there is much evidence emerging regarding inter-tumour heterogeneity in terms of genetic mutations and defective intracellular pathways between the different histological subtypes. More recent work has taken this further and subdivided high grade serous cancer using genomic (TCGA 2011) gene expression (Tothill 2008) and functional (TCGA 2011, Mukhopadhyay 2012) techniques. This has generated at least four distinct gene expression subgroups (Tothill 2008, Tan 2013) and at least two functional subgroups (Mukhopadhyay 2012). The subgroups have distinct prognostic behaviour as well as differences in their sensitivity to conventional and novel chemotherapies.

To date, ovarian cancer is treated as a homogenous disease with platinum-based chemotherapy but effective delivery of novel cytotoxics and the correct selection of patients will require the use of accurate biomarkers capable of predicting response. Ovarian cancer frequently presents at a disseminated stage with multiple sites of disease within the peritoneal cavity and elsewhere. Unless tumours are homogeneous, it is likely that biopsies from a single site of

a tumour may not be representative of the rest of the tumour and therefore such biopsies will be unable to predict response accurately. In particular, most biopsies used for clinical diagnosis are taken from the omentum under radiological guidance and it is rare for disease on the diaphragm or nodal disease to be sampled. Given that there are possible biological differences between disease which disseminates within the peritoneal cavity through direct spread, compared to disease that disseminates by a classical process using lymphatic or haematogenous spread (Lengyel 2010), it can be hypothesised that there will therefore be a systematic bias in reporting of biopsies. This will have an impact as biopsies start to be used to direct therapy both in clinical trials and in clinical practice. The question of spatial heterogeneity and its potential effect upon clinical response to therapy has not been addressed in any prospective study.

There is general consensus that whilst most ovarian cancers are monoclonal in origin with a high degree of genomic parsimony there exists significant heterogeneity within microsatellites and SNPs (single nucleotide polymorphism) (Khalique 2007), copy number and driver mutation status (Bashashati 2013) from anatomically distinct regions (Le Page 2006). This does not however appear to translate into a significant degree of heterogeneity in terms of gene expression (Jochumsen 2007). The significance of this is uncertain. Other possible mechanisms of heterogeneity, including epigenetic changes in methylation, known to be important in determining functional status of the tumour, have not yet been studied.

Evidence for the presence of intra-tumour heterogeneity within EOC is growing. Gene expression studies have indicated different biological profiles in the cancer cells derived from ascites and solid tumour from the same patient in terms of metastasis, invasion and angiogenesis (Le Page 2006). Genetic analysis has provided evidence to suggest that although tumours arise from a single cell, subsequent mutations result in subpopulations with diverse molecular characteristics (Nowell 1976, Khalique 2007). The translational significance of this phenomenon was demonstrated in the robust study undertaken by McAlpine *et al*, where variable response to chemotherapeutic

agents was seen between synchronous samples in 22.4% of the tumours examined (McAlpine 2008). However, this finding is not universally described. Indeed, in the work undertaken by Jochumsen *et al*, minimal genetic intra-tumour heterogeneity was reported (Jochumsen 2007). In this latter study, only three regions of each tumour were examined in a sample size of nine, suggesting that the lack of heterogeneity identified could simply be a manifestation of sampling error. Additionally, this discrepancy could be explained by different opinions amongst authors as to what constitutes a significant quantity of intra-tumour heterogeneity. In fact, Jochumsen *et al* did not report the existence of no variation, simply that they believed the disparity to be 'minimal'. Additionally, phenotypic differences (e.g. antigen status) and functionality (HR status) may vary more than genotypic. Sequence analysis may not pick up epigenetic changes that would affect expression and neither genotypic nor expression analysis will pick up changes in protein levels through changes in stability or post translational modification that affects function. Bashashati *et al* have recently described extensive intra-tumoural mutational diversity in a small panel of HGSC, with TP53 being the only somatic mutation present in all samples and only 51.5% concordance in the presence of other driver mutations across all samples from each patient (Bashashati 2013). This builds upon previous work by Khalique *et al*, who suggested that ovarian cancer develops by a non linear clonal evolutionary process (Khalique 2009). More recently, Scharz *et al* have demonstrated heterogeneity in genomic clonal expansion both spatially and temporally across multiple samples in 14 HGSC patients (Schwarz 2015). Multiple sampling of primary and metastatic sites in breast, pancreas, and renal carcinoma has catalogued genetic divergence and shown that metastases from the same site can show organ-specific phylogenetic branches (Shah 2009, Campbell and McLaren 2010, Navin 2010, Navin 2011, Gerlinger 2012). Taken together, these findings suggest a model in which early divergence gives rise to clones with different driver mutation phenotypes, the only common feature being mutation of TP53.

5.1.2. Reported Solid Culture Methodologies

Normal ovarian epithelium can be cultured by scraping surface cells off the ovary and culturing as epithelial sheets (Auersperg 1984, Auersperg 2001) (Edmondson 2002). However, EOCs do not maintain this structural integrity and few studies have managed to effectively culture EOC.

Several methods for the culture of malignant tissue have been described and include tissue homogenisation using collagenase with a reported success rates of 51% with normal ovary, 45% with benign ovarian tumour material, 66% for malignant tumour and 56% for ascites (Lounis 1994). Mechanical digestion using a Medimachine has also been described and enables rapid processing of solid tumour to a homogenous cell lysate within 15-30 minutes without the need for collagenase digestion (Rodriguez-Casuriaga 2009).

Explant culture of tissue sections has been described for *ex vivo* culture, which maintains cellular architecture, thus mimicking the *in vivo* environment (Vaira 2010). This has been achieved in a heterogeneous group of tumours, with the use of organotypic inserts consisting of Teflon membranes with 0.4 µm pores, which enabled 3D growth for up to 5 days (Vaira 2010). Gene expression profiling and immunofluorescent staining were performed on these tissue sections but application to the current functional HR assay is limited as the current protocol is limited to monolayer cell cultures. Additionally, this methodology is time and resource consuming and highly complex.

More realistic preclinical cancer models are thought to be provided by transplantable, patient-derived cancer tissue xenograft (PDX) lines based on the grafting of fresh cancer tissue specimens subcutaneously, orthotopically or under the kidney capsules of immunodeficient mice (Choi 2014). In one such model by Strauss *et al* (Strauss 2011), solid ovarian tumour was incubated in collagenase/dispase and trypsin before implantation into mammary fat pads of immunodeficient mice. Once growth was established, xenograft tumours were excised and cells cultured as monolayers. This method is time consuming, costly and technically difficult and although this method may preserve the tumour microenvironment, cultivation in mice at a different anatomical location

may not accurately represent original ovarian tumour behaviour. We aimed to develop a method for the culture of solid tumour, which would allow functional testing to be expanded from HGSC ovarian cancer to the other histological subtypes.

Gene expression studies have indicated different biological profiles in the cancer cells derived from ascites and solid tumour from the same patient in terms of metastasis, invasion and angiogenesis(Le Page 2006).

Several methods have also been described to enrich the epithelial cell populations without fibroblast contamination. This includes the use of serum free media devoid of calcium and growth factors needed for fibroblast growth (Hammond 1984); filters with a pore size to separate cellular components; special collagen or extra-cellular matrix (ECM) coated plates and flasks (Crickard 1983); frequent passaging to eliminate fibroblast growth; use of flow-cytometry to segregate cell populations (Chan 2007); and magnetic bead separation of cells tagged to specific binding antibodies.

5.2. Aims

- Explore the feasibility of culturing ovarian cancer solid tumour from various metastatic sites within the abdomen.
- Explore spatial intra-tumoural heterogeneity (ITH) within an individual's cancer by characterising PCO subcultures in terms of antigen expression, growth potential, morphology, with functional HR status and sensitivity to PARP inhibitors and platinum.
- Investigate intra-tumoural heterogeneity itself as a prognostic marker alongside other recognised prognostic markers (histological subtype and surgical cytoreduction).
- Investigate temporal changes in HR status using longitudinally collected samples of ovarian cancer.

5.3. Methods

5.3.1. Characterisation of Solid Tumours

All solid subcultures were characterised in terms of morphology, immunofluorescent detection of antigen expression and HR function at passage 1 as previously described, Section 4.3.1. All subcultures were assessed for growth and sensitivity to cisplatin and rucaparib using standard SRB growth inhibition assays, sections 3.5.2, 3.5.3.

5.4. Results

5.4.1. Culture Method Optimisation

These studies were conducted with Laura Woodhouse, MRes 2012.

Solid tumour culture methodology was optimised using solid tumour samples from six HGSC patients. Single 1 cm³ samples were obtained from the ovarian tumour and, with each sample, one variable was altered to allow measurable protocol optimisation, Table 5.4 - 1. This was assessed by satisfactory epithelial cell growth and confirmed by examination of morphology and cytokeratin staining.

Method	Variable	Results
Sample dissection	Whole	No culture from undiced tumour
	Diced (3M)	Small explant cultures from small solid tumour pieces
Dissociation from connective tissue	Trypsin (0.25%) 30 minutes 1 hour	Minimal dissociation of tumour and poor culture/ high cell death No culture
	Collagenase/Dispase 20 hours 2 hours	Poor culture/ high cell death More rapid formation of explant transforming into monolayer cultures from small diced tumour pieces
Selective seeding to exclude fibroblast	No selective seeding	Mixed morphology within culture with rapid overgrowth of fibroblasts within 24 hours
	Agitation to prevent any seeding for 24 hours*	No culture
	24 hour selective fibroblast seeding~	All cell types seeded in first flask with overgrowth of fibroblasts within 24 hours
	30 minute fibroblast seeding~	Optimal separation of fibroblast and epithelial monolayer cultures

Table 5.4 - 1: Optimisation of Solid Culture Methodology. Dissociation: solid tumour sample was incubated with trypsin or collagenase/dispase for variable times on a rocker, as indicated. Dissociated cells alongside residual solid pieces were collected by centrifugation before PBS washing and plating in culture flasks. Selective fibroblast seeding was incorporated under the assumption that fibroblasts would adhere faster to the hydrophilic surface of the first culture flask and leave an epithelial cell suspension for seeding in the second flask.

To confirm exclusion of fibroblasts using selective seeding, excluded cells were grown to confluence and compared to the epithelial component of the same culture in terms of morphology and CK staining. Epithelial cells grow in a cobblestone monolayer whereas fibroblasts are typically bipolar or multipolar with an elongated shape and grow in a mesenchymal morphological pattern, Figure 5.4 - 1.

The final solid tumour culture method, described in section 3.4.2, used diced tumour, which was dissociated from connective tissue by 2 hour incubation with collagenase/dispase. Selective seeding of the resulting cell suspension excluded fibroblasts before seeding the cell suspension in T75 flasks for further characterisation and use in further experiments.

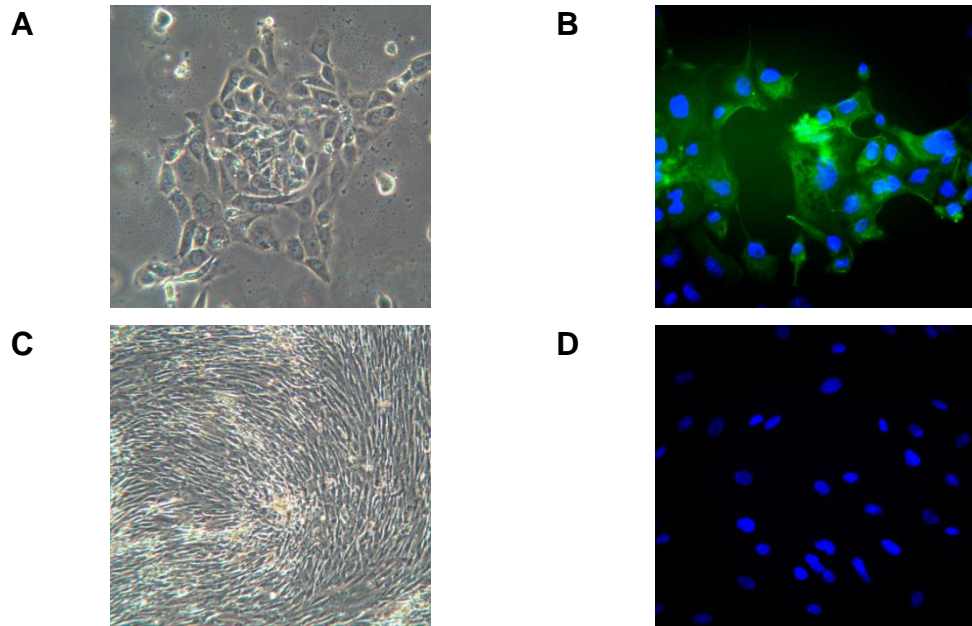


Figure 5.4 - 1: Fibroblast exclusion using selective seeding. A/B: epithelial component; A: cobblestone monolayer; B: CK expression; C/D: fibroblast component, C: mesenchymal morphology; D: No CK expression.

5.5. PCO Solid Culture Case Series

5.5.1. Culture Success

Of the 30 patients with malignant disease from whom solid tumour was sampled, successful culture was achieved in 25 (83%) patients. 3/5 of the patients with unsuccessful cultures had samples taken at the time of interval surgery when chemotherapy had been given in the preceding month. Lack of culture may therefore be a consequence of the cytotoxic effect of chemotherapy.

From the 25 patients included, 98 individual samples were collected of which 68 (69.4%) were successfully grown and used in further experiments. 14 (14.3%) cultures were lost to infection and a further 16 (16.3%) cultures had no growth or were classified as non-epithelial with suboptimal CK expression. Additionally, three cultures were attempted from patients with benign disease but no growth resulted.

5.5.2. Patient Demographics

Demographics of the 25 patients from whom ascites and at least one sample of solid tumour tissue was taken are summarised in Table 5.5 - 1 and in detail in Appendix 7. Solid tumour was sampled from pelvic tumour only in 13 patients and from pelvic and intra-abdominal deposits in the remaining 12 patients.

Demographic	Median (range) / n (%)
Patient age (years)	63 (43 - 83)
FIGO Stage	
Stage 2	1 (4)
Stage 3	19 (76)
Stage 4	5 (20)
Serum CA125 at presentation (U/l)	600 (57 - 9740)
Histology	
High grade serous carcinoma	19 (76)
Clear cell	(8)
Endometrioid	1 (4)
Other	3 (12)
Surgery	
Primary	16 (64)
IDS	9 (36)
Surgical outcome	
Optimal/Complete	22
Suboptimal	2
Progression free survival (PFS) (months)	11 (3 - 26)
Overall survival (OS) (months)	13 (4 - 36)

Table 5.5 - 1: Solid tumour patient demographics. See Appendix 7 for detailed data for individual patients. .

5.5.3. Characterisation

Morphology

Within 24 hours of seeding, adherent cells could be visualised. Cultures initially retained cell-cell adhesions and displayed explant morphology before adopting the typical cobblestone monolayer seen with primary cultures, Figure 5.5 - 1.

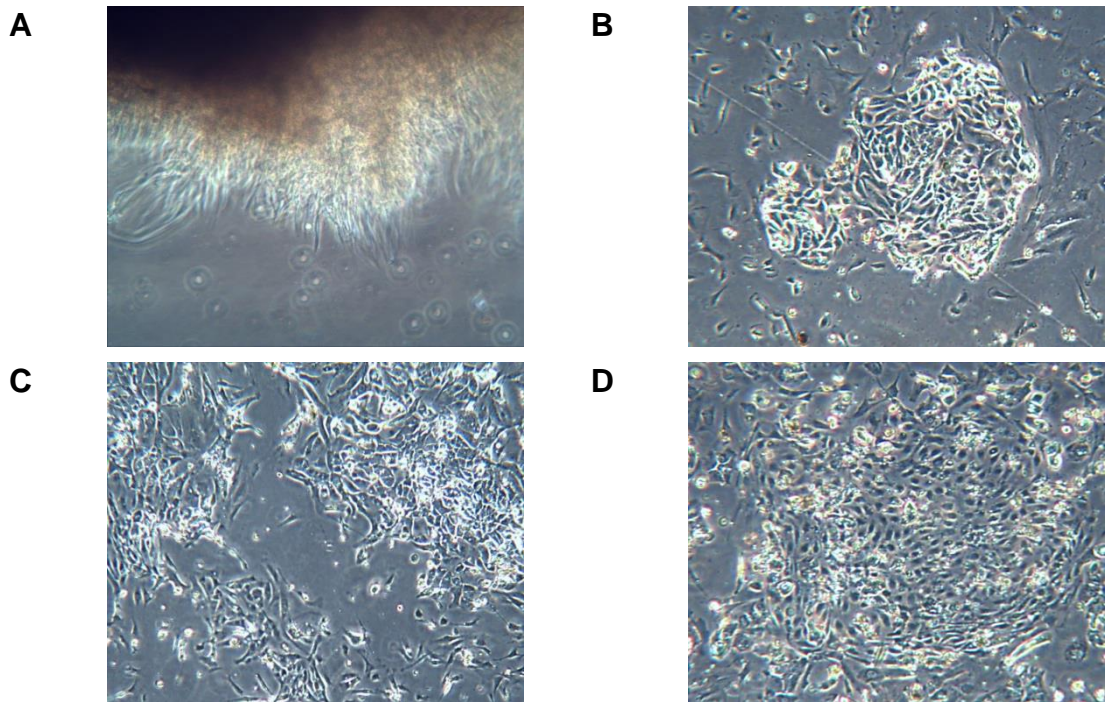


Figure 5.5 - 1: Solid PCO cultures. A: Solid tumour in culture; B: Explant; C/D: Development of cobblestone monolayer .

Morphology of each solid subculture was recorded with 15/45 (33.3%) cultures classified as cobblestone, 29 (64.4%) as mesenchymal and 1 (2.2%) as having spindle morphology. There was no relationship between histological subtype and morphology and no significant difference seen in the proportion of cultures of each morphology within histological groups, Table 5.5 – 2, Figure 5.5 - 2.

Histology	Cobblestone (n=15)	Mesenchymal (n=29)	Spindle (n=1)	Chi ² p
HGSC	12	22	0	0.0863
Clear cell	0	4	0	-
Endometrioid	2	0	0	-
Other ovarian	1	2	1	0.7556
Non-ovarian	0	1	0	-

Table 5.5 – 2: Solid tumour subculture morphological classification by histological subtype.

Immunofluorescent Antigen Expression

All subcultures were assessed in terms of expression of the six characterisation antigens, Chapter 3. Both inter- and intra-tumour heterogeneity was seen, with differences seen between cultures from the same histological subgroup.

Heterogeneity was also seen between cultures taken from different anatomical sites from the same patient, Figure 5.5 - 3. The majority of the cultures showed expression of epithelial as well as mesenchymal markers. Vimentin expression was universal throughout all subcultures, Figure 5.5 - 2. There was no relationship between histology and antigen expression.

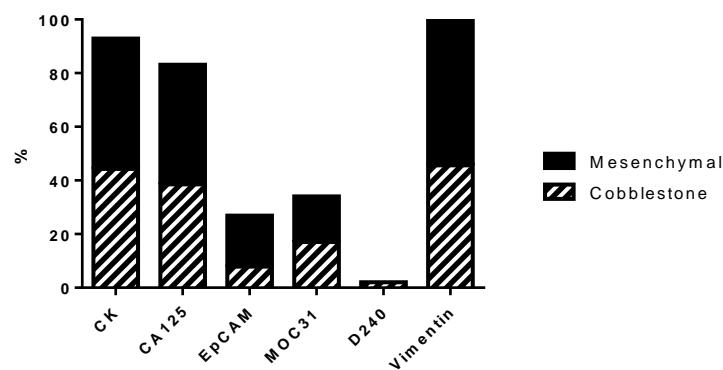


Figure 5.5 - 2: Summary of Characterisation Antigen Detection. All subcultures from 25 patients are combined and antigen status expressed as a % of cultures tested. All cultures used in further experiments were diffusely CK positive. Only 30% of cultures showed expression of EpCAM and MOC31, which may reflect loss of antigen during passage, section 4.7.5. All cultures were diffusely positive for Vimentin, which paralleled ascitic cultures.

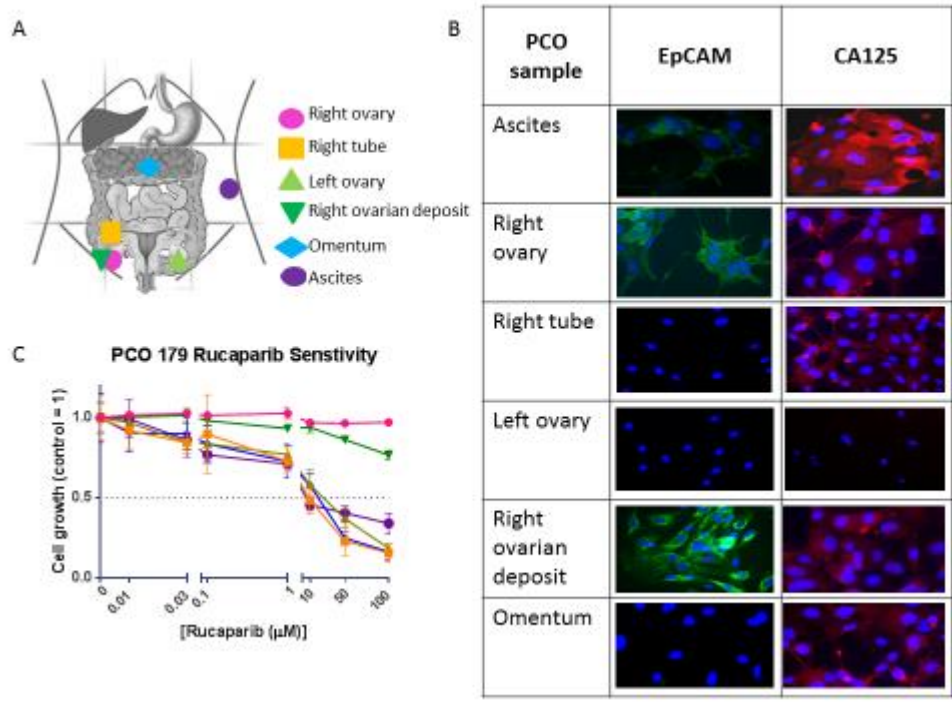


Figure 5.5 - 3: PCO 179. Solid tumour biopsies taken from five intra-abdominal sites cultured, alongside ascites culture (A). (B) Intra-tumoural heterogeneity of antigen detection of EpCAM and CA125 using immunofluorescent microscopy. (C) Variable proliferation following 10-day exposure to rucaparib, assess using SRB assay.

Heterogeneity of expression was seen universally amongst all antigen groups (epithelial, mesenchymal and ovarian). This heterogeneity was not reflected in the histological classification of the tumours, with only 2/16 (12.5%) patients with heterogeneous antigen expression being classified as having mixed histological subtypes on formal pathology. Inter- and intra-tumoural heterogeneity exists for each of the characterisation antigens tested. For future studies, use of the ImageStream characterisation protocol, see Chapter 7, to numerically quantify antigen expression may give a more robust analysis of heterogeneity.

5.5.4. Growth

Once each culture was seen to have established into an adherent monolayer, a standard SRB growth assay was performed to determine doubling time (DT), Chapter 3 Methods. The median DT for all cultures (ascitic and solid tumour cultures combined) was 126 hours, range 55 – 303. The DT for solid cultures (120 hours, 82 – 279) was faster than for ascitic cultures (159 hours, 55 - 303, $p = 0.0142$). All solid tumour and ascites samples were obtained from the patient at the same time, with no differences in culture preparation or handling, and therefore the differences observed can be assumed to reflect differences in the subpopulations themselves. Inter- and intra-tumour DTs were highly variable. When comparing all subcultures from each PCO patient, there was no significant difference in growth between patients (ANOVA, $p = 0.1425$) but there was a significant difference between the SD of each group of subcultures (Brown-Forsythe, $p = 0.0098$), indicating that intra-tumour heterogeneity was greater than inter-tumour heterogeneity in terms of growth, Figure 5.5 - 4. There was no correlation between ascites doubling time and solid tumour subculture doubling time, $r^2 = 0.007$ (95% CI -0.26 – 0.41), $p=0.6361$. All cultures underwent assessment of HR functional status, see section 3.6. There was no difference between the median DT of HRC (126 hours, range 55 - 303) and HRD tumours (128 hours, 81 - 233), $p = 0.2543$, Figure 5.5 - 5.

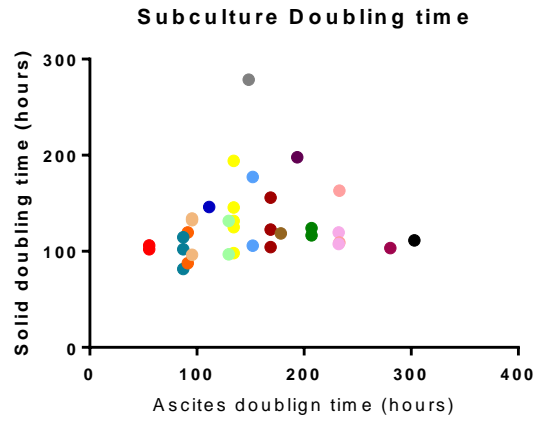
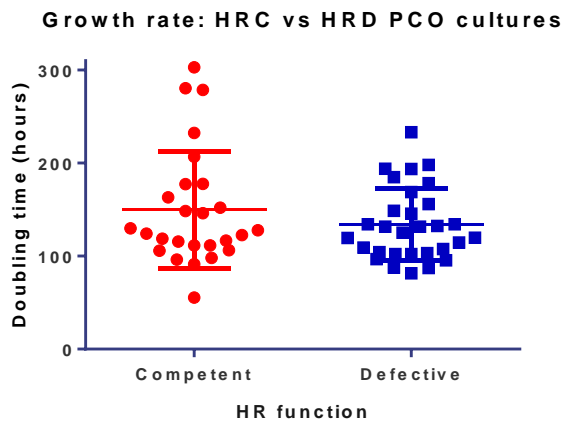


Figure 5.5 - 4: PCO Subculture Doubling Time
 The doubling times (hours) for each ascites sample (x axis) is plotted against the doubling time of each of the solid subcultures (y axis). Where there is more than one solid tumour subculture per PCO patient, subcultures are shown in the same colour.

A



B

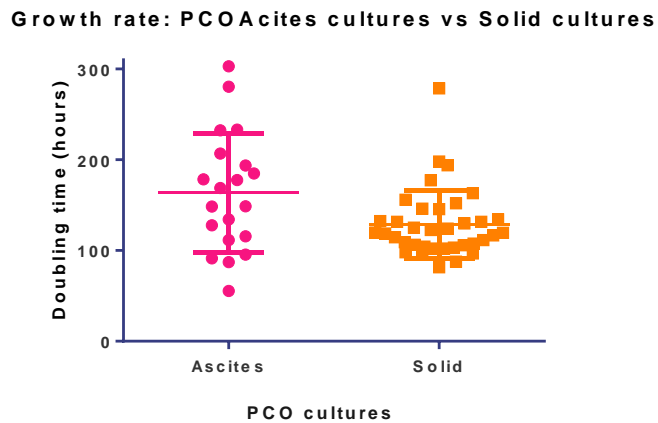


Figure 5.5 - 5: Growth Comparison. A: HRC vs HRD; B: Ascites vs solid cultures

5.5.5. Functional HR Status

When considered individually, 32/68 (47.1%) ascitic and solid subcultures tested were HRC and 36 (52.9%) were HRD, Table 5.5 - 3. HR function was homogeneous in all subcultures from an individual patient in 13/25 PCOs. Of these homogeneous PCOs, 5 were universally HRD and 8 universally HRC.

When considering a single biopsy from the ovary only and comparing the HR function of this culture to that of the paired ascitic culture, concordance was seen in 19/25 (76%) cases. This decreased to 3/12 (25%) when sampling was from two or more spatially distinct areas of solid tumour. Sampling a single solid area, even in conjunction with ascites, will therefore miss ITH in approximately 51% of cases.

PCO	Sample location	HR status	Heterogeneous / Homogeneous	Rucaparib (μM)		Cisplatin (μM)	
				% survival at 100 μM	GI ₅₀	% survival at 10 μM	GI ₅₀
155	Ascites	HRD	Homogeneous	21.5	0.1		
	Ovary	HRD					
156	Ascites	HRD	Homogeneous	33.7	11.1	34.8	1.9
	Ovary	HRD					
157	Ascites	HRC	Homogeneous	99.6	>100		
	Ovary	HRC					
158	Ascites	HRD	Homogeneous	38.3	13.4		
	Ovary	HRD					
162	Ascites	HRC	Homogeneous	33.6	3.3		
	Ovary	HRC					
163	Ascites	HRC	Heterogeneous	30.2	40.3		
	Omentum	HRC					
	Uterus	HRD					
167	Ascites	HRC	Heterogeneous	76.3	>100	36.6	4.6
	Ovary	HRD					
168	Ascites	HRC	Homogeneous	46.7	>100	71.1	>10
	Ovary	HRC					
174	Ascites	HRC	Heterogeneous	58.6	>100	75.6	>10
	Left ovary	HRC		62.2	>100	72.7	>10
	Right ovary	HRD		38.0	15.4	32.9	2.3
175	Ascites	HRC	Heterogeneous	45.0	45.5	53.8	>10
	Left ovary	HRD		36.4	40.5	37.3	1.5
	Right ovary	HRD		62.2	>100	50.6	6.7
179	Ascites	HRD	Heterogeneous	42.1	14.6	61.7	>10
	Left ovary	HRD		18.5	11.2	27.2	1.7
	Omentum	HRD		16.4	7.4	32.3	6.3
	Right ovarian deposit	HRD		76.6	>100	47.5	4.5
	Right ovary	HRC		97.0	>100	29.5	3.1
	Right tube	HRD		15.6	5.8	23.4	2.4
180	Ascites	HRC	Homogeneous	>100	>100	>100	>10
	Left ovary	HRC		63.6	>100	67.2	>10
	Right ovary	HRC		86.9	>100	>100	>10
181	Ascites	HRC	Homogeneous	71.3	>100	79.1	>10
	Ovary	HRC		81.8	>100	91.5	>10
183	Ascites	HRD	Homogeneous	33.7	10.9	41.0	>10
	Ovary	HRD		52.0	>100	42.7	7.8
184	Ascites	HRC	Heterogeneous	25.8	60.3	60.2	>10
	Ovary	HRD		13.1	8.1	49.4	>10
185	Ascites	HRC	Heterogeneous			86.4	>10
	Left tube	HRD		30.2	0.2	34.5	5.9
	Right tube	HRD		24.4	28.8	25.2	5.2
	Omentum	HRC		36.7	6.6	57.9	>10
186	Ascites	HRC	Homogeneous			79.1	>10

	Omentum 1	HRC		66.9	>100	68.9	>10
	Omentum 2	HRC		76.2	>100	72.5	>10
	Pelvic peritoneum	HRC		74.2	>100	69.9	>10
192	Ascites	HRC	Heterogeneous	>100	>100	98.0	>10
	Ovary	HRD		35.7	3.0	33.6	1.8
	Omentum	HRD		36.2	1.7	54.1	2.9
200	Ascites	HRC	Heterogeneous	34.5	0.4	46.2	1.4
	Ovary	HRD		46.6	4.6	44.8	6.7
	Omentum	HRC		>100	>100	>100	>10
201	Ascites	HRC	Heterogeneous	63.1	>100	96.7	>10
	Ovary	HRC		25.7	23.2	96.7	>10
209	Ascites	HRC	Homogeneous	55.3	>100	76.7	>10
	Ovary	HRC		54.9	>100	75.3	>10
217	Ascites	HRD	Heterogeneous	36.2	47.1	32.4	0.9
	Ovary	HRC		57.1	>100	65.9	>10
223	Ascites	HRD	Heterogeneous	37.1	1.3	67.5	>10
	Left ovary	HRD		33.9	11.5	18.5	1.4
	Left tube	HRD		35.4	26.6	32.3	4.4
	Omentum	HRC		59.3	>100	76.6	>10
226	Ascites	HRD	Homogeneous	42.1	14.6	31.9	2.3
	Ovary	HRD		25.0	0.5	23.4	2.4
	Omentum	HRD		20.1	0.2	18.5	1.4
	Bowel mesentery	HRD		16.6	0.1	15.6	0.9
228	Ascites	HRD	Heterogeneous	33.7	10.9	27.3	2.8
	Left ovary	HRD		16.3	5.1	64.3	>10
	Right ovary	HRD		40.1	35.0	34.0	2.8
	Omentum	HRC		43.9	26.4	48.8	3.4

Table 5.5 – 3: PCO solid tumour samples with HR status and corresponding sensitivities to rucaparib and cisplatin, determined using SRB cell proliferation assay. Briefly PCO subcultures from ascites and solid tumour were seeded at density at 1000 cells/well with six replicates per condition and exposed to increasing concentrations of rucaparib or cisplatin for 10 days, corrected for 1% DMSO. After fixation, bound cellular protein was stained using 0.4% SRB and quantified by spectrophotometry.

5.5.6. Sensitivity to Cisplatin and Rucaparib

Sensitivity to cisplatin and rucaparib was assessed for 59/68 subcultures using a standard SRB proliferation assay, Chapter 3 Methods, Table 5.5 - 3. There was 84.7% concordance between HR status and rucaparib sensitivity and 75.5% concordance between HR status and platinum sensitivity between cultures. When subcultures are grouped together according to HR function, HRD cultures were sensitive to both cisplatin and rucaparib with mean GI₅₀ of 4.02 µM (CI 3.2 - 5.1) and 9.73 µM (CI 6.7 - 15.9) respectively, compared to

HRC cultures with mean GI₅₀ of >10 µM and >100 µM, (p < 0.0001), Figure 5.5 - 6, Table 5.5 - 3.

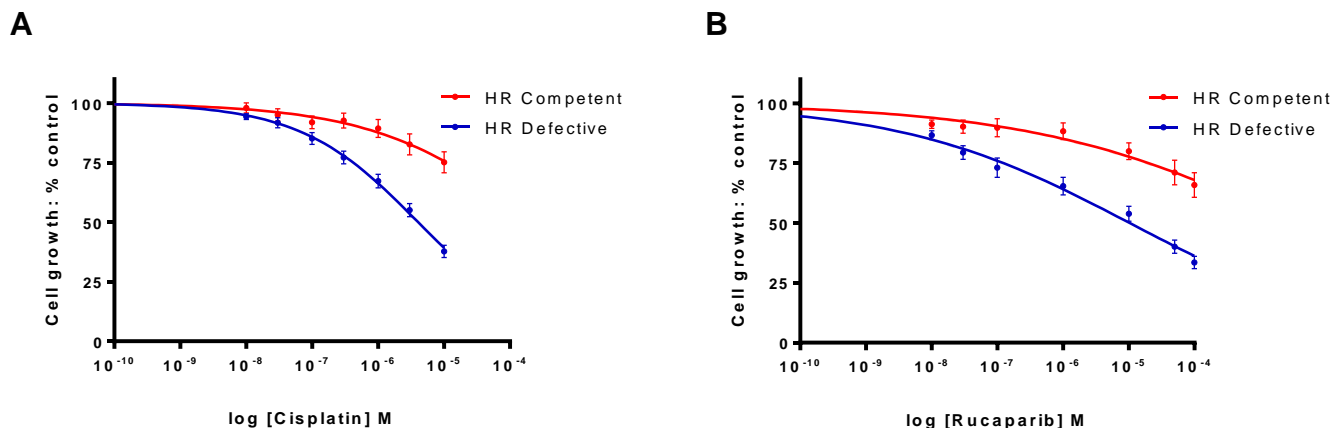


Figure 5.5 - 6: Growth Inhibition
A routine SRB assay was used to determine cytotoxicity to rucaparib and cisplatin stratified by HR function. A total of 59 subcultures were generated and treated with (A) rucaparib or (B) cisplatin. Those cultures deemed HR defective had greater sensitivity to both agents (p < 0.0001).

5.6. Heterogeneity as a Prognostic Marker

Of the 25 patients from whom solid tumour was sampled, 13 patients were found to have homogenous HR status in all subcultures (ascites and solid) tested. The remaining 12 demonstrated discordance in at least one subculture and therefore classified as heterogeneous.

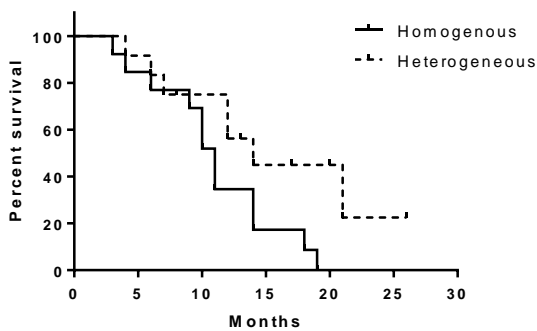
The median PFS of homogenous cultures was 11 (3 - 19) months in comparison to 14 (6 - 26) months for patients with heterogeneous subcultures, (p = 0.0504), Figure 5.6 - 1, Table 5.6 - 1. Median OS for the heterogeneous patients was 272.5 (7 - 1117) months compared to 13 (4 - 36) months for the homogeneous patients. There were no statistically significant differences in event free survival between the heterogeneous and homogenous groups in survival at 6 months, 1 year or 2 years, Table 5.6 - 1, p = 0.0801 at 1 year.

	Median PFS (months)	Median OS (months)	Event free survival n(%)		
			6 months	1 year	2 years
Heterogeneous (n=12)	14 (6 - 26)	272.5 (7 - 1117)	11 (91.7)	3 (25.0)	0 (0)
Homogeneous (n=13)	11 (3 - 19)	13 (4 - 36)	10 (76.9)	5 (38.5)	2 (15.4)
Homogeneous HRD	10 (3 - 19)	13 (4 - 21)	4 (30.7)	3 (23.1)	1 (7.7)
Homogeneous HRC	11 (6 - 18)	36 (9 - 36)	6 (46.2)	2 (15.4)	1 (7.7)

Table 5.6 - 1: Intra-tumoural heterogeneity of HR status and survival (PFS and OS). Each PCO was classified as heterogeneous if subcultures from the donor patient varied in their HR functional status and homogeneous if all subcultures from the same donor PCO patient were concordant.

A

PFS: HR heterogeneous vs homogeneous PCO



B

OS: HR heterogeneous vs homogeneous PCO

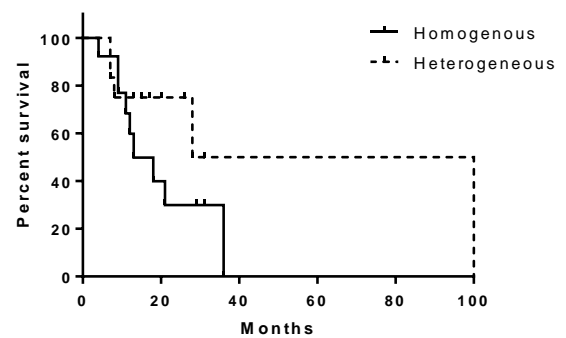


Figure 5.6 - 1: Kaplan Meier: heterogeneous HR cultures vs homogeneous HR cultures.

The differences seen between the heterogeneous and homogeneous are not due to differences in surgical outcome with no significant differences between the proportions of patients with complete, optimal or suboptimal cytoreduction in the two functional groupings, Figure 5.6 - 2.

Homogeneous/Heterogeneous cultures by Surgical Outcome

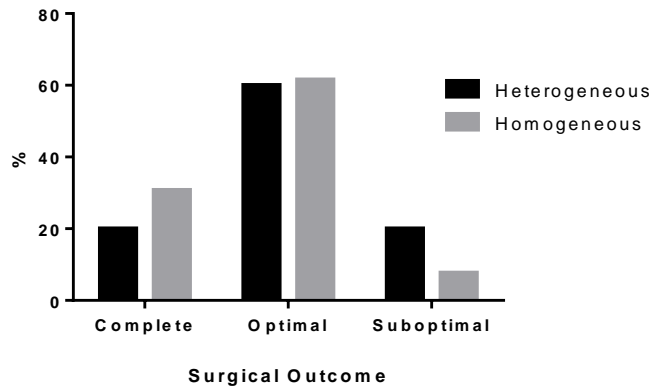


Figure 5.6 - 2: Cytoreductive surgical outcome by homogenous and heterogeneous functional groupings. There was no statistical relationship between heterogeneity and surgical cytoreductive outcome with no statistical difference between the proportion of patients with heterogeneous or homogeneous tumours within each group.

Heterogeneity of HR function may itself be a prognostic marker but this should be considered alongside other recognised prognostic markers. Future clinical trials should be designed and analysed with this in mind, taking into account HR as ascites, histology and surgical cytoreductive success alongside patient factors.

Further exploration of prognostic markers, see Table 5.6 – 2, reveals greater complexity. PCO patients are ordered by progression free survival, heterogeneity and HR function. There is no clear grouping to reveal a single prognostic marker and this suggests that many factors should be taken into account to predict prognosis, perhaps including heterogeneity, HR function, histological subtype and cytoreductive surgical outcome.

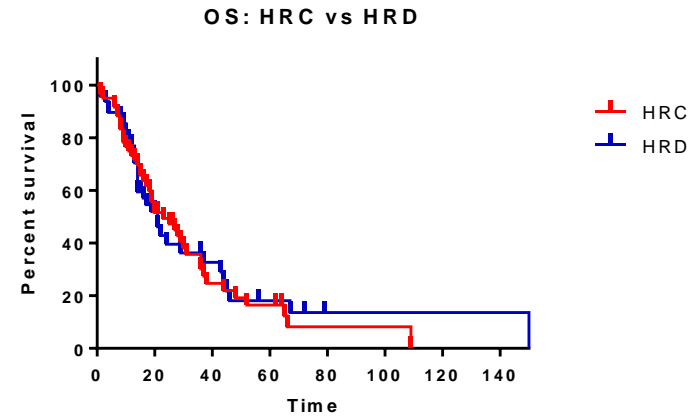
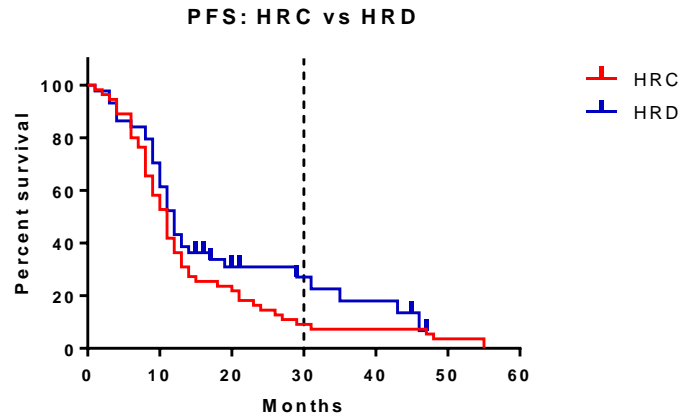
PCO	Age (yrs)	CA1 25 (U/L)	Histological subtype	FIGO Stage	Surgery		NACT	Post-op chemotherapy	PFS (months)	OS	Homogeneous/Heterogeneous	HRC / HRD
					Primary / IDS	Debulking outcome						
192	66	2425	Clear cell	3C	Primary	Optimal	NA	3 carboplatin	4	7	Heterogeneous	
181	72	176	HGSC	3C	IDS	Optimal	3 carboplatin	3 carboplatin	5	7	Homogeneous	HRC
175	66	250	Clear cell	3B	Primary	Optimal	NA	5 carboplatin	5	8	Heterogeneous	
156	49	1320	HGSC	4	IDS	Optimal	4 carboplatin	1 carboplatin	5	8	Homogeneous	HRD
200	59	602	HGSC	3C	IDS	Optimal	4 carboplatin	2 carboplatin	>6	>6	Heterogeneous	
223	43	2074	HGSC	3C	Primary	Optimal	NA	3 carboplatin	>6	>6	Heterogeneous	
228	59	2349	HGSC	4	Primary	Optimal	NA	6 carboplatin	>6	>6	Heterogeneous	
226	83	1964	Low grade serous	3C	Primary	Optimal	NA	Tamoxifen	>6	>6	Homogeneous	HRD
167	63	600	Neuroendocrine	3C	Primary	Optimal	NA	Cisplatin, etoposide	6	>7	Heterogeneous	
209	52	419	HGSC	3C	IDS*	Optimal	4 carboplatin	2 carboplatin	>7	>7	Homogeneous	HRC
217	81	2738	HGSC	3C	No surgery		3 carboplatin	6 carboplatin	>7	>7	Heterogeneous	
180	50	521	HGSC	3C	IDS	Optimal	3 carboplatin	3 carboplatin	8	>9	Homogeneous	HRC
179	66	57	HGSC	4	IDS	Optimal	4 carboplatin	2 carboplatin	8	>14	Heterogeneous	
185	58	500	HGSC	4	IDS	Complete	4 carboplatin	2 carboplatin	>9	>9	Heterogeneous	
186	47	74	HGSC	3C	Primary	Complete	NA	6 carboplatin	>9	>9	Homogeneous	HRC
157	58	500	HGSC	3C	Primary	Suboptimal	NA	6 carboplatin, tamoxifen	10	12	Homogeneous	HRC
201	55	678	HGSC	3C	Primary**	Optimal	NA	6 carboplatin, tamoxifen, rucaparib	11	36	Heterogeneous	
183	82	6388	HGSC	2C	Primary	Complete	NA	4 carboplatin	>13	>13	Homogeneous	HRD
163	77	500	HGSC	3C	Primary	Optimal	NA	5 carboplatin	13	>20	Heterogeneous	
168	66	1500	HGSC	3C	Primary	Complete	NA	6 carboplatin	14	>15	Homogeneous	HRC
155	55	117	Adenocarcinoma	3C	Primary	Optimal	NA	FOLFOX	15	18	Homogeneous	HRD
174	45	552	Endometrioid	3A	Primary	Complete	NA	6 carboplatin, 2 paclitaxol, 4 docetaxol	>16	>16	Heterogeneous	
184	73	9740	HGSC	4	IDS	Suboptimal	4 carboplatin	2 carboplatin	>16	>16	Heterogeneous	
162	68	186	HGSC	3C	Primary	Optimal	NA	6 carboplatin	>21	>21	Homogeneous	HRC
158	68	780	HGSC	3C	Primary	Optimal	NA	6 carboplatin	>22	>22	Homogeneous	HRD

Table 5.6 - 3: PCO patient demographics with heterogeneity of HR function ordered by progression free and overall survival.

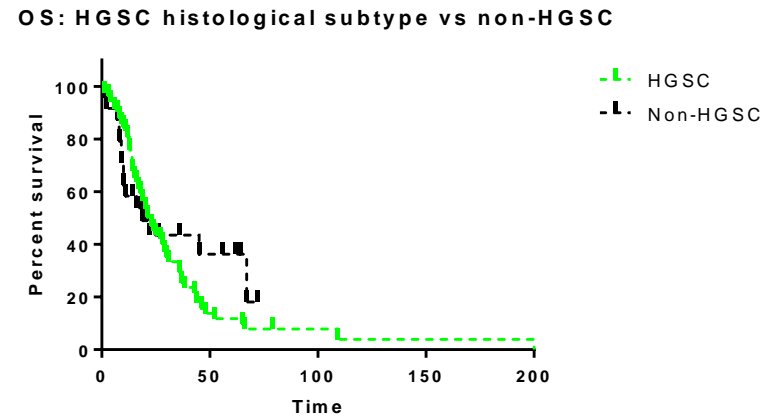
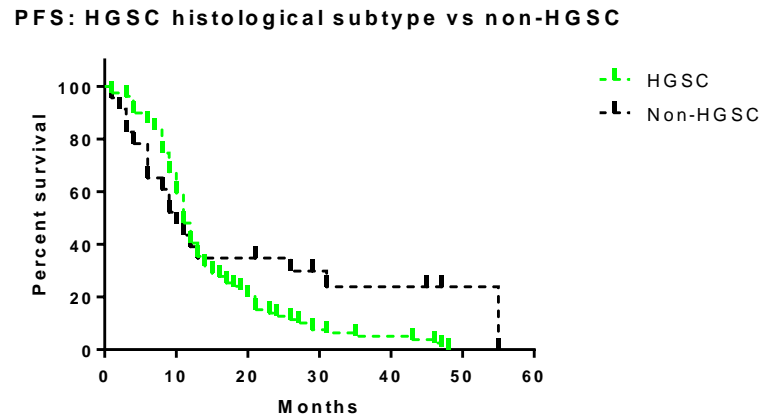
5.7. HR of Ascites as a Prognostic Marker

Sampling multiple areas of tumour in every patient may not be feasible routinely. By hypothesising that cells from all intra-peritoneal areas are released into ascites, we can hypothesise that, collectively, ascitic cells are representative of the entire tumour and therefore functional status of ascitic cultures should correlate with clinical response to therapy and overall outcome. Stratifying patients into HRC and HRD groups reveals separation of the PFS survival curves at 30 months, Figure 5.7 - 1. The median PFS for HRD tumours was 12 months compared to 11 months in the HRC group, (log-rank, $p = 0.0750$). This disease-free benefit is lost with continued follow-up with no significant difference in overall PFS or OS. This may be a reflection of the changing biological function of the tumour with time with possible emergence of resistance in HRD to HRC followed by overgrowth of a new HRC population or growth of a pre-existing HRC population already present in a heterogeneous tumour.

A



B



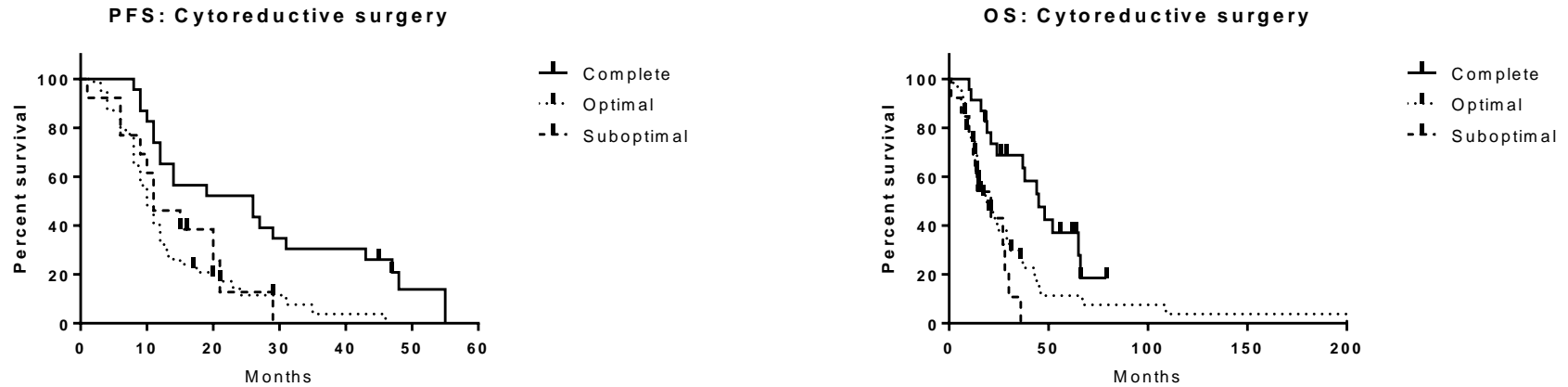
C

Figure 5.7 - 1: Kaplan-Meier survival curves for PFS/OS by HR status (A), histological subtype (B) and outcome of cytoreductive surgery (C)
 A, Overall median PFS in the HRD and HRC groups being (12 vs. 11 months, log-rank, $p = 0.1545$). Median OS was 21 months in HRD group compared with 23 months in HRC group (log-rank, $p = 0.7879$).
 B. Median PFS was 11 months in HGSC, 32 in mucinous disease, 9 in clear cell, 55 for endometrioid cancer and 6 months for mixed tumours ($p = 0.0128$). OS was 23 (HGSC), 30.5 (Mucinous), 13 (clear cell), 60 (endometrioid) and 10 for mixed tumours ($p = 0.0668$). When grouped into HGSC ($n=79$) and non-HGSC ($n=23$), HGSC had a median survival of 11 months compared to 10 months for non-HGSC ($p = 0.0781$). The OS for HGSC was 23 months compared to 19 months for non-HGSC ($p = 0.4426$).
 C. Stratifying patients into surgical outcome (complete, optimal or suboptimal cytoreduction) shows median PFS of 26, 10, 11 months respectively ($p = 0.0011$), OS was 38, 15 and 15 months ($p = 0.0024$).

5.8. Histology as a Prognostic Marker

Combining data from all PCO ascitic cultures with HR status (n=109) collected from 2007 – 2011 (Mukhopadhyay 2010) with that in this thesis (2011 – 2014), demonstrates the relative incidence of HRC and HRD tumours within each histological subtype, Figure 5.7 - 1, Table 5.8 - 1. No relationship can be seen between histological subtype and HR status, with approximately 50% of each subtype being HRC. Although differences can be seen between the PFS and OS of patients subdivided according to histological subtype, numbers within some of the less common subtypes are small. Histological subtype may be a contributory factor to PFS due to the different stages of presentation and the cytoreductive rate achieved with surgery.

Histological Subtype		HR Competent n (%)	HR Defective n (%)	Chi ² P
HGSC	n = 81	43 (53.1)	38 (46.9)	0.5485
Mucinous	n = 4	2 (50.0)	2 (50.0)	-
Clear cell	n = 2	2 (100)	0 (0)	-
Endometrioid	n = 4	2 (50.0)	2 (50.0)	-
Mixed	n = 11	7 (63.6)	4 (36.4)	0.0051 *
Other	n = 7	4 (57.1)	3 (42.9)	0.1615

Table 5.8 – 1: Incidence of HRC and HRD by Histological Subtype. HR status was determined by quantification of nuclear Rad51 foci following induction of DNA DSB with 2 Gy irradiation and incubation with 10 µM rucaparib. HRC was defined as more than a 2 fold increase in Rad51 foci formation, in comparison to untreated controls.

5.9. Surgical Cytoreduction as a Prognostic Marker

Patients underwent primary cytoreductive surgery or NACT followed by interval surgery (IDS). All surgeries were carried out at NGOC by accredited Gynaecologic Oncology consultants. Complete or optimal cytoreduction (residual disease of less than 1 cm in its largest diameter) has been shown to be the best predictor of PFS and OS (Gadducci 2005, Wimberger, Lehmann et al. 2007). This data shows significant differences in PFS and OS in patients with complete/optimal cytoreduction at the time of initial surgery. There was an excess of HRC in both the completely cytoreduced and the suboptimally cytoreduced groups and therefore it is unlikely that HR status affects

cytoreduction or is responsible for the improved survival in the complete/optimal cytoreduced groups, Table 5.9 - 1.

	HRC n (%)	HRD n (%)	Chi ² p
Complete	14 (60.9)	9 (39.1)	0.0278 *
Optimal	34 (54.0)	29 (46.0)	0.4237
Suboptimal	8 (61.5)	5 (38.5)	0.0161 *

Table 5.9 – 1: The Distribution of Cytoreductive Surgical Outcome within the Homogeneous and Heterogeneous Tumour Groups. Complete cytoreduction is defined as no visible macroscopic tumour at the end of the procedure, optimal as visible disease <1cm in greatest diameter and suboptimal cytoreduction as >1cm residual disease.

5.10. Longitudinal Sequential Samples

The majority of patients with ovarian cancer recur despite optimal surgery and aggressive chemotherapy. It is unclear if intratumoural heterogeneity exists following chemotherapy. During the study period, five patients had samples collected at two time points, Figure 5.10 - 1.

In this small mixed series, it can be seen that in one patient (PCO 177/222), the HR status of the PCO culture generated from her ascites preoperatively appears to have converted from HRC to HRD, following 2 lines of chemotherapy. In another patient (PCO 219/234), the PCO culture from ascites appears to have converted from HRD preoperatively to HRC after 4 cycles of carboplatin chemotherapy. These apparent changes in the HR status of ascites may be a result of sampling, inaccurate HR assays but may also reflect the heterogeneous nature of the entire tumour volume with ‘shedding’ of different dominant populations into ascites at any one time.

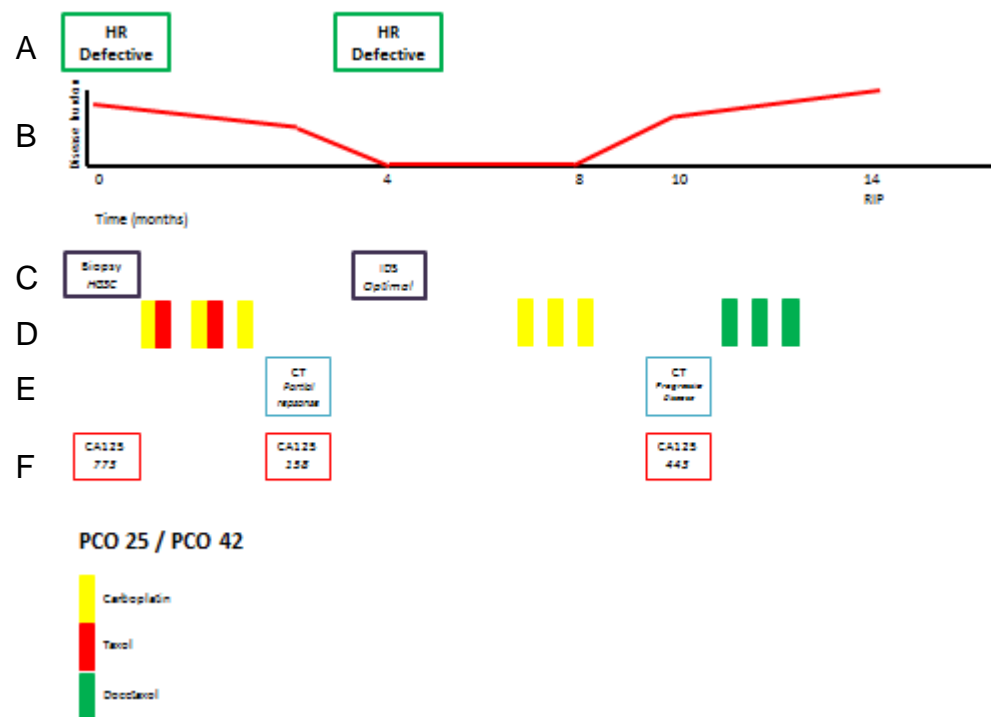
Recurrent disease may represent a regrowth of tumour, which is biologically identical to the original cancer or provision of chemotherapy may induce growth of new subpopulations, biologically distinct to the original tumour. In heterogeneous tumours, recurrence may represent overgrowth of subpopulations that are resistant to the chemotherapy given. Irrespective of the cellular origin of active disease at any one time point, it seems likely that the

growing populations of cells will continue to acquire new mutations that may accumulate to modify tumour behaviour and response to therapy. Therefore, it should not be presumed that a tumour, which was clinically responsive to first line chemotherapy at presentation, should remain responsive at the time of relapse and perhaps serial tumour sampling, with accurate molecular profiling at several time points throughout the course of a patients disease course, should be considered.

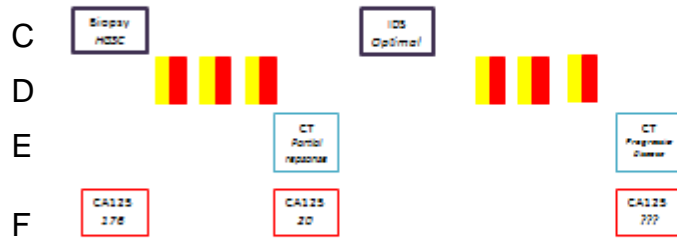
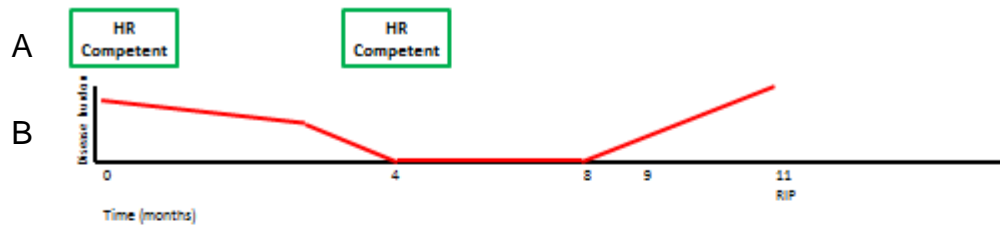
Figure 5.10 - 1: Longitudinal sampling

Key

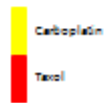
- A: HR functional status (Rad51 assay) from cultured ascites
- B: Graphical representation of volume of disease burden based upon clinical status
- C: Surgical treatment
- D: Chemotherapy regimen
- E: Radiological assessment of disease status
- F: Biochemical measurement of serum CA125 (U/L)



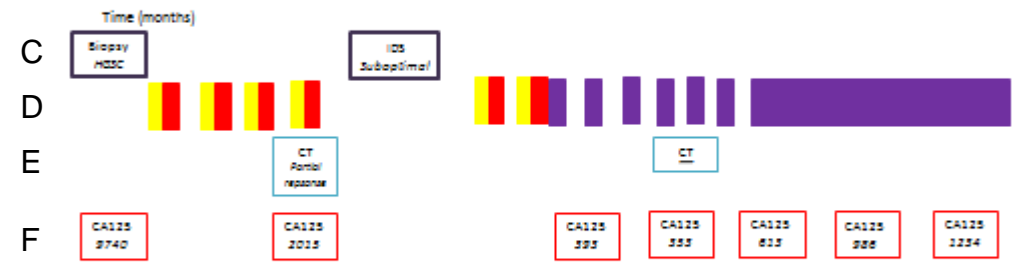
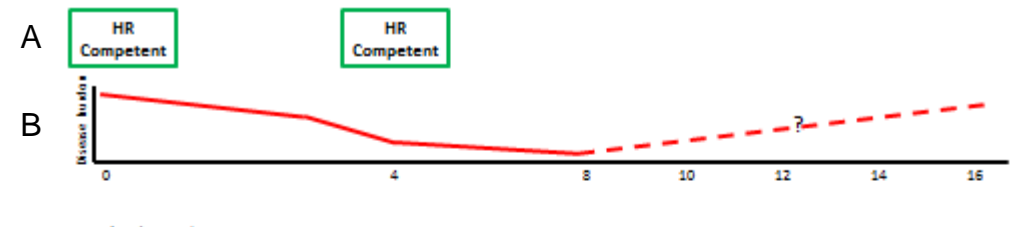
PCO 25: Presented with abdominal distension and ascites (ward paracentesis). NACT (3 carboplatin and 2 taxol). Repeat ascitic sample at IDS – optimal debulking. Post-op 3 carboplatin chemotherapy. Clinical recurrence (PFS 10 months), treated with 3 docetaxol. OS 14 months.



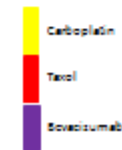
PCO 169 / PCO 181



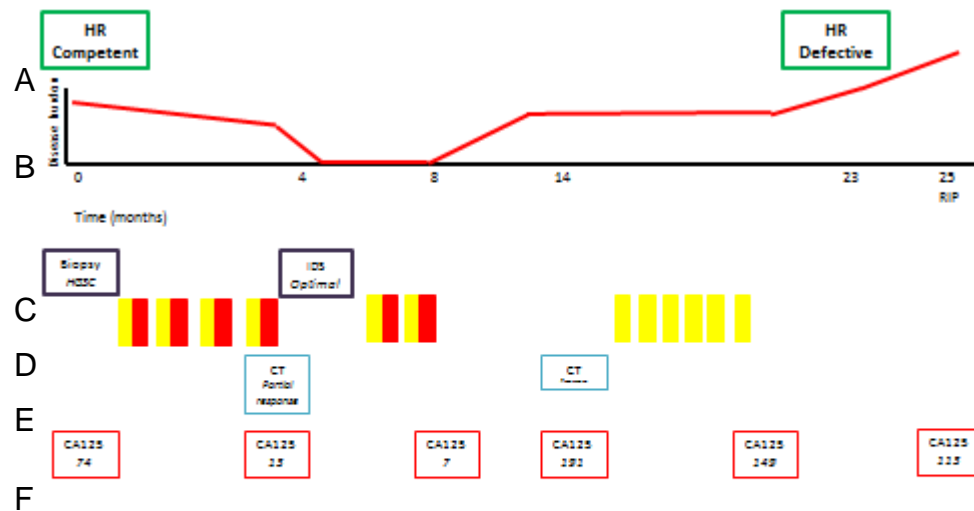
PCO 169: Presented with abdominal distension and ascites (ward paracentesis). NACT (3 carboplatin and taxol). Repeat ascitic sample at IDS – optimal debulking. Post-operative 3 carboplatin and taxol. PFS 9 months, OS 11 months.



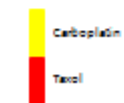
PCO 170 / PCO 184



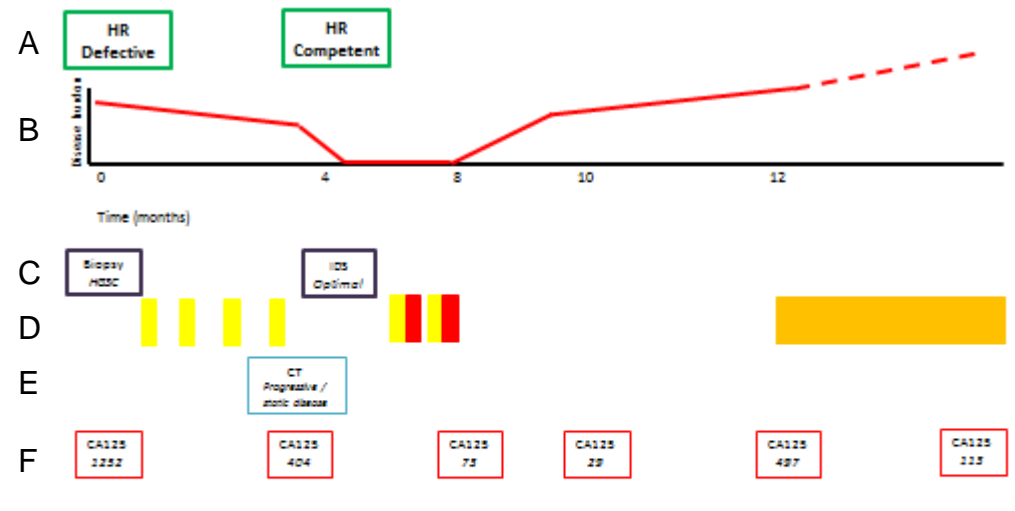
PCO 170: Presented with abdominal distension and ascites (ward paracentesis). NACT (4 carboplatin and taxol). Repeat ascitic sample at IDS –sub optimal debulking with more than 1 cm residual disease. Post-op 2 carboplatin and taxol chemotherapy. Bevacizumab (suboptimal debulk), given as 6 cycles then maintenance therapy. Climbing CA125 suggesting possible development of recurrent disease. OS 27 months.



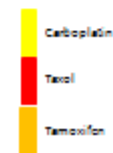
PCO 177 / PCO 222



PCO 177: BRCA 1 carrier. Presented with abdominal distension and ascites (ward paracentesis). NACT (4 carboplatin and taxol). IDS – optimal debulking. Post-op chemotherapy completed with 2 carboplatin and taxol. Clinical recurrence 6 months before re-challenging with 6 further carboplatin. Ascites resampled at 23 months (9 months following diagnosis of recurrence) were HR defective. PFS 13 months, OS 23 months.



PCO 219 / PCO 234



PCO 219: Presented with abdominal distension and weight loss (ward paracentesis). NACT (4 carboplatin). IDS – optimal debulking. HR function of ascitic culture changed from defective to competent. Post-op chemotherapy completed with 2 carboplatin and taxol. Clinical recurrence at 4 months treated with Tamoxifen. Alive and well at 13 months.

5.11. Discussion

5.12.1. *Heterogeneity*

Inter-tumour Heterogeneity

The classification of EOC into histological types is well established and we understand that the observed clinical differences among tumour subtypes are likely to reflect different underlying molecular mechanisms associated with a variety of genetic mutations. The differences seen in survival between the PCO patients with different histological subtypes are small. These differences are independent of HR function (with equal proportions of HRC and HRD within each subtype) and independent of cytoreductive surgery outcome (with equal proportions of optimal cytoreduction in each histological subgroup). Histological subtype may therefore be only a crude marker of some underlying biological differences that contribute to response to chemotherapy and overall prognosis. When assessed in isolation, there is not a statistically significant difference seen in PFS and OS in HRC and HRD groups. The separation of the PFS curves at about 30 months, following treatment between the two functional groups, does however suggest that HR function of ascitic cultures is important in reflecting tumour response to treatment in at least the short term, section 5.7. The initial survival benefit seen in patients with HRD tumours is however lost with time and it may be over ambitious to expect a single measure of the tumour, taken at a single time point to predict overall outcome. We understand that the management of recurrent disease is highly variable and only some patients may go on to receive secondary and tertiary treatments for recurrent disease with variable cytotoxic agents and or surgical strategies used. Additionally, as time goes on, the biology of the tumour may change. None of these factors were taken into account during the simplistic analysis of the data shown in this chapter.

In reality, it is likely that there are several prognostic markers as well as biomarkers of disease response and it may be needed in future clinical practice

to develop an algorithm to combine these markers in order to guide clinical practice accurately. The understanding of intra-tumoural heterogeneity further complicates our ability to accurately combine biomarkers with response to cytotoxic agents.

Intra-tumour Heterogeneity

In this study, we provide evidence that a large proportion of ovarian cancer patients have heterogeneous tumours in terms of antigen expression, cellular growth and HR function, with 12/25 (48%) tumours demonstrating heterogeneity in HR status when two or more samples are taken. This may in fact be an underestimation of intra-tumoural heterogeneity and increased sampling may reveal a higher proportion of heterogeneity in future studies. Functional intra-tumoural heterogeneity was not predictable by assessment of morphology, antigen expression or growth, reinforcing the importance of a novel functional assay to characterise tumour deposits. Antigen expression may just be a marker of the particular site of disease sampled and have no relevance to the underlying biology. The correlation of DNA damage repair status and correlation with cytotoxic sensitivity seen in this study is important as it not only demonstrates the clinical relevance of the approach of functional analysis, section 5.5.6, but also suggests that heterogeneity may have clinical relevance.

The new appreciation of intra-tumoural heterogeneity of HR pathway function may help to explain some of the results in this project, for instance discordance between expression of CA125 using IHC in FFPE tissue and CA125 expression on cultures assessed by IF. It may also explain why some patients with HRD ascitic cultures have short PFS and OS despite optimal cytoreduction (with possible residual microscopic HRC disease). However, it may also mean that the HR result from ascites is not representative of the entire tumour and that a more complex analysis may be required in order to assess the overall impact of HR function in the clinical setting.

The apparent changes in the HR function in ascitic cultures obtained from the same patient at different time intervals in their treatment may be a reflection of the changing biology of the tumour with time or may reflect shedding of different cell subpopulations into ascites at different times, depending upon the predominant proliferating area of tumour. The HR function of ascitic culture from PCO 219 appears to have changed from HRD to HRC in just four months, which is unlikely (but not impossible) to be sufficient time for genomic changes to result in a change in a whole pathway. A more likely explanation is sampling of a different subpopulation. The variable growth and regression of different areas of tumours simultaneously is widely appreciated and often causes difficulties in clinical practice in judging if tumours have responded or progressed over time with chemotherapy treatment. The fact that PCO 177 (section 5.11) expectantly changed from HRC to HRD over 23 months may therefore not necessarily reflect a series of revertant mutations resulting in a change in HR function but instead may reflect overgrowth and shedding of cells from a new area of tumour, which was previously small or dormant. Given that dysfunction of DNA damage repair pathways are also key driver events (Curtin 2012), it is perhaps unsurprising to see variable DNA repair status in different areas of the same tumour representing these different, early divergent clones, Figure 5.12 - 1.

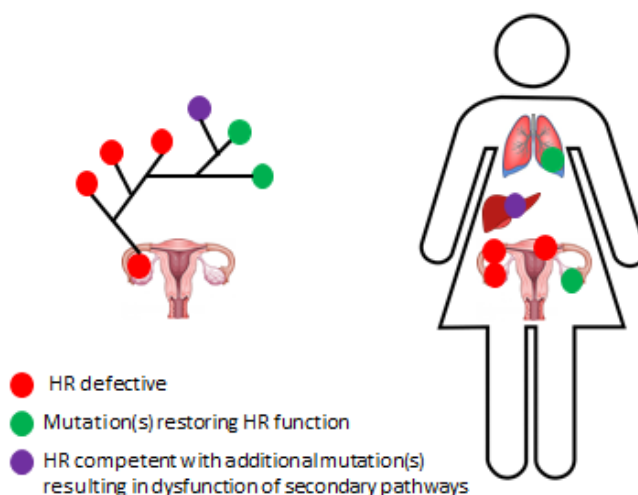


Figure 5.12 - 1: Tumour Evolution and Intra-tumour Heterogeneity

Despite clear differences in response to cisplatin and rucaparib *ex vivo* between the HRD and HRC groups (section 4.13), this did not translate to differences in PFS and OS. The impact of ITH upon PFS and OS is difficult to interpret in this small cohort and is additionally complicated by the many variable clinical factors, many of which have not been taken into account during this analysis. These data suggest that that tumours demonstrating heterogeneity at presentation are more likely to respond to treatment resulting in better PFS and OS. This was unexpected as it was hypothesised that ITH would lead to a greater chance of selecting a drug-resistant sub-population or the genomic instability it reflects would have a greater likelihood of acquiring mutations associated with resistance/progression. Interestingly the homogeneous HRD group had the worst outcome, which but it is unclear if this is a consequence of the small sample size or a true reflection of underlying biology. Further investigation in a larger cohort is essential.

ITH may therefore reflect underlying tumour genomic instability. Homogenous tumour may have acquired driver mutations at an early stage in tumour evolution and is therefore more genetically stable, resulting in less response to chemotherapy. In the series of 14 patients, with 135 samples by Schwarz *et al* greater heterogeneity in terms of genomic clonal expansion correlated with poorer PFS and OS (Schwarz 2015). This cohort of patients was however clinically not comparable to the dataset in this series, with 99% of patients being treated with NACT and almost all samples taken at IDS following chemotherapy. Comparisons to the disease's molecular profile at presentation were based upon a single diagnostic biopsy and did not take into account spatial intra-tumour al heterogeneity that existed before treatment commenced.

We have previously demonstrated a very strong correlation between HR status and *ex vivo* sensitivity to the PARP inhibitor rucaparib, using cells cultured from just one compartment, namely ascites (Mukhopadhyay 2010), with responses seen in approximately 50% of cases (Mukhopadhyay 2012). However, in clinical practice, response rates in non-germline BRCA 1 and 2 patients are only 24% (Gelmon 2011). This may be a result of underlying heterogeneity at

presentation and subsequent clonal selection pressure as a result of initial chemotherapy.

The demonstration in this study that the results of predictive biomarkers will be affected by intra tumour heterogeneity has ramifications for future translational research and biomarker directed therapy. There are several hypotheses that must be considered. The functional status of the ascitic culture may be a reflection of the status of the bulk of the tumour from which tumour cells are shed into the abdominal cavity. Following surgery, the patient's response to subsequent chemotherapy may be more likely to be dependent upon the functional status of the subpopulations of tumour, which has not been excised rather than that of the bulk of the tumour, which has been excised. If the functional status of the residual tumour is different from that of the excised tumour, then the biomarker may be falsely rejected as inaccurate when, in fact, this is a reflection of sampling error. It is therefore crucial that future studies include multiple biopsies to allow assessment of ITH and that protocols that require sequential biopsies, taken before and after treatment, attempt to collect these biopsies from the same tumour site to minimise the risk of selecting non-paired clones.

Further work is required to extend this work. In particular, multi-site longitudinal tissue sampling, integrating functional, genomic and clinical data, has the potential to reveal the composition of subclones and track tumour evolution to address the true effect of heterogeneity upon response to therapy and to begin to define the breadth of genetic diversity. Correlation of molecular heterogeneity with disease location (intra peritoneal versus extra peritoneal) would additionally provide insight into the biology of the metastatic process in ovarian cancer and such studies may provide further evidence for drug-resistance mechanisms informing combinatorial, adaptive, and tumour immune therapies placed within the context of tumour evolution..

5.12.2. Other Factors Which May Impact Upon Survival

The one factor, which is repeatedly reported in the literature and also found in this case series as predictive of outcome is the success of cytoreductive surgery. Complete > optimal > suboptimal cytoreduction has been shown in this data set to be predictive of greater PFS and OS, which is independent of HR function and histological subtype, section 5.7, 5.8, 5.9.

In vitro sensitivity to cytotoxic agents provides an indication of tumour sensitivity but even culturing primary patient samples has limitations and may therefore not be entirely predictive of overall clinical response. The process of culture may select out certain subpopulations and the limited life span of primary cultures and slow growth seen suggests that vital environmental support may be lacking. Future work may explore alternative methodologies to incorporate growth of the tumour's stroma in an attempt to prolong culture lifespan.

The ability of ex vivo culture sensitivity to cisplatin to predict clinical sensitivity was described in Chapter 4 and the AUC (ROC curve) of 0.5530 (95% CI 0.3998 – 0.7062) demonstrated poor test accuracy, Figure 4.13 – 7. The inability of *in vitro* cisplatin sensitivity alone to accurately predict clinical response may in part be a reflection of the variation in surgical management. Unexpected prolonged PFS was seen in women with HRC tumours with *in vitro* resistance to cisplatin and this may be a reflection of the high rate of optimal/complete surgical debulking in this cohort. Complete or optimal cytoreduction (residual disease of less than 1 cm in its largest diameter) remains the best predictor of PFS and OS, Figure 5.7 - 1. It is likely however, that overlooking intra-tumoural heterogeneity by sampling and testing only one area of tumour may significantly distort our interpretation of response to cytotoxic agents when tested clinically.

5.12.3. Evidence of the Fallopian Tube as the Origin of Ovarian Cancer

There is substantial evidence to indicate that HGSC actually arises from the fallopian tube. Within this case series of solid tumour culture, four cultures were successfully created from macroscopically normal tubes. Although numbers are small and therefore no firm conclusions should be drawn, this, alongside the concordance in expression of antigens between the tube and ascitic cultures, suggests that the tube is the likely site of origin. Interestingly, one of the tube cultures was found to be HRD potentially raising the possibility that HRD is an early event in carcinogenesis (providing the genomic instability that is an enabling characteristic of cancer) and these cells were pre-malignant. This possibility warrants further investigation in BRCA carriers undergoing prophylactic surgery to remove ovaries and fallopian tubes. Tumour cells may originate in the tube but are quickly shed into the peritoneal cavity, either depositing on the ovary resulting in formation of an ovarian mass or depositing on other peritoneal surfaces creating ascites. The inability of cells to seed in the fallopian tube may be a result of the unique, and not yet understood, functional ability of the tube epithelium. Comparisons between the antigen expression and functional HR status of each subculture can, in some circumstances, be suggestive of the mode of spread and evolution of the tumour, Figure 5.12 - 1.

5.12.4. The Tumour Microenvironment

In contrast to the prolonged and resilient growth of ovarian cancer *in vivo*, the life span of *ex vivo* cultures is typically short suggesting that there is something uniquely present within the tumour microenvironment required for growth.

It is now known that tumours are complex 'organs' consisting of malignant and many non-malignant cell types including cancer associated fibroblasts (CAFs), tumour associated macrophages (TAMs) and vasculature endothelial cells; all of which contribute to tumour cell survival, proliferation, angiogenesis, metastasis and drug resistance (Rebucci 2013). It is likely that there is a bi-directional interaction between the cancer cells and stroma and there is

significant evidence supporting the role of peri-tumoural tissues in tumour maintenance and the role of the stroma in the acquisition of resistance (Orimo 2006, Patocs 2007). It is also becoming increasingly apparent that the stroma can modify the aggressiveness of tumour cells and that tumour cells re-program the stroma to generate a nurturing environment that is crucial for tumour survival, progression and metastasis (Schauer 2011). This may in fact be an explanation for the poor PFS/OS seen in some patients with HRD cultures. At least some of the intra-tumoural heterogeneity seen in this series may be related to stromal interaction with the tumour.

During the culture of primary tumour, attention has focused upon the reliable isolation of malignant cells separate from the other cell types present in ascites or solid tumour. It is unclear what role, if any, that the stroma plays in maintaining and promoting cancerous, cellular growth or in determining tumour behaviour and ITH. Standard primary cell-culture systems, as used in this study, and cell-line xenografts have advanced our understanding of tumour behaviour. However, these methods have inherent limitations in evaluating the role of the tumour microenvironment. Modification of the culture method to include either growth of the actual tumour stroma or provision of an artificial stroma may create an optimal growth environment to maintain prolonged survival in culture. If culture of stromal cells is possible, it may be of interest to test stromal cultures for their HR function and to assess resistance to cytotoxics with and without concomitant culture with stroma to explore its effects. If the stroma has an impact upon intra-tumoural heterogeneity of HR function that we have found in ovarian cancer then it may be of interest to compare HR function at defined intra-abdominal sites between patients. *Ex vivo* tissue slices seem to be the most promising of techniques (Schmeichel 2003, Guyot 2007). The advantage of this approach is the ability to both maintain organ and cellular architecture, while also preserving the integrity of the tumour–stroma interaction (Umachandran 2006).

The difference seen in the median DT of solid tumour in comparison to ascitic cultures may be a reflection of differences in the cellular components of the

cultures. Solid tumour *in vivo* has a markedly different environment in comparison to malignant cells within ascites and perhaps the malignant component of solid tumour is more vigorous due to better nourishment through the vascular supply. This may result in a more robust primary culture with a greater growth rate. Quantification of Ki-67, an established marker of cell proliferation, and correlation with SRB determined growth rate may clarify if the *ex vivo* growth rate is a true reflection of the tumour's proliferation rate.

5.12. Conclusions

ITH exists in ovarian cancer in terms of function of the HR DNA repair pathway. This results in a variable response to cytotoxic agents between cultures taken from different areas of tumour from within the abdominal cavity and offers one possible explanation for clinical resistance to chemotherapy seen in tumours with HRD cells within the culture from ascitic fluid. Thus ITH is not predictable from morphological appearances or from antigen detection. It is now clear that a single biopsy, from any site, is insufficient if chemotherapy agents are to be stratified based upon tumour biology.

A change in the approach to tumour sampling, classification of tumours and quantification of response to therapy is needed if novel chemotherapies are to result in improvement in PFS and OS.

Chapter 6. Sapacitabine as a Therapeutic Agent in the Treatment of Ovarian Cancer

6.1. Introduction

The ideal agent for the treatment of ovarian cancer would be orally bioavailable, non-toxic, highly targeted and paired with a reliable biomarker capable of accurately predicting the response to therapy. Pairing targeted cytotoxic agents with biomarkers is particularly important in ovarian cancer. Patient frailty and the high frequency of comorbidities prevent polypharmacy and provision of successive ineffective therapies is unlikely to translate into a survival benefit. A biomarker would enable accurate stratification of therapy to those patients who are likely to benefit preventing overtreatment and increasing overall response rates

6.1.1. Nucleoside Analogues: Alternative Targeted Agents

Nucleoside analogues are a major class of antimetabolite cytotoxic agents and were among the first chemotherapeutic agents to be introduced for the treatment of cancer. The anticancer nucleosides include several analogues of pyrimidine and purine that compete with physiological nucleosides and interact with a large number of intracellular targets to induce cytotoxicity. These agents can exert their cytotoxic activity by being incorporated into and altering DNA and RNA macromolecules themselves, by interfering with various enzymes involved in synthesis of nucleic acids or by modifying the metabolism of physiological nucleosides (Galmarini, Mackey et al. 2002).

Nucleoside analogues have been in clinical use for almost 50 years and have become cornerstones of treatment of cancer and viral infections. Following the discovery of fluracil in the 1950s, cytarabine was approved for the treatment of acute myeloid leukaemia (AML) by the FDA in 1969 and since this time numerous nucleoside analogues have been evaluated in patients for the treatment of cancers (Jordheim 2013).

6.2. Sapacitabine

6.2.1. Structure

Sapacitabine is an oral cytosine nucleoside analogue and is the pro-drug of 2'-C-cyano-2'-deoxy-1-β-D-arabino-pentofuranosyl-cytosine (CNDAC).

Sapacitabine has been explored as an alternative agent for the treatment of ovarian cancer (Shapiro 2012). The structure of CNDAC is very similar to that of the other nucleoside analogues but it functions in a different way and therefore arguably should not be included in this class of drug, Figure 6.2 - 1. The incorporation of an additional N4-palmitoyl group (Kaneko 1997, Hanaoka 1999) results in protection of the amino group of CNDAC (reduced inactivation by deamination (Liu 2012)), resulting in better diffusion into the gastrointestinal cells, thereby enabling oral administration (Serova 2007).

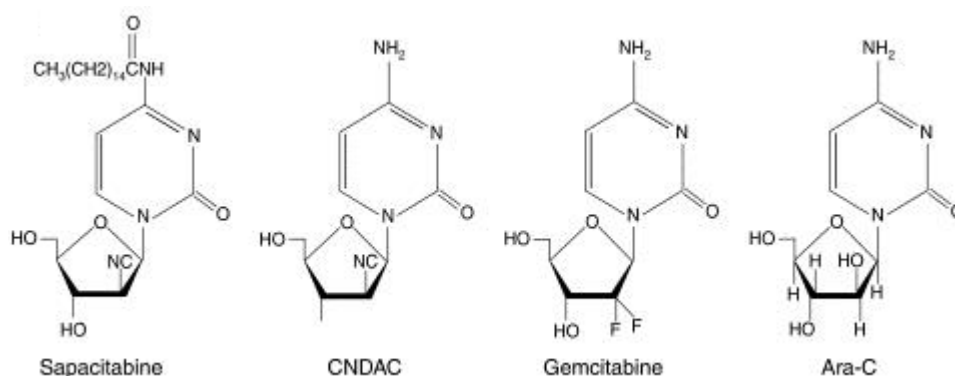


Figure 6.2 - 1: Structure of Sapacitabine, CNDAC, Gemcitabine and Ara-C (Serova 2007).

6.2.2. Function and Mechanism of Action

Sapacitabine is primarily metabolised by plasma, gut and liver amidases into the active metabolite CNDAC, which subsequently enters the cell via the human equilibrative nucleoside transporter (hENT) (Serova 2007). It has a novel mechanism of action by becoming incorporated in the DNA chain and interfering with DNA synthesis by inducing DNA damage.

CNDAC is phosphorylated by deoxycytidine kinase (dCK) to form CNDAC triphosphate, which accumulates in a concentration-dependent manner (Azuma, Huang et al. 2001) and competes with dCTP for incorporation into DNA (Azuma, Huang et al. 2001) by DNA polymerase α (Hayakawa 1998, Hanaoka 1999, Azuma, Huang et al. 2001, Serova 2007). Rather than cause chain termination, like the other nucleoside analogues, resulting in S-phase arrest/collapsed replication forks (Plunkett, Huang et al. 1995) CNDAC causes G2 arrest in a number of cell lines (Liu 2005) through activation of the G2 checkpoint through the canonical Chk1-Cdc25C-Cdk1/CyclinB1 signal pathway following induction of DNA damage (Liu 2012)..

Ligation of the 3'-hydroxyl of the analogue by incorporation of subsequent deoxynucleotides initiates β -elimination (Liu 2010). In DNA, this process cleaves the phosphodiester linkage 3' to the analogue as the CNDAC nucleotide is rearranged to form 2'-C-cyano-2',3'-didehydro-2',3'-dideoxycytidine (CNddC) (Liu 2010), Figure 6.2 - 2. CNddC nucleoside is unique and lacks the 3'hydroxyl group and is subsequently not a substrate for repair by ligation, nor can it be extended without processing to remove the chain-terminating analogue (Liu 2012). This functionally prevents repair until CNddC is removed. The presence of CNddC at the 3' terminus acts as a DNA chain terminator forcing the formation of a single-strand DNA breaks or nicks during first S-phase which are repaired to only a small extent by the TC-NER pathway (Hayakawa 1998, Hanaoka 1999, Azuma, Huang et al. 2001, Wang 2008).

CNDAC has been demonstrated to have potent anti-tumour activity in a number of preclinical trials across multiple tumour types. The antiproliferative effects of CNDAC in terms of IC₅₀ values were more potent than those observed with ara-C (Matsuda, Nakajima et al. 1991, Tanaka 1992). In two separate studies, broad spectrum activity has been demonstrated across a panel of tumour cell lines (Hanaoka 1999, Serova 2007).

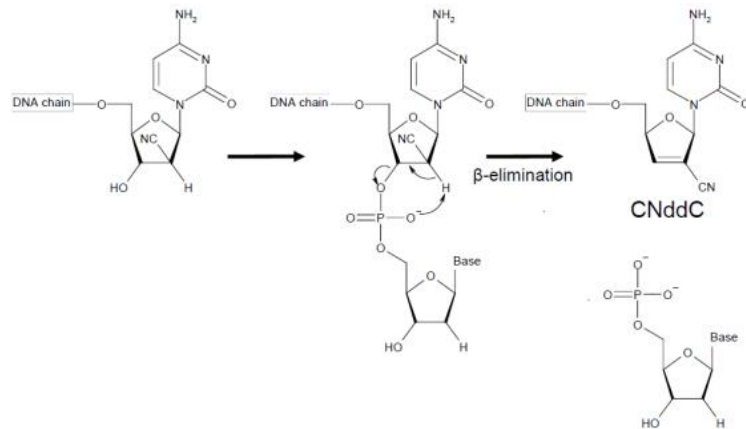


Figure 6.2 - 2: Incorporation of CNDAC into DNA, β -elimination Resulting in CNddC. Adapted from (Azuma, Huang et al. 2001)

During subsequent replication, unrepaired SSB are converted to DSB in second S-phase and, if not repaired, lead to cell death phase (Hanaoka 1999, Azuma, Huang et al. 2001, Liu 2010). Repair of replication-associated DSB or collapsed replication forks is primarily dependent upon the HR pathway, Figure 6.2 - 3.

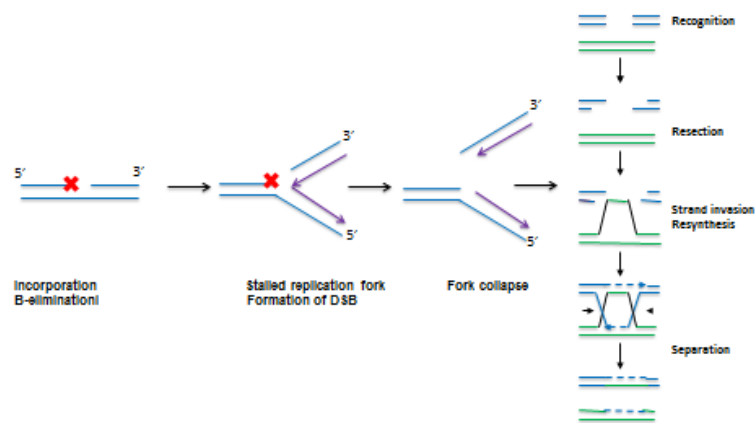


Figure 6.2 - 3: S-Phase stalled replication forks SSB are formed after incorporation of CNDAC into DNA that are converted to stalled replication forks or DSB when cells enter the second S phase during replication. DNA DSB require repair by homologous recombination (HR) repair.

6.2.3. Sapacitabine and DNA Repair Pathways

The repair mechanisms of CNDAC-induced DNA damage are largely unknown.

Sapacitabine and Homologous Recombination Repair

An understanding of the DNA pathways involved in CNDAC-induced damage is important for the identification of reliable biomarkers to facilitate treatment stratification. Several studies have suggested HR (section 1.4.7) as the major pathway for repair of sapacitabine induced DNA damage (Hayakawa 1998, Hanaoka 1999, Azuma, Huang et al. 2001, Wang 2008, Frame 2010, Liu 2010, Frame, Armour et al. 2012).

Inactivation or inhibition of ATM, BRCA2, Rad51 and XRCC3, key components of the HR pathway, has been shown to sensitise cells to sapacitabine (Liu 2010). Depletion of BRCA1 or BRCA2 by siRNA has also been shown to increase sensitivity to CNDAC as well as to platinum and PARPi agents but not to other nucleoside analogues (Frame, Armour et al. 2012). Similarly, BRCA2 mutation enhances CNDAC sensitivity (50x) but does not enhance gemcitabine sensitivity (Frame 2010). Further studies have demonstrated increased levels of components in the HR pathway in response to exposure to CNDAC (Liu 2010) suggesting pathway activation following exposure-related damage. CNDAC has also been shown to have additive or synergistic effects in combination with cisplatin and PARPi (Frame, Armour et al. 2012) indicating that it may have several roles in the management of ovarian cancer.

Sapacitabine and Non-homologous End Joining (NHEJ)

Evidence suggests that NHEJ (section 1.4.6) is not involved in CNDAC cytotoxicity. Cell line models defective in components of the NHEJ pathway are not more sensitive to CNDAC than their matched wild type cell lines and the DNA-PK inhibitor, NU7441, does not sensitise cells to CNDAC, indicating that the NHEJ pathway is unlikely to be critical for repair of CNDAC induced SSB (Liu 2010).

Sapacitabine and Nucleotide Excision Repair

NER (section 1.4.3) is the predominate pathway repairing platinum-DNA adducts, the predominant chemotherapy agent of choice in ovarian cancer. Lack of components of the transcription-coupled nucleotide excision repair (TC-NER) pathway has been shown to render cells 3- to 5-fold more sensitive to CNDAC-induced cytotoxicity, and it is thought that the single-strand nick caused by CNDAC is recognized and, in part, repaired by the TC-NER pathway (Wang 2008). However, the overall removal rate of the analogue from DNA is a relatively slow process and it is thought that single-strand nicks are in fact converted to DSB during mitotic processes prior to initiation of TC-NER repair (Liu 2010). This was supported by biochemical evidence of activation of H2AX phosphorylation and the physical indicators of DSB formation demonstrated by both pulsed-field gel electrophoresis (PFGE) and neutral comet assays following pulsed treatment with CNDAC (Liu 2010).

Sapacitabine and Base Excision Repair

The incorporation of CNDAC into DNA with subsequent collapse of the replication fork also results in damaged DNA bases and SSB, which may require repair by BER, section 1.4.2, at least until they are converted into DSB during replication. However, reports to date suggest it is not important in CNDAC cytotoxicity (Wang 2008).

Sapacitabine in Clinical Trials

Two multicentre Phase I clinical trials of CS-682 (an earlier orally bioavailable compound to sapacitabine) in patients with solid tumours demonstrated disease stabilisation in 11/47 patients with neutropenia limiting further dose escalation (Delaunoy 2006, Green, Choudhary et al. 2010), Table 6.2 - 1. The recommended Phase II dose was 40 mg/m². In the second trial, a range of CS-682 doses from 1.5 to 120 mg/m² were given in 4 weeks cycles (Delaunoy 2006). Six of the 40 patients included experienced stable disease with few non-haematological side effects and the recommended Phase II dose was 30 mg/m². The pharmacokinetic investigations incorporated into these trials

demonstrated oral administration of CS-682 resulted in blood concentrations similar to those of the cytosine nucleoside analogues, cytarabine and gemcitabine, although metabolic clearance by deamination occurred at a lesser rate (Liu 2012). Administered orally at the maximum tolerated dose of 40 mg/m² on the daily times 5 days schedule, the peak plasma concentration of 4.1 ± 1.2 ng/ml (approximately 8 nM) was observed at 2.0 h (Gilbert 2006).

In clinical trials sapacitabine has been shown to be efficacious in the treatment of several haematological malignancies in clinical trials and is currently in “SEAMLESS”, a Phase 3 trial for the first line treatment of acute myeloid leukaemia (AML) in elderly patients, Table 6.2 - 1. Additionally, a trial evaluating its use in various solid tumour malignancies showed measureable tumour shrinkage in 2/7 (28%) patients with ovarian malignancy (Shapiro 2012). TAS-109, a formulation of the parent nucleoside, was studied in solid tumours using 2 different schedules (Sankhala 2008). Myelosuppression was the dose-limiting toxicity but stable disease was observed in several patients within each dose schedule.

These studies, and those described in Table 6.2 - 1, demonstrate that the metabolic pathways observed in models systems are active in human and that several schedules of CS-682/sapacitabine administered orally generate plasma concentrations of CNDAC that have been shown to reduce clonogenicity of cell lines and primary AML cell in vitro (Liu 2010).

Importantly, initial clinical trials demonstrated response in patients who had not responded to treatment with cytarabine or decitabine (Liu 2012). Cross-resistance among these drugs was not apparent, providing rationale for combination strategies.

Study	Study Population	Trial Registration	Phase	Outcome	Reference
Safety and pharmacology study to treat advanced leukaemias or myelodysplastic syndromes	63 patients	NCT00380653	I	Complete remissions were achieved in 6 patients. Median survival was 252 days. 41% of patients received sapacitabine for 4+ cycles. The 30-day mortality rate from all causes was 5%.	(Kantarjian 2010, Garcia-Manero 2012)
Oral sapacitabine for the treatment of AML in elderly patients	105 patients aged 70 years or older treatment naive or at first relapse	NCT00590187	II	Randomisation to 3 schedules: (A) 200 mg bd 7 days, (B) 300 mg bd 7 days, (C) 400 mg bd 3 days. 1-year OS was 35% in (A), 10% in (B), and 30% in (C). 14/105 died <30 days and 27 died <60 days. Grade 3-4 adverse events: anaemia, neutropenia, and thrombocytopenia. Grade 5 events: pneumonia and sepsis.	(Kantarjian 2009, Kantarjian 2012)
A randomized phase 2 study in patients with advanced cutaneous T-cell lymphoma	16 patients after failure of ≥1 systemic therapies	NCT00476554	II	Partial remissions were observed in three patients.	JH Chiao Cyclacel
Study of sapacitabine in AML	Open label trial of patients with newly diagnosed AML	NCT01211457	I/II Recruiting	Sapacitabine in alternating cycles with decitabine. 30-day mortality from all causes was 4.5% and 60-day mortality was 9.5%. The overall response rate was 34.8%.	(Ravandi 2011)
A phase 2 trial for relapsed CLL/SLL with 11q22-23 deletion	40 patients with relapsed CLL / SLL	NCT01253460	II Recruiting	Oral sapacitabine once daily (days 1-3 of 28) with IV cyclophosphamide and IV rituximab. The primary outcome is overall response.	WG Wierda. MD Anderson
A phase 1 study of sapacitabine and seliciclib for solid tumours	124 patients with incurable solid malignancy	NCT00999401	I	Stable disease and tumour shrinkage was seen in 20 patients (5 NSCLC, 4 colorectal, 1 breast, 2/7 ovarian, 2 bladder, 2 GIST, 1 renal, 3 unknown primary, 1 SCLC and 1 parotid tumour).	(Shapiro 2012)
SEAMLESS: First line treatment of AML in elderly patients	485 patients >70 years	NCT01303796	III Recruiting	Multicentre, randomised, open-label trial comparing two drug regimens; sapacitabine sequentially with decitabine vs. decitabine alone. The primary outcome measure is overall survival.	H Kantarjian MD Anderson
A Phase 2 study in patients with previously treated NSCLC		NCT00885963	II	Open label multicentre trial for patients who have progressed after treatment with one or more platinum regimens. The primary outcome measure is rate of response and stable disease.	P Bonomi Rush Uni Med Centre

Table 6.2 - 1: CNDAC in Clinical Trials

AML: Acute myeloid leukaemia; CLL: Chronic lymphocytic leukaemia; SLL: Small lymphocytic lymphoma; NSCLC: Non-small cell lung cancer

Resistance to Sapacitabine

The clinical efficacy of nucleoside drugs depends on a complex interplay of transporters mediating cellular entry, efflux mechanisms that remove drugs from intracellular compartments and cellular metabolism to active metabolites.

Nucleoside transporters (NTs) mediate the uptake of physiologic nucleosides as well as anticancer and antiviral nucleoside drugs (Baldwin 1999) and the interaction between nucleoside drugs and intracellular enzymes (e.g. kinases, deaminases and nucleotidases) may regulate the rate and extent of metabolism of nucleoside drugs to cytotoxic derivatives (Damaraju 2003).

CNDAC is a hydrophilic nucleoside analogue that enters the cell via transmembrane equilibrative nucleoside transporters, ENT1 and ENT2. The abundance and tissue distribution of nucleoside transport proteins contributes to cellular specificity and sensitivity to nucleoside analogies (Mackey, Baldwin et al. 1998). The poor clinical response of patients to treatment with the nucleoside analogues cytarabine and gemcitabine has, through independent clinical research, been correlated with reduced levels or absence of ENT1 (Mackey, Yao et al. 1999, Galmarini 2002, Farrell 2009). In the same study, pancreatic cancer patients with high levels of ENT1 expression had a greater median overall survival following treatment with gemcitabine compared to that for patients with low or no ENT1 expression (Farrell 2009).

ENTs can be pharmacologically inhibited. Nitrobenzyl mercaptopurine ribonucleoside (NBMPR) is a potent inhibitor of ENT1 (IC_{50} of 0.4–8 nM) and a weak inhibitor of ENT2 (IC_{50} of 2.8 μ M) (Ward 2000, SenGupta 2002).

Dipyridamole (DP) inhibits both ENT 1 and 2 (with IC_{50} of 5 and 356 nM, respectively) (Pastor-Anglada 2005) and has been used for many years to prevent strokes and other vascular diseases due to its antiplatelet and vasodilating activities. NBMPR and DP reduce sensitivity to gemcitabine by 39- and 1,800-fold respectively by reducing the cellular uptake of gemcitabine (Mackey, Mani et al. 1998) and both agents have been used in this study to investigate the role of ENT in the sensitivity to CNDAC.

CNDAC activation is by deoxycytidine kinase (dCK) whilst deactivation occurs through deamination by cytidine deaminase (CDA) (Abbruzzese 1991, Owens 1992, Plunkett, Huang et al. 1995) generating the inactive uracil derivative CNDAU, Figure 6.2 - 4. It has previously been shown that cell lines with lower mRNA expression of hENT1 and deoxycytidine kinase (dCK) are more resistant to CNDAC than cell lines with higher expression (Serova 2007). Such cells were not cross resistant to sapacitabine, suggesting other mechanisms of resistance. Other enzymes such as cytidine deaminase (CDA) have recently been shown to play a role in sapacitabine resistance (Fleming 2007).

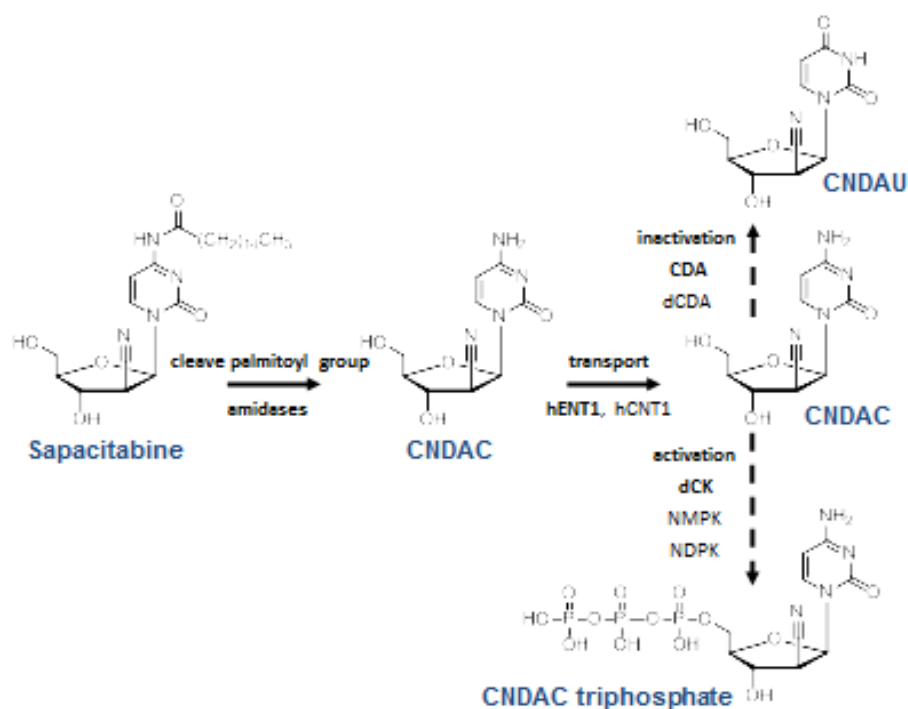


Figure 6.2 - 4: CNDAC metabolism.

CNDAC enters the cell via ENT1 before activation into CNDAC triphosphate by dCK. CNDAC triphosphate is then incorporated into the DNA Deactivation by β elimination. CDA deactivates CNDAC by deamination to CNDAU.

DNA Repair as a Mechanism of Resistance

The incidence of HRD tumours in ovarian cancer is approximately 50% and we would therefore anticipate that 50% of ovarian cancer patients would potentially respond to CNDAC. Testing CNDAC in primary cultures provides a more realistic model to explore the potential use of CNDAC in clinical practice.

6.3. Aims

- Assess the cytotoxic effect of CNDAC and the effect upon proliferation of cell lines with known mutations leading to homologous recombination dysfunction
- Determine the HR status of PCO samples derived from ascitic cultures with corresponding sensitivity to CNDAC, alongside rucaparib and cisplatin
- Establish if defects in other DNA repair pathways are determinants of sensitivity to CNDAC
- Establish a functional assay to test base excision repair status and assess its potential use as a biomarker for stratification of CNDAC therapy
- Explore the effect of variable CNDAC uptake (by ENT receptor), activation (by dCK) and deactivation (by CDA) upon *ex vivo* sensitivity to CNDAC

6.4. Methods

Methods for PCO and cell line culture alongside cell line descriptions and chemical reagents are described in Chapter 3. Detailed methods for colony formation assays, SRB proliferation assay, cell counting assay, the Homologous Recombination (HR) functional assay, PARP activity assay, and RNA analysis are also described in Chapter 3.

6.4.1. Cell lines

A panel of cell lines paired for defective BRCA1 or BRCA2 function with WT (VC8, VC8-BR2, VC8 PIR; UWB1-289 and UWB1-289-BR1) were used in initial experiments to assess the effect of HR status upon sensitivity to CNDAC. See Table 3.4 – 1, Chapter 3 for details of cell lines.

6.4.2. Growth Inhibition of BER Proficient and Deficient Cells by CNDAC With and Without Nucleoside Transport Inhibitors

Paired cell lines (AA8 –BER competent, and EM9 – BER defective with XRCC1 mutation; Chapter 3 methods) were seeded at a concentration of 1000 cells in 100 µl medium per well in 96 well plates. After 24 hours for adherence, media was aspirated and replaced with media containing increasing concentrations of CNDAC (0, 1, 3, 10, 30, 100 µM). NBMPR (0, 0.1, 1, 10 µM), DP (0, 300 nm, 3 µM, 30 µM) or methoxyamine (0, 1 mM, 5 mM, 20 mM) were added and cell density assessed after three doubling times (AA8: 48 hours; EM9: 54 hours), Table 6.4 - 1. All experiments were corrected for 1% DMSO and density normalised to CNDAC-free controls. The potentiation factor (PF), a measure of the increase in growth inhibition in the presence of BER or nucleoside transport inhibitor, was also calculated as stated below.

$$PF_{50} = \frac{GI_{50} \text{ CNDAC}}{GI_{50} \text{ CNDAC} + \text{inhibitor}}$$

Inhibition agent	Mode of action	Hypothesis
Methoxyamine	An alkoxyamine derivative that binds to the AP site after glycosylase-mediated removal of a damaged base. The MX-adducted AP site is resistant to AP endonuclease cleavage and to polymerase β (members of the BER pathway) (Fortini 1993, Horton 2002).	Addition of methoxyamine sensitises BER competent cell lines (AA8) to CNDAC but does not increase sensitivity in BER deficient cell lines (EM9).
Dipyridamole	Inhibitor of equilibrative nucleoside transporters, ENT 1 and ENT 2.	If CNDAC is transported into cells via ENT1 and/or ENT2 inhibition by DP will result in resistance.
S-(4-Nitrobenzyl)-6-thioinosine (NBMPR)	Inhibitor of equilibrative nucleoside transporters, particularly adenosine transporters (ENT1)	If CNDAC is transported by ENT1 but not ENT2 NBMPR will result in resistance to CNDAC

Table 6.4 – 1: Agents for the inhibition of BER or transporter protein, their mode of action and hypothesis for effect with simultaneous treatment with sapacitabine

6.4.3. Development of an Assay of BER Function

Principles of the Assay

Oxidative DNA damage results in production of 8-hydroxy-2'-deoxyguanosine (8-OHdG), without a functional BER pathway, these adducts will accumulate in DNA. The Trevigen ELISA kit is a competitive immunoassay for 8-OHdG quantification in DNA samples.

Extracted DNA yield from PCO cultures is low and therefore the optimum concentration of DNA required for the assay was assessed using the matched BER cells lines, AA8 and EM9. 1.2 $\mu\text{g}/25 \mu\text{l}$ DNA was an achievable DNA concentration from PCO cultures and allowed clear differentiation of 8-OHdG levels from AA8 and EM9 cell lines, data not shown.

Assay Protocol

Equivalent amounts of PCO DNA alongside controls (AA8 and EM9 cell line DNA) were prepared. 2 μl DNase I per 50 μg DNA was added and incubated at 37 °C for 1 hour. 2 μl alkaline phosphatase per 50 μg DNA was added and incubated at 37 °C for 1 further hour. 8-OHdG standards were prepared as per manufacturer's instruction.

25 µl samples and standards were incubated at 25°C for 1 hour in the 96 well plate with 25 µl 1:250 8-OHdG monoclonal antibody. The plate was washed 4 times with 0.1% (v/v) Tween PBS before incubating for 1 hour at 25 °C with 50 µl 1:500 goat HRP conjugate. After washing 4 times with 0.1% Tween PBS, 50 µl TACS-sapphire™ was added and incubated for 5 minutes. 50 µl 0.2 M HCl was added to stop the reaction and the plate read at 450 nm using Spectra Max 250 microplate reader.

Data analysis was performed using the Trevigen online worksheet. Briefly, the mean absorbance of each 8-OHdG standard and a blank was calculated. The log of 8-OHdG standard concentrations (nM) was plotted against the relative absorbance and the sample 8-OHdG concentrations calculated by interpolation from the standard curve.

6.4.4. Western Blotting

The assay protocol described in detail in Chapter 3 was used to quantify protein expression of hENT1, dCK and CDA in PCO samples.

Briefly, 20 mg/ml protein samples were denatured at 100 °C for 5 minutes before proteins separated electrophoretically using the Mini-PROTEAN Tetra cell system. Proteins were transfer to Hybond ECL membrane before blocking. Membranes were incubated in primary antibody in TBST with 1% milk at 4 °C overnight before washing and horseradish peroxidase-conjugated secondary antibodies were applied. Table 6.4 - 2. Bound antibodies were detected using ECL detection solution and chemiluminescence used to quantify protein expression using the Fuji-imager). Total protein was quantified using Ponceau S solution. All immune-blotting experiments were carried out in triplicate.

Protein	Molecular weight (kDa)	Species	Conc
hENT1	55	Rabbit polyclonal anti-hENT-1 (Abcam, UK)	1:100
dCK	31	Rabbit polyclonal anti-dCK antibody (Abcam, UK)	1:500
CDA	16	Rabbit polyclonal anti-CDA (Abcam, UK)	1:100

Table 6.4 - 2: Antibodies for Western blot

6.5. Results

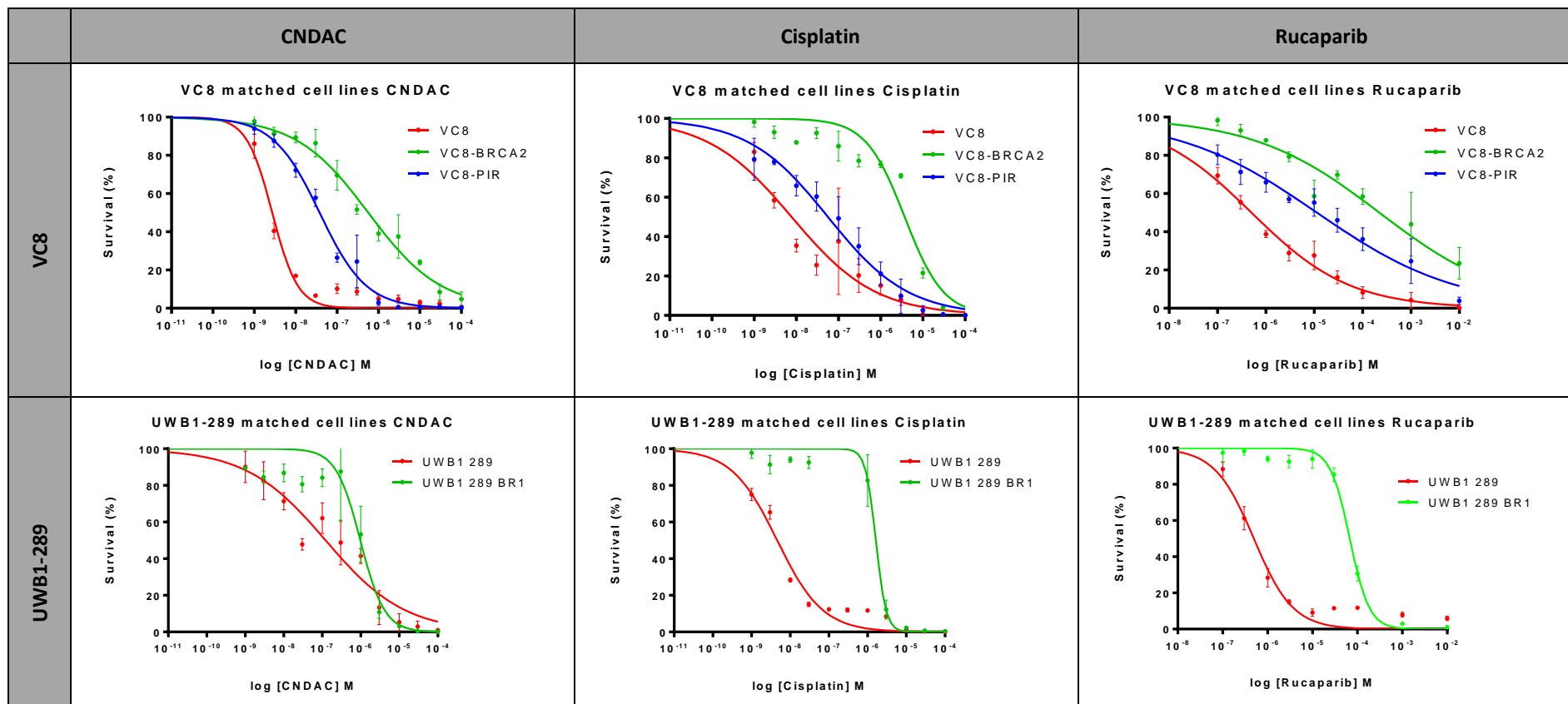
6.5.1. Cell Lines

A panel of cell lines paired for defective BRCA1 or BRCA2 function with WT (VC8, VC8-BR2, VC8 PIR; UWB1-289 and UWB1-289-BR1) were used in initial experiments to assess the effect of HR status upon CNDAC sensitivity. The HR status of each cell line was confirmed using the standard HR Rad51 assay, and sensitivity to CNDAC was assessed using colony formation assays, Table 6.5 - 1. Results clearly demonstrated greater sensitivity in cell lines with BRCA 1/2 mutations and subsequent HR dysfunction in comparison to their matched wild type lines for CNDAC, cisplatin and rucaparib, across different paired cell lines, Table 6.5 – 1,

Figure 6.5 - 1. The LC₅₀ for VC8 BRCA2 cell line (HRC) to CNDAC was 656 nM, which was 243 fold higher than VC8 cell line (HRD, with an LC₅₀ of 3 nM, p = 0.0001. The same trend was seen in UWB1-289 paired cell lines with a 7 fold increase in LC₅₀ in the BRCA1 WT cell lines, p = 0.0001. The PARPi resistant subclone of the VC8 cell line was partially resistant to rucaparib, with an LC₅₀ intermediate to its matched VC8 and VC8 BRCA2. This subclone remained sensitive to cisplatin with an LC₅₀ of 70 nM and CNDAC with an LC₅₀ of 39 nM suggesting that mechanisms, other than the HR pathway, are likely to be involved in resistance to cisplatin and CNDAC.

Cell Line	DNA Repair Status	Doubling Time (hours)	LC ₅₀ CNDAC, nM (mean, SD)	Fold resistant (HRC/HRD)	LC ₅₀ Cisplatin, nM (mean, SD)	Fold resistant (HRC/HRD)	LC ₅₀ Rucaparib, μM (mean, SD)	Fold resistant (HRC/HRD)
VC8	BRCA2 deficient (HR-)	39	3 ± 0.7	-	11 (8.3)	-	0.6 (0.3)	-
VC8 BR2	BRCA2 corrected (HR+)	25	656 ± 434.7	243	3598 (51.4)	327	384.4 (143.5)	641
VC8 PIR	BRCA2 revertant (HR+)	23	39 ± 4.3	14	70 (61.3)	6	11.8 (4.9)	20
UWB1 289	BRCA1 defective (HR-)	53	136 ± 71.8	-	5 (0.9)	-	0.5 (0.1)	-
UWB1 289 BR1	BRCA1 corrected (HR+)	45	971 ± 708.1	7	1786 (865.7)	1984	68.9 (9.5)	138
Capan-1	BRCA2 defective (HR-)	77	128 ± 45.3	-				
MX-1	BRCA1/2 defective (HR-)	27	58 ± 39.1	-				
MCF7	BRCA1/2 WT (HR+)	38	408 ± 99.9	7				

Table 6.5 - 1: Cell line panel: Growth characteristics and cytotoxicity by CNDAC, rucaparib and cisplatin. Doubling time: Cell proliferation was assessed by SRB assay, with six repeats at each time point. Clonogenic survival: cells were treated with cytotoxic agent at various concentrations, as indicated, for 24 hours and survival was determined with colony formation assay. Data are the mean and standard deviation values from three independent experiments, with triplicate values for each concentration. Colony formation assays for MX-1, MCF7 and Capan-1 cell lines completed by James Murray.



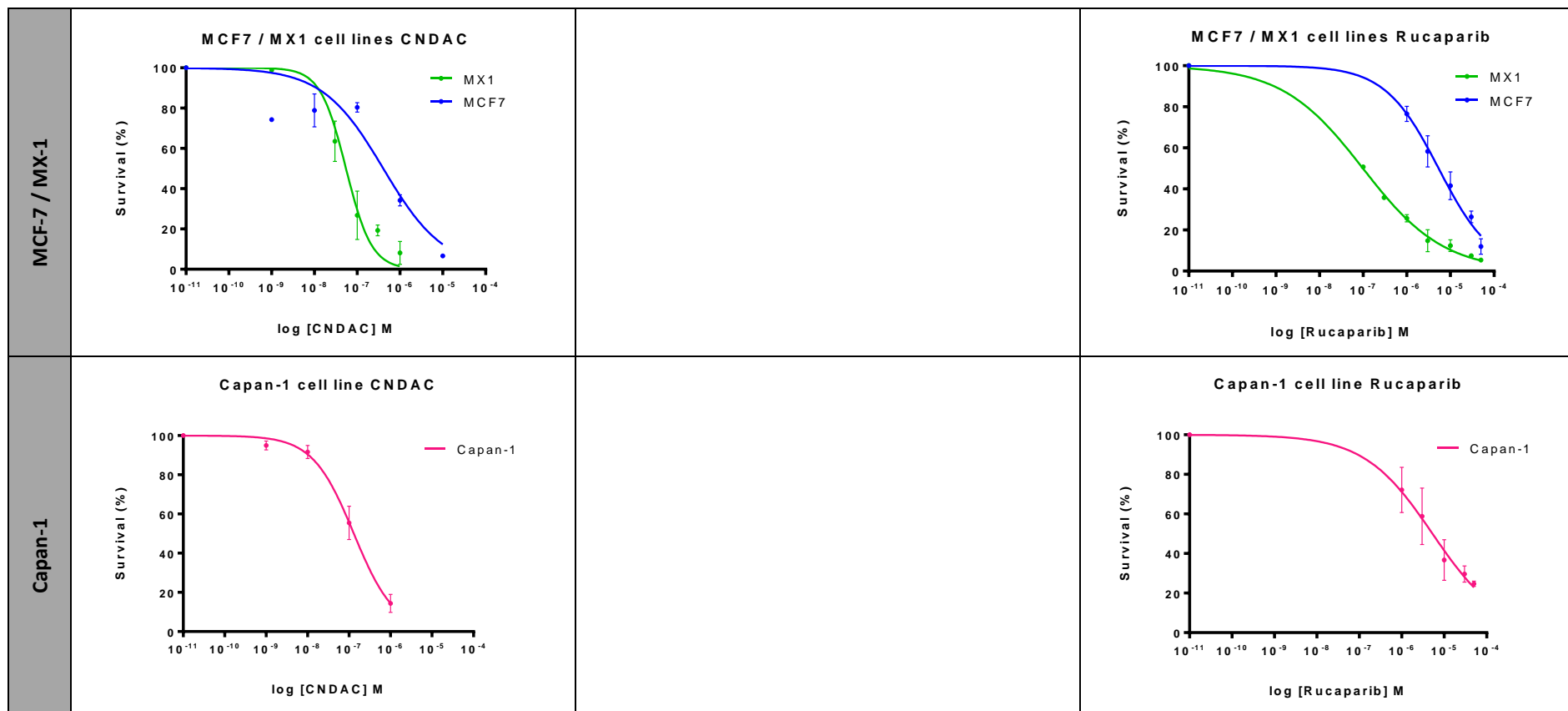


Figure 6.5 - 1: Cytotoxicity of CNDAC and cisplatin in cell lines matched for BRCA1/2 mutations. Cells were treated with CNDAC, rucaparib or cisplatin at various concentrations, as indicated, for 24 hours and survival determined by colony formation assay. Data are the mean values from three independent experiments, with triplicate values for each concentration. Error bars = 95% CI.

6.5.2. Assessing Cytotoxicity in PCO Samples

As described in Chapter 4, the inability of PCO cultures to form colonies in standard or agar colony formation assays prevented accurate assessment of cytotoxicity using this methodology. Evaluation of numerous alternative assays confirmed SRB to be the reproducible and feasible for accurate assessment of cytotoxicity in PCOs, Table 6.5 - 2.

Cell Line	CNDAC Mean \pm SD			
	GI ₅₀ nM SRB	Fold increase	LC ₅₀ nM Colony	Fold resistant (HRC/HRD)
VC8	47 \pm 51	-	3 \pm 0.7	-
VC8 BR2	758 \pm 114	16	656 \pm 434.7	243
VC8 PIR	220 \pm 344	5	39 \pm 4.3	14
UWB1-289	41 \pm 42	-	136 \pm 71.8	-
UWB1-289 BR1	129 \pm 69	3	971 \pm 708.1	7

Table 6.5 - 2: Comparison of SRB with colony formation in cell lines matched for BRCA 1/2. Colony formation. Cells were seeded at low density and treated with CNDAC at various concentrations for 24 hours. Cell proliferation by SRB assay. Cells were seeded at 1000 cells / well and treated with CNDAC at various concentrations for three doubling times. Data are the mean values (95% CI) from three independent experiments, with triplicate values (colony formation) or six replicates (cell proliferation) for each concentration.

6.5.3. Sensitivity of PCO to CNDAC, Cisplatin and Rucaparib in Relation to HR Status

54 PCO cultures that had previously been determined as HRC or HRD and sensitivity to cisplatin and rucaparib determined (Chapter 4) were evaluated for sensitivity to CNDAC. Data are given as percentage control cell growth at a single concentration owing to the high proportion of cultures resistant to the cytotoxic tested, as previously discussed. Sensitivity, quantified by % survival following exposure at a given concentration of cytotoxic agent, is a continuous, variable and therefore strict discrimination between cultures, which are sensitive and resistant is therefore difficult, Figure 6.5 - 2.

Of the 54 PCO cultures tested for sensitivity to CNDAC, cisplatin and rucaparib, 34 (63%) were HRC and 20 (37%) cultures were HRD. When grouping all HRC cultures and comparing to grouped HRD cultures, greater sensitivity to CNDAC was seen in the HRD group, Figure 6.5 - 2, Figure 6.5 - 3. Mean percentage survival following treatment with 100 μ M CNDAC was 63.5% (SD 22.3) in HRC cultures and 43.1% (20.1) in HRD cultures, $p = 0.0015$. The cell line cytotoxicity assays confirm that HRD cell lines with a BRCA mutation are more sensitive to CNDAC as well as cisplatin and rucaparib. However, the ability of HR status alone to reliably determine sensitivity in every culture to CNDAC is not absolute with some outliers as observed for cisplatin and rucaparib (Chapter 4).

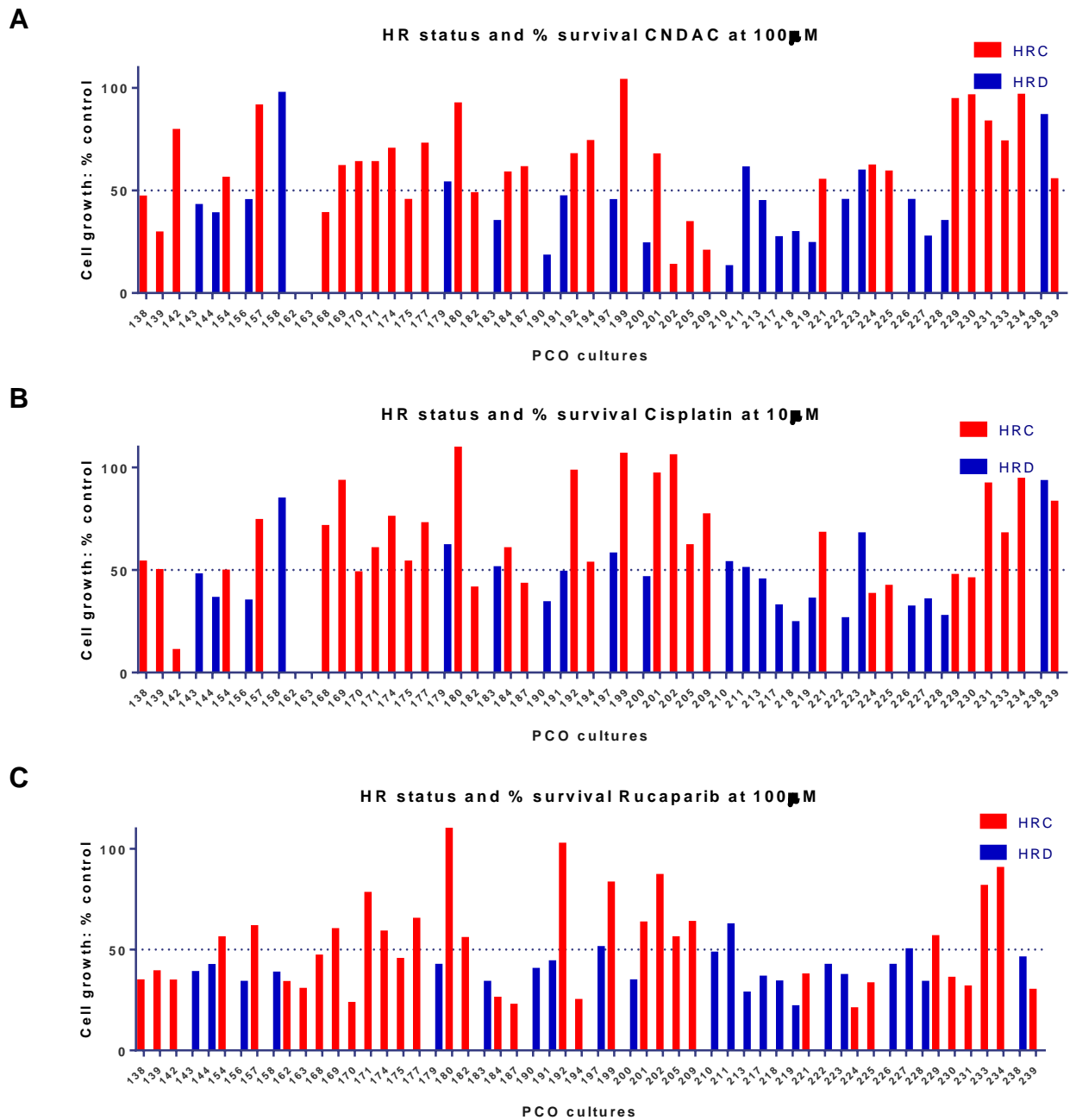
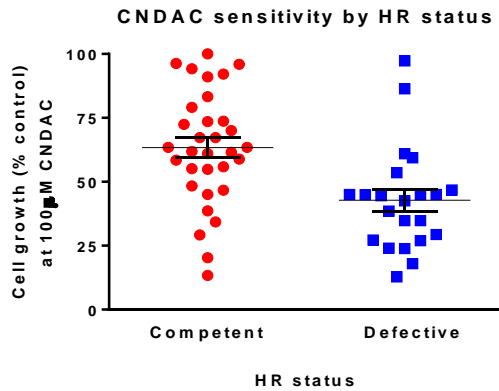
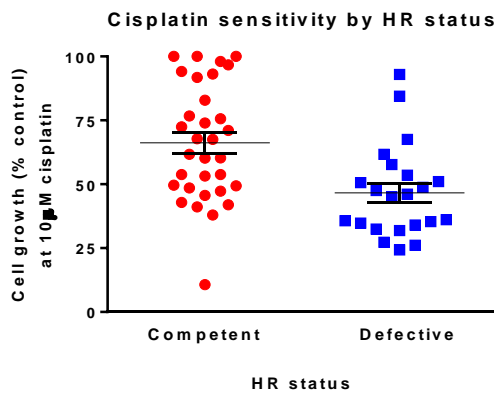


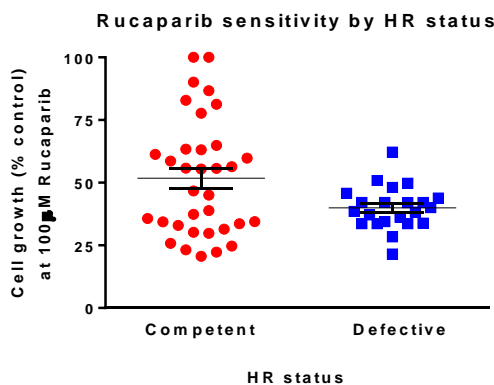
Figure 6.5 - 2: Sensitivity of each PCO culture to CNDAC (A), cisplatin (B), and rucaparib (C). 1000 cells/well were seeded and treated with various concentrations of either rucaparib, CNDAC or cisplatin for 10 days. Cells were fixed before staining with SRB and cell density determined by spectrophotometer. Data are the mean of six replicates for cell density expressed as a percentage of untreated control at the given concentration.



HR	Mean % survival	SEM
HRC n=32	63.5	3.9
HRD n=22	42.8	4.3
p (t-test)	0.0011 *	



HR	Mean % survival	SEM
HRC n=32	66.9	4.2
HRD n=22	46.6	3.8
p (t-test)	0.0014 *	



HR	Mean % survival	SEM
HRC n=32	52.3	4.2
HRD n=22	39.9	1.8
p (t-test)	0.0275 *	

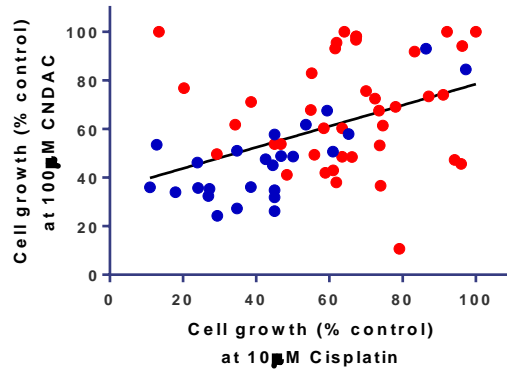
Figure 6.5 - 3: Sensitivity to CNDAC, rucaparib and cisplatin stratified by HR status. Data from Figure 6.5 - 2 describing sensitivity to CNDAC, Rucaparib and cisplatin using SRB cell proliferation assay were grouped into HRC and HRD cultures and analysed for significance. T-test was used to compare the mean percentage survival at a given concentration of cytotoxic agent (see Y-axis) between the HRD and HRC groupings.

This might have been expected as clinically there are highly variable responses to chemotherapy agents between patients and a 50% cell survival in a cytotoxicity assay may reflect a partial response clinically. To assess the relationship between sensitivity across the three agents, correlation studies between percentage survival were performed.

Correlation of Resistance to Cytotoxic Agents

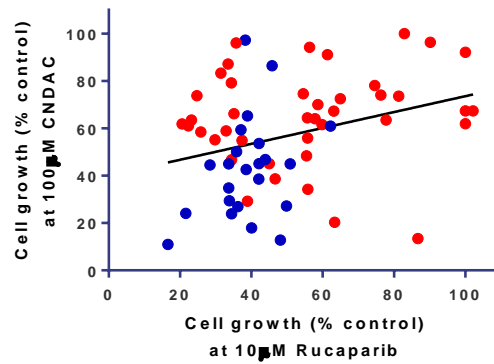
To further assess the relationship between HR status and sensitivity to the three agents tested, sensitivity of each PCO culture was compared across all three agents.

Cell growth at 10 μ M Cisplatin vs cell growth at 100 μ M CNDAC



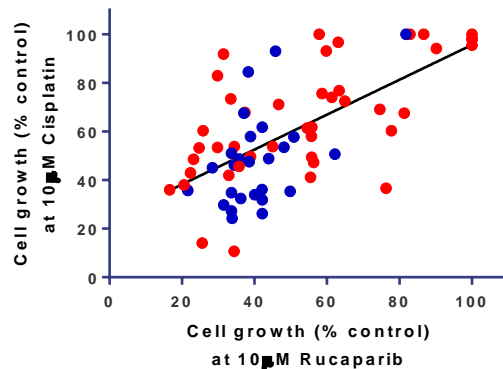
r 0.425
 95% CI 0.194 to 0.611
 p 0.0006 *

Cell growth at 100 μ M Rucaparib vs cell growth at 100 μ M CNDAC



r 0.2925
 95% CI 0.0268 to 0.520
 p 0.0318 *

Cell growth at 100 μ M Rucaparib vs cell growth at 10 μ M Cisplatin



r 0.6457
 95% CI 0.457 to 0.779
 p <0.0001 *

Figure 6.5 - 4: Correlation studies between percentage survival at given concentrations of CNDAC, cisplatin and rucaparib. Percentage survival at given concentrations of cytotoxic agent was determined by cell proliferation SRB assays. HRC cultures are shown by red circles, HRD by blue circles.

Data described in Chapter 4 and summarised in Figure 6.5 - 4, identified a relationship between sensitivity to rucaparib and cisplatin with a strong correlation between antiproliferative activities of each cytotoxic agent. The correlation between CNDAC and rucaparib sensitivity was weak but significant. There was however, a stronger correlation between CNDAC and cisplatin, Figure 6.5 - 5. Nevertheless, there were some outliers, all of which were HRC. Such variable sensitivity in HRC cultures may be due to dysfunction in cellular mechanisms conferring cisplatin sensitivity (e.g. reduced glutathione), or increased CNDAC resistance mechanisms (e.g., reduced ENTs). Sensitivity to CNDAC in cisplatin resistant cultures (purple circle) may be due to high ENT expression or increased cisplatin resistance due to high GSH and/or MRP drug efflux pump. Additionally, unexpectedly there were two HRD cultures that were clearly resistant to both CNDAC and cisplatin.

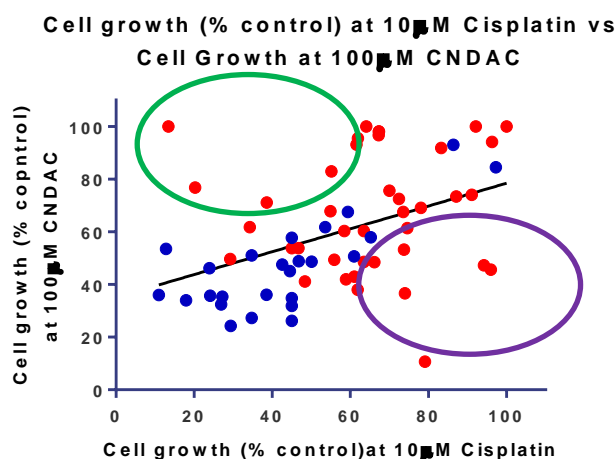
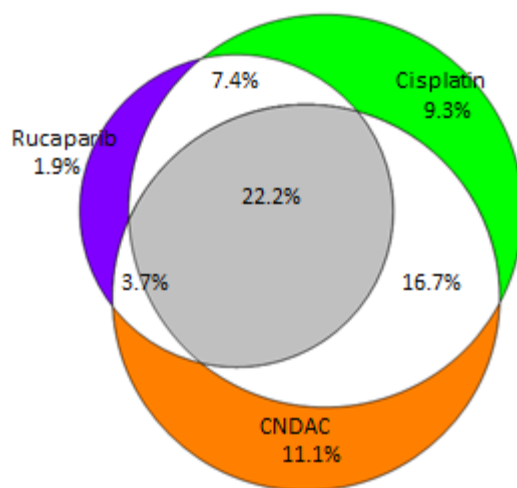


Figure 6.5 - 5: Correlation of sensitivity of PCO cultures to cisplatin and CNDAC. Mean percentage survival at 100 μ M CNDAC assessed using SRB cell proliferation assay is plotted against percentage survival at 10 μ M cisplatin for 54 PCO cultures. Outliers resistant to CNDAC but sensitive to cisplatin (green circle); outliers resistant to cisplatin but sensitive to CNDAC (purple circle). Red dots denote HRC cultures, blue dots, HRD cultures.

The ability of HR function to accurately predict sensitivity to multiple agents was not 100% predictive. Cultures which were resistance to each agent were grouped and the proportions of HRD/HRC calculated, Figure 6.5 – 6.

A



B

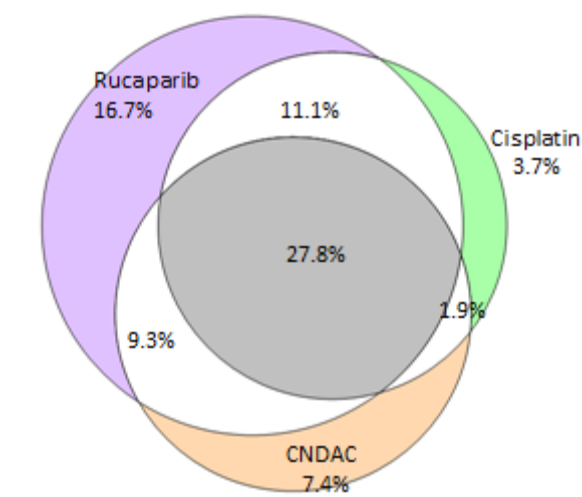


Figure 6.5 - 6: Resistance (A) and sensitivity (B) to CNDAC, cisplatin and rucaparib. SRB cell proliferation assays were used to calculate the percentage survival at 100 μ M CNDAC, 10 μ M cisplatin and 100 μ M rucaparib. $\geq 50\%$ survival of untreated control denoted resistance. The percentage of cultures resistant is shown numerically within the black Venn diagram. The proportion of PCO cultures sensitive to each agent is shown in (B). 27.8% of cultures were sensitive to all three agents.

Grouping the cultures in this way reveals that there are a proportion of cultures, which are resistant to cisplatin that are sensitive to CNDAC ($9.3 + 7.4 = 16.7\%$), Figure 6.5 - 6. 7.4% of all PCO cultures tested were resistant to both cisplatin and rucaparib but were sensitive to CNDAC showing that CNDAC may have a role to play in platinum resistant and PARPi resistant disease. HR function alone however is not a reliable discriminator to identify this group of patients who may benefit.

6.5.4. HR and the Prediction of CNDAC Sensitivity

The ability of HR functional status to accurately predict sensitivity to CNDAC *ex vivo* in PCO cultures was tested by ROC analysis. An AUC of 0.7798 (SE 0.068) demonstrates a significant association with a p value of 0.0005, Figure 6.5 - 7. The PPV of HRC to predict resistance was 83.3% with a NPV of 70.8%. Sensitivity and specificity were shown to be 0.781 and 0.773 respectively, Figure 6.5 - 7.

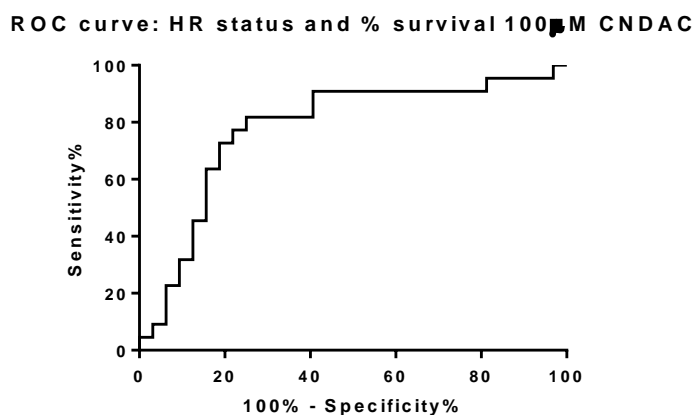


Figure 6.5 - 7: ROC analysis for HR status and CNDAC sensitivity. Sensitivity to CNDAC was determined by SRB cell proliferation assay. Greater than 50% survival in comparison to untreated control after 10 days exposure to 100 μ M CNDAC was used to define resistance. An AUC of 0.7798 confirms a significant association between HR status and percentage survival.

6.5.5. CNDAC in Sequential or Combination Drug Regimes

These studies were conducted by S Frame (Cyclacel).

The ability of CNDAC to be incorporated into nucleic acids during DNA repair makes them interesting candidates for combination therapy with DNA-damaging agents. PCO primary culture data suggests a role for sapacitabine in the treatment of ovarian cancer but it is unclear how this should be offered. Many new agents used in cancer care are often given in trials at the time of relapse following failure of standard therapy. This is unlikely to result in a high rate of response and the possibility of providing sapacitabine earlier in the management of ovarian cancer either as a single agent or in combination was explored, (Frame, Armour et al. 2012).

Data demonstrated that CNDAC could be effectively combined with PARPi inhibitors in ovarian cell lines or given in sequential treatments, although with PARPi, sequential treatments appeared to be better than the concomitant treatment schedule, Table 6.5 - 3.

	ED50	CI	ED75	CI	ED90	CI
CNDAC then PARPi	0.64	<0.5	0.65	<0.5	0.67	<0.5
PARPi then CNDAC	0.83	<0.5	0.68	<0.5	0.57	<0.5
CNDAC plus PARPi	0.81	<0.5	0.75	<0.5	0.72	<0.5

Table 6.5 - 3: CNDAC in combination with PARPi. PEO1 cell lines were seeded at 1000 cells/well, and treated with CNDAC, PARPi or cisplatin in 3 different schedules. For sequential schedules, cells were treated with the first compound for 24 h, followed by the second compound for 72 h. For the combination schedule, cells were treated for 72 h with both compounds. Cell viability was assessed by resazurin assay, and data analysed by Calcsyn. The combination index (CI) is a measure of the nature of the drug interaction, with CI <0.9 showing a synergistic relationship, CI 0.9-1.1 showing additive effect and CI >1.1 showing antagonistic effect. Effective dose values for 50, 75 and 90% reduction in growth (ED50, ED75 and ED90) for each of the combinations are shown (Frame, Armour et al. 2012).

6.5.6. Investigation of Alternative DNA Repair Mechanisms as Possible Determinants of Sensitivity to CNDAC

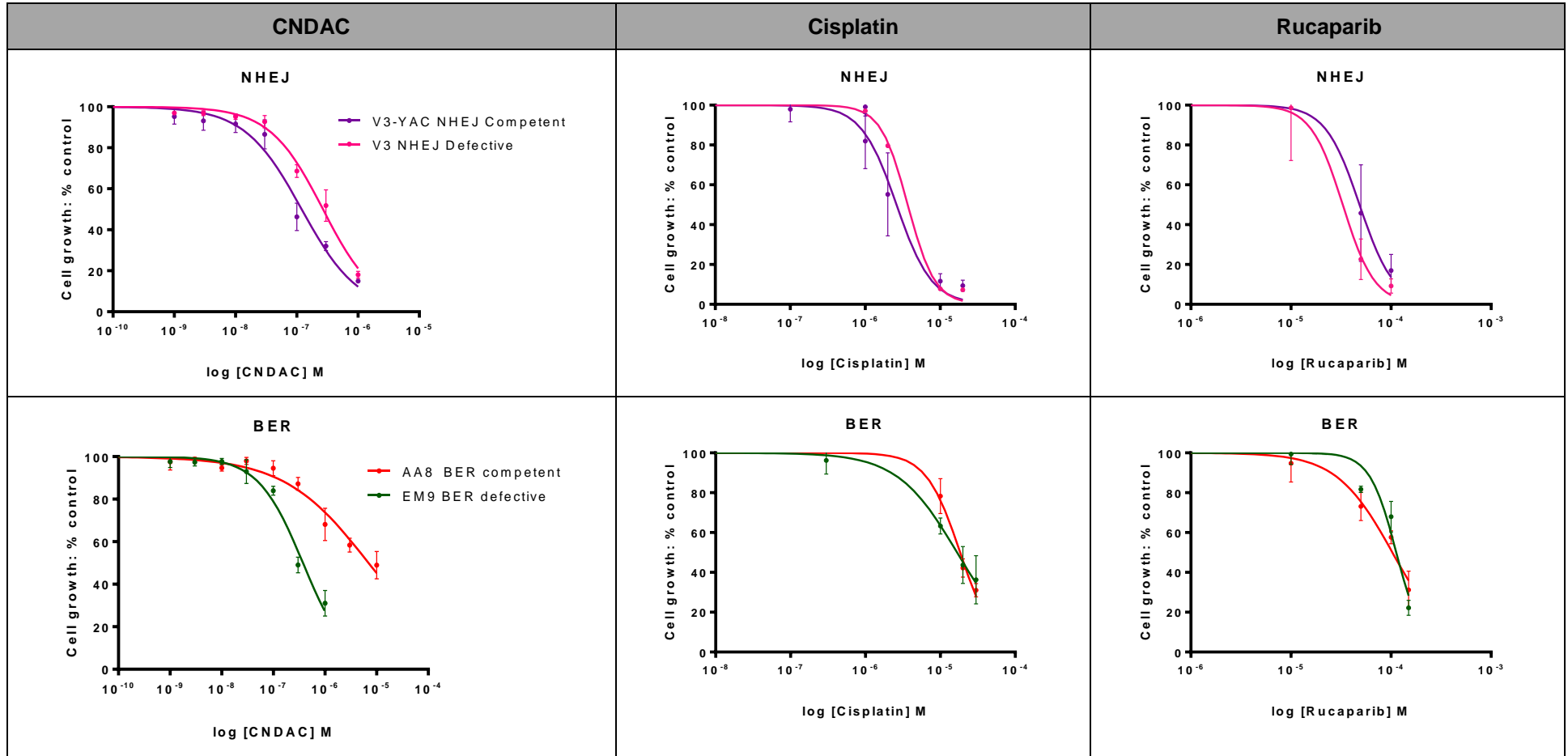
Cell lines with isolated BRCA 1/2 mutations were consistently more sensitive to CNDAC in comparison to their paired WT cell lines suggesting HR status could be used to enrich the population of patients who are likely to be sensitive to CNDAC. However, HR function alone is not entirely predictive of CNDAC sensitivity with several outliers identified indicating that other DNA repair pathways may be important.

To identify any other relevant pathways CNDAC sensitivity in matched cell lines defective in other DNA repair mechanisms was explored using SRB proliferation assays,

Figure 6.5 - 8. Full details of cell lines are given, in Table 3.4 – 1, Chapter 3 and summarised in Table 6.5 - 4.

Cell line	Description
A2780	p53 and MMR-competent
CP70-B1	p53 mutant, MMR competent (chromosome 3 transfer). A2780 derivative
CP70-A2	P53 mutant, MMR defective (transferred chromosome 3 with mutant <i>hMLH1</i>). A2780 derivative
V3	NHEJ defective (DNA-PK _{CS} deficient)
V3-YAC	NHEJ competent (transfected with a yeast artificial chromosome (YAC) carrying DNA-PK _{CS} gene)
AA8	BER competent and NER competent
EM9	BER defective (XRCC1 mutation)
UV5	NER defective (ERCC2 mutation)

Table 6.5 - 4: Cell line panel used to explore the contribution of NHEJ, BER, NER, p53 and MMR in the sensitivity to CNDAC.



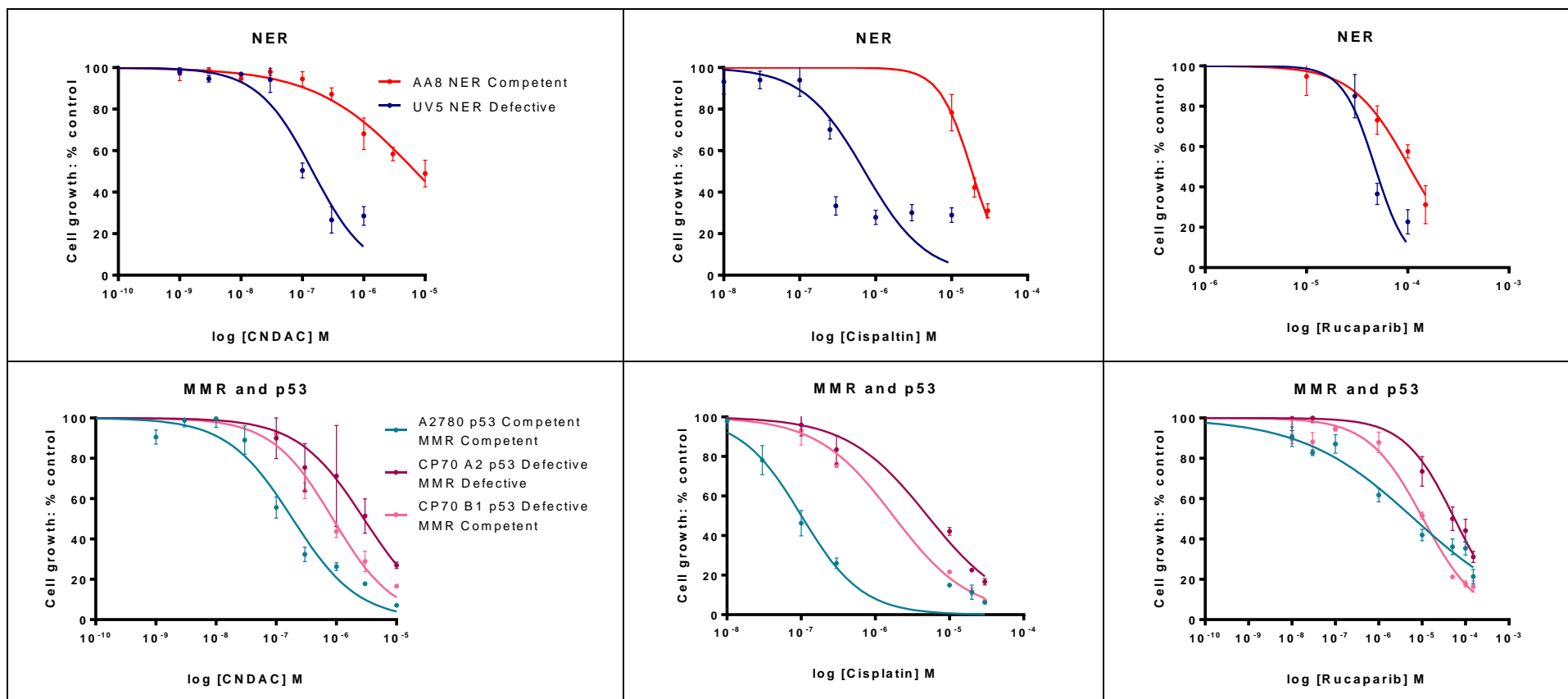


Figure 6.5 - 8: Cell proliferation by CNDAC (SRB assay) with matched cell lines for NHEJ, BER, and NER DNA repair. Cells were seeded at 1000 cells/well and treated with CNDAC at various concentrations, as indicated, for three doubling times. Cell density was measured by SRB assay. Results shown are the mean (SEM) of three independent experiments, each with six repeats.

	GI ₅₀	Competent	Defective	Fold resistance (HRC/HRD)	P value (t-test)
DNA-PK_{CS} (NHEJ)		V3-YAC	V3		
	CNDAC (nM)	120.3 (92.4-157.0)	267.7 (222.4 – 322.1)	0.7	0.0292 *
	Cisplatin (µM)	2.62 (1.69 – 4.06)	3.69 (3.36 – 4.06)	0.7	0.7366
	Rucaparib (µM)	48.5 (24.3 – 96.8)	32.9 (6.5 – 167.9)	1.5	0.9272
XRCC1 (BER)		AA8	EM9		
	CNDAC (nM)	6970 (4540- 10700)	374.4 (303.6 – 461.7)	18.6	<0.0001 *
	Cisplatin (µM)	18.4 (15.6 – 21.8)	16.7 (11.8 – 23.7)	1.1	0.0003 *
	Rucaparib (µM)	103.2 (85.9 – 124.1)	112.9 (102.4 – 124.5)	0.9	0.5039
ERCC2 (NER)		AA8	UV5		
	CNDAC (nM)	6970 (4540- 10700)	147.3 (106.0 – 204.1)	47.3	0.0221 *
	Cisplatin (µM)	18.5 (15.8 – 21.8)	0.72 (0.41 – 1.26)	25.7	<0.0001 *
	Rucaparib (µM)	103.2 (85.9 – 124.1)	47.5 (35.4 – 63.75)	2.2	0.2315
MHLH1 (MMR) / p53		A2780 MMR comp p53 comp	CP70 A2 MMR def p53 def	CP70 B1 MMR comp p53 def	P value (ANOVA)
	CNDAC (nM)	187.4 (138.9 – 252.6)	2869 (1713 – 4805)	872.8 (712 – 1070)	0.0002 *
	Cisplatin (µM)	0.10 (0.08 – 0.13)	5.04 (3.69 – 6.90)	1.74(1.12 – 2.71)	<0.0001 *
	Rucaparib (µM)	6.5 (4.2 – 10.2)	55.8 (44.3 – 70.4)	10.5 (8.0 – 13.8)	<0.0001 *

Table 6.5 - 5: Sensitivity to CNDAC and cisplatin assessed by SRB proliferation assay in cell line panels matched for functional/defective DNA repair pathways. Cells were seeded at a density of 1000 cells/well with six replicates per condition and treated with CNDAC at a variety of concentration normalised to 1% DMSO, as indicated, for three doubling times. Cell proliferation was assessed by SRB assay. Data are the mean values (95% CI) from three independent experiments, with six repeats for each concentration.

Cell lines defective in NER, with ERCC2 mutation (UV5) were also significantly (nearly 50-fold) more sensitive than their WT (AA8), $p=0.0221$. Similarly, the UV5 cells were 26 fold more sensitive to cisplatin than the matched WT AA8 cell line, $p < 0.0001$. No significant difference was seen in these paired cell lines with rucaparib. Cell lines with mutant XRCC1 (EM9), defective in BER were nearly 20x more sensitive to CNDAC than matched WT, $p < 0.0001$, Table 6.5 – 5.

Interestingly, V3 cells (DNA-PK_{CS} deficient) defective in NHEJ was more resistant to CNDAC in comparison to its paired competent cell line (V3-YAC) $p=0.0292$. The fold resistance of 2.23 was however less pronounced than that seen in other pathways. There was no statistical difference in their sensitivities to cisplatin, $p=0.7366$.

Comparing CP70 B1 and A2780 cells the presence of p53 mutation appeared to result in an approximately 5-fold increase in resistance to both CNDAC and cisplatin in comparison to WT, $p < 0.0001$. This requires confirmation by 53 knockdown, The presence of a mutation in hMLH1 (CP70 A2) conferring defective MMR resulted in an additional 3-fold increase in resistance to CNDAC and 1.5 fold increase in resistance to cisplatin, $p < 0.0001$, $p < 0.0001$ respectively.

With only a modest increase in sensitivity in the MMR defective cells and a small fold increase in sensitivity in cell lines with competent NHEJ, these pathways were not investigated further. BER and NER defective cell lines were significantly more sensitive to CNDAC in comparison to their matched wild type cell lines and BER was selected for further evaluation in this study.

6.5.7. Base Excision Repair

The data above have demonstrated that a defective BER DNA repair pathway confers sensitivity to CNDAC. To test prevention of repair by BER pathway results in greater resistance to CNDAC a series of cell proliferation assays were conducted with addition of methoxyamine to inhibit BER.

Inhibition of BER: Methoxyamine

Methoxyamine is an alkoxyamine derivative, which is capable of blocking the short patch nucleotide BER pathway by reacting with the aldehyde group in the acyclic sugar left in the DNA abasic site following removal of a damaged nucleotide (Talpaert-Borle 1983, Liuzzi 1985). The methoxyamine-adducted AP site is a stable intermediate, refractory to the lyase activity of AP endonuclease (Ape1/Ref-1) cleavage and to polymerase (Fortini 1993, Horton 2002).

Incompletely repaired methoxyamine-blocked AP sites lead to increases in SSB, DSB as well as cell death (Taverna 2001, Rinne 2004). Inhibition of BER by methoxyamine is a valid pharmacologic strategy to enhance the cytotoxicity of a methylating chemotherapeutic agent, such as temozolomide, or to overcome temozolomide drug-resistance (Liu 1999, Taverna 2001, Liu 2002). Addition of 6 mM of methoxyamine has been shown to increase sensitivity to temozolomide in colon cell lines by interruption of BER (Liu 1999). It was hypothesised that the addition of methoxyamine would prevent repair of DNA damage by BER and therefore induce resistance in the BER defective cell line EM9.

Methoxyamine is itself a cytotoxic agent with a GI₅₀ of 14.2 mM and 9.4 mM in AA8 and EM9 cell lines respectively.

		Mean (SEM) % cell growth with CNDAC and methoxyamine	
		AA8	EM9
MX	1 mM	72.4 (2.8)	83.5 (2.1)
	5 mM	60.5 (6.8)	66.6 (6.4)
	20 mM	38.0 (2.9)	48.2 (6.3)

Table 6.5 - 6: Cytotoxic effect of methoxyamine (MX): Percentage survival AA8 and EM9 cells with addition of MX. Cells were treated with methoxyamine at 0, 1, 5 and 20 mM concentrations for 48 hours. Cell proliferation was assessed using SRB assay and percentage survival expressed as percentage survival compared to untreated controls.

For drug combination assays data were normalised to methoxyamine or vehicle alone but the inherent growth inhibition by methoxyamine made sensitisation difficult to determine, Figure 6.5 - 9, Table 6.5 - 6.

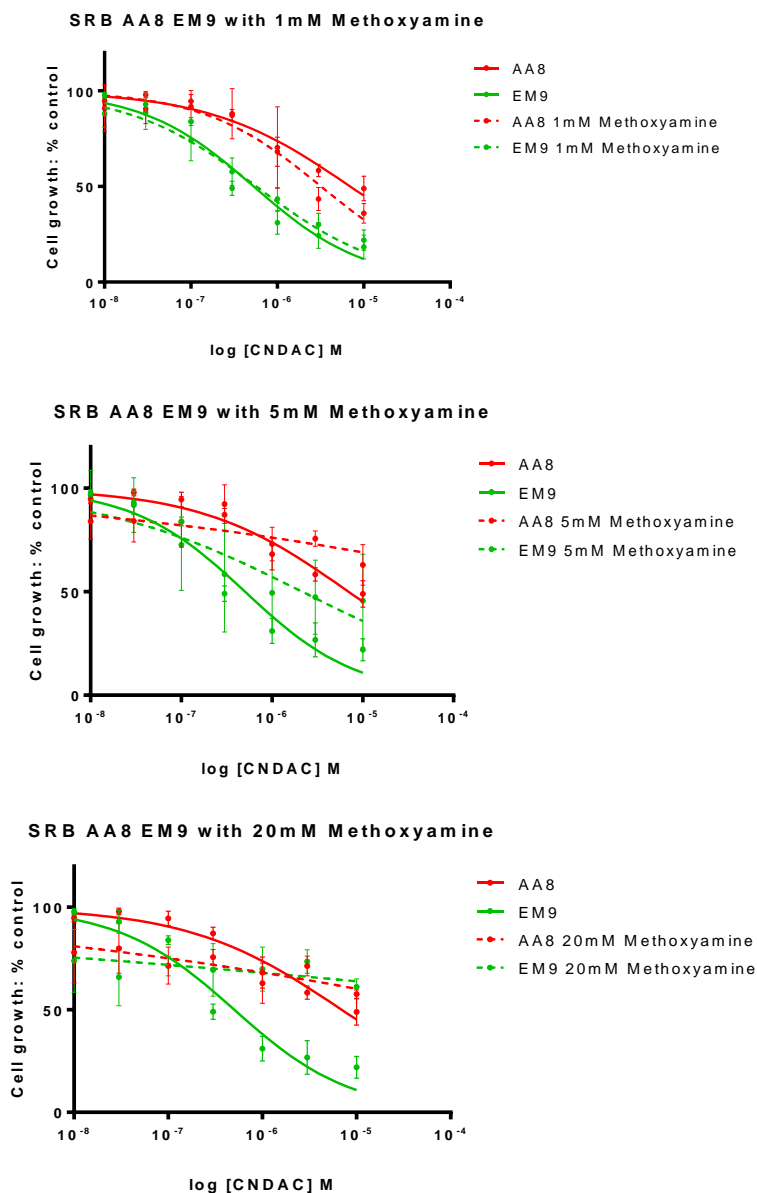


Figure 6.5 - 9: Inhibition of BER using methoxyamine. Cells were treated with CNDAC at various concentrations normalised to 1% DMSO, as indicated, for 48 hours (three doubling times) with addition of 1, 5 or 20 mM methoxyamine. Cell proliferation was assessed by SRB assay and compared to control cells with CNDAC alone, normalised to 1% DMSO or MX alone as appropriate.

Methoxyamine at 1 mM did not potentiate sensitivity to CNDAC significantly in either AA8 or EM9 cell lines. Effect of the addition of higher doses of MX cannot be assessed due to the toxicity of MX.

Functional BER Assay: 8-OHdG ELISA

To further explore the relationship of defective BER pathway with sensitivity to CNDAC, a functional assay was developed to be used in PCO samples. The quantification of 8-OHdG by ELISA testing provides the opportunity to characterise PCO cultures as BER competent or defective using extracted DNA. AA8 and EM9 cells were assayed in parallel with PCOs to provide BER proficient and deficient standards.

8-OHdG is produced during oxidative DNA damage and is removed by BER. Therefore, cells competent in BER (AA8) remove the 8-oxo-dG and have low residual levels, whilst cell lines defective in BER (EM9) fail to remove 8-oxo-dG and have high residual levels. Trevigen's competitive ELISA kit quantifies 8-OHdG in DNA using wells pre-coated with 8-OHdG.

Functional BER Assessment of PCO Samples

58 PCO samples, including four samples run with duplicates during separate experiments, were processed for baseline 8-OHdG levels. All samples were normalised for the concentration of DNA loaded and normalised to EM9 within each assay to eliminate inter-assay variability. Higher measurement of 8-OHdG indicates BER defect, Figure 6.5 - 10.

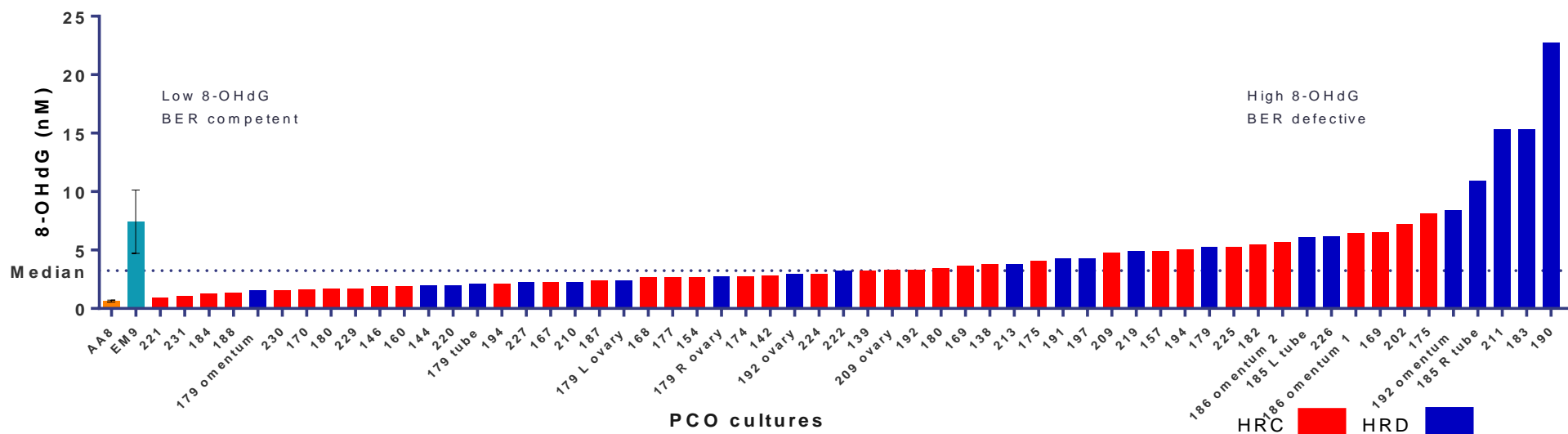


Figure 6.5 - 10: 8-OHdG baseline levels in PCO samples. DNA extracted from PCO ascitic cell cultures, at a concentration of 1.25 µg/25 µl, was added to the Trevigen ELISA plate containing immobilised 8-OHdG before adding 8-OHdG monoclonal antibody followed by HRP with colour conjugate and quantifying by spectrophotometry. Sample 8-OHdG concentrations were calculated by interpolation from the standard curve. Cells competent in BER (AA8) have low residual levels, whilst cells defective in BER (EM9) have high residual levels. Results for cell lines are the mean and SD of three independent experiments.

Correlation 8-OHdG Levels with CNDAC Sensitivity

A negative correlation was seen between 8-OHdG level and percentage survival at 100 μ M CNDAC with a correlation coefficient of $r = -0.3234$, $p=0.0133$, suggesting that 8-OHdG may serve as a marker for sensitivity to CNDAC, Figure 6.5 - 11.

Correlation 8-OHdG with Cell Growth at 100 μ M CNDAC

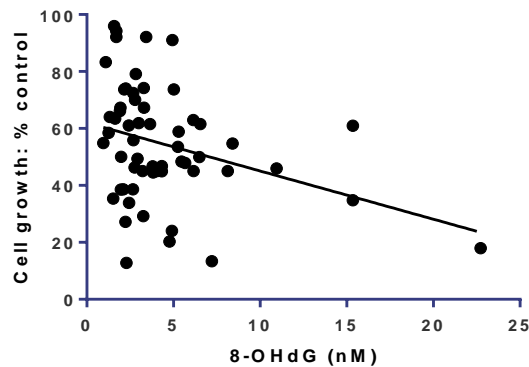


Figure 6.5 - 11: Correlation of 8-OHdG with CNDAC sensitivity.

Analysis of 8-OHdG levels in PCO cultures shows a continuum. There is no clear cut off value at which PCO cultures can be easily stratified into BER competent and defective groups. In order to explore the ability of an isolated 8-OHdG level to predict sensitivity to CNDAC a series of cut-off values were tested using ROC analysis with percentage survival at 100 μ M CNDAC, Table 6.5 - 7. The mean 8-OHdG levels in AA8 cell line (BER competent) was 0.701 and that of EM9 cell line (BER defective) was 5.286. Using a low level of 8-OHdG as the cut-off to allocate PCO cultures into BER competent and defective groups results in the best prediction for sensitivity in this dataset to CNDAC with an AUC of 0.7639, demonstrating this cut-off as having a fair/good predictor for % survival at 100 μ M CNDAC, $p = 0.0803$. However, the ROC analysis does not reach significance, and additionally, using a cut-off of 15 ng in this dataset would mean that only 4/60 (6.7%) of cultures were BER competent. This may be a reflection of the relatively small number of cultures, Figure 6.5 - 12.

8-OHdG Cut-off Value (ng)	Number (%) PCO cultures in group depending upon cut-off		ROC AUC (SE)	95% CI	p
	BER competent	BER defective			
1.5	4	56	0.7639	0.6365 to 0.8913	0.0803
2	13	37	0.5547	0.3802 to 0.7292	0.5508
3 (median)	30	30	0.5886	0.4405 to 0.7366	0.2467
4	36	24	0.5114	0.3603 to 0.6625	0.8853
5	42	18	0.5454	0.3858 to 0.7050	0.5957
6	48	12	0.5048	0.3154 to 0.6943	0.9805
7	52	8	0.5056	0.2953 to 0.7159	0.9619

Table 6.5 - 7: Receiver operator curve (ROC) analysis of predictability of 8-OHdG values (ng) to predict sensitivity to CNDAC, defined as <50% cell survival after 10day exposure to 100 µM CNDAC (determined by SRB assay). .

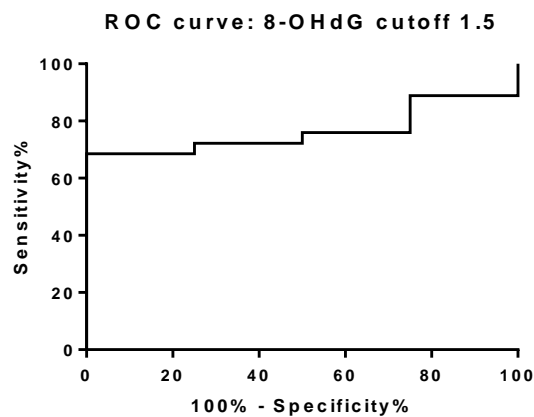


Figure 6.5 - 12: ROC 8-OHdG of 1.5 to predict CNDAC sensitivity. Using 1.5 ng 8-OHdG to stratify PCO samples tested into BER competent and BER defective groups enables accurate prediction of CNDAC sensitivity with an AUC of 0.7639, $p=0.0803$.

Inter-assay Variability

Sample batches of up to 12 samples were run in parallel each with AA8 and EM9 serving as positive and negative controls. There was a 33.5% inter-assay coefficient of variation for AA8 and EM9 and 47.9% in PCO samples. Variability within the PCO repeats may be a reflection of DNA collected at different passages. Using the 8-OHdG cut-off of 1.5 ng interassay variation in PCO did not alter BER functional status.

6.5.8. Interaction of HR and BER Functional Status

The interaction between HR and BER functional status is not yet known and it is not clear if one is more predictive of sensitivity to CNDAC than the other, or of their effect upon sensitivity to other novel cytotoxic agents.

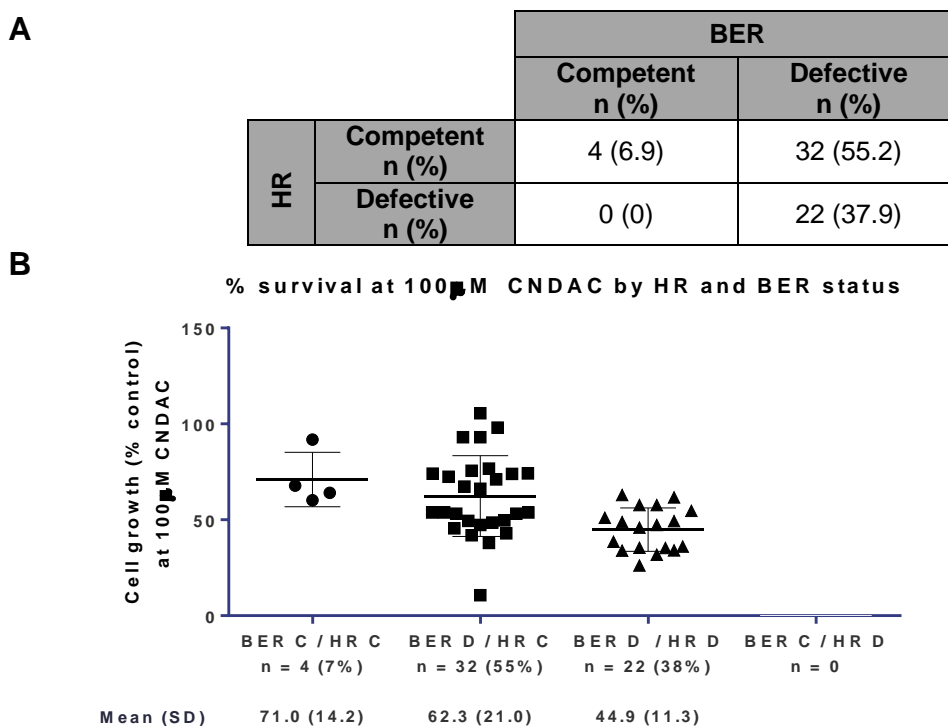


Figure 6.5 - 13: Incidence of BER and HR dysfunction in PCO cultures with corresponding grouped sensitivity to CNDAC. A: HR function determined by Rad51 assay based upon a >2 fold increase in Rad51 foci following induction of DNA DSB, see section 3.6. BER function determined by competitive 8-OHdG ELISA using median 8-OHdG as differential cut-off. B: percentage survival at 100 μ M CNDAC in PCO cultures stratified by HR and BER function. Mean and SD of each of the functional groups are shown on the graph.

Stratifying the PCO cultures according to their combined HR and BER functional status reveals greatest sensitivity to CNDAC in those cultures, which are defective in both HR and BER, with a mean (SD) % growth at 100 μ M CNDAC of 44.9 ± 11.3 , in comparison to cultures with either competent HR or BER function alone, ANOVA $p = 0.0028$, Figure 6.5 - 13.

6.5.9. Investigation of Uptake of CNDAC by Nucleoside Transporters Using Inhibitors

To investigate the relative roles of ENT1 and ENT2 equilibrative nucleoside transporters in the sensitivity to CNDAC, dipyridamole (DP) (which inhibits both ENT1 and ENT2) and NBMPR (which inhibits ENT1) were used. Cell proliferation SRB assays using cell lines paired for BER function (AA8: BER competent; EM9: XRCC1 mutation with BER defective) with addition of DP or NBMPR at various concentrations were undertaken to explore the effect of ENT 1/2 inhibition on sensitivity to CNDAC, Figure 6.5. - 14.

Neither addition of NBMPR nor DP had any effect upon cell growth, (data not shown). Both NBMPR and DP significantly protected the hyper-sensitive EM9 cells from CNDAC and both NBMPR and DP afforded equivalent protection from CNDAC in EM9 cells indicating that inhibition of ENT1 is sufficient and hence this is likely the predominant uptake mechanism of CNDAC, Table 6.5 - 8. Since in these experiments the effect of CNDAC on AA8 was modest it was not possible to determine if DP or NBMPR were protective but it is likely that the same mechanism operated in both cells which may be seen with inhibition of uptake at higher concentrations of CNDAC.

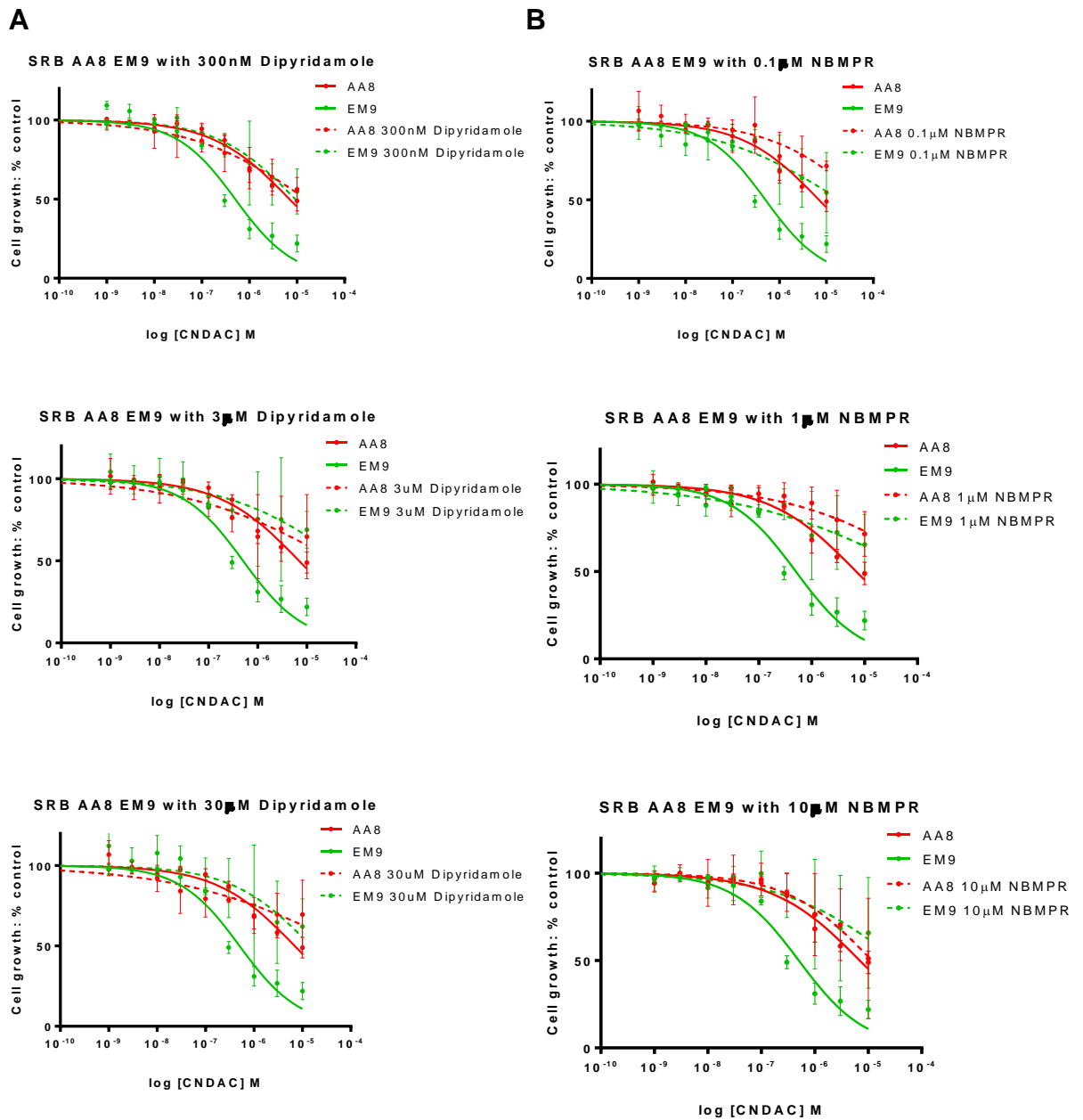


Figure 6.5 - 14: CNDAC cell proliferation assays using AA8 and EM9 cell lines with addition of DP or NBMPR. Cells were treated with CNDAC at various concentrations, normalised for 1% DMSO as indicated, for 48 hours with addition of 0.1, 1, 10 μM NBMPR or 300 nM, 3 μM or 30 μM DP. Cell proliferation was assessed by SRB assay. Data are the mean values and SEM from three independent experiments with six replicates for each concentration.

	Mean GI ₅₀ , μ M (fold increase from control)	
	AA8	EM9
Control	697	50.37
DP 3 μM	3874 (5.56)	5689 (112.94)
NBMPR 1 μM	21300 (30.56)	9893 (196.41)

Table 6.5 - 8: Mean GI₅₀ of paired cell lines following exposure to CNDAC with NBMPR or DP. Cells were treated with CNDAC at various concentrations with NBMPR or DP, as indicated, for 48 hours. Cell proliferation was assessed by SRB assay. Fold increase in GI₅₀ from untreated controls was calculated.

6.5.10. Expression of Proteins Implicated in CNDAC Sensitivity: ENT, dCK, CDA

Levels of protein expression of transporters and enzymes involved in resistance to nucleoside analogues, such as dCK (activation of CNDAC into CNDAC triphosphate), hENT1 (cellular uptake), and CDA (inactivation to CNDAC), were determined in a series of western blots using a panel of cell lines and PCO samples and correlated with CNDAC cytotoxicity, see Chapter 3 for protocol.

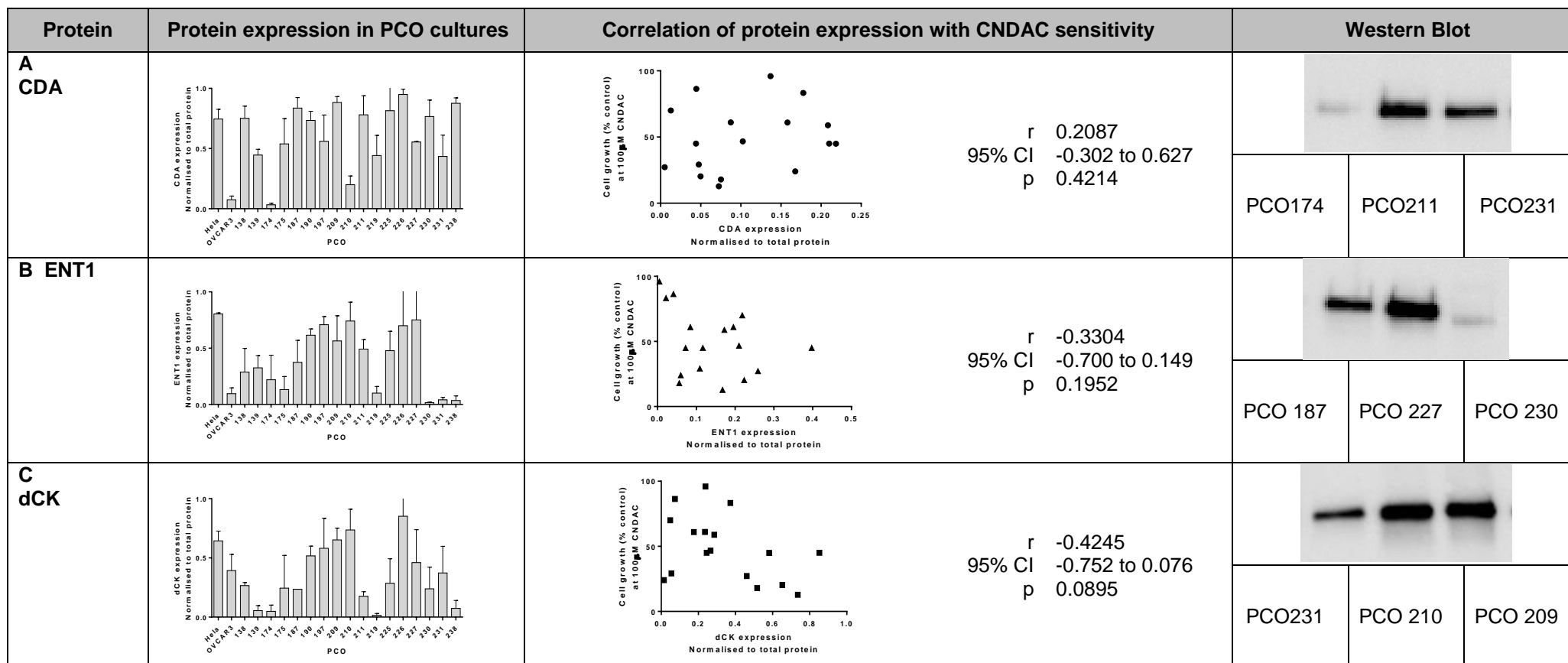


Figure 6.5 - 15: Western blot for protein expression of ENT1, CDA, dCK in PCO cultures. Cell lysates from cultured PCO and cell lines were made from approximately 1 million cells. Proteins were separated using gel electrophoresis, detected using western blotting and visualised using chemiluminescence. Protein levels were normalised to total protein (Ponceau S). Data are from two independent experiments.

Variable expression of ENT, CDA and dCK were detected within the PCO samples tested. As anticipated, there was a modest negative association of CNDAC resistance with dCK expression, indicating that reduced CNDAC activation confers resistance. The same negative association was seen with ENT1 expression. There was however, no significant correlation between levels of expression of any of the proteins tested and sensitivity to CNDAC determined by cell proliferation assays. This suggests that although CNDAC may enter the cells via ENT1 and is phosphorylated by dCK to form CNDAC triphosphate before incorporation into DNA small variations in expression of these proteins is not the major determinant of sensitivity to CNDAC.

Interestingly, ENT1 expression was <0.5 of the normalised protein in 9/17 (53%) of the PCO tested and in comparison to OVCAR3 cell line, known to express low levels of ENT1 (Zhang 2006). It would be expected that this would result in poor uptake of CNDAC into the cell and therefore result in resistance to CNDAC. This was the case in PCO 230, PCO 231 and PC 238 with percentage survival at 100 μ M CNDAC of 96.0, 83.3 and 86.4% respectively but PCO 219 and PCO 175, which also had low expression of ENT1, were sensitive to CNDAC with 24.1 and 45.0 % survival at 100 μ M CNDAC. It is possible that tumours with low ENT have utilised alternative nucleoside transporters that can also carry CNDAC into the cell. As the cell line data demonstrate, there are several determinants of sensitivity to CNDAC and it is possible that one or more of these mechanisms (reduced dCK, increased CDA, increased HR, NER and BER) could confer resistance even if ENT1 was high.

6.5.11. BER Gene Expression as a Surrogate for BER Function

To further evaluate the role of the BER pathway in the sensitivity to CNDAC, RNA expression of key components of the pathway (APE1, PARP1, XRCC1, Pol β , LIGIII, PNK, PCNA, FEN1, LIG1) were examined and correlated to BER function.

The relative expression of genes involved in DNA BER repair was determined by the Oxford genomics centre (Oxford, UK) using Illumina Genome Studio and HumanHT 12v4.0 R1 15002873 array, see Chapter 3. 24 PCO samples with a range of 8-OHdG levels, reflecting variable BER function were tested. The relative expression of each component of the BER DNA repair pathway was calculated and differences between the BER competent and BER defective groups calculated. Groups were defined using the median 8-OHdG value and 2 nM.

No statistically significance difference between RNA expression of any component of the BER pathway was seen when between BER functional groupings using the median 8-OHdG value as the discriminatory cut-off. Significance was seen between the expression of PARP1 and Pol ϵ when the lower discriminatory value of 2 nM was used, Figure 6.5 - 15. However, no correlation between RNA expression and sensitivity to CNDAC was seen. There was however correlation between Pol β expression and sensitivity to CNDAC, $r^2=0.09659$, approaching significance, $p=0.0697$. Correlation between sensitivity to CNDAC and RNA expression of PARP1, LIG1, and Pol ϵ was seen.

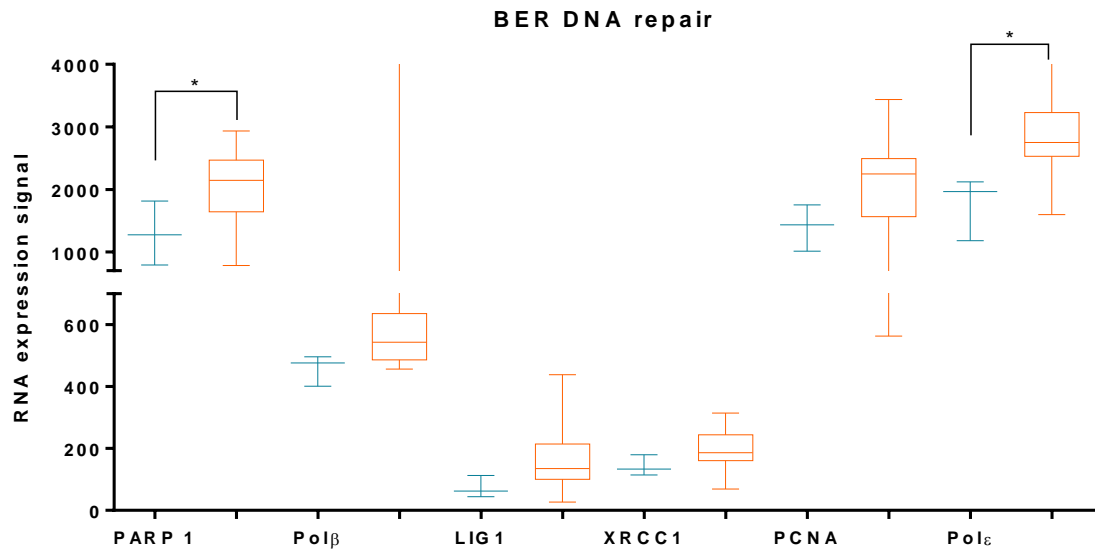


Figure 6.5 - 16: RNA expression of key components of the BER DNA repair pathway in PCO grouped by BER status, $n=24$, (orange = BER competent, Blue = BER defective). RNA was extracted from frozen PCO cell pellets and after quantification, the HumanHT-12 v4 Expression BeadChip used to detect and quantify more than 47,000 probes derived from the National Centre for Biotechnology Information Reference Sequence (NCBI) RefSeq Release 38 (2009). Labelled cRNA are detected by hybridisation to 50-mer probes on the Beadchip. After washing and staining steps using the Direct Hybridization Assay, beadchips are scanned on the HiScan or iScan systems. Illumina Genome Studio Gene expression software is used to extract relative gene expression across samples, clustering them into differential groups. The comparative Ct ($\Delta\Delta C_t$) method was used to assess the expression level of components of each pathway relative to endogenous controls normalized to the reference panel. The fold change differences in expression of each gene between sample categories (HRC and HRD; BER competent and BER defective) was calculated. The mean and SD of the fold change are plotted with HRC cultures shown in red and HRD shown in blue.

6.6. Discussion

6.6.1. Sapacitabine in the Treatment of Ovarian Cancer

Initial cell line and *ex vivo* PCO culture work suggests that there is a role for CNDAC in the treatment of ovarian cancer. A phase 1 study of sapacitabine and seliciclib for advanced solid tumours (NCT00999401), which included 7 patients with end stage ovarian cancer, showed response in 2/7 (29%) when provision of treatment was not stratified. Based upon cell proliferation assays of primary cultures, section 6.5.2, an unstratified approach would result in a response rate of 46% (25/54), with less than 50% cell survival following a 10-day treatment with 100 μ M CNDAC. Exposing patients to the associated morbidity and the NHS to the financial costs of ineffective treatment is not ideal. A stratified approach aims to enrich the patient population who receive the treatment and would at least enable provision of accurate prognostic information to patients and, if biomarkers are used to guide actual therapy, this is likely to result in higher rates of overall response. Successful stratification is dependent upon reliable biomarkers capable of accurately predicting response. This study aimed to further our understanding of the potential effect of CNDAC upon ovarian cancer as well as explore the use of DDR function as biomarkers of response. Cell line studies show greater sensitivity in cell lines with BRCA 1/2 mutations and subsequent HR dysfunction in comparison to their matched wild type lines for CNDAC, as well as for PARPi and cisplatin. A fold increase ranging from 7 to 243 was seen between BRCA mutant and BRCA WT across three sets of paired cell lines, section 6.5.1. The range of levels of sensitisation in different paired cell lines (VC8 were 243 fold and UWB1-289 were 7 fold more sensitive) demonstrated that even within a particular defect (BRCA) there is a spectrum of sensitivity and this may be a consequence of other genetic and epigenetic changes perhaps resulting in dysfunction of other critical pathways. Established cell lines provide an invaluable tool for studying biological functions at the molecular and cellular level. However, their use has several limitations, particularly in ovarian cancer research. We understand that actual ovarian cancer frequently harbours multiple interacting mutations within many cellular pathways and the isolated defects in cell lines underestimate this complexity.

Primary cultures are more accurate in simulating the patient situation more closely and were used in this study to ascertain the frequency of response to CNDAC in ovarian cancer.

6.6.2. HR as a Biomarker of Sensitivity to CNDAC

Each PCO culture was stratified into two groups based upon the Rad51 assay for HR function. 34 (63%) were HRC and 20 (37%) cultures were HRD. When grouping all HRC cultures and comparing to grouped HRD cultures, greater sensitivity to all three agents (CNDAC, rucaparib and cisplatin) was seen in the HRD group, Figure 6.5 – 3, with mean % survival following treatment with 100 μ M CNDAC of 63.5% (SD 22.3) in HRC cultures and 43.1% (20.1) in HRD cultures, $p = 0.0015$. The resistance to CNDAC seen in some HRD PCO cultures may have developed by dysfunction in another cellular pathway and it is important to realise that testing HR function alone will fail to identify some patients who may benefit from treatment with CNDAC and may subject some patients to treatment without clinical benefit. Although there were some outliers with HRD PCO cultures being resistant to CNDAC and HRC cultures showing sensitivity, with the use of HR functional status to stratify treatment response rate rose to 77% with 17/22 cultures classified as HRD showing response to CNDAC. The overall PPV of HRC to predict resistance to CNDAC was 83.3% with a NPV of 70.8%. Sensitivity and specificity were shown to be 0.816 and 0.898 respectively.

The PCO *ex vivo* data presented here suggests that response to sapacitabine could be anticipated in approximately 50% of tumours when used as a first line agent (in PCO samples from chemo-naïve patients) but there is also response seen in a proportion of PCO cultures generated from patients following platinum therapy and in platinum resistant disease, see section 6.5.3. Of the 38 PCO *ex vivo* cultures classified as sensitive to CNDAC, eight of the donor patients had been treated with platinum chemotherapy prior to sample collection and a further four patients had innate platinum resistance indicated by clinical progression of disease within 6 months of treatment. Additionally response to CNDAC was seen in 17 PCO cultures that were resistant to rucaparib. This

initial work suggests that sapacitabine may have a role in both platinum sensitive and platinum resistant disease.

As discussed in Chapter 4, the typical population of patients affected by ovarian cancer is frequently affected by multiple comorbidities and typically, combination treatments would not be tolerated. Sapacitabine can be given as an oral preparation and the reported systemic side effects are minimal. It may therefore be possible to combine sapacitabine with standard treatments.

In BER, PARP-1 mediated recruitment of XRCC1 is followed by nucleotide replacement and their close relationship within the BER pathway and their cross reactivity across the DDR prompts exploration of the combined effect of CNDAC and PARPi. Work undertaken by project collaborators in cell lines aimed to explore the combined effect of CNDAC with PARPi and CNDAC platinum if given sequentially or together upon cytotoxicity. CNDAC can be effectively combined with PARPi in ovarian cell lines or given in sequential treatments, although with PARPi, sequential treatments appeared to be better than the concomitant treatment schedule, Table 6.5 - 3. Synergy was also observed between CNDAC and cisplatin in a schedule-independent manner in non-small cell lung cancer (NSCLC) cell lines, (Frame, Armour et al. 2012). In the same series of work, sequential treatments with CNDAC and PARPi (irrespective of order) in NSCLC cell lines was also synergistic however concomitant treatment with CNDAC and PARPi was antagonistic schedule-independent manner in non-small cell lung cancer cell lines, (Frame, Armour et al. 2012). The synergy observed between CNDAC and rucaparib may be explained, at least in part, by the understanding that although CNDAC and PARPi induced damage is predominantly repaired by the HR pathway, BER is also involved (see section 6.5.6). Induction of damage in both pathways simultaneously results in loss of the synthetically lethal 'backup' pathway resulting in high rates of cell death.

6.6.3. Interaction of Other Cellular Pathways in the Sensitivity to CNDAC

Work to date has utilised cell lines with isolated pathway mutations. In primary ovarian cancers, multiple coexisting mutations may result in dysfunction of several pathways and loss of some elements of one DNA repair pathway may be compensated for by increased activity of others. It may therefore be important to explore other pathways in addition to HR to understand the key pathways involved and identify a possible biomarker of response. It was hypothesised that dysfunction in other important pathways in ovarian cancer may be responsible for the outliers in response to CNDAC, cisplatin and rucaparib in the PCO dataset.

Cell lines defective in NER due to an ERCC2 mutation (UV5) were 47 fold more sensitive than AA8 cells. The increased sensitivity of the NER-defective cells to CNDAC was comparable to their cisplatin sensitivity, Figure 6.5 – 8, Table 6.5 - 5. This is in contrast to work completed by Wang *et al* which demonstrated that cells lacking either XPD (ERCC2), the 3'-helicase, or the 3'-endonuclease XPG were equally as sensitive to CNDAC as wild-type cells (Wang 2008).

Additionally, Wang *et al* showed that cells deficient in the CSB protein, (which initiates TC-NER), exhibited increased sensitivity to CNDAC, whereas cells deficient in XPC, (which initiates GG-NER), were slightly resistant relative to wild-type cells (Wang 2008). It is not clear why these differences exist but may be a reflection of the different paired cell lines and assays used. ERCC2 is involved in both TC- and GG-NER and the greater sensitivity seen in UV5 compared to AA8 cell lines in this study in comparison to the smaller 5 fold difference in TC-NER cell lines previously reported (Wang 2008) may reflect the importance of the difference in the initial DNA damage recognition step with GG-NER may be the major determinant of CNDAC sensitivity. Multiple studies have demonstrated the functional importance of ERCC2 in the repair of cisplatin DNA adducts and in cisplatin sensitivity in human ovarian cancer cells in vitro (Saldivar 2007) and dysfunction of both NER subpathways may be important in the sensitivity of ovarian cancer to CNDAC and the interaction of multiple defective pathways in ovarian cancer requires further exploration.

In this study, the presence of p53 mutation appeared to result in a 4.7 fold increase in resistance to CNDAC in comparison to WT, $p < 0.0001$. Addition of mutation in hMLH1 (CP70 A2) conferring defective MMR resulted in an additional three fold increase in resistance to CNDAC, $p < 0.0001$, reinforcing the lack of understanding of the cross-talk between the different pathways and the unknown summative effects that dysfunction in more than one pathway may have upon sensitivity.

Cells with defective NHEJ are more proficient in HR repair, and it has been suggested that the two DSB DNA repair pathways are in direct competition with one another (Neal, Dang et al. 2011). Interestingly, V3 cell line (DNA-PK_{CS} deficient) defective in NHEJ was more resistant to CNDAC in comparison to its paired competent cell line (V3-YAC) suggesting that NHEJ is not the predominant repair mechanism of CNDAC induced DNA damage. Within the SRB assays used to investigate the role of NHEJ, cell are however in the phase of exponential growth and further investigation of this is essential prior to stratification in clinical trials. It is possible that quiescent cell populations, which are not in active S phase, in which the NHEJ pathway predominates, will be resistant to CNDAC if NHEJ defective. Tumours, which are rapidly growing (in S phase), may therefore show more of a response to CNDAC than more slowly growing tumours. It has been shown that DNA-PK can inhibit HR, which is dependent upon DNA-PKs enzymic activity modulated by phosphorylation (Neal, Dang et al. 2011). Since HR is a determinant of CNDAC sensitivity then a mechanism to increase DNA-PK activity may confer sensitivity by obstructing HR and should be explored as a combination treatment in HR competent cells. Cell lines with mutant XRCC1 (EM9), conferring BER dysfunction were 19 fold more sensitive to CNDAC than matched WT (AA8). The differential sensitivity in the AA8 and EM9 cell lines suggest a central role of XRCC1 in CNDAC sensitivity. This was in contrast to previous work by Wang *et al* who found that XRCC1 defect conferred no difference in sensitivity to CNDAC (Wang 2008). Data in this these was repeated by three people independently (Adriana Buskin and James Murray) with consistent results.

The BER assay described in this work assesses the baseline level of 8-OHdG within PCO samples, and aimed to further assess the relationship of BER dysfunction with sensitivity to CNDAC. It was hypothesised that 8-OHdG serves as a biomarker of BER DNA repair with higher levels of 8-OHdG (indicating defective BER) conferring sensitivity to CNDAC. In the small sample of PCO cultures tested, a negative correlation was seen between 8-OHdG level and percentage survival at 100 μ M CNDAC, $p=0.0133$, Figure 6.5 - 11. However, correlation of XRCC1 (RNA) and BER function in PCO samples with sensitivity to CNDAC was not seen.

The variable level of 8-OHdG detected within the PCO samples tested suggests that different tumours have variable ability to repair using BER but it is also possible that this reflects the different microenvironments of the tumour, with variable levels of oxidative stress. To further evaluate the ability of the tumour to repair using BER, further experiments to quantify the change in levels of 8-OHdG following *ex-vivo* induction of oxidative stress (perhaps with temozolomide), alongside untreated controls may provide a more accurate assessment. Although additional work is required to validate and develop further understanding of the levels of BER in normal cells and the level of 8-OHdG which discriminates between competent and defective BER, this study does however clearly demonstrate the important role of BER in the use of CNDAC in ovarian cancer.

It is perhaps over ambitious to expect that a single marker for a single DNA repair pathway will be capable of predicting overall response to cytotoxic agents in tumours that we understand to have multiple mutations affecting a number of pathways. The development of biomarkers of function of all-important pathways in ovarian cancer is important but further work will be required to understand which of these pathways are predominant and how they interact. The 243 fold increase in mean LC_{50} between HRD and HRC paired cell lines suggests that HR is the predominant pathway of CNDAC DNA damage repair but NER is a key determinant of sensitivity as is BER.

6.6.4. Cellular Uptake and Metabolism of CNDAC

Variable expression of ENT, CDA and dCK were detected within the PCO samples tested. No correlation was seen however between levels of expression of protein with sensitivity to CNDAC determined by cell proliferation assay as previously described. This suggests that although CNDAC may enter the cells via ENT1 and is phosphorylated by dCK to form CNDAC triphosphate before incorporation into DNA small variations in expression of these proteins is not the major determinant of sensitivity to CNDAC.

6.7. Conclusions

CNDAC induced damage is mainly repaired by HR and cell lines deficient in HR are more sensitive to CNDAC than competent cells. This correlated with sensitivity to PARPi and cisplatin. Use of HR functional status may enrich for response to sapacitabine but its PPV and NPV are likely to prevent the isolated use of HR status to stratify treatment in clinical practice. Investigation of the role of alternative DNA repair pathways in the sensitivity to CNDAC using paired cell lines confirmed merit in further investigation of the BER pathway. A functional assessment of this pathway is possible and may aid in future stratification. In reality, it is likely that there are multiple pathways involved in the tumour response to each cytotoxic agent and developing an understanding of if there is a single predominant pathway with a biomarker or if the function of all pathways involved is required to determine sensitivity.

Knowledge of CNDAC mechanisms identifies tumours that may be sensitive to sapacitabine, thus enabling accurate stratification of therapy. It also creates the opportunity to overcome resistance to commonly seen with current platinum based chemotherapies and identifies synergistic interactions. The work in this chapter provides rationale for the design of sapacitabine-based clinical trials in ovarian cancer.

Chapter 7. Circulating Tumour Cells in Ovarian Cancer

7.1. Introduction

The first detection of circulating tumour cells (CTCs) was reported more than a century ago (Ashworth 1869). More recently, interest in the clinical role of CTCs has re-emerged with the development of new technologies.

CTCs potentially represent a substitute for an invasive tissue biopsy. In contrast to functional assessment in tumour biopsies, measuring biomarkers in CTCs offers the potential for more frequent, real time monitoring throughout treatment.

7.1.1. *The Origin of CTCs*

CTCs may originate from the primary tumour or from metastases having acquired properties enabling migration and survival in the circulation. If CTCs are to form metastases, they must also possess the ability to extravasate from the circulation and initiate growth in a secondary site (Kalluri 2009, Allan 2010). The ability of cancer cells to metastasise depends upon their molecular profile as well as the host environment (Coman 1951, Fidler 2008). Epithelial mesenchymal transition (EMT) is considered the crucial event in the metastatic process and involves disruption of epithelial cell homeostasis and acquisition of a migratory mesenchymal phenotype (Thiery 2002, Visvader 2008, Aktas 2009). The molecular profile of CTCs cannot therefore be presumed to be the same as the original tumour (van de Stolpe et al, 2011).

Tumour Metastasis

While the circulatory system is the main route of metastasis in the majority of cancers, ovarian cancer predominantly disseminates by transcoelomic spread. Tumour cells are shed from the tube/ovary releasing proteins resulting in accumulation of ascites that carries floating cancer cells to other intra-peritoneal site. This allows deposition and invasion of tumour cells onto peritoneal surfaces. Different from other malignancies, distant metastasis formed by haematogenous or lymphatic spread, is a late complication and only occurs in about one third of patients (Cormio 2003).

The Clinical Potential of CTCs

CTCs offer the potential to change the way in which we diagnose cancers, stratify available treatments, monitor patients during and following treatment, and provide prognostic information. Research has initially focused on CTC enumeration and, as metastatic disease is the cause of death in 90% of cancer patients (Pantel 2010), it is unsurprising that the presence of CTCs has been linked with poor prognosis in breast, colorectal and prostate cancer (Cohen 2008, De Bono 2008, Krebs 2011). Whilst provision of prognostic information may be of some use to clinicians, the hope for improved survival is dependent upon accurate provision of targeted cytotoxic agents, which in turn relies upon biomarkers. Current biomarker assays in ovarian cancer rely upon surgical resection or invasive biopsies. If CTCs can be identified and used in biomarker assays, they offer the potential for non-invasive real time assessment of an individual's cancer. In some cancer types, it has been shown that cells are shed from tumours into the peripheral circulation well before metastasis occurs (Liotta 1974) and therefore detection of CTCs could be important for screening as well as for detection of recurrence and evaluation of treatment response (Cristofanilli 2006, Hayes 2006, Cristofanilli 2007).

Tumour Microemboli/CTC and WBC Aggregates

There have been reports of clusters of CTCs detected in patients with advanced cancer, which range from 3 to 14 cells (Stott 2010, Hou 2011, Hou 2012). Early studies suggest that CTC clusters may be relatively protected from cell death and the harsh environment and stresses of the vascular circulations. They may also be clinically significant, particularly the number, size or composition of the clusters (Wang 2000, Glinsky 2003, Serrano Fernandez 2009, Stott 2010, Hou 2011, Hou 2012). The presence of clusters may be a better biomarker for increased metastatic potential than single CTCs (Wang 2000, Stott 2010, Hou 2011)

7.1.2. Pharmacodynamic Biomarkers Using CTCs

Bourton *et al* (2012) have demonstrated identification of γ H2AX foci on ImageStream in irradiated immortalised human fibroblast cells. Although the number of foci detected using the ImageStream was lower than those detected in comparable cells using traditional immunofluorescence on fixed cells, the relative difference between the different cell lines used was retained and the difference between control and irradiated samples was also maintained (Bourton 2012). It remains to be seen whether this work can be replicated on primary ovarian samples.

CTCs have also been used as a pharmacodynamic biomarker to study γ H2AX induction after treatment with DNA damaging agents (Wang 2010, Bourton 2012). Results from an initial set of patient data suggest that γ H2AX levels in CTCs may be a more sensitive marker for assessing drug effects in patients than total CTC counts alone (Wang 2010). Similar studies evaluating Rad51 foci formation and other DNA repair proteins in CTCs are on-going (Yap 2011).

7.1.3. CTCs vs. Circulating DNA

Given the many methods and technical challenges that are involved in isolating and characterising CTCs assays, the alternative approach of utilising DNA isolated directly from blood are appealing. Although the majority of circulating extracellular DNA is adsorbed to the surface of leukocytes or erythrocytes, a portion can be identified in the plasma, known as plasma DNA or cfDNA (Kidess 2013). In light of the current advances in next-generation sequencing the availability of cfDNA has ignited interest.

The presence of small amounts of tumour DNA in the plasma of cancer patients was demonstrated several decades ago (Leon 1977). Since then, multiple studies have investigated plasma DNA's potential as a biomarker (Schwarzenbach 2011). Circulating DNA is thought to originate from lytic, apoptotic or necrotic tumour cells or by active secretion from macrophages that have phagocytised necrotic cells, or from CTCs themselves (Schwarzenbach 2011, Payne, Hava *et al.* 2012). However, cfDNA can also be derived from normal cells and therefore cfDNA is also detectable in healthy volunteers,

patients without cancer, patients with benign tumours, as well as cancer patients. cfDNA is typically analysed together with plasma DNA from normal cells. cfDNA fragments represent only a minority of all DNA fragments in the circulation but the actual percentage of cfDNA present may vary considerably and depends on various parameters including the tumour burden. cfDNA isolated from plasma and can be subjected directly to an array for copy number analysis, and or mutations at the nucleotide level. This analysis is independent of epithelial markers, tumour heterogeneity and evolution. On the other hand, CTCs yield information on a cellular level and thus clonality, whereas cfDNA reflects an average of all tumour cells releasing DNA into the circulation (Heitzer 2013). The method selected is likely to therefore depend upon the goal of analysis; whether a biomarker is being sought rather than the biology; identification of a drug target; investigation of tumour response or mechanisms of drug resistance.

Although analysis of cfDNA may be cheaper and technically less challenging its restrictions limit its use in sampling tumour in ovarian cancer for the purposes of functional biomarker assessment and this study has focused upon optimisation of CTC detection, Table 7.1 - 1.

	CTC	cfDNA
Equipment	Special instrumentation for cell identification needed	None, simple blood collection
Isolation of CTC or cfDNA	Complex CTC isolation out of thousands of cells and complex single-cell transfer for further processing	No isolation of cfDNA required; instead, standard preparation of plasma DNA
Information on heterogeneity and clonality	Yes, if enough CTCs are captured and successfully analysed	No, results represent an average from all cells shedding tumour DNA into the circulation
Dependence on EpCAM markers	Yes, for most CTC capture systems, such as the CellSearch system. EpCAM-independent CTC capture systems exist but await validation in clinical studies	Independent of any marker
Applicability for basic metastasis research	Instrumental, as it enables cell-by-cell analyses, generation of cell lines and analyses in animal models	Provides only a snapshot of the current status of the tumour genome
Applicability for diagnostic or monitoring purposes	Established for CTC enumeration; advancements will depend on improvements in CTC capturing, analysis tools and associated costs	Appears to be very attractive because of the simplicity of obtaining plasma DNA; needs to be determined in clinical studies

Table 7.1 - 1 Differences between CTC and ctDNA analyses, (Heitzer 2013)

7.1.4. CTCs in Ovarian Cancer

There are several reports of the identification of CTCs in ovarian cancer patients (Marth 2002, Judson 2003, Wimberger, Heubner et al. 2007, He 2008, Fan 2009), which have mainly used cytological detection methods. These antibody-based methods resulted in variable CTC detection rates, ranging from detection in 12% - 100% of all patients tested. Cellular yields were also variable, ranging from 0 - 3118 CTC/ml in one study (He 2008) and as expected, higher detection rates have been associated with higher stage of disease (CTC present in 100% of stage IV patients tested compared to 35% for stage III) (Sapi 2002). There have also been reports of metastatic cells in the bone marrow of 20 - 30% patients with ovarian cancer, providing further evidence for the existence of CTCs in at least a proportion of patients (Braun 2001, Marth 2001, Marth 2002).

The study by Marth *et al* 2002 identified CTCs using immunomagnetic beads conjugated to an epithelial glycoprotein (EGP-2 / MOC31). Samples that

demonstrated at least two cells with antibody-bound beads were considered positive but this was the only criteria used to select a CTC from the other nucleated cells in the sample. The study by Judson *et al* (2003) used immunomagnetic beads conjugated to a mixture of epithelial markers (anti-cytokeratin 8 and 18, TFS02, CK-7, CK-10 and EGFR), following gradient separation of the mononuclear cell fraction to enrich tumour cells, and then used microscopic evaluation to identify and count CTCs based on specific cytoplasmic staining and tumour cell morphology. This study did not include a leucocyte specific marker and it is possible that the cells found to be positive for one or more of the epithelial antigens were in fact false positive antigen expression in apoptotic / activated WBC or contaminated epithelial skin cells. The study by Tan *et al* (2010) describes antibody enrichment of the mononuclear cell fraction, following density gradient separation, and enumerates epithelial positive (CAM+ and [EPCAM+ or ESA+ or CK+]), CD45 negative cells. None of the five benign samples tested had detectable CTCs and CTC counts ranged from 0 - 149 CTC/ml, with Stage III and IV patients exhibiting significantly higher mean counts (41.3 CTC/ml). These antibody-based methods resulted in CTC detection in a small proportion of patients ranging from 12% - 18.7% and the presence of CTC defined by anti-epithelial antibody markers alone was not found to correlate with survival or disease recurrence.

One potential explanation for the variation reported is the multiple different detection platforms used, which all utilise varying definitions of what constitutes a CTC. Of concern, a number of these platforms, including Veridex, have been reported to detect objects, classified by their definition as CTCs, in healthy volunteer blood or those with non-malignant disease, (Allard and Tibbe 2004, Obermayr 2013). CellSearch™ state that it is only abnormal to have >2 'CTC' (Allard and Tibbe 2004).

7.1.5. CTC Challenges

Effective enumeration and characterisation depend upon a reliable method for detection. Detection of small populations of CTCs within the large number of normal blood cells represents a significant technical challenge.

Rare Cell Population

Whole blood contains $4 - 11 \times 10^9$ /L WBC, $3 - 7 \times 10^{12}$ /L RBC and $150 - 450 \times 10^9$ /L platelets. The ideal method for CTC analysis would enable 100% detection with no CTC loss. However, imaging and sorting millions of cells is unlikely to be clinically reproducible and evidence suggests that enrichment is necessary to prevent underestimation of CTCs (Pantel 1999). Enrichment may consist of positive selection of CTCs, negative depletion of blood cells or a combination of the two methods. The majority of studies have relied on positive enrichment using a single tumour cell antigen, most commonly EpCAM (Tibbe 1999, Nagrath 2007, Riethdorf 2007, Maheswaran 2008, Sequist 2009, Talasz 2009, Gleghorn 2010, Stott 2010). The problem with this approach is tumour heterogeneity and there are currently no known markers expressed by every tumour cell within a given tumour type (Allan 2010). Use of a single antigen is likely to result in underestimation of the number of CTCs as well as biased selection of a single subpopulation. Negative enrichment options include lysis or filtration of RBCs, alongside negative selection of WBCs labelled with specific antigens, for example the highly conserved marker CD45 (Goodale 2009).

CTC Definition

There is much debate about what constitutes a CTC with various definitions being used across different CTC platforms. It seems unlikely that CTCs from ovarian cancer will have the same phenotype as CTCs from other tissue types and therefore the definition must be cancer-site specific. The Lorentz Workshop; CTC Isolation and Diagnostics: Toward Routine Clinical Use, created a standard CTC definition combining parameters to increase specificity (Van de Stolpe 2011):

“A nucleated cell larger than 4 μ m, expressing epithelial proteins EpCAM and cytokeratins 8/18/19, while being negative for the leukocyte-specific antigen CD45”.

Heterogeneity of CTCs

We have shown that inter- and intra-tumoural heterogeneity exists within intra-abdominal ovarian tumour and the same heterogeneity may exist in CTCs.

Terstappen *et al* (2000) showed, using retrospective analysis of prostate CTC images, that different CTC definitions resulted in different counts with varying degrees of clinical significance. The use of a single parameter to define a CTC is problematic as no single parameter is essential, or sufficiently distinctive, to define a true CTC without overlapping with WBC and/or the presence in healthy volunteers (Van de Stolpe 2011).

EpCAM is widely used in many CTC platforms and is theoretically expressed by all epithelial cells. As discussed in this thesis, CTCs may lose their epithelial antigens as they undergo EMT. EMT constitutes a spectrum and it therefore seems likely that CTCs can express both epithelial and mesenchymal antigens to varying degrees, giving rise to heterogeneous CTC populations (Christiansen 2006). The use of a panel of antigens for the positive detection of CTCs may overcome these problems.

7.1.6. CTC Detection Techniques

Technologies available can be broadly divided into nucleic acid based and cytometric approaches. In the 1990s, nucleic acid based methods predominated, relying upon the detection of DNA/RNA sequences differentially expressed by tumour cells (Paterlini-Brechot 2007, Alunni-Fabbroni 2010).

Circulating free DNA may however be released from non-viable cells and cytometric techniques examining intact CTCs enables assessment of morphology, enumeration of CTCs and has potential for further analysis, Table 7.1 - 2.

Technique		Description	Enrichment	References
ImageStream, Amnis	High resolution immunofluorescent microscopy with flow cytometry	See section 7.2.6 Cells are stained for a panel of antibodies to positively identify epithelial tumour cells, whilst simultaneously excluding WBCs and un-nucleated objects.	Negative enrichment of RBC +/- WBCs.	
CellSearch™, Veridex	Immunological selective isolation	EpCAM antibody coated magnetic beads to select epithelial cells subsequently labelled with anti-CK antibody. Negative exclusion of anti-CD45 labelled WBC.	Positive enrichment for EpCAM.	(Cristofanilli 2004, De Bono 2008, Krebs 2011)
Magsweeper		Anti-EpCAM coated magnetic beads dispersed in the sample and collected by sweeping rods.	Positive enrichment for EpCAM.	(Talasaz 2009)
CTC-Chip	Microfluidic technologies	Silicon microchip containing chambers lined with microposts coated with EpCAM antibodies with flow patterns to optimise cell antibody contact while preserving cell viability. Microfluidics push whole blood over the chip to capture EpCAM-positive CTCs, which are confirmed to be CTC with CK immunofluorescence.	Positive enrichment for EpCAM.	(Kobayashi 2005, Nagrath 2007, Maheswaran 2008, Sequist 2009, Tewes 2009, Gleghorn 2010, Stott 2010)
IMEC	Molecular selective isolation	Immunomagnetic bead capture with di-electrophoresis-based transport combined with a PCR assay.	Positive enrichment for CTC	(Stakenborg 2010)
Isolation by size of epithelial tumour cells (ISET) 3D microfilter	Filter technologies	Filter technique based upon differentiation of CTCs by size using an 8 um pore, pressure driven polycarbonate filter (ISET 29) or 3-dimensional parylene microfilter containing homogeneous posers, enabling direct visualisation/analysis on the filter.	Positive enrichment for CTC	(Vona 2000, Krebs 2011, Zheng 2011)
Epithelial immunospot (EPISPOT)		Antibody-based approach based upon the ELISPOT technology. Based upon the identification of cells able to secrete epithelial specific or tumour type-specific soluble proteins.	Positive enrichment for CTC based upon epithelial markers (MUC1 – breast; PSA-prostate)	(Alix-Panabieres 2007)

Table 7.1 - 2: CTC detection technologies. Adapted from (Alunni-Fabbroni 2010).

CellSearch™

CellSearch™ is FDA approved for CTC detection in patients with metastatic breast, colorectal and prostate cancer (Cristofanilli 2004, Cristofanilli 2005, De Bono 2008, Plummer, Woll et al. 2008, Miller 2010). Its advantages include its semi-automation, reported reproducibility and sensitivity. However, dependence upon EpCAM enrichment means CTC subpopulations may go undetected (Fischer 2009). Briefly, blood is diluted and incubated with anti-EpCAM antibody coated ferrofluid particles. Then, following immunomagnetic enrichment, cells are permeabilised and fluorescently labelled using anti-CK antibodies (epithelial cells) and anti-CD45 antibody to exclude WBCs (Hou 2009).

The first publication from CellSearch compared CTC numbers in 964 metastatic cancer patients to 145 healthy volunteer and 199 non-malignant disease samples (Allard and Tibbe 2004). Only one sample from the non-cancer samples had more than 2 CTC/7.5 ml whole blood in comparison to 36% of samples from metastatic cancer patients, (range 0 - 23618 CTC/7.5 ml blood) (Allard and Tibbe 2004). The presence of CTCs varied widely in samples from different carcinomas, with highest frequency in metastatic prostate, unknown primary, ovary and breast cancers (Allard and Tibbe 2004). Three seminal studies in breast (Cristofanilli 2004), prostate (De Bono 2008) and colorectal cancer (Cohen 2008) have subsequently shown that the number of CTCs, over a specified cut-off, predicted worse prognosis and a change in CTC number following initiation of therapy demonstrated predictive value for survival outcome (Krebs 2010).

7.1.7. ImageStream

Technology

ImageStream is a multispectral imaging flow cytometer that produces high-resolution images of individual cells in flow, allowing assessment of morphology as well as intensity and location of fluorochrome labelled antigens.

ImageStream has five lasers and can collect up to 12 simultaneous images, with three lenses and two cameras. The sample is run at up to 5000 objects/second allowing rapid processing. Inclusion of SpeedBeads in the

sample enables hydrodynamic focusing of the cell suspension as well as synchronisation of pixel resolution with flow rate, resulting in preservation of image quality. Inspire™ data acquisition software is integrated with the ImageStream and is used to capture objects defined by cell classifier parameters. Sub-populations can then be identified and further characterised based on numerous variables using IDEAS Software. These features potentially allow for the quantification and characterisation of CTCs as well as quantification of nuclear γ H2AX and Rad51 foci, offering the potential of performing the HR assay on such cells.

Published Evidence

Multiple publications have demonstrated the imaging capabilities of the ImageStream system but there has been no published work using this technology for detection of CTCs in any cancer.

7.2. Aims

- Develop a method for sample preparation of whole blood to positively identify ovarian cancer cells from blood cells using cell lines and healthy volunteer blood.
- Develop a method for data handling and analysis of such samples.
- Develop a method for the accurate identification, quantification and characterisation of CTCs from whole blood taken from ovarian cancer patients
- Correlate enumeration of CTCs with stage of disease/PFS/OS
- Develop a method for application of the HR functional assay based upon γ H2AX and Rad51 foci formation to cell lines, PCO cultures, and CTC using ImageStream.
- Explore the alternative approach of using ImageStream technology to directly characterise and functionally assess the cellular component of malignant ascites.

7.3. Method Development

A method was developed for processing whole blood for CTC enumeration and characterisation. Prior to ImageStream sample processing, cell suspensions required fixation, permeabilisation and antigen labelling. Details of method development using cell lines, and PCO cultures are shown in Appendix 8. Optimised methods and patient results are shown below.

7.3.1. Antibody Selection

Three antigens (EpCAM, CK and CA125) were selected for positive selection of CTCs, alongside CD45 to identify WBCs and DRAQ5 as a generic nuclear stain. Commercially available fluorochrome conjugated antibodies were selected ensuring those with similar emission spectra were in separate cellular compartments and ImageStream channels. Fluorochrome-conjugated CA125 was not available commercially and was manually conjugated, see Appendix 8.

7.3.2. ImageStream Settings

Excitation of fluorochromes was achieved with 405, 488, 561 and 642 nm lasers and images collected through a 40 x objective. Of the 12 channels, 1 and 9 were reserved for Brightfield images. The other channels collected emitted light over a range of wavelengths between 430 and 745 nm. Only images of objects with an area larger than 50 μm^2 were retained for analysis. ImageStream laser settings were manually selected to achieve optimal live image quality with identifiable labelling of the corresponding antigens in cell line samples, aiming for signal intensity between 100 and 4000, Table 7.3 – 1.

Antibody	Concentration	Fluorochrome	Colour	Excitation Laser	Intensity	Channel
EpCAM	1:50	AF 488	Green	488	0.5	2
CA125	1:10	AF595	Orange	561	40	4
CK	1:20	PE	Yellow	488	0.5	3
DRAQ5	1:50000	DRAQ5	Far-red	658	60	11
CD45	1:20	V450	Blue	405	20	7

Table 7.3 - 1: ImageStream laser and channel settings for flourochrome conjugated antibodies.

Antibody	Fixed immunofluorescence	ImageStream
Pancytokeratin		
CA125		
DRAQ5 nuclear stain (FITC panCK)		
EpCAM		
Composite		

Table 7.3 - 2: Characterisation of OVCAR3 cell line using traditional fixed immunofluorescent microscopy and ImageStream. Representative images obtained from a single cell are shown in each horizontal panel. The bright field image of the cell shown on the left hand side of each panel allows visualisation of the nucleus, plasma membrane and overall cell morphology. The fluorescent detected expression of EpCAM/CK/CA125 are shown. The composite images shown on the right hand side of the panels confirm membrane localisation of EpCAM and CA125 as well as cytoplasmic localisation of CK.

7.3.3. Characterisation of OVCAR3 Cell Line and PCO Cultures

Validation of the final protocol for sample preparation and data analysis was undertaken by characterisation of a panel of cell lines (with known antigen expression of EpCAM, CK and CA125) as well as assessment of PCO cultures, Table 7.3 - 2.

Cell cultures were trypsinised, cytospun and PBS washed, prior to fixation (methanol, -20 °C for 20 minutes). Cells were permeabilised with BD Phosflow Perm/Wash Buffer I for 12 hours before incubating with EpCAM, CK, CA125 and DRAQ 5 antibodies for 12 hours, as above. A population of single, focused cells was selected using a scatterplot of area with aspect ratio and histogram of gradient root mean square (RMS – an average measure of a dynamic sample), Figure 7.3 - 1.

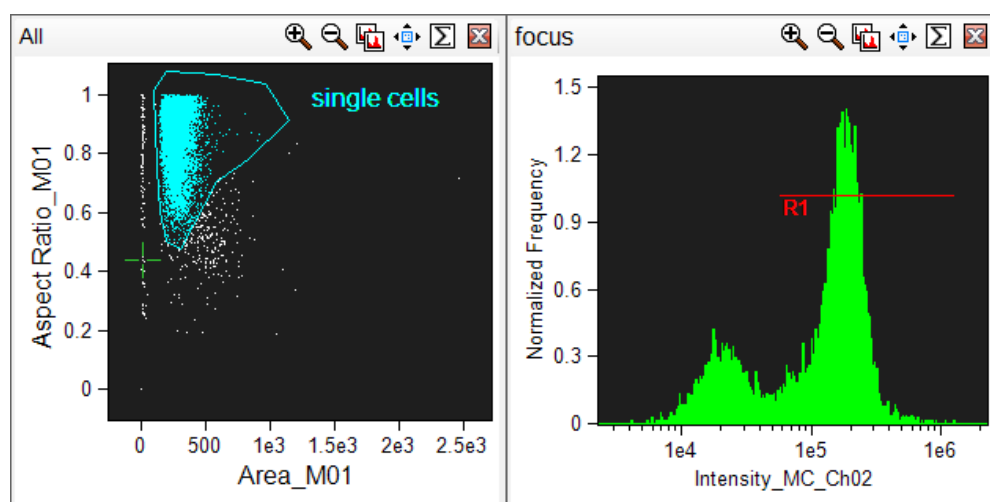


Figure 7.3 - 1: A: Scatterplot showing the area and aspect ratio of OVCAR3 cell line sample (incubate with EpCAM, CK, CA125 and DRAQ5) based upon brightfield image (MO1). A single cell population can be gated based on these parameters as demonstrated here. B: A histogram plot of the gated single, focused cell population demonstrating the intensity gradient of immunofluorescent signal of EpCAM (detected within Channel 2) in this population. The cut-off denoting positive expression is marked by R1 and the cell quantifier function used to calculate the proportion of cells expressing the EpCAM antigen.

Morphology was studied using the Brightfield images from channels 1 and 9. Intensity histograms for EpCAM, CK and CA-125 were drawn and the proportion of cells positive defined using parameters set from positive (OVCAR3) and negative (A2780) controls, Figure 7.3 - 2.

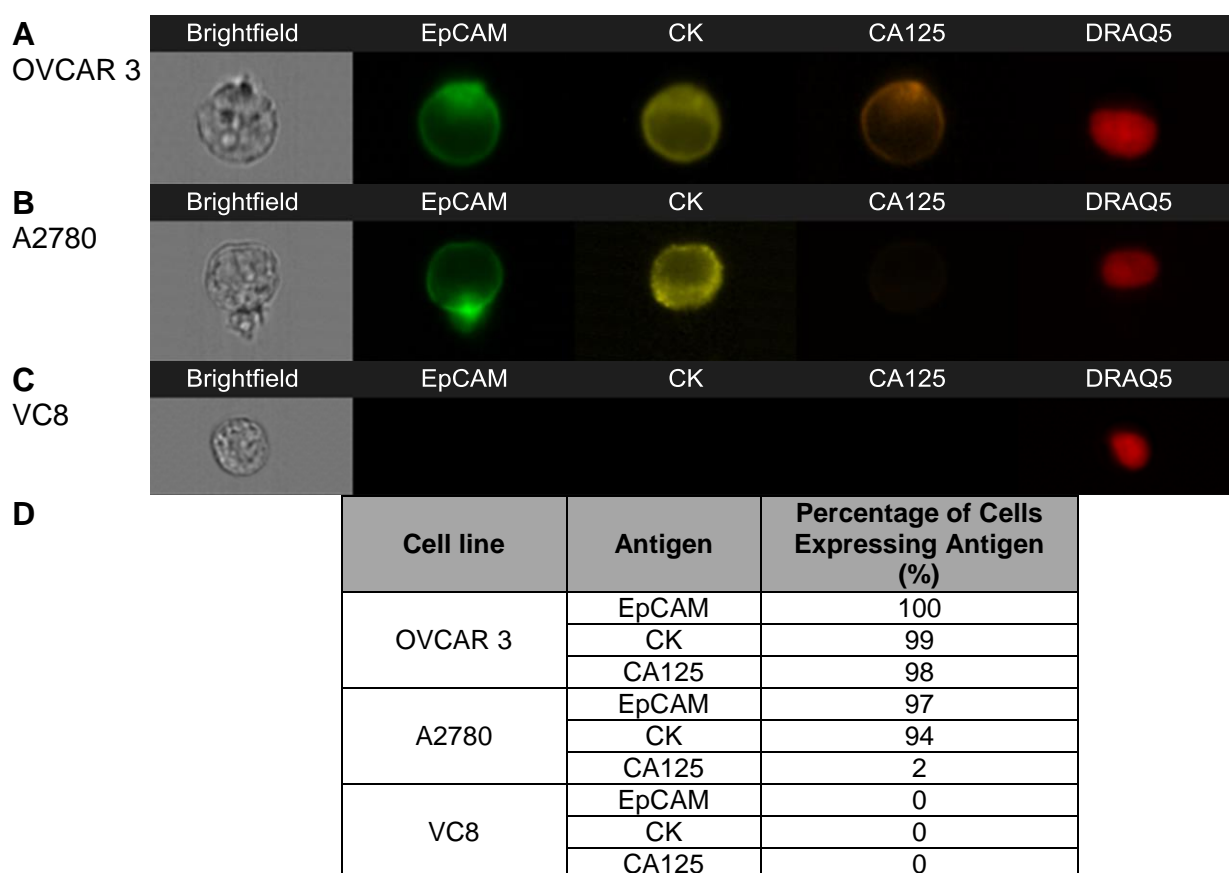


Figure 7.3 - 2: ImageStream cell Line characterisation results. A: Cell plot of OVCAR 3 with a nucleated cell (DRAQ 5 nuclear stain) expressing EpCAM, CK and CA125. B: Cell plot of ovarian cell line A2780 showing expression of CK with no expression of EpCAM or CA125. C: Cell plot of VC8 lung fibroblast cell line showing nucleated cell with no expression of EpCAM, CK or CA125. D: Quantification of antigen expression in cell line panel.

7.3.4. Retrieval of Spiked 'CTC'

A series of retrieval experiments spiking OVCAR3 cells into healthy volunteer whole blood were undertaken.

Principle of the Assay

In order to minimise biased selection of subpopulations of CTCs, a method for CTC selection was based upon expression of any of a panel of three antigens.

Method

Following informed consent, venous blood samples were collected using the Vacutainer system. The initial 4 ml of blood drawn was discarded to minimise the risk of epithelial skin cell contamination. Blood for analysis was then collected in EDTA tubes (no fixative agent) or a single 7.5 ml Transfix tube (with fixative). Samples were maintained at room temperature and processed within four hours of collection.

Assay Protocol

Trypsinised OVCAR3 cells re-suspended in PBS were counted and diluted twice by 1 in 10 and the appropriate volume of cells containing 2000, 200, 20 or 0 cells was added to four 4 ml blood samples equating to 500, 50, 5 and 0 cells per ml whole blood. Samples were transferred into 50 ml Falcon tubes, blocked in 5% BSA autoMACS solution. Human FcR Blocking Reagent was added directly to the blood to a final dilution of 1:40 to prevent non-specific antibody binding (Daeron 1997). RBCs were lysed, and all other cells fixed, by incubation in BD Phosflow Lyse/Fix Buffer 1:20 (v:v) for 15 min at 37 °C. Fixed cells were collected by centrifugation at 500 g at room temperature for 8 min and permeabilised in 1 ml BD Phosflow Perm/Wash Buffer I for 1 hour. Following centrifugation cells were resuspended in 100 µl of Perm/Wash Buffer I and incubated with 1:20 anti-pan cytokeratin phycoerythrin (PE) for 30 minutes at 4°C. Membrane antibodies (1:10 anti-CA125 conjugated to Alexa Fluor® 594, 1:50 anti-EpCAM CD326 Alexa Fluor® 488 and 1:20 anti-CD45 V450) were added with nuclear stain (1:50000 DRAQ5) and incubated for 1 h at 4°C. Cells were washed in 500 µl of BD Phosflow Perm/Wash Buffer I and centrifuged at 500 g for 5 min.

Experimental samples were divided into 60 µl aliquots and processed alongside single-colour controls (SCC), generated from OVCAR3 cells, that had been incubated with each antibody separately.

7.3.5. ImageStream Data Analysis Algorithm

An algorithm for a series of scatter and histogram plots was developed to enable identification and enumeration of CTCs based on size, morphology and expression of CD45, EpCAM, CK and CA125. CTCs were defined as:

“CK/EpCAM/CA125 positive, CD45 negative with a consistent cellular morphology

(aspect ratio >0.8; size >WBC; 3-D appearance) and nucleated.

WBCs were defined as nucleated cells with CD45 expression”.

The first selection was based upon the intensity of the nuclear dye retained by the cells,

Figure 7.3 - 3. The sharp peak above zero contains beads and small particles of debris and can be excluded from further analysis. The largest peak of intensity between $3 - 4 \times 10^5$ typically contains single leukocytes. The second peak of intensity between $5 - 8 \times 10^5$, which contains malignant cells and doublets of white blood cells gating the population of cells at 0.2×10^5 , selects these two populations for further analysis.

Subsequent selection aimed to exclude WBC (with expression of only CD45) and include other cells expressing EpCAM, cytokeratin and CA125. The selection was based upon absence of CD45 expression and presence of expression of EpCAM, cytokeratins and CA125.

Intensity histograms of each of the CTC antigens were created and visual inspection of cells within each histogram bar ('bucket') enabled discriminatory values to be selected for positive and negative expression. Gating varied marginally within each experiment due to the variable intensity of

immunofluorescence detected. Typically gating a cell population with intensity of antigen detection above $3 - 4 \times 10^4$ resulted in accurate discrimination between the presence of antigen but ensured inclusion of even weakly positive cells. Three separate dot plots were then configured, plotting intensity of CD45 (y axis) against intensity of each of the antigens of interest (EpCAM, CK, CA125), see Figure 7.7 – 3B. The gating determined by histogram plot was used to gate off cell populations with detected expression of the antigen of interest whilst excluding cells, which were only CD45 positive and therefore presumed to be WBC. The effectiveness of the discrimination is illustrated in Figure 7.3 - 3C; one population of cells expresses CD45 but not EpCAM while the second population expresses EpCAM but not CD45. Cell populations that express one or more of the epithelial or tumour specific antigens and do not express CD45 were selected automatically with the IDEAS Software and combined for further visual inspection. The images of each of these cells are examined visually to confirm that they have a cellular morphology and that the IDEAS Software is able to distinguish the malignant cells from any residual haematopoietic cells.

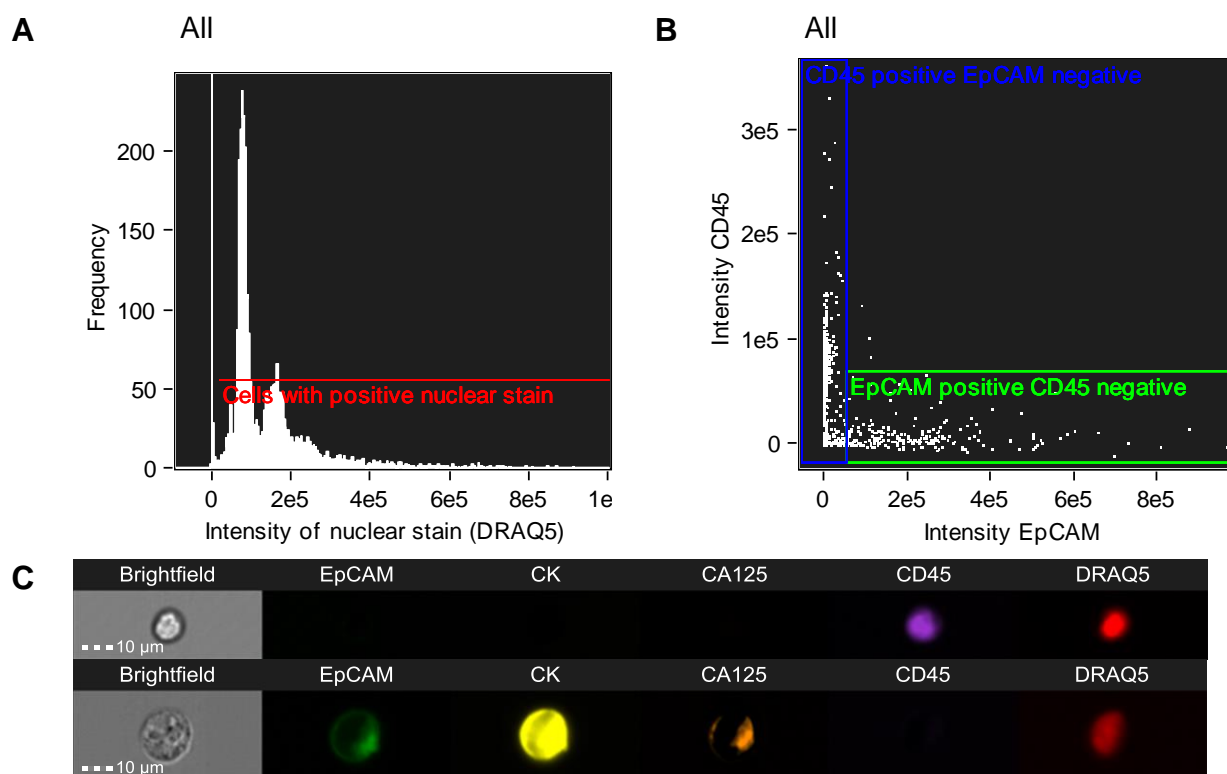


Figure 7.3 - 3: CTC analysis algorithm. A: Histogram plot of intensity of immunofluorescence of DRAQ5 in all objects detected, identifying the nucleated cell fraction; B: Scatterplot of immunofluorescent intensity of CD45 (Channel 7) and EpCAM (Channel 2) to enable broad discrimination of haematopoietic and epithelial cells (positive expression cut-off of 4×10^4). Cell populations which are EpCAM or CK or CA125 positive were combined to create a second population before the CTC population was defined following visual inspection of bright field images (C).

7.3.6. Retrieval Results Without Enrichment

Despite the ability of the ImageStream flow cytometer to image 5,000 cells per second, the large number of leukocytes in whole blood means that analysis of each ml of blood takes approximately six hours and produces an enormous amount of data for analysis and storage. A standard 8 – 10 ml sample may therefore take 4 days to process. Additionally, retrieval in unenriched spiked samples across three separate experiments was low with a mean retrieval of 13% (13.3% of 500 cells, 15.3% of 50 cells and 13.3% of 5 cells), Figure 7.3 - 4. Enrichment for non-haematopoietic cells is therefore required before identification of CTCs can occur, ensuring that a sufficient volume of whole blood could be processed within a reasonable timeframe.

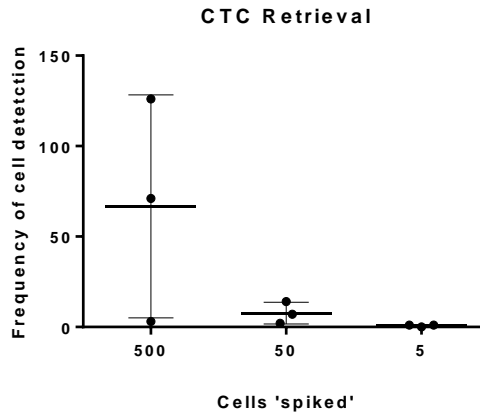


Figure 7.3 - 4: CTC retrieval without WBC enrichment. 500, 50 and 5 cells per 1 ml were spiked into healthy volunteer blood. Following fixation, permeabilisation and incubation with EpCAM, CK, CA125, DRAQ5 and CD45, the percentage retrieval following ImageStream processing and data analysis was calculated. Results shown are the mean and SD of three independent experiments.

7.3.7. Enrichment

Enrichment may consist of positive selection of CTCs, negative depletion of blood cells or a combination of both methods. A series of depletion and retrieval experiments were undertaken to evaluate several techniques. Table 7.3 – 3 summarises the principles of each method as well as the protocol used. Positive selection of CTCs involved identification of a universally expressed antigen or differential separation based on density. Methods tested gave low recovery of spiked CTCs and the cells that were recovered were damaged physically as assessed by the images produced (data not shown). Depletion methods of haematopoietic cells were therefore evaluated.

Depletion Method

4 ml of healthy volunteer blood was depleted of RBCs by incubating the sample with 40 ml BD Phosflow Lyse/Fix Buffer for 15 minutes at 37 °C. The sample was centrifuged at 500 g for 5 minutes, supernatant discarded and resulting cell pellet resuspended in 10 ml PBS. The sample was counted using the Coulter counter. Briefly, 100 µl of cell suspension was added to 4900 µl FACS Buffer. After mixing well, the mean of three counts was used as the pre-depletion count. Following depletion, utilising one of the methods described in Table 7.3 – 3, the mean of three readings gave the post-depletion count and percentage depletion calculated.

Method	Principle	Protocol
MACS	Antibody directly coupled to magnetic microbead particles is used for either positive (EpCAM) or negative (CD45) enrichment. The sample is passed through the MiniMACS™ Separator, a high-gradient magnetic field, which retains cells labelled with the microbeads. Unlabelled and labelled cells can be collected for use in further experiments.	Following red cell lysis, the cell pellet was resuspended in 500 µl MACS buffer solution and incubated with variable quantities of MACS CD45 or MACS EpCAM microbeads (50 - 200 µl) at 4 °C for 20 minutes. The column was prepped with 2 ml MACS buffer, followed by the sample, before washing twice with MACS buffer.
Dynabeads	The Dynabeads system is based upon depletion of CD45 positive cells using magnetically labelled anti-CD45 antibody. Beads bind to target cells during a short incubation. Bead bound cells are separated using a DynaMag™ magnet.	The cell pellet was resuspended in isolation buffer (PBS with 0.1% [v/v] BSA, 3 mM EDTA, pH 7.4) and incubated with variable volumes (100 - 200 µl) of prewashed Dynabeads at 4 °C for 30 minutes before pouring off the unbound cellular fraction and counting.
Magnet	In an attempt to avoid the complexities of some of the preceding techniques, a simplified method of magnet incubation within a sample mixed with MACS CD45 microbeads was explored. This assay relies upon the positive exclusion of cells, which express CD45 antigen, using magnetically labelled anti-CD45 antibodies.	The cell pellet was resuspended in 20 ml PBS in a 50 ml falcon tube and variable quantities of MACS CD45 microbeads (50 - 200 µl) added. An 8 x 30 mm neodymium magnet within a glass FACS tube was inserted into the sample and incubated for 1 - 12 hours, 3 times.
RosetteSep™ <i>Work done by Emma Rouke (MRes 2012)</i>	The RosetteSep™ system combines immunodensity cell isolation reagent with a cell processing tube (SepMate™) for cell separation directly from whole blood. The RosetteSep® cocktail crosslinks unwanted cells to multiple RBCs forming immunorosettes. When centrifuged over Ficoll™, the unwanted (rosetted) cells pellet, along with RBCs, leaving the CTC fraction untouched at the density medium: plasma interface.	4 ml whole blood was spiked with SKBR3 cells and enriched with the RosetteSep CD45+ negative selection cocktail, according to manufacturer instructions. Briefly, whole blood was incubated with 100 µl RosetteSep antibody cocktail for 20 minutes at room temperature. The blood was then diluted 1:1 with PBS containing 2% FBS, layered over Ficoll™ and centrifuged for 20 minutes at 1200 g. The non-RBC/WBC cell layer was extracted and analysed further with ImageStream.
EasySep™	See section 7.3.7 below	

Table 7.3 – 3: Methods for depletion of white blood cells.

EasySep™

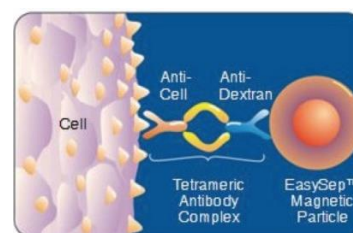
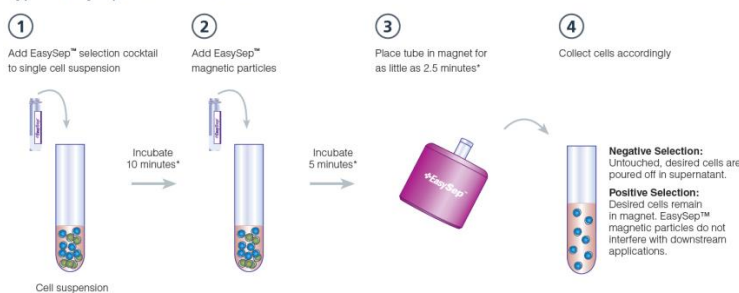
Principle of the Assay

The EasySep™ system uses a cocktail of antibodies against CD45 and dextran coated magnetic tetrameric complexes to negatively enrich blood samples. Incubation in the EasySep™ magnet removes the unwanted CD45 antibody bound cells, leaving unbound CTCs in the cellular fraction poured off.

Assay Protocol

WBCs were removed with an EasySep™ Human Whole Blood CD45 Depletion Kit according to the manufacturer's instructions (STEMCELL Technologies, 2013), Figure 7.3 - 5. Briefly, EasySep™ Whole Blood Depletion Cocktail was added at 100 µl/ml of sample and incubated at room temperature for 15 minutes. EasySep™ dextran-coated Magnetic Nanoparticles were then added at 50 µl/ml of sample and incubated at room temperature for a further 10 minutes. The cell suspension was diluted to 5 ml with RoboSep Buffer and placed in a "Big Easy" EasySep™ Magnet for 10 minutes. The magnetically labelled CD45 cells were held in the tube by the magnetic field and the un-retained cell fraction (containing non-CD45 cells) was decanted into a clean tube by inversion of the sample and magnet. The recovered cells were centrifuged at 250 g for 5 min, re-suspended in 1 ml Perm/Wash buffer (10% (v/v) with ddH₂O) for 1 h at room temperature in preparation for antibody labelling.

Typical EasySep™ Human Cell Isolation Protocol



*Times are typical for negative selection kits. Times for each kit will vary depending on the exact isolation protocol.

Figure 7.3 - 5: EasySep™ CD45 depletion of WBC (STEMCELL Technologies, 2013).

7.3.8. Enrichment Results

The concentration of WBCs was counted pre- and post- depletion using the methods described in section 7.3.7. Percentage depletion across three separate experiments was calculated. Consistent depletion was achieved with EasySep™, with a median depletion of 96% (92 - 99%), Figure 7.3 - 6, EasySep™ was adopted as the method to be used in further experiments.

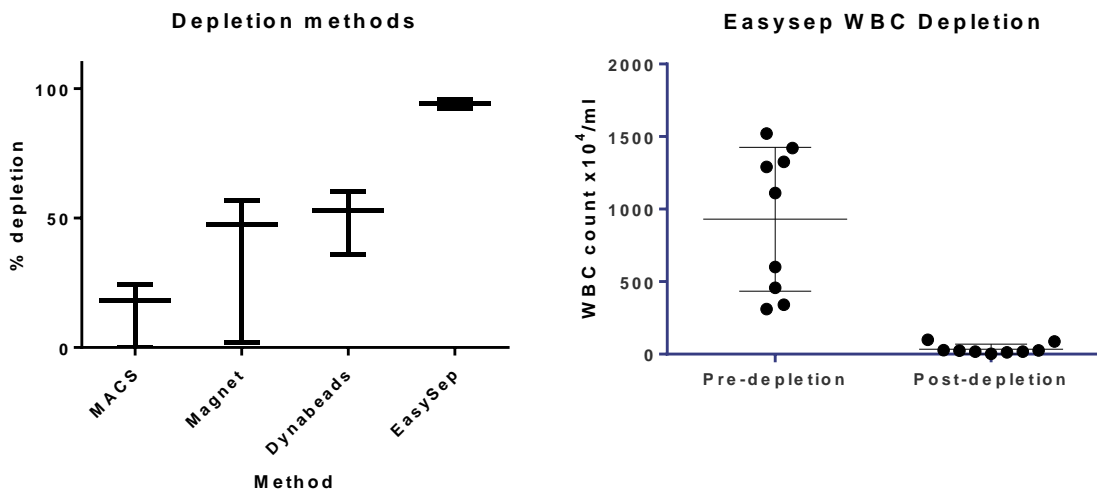


Figure 7.3 - 6: A: Comparison of depletion methods. The mean and range from three separate experiments are shown. B: EasySep™ WBC Depletion. Enrichment for non-haematopoietic cells. Cultured malignant cells were added to 4 ml of whole blood and cells were incubated with tetrameric antibody complexes against CD45 and dextran-coated magnetic particles for 1 h and placed in an EasySep™ Big Easy magnet. Cells not attracted to the magnet were recovered. The number of leukocytes was counted with a haemocytometer prior to and after depletion. Erythrocytes were removed by lysis and platelets by centrifugation at 250 g.

7.3.9. Retrieval Results with Enrichment

Mean percentage retrieval, following enrichment with RosetteSep, was 48% but this was highly variable and resulted in substantial debris, which prolonged sample running and processing time (data not shown). Retrieval experiments were repeated with spiked OVCAR3 cells with the addition of EasySep™ WBC depletion. Depletion was consistent and images of the malignant cells and residual leukocytes were similar to those shown in

Figure 7.3 - 3, confirming minimal damage to the malignant cells by depletion of the blood cells. Validation of the methodology on samples from patients with oesophageal (Barry Dent), hepatocellular (Laura Ogle) and thyroid (David Jamieson) cancers confirmed its utility and indicated that it has comparable or greater sensitivity to published methods, Figure 7.3 - 7. The recovery after analysis of known numbers of cells by image flow cytometry was $59.2 \pm 6.2\%$. This means that the recovery during the red blood cell lysis, white blood cell depletion, centrifugation and antibody labelling steps was 61.9% to give an overall recovery of 55.2%. The sample processing and analysis time was dramatically reduced from in excess of six hours/ml whole blood analysed (see Section 7.4.6) for unenriched samples, to approximately one hour per/ml blood processed.

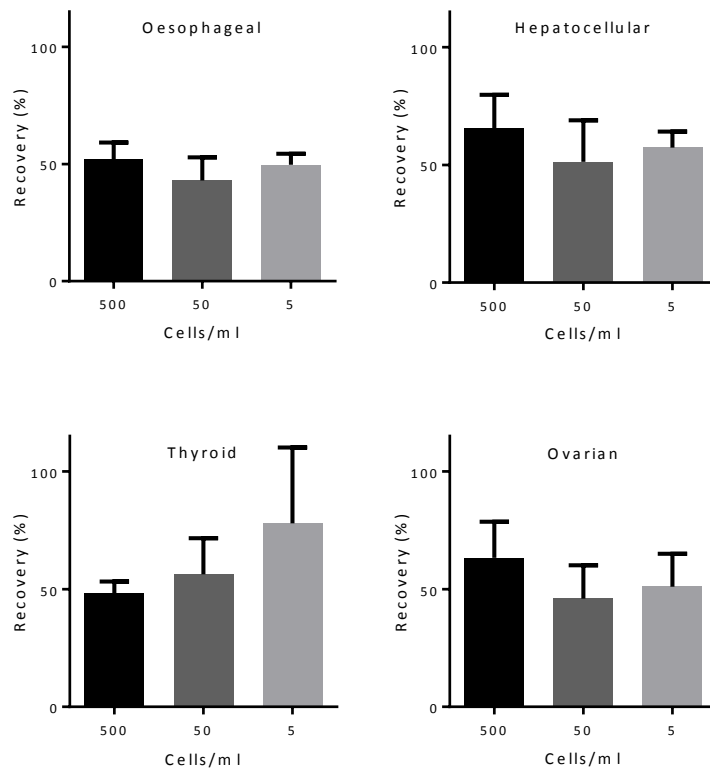


Figure 7.3 - 7: Retrieval of malignant cells from whole blood. SK-GT-4, Huh-7, ML1 and OVCAR 3 cells were added to 5 ml of whole blood to give a final concentration of 500, 50 and 5 malignant cells per ml. The samples were enriched for malignant cells by depletion of blood cells and the residual cells were incubated with fluorescent antibodies and nuclear dye and analysed by high-resolution flow cytometry as described as described in the Materials and Methods. The mean recoveries of malignant cells \pm SEM from three experiments are shown.

7.4. Results: Ovarian Cancer Patient Sample Results

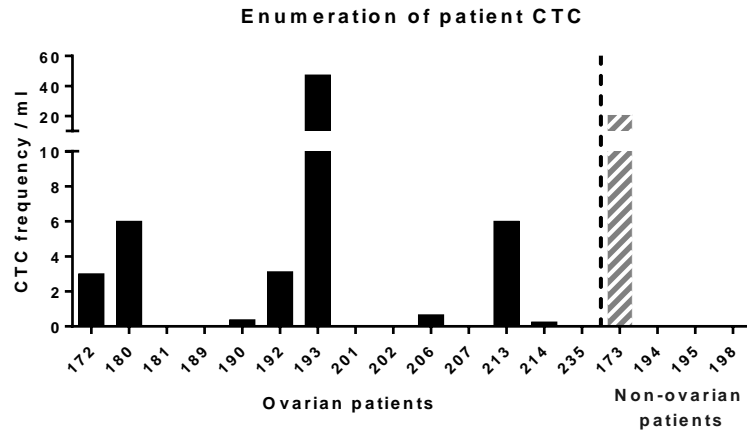
Blood samples were collected in Transfix collection tubes for storage up to 24 hours at 4 °C or in BD Vacutainer EDTA tubes for immediate use from 18 patients (14 with confirmed ovarian malignancy). Samples were transferred into 50 ml Falcon tubes, blocked in 5% BSA and FcR Blocking Reagent added. RBCs were lysed and WBCs depleted, with EasySep, as above. Cells were incubated with anti-pan cytokeratin, followed by anti-CA125, anti-EpCAM, anti-CD45 antibodies and DRAQ5. Cells were washed before ImageStream processing, alongside OVCAR3 single-colour controls.

7.4.1. Enumeration

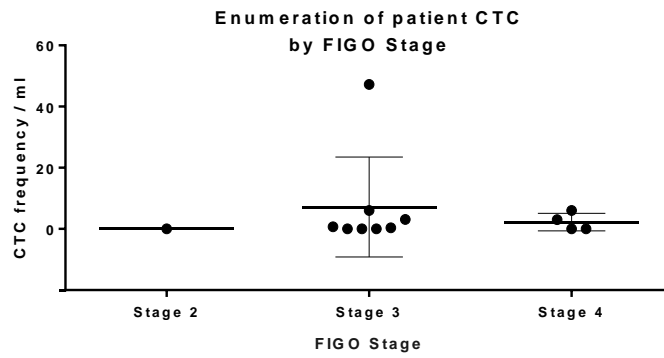
Using the CTC definition in Section 7.3.5, “CK/EpCAM/CA125 positive, CD45 negative negative with a consistent cellular morphology (aspect ratio >0.8; size >WBC; 3-D appearance) and nucleated”, CTCs were detected in 9/18 samples tested (7/14 (7/14 ovarian cancer samples), Table 7.4 - 1. The frequency of ovarian CTCs was highly variable with a median count of 1 CTC per ml blood tested in all samples and 5.3 CTC per ml in ovarian cancer patients (0 - 47),

Figure 7.4 - 1A. There was no relationship seen between frequency of CTCs and FIGO Stage at presentation or presence of intra- or extra-peritoneal metastases, Figure 7.4 - 1B/C. The highest concentration of CTCs (47 per ml) was detected in a patient who had completed 4 cycles of dual agent chemotherapy just 4 weeks earlier, with a significant reduction in tumour volume on CT imaging. CTCs from this patient were highly homogeneous. Despite the high frequency of CTCs, the patient remains alive and well at 30 months.

A



B



C

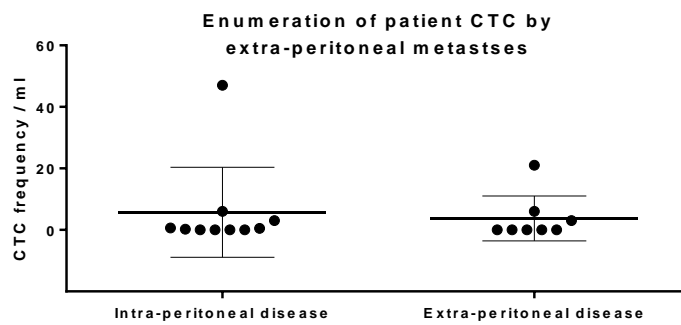


Figure 7.4 - 1: CTC frequency and relation to stage of disease and extra-peritoneal disease. A: CTC Frequency per ml Whole Blood Tested in PCO samples and non-ovarian patients; B: CTC frequency by FIGO stage of disease; C: CTC frequency by presence of intra- and extra-peritoneal spread of disease

PCO	Age	Histology	FIGO Stage	CA125		Treatment Prior to CTC Sampling		Last Chemo (wks)	Timing of Sample	Total CTC No.	Vol blood (ml)	CTC/ml	Total No. cells	Total No. WBC	Total No. 'Other'	PFS	OS
				Diagnosis	Sample Collection	Surgery	Chemo										
235	71	HGSC	2C	254		Complete	6 carboplatin and taxol	208	Relapse	0	8	0	391620	390337	1283	35	68+
189	65	HGSC	3C	289	65	None	3 carboplatin ad taxol	4	IDS	0	4	0	216504	213025	3479	28+	28+
201	55	HGSC	3C	678	ND	Optimal	6 carboplatin and taxol, tamoxifen, rucaparib	26	Relapse	0	7.5	0	449327	442543	6784	10	36
206	54	HGSC	3C	1197	562	Optimal	6 carboplatin and taxol, tamoxifen, radiotherapy, 3 carboplatin and taxol	16	Relapse	0	7.5	0	364817	363783	1034	11	27
202	52	HGSC	3C	1352	155	None	3 carboplatin and taxol	4	IDS	5	7.5	<1	749676	744384	5292	23	25+
214	72	HGSC	3C	571	NA	None	None	NA	Presentation	2	8	<1	893092	835670	57422	18+	18+
192	66	HGSC	3C	2425	NA	None	None	NA	Presentation	25	8	3	214825	213970	855	4	7
180	50	HGSC	3C	521	NA	None	None	NA	Presentation	12	2	6	355912	343290	12622	11	12+
193	66	HGSC	3C	2800	548	None	6 carboplatin and taxol	4	IDS	378	8	47	545300	539053	6247	7	30+
181	72	HGSC	4	180	20	None	3 carboplatin and taxol	5	IDS	0	2	0	108252	99384	8868	10	11
207	63	HGSC	4	371	60	None	3 carboplatin and taxol	6	IDS	0	4	0	197138	184466	12672	5	5
213	85	HGSC	4	1295	NA	None	None	NA	Presentation	48	8	6	279883	271351	8532	4	4
172	73	HGSC	4	2494	115	Optimal	6 carboplatin and taxol	9	Relapse	19	2	10	22800	18502	4298	8	38+
190	75	Mucinous	3C	135	NA	None	None	NA	Presentation	3	8	<1	787144	212508	54636	9	11
195	75	<i>Pseudomyxoma peritonei</i>	<i>Non-malignant</i>	30	NA	<i>None</i>	<i>None</i>	NA	<i>Presentation</i>	0	8	0					
194	59	<i>Gastric adenocarcinoma</i>	<i>Metastatic</i>	1000	NA	<i>None</i>	<i>None</i>	NA	<i>Presentation</i>	0	8	0					
198	52	<i>Gastric adenocarcinoma</i>	<i>Metastatic</i>	385	NA	<i>None</i>	<i>None</i>	NA	<i>Presentation</i>	0	8	0					
173	58	<i>Gastric adenocarcinoma</i>	<i>Metastatic</i>	164	NA	<i>None</i>	<i>None</i>	NA	<i>Presentation</i>	42	2	21					

Table 7.4 - 1: Patient demographics and numbers of circulating tumour cells in blood from patients with ovarian cancers. Grey patients with suspected ovarian malignancy at time of blood collection but proven to be non-ovarian in origin following histological examination.

PCO	Representative Images of CTC						
172	Brightfield	EpCAM	CK	CA125	CD45	DRAQ5	Composite
173	Brightfield	EpCAM	CK	CA125	CD45	DRAQ5	Composite
180	Brightfield	EpCAM	CK	CA125	CD45	DRAQ5	Composite
190	Brightfield	EpCAM	CK	CA125	CD45	DRAQ5	Composite
192	Brightfield	EpCAM	CK	CA125	CD45	DRAQ5	Composite
193	Brightfield	EpCAM	CK	CA125	CD45	DRAQ5	Composite
202	Brightfield	EpCAM	CK	CA125	CD45	DRAQ5	Composite
213	Brightfield	EpCAM	CK	CA125	CD45	DRAQ5	Composite

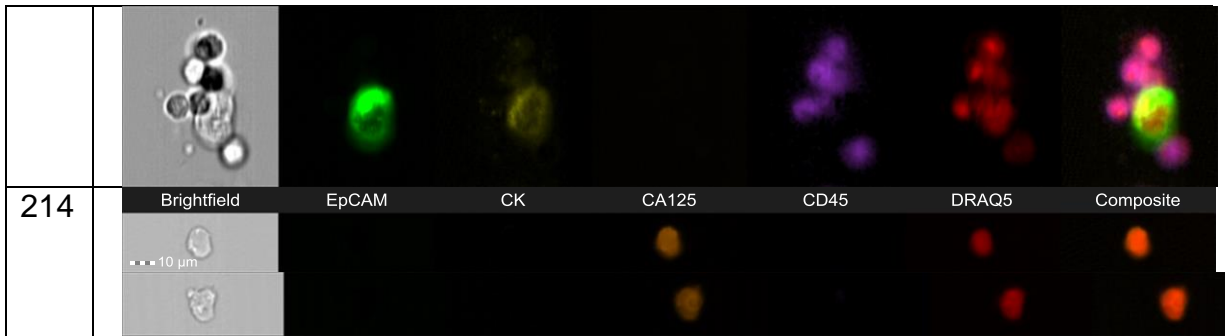


Figure 7.4 - 1: Ovarian cancer CTC. ImageStream. Cell plot of ovarian cancer CTC with nucleated cells (DRAQ5 nuclear stain) with variable expression of EpCAM, CK and CA125.

7.4.2. Characterisation

Antigen Expression

Representative images from all ovarian cancer patients with detectable CTCs are shown in

Figure 7.4 - 1. The different images obtained from a single cell are shown in each horizontal panel. The bright field image of the cell shown on the left hand side of each panel allows visualisation of the nucleus, plasma membrane and overall cell morphology. CTCs detected have variable membrane immunoreaction for EpCAM, with some evidence of intracellular vesicular accumulation and membrane localisation. The immuno-reaction for the cytokeratins was evident in the cytoplasmic compartment of cells. CA125 expression was also variable with localisation predominantly in the membrane. The composite images shown on the right and confirm localisation of EpCAM and CA125 in the membrane and cytokeratin in the cytoplasm. Expression of CD45 was not detected in CTCs but many CTC were captured in association with CD45 expressing WBC. It is unclear if it is by chance that they are captured within the same field, whether this is a consequence of the assay protocol or whether this is as a result of a true immunological reaction. A summary of the total proportion of CTCs expressing EpCAM, CK and CA125 is shown in Figure 7.4 - 2 which shows heterogeneity in the expression of all three markers reinforcing the importance of a multi-marker panel.

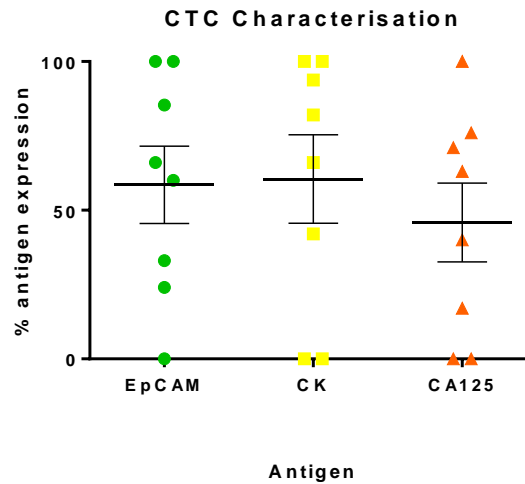


Figure 7.4 - 2: CTC characterisation. Proportion of cells with detectable expression of EpCAM, CK and CA125.

Are CTCs Representative of Ascitic PCO Cultures?

It was possible to compare the expression of EpCAM, CK and CA125 in CTCs. Comparison of expression of the same antigens in cultured ascites from the same patient was possible in 5/8 patients with CTC. Discordance in characterisation of CTC and primary tumour culture was present in 9/15 (60%) tests. Additionally, heterogeneity in expression of antigens was seen within the CTC population from individual patients, Figure 7.4 - 3, further demonstrating the intra-tumoural heterogeneity within ovarian cancer.

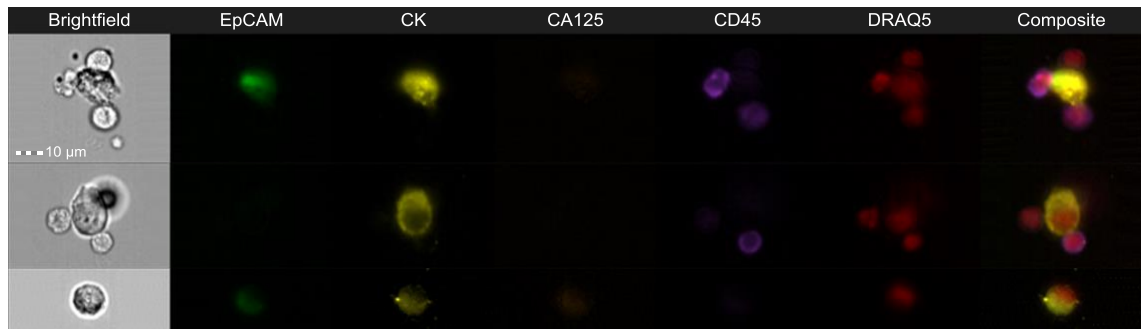


Figure 7.4 - 3: Three representatives CTC from PCO 202. Heterogeneity of EpCAM expression with 2/3 cells shown expressing EpCAM and 1/3 with no expression. Additionally in two of the cells seen are surrounded by WBC, which may be representative of an immune response against CTC.

CTC Size

Quantification of CTC size using diameter alone results in over- or under-estimation in elongated cells and is dependent upon orientation. CTC size was best assessed using cell area and calculated by IDEAS Software utilising a basic cell outline mask (Erode(M01, 1)) and cell area functions.

Mean cell area across all PCO samples was $61.48 \mu\text{m}^2$, SD $45.27 \mu\text{m}^2$. This was significantly larger than the mean cell area of WBCs (20.3 , SD 1.0), $p < 0.0001$, and significantly smaller than ovarian cancer cell line areas (98.5 , SEM 5.8), $p < 0.0001$.

The morphologic characteristics exhibited by the captured CTCs were consistent with malignant cells, including large cellular size with high nuclear:cytoplasmic ratios and visible nucleoli and were similar to that of the cultured ovarian cells, Figure 7.4 - 4. CTCs detected were highly heterogeneous in their expression of EpCAM, cytokeratins and CA125.

7.4.4. Objects of Interest

There are several populations of circulating objects, which do not fulfil the definition for WBCs nor CTCs and have not previously been well described, Figure 7.4 - 6.

Cellular Debris

Cellular debris (consistently less than 2% of total objects) can be recognised by its atypical morphology with non-discriminatory uptake of fluorescence antibodies. Quantities of cellular debris were considerably less with use of EasySep™ enrichment in comparison to use of other depletion methodologies, thereby reducing the time spent on manually sorting cellular debris from true CTCs.

Atypical WBCs

Within each patient sample, there was a population of cells (3-15% of all WBC) whose morphology and size is akin to WBCs but that appeared to express all tumour antigens alongside WBC antigens. There are several subtypes of WBCs, including those from the myeloid lineage (neutrophils, monocytes, eosinophils and basophils) and lymphocytes (including T cells, B cells and natural killer cells). Neutrophils are the most abundant WBC, constituting 60 - 70% of the circulating leukocytes. It is unclear if the cells identified with expression of all antigens are one of the other subpopulations of circulating WBCs or if they represent activated or apoptotic neutrophils. Another, less likely, possibility is that they represent CTCs, which have developed a leucocyte phenotype as they adapt to the circulating environment. It has been acknowledged that although the majority of leukocytes do not express epithelial markers, they have been observed to be EpCAM positive when in an activated state (Jung 1998, Sleijfer 2007).

Macrophages

Circulating nucleated cells, which appear to be distinctly different from CTCs and WBCs morphologically and which do not express epithelial antigens, may represent circulating macrophages (0.5 – 3% of all objects). Tumour-associated circulating macrophages have been previously described and are believed to facilitate CTC seeding of distant metastases (Adams 2014). This study described circulating macrophages in 86% of patients with prostate cancer, 93% of patients with pancreatic cancer, and 97% of patients with breast cancer (Adams 2014). Mean macrophage count was 22/ml whole blood tested in patients from all tumour types with stage IV disease, with a mean CTC count in the same group of 59.7/ml (Adams 2014).

Tumour-associated macrophages (TAMs) are found within most tumours and have been shown to be prognostic indicators of tumour invasiveness (Shih, Yuan et al. 2006). TAMs, recruited to the stroma from circulating monocytes, are required for tumour cell intravasation, migration, extravasation and angiogenesis (Condeelis 2006, Shih, Yuan et al. 2006). Highly differentiated giant circulating macrophage-like cells, with expression of CD14 (macrophage antigen) and containing vacuoles of phagocytosed material, have been isolated from the peripheral blood of patients with breast, prostate and pancreatic cancer (Adams 2014). This cell population, not detected in healthy individuals, has been hypothesised to serve as a cellular biomarker of innate immune response to the presence of cancer and of cancer aggressiveness and may be useful in monitoring chemotherapy-induced responses (Adams 2014).

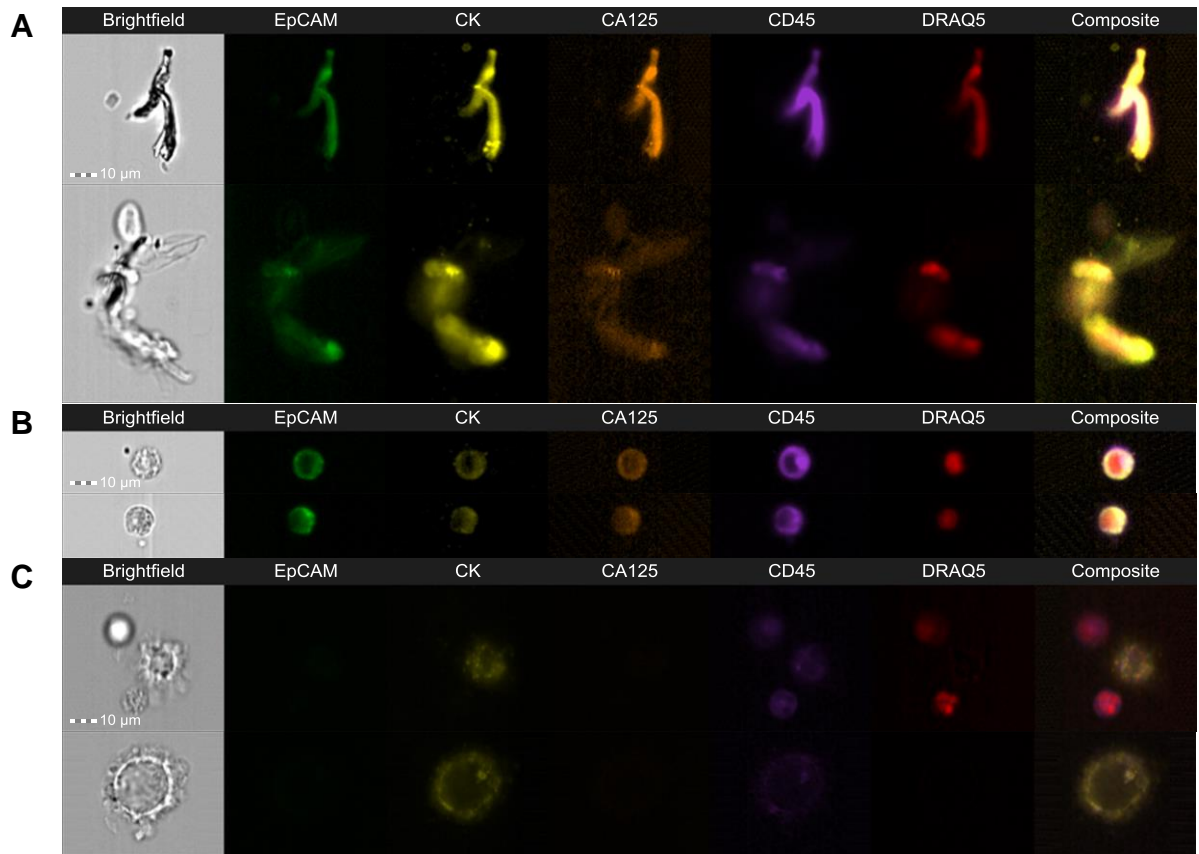


Figure 7.4 - 6: Objects of interest from healthy volunteer sample. A: Cellular debris – identifiable by its atypical morphology and saturation for all fluorescence markers. B: Atypical WBC, C: Circulating macrophages; see section 7.4.4.

Tumour Microemboli/CTC and WBC Aggregates

There have been reports of clusters of CTCs detected in patients with advanced cancer which range from 3 to 14 cells (Stott 2010, Hou 2011, Hou 2012). Early studies suggest that CTC clusters may be relatively protected from cell death and the harsh environment and stresses of the vascular circulations. They may also be clinically significant, particularly the number, size or composition of the clusters (Wang 2000, Glinsky 2003, Serrano Fernandez 2009, Stott 2010, Hou 2011, Hou 2012). The presence of clusters itself has therefore been hypothesised to be a biomarker for increased metastatic potential than enumeration of single CTCs (Wang 2000, Stott 2010, Hou 2011). However, no clusters of CTCs were found with ImageStream in this series and it is unclear if the clusters seen in other studies are an artefact of the cell preparation method or whether the clusters are disaggregated during the preparation and processing for the ImageStream.

Several samples did however demonstrate clustering of WBC with CTC, Figure 7.4 - 7.

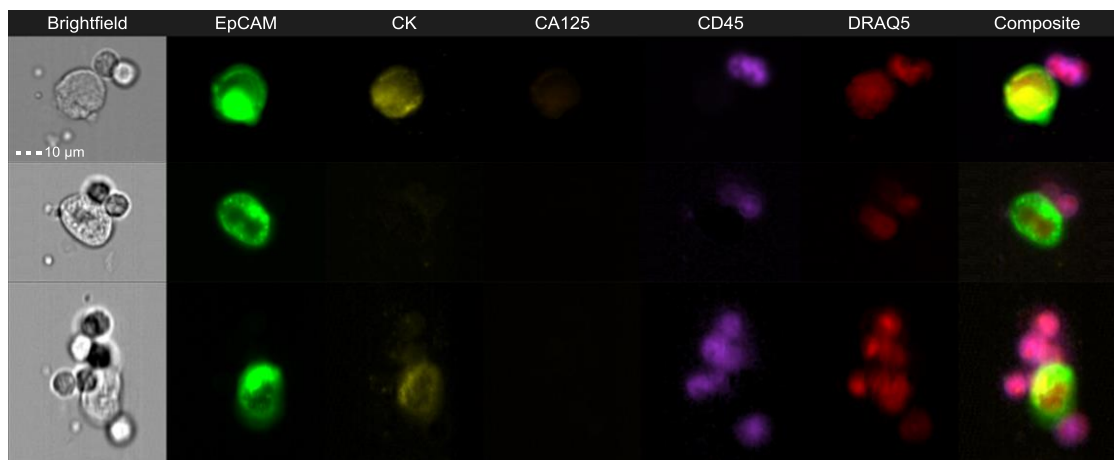


Figure 7.4 - 7: CTC from PCO 173, 180 and 213 showing CTC surrounded by WBC.

7.4.5. Healthy Volunteer Blood without Spiked 'CTC'

It was important to demonstrate that the method did not detect cells in whole blood from healthy individuals. Collectively, over fifty healthy volunteer samples have been analysed without detection of cells with the morphology shown in Figure 7.4 - 1 or expression of the markers chosen indicating that the method described provides a robust measure of non-haematopoietic cells. Furthermore, cellular debris, apoptotic WBCs, non-staining WBCs and circulating macrophages have been seen in healthy volunteer blood, Figure 7.4 - 6 reinforcing the importance of their exclusion from CTC counts.

7.4.6. ImageStream HR Assay

Although enumeration of CTCs in ovarian cancer in this cohort does not have prognostic value, characterisation, including functional characterisation of CTCs may have more clinical relevance. The homologous recombination repair (HR) assay, based upon quantification of nuclear γ H2AX and Rad51 foci has been shown to be of importance in prediction and prognosis.

ImageStream HR Assay using Cell Lines

A panel of cell lines, with known HR status, underwent HR evaluation using ImageStream, Figure 7.4 - 8. The optimised ImageStream settings for fluorescence intensity, nuclear and foci mask formation as well as counting of foci were used.

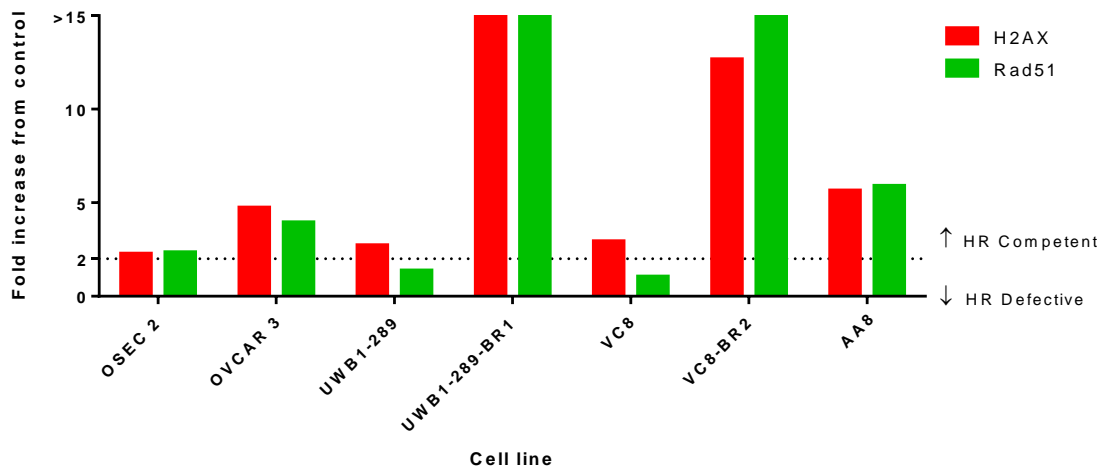


Figure 7.4 - 8: ImageStream assessment of HR function in a panel of cell lines. Fold increase from untreated controls in γ H2AX and Rad51 foci count are shown in red and green respectively. The two fold cut-off of γ H2AX foci, above which signifies induction of adequate DNA DSB (following 2 Gy IR). The 2-fold increase in Rad51 foci count, above which denotes HR competence is shown by a dotted line.

Cell lines known to be competent in HR function (OSEC2, OVCAR3, UWB1-289-BRCA1, VC8-BR2, AA8) showed a greater than 2-fold increase in Rad51 foci in response to irradiation induced of DNA DSB, assessed using the optimised ImageStream methodology, Figure 7.4 - 9. HR defective cell lines (UWB1-289 and VC8) had a less than 2-fold increase in Rad51 foci.

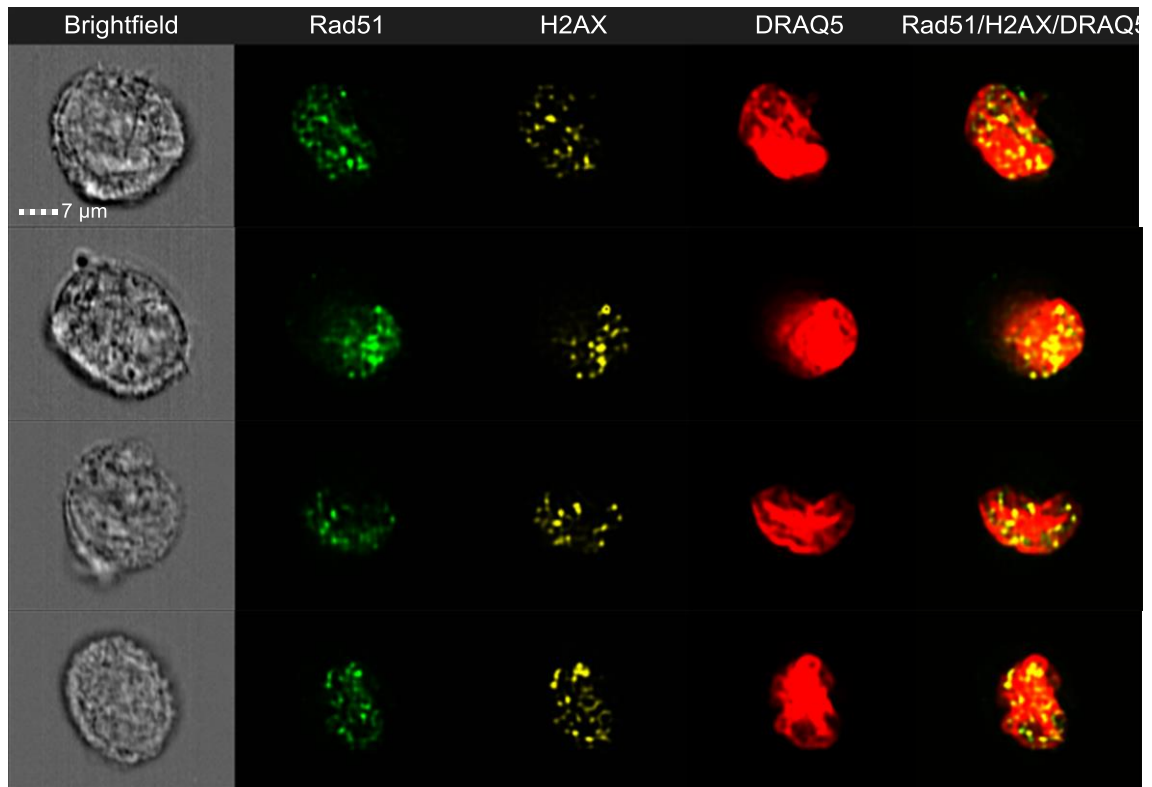


Figure 7.4 - 9: γ H2AX and Rad51 nuclear foci. Representative images from HR assay using OSEC2 cell line. Cultured cells were treated with 2 Gy irradiation and 10 μ M rucaparib to induce DNA DSB, alongside untreated controls. After 24 hours, cells were trypsinised and the fixed with methanol before permeabilising with BD Phosflow Perm/Wash Buffer. Samples were incubated with primary γ H2AX and Rad51 antibodies for 12 hours at 4 °C followed by corresponding secondary antibodies and DRAQ5.

γ H2AX Fold Increase in PCO Cultures

The optimised protocol was used to count the γ H2AX focus formation in irradiated and control PCO samples (n = 4). All irradiated samples showed a rise in the mean number of γ H2AX foci present, with 3 out of the 4 samples achieving a greater than 2-fold increase, Figure 7.4 - 10.

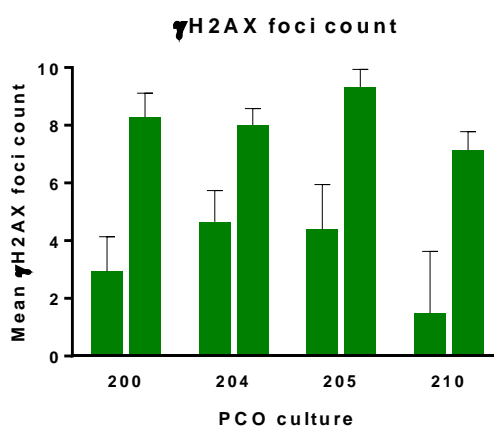


Figure 7.4 - 10: Mean γ H2AX foci count in PCO cultures using ImageStream. PCO cultures were irradiated with 2 Gy, trypsinised and fixed at 6 hours alongside un-irradiated controls. The mean γ H2AX foci count using the optimised protocols, described above and fold increase from control were calculated. PCO200, PCO205 and PCO210 irradiated samples all achieved a greater than 2-fold increase.

7.4.7. HR Assay in CTCs

Principles of the Assay

The HR assay is based upon quantification of nuclear γ H2AX and Rad51 foci in response to induction of DNA DSB, section 3.6. ImageStream's extended depth of field function (EDF) enables discrimination of cellular features and more precise quantification of nucleic foci. The method for sample processing and analysis was optimised using cell lines, before applying to PCO cultures.

Assay Protocol

Cultured cell lines were treated with 2 Gy irradiation and 10 μ M rucaparib to induce DNA DSB, alongside untreated controls. After 24 hours, cells were trypsinised and the resulting cell suspension fixed with methanol for 20 minutes at -20 °C and then permeabilised with BD Phosflow Perm/Wash Buffer I for 1 hour at room temperature. Samples were incubated with primary γ H2AX and

Rad51 antibodies for 12 hours at 4 °C (see Chapter 3 for antibody details). Following 3 x 15 minute washes with KCM wash buffer, corresponding secondary antibodies and DRAQ5 were added for 1 hour at room temperature. Cells were washed and resuspended in PBS before analysis with ImageStream. Samples were run at 60x magnification with the EDF filter enabled.

Laser (nm)	Intensity Setting
405	120 (with CD45 antibody)
488	20
561	50
658	150
785	2.17

Table 7.4 – 2: ImageStreamlaser settings for the HR assay.

Mask Optimisation

Mask optimisation was undertaken by manual adjustment of mask features and visual confirmation of correct outlining the fluorescence antigen of interest, see Appendix 8.

Method Optimisation in PCO

When applied to cell suspensions of trypsinised PCO cultures, the method described for HR assessment above resulted in poor intra-nucleic permeabilisation and non-specific cytoplasmic staining. Numerous optimisation steps were undertaken, Appendix 8. For the final protocol, cells were fixed with methanol and permeabilised with 0.1% Triton X-100. Addition of a blocking buffer resulted in reduced non-specific antibody binding.

7.4.8. *ImageStream for the Characterisation of Ascites*

Principles of the Assay

ImageStream, with its ability to simultaneously assess multiple immunofluorescent labelled antigens offers a unique opportunity to directly characterise the cellular component of ascitic fluid, avoiding the need for cell culture. Additionally assessment of the cell suspension avoids culture induced selection of subpopulations. Before ascitic samples could be analysed with

ImageStream, the cellular components of ascites were filtered from other debris. RBCs and WBCs were depleted before the sample was fixed, permeabilised and labelled with a panel of immunofluorescent antibodies.

Characterisation Assay Protocol

10 ml of ascitic fluid was filtered using a 180 μ m nylon filter into a 50 ml Falcon tube. Following centrifugation at 50 g for 5 minutes, the cell pellet was incubated with BD Phosflow Lyse/Fix Buffer (1:20 v/v) for 15 minutes at 37 °C. After centrifugation, the cell pellet was resuspended in 500 μ l RoboSep buffer in a 14 ml Falcon tube. The sample was then depleted of WBCs with EasySep™ Human Whole Blood CD45 Depletion Kit, section 7.3.7. Cells were permeabilised with BD Phosflow Perm/Wash Buffer before incubation with EpCAM, CK, CA125, CD45 and DRAQ5 antibodies, as previously described section 7.3.6. Cell pellets were resuspended in PBS for ImageStream processing.

HR Assay Protocol

Two 10 ml of ascitic fluid was filtered into 50 ml Falcon tubes. DNA DSB was induced in one sample with 2 Gy irradiation, alongside untreated controls. Two hours after irradiation, samples underwent red cell lysis and fixation as previously described. Following cell pelleting, 2 ml methanol was added for 20 minutes at -20 °C before enriching for WBCs with EasySep™ Human Whole Blood CD45 Depletion Kit, as above. The cell pellet was blocked in 10% blocking buffer for 1 hour, prior to incubation with primary γ H2AX and Rad51 antibodies for 12 hours at 4 °C. Following three washes with KCM wash buffer, the sample was incubated with the corresponding secondary antibodies, DRAQ5 and CD45 antibodies for 1 hour. Following three further 15 minute washes, the cell pellet was resuspended in PBS and processed with ImageStream.

7.4.9. Ascitic Fluid

ImageStream has been shown to be efficient at characterising cell lines and PCO culture suspensions as well as identifying CTCs. Low numbers of CTCs in ovarian cancer are likely to hinder the potential for their use in meaningful functional assays and ImageStream was therefore considered for the characterisation and functional assessment of fresh ascites.

Characterisation of the Cellular Components of Ascitic Fluid

Ascites from seven patients with ovarian cancer was characterised.

Cellular Classification

Following exclusion of debris and WBCs that had escaped the depletion process, the total number of epithelial and non-epithelial cells within each 10 ml ascitic sample was calculated. Non-epithelial cells (no CD45/EpCAM/CK/CA125 expression) were excluded from further analysis. The concentration and proportion of epithelial and non-epithelial cells differed between samples, demonstrating a clear inter-patient variability of the ascitic fluid composition, Figure 7.4 – 12.

Division of the epithelial cell population into further subpopulations based upon expression of EpCAM, CK, and CA125 demonstrated great inter- and intra-sample heterogeneity, Figure 7.4 - 11. Collating all samples, 76.9% of epithelial cells expressed EpCAM, 26.2% expressed CK and 17.2% expressed CA125. Only 5.4% of all epithelial cells co-expressed all three antigens, Figure 7.4 - 12 and

Figure 7.4 - 13.

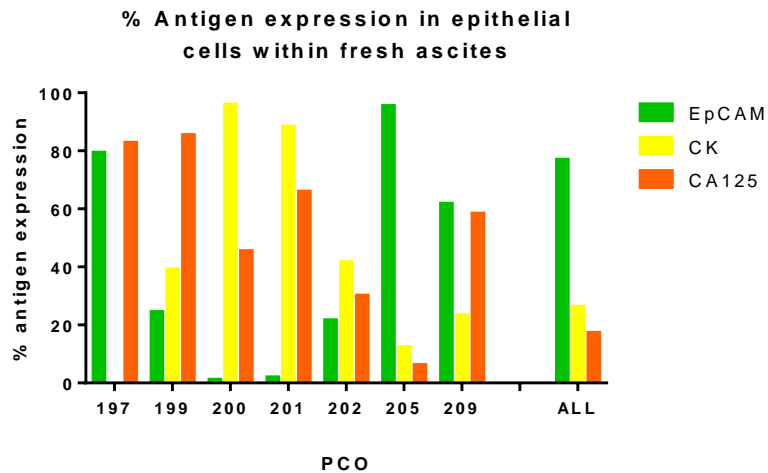


Figure 7.4 - 11: ImageStream antigen characterisation of PCO ascites. Percentage expression of EpCAM, CK and CA125 for each of the seven ascitic samples tested.

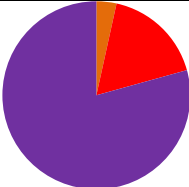
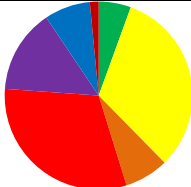
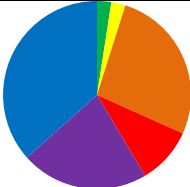
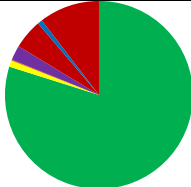
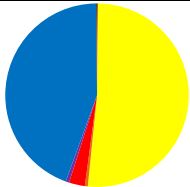
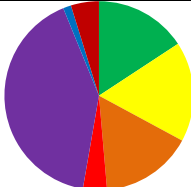
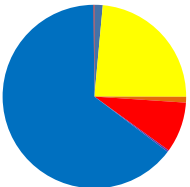
PCO	Epithelial	Non-Epithelial	Antigen Expression within the epithelial cellular component	PCO	Epithelial	Non-Epithelial	Antigen Expression within the epithelial cellular component
	n (%) in 10ml Ascitic Sample				n (%) in 10ml Ascitic Sample		
197	236 (56.9)	179 (43.1)		202	595 (56.8)	453 (43.2)	
199	410 (22.3)	1428 (77.7)		205	5345 (95.9)	229 (4.1)	
200	1174 (86.8)	179 (13.2)		209	146 (9.5)	1391 (90.5)	
201	683 (63.8)	384 (36.2)		<ul style="list-style-type: none"> ■ EpCAM positive ■ CK positive ■ Ca125 positive ■ EpCAM and Ca125 positive ■ CK and Ca125 positive ■ EpCAM and CK positive ■ All positive 			

Figure 7.4 - 12: ImageStream characterisation of ascitic PCO samples. The sub-populations identified in the epithelial cell population present in 10 ml ascitic fluid of patients with EOC.

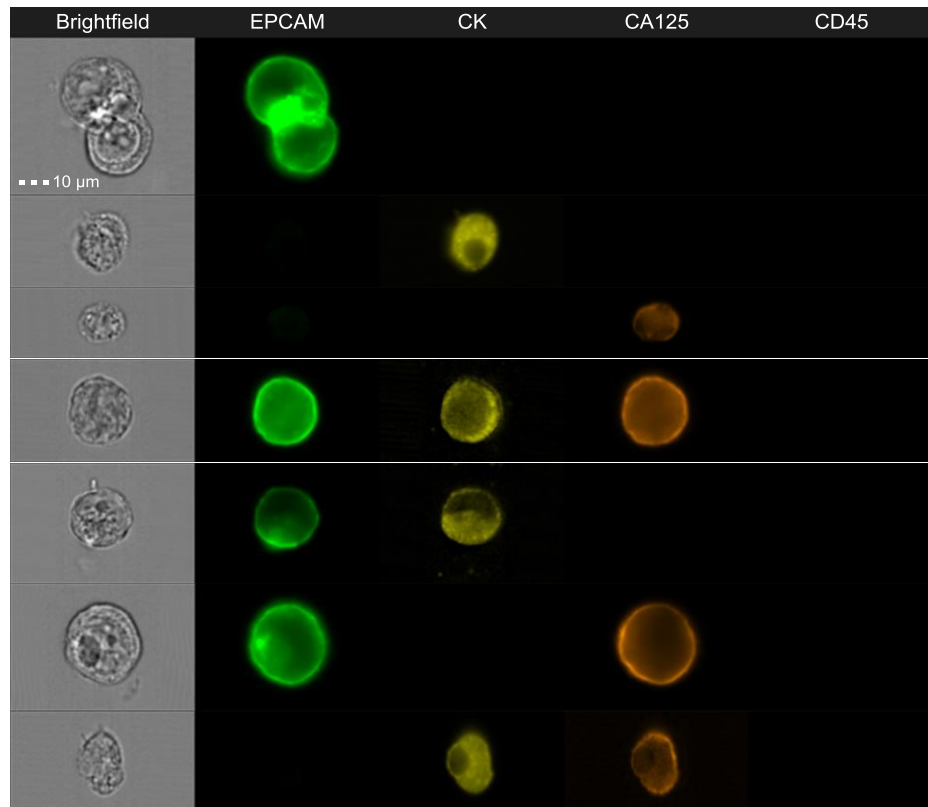


Figure 7.4 - 13: ImageStream cell plot of the major sub-populations of cells identified within the ascitic fluid of PCO209. A: EpCAM only. B: CK only. C: CA125 only. D: All. E: EpCAM and CK. F: EpCAM and CA125. G: CK and CA125.

HR Assay Ascites

Quantification of γ H2AX foci was initially attempted in the tumour cell population identified within ascitic fluid. Optimisation with addition fixation/permeabilisation with methanol alongside RCLB, permeabilisation with 0.1% Triton and addition of a blocking buffer resulted in less non-specific binding. In addition, use of a nuclear mask excluded non-specific cytoplasmic binding and resulted in quantifiable γ H2AX foci, Figure 7.4 - 14, indicating that application of the HR assay to fresh ascites may be achieved. Time prevented inclusion of Rad51.

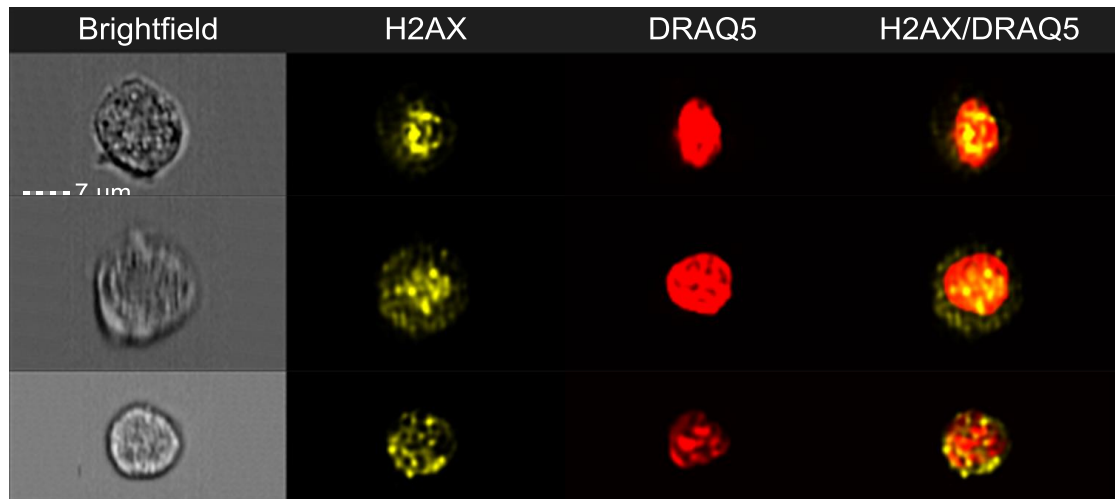


Figure 7.4 - 14: γ H2AX foci in fresh ascites. Fresh ascites was depleted of RBC and WBC using Phosflow RCLB and EasySep™ CD45 depletion. The remaining cellular component was permeabilised with methanol and 0.1% Triton before blocking and incubating with anti- γ H2AX antibody and corresponding fluorescent antibody in a 2 step process. Foci were counted using IDEAS software.

7.5. Summary

- It is possible to detect CTCs in ovarian cancer patients
- CTC enumeration is variable but typically low with no correlation with survival
- CTCs have heterogeneous expression of tumour antigens
- HR function can be determined using ImageStream
- Adaptation of CTC methodologies to direct assessment of tumour cells in ascites offers the potential for real time assessment of tumour biology with minimal intervention.

7.6. Discussion

ImageStream technology has been used in this project for characterisation of cell lines, PCO cultures and fresh ascites as well as CTC detection. Before sample processing with the ImageStream, cell suspensions were fixed, permeabilised and antigens labelled with a panel of antibodies. Initial validation of antibody selection and sample preparation was performed using commercial cell lines and PCO cultures. Evaluation of depletion methods and retrieval was performed using healthy volunteer whole blood spiked with cell lines. Method optimisation has been described, followed by the results of patient sample assessment. Adapting the HR assay for analysis on the ImageStream, offers the potential to simultaneously identify, characterise and functionally assess CTCs. HR method optimisation was undertaken using cell line suspensions and PCO cultures. Realisation that application of the HR assay to the low number of CTCs in ovarian cancer may not be feasible led to exploration of application of the assay to cells circulating within ascites.

An ideal method for analysis of CTCs would be one without enrichment, which has the associated risk of CTC depletion. This approach is achievable with ImageStream but the time required to process an unenriched sample (more than 6 hours per ml blood processed, see section 7.3.6) prevents its routine use. CTC detection therefore requires enrichment to reduce the large number of haematological cells. The enrichment described is based exclusively on depletion of haematological cells, section 7.3.7. Consequently, the method does not rely on any single physical or molecular characteristic of the malignant CTC. The method has been shown to be simple and reproducible with consistent depletion of more than 90% of WBC and patient CTCs detected in samples from different tumour types, see section 7.3.9. The recovery after analysis of known numbers of cells by ImageStream was $59.2 \pm 6.2\%$ (combining data from other tumour cell types). Recovery rates of 40-80% achieved in this study are comparable with previously described methods (Marth 2002, Judson 2003, Wimberger, Heubner et al. 2007, He 2008, Fan 2009). The overall loss from the procedure is 44.8%, of which 38.1% is lost during the enrichment and 6.7%

during the image collection. The majority of these studies used density gradient solutions to isolate a mononuclear cell fraction followed by positive selection of CTC using a variety of epithelial antigens, usually in isolation. Few studies have reported co-expression of epithelial and leucocyte specific antigens and it is possible that many of these studies are in fact enumerating activated or apoptotic WBC with non-specific antigen binding. The study by Tan *et al* however describes antibody enrichment of the mononuclear cell fraction following density gradient separation and enumerates epithelial positive (CAM+ and [EPCAM+ or ESA+ or CK+]), CD45 negative cells. None of the five benign samples tested had detectable CTCs and CTC counts ranged from 0–149 CTCs/ml with stage III/IV patients exhibiting significantly higher mean counts (41.3 CTCs/ml).

These antibody-based methods resulted in variable CTC detection rates ranging from 12%–100% (Marth 2002, Sapi 2002, Allard and Tibbe 2004, Ntouroupi 2008, Fan 2009, Obermayr 2013), and cellular yields also tend to be variable ranging from 0 to 3118 CTCs/ml in one study (He 2008). The presence of CTCs defined by anti-epithelial antibody markers alone has not been found to significantly affect survival or disease recurrence.

Heterogeneity in EpCAM expression in established cell lines (Sieuwerds 2009) as well as epithelial ovarian tumours is well documented and it is appreciated that this heterogeneity is a likely consequence of EMT. Enrichment based on any single molecular characteristic prohibits analysis of CTC heterogeneity. In the described method, CTCs were distinguished from residual leukocytes and cellular debris by antigen expression of four antigens with a nuclear stain and additionally by visual examination of cellular morphology with high quality microscopy images. This prevented inclusion and enumeration of activated WBC or debris and crucially permits detection of CTC heterogeneity. If CTC research is to translate into changes in clinical practice, it is important that the specificity of CTC detection is high. The majority of studies define CTCs based upon positive and negative antigen expression. In some studies, molecular definition is combined with cell morphology. The high resolution imaging that we describe allows us to discriminate objects, such as circulating macrophages,

that might have been included in enumeration of CTCs had detection relied on a lower resolution method. Scrutiny of the high resolution images of these objects demonstrate that they are not cells. It has been proposed that some of these objects may be apoptotic CTCs or fragmented CTCs but this supposition is unproven. We have identified a small number of these objects in healthy volunteer samples further supporting the hypothesis that they represent cellular debris, possibly created during enrichment.

In this study CTC were detected in 7/14 ovarian cancer patients tested with a median count of 5.3 CTC/ml blood tested (0 - 47). Some published studies have reported substantially larger numbers of CTCs (Marth 2002, Judson 2003, Wimberger, Heubner et al. 2007, He 2008, Fan 2009), than identified in this study or in other reports. It is possible that such high numbers reflect inclusion of non-cellular objects and cellular debris in the enumeration. There is no consensus definition within the literature as to what constitutes a CTC. In part, this reflects the large number of techniques used for their detection. Terstappen *et al* (2000) demonstrated that different definitions of the CTC phenotype resulted in different CTC counts with varying degrees of clinical significance (Coumans 2010).

The ability to select different antigens for detection based upon the tumour type to be investigated means that our method could be adapted to multiple tumour types. Consistent results were obtained between the four tumour types studied to date. EpCAM was included within our panel of antigens but could be replaced with any other malignant antigen for detection of non-epithelial malignant cells. Similarly, as novel biomarkers are discovered, analysis of these could be incorporated into this method by inclusion of appropriate antibodies. The method also leaves space for the inclusion of pharmacodynamic biomarkers. The current focus of CTC research is enumeration of CTCs in patients with metastatic disease and the potential association of CTC numbers with prognosis or response to systemic therapy. In this small dataset no correlation was seen between CTC frequency and PFS or OS, section 7.4.3. The 50% retrieval rate, quantified during retrieval experiments, combined with the generally small number of CTC detected in this dataset makes tracking of

changes in CTC frequency with treatment unreliable. In patients with metastatic breast cancer, metastatic colorectal cancer and castration-resistant prostate cancer, CTC levels have been shown to be associated with overall survival in pre- and on-treatment samples (Cristofanilli 2004, Cristofanilli 2005, Budd 2006, Hayes 2006, De Bono 2008, Cohen 2009, Olmos 2009, Tol 2010). These tumours do however predominately metastasise haematogenously and CTC frequency is therefore considerably higher than those seen in ovarian patients. There is considerable interest in the potential to analyse CTCs as a means of studying the biology and behaviour of metastatic cancer. Traditionally, molecular assessments of tumours are based on tissue biopsies. In the majority of cases, these biopsies are from the primary tumour. Metastatic disease is frequently more difficult to biopsy and treatment of metastatic disease is therefore based on analysis of the original biopsy. There is increasing evidence that metastatic disease may differ from the primary tumour. As CTCs are thought to represent an interim step in the metastatic process in the majority of tumour types, sampling of CTCs may allow a more accurate assessment of the metastatic disease without the requirement to invasively biopsy metastatic deposits. This is complicated in ovarian cancer. The work described in Chapter 5 has shown the presence of multiple subpopulations (in terms of antigen expression, HR pathway function and response to cytotoxic agents) within different areas of intra-peritoneal tumour and it is therefore impossible for the CTC population in ovarian cancer to represent the entire tumour. Ovarian cancer CTCs may however represent a clinically aggressive subpopulation whose biology may reflect extra-peritoneal deposits.

7.6.1. *Why are there so few CTCs in Ovarian Cancer?*

Within 14 ovarian cancer patients the median frequency of CTC detected per ml of blood tested was 5.3, ranging from 0 – 47. CTC enumeration in this study, alongside other CTC ovarian cancer series have failed to correlate CTC frequency with clinical outcome, (Marth 2002, Judson 2003). This is likely to reflect the aetiology and natural course of the disease rather than the technologies utilised.

Ovarian cancer is thought to originate in the distal fallopian tube with tumour implanting onto peritoneal surfaces by transcoelomic spread. Even at the advanced stage of presentation, haematogenous or lymphatic spread may not have occurred with very few tumour cells shed into the circulation. In contrast, the majority of other tumours, including prostate and breast, in which CTC enumeration has been shown to correlate with prognosis predominately metastasise haematogenously. The prognosis of CTC enumeration may therefore only be of significance in the subset of malignancies which spread via the circulation.

The biggest limitation of the CTC data set is that blood sampling in this cohort has been opportunistic and has sometimes taken place following delivery of chemotherapy or at times of disease relapse. Chemotherapy is given intravenously and therefore we would expect that any cancer cells within the circulation would be the first to die. In fact, the highest frequency of CTCs was detected in a patient who had undergone chemotherapy treatment just 4 weeks (with a good clinical response) before sampling and it therefore appears that other factors may be more important. The presence and quantity of CTCs may not be dependent upon FIGO stage, which essentially describes the distance of the metastasis from the pelvis, but perhaps more upon the actual volume of disease and its location in respect to major blood vessels?

In Chapter 4, evidence for EMT in the ovarian cancer patient samples tested was presented. Many cultured samples expressed vimentin and lost expression of typical epithelial markers (EpCAM and MOC31), section 4.7.4. It was shown that this was independent of *ex vivo* culture and further supported by the characterisation profiling of ascitic cells assessed using ImageStream protocol, section 7.4.2. Additionally, these data showed that EMT was not universal throughout the whole tumour with multiple subpopulations of cells with different phenotypes. The process of EMT is dynamic and highly variable and it may be that although EMT is thought to take place early in the development of ovarian cancer, cells have not yet acquired the ability to invade through the serosal surfaces of the intra-abdominal organs or blood vessels and therefore access to the circulation is limited. This may not be the case in other cancers from

different origins, which may spread predominantly via the circulation and may develop the ability to invade blood vessels during their development. Hence, this may be one explanation to the reported variability of enumeration of CTCs in other tumour types. Additionally, even if tumour cells can access the blood stream, survival in this hostile environment is challenging. Preclinical models demonstrate that within 24 hours of intravenous administration of tumour cells, less than 0.1% of cells remain viable and that less than 0.01% of these surviving CTCs can produce metastasis (Fidler 1970).

Perhaps CTCs in ovarian cancer are in fact plentiful but are rapidly identified by the immune system as foreign and are removed promptly before detection is possible, Figure 7.4 - 7.

7.6.2. *Can ImageStream Assessment of Ascites make Real Time HR Assessment Possible?*

This study shows that identification and characterisation of epithelial tumour cells within just 10 ml of patient ascites is possible. Additionally, using the principles of the HR assay, we have demonstrated that DNA damage can be estimated in tumour cells within ascites by quantification of γ H2AX foci. The ability to identify and characterise the multiple subpopulations of cells present in ascites using a relatively small volume of ascites is an appealing prospect and offers the major advantage of immediate assessment of tumour cells bypassing culture and also enabling recognition and assessment of all sub-populations.

7.7. Conclusions

It is clear that CTCs cannot currently replace the diagnostic tests for ovarian cancer. Perhaps for ovarian cancer, unlike other malignancies which predominantly spread haematogenously, simple enumeration of CTCs is less useful owing to their typically low numbers. If it is appreciated that only small numbers of ovarian cancer cells are capable of gaining entry into the circulation and that an even smaller proportion are capable of survival and initiation of distant metastasis, then any CTCs detected are likely to represent one small subpopulation. It is therefore unlikely that any characterisation (antigen or molecular profiling) of them should be interpreted with care.

It has been shown that sophisticated molecular testing to determine HR function of cell populations using ImageStream technology is possible and although this is not feasible with the typical small numbers of CTC detected in ovarian cancers, these techniques are adaptable to other tumour types for antigen and biological characterisation. Additionally, the technology is applicable to analysis of ascitic fluid and the option for a large number of antibodies to be used simultaneously in combination with high resolution microscopy allows for very accurate identification and localisation of specific target antigens within the cells enabling assessment of the multiple subpopulations within ovarian cancer.

Chapter 8: Discussion

Ovarian cancer is a complex disease. As we begin to unravel the complexity of its aetiology and underlying genetics, the hope of discovering a single chemotherapy adjunct to surgery, which is capable of significantly improving survival, dissipates. Instead, the developing insight into this mysterious disease helps us to strive towards a more realistic goal. A cure for ovarian cancer is unlikely unless we can shift the timing of diagnosis to an earlier stage. The search for effective screening tools has yet to identify any factors that enable accurate identification of early stage disease and therefore we can anticipate that women will continue to present with non-specific symptoms at a late stage of disease. It is therefore more realistic to, at least initially, aim to turn ovarian cancer into a chronic disease rather than the 'silent killer', which it is currently regarded.

It is not refuted that surgery plays an essential role in the management of ovarian cancer and that this should be undertaken only at a time when complete cytoreduction is thought to be achievable. Further discussion of judging the timing of surgery and the accuracy of predicting complete cytoreduction is not covered within the scope of this thesis. Polypharmacy of adjuvant chemotherapy in the typical population of women affected by ovarian cancer is an unrealistic goal owing to the toxic profile of most available agents and the typical advanced age of patients, who often have multiple comorbid conditions, which limits chemotherapy options. It is perhaps unrealistic to expect a single targeted agent to offer the hope of a 'magic bullet' for ovarian cancer but it may be possible to increase PFS with the use of sequential novel agents, which may cumulatively add overall survival benefit.

An alternative treatment strategy for ovarian cancer is long overdue but implementation is massively restricted by our limited ability to accurately predict response to treatment and the availability of effective agents. Additionally, for alternative treatment strategies to be implemented into routine practice, the

importance of the influence of tumour biology upon response to treatment and survival needs to be accepted by the clinical team and communicated effectively to our patients.

8.1. Summary of Results

The aim of this study was to explore the ability of a functional HR assay to predict sensitivity to various cytotoxic agents, including CNDAC - a novel nucleoside analogue, and the prediction of disease outcome. Additionally, project aimed to address the question of the optimal way to sample cancer in order to provide accurate, clinically relevant biological about an individual's tumour by exploring sampling of the circulating cells as an alternative non-invasive biopsy to the sampling of ascites and tumour. A summary of the main objectives and the additional objectives during evolution of the project are shown in

Table 8.1 - 1.

Aim	Results Achieved	Comment
Characterise PCO cultures (antigen expression, growth potential, morphology) to further understand validity of <i>ex vivo</i> cultures	Yes	Ovarian cancer is highly heterogeneous in terms of antigen expression, growth and morphology. Selection bias and antigen expression changes with the process of <i>ex vivo</i> culture
Determine HR status of ascitic PCO samples and explore relationship with sensitivity to rucaparib and cisplatin	Yes	HR status of ascites, with <i>ex vivo</i> sensitivity data with PF/OS data completed for 56 patients.
Develop a method for culture and HR characterisation of solid tumour	Yes	Culture success rate of 86%
Explore spatial heterogeneity within an individual's cancer by assessing variability of functional HR status	Yes	Heterogeneity exists in terms of antigen expression, growth, HR function and sensitivity to cytotoxic agents
Determine the proportion of PCO cultures sensitive to CNDAC and assess HR status as a biomarker of sensitivity	Yes	46% PCO cultures sensitivity to CNDAC. Stratification using HR function is likely to enrich for sensitivity to CNDAC. Additionally defective BER, is also likely to enrich for sensitivity
Develop and validate a method for accurate identification, quantification and characterisation of CTCs from whole blood	Yes	CTC frequency is variable but typically low with a median frequency of 5.3 CTC/ml whole blood tested
Explore relationship of enumeration with outcome	Yes	Small numbers but no clear relationship with stage or disease outside of the abdomen
Develop a method for application of the HR assay to CTCs	Yes	HR assay using ImageStream developed and validated on cell lines and PCO samples. Method can be applied to ascitic cells and CTCs (in cases with greater numbers of CTCs)

Table 8.1 - 1: Summary of objectives and project outcomes

The use of PCO ascitic cultures described in this project has provided a valuable resource for the study of ovarian cancer tumour biology. Use of this model has many advantages over commercially available cell lines but also has several limitations. In this project, we have increased our understanding of the effect of culture on the phenotype of the PCO culture in terms of change in antigen detection, growth rate and morphology. We now appreciate the inability of ascites in isolation to accurately represent the entire tumour without further assessment of other areas of the tumour and, additionally, acknowledge the

high levels of resources and specialist expertise needed in order to create and maintain cultures for biological assessments. In the absence of a simple and reproducible alternative, this model should continue to be used to test the molecular profile of tumours and, whilst we continue to assess the validity of genomic profiling in predicting response, we should incorporate ascites assessment into clinical trials.

This study confirms the high incidence of defective HR within ovarian cancer and also provides growing evidence of dysfunction within other DNA repair pathways. A functional biomarker utilising live cultured cells remains the most reliable way to stratify patients into functional groups, with good evidence that this correlates with sensitivity *ex vivo* and patient outcome (PFS). Irrespective of the specific genetic defect, the HR functional assay was able to predict the group of women who could potentially benefit from PARP inhibitors. Attempts to simplify the functional assay or provide alternative surrogate assays are promising but require further evaluation within trials to assess their PPV, NPV and application to the clinical setting.

Additional cytotoxic agents are required if sequential targeted therapies are to be given and the sensitivity seen in *ex vivo* primary cultures in this study provides evidence for sapacitabine to progress to phase 1/2 clinical trials in ovarian cancer. Incorporation of translational research into these trials will be able to further evaluate the usefulness of HR, or perhaps BER, as markers of sensitivity.

We have developed a technique for the successful culture of tumour from solid samples and have been able to perform subsequent characterisation and assessment of HR function and sensitivity to various cytotoxic agents. The greatest challenge that this project has identified is the question of how to adequately sample a tumour. We now appreciate the functional heterogeneity of ovarian cancer between individual patients, even those with tumours of the same histological subtype, and additionally within an individual patient with different areas of tumour having different abilities to repair DNA damage and

subsequent variable response to cytotoxic agents. Without assessing the intra-tumoural heterogeneity, it is unrealistic to expect a single assay to accurately predict response to any cytotoxic agent and there is a danger that clinical trials that do not take this into account may underestimate the actual clinical benefit.

Development of a novel technique to identify and characterise circulating tumour cells (CTCs) has enabled exploration of the ability to sample CTCs as a minimally invasive way to sample a tumour and assess its HR functional status. The limited number of CTCs identified even in advanced disease limits the use of this technique out of the academic setting. Additionally, it is impossible for CTCs alone to represent the multiple subpopulations of tumour and although we can hypothesise that the cells capable of gaining access and surviving within the harsh environment of the circulation are likely to be the most clinically aggressive, we as yet have no evidence to confirm this. The adaptation of the technique to use ImageStream to assess ascites may however offer the opportunity for rapid and detailed characterisation of ascites without labour intensive culture.

It is becoming clear that ovarian cancer is a broad and diverse group of diseases and that, even within an individual's tumour, there exists heterogeneity. This heterogeneity may be responsible for determining the variable response to chemotherapy seen and the inaccuracy of single biopsy determined biomarkers to precisely predict disease response.

The major outcome from this project is the identification of the need for development of sampling regimes and the ability to map tumour according to its biological profile. This will require total revision of the definitions of 'response' and 'relapse' and of management pathways.

8.2. A New Treatment Strategy for Ovarian Cancer

If the knowledge of intra-tumoural heterogeneity (ITH) is to be translated into clinical practice, it necessitates a new approach to treatment. It is likely that the different regions of heterogeneous tumours require treatment with multiple targeted agents. As discussed, simultaneous provision of multiple therapies ensuring a broad coverage of all subpopulations is not practical in ovarian cancer. If chemotherapies cannot be given in combination, sequential provision of therapy should be considered with re-stratification at each relapse.

A combination of debulking surgery paired with the proven most effective cytotoxic agent for ovarian cancer, platinum, should remain central to our management. Following debulking surgery, whether this is primary surgery or interval surgery, all tumours should be sampled and characterised in terms of biomarkers indicative of sensitivity to novel targeted cytotoxic agents. In particular, any residual tumour that cannot be excised at the time of surgery should be sampled, as it is most likely that the residual tumour is the subpopulation that will expand and cause relapse/recurrence.

At the time of relapse, the tumour should be re-biopsied and re-characterised with regards to a biomarker panel to enable selection of the targeted cytotoxic agent that should be used. This would enable provision of effective therapy whilst minimising side effects and, hopefully, improving PFS and OS, Figure 8.2 - 1.

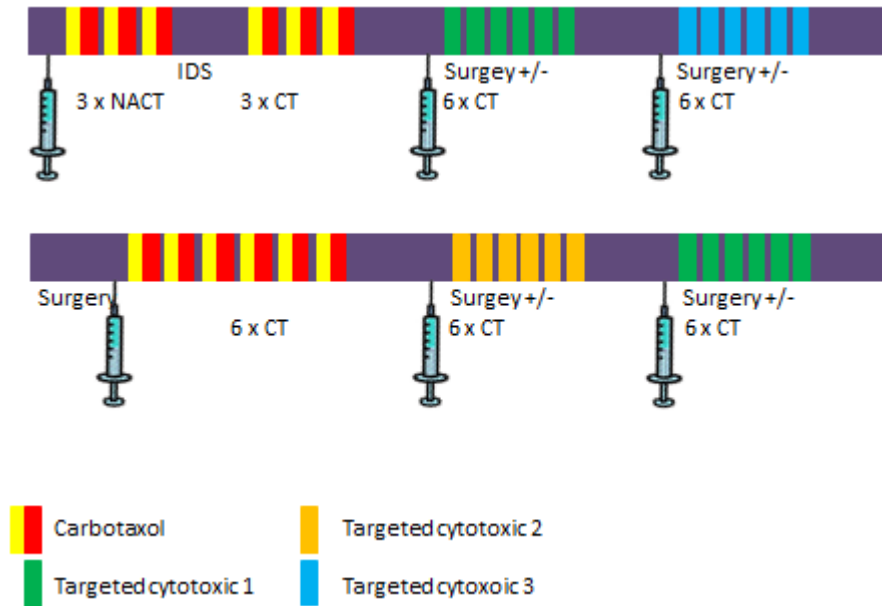


Figure 8.2 - 1: Schematic for the sequential Provision of Targeted Agents following Interim Tumour Sampling and Biomarker Testing

Intra-tumour heterogeneity does however add a further complicating factor to this concept and a single biopsy will not be sufficient. Multiple biopsies from all areas of relapse within the abdomen will be required. This is likely to be best achieved laparoscopically, allowing multiple biopsies to be taken whilst assessing operability. The role of secondary, tertiary and quaternary surgery should not be overlooked, particularly in cases of isolated recurrences.

The likely key to the successful treatment of the heterogeneous disease of ovarian cancer is sequential provision of cytotoxic agents. The current choice of cytotoxic agents available for the treatment of ovarian cancer is relatively limited and no current treatments have been paired with a reliable biomarker. Future treatments need to be selectively cytotoxic to cancer cells with minimal systemic side effects. They should work predictably in cancers identified to be sensitive to the agent, using a clinically useful assay.

8.3. Redefining Ovarian Cancer

If the way in which we investigate and treat ovarian cancer is evolving then the definitions that we currently use for progression and relapse will shortly become inapplicable. The current clinical definitions are based upon clinical symptoms or multiple measurements of the tumour but are broad and consider the overall tumour, Table 8.3 - 1.

Category	Definition	
NCI (Institute 2014)		
Relapse	The return of a disease or the signs and symptoms of a disease after a period of improvement.	
Recurrence	Cancer that has returned usually after a period of time during which the cancer could not be detected	
Progression	The course of a disease as it becomes worse or spreads in the body	
RECIST (Eisenhauer 2009)		
	Target lesions	Non-target lesions
Complete response (CR)	Disappearance of all target lesions. Any pathological lymph nodes (target or non-target) must have reduced in short axis to <10 mm	Disappearance of all non-target lesions and normalisation of tumour marker level. All lymph nodes must be non-pathological in size (<10 mm short axis)
Partial response (PR)	At least a 30% decrease in the sum of diameters of target lesions	Non-CR/Non-PD Persistence of one or more non-target lesion(s) and/or maintenance of tumour marker level above the normal limits
Stable disease (SD)	Neither sufficient shrinkage to qualify for PR nor sufficient increase to qualify for PD	
Progressive disease (PD)	At least a 20% increase in the sum of diameters of target lesions with an absolute increase of at least 5 mm. The appearance of one or more new lesions is also considered progression.	Unequivocal progression of existing non-target lesions. The appearance of one or more new lesions is also considered progression.

Table 8.3 - 1: Ovarian Cancer Clinical and Radiological Definitions of Disease Response

RECIST (response evaluation criteria in solid tumours) is a set of published rules that define responsive, stable or progressive disease during treatment (Eisenhauer 2009). The original criteria were published in 2000 by an international collaboration, which included the European Organisation for Research and Treatment of Cancer (EORTC), National Cancer Institute (NCI) of the United States and the National Cancer Institute of Cancer Clinical Trials

group. RECIST helps to categorise tumours based upon their radiological appearance, giving an overall summary of the changes seen. With the knowledge of the presence of intra-tumoural heterogeneity and the appreciation that distinct areas of tumour are likely to behave differently to a single cytotoxic agent, then it is likely that we are to anticipate response in one targeted area only. Modification to RECIST or an alternative system may therefore be needed to enable description of the individual tumour areas. This method heavily relies upon measurement of tumour size from CT imaging and, in fact, alternatives to this may need to be considered.

8.4. Ovarian Cancer Heterogeneity: Implications for Academia

The provision of clinical samples, with time, will help to unravel the difficulties in understanding the importance of adequate sampling of tumour. As the ability to molecular profile tumours continues to grow and we begin to understand the effects of molecular aberrations on overall function of the cells and subsequent response to therapy, then more questions are likely to arise. If multiple pathways are dysfunctional, then how will the dysfunctional pathways interact and are there 'dominant' mutations that are known to be the most important and, if present, should dictate management irrespective of their prevalence or presence of other mutations? Understanding the interplay of all the important pathways in ovarian cancer, alongside the highly variable and influential clinical factors, is a sizable and daunting challenge and perhaps unachievable using current technologies. This should however be readdressed with the introduction of biological programming with artificial intelligence systems (Enshaei 2015).

8.5. Strengths and Weaknesses

The mixed nature of the patients, histological subtypes, timing and outcome of surgery initially appears to be a limitation of this work as this heterogeneous group of patients and samples may not be considered directly comparable. However, this may also be one of the greatest strengths of this project as it demonstrates that categorisation of tumours based upon histology alone is largely unhelpful and does not reliably predict outcome or response to treatment.

Categorisation of tumours using functional status of the DDR does however appear to enable more accurate prediction of outcomes and should be used to inform provision of additional cytotoxic agents.

One strength of our study, in terms of clinicopathological and survival data, is that it was a prospective observational study. Although not randomised, clinicians involved in managing the patients were not aware of the HR status of cultures.

The number of women from whom multiple solid tumour biopsies were taken may be considered small but the data included demonstrates the variability of heterogeneity and provides sufficient pilot data to justify a larger trial. Clearly, standardisation of the number and location of biopsies would be needed and large numbers of participants would be required for meaningful analysis of the effect of heterogeneity upon outcome to be undertaken.

The work in this study adds to the growing evidence regarding the importance of the HR pathway within ovarian cancer and, at present, there are no reliable alternatives to the labour intensive functional Rad51 assay. Ongoing efforts to identify a reliable and rapid alternative are still needed but require validation alongside the functional assay in paired samples from the same tumour site as previous genomic signatures may have been falsely excluded due to incorrect sampling of heterogeneous tumours.

8.6. Future Work

1. Validation of a genomic sequence for HR function using RNA extracted from FFPE tissue matched for biopsy location of solid cultures with HR function determined by Rad51 assay (FFPE blocks available).
2. Development of a database and tissue bank to enable accurate documentation and storage of multiple biopsies from multiple sites in patients recruited to research.
3. Continued collection of serial samples from the same patient at different time points to explore tumour evolution with time and therapy.
4. Exploration of the fallopian tube as the site of origin of ovarian/primary peritoneal cancer using historical FFPE of STIC lesions. The gene signature created from HRD cultures will be applied and used to stratify STIC lesions into functional HR groups and correlate with PFS/OS and other clinical features. Collaboration with Dr James Bierne (Centre for Cancer Research and Cell Biology, Queens University Belfast).
5. Feasibility of alternative culture methods (splice tumour culture) will be tested with solid ovarian tumour to assess if a higher yield of cells will result which can be used in a wider variety of assays. This will incorporate the per-tumour stroma allowing the impact of this to be assessed in terms of growth.
6. Studying protein expression by IHC in the tumour incorporated into FFPE has failed to identify a marker capable of reliably predicting HR functional status (although tumour biopsies have been compared to HR status of ascites, not a solid tissue culture from the corresponding area of tumour from which the biopsy was taken). Assessment of the stroma alongside tumour can be undertaken in FFPE tissues already available to explore the ability of a stromal score to predict HR function of tumour.
7. Further quantification of BER dysfunction in ovarian cancer with exploration of manipulation of activating/deactivating agents as well as APE1 inhibitors.

8. The low number of CTCs detected in ovarian cancer alongside the heterogeneous nature of the disease, limit the validity of any biological assessment performed upon CTCs. Instead of studying molecular biology of these cells, the response to treatment will be assessed in real time by assessing the impact of cytotoxic agents on CTC cell cycle. For examples, platinum is known to induce G2 arrest. CTC blood sample obtained pre-chemo can be compared to a sample collected during chemo and any changes in cell cycle assessed. This may be an early indicator of likely response alongside enumeration.

Appendices

Appendix 1: PhD Publications

- RL O'Donnell, A McCormick, A Mukhopadhyay, LC Woodhouse, M Moat, A Grundy, M Dixon, A Kaufman, S Soohoo, A Elattar, B Uzir, NJ Curtin, RJ Edmondson. The use of ovarian cancer cells from patients undergoing surgery to generate primary cultures capable of undergoing functional analysis. Plos One. 6; 9 (3):e90604. 2014
- MJ Patterson, RE Sutton, I Forrest, R Sharrock, M Lane, A Kaufmann, R O'Donnell, RJ Edmondson, BT Wilson, NJ Curtin. Assessing the function of homologous recombination DNA repair in malignant pleural effusion (MPE) samples. British Journal of Cancer. 111: 94-100. 2014
- BM Dent, RL O'Donnell, LF Ogle, E Rouke, H Ramesh, M Moat, N Hayes, U Malik, NJ Curtin, AV Boddy, ER Plummer, RJ Edmondson, HL Reeves, FEB May, D Jamieson. High-resolution imaging for the detection and characterisation of circulating tumour cells from patients with oesophageal, hepatocellular, thyroid and ovarian cancers. In press
- RL O'Donnell, A Kaufmann, L Woodhouse, A McCormick, RJ Edmondson, NJ Curtin. Advanced ovarian cancer displays functional intra-tumour heterogeneity which correlates to *ex vivo* drug sensitivity. SUBMITTED TO IJGC – IN PRESS
- RL O'Donnell, J Murray, A Buskin, MJ Paterson, A McCormick, A Kaufmann, S Frame, D Blake, RJ Edmondson, NJ Curtin. The stratified use of Sapacitabine in the management of ovarian cancer. Manuscript prepared. FOR SUBMISSION TO MOLECULAR ONCOLOGY following review by Cyclacel.

Appendix 2: Published Abstracts

- B Dent, RL O'Donnell, LF Ogle, ED Rourke, HP Ramesh, M Moat, N Hayes, UK Mallick, FE May, HL Reeves, NJ Curtin, RJ Edmondson, AV Boddy, R Plummer, D Jamieson. Detection and characterization of circulating tumour cells by imaging flow cytometry. *Cancer Research*. 74(19 Supplement):3059-3059.2014.
- L Ogle, D Jamieson, R O'Donnell, B Dent, A Boddy, NJ Curtin, R Plummer, H Reeves. Detection of circulating tumour cells (CTCs) in hepatocellular cancer (HCC) patients using ImageStream. *Journal of Hepatology*. 60 (1): S95. 2014
- RL O'Donnell, LC Woodhouse, A McCormick, A Kaufmann, M Dixon, A Mukhopadhyay, NJ Curtin, RJ Edmondson. Intra- and inter-tumour heterogeneity in epithelial ovarian cancer: Consequences for biomarker-dependent stratification of therapies. *Clinical Cancer Research*. 19: PR10. 2013
- A McCormick, M Dixon, RL O'Donnell, NJ Curtin, RJ Edmondson. Ovarian cancers harbour defects in non-homologous end joining resulting in error prone repair and resistance to rucaparib. *Clinical Cancer Research*. 19: PR06, 2013.
- A McCormick, E Earp, C Leeson, M Dixon, RL O'Donnell, RJ Edmondson. PTEN expression level is important in determining sensitivity to cytotoxic agents in vitro, but is not representative of PTEN function observed in primary ovarian cancer cultures. *Clinical Cancer Research*. 19: B9. 2013
- RL O'Donnell, JCC Murray, ABG Buskin, S Frame, DG Blake, A Kaufmann, M Dixon, ER Plummer, NJ Curtin, RJ Edmondson. Therapeutic potential of sapacitabine in ovarian cancer defective in homologous recombination. *Clinical Cancer Research*. 19:A33. 2013.

Appendix 3: Oral Presentations

- RL O'Donnell, A Kaufmann, L Woodhouse, A McCormick, NJ Curtin, RJ Edmondson. Intra- And Inter-tumour Heterogeneity In Epithelial Ovarian Cancer: Consequences For Biomarker-dependent Stratification Of Therapies. RCOG Annual Academic Meeting, 2014
- RL O'Donnell, L Woodhouse, A McCormick, A Mukhopadhyay, M Dixon, A Kaufmann, NJ Curtin, RJ Edmondson. Intra- And Inter-tumour Heterogeneity In Epithelial Ovarian Cancer: Consequences for Biomarker-dependent Stratification of Therapies. BGCS, 2014
- BGCS PRIZE
- RL O'Donnell, M Moat, B Dent, L Ogle, D Jamieson, NJ Curtin, RJ Edmondson. Detection and characterisation of circulating tumour cells in ovarian cancer: can we functionally assess this population? UK Imaging Flow Cytometry Interest Group Meeting 2013.
- RL O'Donnell, L Woodhouse, A McCormick, A Mukhopadhyay, M Dixon, A Kaufmann, NJ Curtin, RJ Edmondson. Functional intra-tumour heterogeneity in ovarian cancer: what is a representative sample? ESGO, 2013
- RL O'Donnell, LC Woodhouse, A McCormick, A Kaufmann, M Dixon, A Mukhpadhyay, NJ Curtin, RJ Edmondson. Intra- and inter-tumour heterogeneity in epithelial ovarian cancer: Consequences for biomarker-dependent stratification of therapies. AACR: Ovarian cancer – concept to clinic, 2013

Appendix 4: Poster Presentations

- RL O'Donnell, M Moat, BM Dent, LF Ogle, D Jamieson, AV Boddy, ER Plummer, HL Reeves, FEB May, NJ Curtin, RJ Edmondson. Detection and characterisation of circulating tumour cells in Ovarian Cancer: are CTCs clinically useful for functional biomarker analysis? BGCS 2015
- J Burgon, A Herriott, D Jamieson, A McCormick, M Moat, R O'Donnell, NJ Curtin, Y Drew. Targeting the Mismatch Repair Pathway in Ovarian Cancer. NCRI 2015
- RL O'Donnell, K Broome, I Biliatis, N Ratnavelu, A Mukhopadhyay, C Ang, A Fisher, KA Godfrey, CW Helm, A Kucukmetin, R Naik. 30-day Post-Operative Mortality (POM) Following Laparotomy in Gynaecological Oncology: What Lessons Can Be Learnt From Prospectively Collecting Data? BGCS, 2014
- B Dent, RL O'Donnell, L Ogle, E Rourke, H Ramesh, M Moat, N Hayes, U Mallick, F May, H Reeves, N Curtin, R Edmondson, A Boddy, R Plummer, D Jamieson. Detection and characterization of circulating tumour cells by imaging flow cytometry. AACR, San Diego, 2014
- M Moat, RL O'Donnell, B Dent, L Ogle, NJ Curtin, D Jamieson, RJ Edmondson. A novel use of ImageStreamX: The characterisation and functional assessment of epithelial ovarian cancer cells derived from ascitic fluid using ImageStreamX. UK Imaging Flow Cytometry Interest Group Meeting 2013.
- M Moat, RL O'Donnell, B Dent, L Ogle, N Curtin, D Jamieson, RJ Edmondson. The characterisation and functional assessment of epithelial ovarian cancer cells derived from ascitic fluid using ImageStreamX. NCRI Cancer Conference, 2013
- RL O'Donnell, L Woodhouse, A McCormick, A Mukhopadhyay, M Dixon, A Kaufmann, NJ Curtin, RJ Edmondson. Functional intra-tumour heterogeneity in ovarian cancer: what is a representative sample? ESGO, 2013

- M Moat, R O'Donnell, B Dent, L Ogle, NJ Curtin RJ Edmondson. The characterisation and functional assessment of epithelial ovarian cancer cells derived from ascitic fluid using ImageStreamX. ESGO, 2013
- RL O'Donnell, LC Woodhouse, A McCormick, A Kaufmann, M Dixon, A Mukhpadhyay, NJ Curtin, RJ Edmondson. Intra- and inter-tumour heterogeneity in epithelial ovarian cancer: Consequences for biomarker-dependent stratification of therapies. AACR: Ovarian cancer – concept to clinic, 2013
- RL O'Donnell, JCC Murray, AGB Buskin, S Frame, DG Blake, M Dixon, A McCormick, A Kaufmann, ER Plummer, RJ Edmondson, NJ Curtin. Therapeutic potential of sapacitabine in ovarian cancers defective in homologous recombination. AACR: Ovarian cancer – concept to clinic, 2013
- A McCormick, M Dixon, R O'Donnell, NJ Curtin, RJ Edmondson. Ovarian cancers harbour defect in non-homologous end-joining resulting in error prone repair and resistance to rucaparib. AACR: Ovarian cancer – concept to clinic, 2013
- A McCormick, E Earp, C Leeson, M Dixon, R O'Donnell, RJ Edmondson. PTEN expression level is important in determining sensitivity to cytotoxic agents in vitro, but is not representative of PTEN function observed in primary ovarian cancer cultures. AACR: Ovarian cancer – concept to clinic, 2013
- RL O'Donnell, L Woodhouse, A McCormick, A Mukhopadhyay, M Dixon, A Kaufmann, NJ Curtin, RJ Edmondson. Functional intra-tumour heterogeneity in ovarian cancer: are our expectations of novel therapies too high? BGCS 2013
- RL O'Donnell, AGB Buskin, JCC Murray, A McCormick, S Frame, A Mukhopadhyay, ER Plummer, BG Blake, RJ Edmondson, NJ Curtin. Therapeutic potential of sapacitabine in cancers defective in homologous recombination. National Cancer Research Institute Annual conference, Liverpool. 2012.

- L Woodhouse, A Grundy, A McCormick, RL O'Donnell, NJ Curtin, RJ Edmondson. Validating the use of solid tissue explants to determine homologous recombination status in epithelial ovarian carcinomas. National Cancer Research Institute Annual conference, Liverpool. 2012.
- A Grundy, L Woodhouse, A McCormick, RL O'Donnell. NJ Curtin, RJ Edmondson. Development of a more clinically applicable method to determine the homologous recombination status of human epithelial ovarian cancers. National Cancer Research Institute Annual conference, Liverpool. 2012
- A McCormick, R O'Donnell, A Grundy, L Woodhouse, NJ Curtin, RJ Edmondson. Ovarian cancers harbour defects in non-homologous end-joining. National Cancer Research Institute Annual conference, Liverpool, 2012.

Appendix 5: Consent Form for Tissue Collection



Cancer Research Involving Tumour Samples Blood and Patient Information

CONSENT FORM

Please
initial
box

1. I have read the attached information sheet on the above project and have been given a copy to keep. I have had the opportunity to ask questions and understand why tumour samples, blood and patient information is being collected.
2. I agree to donate a sample of tumour tissue and blood for research. I understand how the sample will be collected, that giving the sample for this research is voluntary and that I am free to withdraw my approval at any time without giving a reason and without my medical treatment or legal rights being affected.
3. I give permission for certain anonymised medical details, as have been explained to me, to be looked at and information taken from them to be analysed in strict confidence by staff at the Northern Gynaecological Oncology Centre or from organisations supervising the research.
4. I understand that future research using the sample I have given may include genetic research aimed at understanding the genetic influences relating to cancer, but that the results of these investigations are unlikely to have any implications for me personally.
5. I agree that the samples I have given and the information gathered about me can be looked after and stored in the Northern Gynaecological Oncology Centre for use in future projects, as described in the attached information sheet. I understand that some of these projects may be carried out by researchers other than from the NGOC.
6. I understand that all studies will be anonymised, coded and unlinked. This means that no results will be given to me directly of any research carried out on tissue, blood or data that I donate.
7. I understand some research may take part in conjunction with commercial organisations. I will not benefit financially if this research leads to the development of a new treatment or medical test.
8. I know how to contact the research team if I need to.

Name of patient: Signature: Date:

Name of doctor: Signature: Date:

Thank you for agreeing to participate

White Copy – Patient Copy

Appendix 6: Detailed Patient Demographics

PCO	Date of Collection	Age (yrs)	FIGO Stage	Histological subtype	Pre-op CA125 (U/L)	Surgery	Cytoreduction	NACT	Adjuvant Chemo	PFS	OS
										(months)	
138	12/10/2011	70	3C	HGSC	1412	Primary	Suboptimal	NA	6 x carbo/taxol	29	30
139	21/10/2011	77	4	Endometrioid/Clear	1445	Primary	Optimal	NA	NA	9	9
142	31/10/2011	62	3C	HGSC /Endometrioid/Clear	896	Primary	Optimal	NA	NA	2	2
143	21/11/2011	46	3C	HGSC	1465	Primary	Optimal	NA	6 x carbo/taxol	10	10
144	02/12/2011	60	1A	Endometrioid/Clear	1317	Primary	Optimal	NA	6 x carbo/taxol	29	36
154	22/02/2012	78	3C	Carcinosarcoma	618	Primary	Complete	NA	NA	10	10
155	22/02/2012	55	NA	Appendix adenocarcinoma	117	Primary	Optimal	NA	FOLFOX	14	18
156	27/02/2012	49	4	HGSC	1320	IDS	Optimal	4 x carbo/taxol	1 x carbo/taxol	9	13
157	02/03/2012	58	3C	HGSC	500	Primary	Suboptimal	NA	6 x carbo/taxol; tamoxifen	11	12
158	05/03/2012	68	3C	HGSC	780	Primary	Optimal	NA	4 x carboplatin	4	4
162	23/04/2012	68	3C	HGSC	186	Primary	Optimal	NA	6 x carbo/taxol	18	31
163	02/05/2012	77	3C	HGSC	500	Primary	Optimal	NA	5 x carbo/taxol	14	31
167	18/06/2012	63	3C	HG Neuroendocrine tumour	600	Primary	Optimal	NA	Cisplatin/etoposide	7	7
168	19/06/2012	66	3C	HGSC	1500	Primary	Complete	NA	6 x carbo/taxol	14	29
169	13/07/2012	72	3C	HGSC	176	IDS	Optimal	3 x carbo/taxol	3 x carbo/taxol	10	11
170	03/08/2012	73	3C	HGSC	10000	IDS	Suboptimal	4 x carbo/taxol	2 x carbo/taxol; bevacizumab	20	27
171	22/08/2012	75	3C	HGSC	1285	IDS	Optimal	4 x carbo/taxol	2 x carbo/taxol	24	31
174	12/09/2012	45	3A	Endometrioid	552	Primary	Complete	NA	6 x carbo, 2 x taxol, 4 x docetaxol	15	26
175	12/09/2012	66	3B	Clear cell	250	Primary	Optimal	NA	5 x carbo/taxol	6	8
177	16/10/2012	46	3C	HGSC	6	IDS	Optimal	4 x carbo/taxol	2 x carbo/taxol	13	23
179	09/11/2012	66	4	HGSC	800	IDS	Optimal	4 x carbo/taxol	2 x carbo/taxol	12	1117

180	19/11/2012	50	3C	HGSC	521	IDS	Optimal	3 x carbo/taxol	3 x carbo/taxol	11	12
181	19/11/2012	72	3C	HGSC	180	IDS	Optimal	3 x carbo/taxol	3 x carbo/taxol	10	11
182	23/11/2012	61	3C	HGSC	286	IDS	Complete	3 x carbo/taxol	3 x carbo/taxol; tamoxifen; 5 x rucaparib	11	38
183	28/11/2012	82	2C	HGSC	6388	Primary	Complete	NA	4 x carbo/taxol	19	21
184	05/12/2012	73	3C	HGSC	10,000	IDS	Suboptimal	4 x carbo/taxol	2 x carbo/taxol	21	28
185	07/01/2013	58	4	HGSC	500	IDS	Complete	4 x carbo/taxol	2 x carbo/taxol	10	13
186	09/01/2013	47	3C	HGSC	74	Primary	Complete	NA	6 x carbo/taxol	7	9
187	10/01/2013	71	3C	HGSC	2013	Primary	Optimal	NA	6 x carbo/taxol	12	20
190	28/01/2013	75	3C	Mucinous	135	Primary	Complete	NA	6 x carbo/taxol	9	11
191	31/01/2013	75	3C	HGSC	346	Primary	Optimal	NA	6x carbo/taxol	12	16
192	06/02/2013	66	3C	Endometrioid/Clear	2425	Primary	Optimal	NA	3 x carbo/taxol	4	7
194	25/02/2013	59	NA	Adenocarcinoma (enteric type) in mature teratoma	1000	Primary	Suboptimal	NA	NA	2	2
197	06/03/2013	63	3C	HGSC	2000	primary	Optimal	NA	6 x carboplatin	21	21
199	09/12/1949	63	3C	HGSC	69	primary	Complete	NA	NA	26	66
200	20/03/2013	59	3C	HGSC	602	IDS	Optimal	4 x carbo/taxol	2 x carbo/taxol	10	20
201	20/03/2013	55	3C	HGSC	678	primary	Optimal	NA	6 x carbo/taxol; tamoxifen; rucaparib	10	36
202	27/03/2013	52	3C	HGSC	1352	IDS	Optimal	ICON8	3 x carbo/taxol	23	25
205	15/04/2013	67	1C	Clear	203	Primary	Complete	NA	6 x carbo/taxol	12	18
209	26/04/2013	52	3C	HGSC	419	Primary	Optimal	4 x carbo/taxol	2 x carbo/taxol	5	9
210	04/05/2013	63	3C	HGSC	420	Primary	Optimal	NA	6 x carbo/taxol	21	21
211	04/05/2013	53	3C	HGSC	869	Primary	Optimal	NA	6 x carbo/taxol	20	20
213	10/05/2013	85	4	HGSC	1295	NA	NA	NA	NA	4	4
217	31/05/2013	81	3C	HGSC	2738	IDS	Optimal	6 x carbo/taxol	NA	5	8
218	31/05/2013	62	3C	HGSC	150	Primary	Optimal	NA	6 x carbo/taxol	35	43
219	03/06/2013	60	3C	HGSC	1445	IDS	Optimal	4 x carbo/taxol	2 x carboplatin	4	13
221	05/06/2013	72	2C	Carcinosarcoma	1000	IDS	Optimal	4 x carbo/taxol	2 x carbo/taxol	14	21
222	07/06/2013	47	3C	HGSC	6	IDS	optimal	4 x carbo/taxol	2 x carbo/taxol	13	25
223	05/07/2013	43	3C	HGSC	2074	Primary	Optimal	NA	3 x carbo/taxol	17	17

224	12/07/2013	70	3C	HGSC	325	Primary	optimal	NA	5 x carbo/taxol	8	9
225	15/07/2013	48	3C	HGSC	2852	Primary	Optimal	NA	6 x carbo/taxol; bevacizumab	8	15
226	24/07/2013	83	3C	Low grade serous	1964	Primary	Optimal	NA	Tamoxifen	3	9
227	26/07/2013	63	3C	HGSC	8430	Primary	Suboptimal	NA	6 x carbo/taxol	16	16
228	12/08/2013	59	4	HGSC	2349	Primary	Optimal	NA	6 x carbo/taxol	12	15
229	11/09/2013	71	4	HGSC	6521	Primary	Optimal	NA	2 x carbo/taxol; 4 x carboplatin	13	14
230	11/09/2013	41	3C	HGSC/Clear cell	1743	Primary	Optimal	NA	6 x carbo/taxol	11	14
231	01/10/2013	69	3C	HGSC	388	NA	NA	6 x carbo/taxol	NA	11	13
233	02/10/2013	69	4	HGSC	8407	IDS	Suboptimal	6 x carbo/taxol	NA	13	14
234	02/10/2013	60	3C	HGSC	1252	IDS	Optimal	4 x carbo/taxol	2 x carboplatin	4	13
238	25/10/2013	76	3C	HGSC	1317	IDS	Suboptimal	4 x carbo/taxol	2 x carbo/taxol; bevacizumab	15	15
239	25/10/2013	77	3C	HGSC	4361	NA	NA	no chemo (too frail)	NA	1	1

PCO	Morphology	Antigen Characterisation (Immuofluorescent panel)						FFPE IHC	Doubling time	HR	BER	GI50 (SRB proliferation assay)			% Survival at * (SRB proliferation assay)		
		CK	EpCAM	CA125	MOC31	D240	Vimentin	CA125	(hrs)	(Rad51)	(8-OHdG)	Rucaparib (µM)	CNDAC (µM)	Cisplatin (µM)	Rucaparib (*100µM)	CNDAC (*100µM)	Cisplatin (*10µM)
221	Mes	+	+	-	-	-	+	-	105.0	Comp	50.54	26.6	>100	>10	37.4	54.9	67.8
231	Cob	+	-	-	-	-	+	+		Comp	34.16	17.6	>100	>10	31.4	83.3	91.8
184	Mes	+	+	+	+	-	+	+	280.5	Comp	34.16	60.3	>100	>10	25.8	58.4	60.2
230	Cob	+	-	-	-	-	+	+	65.1	Comp	18.07	34.6	>100	7.8	35.7	96.0	45.6
229	Cob	+	-	-	-	-	+	ND	80.6	Comp	14.44	>100	>100	8.8	56.3	94.2	47.3
187	Cob	+	+	+	+	-	+	ND	153.1	Comp	10.62	21.7	>100	8.4	22.3	61.0	42.9
154	Cob	+	-	+	-	-	+	ND	93.3	Comp	8.50	>100	>100	>10	55.7	55.9	49.4
170	Cob	+	-	+	-	-	+	+	211.2	Comp	7.83	53.1	>100	>10	23.2	63.5	48.6
209	Cob	+	-	+	-	-	+	+	148.4	Comp	5.40	>100	2.5	>10	63.4	20.3	76.7
202	Cob	+	-	-	-	-	+	+	87.5	Comp	3.63	0.0	0.6	>10	86.7	13.4	105.5
142	Cob	+	+	+	ND	ND	ND	ND	130.2	Comp	3.42	14.3	>100	0.6	34.4	79.1	10.7
175	Cob	+	-	+	+	-	+	ND	91.3	Comp	3.20	45.5	42.8	>10	45.0	45.0	53.8
177	Mes	+	patchy	+	+	-	+	ND	112.6	Comp	3.15	>100	>100	>10	64.9	72.4	72.4
181	Cob	+	-	-	ND	-	+	+	111.4	Comp	3.13	>100	>100	>10	59.8	61.6	93.1
186	Cob	+	-	+	-	-	+	ND	ND	Comp	3.13	ND	ND	>10	ND	ND	79.1
185	Cob	+	+	+	+	-	+	ND	ND	Comp	3.00	ND	ND	>10	ND	ND	86.4
182	Cob	+	+	+	+	-	+	+	125.8	Comp	2.98	>100	42.9	4.7	55.5	48.4	41.1
225	Cob	+	-	-	-	-	+	+	123.6	Comp	2.92	10.3	>100	>10	32.9	58.9	42.0
139	Mes	+	ND	ND	ND	ND	ND	ND	ND	Comp	2.88	73.4	11.6	6.6	38.9	29.2	49.6
157	Cob	+	ND	+	ND	ND	ND	ND	310.7	Comp	2.87	>100	>100	>10	61.3	91.1	74.0
138	Mes	+	-	-	ND	ND	ND	+	ND	Comp	2.68	5.5	37.2	>10	34.4	46.7	53.8
192	Cob	+	-	patchy	-	-	+	+	232.4	Comp	2.62	>100	>100	>10	102.1	67.3	98.0
224	Cob	+	-	patchy	-	-	+	ND	90.3	Comp	2.52	7.8	>100	8.0	20.6	61.9	38.0
194	Cob	+	-	patchy	-	-	+	-	79.3	Comp	2.13	12.6	>100	>10	24.7	73.7	53.2
174	Cob	+	-	+	-	-	+	-	35.0	Comp	2.05	>100	>100	>10	58.6	70.0	75.6
167	Cob	+	ND	-	ND	ND	+	-	115.7	Comp	1.89	>100	>100	4.6	76.3	74.0	36.6
180	Cob	+	-	+	-	-	+	+	206.9	Comp	1.61	>100	>100	>10	116.0	92.1	109.7
169	Cob	+	-	-	ND	-	+	+	111.4	Comp	1.61	>100	>100	>10	59.8	61.6	93.1
168	Mes	+	-	+	ND	ND	+	ND	127.7	Comp	1.61	>100	30.3	>10	46.7	38.6	71.1
227	Cob	+	-	patchy	-	-	+	+	131.1	Def	11.18	72.4	8.7	2.1	49.8	27.2	35.4
210	Cob	+	-	-	-	-	+	+	135.0	Def	10.91	84.2	6.8	>10	48.2	12.8	53.5
222	Cob	+	+	patchy	+	-	+	ND	268.5	Def	7.23	14.6	28.3	0.6	42.1	45.0	26.2
226	Cob	+	-	patchy	patchy	-	+	ND	160.5	Def	4.25	14.6	28.3	2.3	42.1	45.0	31.9
144	Cob	+	-	+	-	-	+	+		Def	3.46	58.9	34.9	3.6	42.1	38.5	36.1
211	Cob	+	-	patchy	-	-	+	ND	97.6	Def	3.43	>100	>100	9.9	62.2	61.0	50.6
219	Cob	+	-	+	-	-	+	+	83.0	Def	2.85	2.2	14.4	4.6	21.6	24.1	35.7
197	Cob	+	-	-	-	-	+	+	95.3	Def	2.79	>100	53.9	>10	50.9	45.0	57.7
191	Cob	+	+	+	+	-	+	+	277.9	Def	2.71	26.4	27.8	3.4	43.9	46.8	48.8
213	Cob	+	-	-	-	-	+	ND	98.2	Def	2.70	2.4	58.2	6.0	28.4	44.5	45.1
183	Mes	+	-	+	-	-	+	+	193.6	Def	2.43	10.9	18.5	>10	33.7	34.8	51.0

179	Mes	+	+	+	+	-	+	+	134.3	Def	2.16	14.6	>100	>10	42.1	53.6	61.7
190	Cob	+	-	patchy	-	-	+	-	112.5	Def	2.12	35.0	1.5	3.2	40.1	17.9	34.0
234	Mes	+	+	-	-	-	+	+	196.8	Comp	ND	>100	>100	>10	90.2	96.3	94.1
199	Cob	+	-	patchy	-	-	+	ND	486.7	Comp	ND	>100	>100	>10	82.9	103.6	106.2
233	Cob	+	-	-	-	-	+	ND	303.1	Comp	ND	>100	>100	>10	81.3	73.6	67.5
171	Cob	+	-	+	ND	ND	ND	ND	273.7	Comp	ND	>100	>100	>10	77.7	63.5	60.3
201	Cob	+	-	-	+	-	+	ND	272.8	Comp	ND	>100	>100	>10	63.1	67.3	96.7
205	Cob	+	pathy	+	-	-	+	ND	118.5	Comp	ND	>100	12.8	>10	55.8	34.3	61.7
162	Cob	+	ND	+	ND	ND	ND	ND	ND	Comp	ND	52.6	ND	ND	33.6	ND	ND
163	Mes	+	ND	+	ND	ND	ND	ND	ND	Comp	ND	27.5	ND	ND	30.2	ND	ND
239	Cob	+	-	-	-	-	+	+	200.7	Comp	ND	24.6	>100	>10	29.8	55.1	82.9
238	Cob	+	-	patchy	-	-	+	ND	110.9	Def	ND	78.7	>100	>10	45.8	86.4	93.0
143	Cob	+	-	-	ND	ND	ND	+	87.5	Def	ND	72.3	39.0	9.1	38.5	42.5	47.6
158	Cob	+	ND	+	ND	ND	ND	+	148.7	Def	ND	13.4	>100	>10	38.3	97.3	84.5
223	Cob	+	-	patchy	-	-	+	+	129.3	Def	ND	1.3	>100	>10	37.1	59.3	67.5
217	Cob	+	-	+	-	-	+	ND	178.3	Def	ND	47.1	13.6	0.9	36.2	26.9	32.4
200	Cob	+	+	+	+	-	+	+	312.4	Def	ND	0.4	0.5	1.4	34.5	23.9	46.2
218	Cob	+	+	patchy	+	-	+	+	284.2	Def	ND	1.2	1.5	0.2	33.8	29.4	24.3
156	Mes	+	-	+	+	-	+	+	168.7	Def	ND	11.1	44.2	1.9	33.7	45.0	34.8
228	Mes	+	-	+	+	-	+	ND	168.7	Def	ND	10.9	18.5	2.8	33.7	34.8	27.3
155	Cob	+	-	-	-	-	-	-	ND	Def	ND	0.0	ND	ND	21.5	ND	ND

Morphology: Cob = cobblestone; Mes = mesenchymal. ND = Not done. GI50 and % survival determined by SRB cell proliferation assays. PCO cultures are ordered by HR status (HRC = Red; HRD= Blue), then by BER status (BERC = Orange; BERD = Pale blue), then by sensitivity to rucaparib, CNDAC and cisplatin (Resistant = hatched red, sensitive = hatched green).

Appendix 7: Solid Tumour Case Series

PCO	Age (years)	CA125 (U/L)	Histological subtype	FIGO Stage	Surgery		Sample timing (pre-post chemo)	NACT	Post-op chemotherapy	PFS	OS
					Primary / IDS	Debulking outcome				(months)	
155	55	117	Adenocarcinoma	3C	Primary	Optimal	Pre	NA	FOLFOX	15	18
156	49	1320	HGSC	4	IDS	Optimal	Post	4 carboplatin	1 carboplatin	5	8
157	58	500	HGSC	3C	Primary	Suboptimal	Pre	NA	6 carboplatin, tamoxifen	10	12
158	68	780	HGSC	3C	Primary	Optimal	Pre	NA	6 carboplatin	(>22)	(>22)
162	68	186	HGSC	3C	Primary	Optimal	Pre	NA	6 carboplatin	(>21)	(>21)
163	77	500	HGSC	3C	Primary	Optimal	Pre	NA	5 carboplatin	13	(>20)
167	63	600	Neuroendocrine	3C	Primary	Optimal	Pre	NA	Cisplatin, etoposide	6	7
168	66	1500	HGSC	3C	Primary	Complete	Pre	NA	6 carboplatin	14	(>15)
174	45	552	Endometrioid	3A	Primary	Complete	Pre	NA	6 carboplatin, 2 paclitaxel, 4 docetaxel	(>16)	(>16)
175	66	250	Clear cell	3B	Primary	Optimal	Pre	NA	5 carboplatin	5	8
179	66	57	HGSC	4	IDS	Optimal	Post	4 carboplatin	2 carboplatin	8	(>14)
180	50	521	HGSC	3C	IDS	Optimal	Post	3 carboplatin	3 carboplatin	8	(>9)
181	72	176	HGSC	3C	IDS	Optimal	Post	3 carboplatin	3 carboplatin	5	7
183	82	6388	HGSC	2C	Primary	Complete	Pre	NA	4 carboplatin	(>13)	(>13)
184	73	9740	HGSC	4	IDS	Suboptimal	Post	4 carboplatin	2 carboplatin	(>16)	(>16)
185	58	500	HGSC	4	IDS	Complete	Post	4 carboplatin	2 carboplatin	(>9)	(>9)
186	47	74	HGSC	3C	Primary	Complete	Pre	NA	6 carboplatin	(>9)	(>9)
192	66	2425	Clear cell	3C	Primary	Optimal	Pre	NA	3 carboplatin	4	7
200	59	602	HGSC	3C	IDS	Optimal	Post	4 carboplatin	2 carboplatin	(>6)	(>6)
201	55	678	HGSC	3C	Primary**	Optimal	Pre	NA	6 carboplatin, tamoxifen, rucaparib	11	36
209	52	419	HGSC	3C	IDS*	Optimal	Post	4 carboplatin	2 carboplatin	(>7)	(>7)
217	81	2738	HGSC	3C	No surgery		Post	3 carboplatin	6 carboplatin	(>7)	(>7)
223	43	2074	HGSC	3C	Primary	Optimal	Pre	NA	3 carboplatin	(>6)	(>6)
226	83	1964	Low grade serous	3C	Primary	Optimal	Pre	NA	Tamoxifen	(>6)	(>6)
228	59	2349	HGSC	4	Primary	Optimal	Pre	NA	6 carboplatin	(>6)	(>6)

Appendix 8: CTC Method Development

Sample preparation methods were evaluated by assessing uniformity and consistency of fluorochrome staining for both cell surface and intracellular antigens in comparison to parallel experiments using traditional fixed cell immunofluorescent microscopy.

CA125 Antibody Fluorochrome Conjugation

The APEX™ antibody labelling kit was used to covalently bind AlexaFluor-594 to anti-CA125 antibody, as per manufacturer's instructions (Life Technologies, 2013). Briefly, the hydrated resin filled APEX tip was incubated for 2 hours with 10 µg of IgG CA125 antibody and 10 µl of fluorochrome dye solution before washing twice with 50 µl wash buffer. Conjugated antibody was eluted with 40 µl elution buffer and stored with 10 µl neutralisation buffer at -20 °C. Uniformity and intensity of antigen detection, using conjugated CA125 antibody, was compared to a 2-step process using traditional immunofluorescent microscopy and ImageStream cell suspensions. Consistent results (n = 5) were seen and the method adopted for all ImageStream characterisation.

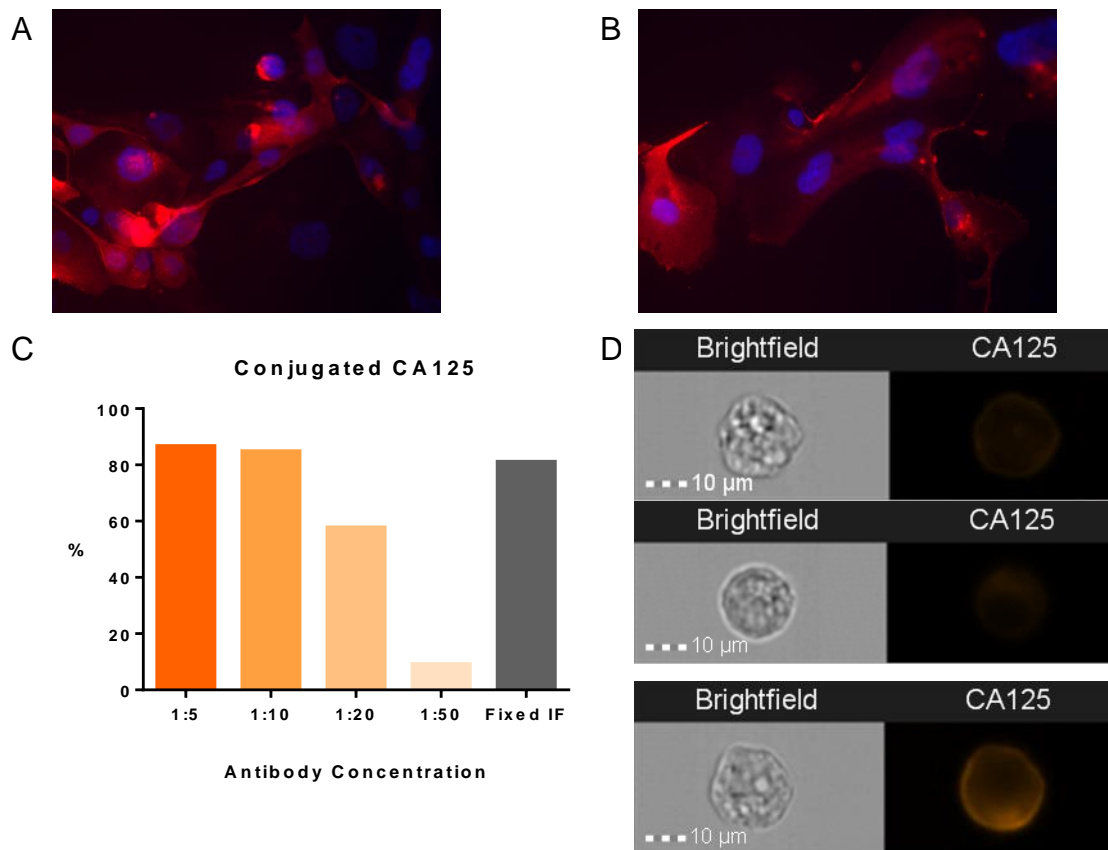


Figure 9.1 – 1: CA125 conjugation validation. A: Immunofluorescent microscopy showing PCO 142 stained with anti-CA125 conjugated with AF594. B: PCO 142 stained with anti-CA125 and secondary AF594 in a 2-step process. C: ImageStream assessment of % of OVCAR 3 cells with detected expression of CA125 using conjugated CA125 at variable concentrations as indicated. D: ImageStream images of OVCAR 3 cells using 1:10, 1:20 and 1:50 concentration.

Fixation and Permeabilisation

OVCAR3 cells were trypsinised and PBS washed prior to fixation. All cells were permeabilised with BD Phosflow Perm/Wash Buffer I for 12 hours before incubating with EpCAM, CK, CA125 and DRAQ 5 antibodies for 12 hours. Five fixatives were investigated, Table 9.1 - 1. Methanol fixation resulted in consistent detection of both surface and intracellular antigens and was adopted for use in cell line experiments. Comparable results were achieved with BD Phosflow Lyse/Fix Buffer and this was adopted for use in blood sample processing due to simultaneous fixation and lysis of RBC.

Fixative	Method	Results
Methanol	2 ml 100% methanol at -20 °C for 20 minutes	Preservation of cell morphology, surface, intracellular and nuclear antigens. Good cell recovery.
Paraformaldehyde	2 ml 0.4% at 4 °C for 20 minutes	Preservation of cell morphology, surface and internal antigens as well as good cell recovery.
BD Phosflow Lyse/Fix buffer	1:20 (2 ml PBS: 40 ml buffer) at 37 °C for 15 minutes	Preservation of cell morphology, surface and internal antigens as well as good cell recovery. Simultaneous red cell lysis.
Acetone	2 ml 80% at -20 °C for 20 minutes	Shrinking effect with distortion of cellular morphology.
Acetone/Methanol	2 ml v:v at 4 °C	Shrinking effect with distortion of cellular morphology.

Table 9.1 - 1: Optimisation of cell suspension fixation.

Nuclear Foci Mask Optimisation

Mask optimisation was undertaken by manual adjustment of mask features and visual confirmation of correct outlining the fluorescence antigen of interest, Table 9.2 - 1. Two reviewers independently ranked 5 mask options and three were selected for further assessment. The method for accurate quantification of foci using IDEAS Software was optimised by counting γ H2AX foci in a series of OSEC2 cells, fixed at varying times, following induction of DSB by irradiation. Using the various nuclear mask and spot count functions, ImageStream counts were compared to counts obtained in parallel samples assessed with conventional IF microscopy, counted with ImageJ Software and to a series counted manually, Figure 9.2 - 1.

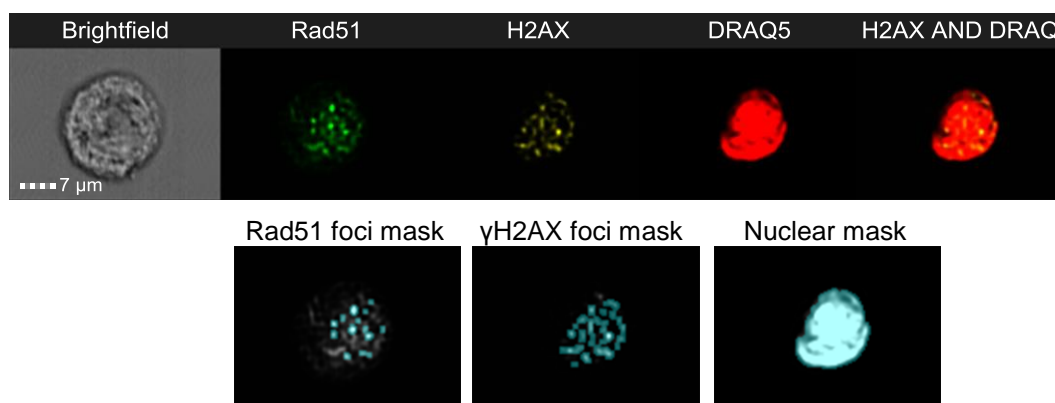


Figure 9.2 - 1: HR assay optimisation of nuclear, γ H2AX and Rad51 foci masks DRAQ5 and γ H2AX antibody labelling on an OSEC2 cell and their respective optimised masks.

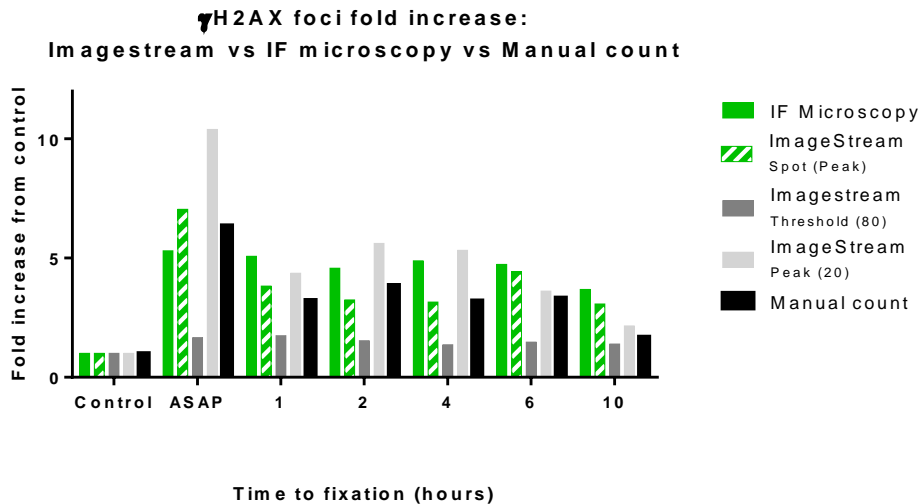


Figure 9.3 - 1: γ H2AX focus dose response comparing three ImageStream masks with traditional immunofluorescent microscopy and manual counting. Fold increase of mean γ H2AX focus count in OSEC2 cells, fixed at various time points following induction of DS DNA with 2 Gy irradiation, in comparison to control. The results are from parallel experiments comparing traditional IF microscopy to ImageStream.

Foci Count Method	ImageStream settings	Correlation with IF count	
		r	p
Spot (Peak)	Spot Count [Peak(M03,Ch03, Bright, 50)]	0.7738	0.0142*
Threshold (80)	Threshold(M03, Ch03, 80)	0.8947	0.0065**
Peak (20)	Peak(M03,Ch03, Bright 50)	0.7127	0.0722
Spot (5.5:1)	Spot(M03,Ch03,Bright 5.5,1)	0.5298	0.2213
Manual Count	NA	0.7616	0.0466*

Table 9.2 - 1: Imagestream IDEAS settings for Rad51 foci HR assay.

Positive correlation was seen between the fold increases from control between conventional IF results and results using ImageStream Spot (Peak) and Threshold functions. Additionally, Spot (Peak) function gave the most accurate outline of actual foci confirmed visually and was used as the optimum mask for γ H2AX foci quantification and these settings used for the analysis of all further experimental samples.

The same analysis was repeated for Rad51 foci and Spot Count [Peak(Ch02, Bright, 50)] used for further analysis.

Data Analysis

A population of single focused cells was gated for further analysis before creating a nuclear mask based upon intensity of DRAQ5 nuclear stain [Fill(Intensity(M11, Ch11, 400-4095))]. This was combined with a peak intensity mask [γ H2AX: Peak(Ch03, Bright, 20) or Rad51: [Peak(Ch02, Bright, 50)] to identify the foci and combined with the Spot function used to quantify foci. The mean Spot Count was used to calculate the fold-increase between the irradiated and control samples.

Dose Response Curve

To further validate ImageStream assessed focus count, a series of OVCAR3 cells were irradiated at varying doses of IR and γ H2AX focus quantified. Mean foci count per cell assessed using ImageStream was compared with mean foci count per cell counted using ImageJ and IF. Poor correlation was seen and this lack of correlation of actual focus count between the two methods is in keeping with previous published work (Bourton 2012). Alternative methodologies for quantification of foci were explored. The change in proportion of cells counted with mean foci counts above a threshold level of 5, 10 or 15 foci per cell from control was compared to traditional IF and strong correlation seen between ImageStream assessment of the proportion of cells foci count >15 and traditional counting methods using ImageJ, $r = 0.9094$, $p < 0.0001$. This counting method was adopted for further experiments.

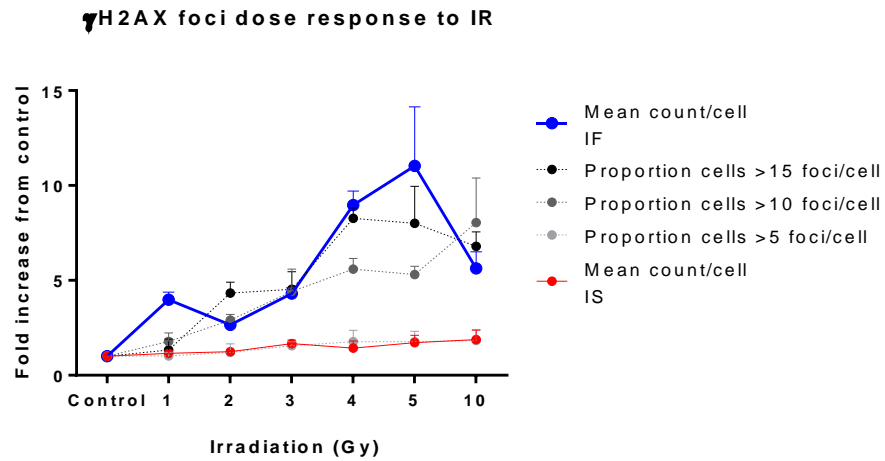


Figure 9.4 - 1: γ H2AX foci following irradiation at different doses. Assessment of count using ImageStream.

Method Optimisation in PCO

When applied to cell suspensions of trypsinised PCO cultures, the method described for HR assessment above resulted in poor intra-nucleic permeabilisation and non-specific cytoplasmic staining. Numerous optimisation steps were undertaken, Figure 9.5 - 1.

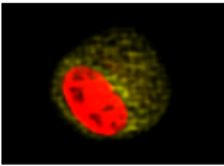
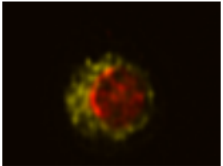
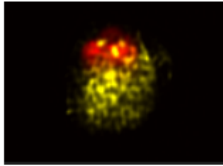
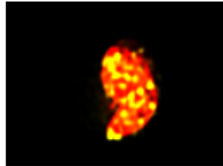
	Optimisation Steps			
	1	2	3	4
Composite images of DRAQ5 and γ H2AX				
Fixative	PFA	Methanol	Methanol	Methanol
Permeabilisation	Saponin	Saponin	0.1% Triton X-100	0.1% Triton X-100
Blocking Buffer	No	No	No	Yes
Washes	No	No	No	3 x15 minutes washes KCM wash buffer
Results	No intra-nuclear foci identified	Improvement in permeabilisation not obvious	Intra-nuclear foci identified but non-specific binding present	The majority of non-specific binding eliminated

Figure 9.5 - 1: HR method optimisation in PCO cultures. Demonstrating the experiments undertaken to optimise the protocol for the identification of γ H2AX foci in PCO cultures using ImageStream. Cells were irradiated at 2 Gy and labelled with γ H2AX and DRAQ5 antibodies. The optimisation steps made in each experiment are highlighted in red.

References

- Abbruzzese, J. L., Grunewald, R., Weeks, E. A., Gravel, D., Adams, T., Nowak, B., Mineishi, S., Tarassoff, P., Satterlee, W., Raber, M. N., et al., (1991). "A phase I clinical, plasma, and cellular pharmacology study of gemcitabine." J Clin Oncol **9**(3): 491-498.
- Abkevich, V., Timms, K. M., Hennessy, B. T., Potter, J., Carey, M. S., Meyer, L. A., Smith-McCune, K., Broaddus, R., Lu, K. H., Chen, J., Tran, T. V., Williams, D., Iliev, D., Jammulapati, S., FitzGerald, L. M., Krivak, T., DeLoia, J. A., Gutin, A., Mills, G. B., Lanchbury, J. S. (2012). "Patterns of genomic loss of heterozygosity predict homologous recombination repair defects in epithelial ovarian cancer." Br J Cancer **107**(10): 1776-1782.
- Abraham, R. T. (2001). "Cell cycle checkpoint signaling through the ATM and ATR kinases." Genes Dev **15**(17): 2177-2196.
- Abramoff, M., Magelhaes, P., Ram, S. (2004). "Image processing with ImageJ." Biophoton Int **11**: 36-42.
- Acharya, S., Wilson, T., Gradia, S., Kane, M. F., Guerrette, S., Marsischky, G. T., Kolodner, R., Fishel, R. (1996). "hMSH2 forms specific mismatch-binding complexes with hMSH3 and hMSH6." Proc Natl Acad Sci U S A **93**(24): 13629-13634.
- Adams, D. L., Martin, S. S., Alpaugh, R. K., Charpentier, M., Tsai, S., Bergan, R. C., Ogden, I. M., Catalona, W., Chumsri, S., Tang, C. M., Cristofanilli, M. (2014). "Circulating giant macrophages as a potential biomarker of solid tumors." Proc Natl Acad Sci U S A **111**(9): 3514-3519.
- Aebi, S., Kurdi-Haidar, B., Gordon, R., Cenni, B., Zheng, H., Fink, D., Christen, R. D., Boland, C. R., Koi, M., Fishel, R., Howell, S. B. (1996). "Loss of DNA mismatch repair in acquired resistance to cisplatin." Cancer Res **56**(13): 3087-3090.
- Agarwal, R. and S. B. Kaye (2005). "Prognostic factors in ovarian cancer: how close are we to a complete picture?" Ann Oncol **16**(1): 4-6.
- Aghajanian, C., Blank, S. V., Goff, B. A., Judson, P. L., Teneriello, M. G., Husain, A., Sovak, M. A., Yi, J., Nycum, L. R. (2012). "OCEANS: a randomized, double-blind, placebo-controlled phase III trial of chemotherapy with or without bevacizumab in patients with platinum-sensitive recurrent epithelial ovarian, primary peritoneal, or fallopian tube cancer." J Clin Oncol **30**(17): 2039-2045.
- Ahmed, A. A., Becker, C. M., Bast, R. C., Jr. (2012). "The origin of ovarian cancer." BJOG **119**(2): 134-136.
- Ahmed, A. A., Etemadmoghadam, D., Temple, J., Lynch, A. G., Riad, M., Sharma, R., Stewart, C., Fereday, S., Caldas, C., Defazio, A., Bowtell, D., Brenton, J. D. (2010). "Driver mutations in TP53 are ubiquitous in high grade serous carcinoma of the ovary." J Pathol **221**(1): 49-56.
- Aktas, B., Tewes, M., Fehm, T., Hauch, S., Kimmig, R., Kasimir-Bauer, S. (2009). "Stem cell and epithelial-mesenchymal transition markers are frequently overexpressed in circulating tumor cells of metastatic breast cancer patients." Breast Cancer Res **11**(4): R46.
- Al-Attar, A., L. Gossage, K. R. Fareed, M. Shehata, M. Mohammed, A. M. Zaitoun, I. Soomro, D. N. Lobo, R. Abbotts, S. Chan and S. Madhusudan (2010). "Human

- apurinic/aprimidinic endonuclease (APE1) is a prognostic factor in ovarian, gastro-oesophageal and pancreato-biliary cancers." Br J Cancer **102**(4): 704-709.
- Al Rawahi, T., Lopes, A. D., Bristow, R. E., Bryant, A., Elattar, A., Chattopadhyay, S., Galaal, K. (2013). "Surgical cytoreduction for recurrent epithelial ovarian cancer." Cochrane Database Syst Rev **2**: CD008765.
- Alix-Panabieres, C., Vendrell, J. P., Pelle, O., Rebillard, X., Riethdorf, S., Muller, V., Fabbro, M., Pantel, K. (2007). "Detection and characterization of putative metastatic precursor cells in cancer patients." Clin Chem **53**(3): 537-539.
- Alizadeh, A. A., Ross, D. T., Perou, C. M., van de Rijn, M. (2001). "Towards a novel classification of human malignancies based on gene expression patterns." J Pathol **195**(1): 41-52.
- Allan, A. L., Keeney, M. (2010). "Circulating tumor cell analysis: technical and statistical considerations for application to the clinic." J Oncol **2010**: 426218.
- Allard, W. J., Matera, J., Miller, M. C., Repollet, M., Connelly, M. C., Rao, C. and A. G. Tibbe, Uhr, J. W., Terstappen, L. W. (2004). "Tumor cells circulate in the peripheral blood of all major carcinomas but not in healthy subjects or patients with nonmalignant diseases." Clin Cancer Res **10**(20): 6897-6904.
- Almeida, K. H., Sobol, R. W. (2007). "A unified view of base excision repair: lesion-dependent protein complexes regulated by post-translational modification." DNA Repair (Amst) **6**(6): 695-711.
- Althaus, F. R., Hofferer, L., Kleczkowska, H. E., Malanga, M., Naegeli, H., Panzeter, P., Realini, C. (1993). "Histone shuttle driven by the automodification cycle of poly(ADP-ribose)polymerase." Environ Mol Mutagen **22**(4): 278-282.
- Alunni-Fabbroni, M., Sandri, M. T. (2010). "Circulating tumour cells in clinical practice: Methods of detection and possible characterization." Methods **50**(4): 289-297.
- Alvarez, A. A., Krigman, H. R., Whitaker, R. S., Dodge, R. K., Rodriguez, G. C. (1999). "The prognostic significance of angiogenesis in epithelial ovarian carcinoma." Clin Cancer Res **5**(3): 587-591.
- Anacleto, C., Leopoldino, A. M., Rossi, B., Soares, F. A., Lopes, A., Rocha, J. C., Caballero, O., Camargo, A. A., Simpson, A. J., Pena, S. D. (2005). "Colorectal cancer "methylator phenotype": fact or artifact?" Neoplasia **7**(4): 331-335.
- Anglesio, M. S., Kommoss, S., Tolcher, M. C., Clarke, B., Galletta, L., Porter, H., Damaraju, S., Fereday, S., Winterhoff, B. J., Kalloger, S. E., Senz, J., Yang, W. N., Steed, H., Allo, G., Ferguson, S., Shaw, P., Teoman, A., Garcia, J. J., Schoolmeester, J. K., Bakkum-Gamez, J., Tinker, A. V., Bowtell, D. D., Huntsman, D. G., Gilks, C. B., McAlpine, J. N. (2013). "Molecular characterization of mucinous ovarian tumours supports a stratified treatment approach with HER2 targeting in 19% of carcinomas." Journal of Pathology **229**(1): 111-120.
- Anthoney, D. A., McIlwrath, A. J., Gallagher, W. M., Edlin, A. R., Brown, R. (1996). "Microsatellite instability, apoptosis, and loss of p53 function in drug-resistant tumor cells." Cancer Res **56**(6): 1374-1381.
- Antonia, S. J., Mirza, N., Fricke, I., Chiappori, A., Thompson, P., Williams, N., Bepler, G., Simon, G., Janssen, W., Lee, J. H., Menander, K., Chada, S., Gabrilovich, D. I. (2006). "Combination of p53 cancer vaccine with chemotherapy in patients with extensive stage small cell lung cancer." Clin Cancer Res **12**(3 Pt 1): 878-887.

- Arias-Lopez, C., Lazaro-Trueba, I., Kerr, P., Lord, C. J., Dexter, T., Iravani, M., Ashworth, A., Silva, A. (2006). "p53 modulates homologous recombination by transcriptional regulation of the RAD51 gene." EMBO Rep **7**(2): 219-224.
- Ashworth, A. (1869). "A case of cancer in which cells similar to those in the tumours were seen in the blood after death." Aus Med J(14): 146-149.
- Audeh, M. W., Carmichael, J., Penson, R. T., Friedlander, M., Powell, B., Bell-McGuinn, K. M., Scott, C., Weitzel, J. N., Oaknin, A., Loman, N., Lu, K., Schmutzler, R. K., Matulonis, U., Wickens, M., Tutt, A. (2010). "Oral poly(ADP-ribose) polymerase inhibitor olaparib in patients with BRCA1 or BRCA2 mutations and recurrent ovarian cancer: a proof-of-concept trial." Lancet **376**(9737): 245-251.
- Auer, B., Nagl, U., Herzog, H., Schneider, R., Schweiger, M. (1989). "Human nuclear NAD⁺ ADP-ribosyltransferase(polymerizing): organization of the gene." DNA **8**(8): 575-580.
- Auersperg, N., Siemens, C.H., Myrdal, S.E. (1984). "Human ovarian surface epithelium in primary culture." In Vitro **20**(10): 743-755.
- Auersperg, N., Wong, S.T., Choi, K.C., Yang, S.K., Leung, P.C.K., (2001). "Ovarian surface epithelium: biology, endocrinology and pathology." Endocrine Reviews **22**(2): 255-288.
- Ayoub, N., Rajendra, E., Su, X., Jeyasekharan, A. D., Mahen, R., Venkitaraman, A. R. (2009). "The carboxyl terminus of Brca2 links the disassembly of Rad51 complexes to mitotic entry." Curr Biol **19**(13): 1075-1085.
- Azuma, A., P. Huang, A. Matsuda and W. Plunkett (2001). "2'-C-cyano-2'-deoxy-1-beta-D-arabino-pentofuranosylcytosine: a novel anticancer nucleoside analog that causes both DNA strand breaks and G(2) arrest." Mol Pharmacol **59**(4): 725-731.
- Azuma, A., P. Huang, A. Matsuda and W. Plunkett (2001). "Cellular pharmacokinetics and pharmacodynamics of the deoxycytidine analog 2'-C-cyano-2'-deoxy-1-beta-D-arabino-pentofuranosylcytosine (CNDAC)." Biochem Pharmacol **61**(12): 1497-1507.
- Baldwin, S. A., Mackey, J. R., Cass, C. E., Young, J. D. (1999). "Nucleoside transporters: molecular biology and implications for therapeutic development." Mol Med Today **5**(5): 216-224.
- Bamias, A., Sotiropoulou, M., Zagouri, F., Trachana, P., Sakellariou, K., Kostouros, E., Kakoyianni, K., Rodolakis, A., Vlahos, G., Haidopoulos, D., Thomakos, N., Antsaklis, A., Dimopoulos, M. A. (2011). "Prognostic evaluation of tumour type and other histopathological characteristics in advanced epithelial ovarian cancer, treated with surgery and paclitaxel/carboplatin chemotherapy: Cell type is the most useful prognostic factor." Eur J Cancer.
- Banasik, M., Komura, H., Shimoyama, M., Ueda, K. (1992). "Specific inhibitors of poly(ADP-ribose) synthetase and mono(ADP-ribosyl)transferase." J Biol Chem **267**(3): 1569-1575.
- Barak, V., Goike, H., Panaretakis, K. W., Einarsson, R. (2004). "Clinical utility of cytokeratins as tumor markers." Clin Biochem **37**(7): 529-540.
- Barretina, J., Caponigro, G., Stransky, N., Venkatesan, K., Garraway, L. A. (2012). "The Cancer Cell Line Encyclopedia enables predictive modelling of anticancer drug sensitivity." Nature **483**(7391): 603-607.

- Bashashati, A., Ha, G., Tone, A., Ding, J., Huntsman, D. G., McAlpine, J. N., Shah, S. P. (2013). "Distinct evolutionary trajectories of primary high-grade serous ovarian cancers revealed through spatial mutational profiling." J Pathol **231**(1): 21-34.
- Baskaran, R., Wood, L. D., Whitaker, L. L., Canman, C. E., Morgan, S. E., Xu, Y., Barlow, C., Baltimore, D., Wynshaw-Boris, A., Kastan, M. B., Wang, J. Y. (1997). "Ataxia telangiectasia mutant protein activates c-Abl tyrosine kinase in response to ionizing radiation." Nature **387**(6632): 516-519.
- Bast, R. C., Jr., Hennessy, B., Mills, G. B. (2009). "The biology of ovarian cancer: new opportunities for translation." Nat Rev Cancer **9**(6): 415-428.
- Bast, R. C., Jr., Mills, G. B. (2010). "Personalizing therapy for ovarian cancer: BRCAness and beyond." J Clin Oncol **28**(22): 3545-3548.
- Baumann, P., Benson, F. E., West, S. C. (1996). "Human Rad51 protein promotes ATP-dependent homologous pairing and strand transfer reactions in vitro." Cell **87**(4): 757-766.
- Baumann, P., West, S. C. (1998). "Role of the human RAD51 protein in homologous recombination and double-stranded-break repair." Trends Biochem Sci **23**(7): 247-251.
- Baute, J., Depicker, A. (2008). "Base excision repair and its role in maintaining genome stability." Crit Rev Biochem Mol Biol **43**(4): 239-276.
- Bergmann, L., Hirschfield, S., Morris, C., Palmeri, S., Stone, A., Biotherapy Development Association (BDA). (2007). "Progression-free survival as an end-point in clinical trials of biotherapeutic agents." Eur J Cancer **5**(9): 23-28.
- Bernstein, C., Bernstein, H., Payne, C. M., Garewal, H. (2002). "DNA repair/pro-apoptotic dual-role proteins in five major DNA repair pathways: fail-safe protection against carcinogenesis." Mutation Research-Reviews in Mutation Research **511**(2): 145-178.
- Berridge, M. V., Herst, P. M., Tan, A. S. (2005). "Tetrazolium dyes as tools in cell biology: new insights into their cellular reduction." Biotechnol Annu Rev **11**: 127-152.
- Blandino, G., Levine, A. J., Oren, M. (1999). "Mutant p53 gain of function: differential effects of different p53 mutants on resistance of cultured cells to chemotherapy." Oncogene **18**(2): 477-485.
- Boland, C. R., Goel, A. (2010). "Microsatellite instability in colorectal cancer." Gastroenterology **138**(6): 2073-2087 e2073.
- Bonner, W. M., C. E. Redon, J. S. Dickey, A. J. Nakamura, O. A. Sedelnikova, S. Solier and Y. Pommier (2008). "GammaH2AX and cancer." Nat Rev Cancer **8**(12): 957-967.
- Bookman, M. A., Brady, M. F., McGuire, W. P., Harper, P. G., Alberts, D. S., Friedlander, M., Colombo, N., Fowler, J. M., Argenta, P. A., De Geest, K., Mutch, D. G., Burger, R. A., Swart, A. M., Trimble, E. L., Accario-Winslow, C., Roth, L. M. (2009). "Evaluation of new platinum-based treatment regimens in advanced-stage ovarian cancer: a Phase III Trial of the Gynecologic Cancer Intergroup." J Clin Oncol **27**(9): 1419-1425.
- Bookman, M. A., Greer, B. E., Ozols, R. F. (2003). "Optimal therapy of advanced ovarian cancer: carboplatin and paclitaxel versus cisplatin and paclitaxel (GOG158) and an update on GOG0182-ICON5." Int J Gynecol Cancer **13 Suppl 2**: 149-155.

- Bourton, E. C., Plowman, P. N., Zahir, S. A., Senguloglu, G. U., Serrai, H., Bottley, G., Parris, C. N. (2012). "Multispectral imaging flow cytometry reveals distinct frequencies of gamma-H2AX foci induction in DNA double strand break repair defective human cell lines." Cytometry Part A **81A**(2): 130-137.
- Bouwman, P., Aly, A., Escandell, J. M., Pieterse, M., Bartkova, J., van der Gulden, H., Tarsounas, M., Ganesan, S., Jonkers, J. (2010). "53BP1 loss rescues BRCA1 deficiency and is associated with triple-negative and BRCA-mutated breast cancers." Nat Struct Mol Biol **17**(6): 688-695.
- Braun, S., Schindlbeck, C., Hepp, F., Janni, W., Kantenich, C., Riethmuller, G., Pantel, K. (2001). "Occult tumor cells in bone marrow of patients with locoregionally restricted ovarian cancer predict early distant metastatic relapse." J Clin Oncol **19**(2): 368-375.
- Bristow, R. E., Tomacruz, R. S., Armstrong, D. K., Trimble, E. L., Montz, F. J. (2002). "Survival effect of maximal cytoreductive surgery for advanced ovarian carcinoma during the platinum era: a meta-analysis." J Clin Oncol **20**(5): 1248-1259.
- Brown, R., Clugston, C., Burns, P., Edlin, A., Vasey, P., Vojtesek, B., Kaye, S. B. (1993). "Increased accumulation of p53 protein in cisplatin-resistant ovarian cell lines." Int J Cancer **55**(4): 678-684.
- Brown, R., Hirst, G. L., Gallagher, W. M., McIlwrath, A. J., Margison, G. P., van der Zee, A. G., Anthoney, D. A. (1997). "hMLH1 expression and cellular responses of ovarian tumour cells to treatment with cytotoxic anticancer agents." Oncogene **15**(1): 45-52.
- Bryant, H. E., Schultz, N., Thomas, H. D., Parker, K. M., Flower, D., Lopez, E., Kyle, S., Meuth, M., Curtin, N. J., Helleday, T. (2005). "Specific killing of BRCA2-deficient tumours with inhibitors of poly(ADP-ribose) polymerase." Nature **434**(7035): 913-917.
- Budd, G. T., Cristofanilli, M., Ellis, M. J., Stopeck, A., Borden, E., Miller, M. C., Matera, J., Repollet, M., Doyle, G. V., Terstappen, L. W., Hayes, D. F. (2006). "Circulating tumor cells versus imaging--predicting overall survival in metastatic breast cancer." Clin Cancer Res **12**(21): 6403-6409.
- Bugreev, D. V., Mazina, O. M., Mazin, A. V. (2006). "Rad54 protein promotes branch migration of Holliday junctions." Nature **442**(7102): 590-593.
- Buller, R. E., I. B. Runnebaum, B. Y. Karlan, J. A. Horowitz, M. Shahin, T. Buekers, S. Petrauskas, R. Kreienberg, D. Slamon and M. Pegram (2002). "A phase I/II trial of rAd/p53 (SCH 58500) gene replacement in recurrent ovarian cancer." Cancer Gene Ther **9**(7): 553-566.
- Buller, R. E., Shahin, M. S., Holmes, R. W., Hatterman, M., Kirby, P. A., Sood, A. K. (2001). "p53 Mutations and microsatellite instability in ovarian cancer: Yin and yang." Am J Obstet Gynecol **184**(5): 891-902; discussion 902-893.
- Burger, R. A., Brady, M. F., Bookman, M. A., Fleming, G. F., Monk, B. J., Huang, H., Mannel, R. S., Homesley, H. D., Fowler, J., Greer, B. E., Boente, M., Birrer, M. J., Liang, S. X., Gynecologic Oncology, Group (2011). "Incorporation of bevacizumab in the primary treatment of ovarian cancer." N Engl J Med **365**(26): 2473-2483.
- Burger, R. A., Sill, M. W., Monk, B. J., Greer, B. E., Sorosky, J. I. (2007). "Phase II trial of bevacizumab in persistent or recurrent epithelial ovarian cancer or primary peritoneal cancer: a Gynecologic Oncology Group Study." J Clin Oncol **25**(33): 5165-5171.

- Calabrese, C. R., Almassy, R., Barton, S., Batey, M. A., Calvert, A. H., Canan-Koch, S., Wang, L. Z., Webber, S. E., Williams, K. J., Curtin, N. J. (2004). "Anticancer chemosensitization and radiosensitization by the novel poly(ADP-ribose) polymerase-1 inhibitor AG14361." J Natl Cancer Inst **96**(1): 56-67.
- Campbell, P. J., Yachida, S., Mudie, L. J., Stephens, P. J., Pleasance, E. D., Stebbings, L. A., Morsberger, L. A., Latimer, C. and S. McLaren, Lin, M. L., Stratton, M. R., Iacobuzio-Donahue, C., Futreal, P. A. (2010). "The patterns and dynamics of genomic instability in metastatic pancreatic cancer." Nature **467**(7319): 1109-1113.
- Campos, S. M., Humphreys, B.D. (2009). "Safety of Bevacizumab in advanced ovarian and mullerian cancers: a review." Clin Cancer Res.
- Cannistra, S. A., Matulonis, U. A., Penson, R. T., Hambleton, J., Dupont, J., Mackey, H., Douglas, J., Burger, R. A., Armstrong, D., Wenham, R., McGuire, W. (2007). "Phase II study of bevacizumab in patients with platinum-resistant ovarian cancer or peritoneal serous cancer." J Clin Oncol **25**(33): 5180-5186.
- Carreira, A., Hilario, J., Amitani, I., Baskin, R. J., Shivji, M. K., Venkitaraman, A. R., Kowalczykowski, S. C. (2009). "The BRC repeats of BRCA2 modulate the DNA-binding selectivity of RAD51." Cell **136**(6): 1032-1043.
- Celeste, A., Fernandez-Capetillo, O., Kruhlak, M. J., Pilch, D. R., Staudt, D. W., Lee, A., Bonner, R. F., Bonner, W. M., Nussenzweig, A. (2003). "Histone H2AX phosphorylation is dispensable for the initial recognition of DNA breaks." Nat Cell Biol **5**(7): 675-679.
- Cerbinskaite, A., Mukhopadhyay, A., Plummer, E. R., Curtin, N. J., Edmondson, R. J. (2012). "Defective homologous recombination in human cancers." Cancer Treat Rev **38**(2): 89-100.
- Chan, J. K., Hamilton, C. A., Anderson, E. M., Cheung, M. K., Baker, J., Husain, A., Teng, N. N., Kong, C. S., Negrin, R. S. (2007). "A novel technique for the enrichment of primary ovarian cancer cells." Am J Obstet Gynecol **197**(5): 507 e501-505.
- Chapman, J. R., Barral, P., Vannier, J. B., Borel, V., Steger, M., Tomas-Loba, A., Sartori, A. A., Adams, I. R., Batista, F. D., Boulton, S. J. (2013). "RIF1 Is Essential for 53BP1-Dependent Nonhomologous End Joining and Suppression of DNA Double-Strand Break Resection." Molecular Cell **49**(5): 858-871.
- Chapman, J. R., Sossick, A. J., Boulton, S. J., Jackson, S. P. (2012). "BRCA1-associated exclusion of 53BP1 from DNA damage sites underlies temporal control of DNA repair." J Cell Sci **125**(Pt 15): 3529-3534.
- Chen, H. C. and J. L. Guan (1994). "Association of focal adhesion kinase with its potential substrate phosphatidylinositol 3-kinase." Proc Natl Acad Sci U S A **91**(21): 10148-10152.
- Cheng, C. X., Xue, M., Li, K., Li, W. S. (2012). "Predictive value of XRCC1 and XRCC3 gene polymorphisms for risk of ovarian cancer death after chemotherapy." Asian Pac J Cancer Prev **13**(6): 2541-2545.
- Chetrit, A., Hirsh-Yechezkel, G., Ben-David, Y., Lubin, F., Friedman, E., Sadetzki, S. (2008). "Effect of BRCA1/2 mutations on long-term survival of patients with invasive ovarian cancer: the national Israeli study of ovarian cancer." J Clin Oncol **26**(1): 20-25.
- Chi, P., Kwon, Y., Seong, C., Epshtein, A., Lam, I., Sung, P., Klein, H. L. (2006). "Yeast recombination factor Rdh54 functionally interacts with the Rad51

recombinase and catalyzes Rad51 removal from DNA." J Biol Chem **281**(36): 26268-26279.

Chiou, C. C., Chang, P. Y., Chan, E. C., Wu, T. L., Tsao, K. C., Wu, J. T. (2003). "Urinary 8-hydroxydeoxyguanosine and its analogs as DNA marker of oxidative stress: development of an ELISA and measurement in both bladder and prostate cancers." Clin Chim Acta **334**(1-2): 87-94.

Chistiakov, D. A., Voronova, N. V., Chistiakov, P. A. (2008). "Genetic variations in DNA repair genes, radiosensitivity to cancer and susceptibility to acute tissue reactions in radiotherapy-treated cancer patients." Acta Oncol **47**(5): 809-824.

Choi, S. Y., Lin, D., Gout, P. W., Collins, C. C., Xu, Y., Wang, Y. (2014). "Lessons from patient-derived xenografts for better in vitro modeling of human cancer." Adv Drug Deliv Rev **79-80**: 222-237.

Christiansen, J. J., Rajasekaran, A. K. (2006). "Reassessing epithelial to mesenchymal transition as a prerequisite for carcinoma invasion and metastasis." Cancer Res **66**(17): 8319-8326.

Christmann, M., Tomicic, M. T., Roos, W. P., Kaina, B. (2003). "Mechanisms of human DNA repair: an update." Toxicology **193**(1-2): 3-34.

ClinicalTrials.gov. (NCT00628251). "Dose-finding Study Comparing Efficacy and Safety of a PARP Inhibitor Against Doxil in BRCA+ve Advanced Ovarian Cancer (ICEBERG 3)."

ClinicalTrials.gov. (NCT00664781). "Rucaparib(CO-338;Formally Called AG-014699 or PF-0136738) in Treating Patients With Locally Advanced or Metastatic Breast Cancer or Advanced Ovarian Cancer."

ClinicalTrials.gov (NCT01891344). "A Study of Rucaparib in Patients With Platinum-Sensitive, Relapsed, High-Grade Epithelial Ovarian, Fallopian Tube, or Primary Peritoneal Cancer (ARIEL2)."

ClinicalTrials.gov (NCT01968213). "A Study of Rucaparib as Switch Maintenance Following Platinum-Based Chemotherapy in Patients With Platinum-Sensitive, High-Grade Serous or Endometrioid Epithelial Ovarian, Primary Peritoneal or Fallopian Tube Cancer (ARIEL3)."

Cohen, S. J., Punt, C. J. A., Iannotti, N., Saidman, B. H., Sabbath, K. D., Gabrail, N. Y., Picus, J., Morse, M., Mitchell, E., Miller, M. C., Doyle, G. V., Tissing, H., Terstappen, L. W. M., Meropol, N. J. (2008). "Relationship of circulating tumor cells to tumor response, progression-free survival, and overall survival in patients with metastatic colorectal cancer." Journal of Clinical Oncology **26**(19): 3213-3221.

Cohen, S. J., Punt, C. J., Iannotti, N., Saidman, B. H., Sabbath, K. D., Gabrail, N. Y., Picus, J., Morse, M. A., Mitchell, E., Miller, M. C., Doyle, G. V., Tissing, H., Terstappen, L. W., Meropol, N. J. (2009). "Prognostic significance of circulating tumor cells in patients with metastatic colorectal cancer." Ann Oncol **20**(7): 1223-1229.

Collaborators, I. (2002). "Paclitaxel plus carboplatin versus standard chemotherapy with either single-agent carboplatin or cyclophosphamide, doxorubicin, and cisplatin in women with ovarian cancer: the ICON3 randomised trial." Lancet **360**(9332): 505-515.

Collins, N., R. McManus, R. Wooster, J. Mangion, S. Seal, S. R. Lakhani, W. Ormiston, P. A. Daly, D. Ford, D. F. Easton and et al. (1995). "Consistent loss of the

- wild type allele in breast cancers from a family linked to the BRCA2 gene on chromosome 13q12-13." Oncogene **10**(8): 1673-1675.
- Coman, D. R., de Long, R.P., McCutcheon, M. (1951). "Studies on the mechanisms of metastasis; the distribution of tumors in various organs in relation to the distribution of arterial emboli." Cancer Res **11**(8): 648-651.
- Condeelis, J., Pollard, J. W. (2006). "Macrophages: obligate partners for tumor cell migration, invasion, and metastasis." Cell **124**(2): 263-266.
- Cooke, S. L., Brenton, J. D. (2011). "Evolution of platinum resistance in high-grade serous ovarian cancer." Lancet Oncol **12**(12): 1169-1174.
- Cormio, G., Rossi, C., Cazzolla, A., Resta, L., Loverro, G., Greco, P., Selvaggi, L. (2003). "Distant metastases in ovarian carcinoma." Int J Gynecol Cancer **13**(2): 125-129.
- Cortez, D., Wang, Y., Qin, J., Elledge, S. J. (1999). "Requirement of ATM-dependent phosphorylation of brca1 in the DNA damage response to double-strand breaks." Science **286**(5442): 1162-1166.
- Coumans, F. A., Doggen, C. J., Attard, G., de Bono, J. S., Terstappen, L. W. (2010). "All circulating EpCAM+CK+CD45- objects predict overall survival in castration-resistant prostate cancer." Ann Oncol **21**(9): 1851-1857.
- Covens, A. L. (2000). "A critique of surgical cytoreduction in advanced ovarian cancer." Gynecol Oncol **78**(3 Pt 1): 269-274.
- Cramer, S. F., Roth, L. M., Ulbright, T. M., Mazur, M. T., Nunez, C. A., Gersell, D. J., Mills, S. E., Kraus, F. T. (1987). "Evaluation of the reproducibility of the World Health Organization classification of common ovarian cancers. With emphasis on methodology." Arch Pathol Lab Med **111**(9): 819-829.
- Crickard, K., Crickard, U., Yoonessi, M. (1983). "Human ovarian carcinoma cells maintained on extracellular matrix versus plastic." Cancer Res **43**(6): 2762-2767.
- Cristofanilli, M., Broglio, K. R., Guarneri, V., Jackson, S., Fritsche, H. A., Islam, R., Dawood, S., Reuben, J. M., Kau, S. W., Lara, J. M., Krishnamurthy, S., Ueno, N. T., Hortobagyi, G. N., Valero, V. (2007). "Circulating tumor cells in metastatic breast cancer: biologic staging beyond tumor burden." Clin Breast Cancer **7**(6): 471-479.
- Cristofanilli, M., Budd, G. T., Ellis, M. J., Stopeck, A., Matera, J., Miller, M. C., Reuben, J. M., Doyle, G. V., Allard, W. J., Terstappen, L. W., Hayes, D. F. (2004). "Circulating tumor cells, disease progression, and survival in metastatic breast cancer." N Engl J Med **351**(8): 781-791.
- Cristofanilli, M., Hayes, D. F., Budd, G. T., Ellis, M. J., Stopeck, A., Reuben, J. M., Doyle, G. V., Matera, J., Allard, W. J., Miller, M. C., Fritsche, H. A., Hortobagyi, G. N., Terstappen, L. W. (2005). "Circulating tumor cells: a novel prognostic factor for newly diagnosed metastatic breast cancer." J Clin Oncol **23**(7): 1420-1430.
- Cristofanilli, M., Mendelsohn, J. (2006). "Circulating tumor cells in breast cancer: Advanced tools for "tailored" therapy?" Proc Natl Acad Sci U S A **103**(46): 17073-17074.
- Csete, B., Lengyel, Z., Kadar, Z., Battyani, Z. (2009). "Poly(adenosine diphosphate-ribose) polymerase-1 expression in cutaneous malignant melanomas as a new molecular marker of aggressive tumor." Pathol Oncol Res **15**(1): 47-53.

- Curtin, N. J. (2005). "PARP inhibitors for cancer therapy." Expert Rev Mol Med **7**(4): 1-20.
- Curtin, N. J. (2012). "DNA repair dysregulation from cancer driver to therapeutic target." Nat Rev Cancer **12**(12): 801-817.
- Dabholkar, M., Thornton, K., Vionnet, J., Bostick-Bruton, F., Yu, J. J., Reed, E. (2000). "Increased mRNA levels of xeroderma pigmentosum complementation group B (XPB) and Cockayne's syndrome complementation group B (CSB) without increased mRNA levels of multidrug-resistance gene (MDR1) or metallothionein-II (MT-II) in platinum-resistant human ovarian cancer tissues." Biochem Pharmacol **60**(11): 1611-1619.
- Dabholkar, M., Vionnet, J., Bostick-Bruton, F., Yu, J. J., Reed, E. (1994). "Messenger RNA levels of XPAC and ERCC1 in ovarian cancer tissue correlate with response to platinum-based chemotherapy." J Clin Invest **94**(2): 703-708.
- Daeron, M. (1997). "Fc receptor biology." Annu Rev Immunol **15**: 203-234.
- Damaraju, V. L., Damaraju, S., Young, J. D., Baldwin, S. A., Mackey, J., Sawyer, M. B., Cass, C. E. (2003). "Nucleoside anticancer drugs: the role of nucleoside transporters in resistance to cancer chemotherapy." Oncogene **22**(47): 7524-7536.
- Damia, G., Guidi, G., D'Incalci, M. (1998). "Expression of genes involved in nucleotide excision repair and sensitivity to cisplatin and melphalan in human cancer cell lines." Eur J Cancer **34**(11): 1783-1788.
- Dantzer, F., de La Rubia, G., Menissier-De Murcia, J., Hostomsky, Z., de Murcia, G., Schreiber, V. (2000). "Base excision repair is impaired in mammalian cells lacking Poly(ADP-ribose) polymerase-1." Biochemistry **39**(25): 7559-7569.
- Dantzer, F., Schreiber, V., Niedergang, C., Trucco, C., Flatter, E., De La Rubia, G., Oliver, J., Rolli, V., Menissier-de Murcia, J., de Murcia, G. (1999). "Involvement of poly(ADP-ribose) polymerase in base excision repair." Biochimie **81**(1-2): 69-75.
- David, S. S., O'Shea, V. L., Kundu, S. (2007). "Base-excision repair of oxidative DNA damage." Nature **447**(7147): 941-950.
- Davies, A. A., Masson, J. Y., McIlwraith, M. J., Stasiak, A. Z., Stasiak, A., Venkitaraman, A. R., West, S. C. (2001). "Role of BRCA2 in control of the RAD51 recombination and DNA repair protein." Mol Cell **7**(2): 273-282.
- Davies, H., Bignell, G. R., Cox, C., Stephens, P., Edkins, S., Clegg, S., Teague, J., Woffendin, H., Garnett, M. J., Bottomley, W., Davis, N., Darrow, T. L., Paterson, H., Marais, R., Marshall, C. J., Wooster, R., Stratton, M. R., Futreal, P. A. (2002). "Mutations of the BRAF gene in human cancer." Nature **417**(6892): 949-954.
- De Bono, J. S., Scher, H. I., Montgomery, R. B., Parker, C., Miller, M. C., Tissing, H., Doyle, G. V., Terstappen, L. W., Pienta, K. J., Raghavan, D. (2008). "Circulating tumor cells predict survival benefit from treatment in metastatic castration-resistant prostate cancer." Clin Cancer Res **14**(19): 6302-6309.
- De Murcia, G., Menissier de Murcia, J. (1994). "Poly(ADP-ribose) polymerase: a molecular nick-sensor." Trends Biochem Sci **19**(4): 172-176.
- De Vos, M., Schreiber, V., Dantzer, F. (2012). "The diverse roles and clinical relevance of PARPs in DNA damage repair: current state of the art." Biochem Pharmacol **84**(2): 137-146.

- Delaunoy, T., Burch, P. A., Reid, J. M., Camoriano, J. K., Kobayash, T., Braich, T. A., Kaur, J. S., Rubin, J., Erlichman, C. (2006). "A phase I clinical and pharmacokinetic study of CS-682 administered orally in advanced malignant solid tumors." Invest New Drugs **24**(4): 327-333.
- DelloRusso, C., Welch, P. L., Wang, W., Garcia, R. L., King, M. C., Swisher, E. M. (2007). "Functional characterization of a novel BRCA1-null ovarian cancer cell line in response to ionizing radiation." Mol Cancer Res **5**(1): 35-45.
- Demokan, S., Suoglu, Y., Demir, D., Gozeler, M., Dalay, N. (2006). "Microsatellite instability and methylation of the DNA mismatch repair genes in head and neck cancer." Ann Oncol **17**(6): 995-999.
- Dennis, M. J., Beijnen, J. H., Grochow, L. B., van Warmerdam, L. J. (1997). "An overview of the clinical pharmacology of topotecan." Semin Oncol **24**(1 Suppl 5): S5-12-S15-18.
- Dimova, I., Raitcheva, S., Dimitrov, R., Doganov, N., Toncheva, D. (2006). "Correlations between c-myc gene copy-number and clinicopathological parameters of ovarian tumours." Eur J Cancer **42**(5): 674-679.
- Dobzhansky, T. (1946). "Genetics of Natural Populations. Xiii. Recombination and Variability in Populations of *Drosophila Pseudoobscura*." Genetics **31**(3): 269-290.
- Doe, C. L., Ahn, J. S., Dixon, J., Whitby, M. C. (2002). "Mus81-Eme1 and Rqh1 involvement in processing stalled and collapsed replication forks." J Biol Chem **277**(36): 32753-32759.
- Dong, C., Davis, R. J., Flavell, R. A. (2002). "MAP kinases in the immune response." Annu Rev Immunol **20**: 55-72.
- Drew, Y., Mulligan, E. A., Vong, W. T., Thomas, H. D., Kahn, S., Kyle, S., Mukhopadhyay, A., Los, G., Hostomsky, Z., Plummer, E. R., Edmondson, R. J., Curtin, N. J. (2011). "Therapeutic potential of poly(ADP-ribose) polymerase inhibitor AG014699 in human cancers with mutated or methylated BRCA1 or BRCA2." J Natl Cancer Inst **103**(4): 334-346.
- Drew, Y., Plummer, R. (2009). "PARP inhibitors in cancer therapy: Two modes of attack on the cancer cell widening the clinical applications." Drug Resistance Updates **12**(6): 153-156.
- Drouet, J., Frit, P., Delteil, C., de Villartay, J. P., Salles, B., Calsou, P. (2006). "Interplay between Ku, Artemis, and the DNA-dependent protein kinase catalytic subunit at DNA ends." J Biol Chem **281**(38): 27784-27793.
- Drummond, J. T., Anthony, A., Brown, R., Modrich, P. (1996). "Cisplatin and adriamycin resistance are associated with MutLalpha and mismatch repair deficiency in an ovarian tumor cell line." J Biol Chem **271**(33): 19645-19648.
- Du Bois, A., Weber, B., Rochon, J., Meier, W., Goupil, A., Olbricht, S., Barats, J. C., Costa, S., Schroeder, W., Kimmig, R., Pujade-Lauraine, E., Arbeitsgemeinschaft Gynaekologische, Onkologie, Ovarian Cancer Study, Group, Groupe d'Investigateurs Nationaux pour l'Etude des Cancers, Ovariens (2006). "Addition of epirubicin as a third drug to carboplatin-paclitaxel in first-line treatment of advanced ovarian cancer: a prospectively randomized gynecologic cancer intergroup trial by the Arbeitsgemeinschaft Gynaekologische Onkologie Ovarian Cancer Study Group and the Groupe d'Investigateurs Nationaux pour l'Etude des Cancers Ovariens." J Clin Oncol **24**(7): 1127-1135.

- Dubeau, L. (1999). "The cell of origin of ovarian epithelial tumors and the ovarian surface epithelium dogma: does the emperor have no clothes?" Gynecol Oncol **72**(3): 437-442.
- Dumont, N., M. B. Wilson, Y. G. Crawford, P. A. Reynolds, M. Sigaroudinia and T. D. Tlsty (2008). "Sustained induction of epithelial to mesenchymal transition activates DNA methylation of genes silenced in basal-like breast cancers." Proc Natl Acad Sci U S A **105**(39): 14867-14872.
- Duncan, T. J., Al-Attar, A., Rolland, P., Scott, I. V., Deen, S., Liu, D. T., Spendlove, I., Durrant, L. G. (2008). "Vascular endothelial growth factor expression in ovarian cancer: a model for targeted use of novel therapies?" Clin Cancer Res **14**(10): 3030-3035.
- Dunfield, L. D., Shepherd, T. G., Nachtigal, M. W. (2002). "Primary culture and mRNA analysis of human ovarian cells." Biol Proced Online **4**: 55-61.
- Durkacz, B. W., Omidiji, O., Gray, D. A., Shall, S. (1980). "(ADP-ribose)_n participates in DNA excision repair." Nature **283**(5747): 593-596.
- Edmondson, R. J., Monaghan, J. M., Davies, B. R. (2002). "The human ovarian surface epithelium is an androgen responsive tissue." Br J Cancer **86**(6): 879-885.
- Eisenhauer, E. A., Therasse, P., Bogaerts, J., Schwartz, L. H., Sargent, D., Ford, R., Dancey, J., Arbuck, S., Gwyther, S., , Mooney, M., Rubinstein, L., Shankar, L., Dodd, L., Kaplan, R., Lacombe, D., Verweij, J. (2009). "New response evaluation criteria in solid tumours: revised RECIST guideline (version 1.1)." Eur J Cancer **45**(2): 228-247.
- Elattar, A., Bryant, A., Winter-Roach, B. A., Hatem, M., Naik, R. (2011). "Optimal primary surgical treatment for advanced epithelial ovarian cancer." Cochrane Database Syst Rev(8): CD007565.
- Elstrodt, F., Hollestelle, A., Nagel, J. H., Gorin, M., Wasielewski, M., van den Ouweland, A., Merajver, S. D., Ethier, S. P., Schutte, M. (2006). "BRCA1 mutation analysis of 41 human breast cancer cell lines reveals three new deleterious mutants." Cancer Res **66**(1): 41-45.
- Enshaei, A., Robson, C. N., Edmondson, R. J. (2015). "Artificial Intelligence Systems as Prognostic and Predictive Tools in Ovarian Cancer." Ann Surg Oncol.
- Esashi, F., Galkin, V. E., Yu, X., Egelman, E. H., West, S. C. (2007). "Stabilization of RAD51 nucleoprotein filaments by the C-terminal region of BRCA2." Nat Struct Mol Biol **14**(6): 468-474.
- Essers, J., Hendriks, R. W., Swagemakers, S. M., Troelstra, C. and J. de Wit, Bootsma, D., Hoeijmakers, J. H., Kanaar, R. (1997). "Disruption of mouse RAD54 reduces ionizing radiation resistance and homologous recombination." Cell **89**(2): 195-204.
- Esteller, M. (2000). "Epigenetic lesions causing genetic lesions in human cancer: promoter hypermethylation of DNA repair genes." Eur J Cancer **36**(18): 2294-2300.
- Fagotti, A., Ferrandina, G., Fanfani, F., Garganese, G., Vizzielli, G., Carone, V., Salerno, M. G., Scambia, G. (2008). "Prospective validation of a laparoscopic predictive model for optimal cytoreduction in advanced ovarian carcinoma." Am J Obstet Gynecol **199**(6): 642 e641-646.

- Fan, T., Zhao, Q., Chen, J. J., Chen, W. T., Pearl, M. L. (2009). "Clinical significance of circulating tumor cells detected by an invasion assay in peripheral blood of patients with ovarian cancer." Gynecol Oncol **112**(1): 185-191.
- Faratian, D., Christiansen, J., Gustavson, M., Jones, C. Scott, C., Um, I., Harrison, D. J. (2011). "Heterogeneity Mapping of Protein Expression in Tumors using Quantitative Immunofluorescence." J Vis Exp(56).
- Farley, J., Brad, W. E., Vathipadiakal, V., Lankes, H. A., Coleman, R., Morgan, M. A., Mannel, R., Yamada, S. D., Mutch, D., Rodgers, W. H., Birrer, M., Gershenson, D. M. (2013). "Selumetinib in women with recurrent low-grade serous carcinoma of the ovary or peritoneum: an open-label, single-arm, phase 2 study." Lancet Oncology **14**(2): 134-140.
- Farley, J., W. E. Brady, V. Vathipadiakal, H. A. Lankes, R. Coleman, M. A. Morgan, R. Mannel, S. D. Yamada, D. Mutch, W. H. Rodgers, M. Birrer and D. M. Gershenson (2013). "Selumetinib in women with recurrent low-grade serous carcinoma of the ovary or peritoneum: an open-label, single-arm, phase 2 study." Lancet Oncol **14**(2): 134-140.
- Farmer, H., McCabe, N., Lord, C. J., Tutt, A. N., Johnson, D. A., Richardson, T. B., Santarosa, M., Dillon, K. J., Hickson, I., Knights, C., Martin, N. M., Jackson, S. P., Smith, G. C., Ashworth, A. (2005). "Targeting the DNA repair defect in BRCA mutant cells as a therapeutic strategy." Nature **434**(7035): 917-921.
- Farrell, J. J., Elsaleh, H., Garcia, M., Lai, R., Ammar, A., Regine, W. F., Abrams, R., Benson, A. B., Macdonald, J., Cass, C. E., Icker, A. P., Mackey, J. R. (2009). "Human equilibrative nucleoside transporter 1 levels predict response to gemcitabine in patients with pancreatic cancer." Gastroenterology **136**(1): 187-195.
- Fathalla, M. F. (1971). "Incessant ovulation--a factor in ovarian neoplasia?" Lancet **2**(7716): 163.
- Fekete, T., Raso, E., Pete, I., Tegze, B., Liko, I., Munkacsy, G., Sipos, N., Rigo, J., Jr., Gyorffy, B. (2011). "Meta-analysis of gene expression profiles associated with histological classification and survival in 829 ovarian cancer samples." Int J Cancer.
- Ferraris, D. V. (2010). "Evolution of poly(ADP-ribose) polymerase-1 (PARP-1) inhibitors. From concept to clinic." J Med Chem **53**(12): 4561-4584.
- Ferry, K. V., Hamilton, T. C., Johnson, S. W. (2000). "Increased nucleotide excision repair in cisplatin-resistant ovarian cancer cells: role of ERCC1-XPF." Biochem Pharmacol **60**(9): 1305-1313.
- Fidler, I. J. (1970). "Metastasis: quantitative analysis of distribution and fate of tumour emolilabeled with 125 I-5-iodo-2'-deoxyuridine." J Natl Cancer Inst **45**: 773-782.
- Fidler, I. J., Poste, G. (2008). "The "seed and soil" hypothesis revisited." Lancet Oncol **9**(8): 808.
- Fink, D., Aebi, S., Howell, S. B. (1998). "The role of DNA mismatch repair in drug resistance." Clin Cancer Res **4**(1): 1-6.
- Fischer, A. H. (2009). "Circulating Tumor Cells Seeing Is Believing." Archives of Pathology & Laboratory Medicine **133**(9): 1367-1369.
- Fishel, M. L., He, Y., Smith, M. L., Kelley, M. R. (2007). "Manipulation of base excision repair to sensitize ovarian cancer cells to alkylating agent temozolomide." Clin Cancer Res **13**(1): 260-267.

Fleming, I. N., Gudmundsdottir, E., Sleigh, R., Green, S.R. (2007). "Identification of biomarkers and drug combinations to aid clinical development of sapacitabine (CYC682), a novel nucleoside analogue." AACR Annual meeting. Proc AM Assoc Cancer Res abstract 3138: 756.

Folkins, A. K., Saleemuddin, A., Garrett, L. A., Garber, J. E., Muto, M. G., Tworoger, S. S., Crum, C. P. (2009). "Epidemiologic correlates of ovarian cortical inclusion cysts (CICs) support a dual precursor pathway to pelvic epithelial cancer." Gynecol Oncol **115**(1): 108-111.

Fong, P. C., Boss, D. S., Yap, T. A., Tutt, A., Wu, P., Mergui-Roelvink, M., Mortimer, P., Swaisland, H., Lau, A., O'Connor, M. J., Ashworth, A., Carmichael, J., Kaye, S. B., Schellens, J. H., de Bono, J. S. (2009). "Inhibition of poly(ADP-ribose) polymerase in tumors from BRCA mutation carriers." N Engl J Med **361**(2): 123-134.

Fong, P. C., Yap, T. A., Boss, D. S., Carden, C. P., Mergui-Roelvink, M., Gourley, C., De Greve, J., Lubinski, J., Shanley, S., Messiou, C., A'Hern, R., Tutt, A., Ashworth, A., Stone, J., Carmichael, J., Schellens, J. H. M., de Bono, J. S., Kaye, S. B. (2010). "Poly(ADP)-Ribose Polymerase Inhibition: Frequent Durable Responses in BRCA Carrier Ovarian Cancer Correlating With Platinum-Free Interval." Journal of Clinical Oncology **28**(15): 2512-2519.

Forget, A. L., Bennett, B. T., Knight, K. L. (2004). "Xrcc3 is recruited to DNA double strand breaks early and independent of Rad51." J Cell Biochem **93**(3): 429-436.

Fortini, P., Calcagnile, A., Vrieling, H., van Zeeland, A. A., Bignami, M., Dogliotti, E. (1993). "Mutagenic processing of ethylation damage in mammalian cells: the use of methoxyamine to study apurinic/apyrimidinic site-induced mutagenesis." Cancer Res **53**(5): 1149-1155.

Foulkes, W. D. (2006). "BRCA1 and BRCA2: chemosensitivity, treatment outcomes and prognosis." Fam Cancer **5**(2): 135-142.

Frame, S., S. Armour, D. Zheleva, S. Green and D. Blake (2012). Sapacitabine efficacy is enhanced in homologous recombination defective tumours. . AACR. Liverpool. **Abstract B12**.

Frame, S., S. Armour, D. I. Zheleva, S. R. Green and D. G. Blake (2012). "DNA repair defects enhance tumor cell sensitivity to sapacitabine." Cancer Res **72**(5666).

Frame, S., Armour, S., Munro, C., Hogben, M., Jones, R., Blake, D.G., MacCallum, D.E., Green, S.R. (2010). "Understanding the pathways involved in the reepair of CNDAC induced DNA damage." AACR.

Fujita, M., Enomoto, T., Yoshino, K., Nomura, T., Buzard, G. S., Inoue, M., Okudaira, Y. (1995). "Microsatellite instability and alterations in the hMSH2 gene in human ovarian cancer." Int J Cancer **64**(6): 361-366.

Gadducci, A., Sartori, E., Landoni, F., Zola, P., Maggino, T., Maggioni, A., Cosio, S., Frassi, E., LaPresa, M. T., Fuso, L., Cristofani, R. (2005). "Relationship between time interval from primary surgery to the start of taxane- plus platinum-based chemotherapy and clinical outcome of patients with advanced epithelial ovarian cancer: results of a multicenter retrospective Italian study." J Clin Oncol **23**(4): 751-758.

Gaitanis, A., Staal, S. (2010). "Liposomal doxorubicin and nab-paclitaxel: nanoparticle cancer chemotherapy in current clinical use." Methods Mol Biol **624**: 385-392.

- Galmarini, C. M., J. R. Mackey and C. Dumontet (2002). "Nucleoside analogues and nucleobases in cancer treatment." Lancet Oncol **3**(7): 415-424.
- Galmarini, C. M., Thomas, X., Calvo, F., Rousselot, P., Rabilloud, M., El Jaffari, A., Cros, E., Dumontet, C. (2002). "In vivo mechanisms of resistance to cytarabine in acute myeloid leukaemia." Br J Haematol **117**(4): 860-868.
- Garcia-Manero, G., Lugar, S.M., Goldberg, S., Altman, J.K., Arellano, M.L., wetzler, M., Seiter, K., Chiao, J.H., Kantarjian, H. (2012). "A randomized phase II study of sapacitabine in MDS refractory to hypomethylating agents." J Clin Oncol **30**: Suppl; abstr 6520.
- Garnett, M. J., Edelman, E. J., Heidorn, S. J., Greenman, C. D., Dastur, A., Lau, K. W., Greninger, P., Taber, L. D., Stratton, M. R., Ramaswamy, S., McDermott, U., Benes, C. H. (2012). "Systematic identification of genomic markers of drug sensitivity in cancer cells." Nature **483**(7391): 570-575.
- Gatei, M., Young, D., Cerosaletti, K. M., Desai-Mehta, A., Spring, K., Kozlov, S., Lavin, M. F., Gatti, R. A., Concannon, P., Khanna, K. (2000). "ATM-dependent phosphorylation of nibrin in response to radiation exposure." Nat Genet **25**(1): 115-119.
- Gayther, S. A., Pharoah, P.D., (2010). "The inherited genetics of ovarian and endometrial cancer." Current Opinions in Genetics & Development **20**(3): 231-238.
- Gayther, S. A., Russell, P., Harrington, P., Antoniou, A. C., Easton, D. F., Ponder, B. A. (1999). "The contribution of germline BRCA1 and BRCA2 mutations to familial ovarian cancer: no evidence for other ovarian cancer-susceptibility genes." Am J Hum Genet **65**(4): 1021-1029.
- Geisler, H. E., Geisler, J. P., Miller, G. A., Geisler, M. J., Wiemann, M. C., Zhou, Z., Crabtree, W. (2001). "p21 and p53 in ovarian carcinoma: their combined staining is more valuable than either alone." Cancer **92**(4): 781-786.
- Gelmon, K. A., Hirte, H.W., Robidoux, A., Tonkin, K.S., Tischkowitz, M., Swenerton, K., Huntsman, D., Carmichael, J., Macpherson, E., Oza, A.M. (2010). "Can we define tumors that will respond to PARP inhibitors? A phase II correlative study of olaparib in advanced serous ovarian cancer and triple-negative breast cancer." J Clin Oncol **28** (15s): p Abstract 3002.
- Gelmon, K. A., Tischkowitz, M., Mackay, H., Swenerton, K., Robidoux, A., Tonkin, K., Hirte, H., Huntsman, D., Clemons, M., Gilks, B., Yerushalmi, R., Macpherson, E., Carmichael, J., Oza, A. (2011). "Olaparib in patients with recurrent high-grade serous or poorly differentiated ovarian carcinoma or triple-negative breast cancer: a phase 2, multicentre, open-label, non-randomised study." Lancet Oncol **12**(9): 852-861.
- Gerlinger, M., Rowan, A. J., Horswell, S., Larkin, J., Endesfelder, J., Gronroos, E., Szallasi, Z., Downward, J., Futreal, P. A., Swanton, C. (2012). "Intratumor heterogeneity and branched evolution revealed by multiregion sequencing." N Engl J Med **366**(10): 883-892.
- Gershenson, D. M., C. C. Sun, D. Bodurka, R. L. Coleman, K. H. Lu, A. K. Sood, M. Deavers, A. L. Malpica and J. J. Kavanagh (2009). "Recurrent low-grade serous ovarian carcinoma is relatively chemoresistant." Gynecol Oncol **114**(1): 48-52.
- Gershenson, D. M., C. C. Sun, R. B. Iyer, A. L. Malpica, J. J. Kavanagh, D. C. Bodurka, K. Schmeler and M. Deavers (2012). "Hormonal therapy for recurrent low-

grade serous carcinoma of the ovary or peritoneum." Gynecol Oncol **125**(3): 661-666.

Geyer, J. T., Lopez-Garcia, M. A., Sanchez-Estevez, C., Sarrío, D., Moreno-Bueno, G., Franceschetti, I., Palacios, J., Oliva, E. (2009). "Pathogenetic pathways in ovarian endometrioid adenocarcinoma: a molecular study of 29 cases." Am J Surg Pathol **33**(8): 1157-1163.

Gifford, G., Paul, J., Vasey, P. A., Kaye, S. B., Brown, R. (2004). "The acquisition of hMLH1 methylation in plasma DNA after chemotherapy predicts poor survival for ovarian cancer patients." Clin Cancer Res **10**(13): 4420-4426.

Gilbert, J., Carducci, M. A., Baker, S. D., Dees, E. C., Donehower, R. (2006). "A Phase I study of the oral antimetabolite, CS-682, administered once daily 5 days per week in patients with refractory solid tumor malignancies." Invest New Drugs **24**(6): 499-508.

Gleghorn, J. P., Pratt, E. D., Denning, D., Liu, H., Bander, N. H., Tagawa, S. T., Nanus, D. M., Giannakakou, P. A., Kirby, B. J. (2010). "Capture of circulating tumor cells from whole blood of prostate cancer patients using geometrically enhanced differential immunocapture (GEDI) and a prostate-specific antibody." Lab Chip **10**(1): 27-29.

Glinsky, V. V., Glinsky, G. V., Glinskii, O. V., Huxley, V. H., Turk, R., Mossine, V. V., Deutscher, S. L., Pienta, K. J., Quinn, T. P. (2003). "Intravascular metastatic cancer cell homotypic aggregation at the sites of primary attachment to the endothelium." Cancer Res **63**(13): 3805-3811.

Goggins, M., Schutte, M., Lu, J., Moskaluk, C. A., Weinstein, C. L., Petersen, G. M., Yeo, C. J., Jackson, C. E., Lynch, H. T., Hruban, R. H., Kern, S. E. (1996). "Germline BRCA2 gene mutations in patients with apparently sporadic pancreatic carcinomas." Cancer Res **56**(23): 5360-5364.

Goodale, D., Phay, C., Brown, W., Gray-Statchuk, L., Furlong, P., Lock, M., Chin-Yee, I., Keeney, M., Allan, A. L. (2009). "Flow cytometric assessment of monocyte activation markers and circulating endothelial cells in patients with localized or metastatic breast cancer." Cytometry B Clin Cytom **76**(2): 107-117.

Gottipati, P., Vischioni, B., Schultz, N., Solomons, J., Bryant, H. E., Djureinovic, T., Issaeva, N., Sleeth, K., Sharma, R. A., Helleday, T. (2010). "Poly(ADP-ribose) polymerase is hyperactivated in homologous recombination-defective cells." Cancer Res **70**(13): 5389-5398.

Gowen, L. C., Johnson, B. L., Latour, A. M., Sulik, K. K., Koller, B. H. (1996). "Brca1 deficiency results in early embryonic lethality characterized by neuroepithelial abnormalities." Nat Genet **12**(2): 191-194.

Gras, E., Catusus, L., Arguelles, R., Moreno-Bueno, G., Palacios, J., Gamallo, C., Matias-Guiu, X., Prat, J. (2001). "Microsatellite instability, MLH-1 promoter hypermethylation, and frameshift mutations at coding mononucleotide repeat microsatellites in ovarian tumors." Cancer **92**(11): 2829-2836.

Green, S. R., A. K. Choudhary and I. N. Fleming (2010). "Combination of sapacitabine and HDAC inhibitors stimulates cell death in AML and other tumour types." Br J Cancer **103**(9): 1391-1399.

- Griffin, R. J., Curtin, N. J., Newell, D. R., Golding, B. T., Durkacz, B. W., Calvert, A. H. (1995). "The role of inhibitors of poly(ADP-ribose) polymerase as resistance-modifying agents in cancer therapy." Biochimie **77**(6): 408-422.
- Griffiths, C. T. (1975). "Surgical resection of tumor bulk in the primary treatment of ovarian carcinoma." Natl Cancer Inst Monogr **42**: 101-104.
- Gudmundsdottir, K., Ashworth, A. (2006). "The roles of BRCA1 and BRCA2 and associated proteins in the maintenance of genomic stability." Oncogene **25**(43): 5864-5874.
- Gui, T., Shen, K. (2012). "The epidermal growth factor receptor as a therapeutic target in epithelial ovarian cancer." Cancer Epidemiol **36**(5): 490-496.
- Guppy, A. E., Nathan, P. D., Rustin, G. J. S. (2005). "Epithelial Ovarian Cancer: A Review of Current Management." Clinical Oncology **17**(6): 399-411.
- Gurin, C. C., Federici, M. G., Kang, L., Boyd, J. (1999). "Causes and consequences of microsatellite instability in endometrial carcinoma." Cancer Res **59**(2): 462-466.
- Gustafsson, J. O., Oehler, M. K., Ruzkiewicz, A., McColl, S. R., Hoffmann, P. (2011). "MALDI Imaging Mass Spectrometry (MALDI-IMS)-Application of Spatial Proteomics for Ovarian Cancer Classification and Diagnosis." Int J Mol Sci **12**(1): 773-794.
- Guyot, C., Combe, C., Clouzeau-Girard, H., Moronvalle-Halley, V., Desmouliere, A. (2007). "Specific activation of the different fibrogenic cells in rat cultured liver slices mimicking in vivo situations." Virchows Arch **450**(5): 503-512.
- Hacker, N. F., Berek, J. S., Lagasse, L. D., Nieberg, R. K., Elashoff, R. M. (1983). "Primary cytoreductive surgery for epithelial ovarian cancer." Obstet Gynecol **61**(4): 413-420.
- Hamilton, T. C., Young, R. C., McKoy, W. M., Grotzinger, K. R., Green, J. A., Chu, E. W., Whang-Peng, J., Rogan, A. M., Green, W. R., Ozols, R. F. (1983). "Characterization of a human ovarian carcinoma cell line (NIH:OVCAR-3) with androgen and estrogen receptors." Cancer Res **43**(11): 5379-5389.
- Hammond, S. L., Ham, R. G., Stampfer, M. R. (1984). "Serum-free growth of human mammary epithelial cells: rapid clonal growth in defined medium and extended serial passage with pituitary extract." Proc Natl Acad Sci U S A **81**(17): 5435-5439.
- Hanahan, D., Weinberg, R. A. (2000). "The hallmarks of cancer." Cell **100**(1): 57-70.
- Hanaoka, K., Suzuki, M., Kobayashi, T., Tanzawa, F., Tanaka, K., Shibayama, T., Miura, S., Ikeda, T., Iwabuchi, H., Nakagawa, A., Mitsuhashi, Y., Hisaoka, M., Kaneko, M., Tomida, A., Wataya, Y., Nomura, T., Sasaki, T., Matsuda, A., Tsuruo, T., Kurakata, S. (1999). "Antitumor activity and novel DNA-self-strand-breaking mechanism of CNDAC (1-(2-C-cyano-2-deoxy-beta-D-arabino-pentofuranosyl) cytosine) and its N4-palmitoyl derivative (CS-682)." Int J Cancer **82**(2): 226-236.
- Harkin, D. P., J. M. Bean, D. Miklos, Y. H. Song, V. B. Truong, C. Englert, F. C. Christians, L. W. Ellisen, S. Maheswaran, J. D. Oliner and D. A. Haber (1999). "Induction of GADD45 and JNK/SAPK-dependent apoptosis following inducible expression of BRCA1." Cell **97**(5): 575-586.
- Hartenbach, E. M., Olson, T. A., Goswitz, J. J., Mohanraj, D., Twigg, L. B., Carson, L. F., Ramakrishnan, S. (1997). "Vascular endothelial growth factor (VEGF)

expression and survival in human epithelial ovarian carcinomas." Cancer Lett **121**(2): 169-175.

Harter, P., du Bois, A., Hahmann, M., Hasenburg, A., Burges, A., Loibl, S., Gropp, M., Preitbach, G. P., Tanner, B., Sehouli, J., Arbeitsgemeinschaft Gynaekologische Onkologie Ovarian, Committee, A. G. O. Ovarian Cancer Study Group (2006).

"Surgery in recurrent ovarian cancer: the Arbeitsgemeinschaft Gynaekologische Onkologie (AGO) DESKTOP OVAR trial." Ann Surg Oncol **13**(12): 1702-1710.

Hartlerode, A. J., Scully, R. (2009). "Mechanisms of double-strand break repair in somatic mammalian cells." Biochem J **423**(2): 157-168.

Hay, E. D. (1995). "An overview of epithelio-mesenchymal transformation." Acta Anat (Basel) **154**(1): 8-20.

Hayakawa, Y., Kawai, R., Otsuki, K., Kataoka, M., Matsuda, A. (1998). "Evidence supporting the activity of 2'-C-cyano-2'-deoxy-1-beta-D-arabino-pentafuranosylcytosine as a terminator in enzymatic DNA-chain elongation." Bioorg Med Chem Lett **8**(18): 2559-2562.

Hayashi, M., Tamura, G., Jin, Z., Kato, I., Sato, M., Shibuya, Y., Yang, S., Motoyama, T. (2003). "Microsatellite instability in esophageal squamous cell carcinoma is not associated with hMLH1 promoter hypermethylation." Pathol Int **53**(5): 270-276.

Hayes, D. F., Cristofanilli, M., Budd, G. T., Ellis, M. J., Stopeck, A., Miller, M. C., Matera, J., Allard, W. J., Doyle, G. V., Terstappen, L. W. (2006). "Circulating tumor cells at each follow-up time point during therapy of metastatic breast cancer patients predict progression-free and overall survival." Clin Cancer Res **12**(14 Pt 1): 4218-4224.

He, W., Kularatne, S. A., Kalli, K. R., Prendergast, F. G., Amato, R. J., Klee, G. G., Hartmann, L. C., Low, P. S. (2008). "Quantitation of circulating tumor cells in blood samples from ovarian and prostate cancer patients using tumor-specific fluorescent ligands." Int J Cancer **123**(8): 1968-1973.

Hecht, J. L., Pinkus, J. L., Pinkus, G. S. (2006). "Monoclonal antibody MOC-31 reactivity as a marker for adenocarcinoma in cytologic preparations." Cancer **108**(1): 56-59.

Heinzelmann-Schwarz, V. A., Gardiner-Garden, M., Henshall, S. M., Scurry, J. P., Scolyer, R. A., Smith, A. N., Bali, A., Vanden Bergh, P., Baron-Hay, S., Scott, C., Fink, D., Hacker, N. F., Sutherland, R. L., O'Brien, P. M. (2006). "A distinct molecular profile associated with mucinous epithelial ovarian cancer." Br J Cancer **94**(6): 904-913.

Helleday, T. (2010). "Homologous recombination in cancer development, treatment and development of drug resistance." Carcinogenesis **31**(6): 955-960.

Helleday, T., Petermann, E., Lundin, C., Hodgson, B., Sharma, R. A. (2008). "DNA repair pathways as targets for cancer therapy." Nat Rev Cancer **8**(3): 193-204.

Helleman, J., van Staveren, I. L., Dinjens, W. N., van Kuijk, P. F., Ritstier, K., Ewing, P. C., van der Burg, M. E., Stoter, G., Berns, E. M. (2006). "Mismatch repair and treatment resistance in ovarian cancer." BMC Cancer **6**: 201.

Hennessy, B. T., Murph, M., Nanjundan, M., Carey, M., Auersperg, N., Almeida, J., Coombes, K. R., Liu, J., Lu, Y., Gray, J. W., Mills, G. B. (2008). "Ovarian cancer: linking genomics to new target discovery and molecular markers--the way ahead." Adv Exp Med Biol **617**: 23-40.

- Herrington, C. S., McCluggage, W. G. (2010). "The emerging role of the distal Fallopian tube and p53 in pelvic serous carcinogenesis." J Pathol **220**(1): 5-6.
- Herzog, T. J. (2004). "Recurrent ovarian cancer: how important is it to treat to disease progression?" Clin Cancer Res **10**(22): 7439-7449.
- Hibbs, K., Skubitz, K. M., Pambuccian, S. E., Casey, R. C., Bureson, K. M., Oegema, T. R., Jr., Thiele, J. J., Grindle, S. M., Bliss, R. L., Skubitz, A. P. (2004). "Differential gene expression in ovarian carcinoma: identification of potential biomarkers." Am J Pathol **165**(2): 397-414.
- Hirte, H. W., Clark, D. A., Mazurka, J., O'Connell, G., Rusthoven, J. (1992). "A rapid and simple method for the purification of tumor cells from ascitic fluid of ovarian carcinoma." Gynecol Oncol **44**(3): 223-226.
- Hoeijmakers, J. H. (2001). "Genome maintenance mechanisms for preventing cancer." Nature **411**(6835): 366-374.
- Hollingsworth, H. C., Kohn, E. C., Steinberg, S. M., Rothenberg, M. L., Merino, M. J. (1995). "Tumor angiogenesis in advanced stage ovarian carcinoma." Am J Pathol **147**(1): 33-41.
- Horton, J. K., Baker, A., Berg, B. J., Sobol, R. W., Wilson, S. H. (2002). "Involvement of DNA polymerase beta in protection against the cytotoxicity of oxidative DNA damage." DNA Repair (Amst) **1**(4): 317-333.
- Hoskins, P., Vergote, I., Cervantes, A., Tu, D., Stuart, G., Zola, P., Poveda, A., Provencher, D., Katsaros, D., Ojeda, B., Ghatage, P., Grimshaw, R., Casado, A., Elit, L., Mendiola, C., Sugimoto, A., D'Hondt, V., Oza, A., Germa, J. R., Roy, M., Brotto, L., Chen, D., Eisenhauer, E. A. (2010). "Advanced ovarian cancer: phase III randomized study of sequential cisplatin-topotecan and carboplatin-paclitaxel vs carboplatin-paclitaxel." J Natl Cancer Inst **102**(20): 1547-1556.
- Hoskins, W. J., Bundy, B. N., Thigpen, J. T., Omura, G. A. (1992). "The influence of cytoreductive surgery on recurrence-free interval and survival in small-volume stage III epithelial ovarian cancer: a Gynecologic Oncology Group study." Gynecol Oncol **47**(2): 159-166.
- Hoskins, W. J., McGuire, W. P., Brady, M. F., Homesley, H. D., Creasman, W. T., Berman, M., Ball, H., Berek, J. S. (1994). "The effect of diameter of largest residual disease on survival after primary cytoreductive surgery in patients with suboptimal residual epithelial ovarian carcinoma." Am J Obstet Gynecol **170**(4): 974-979; discussion 979-980.
- Hou, J. M., Greystoke, A., Lancashire, L., Cummings, J., Ward, T., Board, R., Amir, E., Hughes, S., Krebs, M., Hughes, A., Ranson, M., Lorigan, P., Dive, C., Blackhall, F. H. (2009). "Evaluation of circulating tumor cells and serological cell death biomarkers in small cell lung cancer patients undergoing chemotherapy." Am J Pathol **175**(2): 808-816.
- Hou, J. M., Krebs, M. G., Lancashire, L., Sloane, R., Backen, A., Swain, R. K., Priest, L. J., Greystoke, A., Zhou, C., Morris, K., Ward, T., Blackhall, F. H., Dive, C. (2012). "Clinical significance and molecular characteristics of circulating tumor cells and circulating tumor microemboli in patients with small-cell lung cancer." J Clin Oncol **30**(5): 525-532.

Hou, J. M., Krebs, M., Ward, T., Sloane, R., Priest, L., Hughes, A., Clack, G., Ranson, M., Blackhall, F., Dive, C. (2011). "Circulating tumor cells as a window on metastasis biology in lung cancer." Am J Pathol **178**(3): 989-996.

Huncharek, M., Geschwind, J. F., Kupelnick, B. (2003). "Perineal application of cosmetic talc and risk of invasive epithelial ovarian cancer: a meta-analysis of 11,933 subjects from sixteen observational studies." Anticancer Res **23**(2C): 1955-1960.

Ince, T. A., Sousa, A. D., Jones, M. A., Harrell, J. C., Agoston, E. S., Krohn, M., Selfors, L. M., Liu, W., Chen, K., Yong, M., Buchwald, P., Foster, R., Rueda, B. R., Crum, C. P., Brugge, J. S., Mills, G. B. (2015). "Characterization of twenty-five ovarian tumour cell lines that phenocopy primary tumours." Nat Commun **6**: 7419.

Institute, N. C. "Surveillance, Epidemiology, and End Results Program. SEER Stat Fact Sheets: Ovary Cancer." Retrieved November, 2014.

Institute, N. C. (2014). "National Cancer Institute at the National Institute of Health " Dictionary for Cancer Terms Retrieved 6/4/14, 2014.

Isakoff, S. J., Overmoyer, B., Tung, N.M., Gelman, R.S., Giranda, V.L., Bernhard, K.M., Habin, K.R., Ellisen, L.W., Winer, E.P., Goss, P.E. (2010). "A phase II trial of the PARP inhibitor veliparib (ABT888) and temozolomide for metastatic breast cancer." J Clin Oncol **28 (15s)**: Abstract 1019.

Isobe, M., Emanuel, B. S., Givol, D., Oren, M., Croce, C. M. (1986). "Localization of gene for human p53 tumour antigen to band 17p13." Nature **320**(6057): 84-85.

Itamochi, H., Kigawa, J., Sugiyama, T., Kikuchi, Y., Suzuki, M., Terakawa, N. (2002). "Low proliferation activity may be associated with chemoresistance in clear cell carcinoma of the ovary." Obstet Gynecol **100**(2): 281-287.

Iwashita, A., K. Mihara, S. Yamazaki, S. Matsuura, J. Ishida, H. Yamamoto, K. Hattori, N. Matsuoka and S. Mutoh (2004). "A new poly(ADP-ribose) polymerase inhibitor, FR261529 [2-(4-chlorophenyl)-5-quinoxalinecarboxamide], ameliorates methamphetamine-induced dopaminergic neurotoxicity in mice." J Pharmacol Exp Ther **310**(3): 1114-1124.

Jacquemont, C., Taniguchi, T. (2007). "Proteasome function is required for DNA damage response and fanconi anemia pathway activation." Cancer Res **67**(15): 7395-7405.

Jagtap, P. G., E. Baloglu, G. J. Southan, J. G. Mabley, H. Li, J. Zhou, J. van Duzer, A. L. Salzman and C. Szabo (2005). "Discovery of potent poly(ADP-ribose) polymerase-1 inhibitors from the modification of indeno[1,2-c]isoquinolinone." J Med Chem **48**(16): 5100-5103.

Jamieson, E. R., Lippard, S. J. (1999). "Structure, Recognition, and Processing of Cisplatin-DNA Adducts." Chem Rev **99**(9): 2467-2498.

Jazaeri, A. A., Yee, C. J., Sotiriou, C., Brantley, K. R., Boyd, J., Liu, E. T. (2002). "Gene expression profiles of BRCA1-linked, BRCA2-linked, and sporadic ovarian cancers." J Natl Cancer Inst **94**(13): 990-1000.

Jemal, A., Siegel, R., Ward, E., Hao, Y., Xu, J., Thun, M. J. (2009). "Cancer statistics, 2009." CA Cancer J Clin **59**(4): 225-249.

Jensen, R. B., Carreira, A., Kowalczykowski, S. C. (2010). "Purified human BRCA2 stimulates RAD51-mediated recombination." Nature **467**(7316): 678-683.

Jiang, B. H., Aoki, M., Zheng, J. Z., Li, J., Vogt, P. K. (1999). "Myogenic signaling of phosphatidylinositol 3-kinase requires the serine-threonine kinase Akt/protein kinase B." Proc Natl Acad Sci U S A **96**(5): 2077-2081.

Jochumsen, K. M., Tan, Q., Holund, B., Kruse, T. A., Mogensen, O. (2007). "Gene expression in epithelial ovarian cancer: a study of intratumor heterogeneity." Int J Gynecol Cancer **17**(5): 979-985.

Jordan, S. J., D. C. Whiteman, D. M. Purdie, A. C. Green and P. M. Webb (2006). "Does smoking increase risk of ovarian cancer? A systematic review." Gynecol Oncol **103**(3): 1122-1129.

Jordan, V. C. (2006). "Tamoxifen (ICI46,474) as a targeted therapy to treat and prevent breast cancer." Br J Pharmacol **147 Suppl 1**: S269-276.

Jordheim, L. P., Durantel, D., Zoulim, F., Dumontet, C. (2013). "Advances in the development of nucleoside and nucleotide analogues for cancer and viral diseases." Nat Rev Drug Discov **12**(6): 447-464.

Judson, P. L., Geller, M. A., Bliss, R. L., Boente, M. P., Downs, L. S., Jr., Argenta, P. A., Carson, L. F. (2003). "Preoperative detection of peripherally circulating cancer cells and its prognostic significance in ovarian cancer." Gynecol Oncol **91**(2): 389-394.

Jung, R., Kruger, W., Hosch, S., Holweg, M., Kroger, N., Gutensohn, K., Wagener, C., Neumaier, M., Zander, A. R. (1998). "Specificity of reverse transcriptase polymerase chain reaction assays designed for the detection of circulating cancer cells is influenced by cytokines in vivo and in vitro." Br J Cancer **78**(9): 1194-1198.

Kaku, T., Ogawa, S., Kawano, Y., Ohishi, Yoshihiro., Kobayashi, Hiroaki., Hirakawa, Toshio., Nakano, Hitoo (2003). "Histological classification of ovarian cancer." Medical Electron Microscopy **36**(1): 9-17.

Kalluri, R., Neilson, E. G. (2003). "Epithelial-mesenchymal transition and its implications for fibrosis." J Clin Invest **112**(12): 1776-1784.

Kalluri, R., Weinberg, R. A. (2009). "The basics of epithelial-mesenchymal transition." J Clin Invest **119**(6): 1420-1428.

Kaneko, M., Koga, R., Murayama, K., Shibata, T., Hotoa H, Suziki M, Manaoka K, Tanazawa F, Kurakata S, Kobayashi T, Sasaki T, Matsuda A (1997). "Synthesis and antitumor activity of a novel antitumor nucleoside 1-(2-C-cyano-2-deoxy-B-D-arabino-pentofuranosyl)-N4-palmitoylcytosine (CS-682). Eighty-Eighth Annual Meeting of the American Association for Cancer research. ." Proc Am Assoc Cancer Res **38**(101 Abstract).

Kang, J., D'Andrea, A. D., Kozono, D. (2012). "A DNA repair pathway-focused score for prediction of outcomes in ovarian cancer treated with platinum-based chemotherapy." J Natl Cancer Inst **104**(9): 670-681.

Kantarjian, H., F, Faderl, S., Garcia-Manero, G., Luger, S., Venugopal, P., Maness, L., Wetzler, M., Coutre, S., Stock, W., Claxton, D., Goldberg, S. L., Arellano, M., Strickland, S. A., Seiter, K., Schiller, G., Jabbour, E., Chiao, J., Plunkett, W. (2012). "Oral sapacitabine for the treatment of acute myeloid leukaemia in elderly patients: a randomised phase 2 study." Lancet Oncol **13**(11): 1096-1104.

Kantarjian, H., Garcia-Manero, G., O'Brien, S., Faderl, S., Ravandi, F., Westwood, R., Green, S. R., Chiao, J. H., Boone, P. A., Cortes, J., Plunkett, W. (2010). "Phase I

clinical and pharmacokinetic study of oral sapacitabine in patients with acute leukemia and myelodysplastic syndrome." J Clin Oncol **28**(2): 285-291.

Kantarjian, H. M., Garcia-Manero, G., Lugar, S., Venugopal, P., Maness, L.J., Wetzler, M., Stock, W., Coutre, S., Borthakur, G., Chiao, J. (2009). "A Randomized Phase 2 Study of Sapacitabine, An Oral Nucleoside Analogue, in Elderly Patients with AML Previously Untreated or in First Relapse." Blood **114**(22): Abstr 1061.

Kehoe, S., Hook, J., Nankivell, M., Jayson, G. C., Kitchener, H., Lopes, T., Luesley, D., Perren, T., Bannoo, S., Mascarenhas, M., Dobbs, S., Essapen, S., Twigg, J., Herod, J., McCluggage, G., Parmar, M., Swart, A. M. (2015). "Primary chemotherapy versus primary surgery for newly diagnosed advanced ovarian cancer (CHORUS): an open-label, randomised, controlled, non-inferiority trial." Lancet **386**(9990): 249-257.

Kennedy, R. D., D'Andrea, A. D. (2006). "DNA repair pathways in clinical practice: lessons from pediatric cancer susceptibility syndromes." J Clin Oncol **24**(23): 3799-3808.

Khalique, L., Ayhan, A., Weale, M. E., Jacobs, I. J., Ramus, S. J., Gayther, S. A. (2007). "Genetic intra-tumour heterogeneity in epithelial ovarian cancer and its implications for molecular diagnosis of tumours." J Pathol **211**(3): 286-295.

Khalique, L., Ayhan, A., Whittaker, J. C., Singh, N., Jacobs, I. J., Gayther, S. A., Ramus, S. J. (2009). "The clonal evolution of metastases from primary serous epithelial ovarian cancers." Int J Cancer **124**(7): 1579-1586.

Khanna, K. K., Jackson, S. P. (2001). "DNA double-strand breaks: signaling, repair and the cancer connection." Nat Genet **27**(3): 247-254.

Kindelberger, D. W., Lee, Y., Miron, A., Hirsch, M. S., Feltmate, C., Medeiros, F., Callahan, M. J., Garner, E. O., Gordon, R. W., Birch, C., Berkowitz, R. S., Muto, M. G., Crum, C. P. (2007). "Intraepithelial carcinoma of the fimbria and pelvic serous carcinoma: Evidence for a causal relationship." Am J Surg Pathol **31**(2): 161-169.

King, B. L., Carcangiu, M. L., Carter, D., Kiechle, M., Pfisterer, J., Pfeleiderer, A., Kacinski, B. M. (1995). "Microsatellite instability in ovarian neoplasms." Br J Cancer **72**(2): 376-382.

Kitchener, H. C. (2008). "Survival from cancer of the ovary in England and Wales up to 2001." Br J Cancer **99** **Suppl 1**: S73-74.

Knappskog, S., Lonning, P. E. (2012). "P53 and its molecular basis to chemoresistance in breast cancer." Expert Opin Ther Targets **16** **Suppl 1**: S23-30.

Kobayashi, S., Boggon, T. J., Dayaram, T., Janne, P. A., Kocher, O., Meyerson, M., Johnson, B. E., Eck, M. J., Tenen, D. G., Halmos, B. (2005). "EGFR mutation and resistance of non-small-cell lung cancer to gefitinib." N Engl J Med **352**(8): 786-792.

Koi, M., Umar, A., Chauhan, D. P., Herian, S. P., Carethers, J. M., Kunkel, T. A., Boland, C. R. (1994). "Human chromosome 3 corrects mismatch repair deficiency and microsatellite instability and reduces N-methyl-N'-nitro-N-nitrosoguanidine tolerance in colon tumor cells with homozygous hMLH1 mutation." Cancer Res **54**(16): 4308-4312.

Kollmannsberger, C., Mross, K., Jakob, A., Kanz, L., Bokemeyer, C. (1999). "Topotecan - A novel topoisomerase I inhibitor: pharmacology and clinical experience." Oncology **56**(1): 1-12.

- Konstantinopoulos, P. A., Spentzos, D., Karlan, B. Y., Taniguchi, T., Fountzilias, E., Francoeur, N., Levine, D. A., Cannistra, S. A. (2010). "Gene expression profile of BRCAness that correlates with responsiveness to chemotherapy and with outcome in patients with epithelial ovarian cancer." J Clin Oncol **28**(22): 3555-3561.
- Korch, C., Spillman, M. A., Jackson, T. A., Jacobsen, B. M., Murphy, S. K., Lessey, B. A., Jordan, V. C., Bradford, A. P. (2012). "DNA profiling analysis of endometrial and ovarian cell lines reveals misidentification, redundancy and contamination." Gynecol Oncol **127**(1): 241-248.
- Krahn, J. M., Beard, W. A., Miller, H., Grollman, A. P., Wilson, S. H. (2003). "Structure of DNA polymerase beta with the mutagenic DNA lesion 8-oxodeoxyguanine reveals structural insights into its coding potential." Structure **11**(1): 121-127.
- Krebs, M. G., Hou, J. M., Ward, T. H., Blackhall, F. H., Dive, C. (2010). "Circulating tumour cells: their utility in cancer management and predicting outcomes." Ther Adv Med Oncol **2**(6): 351-365.
- Krebs, M. G., Sloane, R., Priest, L., Lancashire, L., Hou, J. M., Greystoke, A., Ward, T. H., Ferraldeschi, R., Hughes, A., Clack, G., Ranson, M., Dive, C., Blackhall, F. H. (2011). "Evaluation and prognostic significance of circulating tumor cells in patients with non-small-cell lung cancer." J Clin Oncol **29**(12): 1556-1563.
- Krupa, R., Sliwinski, T., Morawiec, Z., Pawlowska, E., Zadrozny, M., Blasiak, J. (2009). "Association between polymorphisms of the BRCA2 gene and clinical parameters in breast cancer." Exp Oncol **31**(4): 250-251.
- Kummar, S., Ji, J., Morgan, R., Lenz, H. J. Puhalla, S. L., Belani, C. P., Gandara, D. R., Allen, D., Kiesel, B., Beumer, J. H., Newman, E. M., Rubinstein, L., Chen, A., Zhang, Y., Wang, L., Kinders, R. J., Parchment, R. E., Tomaszewski, J. E., Doroshow, J. H. (2012). "A phase I study of veliparib in combination with metronomic cyclophosphamide in adults with refractory solid tumors and lymphomas." Clin Cancer Res **18**(6): 1726-1734.
- Kundu, U. R., Krishnamurthy, S. (2011). "Use of the monoclonal antibody MOC-31 as an immunomarker for detecting metastatic adenocarcinoma in effusion cytology." Cancer Cytopathol **119**(4): 272-278.
- Kurian, A. W., Balise, R. R., McGuire, V., Whittemore, A. S. (2005). "Histologic types of epithelial ovarian cancer: have they different risk factors?" Gynecol Oncol **96**(2): 520-530.
- Kurman, R. J., Shih, I.M. (2011). "Molecular pathogenesis and extraovarian origin of epithelial ovarian cancer--shifting the paradigm." Hum Pathol **42**(7): 918-931.
- Kurman, R. J., Shih, I.M., (2010). "The Origin and Pathogenesis of Epithelial Ovarian Cancer- a Proposed Unifying Theory " Surgical Pathology **34**(3): 433-443.
- Lahmann, P. H., Cust, A. E., Friedenreich, C. M., Schulz, M., Lukanova, A., Kaaks, R., Lundin, E., Tjonneland, A., Halkjaer, J., Spencer, E., Rinaldi, S., Slimani, N., Chajes, V., Michaud, D., Norat, T., Riboli, E. (2010). "Anthropometric measures and epithelial ovarian cancer risk in the European Prospective Investigation into Cancer and Nutrition." Int J Cancer **126**(10): 2404-2415.
- Lai, D., Visser-Grieve, S., Yang, X. (2012). "Tumour suppressor genes in chemotherapeutic drug response." Biosci Rep **32**(4): 361-374.

- Lawrenson, K., Gayther, S. A. (2009). "Ovarian cancer: a clinical challenge that needs some basic answers." PLoS Med **6**(2): e25.
- Le Page, C., Ouellet, V., Madore, J., Ren, F., Hudson, T. J., Tonin, P. N., Provencher, D. M., Mes-Masson, A. M. (2006). "Gene expression profiling of primary cultures of ovarian epithelial cells identifies novel molecular classifiers of ovarian cancer." Br J Cancer **94**(3): 436-445.
- Le Page, F., Kwoh, E. E., Avrutskaya, A., Gentil, A., Leadon, S. A., Sarasin, A., Cooper, P. K. (2000). "Transcription-coupled repair of 8-oxoguanine: requirement for XPG, TFIIH, and CSB and implications for Cockayne syndrome." Cell **101**(2): 159-171.
- Ledermann, J., Harter, P., Gourley, C., Friedlander, M., Vergote, I., Rustin, G., Scott, C., Meier, W., Shapira-Frommer, R., Safra, T., Matei, D., Macpherson, E., Watkins, C., Carmichael, J., Matulonis, U. (2012). "Olaparib Maintenance Therapy in Platinum-Sensitive Relapsed Ovarian Cancer." New England Journal of Medicine **366**(15): 1382-1392.
- Ledermann, J. A., Kristeleit, R. S. (2010). "Optimal treatment for relapsing ovarian cancer." Ann Oncol **21 Suppl 7**: vii218-222.
- Lee, S. A., C. Roques, A. C. Magwood, J. Y. Masson and M. D. Baker (2009). "Recovery of deficient homologous recombination in Brca2-depleted mouse cells by wild-type Rad51 expression." DNA Repair (Amst) **8**(2): 170-181.
- Lee, Y., Medeiros, F., Kindelberger, D., Callahan, M. J., Muto, M. G., Crum, C. P. (2006). "Advances in the recognition of tubal intraepithelial carcinoma: applications to cancer screening and the pathogenesis of ovarian cancer." Adv Anat Pathol **13**(1): 1-7.
- Lee, Y., Miron, A., Drapkin, R., Nucci, M. R., Medeiros, F., Saleemuddin, A., Garber, J., Birch, C., Mou, H., Gordon, R. W., Cramer, D. W., McKeon, F. D., Crum, C. P. (2007). "A candidate precursor to serous carcinoma that originates in the distal fallopian tube." J Pathol **211**(1): 26-35.
- Leffers, N., Vermeij, R., Hoogeboom, B. N., Schulze, U. R., Wolf, R., Hamming, I. E., van der Zee, A. G., Melief, K. J., van der Burg, S. H., Daemen, T., Nijman, H. W. (2012). "Long-term clinical and immunological effects of p53-SLP(R) vaccine in patients with ovarian cancer." Int J Cancer **130**(1): 105-112.
- Lengyel, E. (2010). "Ovarian Cancer Development and Metastasis." The American Journal of Pathology **177**(3): 1053-1064.
- Levine, A. J. (1997). "p53, the cellular gatekeeper for growth and division." Cell **88**(3): 323-331.
- Li, Q., Yu, J. J., Mu, C., Yunmbam, M. K., Slavsky, D., Cross, C. L., Bostick-Bruton, F., Reed, E. (2000). "Association between the level of ERCC-1 expression and the repair of cisplatin-induced DNA damage in human ovarian cancer cells." Anticancer Res **20**(2A): 645-652.
- Li, X., Heyer, W. D. (2008). "Homologous recombination in DNA repair and DNA damage tolerance." Cell Res **18**(1): 99-113.
- Lieber, M. R. (2008). "The mechanism of human nonhomologous DNA end joining." J Biol Chem **283**(1): 1-5.

- Lieber, M. R. (2010). "The mechanism of double-strand DNA break repair by the nonhomologous DNA end-joining pathway." Annu Rev Biochem **79**: 181-211.
- Lindhahl, T. (1993). "Instability and decay of the primary structure of DNA." Nature **362**(6422): 709-715.
- Liotta, L. A., Kleinerman, J., Saidel, G. M. (1974). "Quantitative relationships of intravascular tumor cells, tumor vessels, and pulmonary metastases following tumor implantation." Cancer Res **34**(5): 997-1004.
- Liu, L., Nakatsuru, Y., Gerson, S. L. (2002). "Base excision repair as a therapeutic target in colon cancer." Clin Cancer Res **8**(9): 2985-2991.
- Liu, L., Taverna, P., Whitacre, C. M., Chatterjee, S., Gerson, S. L. (1999). "Pharmacologic disruption of base excision repair sensitizes mismatch repair-deficient and -proficient colon cancer cells to methylating agents." Clin Cancer Res **5**(10): 2908-2917.
- Liu, N., Lamerdin, J. E., Tebbs, R. S., Schild, D., Tucker, J. D., Shen, M. R., Brookman, K. W., Siciliano, M. J., Walter, C. A., Fan, W., Narayana, L. S., Zhou, Z. Q., Adamson, A. W., Sorensen, K. J., Chen, D. J., Jones, N. J., Thompson, L. H. (1998). "XRCC2 and XRCC3, new human Rad51-family members, promote chromosome stability and protect against DNA cross-links and other damages." Mol Cell **1**(6): 783-793.
- Liu, N., Lim, C. S. (2005). "Differential roles of XRCC2 in homologous recombinational repair of stalled replication forks." J Cell Biochem **95**(5): 942-954.
- Liu, X., Guo, Y., Li, Y., Jiang, Y., Chubb, S., Azuma, A., Huang, P., Matsuda, A., Hittelman, W., Plunkett, W. (2005). "Molecular basis for G2 arrest induced by 2'-C-cyano-2'-deoxy-1-beta-D-arabino-pentofuranosylcytosine and consequences of checkpoint abrogation." Cancer Res **65**(15): 6874-6881.
- Liu, X., Kantarjian, H., Plunkett, W. (2012). "Sapacitabine for cancer." Expert Opin Investig Drugs **21**(4): 541-555.
- Liu, X., Wang, Y., Benaissa, S., Matsuda, A., Kantarjian, H., Estrov, Z., Plunkett, W. (2010). "Homologous recombination as a resistance mechanism to replication-induced double-strand breaks caused by the antileukemia agent CNDAC." Blood **116**(10): 1737-1746.
- Liu, Z., Phan, S., Famili, F., Pan, Y., Lenferink, A. E., Cantin, C., Collins, C., O'Connor-McCourt, M. D. (2010). "A multi-strategy approach to informative gene identification from gene expression data." J Bioinform Comput Biol **8**(1): 19-38.
- Liuzzi, M., Talpaert-Borle, M. (1985). "A new approach to the study of the base-excision repair pathway using methoxyamine." J Biol Chem **260**(9): 5252-5258.
- Loh, V. M., Jr., Cockcroft, X. L., Dillon, K. J., Dixon, L., Drzewiecki, J., Eversley, P. J., Gomez, S., Hoare, J., Kerrigan, F., Matthews, I. T., Menear, K. A., Martin, N. M., Newton, R. F., Paul, J., Smith, G. C., Vile, J., Whittle, A. J. (2005). "Phthalazinones. Part 1: The design and synthesis of a novel series of potent inhibitors of poly(ADP-ribose)polymerase." Bioorg Med Chem Lett **15**(9): 2235-2238.
- Lounis, H., Provencher, D., Godbout, C., Fink, D., Milot, M. J., Mes-Masson, A. M. (1994). "Primary cultures of normal and tumoral human ovarian epithelium: a powerful tool for basic molecular studies." Exp Cell Res **215**(2): 303-309.

- Lowe, S. W., Bodis, S., McClatchey, A., Remington, L., Ruley, H. E., Fisher, D. E., Housman, D. E., Jacks, T. (1994). "p53 status and the efficacy of cancer therapy in vivo." Science **266**(5186): 807-810.
- Lu, X., J. Errington, N. J. Curtin, J. Lunec and D. R. Newell (2001). "The impact of p53 status on cellular sensitivity to antifolate drugs." Clin Cancer Res **7**(7): 2114-2123.
- Lundin, C., Schultz, N., Arnaudeau, C., Mohindra, A., Hansen, L. T., Helleday, T. (2003). "RAD51 is involved in repair of damage associated with DNA replication in mammalian cells." J Mol Biol **328**(3): 521-535.
- Lynch, H. T., Lynch, P. M., Lanspa, S. J., Snyder, C. L., Lynch, J. F., Boland, C. R. (2009). "Review of the Lynch syndrome: history, molecular genetics, screening, differential diagnosis, and medicolegal ramifications." Clin Genet **76**(1): 1-18.
- Mackey, J. R., S. A. Baldwin, J. D. Young and C. E. Cass (1998). "Nucleoside transport and its significance for anticancer drug resistance." Drug Resist Updat **1**(5): 310-324.
- Mackey, J. R., R. S. Mani, M. Selner, D. Mowles, J. D. Young, J. A. Belt, C. R. Crawford and C. E. Cass (1998). "Functional nucleoside transporters are required for gemcitabine influx and manifestation of toxicity in cancer cell lines." Cancer Res **58**(19): 4349-4357.
- Mackey, J. R., S. Y. Yao, K. M. Smith, E. Karpinski, S. A. Baldwin, C. E. Cass and J. D. Young (1999). "Gemcitabine transport in xenopus oocytes expressing recombinant plasma membrane mammalian nucleoside transporters." J Natl Cancer Inst **91**(21): 1876-1881.
- Maheswaran, S., Sequist, L. V., Nagrath, S., Ulkus, L., Brannigan, B., Collura, C. V., Inserra, E., Diederichs, S., Iafrate, A. J., Bell, D. W., Digumarthy, S., Muzikansky, A., Irimia, D., Settleman, J., Tompkins, R. G., Lynch, T. J., Toner, M., Haber, D. A. (2008). "Detection of mutations in EGFR in circulating lung-cancer cells." N Engl J Med **359**(4): 366-377.
- Markman, M. (2009). "Optimal management of recurrent ovarian cancer." International Journal of Cancer **19**(Suppl 2): S40-43.
- Marks, A., Sutherland, D. R., Bailey, D., Iglesias, J., Law, J., Lei, M., Yeger, H., Banerjee, D., Baumal, R. (1999). "Characterization and distribution of an oncofetal antigen (M2A antigen) expressed on testicular germ cell tumours." Br J Cancer **80**(3-4): 569-578.
- Martensson, S., Hammarsten, O. (2002). "DNA-dependent protein kinase catalytic subunit. Structural requirements for kinase activation by DNA ends." J Biol Chem **277**(4): 3020-3029.
- Marth, C., Hoifodt, H., Walberg, L., Kaern, J., Mathiesen, O., Andresen, M. (2001). Detection of circulating tumor cells in the peripheral blood and bone marrow of patients with ovarian cancer. Textbook of Ovarian Cancer. H. JacobsI, ShepardJ, OramD, BlackettA, LuelseyD. Oxford, Oxford University Press: 279-283.
- Marth, C., Kistic, J., Kaern, J., Trope, C., Fodstad, O. (2002). "Circulating tumor cells in the peripheral blood and bone marrow of patients with ovarian carcinoma do not predict prognosis." Cancer **94**(3): 707-712.
- Matsuda, A., Y. Nakajima, A. Azuma, M. Tanaka and T. Sasaki (1991). "Nucleosides and nucleotides. 100. 2'-C-cyano-2'-deoxy-1-beta-D-arabinofuranosyl-cytosine

- (CNDAC): design of a potential mechanism-based DNA-strand-breaking antineoplastic nucleoside." J Med Chem **34**(9): 2917-2919.
- Mazin, A. V., Alexeev, A. A., Kowalczykowski, S. C. (2003). "A novel function of Rad54 protein. Stabilization of the Rad51 nucleoprotein filament." J Biol Chem **278**(16): 14029-14036.
- Mazzoletti, M., Broggin, M. (2010). "PI3K/AKT/mTOR Inhibitors In Ovarian Cancer." Current Medicinal Chemistry **17**(36): 4433-4447.
- McAlpine, J. N., Eisenkop, S. M., Spirtos, N. M. (2008). "Tumor heterogeneity in ovarian cancer as demonstrated by in vitro chemoresistance assays." Gynecol Oncol **110**(3): 360-364.
- McCabe, N., N. C. Turner, C. J. Lord, K. Kluzek, A. Bialkowska, S. Swift, S. Giavara, M. J. O'Connor, A. N. Tutt, M. Z. Zdzienicka, G. C. Smith and A. Ashworth (2006). "Deficiency in the repair of DNA damage by homologous recombination and sensitivity to poly(ADP-ribose) polymerase inhibition." Cancer Res **66**(16): 8109-8115.
- McCluggage, W. G. (2011). "Morphological subtypes of ovarian carcinoma: a review with emphasis on new developments and pathogenesis." Pathology **43**(5): 420-432.
- McCormick, A., Donoghue, P., Dixon, M., O'Sullivan, R., O'Donnell, R.L., Kaufmann, A., Curtin, N.J., Edmondson, R.J. (2015). "Ovarian cancers harbour defects in non homologous end joining resulting in error prone repair and resistance to rucaparib." Unpublished.
- McGowan, C. H., Russell, P. (2004). "The DNA damage response: sensing and signaling." Curr Opin Cell Biol **16**(6): 629-633.
- McGuire, W. P., Hoskins, W. J., Brady, M. F., Kucera, P. R., Partridge, E. E., Look, K. Y., Clarke-Pearson, D. L., Davidson, M. (1996). "Cyclophosphamide and cisplatin compared with paclitaxel and cisplatin in patients with stage III and stage IV ovarian cancer." N Engl J Med **334**(1): 1-6.
- Medeiros, F., Muto, M. G., Lee, Y., Elvin, J. A., Callahan, M. J., Feltmate, C., Garber, J. E., Cramer, D. W., Crum, C. P. (2006). "The tubal fimbria is a preferred site for early adenocarcinoma in women with familial ovarian cancer syndrome." Am J Surg Pathol **30**(2): 230-236.
- Meng, Q., Xia, C., Fang, J., Rojanasakul, Y., Jiang, B. H. (2006). "Role of PI3K and AKT specific isoforms in ovarian cancer cell migration, invasion and proliferation through the p70S6K1 pathway." Cell Signal **18**(12): 2262-2271.
- Michel, B., Grompone, G., Flores, M. J., Bidnenko, V. (2004). "Multiple pathways process stalled replication forks." Proc Natl Acad Sci U S A **101**(35): 12783-12788.
- Miller, M. C., Doyle, G. V., Terstappen, L. W. (2010). "Significance of Circulating Tumor Cells Detected by the CellSearch System in Patients with Metastatic Breast Colorectal and Prostate Cancer." J Oncol **2010**: 617421.
- Monteiro, A. N. (2000). "BRCA1: exploring the links to transcription." Trends Biochem Sci **25**(10): 469-474.
- Morgan, R. L., De Young, B. R., McGaughy, V. R., Niemann, T. H. (1999). "MOC-31 aids in the differentiation between adenocarcinoma and reactive mesothelial cells." Cancer **87**(6): 390-394.

- Moynahan, M. E., Chiu, J. W., Koller, B. H., Jasin, M. (1999). "BRCA1 controls homology-directed DNA repair." Mol Cell **4**(4): 511-518.
- Moynahan, M. E., Pierce, A. J., Jasin, M. (2001). "BRCA2 is required for homology-directed repair of chromosomal breaks." Mol Cell **7**(2): 263-272.
- Muggia, F. M., Braly, P. S., Brady, M. F., Sutton, G., Niemann, T. H., Lentz, S. L., Alvarez, R. D., Kucera, P. R., Small, J. M. (2000). "Phase III randomized study of cisplatin versus paclitaxel versus cisplatin and paclitaxel in patients with suboptimal stage III or IV ovarian cancer: a gynecologic oncology group study." J Clin Oncol **18**(1): 106-115.
- Mukhopadhyay, A., Elattar, A., Cerbinskaite, A., Wilkinson, S. J., Drew, Y., Kyle, S., Los, G., Hostomsky, Z., Edmondson, R. J., Curtin, N. J. (2010). "Development of a functional assay for homologous recombination status in primary cultures of epithelial ovarian tumor and correlation with sensitivity to poly(ADP-ribose) polymerase inhibitors." Clin Cancer Res **16**(8): 2344-2351.
- Mukhopadhyay, A., E. R. Plummer, A. Elattar, S. Soohoo, B. Uzir, J. E. Quinn, W. G. McCluggage, P. Maxwell, H. Aneke, N. J. Curtin and R. J. Edmondson (2012). "Clinicopathological features of homologous recombination deficient epithelial ovarian cancers: Sensitivity to PARP inhibitors, platinum and survival." Cancer Research **72**: 5675.
- Mukhopadhyay, A., Plummer, E. R., Elattar, A., Soohoo, S., Uzir, B., Quinn, J. E., McCluggage, W. G., Maxwell, P., Aneke, H., Curtin, N. J., Edmondson, R. J. (2012). "Clinicopathological features of homologous recombination-deficient epithelial ovarian cancers: sensitivity to PARP inhibitors, platinum, and survival." Cancer Res **72**(22): 5675-5682.
- Munz, M., Kieu, C., Mack, B., Schmitt, B., Zeidler, R., Gires, O. (2004). "The carcinoma-associated antigen EpCAM upregulates c-myc and induces cell proliferation." Oncogene **23**(34): 5748-5758.
- Nagaraju, G., Hartlerode, A., Kwok, A., Chandramouly, G., Scully, R. (2009). "XRCC2 and XRCC3 regulate the balance between short- and long-tract gene conversions between sister chromatids." Mol Cell Biol **29**(15): 4283-4294.
- Nagata, Y., Lan, K. H., Zhou, X., Tan, M., Esteva, F. J., Sahin, A. A., Klos, K. S., Li, P., Monia, B. P., Nguyen, N. T., Hortobagyi, G. N., Hung, M. C., Yu, D. (2004). "PTEN activation contributes to tumor inhibition by trastuzumab, and loss of PTEN predicts trastuzumab resistance in patients." Cancer Cell **6**(2): 117-127.
- Nagrath, S., Sequist, L. V., Maheswaran, S., Bell, D. W., Irimia, D., Ulkus, L., Smith, M. R., Kwak, E. L., Digumarthy, S., Muzikansky, A., Ryan, P., Balis, U. J., Tompkins, R. G., Haber, D. A., Toner, M. (2007). "Isolation of rare circulating tumour cells in cancer patients by microchip technology." Nature **450**(7173): 1235-1239.
- Nakayama, K., Nakayama, N., Kurman, R. J., Cope, L., Pohl, G., Samuels, Y., Velculescu, V. E., Wang, T. L., Shih Ie, M. (2006). "Sequence mutations and amplification of PIK3CA and AKT2 genes in purified ovarian serous neoplasms." Cancer Biol Ther **5**(7): 779-785.
- Nakayama, N., Nakayama, K., Yeasmin, S., Ishibashi, M., Katagiri, A., Iida, K., Fukumoto, M., Miyazaki, K. (2008). "KRAS or BRAF mutation status is a useful predictor of sensitivity to MEK inhibition in ovarian cancer." Br J Cancer **99**(12): 2020-2028.

Naumann, R. W., Coleman, R. L., Burger, R. A., Sausville, E. A., Kutarska, E., Ghamande, S. A., Gabrail, N. Y., Penson, R. T., Symanowski, J. T., Lovejoy, C. D., Leaman, C. P., Morgenstern, D. E., Messmann, R. A. (2013). "PRECEDENT: A Randomized Phase II Trial Comparing Vintafolide (EC145) and Pegylated Liposomal Doxorubicin (PLD) in Combination Versus PLD Alone in Patients With Platinum-Resistant Ovarian Cancer." Journal of Clinical Oncology **31**(35): 4400-+.

Navin, N., Kendall, J., Troge, J., Andrews, P., Rodgers, L., McIndoo, J., Cook, K., Stepansky, A., Levy, D., Esposito, D., Muthuswamy, L., Krasnitz, A., McCombie, W. R., Hicks, J., Wigler, M. (2011). "Tumour evolution inferred by single-cell sequencing." Nature **472**(7341): 90-94.

Navin, N., Krasnitz, A., Rodgers, L., Cook, K., Meth, J., Kendall, J., Riggs, M., Eberling, Y., Troge, J., Grubor, V., Levy, D., Lundin, P., Maner, S., Zetterberg, A., Hicks, J., Wigler, M. (2010). "Inferring tumor progression from genomic heterogeneity." Genome Res **20**(1): 68-80.

Neal, J. A., V. Dang, P. Douglas, M. S. Wold, S. P. Lees-Miller and K. Meek (2011). "Inhibition of homologous recombination by DNA-dependent protein kinase requires kinase activity, is titratable, and is modulated by autophosphorylation." Mol Cell Biol **31**(8): 1719-1733.

Network, C. G. A. R. (2011). "Integrated genomic analyses of ovarian carcinoma." Nature **474**(7353): 609-615.

New, J. H., Sugiyama, T., Zaitseva, E., Kowalczykowski, S. C. (1998). "Rad52 protein stimulates DNA strand exchange by Rad51 and replication protein A." Nature **391**(6665): 407-410.

Nielsen, L. L., Dell, J., Maxwell, E., Armstrong, L., Maneval, D., Catino, J. J. (1997). "Efficacy of p53 adenovirus-mediated gene therapy against human breast cancer xenografts." Cancer Gene Ther **4**(2): 129-138.

Nielsen, L. L., Maneval, D. C. (1998). "P53 tumor suppressor gene therapy for cancer." Cancer Gene Ther **5**(1): 52-63.

Nowell, P. C. (1976). "The clonal evolution of tumor cell populations." Science **194**(4260): 23-28.

Ntouroupi, T. G., Ashraf, S. Q., McGregor, S. B., Turney, B. W., Seppo, A., Kim, Y., Wang, X., Kilpatrick, M. W., Tsipouras, P., Tafas, T., Bodmer, W. F. (2008). "Detection of circulating tumour cells in peripheral blood with an automated scanning fluorescence microscope." Br J Cancer **99**(5): 789-795.

Obermayr, E., Castillo-Tong, D. C., Pils, D., Speiser, P., Braicu, I., Van Gorp, T., Mahner, S., Sehouli, J., Vergote, I., Zeillinger, R. (2013). "Molecular characterization of circulating tumor cells in patients with ovarian cancer improves their prognostic significance - A study of the OVCAD consortium." Gynecologic Oncology **128**(1): 15-21.

Olmos, D., Arkenau, H. T., Ang, J. E., Ledaki, I., Attard, G., Carden, C. P., Reid, A. H., A'Hern, R., Fong, P. C., Oomen, N. B., Molife, R., Dearnaley, D., Parker, C., Terstappen, L. W., de Bono, J. S. (2009). "Circulating tumour cell (CTC) counts as intermediate end points in castration-resistant prostate cancer (CRPC): a single-centre experience." Ann Oncol **20**(1): 27-33.

Olsen, C. M., C. M. Nagle, D. C. Whiteman, R. Ness, C. L. Pearce, M. C. Pike, M. A. Rossing, K. L. Terry, A. H. Wu, S. Australian Cancer, G. Australian Ovarian Cancer

Study, H. A. Risch, H. Yu, J. A. Doherty, J. Chang-Claude, R. Hein, S. Nickels, S. Wang-Gohrke, M. T. Goodman, M. E. Carney, R. K. Matsuno, G. Lurie, K. Moysich, S. K. Kjaer, A. Jensen, E. Hogdall, E. L. Goode, B. L. Fridley, R. A. Vierkant, M. C. Larson, J. Schildkraut, C. Hoyo, P. Moorman, R. P. Weber, D. W. Cramer, A. F. Vitonis, E. V. Bandera, S. H. Olson, L. Rodriguez-Rodriguez, M. King, L. A. Brinton, H. Yang, M. Garcia-Closas, J. Lissowska, H. Anton-Culver, A. Ziogas, S. A. Gayther, S. J. Ramus, U. Menon, A. Gentry-Maharaj, P. M. Webb and C. Ovarian Cancer Association (2013). "Obesity and risk of ovarian cancer subtypes: evidence from the Ovarian Cancer Association Consortium." Endocr Relat Cancer **20**(2): 251-262.

Omura, G. A., Brady, M. F., Homesley, H. D., Yordan, E., Major, F. J., Buchsbaum, H. J., Park, R. C. (1991). "Long-term follow-up and prognostic factor analysis in advanced ovarian carcinoma: the Gynecologic Oncology Group experience." J Clin Oncol **9**(7): 1138-1150.

Orimo, A., Weinberg, R. A. (2006). "Stromal fibroblasts in cancer: a novel tumor-promoting cell type." Cell Cycle **5**(15): 1597-1601.

Owens, J. K., Shewach, D. S., Ullman, B., Mitchell, B. S. (1992). "Resistance to 1-beta-D-arabinofuranosylcytosine in human T-lymphoblasts mediated by mutations within the deoxycytidine kinase gene." Cancer Res **52**(9): 2389-2393.

Pantel, K., Alix-Panabières, Catherine (2010). "Circulating tumour cells in cancer patients: challenges and perspectives." Trends in Molecular Medicine **16**(9): 398-406.

Pantel, K., Cote, R. J., Fodstad, O. (1999). "Detection and clinical importance of micrometastatic disease." J Natl Cancer Inst **91**(13): 1113-1124.

Pastor-Anglada, M., Cano-Soldado, P., Molina-Arcas, M., Lostao, M. P., Larrayoz, I., Martinez-Picado, J., Casado, F. J. (2005). "Cell entry and export of nucleoside analogues." Virus Res **107**(2): 151-164.

Paterlini-Brechot, P., Benali, N. L. (2007). "Circulating tumor cells (CTC) detection: clinical impact and future directions." Cancer Lett **253**(2): 180-204.

Patocs, A., Zhang, L., Xu, Y., Weber, F., Caldes, T., Mutter, G. L., Platzer, P., Eng, C. (2007). "Breast-cancer stromal cells with TP53 mutations and nodal metastases." N Engl J Med **357**(25): 2543-2551.

Paull, T. T., Lee, J. H. (2005). "The Mre11/Rad50/Nbs1 complex and its role as a DNA double-strand break sensor for ATM." Cell Cycle **4**(6): 737-740.

Pellegrini, L., Yu, D. S., Lo, T., Anand, S., Lee, M., Blundell, T. L., Venkitaraman, A. R. (2002). "Insights into DNA recombination from the structure of a RAD51-BRCA2 complex." Nature **420**(6913): 287-293.

Peltomaki, P. (2003). "Role of DNA mismatch repair defects in the pathogenesis of human cancer." J Clin Oncol **21**(6): 1174-1179.

Peltomaki, P. and H. Vasen (2004). "Mutations associated with HNPCC predisposition -- Update of ICG-HNPCC/INSIGHT mutation database." Dis Markers **20**(4-5): 269-276.

Pennington, K. P., Walsh, T., Harrell, M. I., Lee, M. K., Pennil, C. C., Rendi, M. H., Thornton, A., Norquist, B. M., Casadei, S., Nord, A. S., Agnew, K. J., Pritchard, C. C., Scroggins, S., Garcia, R. L., King, M. C., Swisher, E. M. (2014). "Germline and somatic mutations in homologous recombination genes predict platinum response

and survival in ovarian, fallopian tube, and peritoneal carcinomas." Clin Cancer Res **20**(3): 764-775.

Perren, T. J., Swart, A. M., Pfisterer, J., Ledermann, J. A., Pujade-Lauraine, E., Kristensen, G., Carey, M. S., Beale, P., Qian, W., Parmar, M. K., Oza, A. M., Icon Investigators (2011). "A phase 3 trial of bevacizumab in ovarian cancer." N Engl J Med **365**(26): 2484-2496.

Petrini, J. H., Bressan, D. A., Yao, M. S. (1997). "The RAD52 epistasis group in mammalian double strand break repair." Semin Immunol **9**(3): 181-188.

Pfisterer, J., Weber, B., Reuss, A., Kimmig, R., du Bois, A., Wagner, U., Bourgeois, H., Meier, W., Costa, S., Meden, H., Nitz, U., Pujade-Lauraine, E., Ago, Ovar, Gineco, (2006). "Randomized phase III trial of topotecan following carboplatin and paclitaxel in first-line treatment of advanced ovarian cancer: a gynecologic cancer intergroup trial of the AGO-OVAR and GINECO." J Natl Cancer Inst **98**(15): 1036-1045.

Pharoah, P. D., Easton, D. F., Stockton, D. L., Gayther, S., Ponder, B. A. (1999). "Survival in familial, BRCA1-associated, and BRCA2-associated epithelial ovarian cancer. United Kingdom Coordinating Committee for Cancer Research (UKCCCR) Familial Ovarian Cancer Study Group." Cancer Res **59**(4): 868-871.

Piccart, M. J., Bertelsen, K., James, K., Cassidy, J., Mangioni, C., Simonsen, E., Stuart, G., Kaye, S., Vergote, I., Andersen, J. E., Zee, B., Paul, J., Baron, B., Pecorelli, S. (2000). "Randomized intergroup trial of cisplatin-paclitaxel versus cisplatin-cyclophosphamide in women with advanced epithelial ovarian cancer: three-year results." J Natl Cancer Inst **92**(9): 699-708.

Piek, J. M., Kenemans, P., Zweemer, R. P., van Diest, P. J., Verheijen, R. H. (2007). "Ovarian carcinogenesis, an alternative theory." Gynecol Oncol **107**(2): 355.

Piek, J. M., van Diest, P. J., Zweemer, R. P., Kenemans, P., Verheijen, R. H. (2001). "Tubal ligation and risk of ovarian cancer." Lancet **358**(9284): 844.

Pieretti, M., Hopenhayn-Rich, C., Khatrar, N. H., Cao, Y., Huang, B., Tucker, T. C. (2002). "Heterogeneity of ovarian cancer: relationships among histological group, stage of disease, tumor markers, patient characteristics, and survival." Cancer Invest **20**(1): 11-23.

Plumb, J. A., Aherne, W., Lee, D., Westwood, N., O'Brien, V., McDonald, E., Brown, R. (2006). "MMR201: a novel small molecule that selectively inhibits growth of MLH1 deficient tumour cells." Proc Am Assoc Cancer Res Res **47**(Abs 2435).

Plummer, E. R., Calvert, Hilary (2007). "Targeting Poly(ADP-Ribose) Polymerase: A Two-Armed Strategy for Cancer Therapy." Clinical Cancer Research **13**(21): 6252-6256.

Plummer, E. R., Middleton, M. R., Jones, C., Olsen, A., Hickson, I., McHugh, P., Margison, G. P., McGown, G., Thorncroft, M., Watson, A. J., Boddy, A. V., Calvert, A. H., Harris, A. L., Newell, D. R., Curtin, N. J. (2005). "Temozolomide pharmacodynamics in patients with metastatic melanoma: dna damage and activity of repair enzymes O6-alkylguanine alkyltransferase and poly(ADP-ribose) polymerase-1." Clin Cancer Res **11**(9): 3402-3409.

Plummer, R., C. Jones, M. Middleton, R. Wilson, J. Evans, A. Olsen, N. Curtin, A. Boddy, P. McHugh, D. Newell, A. Harris, P. Johnson, H. Steinfeldt, R. Dewji, D. Wang, L. Robson and H. Calvert (2008). "Phase I study of the poly(ADP-ribose)

polymerase inhibitor, AG014699, in combination with temozolomide in patients with advanced solid tumors." Clin Cancer Res **14**(23): 7917-7923.

Plummer, R., Lorigan, P., Steven, N., Scott, L., Middleton, M. R., Wilson, R. H., Mulligan, E., Curtin, N., Wang, D., Dewji, R., Abbattista, A., Gallo, J., Calvert, H. (2013). "A phase II study of the potent PARP inhibitor, Rucaparib (PF-01367338, AG014699), with temozolomide in patients with metastatic melanoma demonstrating evidence of chemopotential." Cancer Chemother Pharmacol **71**(5): 1191-1199.

Plummer, R., P. Woll, D. Fyfe, A. V. Boddy, M. Griffin, P. Hewitt, J. Carmichael, F. Namouni, M. Cohen and M. Verrill (2008). "A phase I and pharmacokinetic study of ixabepilone in combination with Carboplatin in patients with advanced solid malignancies." Clin Cancer Res **14**(24): 8288-8294.

Plunkett, W., P. Huang, Y. Z. Xu, V. Heinemann, R. Grunewald and V. Gandhi (1995). "Gemcitabine: metabolism, mechanisms of action, and self-potential." Semin Oncol **22**(4 Suppl 11): 3-10.

Polyak, K., Weinberg, R. A. (2009). "Transitions between epithelial and mesenchymal states: acquisition of malignant and stem cell traits." Nat Rev Cancer **9**(4): 265-273.

Prat, J., FIGO Committee on Gynecologic Oncology (2013). "Staging classification for cancer of the ovary, fallopian tube, and peritoneum." Int J Gynaecol Obstet.

Przybycin, C. G., urman, R. J., Ronnett, B. M., Shih le, M., Vang, R. (2010). "Are all pelvic (nonuterine) serous carcinomas of tubal origin?" Am J Surg Pathol **34**(10): 1407-1416.

Pujade-Lauraine, E., Hilpert, F., Weber, B., Reuss, A., Poveda, A., Kristensen, G., Sorio, R., Vergote, I. B., Witteveen, P., Bamias, A., Pereira, D., Wimberger, P., Oaknin, A., Mirza, M. R., Follana, P., Bollag, D. T., Ray-Coquard, I., AURELIA Investigators (2012). "AURELIA: A randomized phase III trial evaluating bevacizumab (BEV) plus chemotherapy (CT) for platinum (PT)-resistant recurrent ovarian cancer (OC)." Journal of Clinical Oncology **30**(18).

Purnell, M. R., Whish, W. J. (1980). "Novel inhibitors of poly(ADP-ribose) synthetase." Biochem J **185**(3): 775-777.

Ramus, S. J., Pharoah, P. D., Harrington, P., Pye, C., Werness, B., Bobrow, L., Ayhan, A., Wells, D., Fishman, A., Gore, M., DiCioccio, R. A., Piver, M. S., Whittemore, A. S., Ponder, B. A., Gayther, S. A. (2003). "BRCA1/2 mutation status influences somatic genetic progression in inherited and sporadic epithelial ovarian cancer cases." Cancer Res **63**(2): 417-423.

Rao, C. G., Chianese, D., Doyle, G. V., Miller, M. C., Russell, T., Sanders, R. A., Jr., Terstappen, L. W. (2005). "Expression of epithelial cell adhesion molecule in carcinoma cells present in blood and primary and metastatic tumors." Int J Oncol **27**(1): 49-57.

Ratner, E. S., Keane, F. K., Lindner, R., Tassi, R. A., Paranjape, T., Glasgow, M., Nallur, S., Deng, Y., Lu, L., Steele, L., Sand, S., Muller, R. U., Bignotti, E., Neuhausen, S. L., Schwartz, P. E., Slack, F. J., Santin, A. D., Weidhaas, J. B. (2011). "A KRAS variant is a biomarker of poor outcome, platinum chemotherapy resistance and a potential target for therapy in ovarian cancer." Oncogene.

Ravandi, F., Faderl, S., Cortes, J.E., Garcia-Manero, G., Jabbour, E., Boone, P.A., Kadia, T., Borthakur, G., Wierda, W.G., Wetzler, M., Venugopal, P., Chiao, J.,

- Kantarjian, H.M. (2011). "Phase 1/ 2 Study of Sapacitabine and Decitabine Administered Sequentially in Elderly Patients with Newly Diagnosed AML." Blood **118**(Abstract 3630).
- Rebucci, M., Michiels, C. (2013). "Molecular aspects of cancer cell resistance to chemotherapy." Biochem Pharmacol **85**(9): 1219-1226.
- Riethdorf, S., Fritsche, H., Muller, V., Rau, T., Schindlbeck, C., Rack, B., Janni, W., Coith, C., Beck, K., Janicke, F., Jackson, S., Gornet, T., Cristofanilli, M., Pantel, K. (2007). "Detection of circulating tumor cells in peripheral blood of patients with metastatic breast cancer: a validation study of the CellSearch system." Clin Cancer Res **13**(3): 920-928.
- Righetti, S. C., Della Torre, G., Pilotti, S., Menard, S., Ottone, F., Colnaghi, M. I., Pierotti, M. A., Lavarino, C., Cornarotti, M., Oriana, S., Bohm, S., Bresciani, G. L., Spatti, G., Zunino, F. (1996). "A comparative study of p53 gene mutations, protein accumulation, and response to cisplatin-based chemotherapy in advanced ovarian carcinoma." Cancer Res **56**(4): 689-693.
- Rinne, M., Caldwell, D., Kelley, M. R. (2004). "Transient adenoviral N-methylpurine DNA glycosylase overexpression imparts chemotherapeutic sensitivity to human breast cancer cells." Mol Cancer Ther **3**(8): 955-967.
- Risch, H. A., McLaughlin, J. R., Cole, D. E., Rosen, B., Bradley, L., Kwan, E., Jack, E., Vesprini, D. J., Kuperstein, G., Abrahamson, J. L., Fan, I., Wong, B., Narod, S. A. (2001). "Prevalence and penetrance of germline BRCA1 and BRCA2 mutations in a population series of 649 women with ovarian cancer." Am J Hum Genet **68**(3): 700-710.
- Robles-Diaz, L., Goldfrank, D. J., Kauff, N. D., Robson, M., Offit, K. (2004). "Hereditary ovarian cancer in Ashkenazi Jews." Fam Cancer **3**(3-4): 259-264.
- Rodriguez-Casuriaga, R., Geisinger, A., Lopez-Carro, B., Porro, V., Wettstein, R., Folle, G. A. (2009). "Ultra-fast and optimized method for the preparation of rodent testicular cells for flow cytometric analysis." Biol Proced Online **11**: 184-195.
- Rogakou, E. P., Pilch, D. R., Orr, A. H., Ivanova, V. S., Bonner, W. M. (1998). "DNA double-stranded breaks induce histone H2AX phosphorylation on serine 139." J Biol Chem **273**(10): 5858-5868.
- Rosen, D. G., Wang, L., Atkinson, J. N., Yu, Y., Lu, K. H., Diamandis, E. P., Hellstrom, I., Mok, S. C., Liu, J., Bast, R. C., Jr. (2005). "Potential markers that complement expression of CA125 in epithelial ovarian cancer." Gynecol Oncol **99**(2): 267-277.
- Roth, J. A., Nguyen, D., Lawrence, D. D., Kemp, B. L., Carrasco, C. H., Ferson, D. Z., Hong, W. K., Komaki, R., Lee, J. J., Stephens, L. C., McDonnell, T. J., Mukhopadhyay, T., Cai, D. (1996). "Retrovirus-mediated wild-type p53 gene transfer to tumors of patients with lung cancer." Nat Med **2**(9): 985-991.
- Ruitenbeek, T., Gouw, A. S., Poppema, S. (1994). "Immunocytology of body cavity fluids. MOC-31, a monoclonal antibody discriminating between mesothelial and epithelial cells." Arch Pathol Lab Med **118**(3): 265-269.
- Russell, S. E., McCluggage, W. G. (2004). "A multistep model for ovarian tumorigenesis: the value of mutation analysis in the KRAS and BRAF genes." J Pathol **203**(2): 617-619.

- Rustin, G. J. (2004). "Can we now agree to use the same definition to measure response according to CA-125?" J Clin Oncol **22**(20): 4035-4036.
- Rustin, G. J., Vergote, I., Eisenhauer, E., Pujade-Lauraine, E., Quinn, M., Thigpen, T., du Bois, A., Kristensen, G., Jakobsen, A., Sagae, S., Greven, K., Parmar, M., Friedlander, M., Cervantes, A., Vermorken, J., Gynecological Cancer, Intergroup (2011). "Definitions for response and progression in ovarian cancer clinical trials incorporating RECIST 1.1 and CA 125 agreed by the Gynecological Cancer Intergroup (GCIg)." Int J Gynecol Cancer **21**(2): 419-423.
- Sabbah, M., Emami, S., Redeuilh, G., Julien, S., Prevost, G., Zimber, A., Ouelaa, R., Bracke, M., De Wever, O., Gespach, C. (2008). "Molecular signature and therapeutic perspective of the epithelial-to-mesenchymal transitions in epithelial cancers." Drug Resist Updat **11**(4-5): 123-151.
- Saffhill, R., Margison, G. P., O'Connor, P. J. (1985). "Mechanisms of carcinogenesis induced by alkylating agents." Biochim Biophys Acta **823**(2): 111-145.
- Saldivar, J. S., Wu, X., Follen, M., Gershenson, D. (2007). "Nucleotide excision repair pathway review I: implications in ovarian cancer and platinum sensitivity." Gynecol Oncol **107**(1 Suppl 1): S56-71.
- Salehi, F., Dunfield, L., Phillips, K. P., Krewski, D., Vanderhyden, B. C. (2008). "Risk factors for ovarian cancer: an overview with emphasis on hormonal factors." J Toxicol Environ Health B Crit Rev **11**(3-4): 301-321.
- Sankhala, K., Takimoto, C.H., Mita, A.C. (2008). "Two phase I, pharmacokinetic and pharmacodynamics studies of TAS-109, a novel nucleotide analogue with 14 days and 7 days continuous infusion schedules. ." Proc Am Soc Clin Oncol **26**.
- Sapi, E., Okpokwasili, N. I., Rutherford, T. (2002). "Detection of telomerase-positive circulating epithelial cells in ovarian cancer patients." Cancer Detection and Prevention **26**(2): 158-167.
- Scartozzi, M., De Nicolis, M., Galizia, E., Carassai, P., Bianchi, F., Berardi, R., Gesuita, R., Piga, A., Cellierino, R., Porfiri, E. (2003). "Loss of hMLH1 expression correlates with improved survival in stage III-IV ovarian cancer patients." Eur J Cancer **39**(8): 1144-1149.
- Schauer, I. G., Sood, A. K., Mok, S., Liu, J. (2011). "Cancer-associated fibroblasts and their putative role in potentiating the initiation and development of epithelial ovarian cancer." Neoplasia **13**(5): 393-405.
- Schmeichel, K. L., Bissell, M. J. (2003). "Modeling tissue-specific signaling and organ function in three dimensions." J Cell Sci **116**(Pt 12): 2377-2388.
- Schondorf, T., Gohring, U. J., Roth, G., Middel, I., Becker, M., Moser, N., Valter, M. M., Hoopmann, M. (2003). "Time to progression is dependent on the expression of the tumour suppressor PTEN in ovarian cancer patients." Eur J Clin Invest **33**(3): 256-260.
- Schreiber, V., Ame, J. C., Dolle, P., Schultz, I., Rinaldi, B., Fraulob, V., Menissier-de Murcia, J., de Murcia, G. (2002). "Poly(ADP-ribose) polymerase-2 (PARP-2) is required for efficient base excision DNA repair in association with PARP-1 and XRCC1." J Biol Chem **277**(25): 23028-23036.
- Schreiber, V., Dantzer, F., Ame, J. C., de Murcia, G. (2006). "Poly(ADP-ribose): novel functions for an old molecule." Nat Rev Mol Cell Biol **7**(7): 517-528.

- Schultz, N., Lopez, E., Saleh-Gohari, N., Helleday, T. (2003). "Poly(ADP-ribose) polymerase (PARP-1) has a controlling role in homologous recombination." Nucleic Acids Res **31**(17): 4959-4964.
- Schwarz, R. F., Ng, C. K., Cooke, S. L., Newman, S., Temple, J., Piskorz, A. M., Gale, D., Sayal, K., Murtaza, M., Baldwin, P. J., Rosenfeld, N., Earl, H. M., Sala, E., Jimenez-Linan, M., Parkinson, C. A., Markowitz, F., Brenton, J. D. (2015). "Spatial and temporal heterogeneity in high-grade serous ovarian cancer: a phylogenetic analysis." PLoS Med **12**(2): e1001789.
- Scully, R. and D. M. Livingston (2000). "In search of the tumour-suppressor functions of BRCA1 and BRCA2." Nature **408**(6811): 429-432.
- Scully, R. E. (1975). "World Health Organization classification and nomenclature of ovarian cancer." Natl Cancer Inst Monogr **42**: 5-7.
- Sedelnikova, O. A., Rogakou, E. P., Panyutin, I. G., Bonner, W. M. (2002). "Quantitative detection of (125)IdU-induced DNA double-strand breaks with gamma-H2AX antibody." Radiat Res **158**(4): 486-492.
- Selvakumaran, M., Pisarcik, D. A., Bao, R., Yeung, A. T., Hamilton, T. C. (2003). "Enhanced cisplatin cytotoxicity by disturbing the nucleotide excision repair pathway in ovarian cancer cell lines." Cancer Res **63**(6): 1311-1316.
- SenGupta, D. J., Lum, P. Y., Lai, Y., Shubochkina, E., Bakken, A. H., Schneider, G., Unadkat, J. D. (2002). "A single glycine mutation in the equilibrative nucleoside transporter gene, hENT1, alters nucleoside transport activity and sensitivity to nitrobenzylthioinosine." Biochemistry **41**(5): 1512-1519.
- Sequist, L. V., Nagrath, S., Toner, M., Haber, D. A., Lynch, T. J. (2009). "The CTC-chip: an exciting new tool to detect circulating tumor cells in lung cancer patients." J Thorac Oncol **4**(3): 281-283.
- Serova, M., Galmarini, C. M., Ghoul, A., Benhadji, K., Green, S. R., Chiao, J., Faivre, S., Cvitkovic, E., Le Tourneau, C., Calvo, F., Raymond, E. (2007). "Antiproliferative effects of sapacitabine (CYC682), a novel 2'-deoxycytidine-derivative, in human cancer cells." Br J Cancer **97**(5): 628-636.
- Serrano Fernadez, M. J., Alvarez Merino, J. C., Martinez Zubiaurre, I., Fernandez Garcia, A., Sanchez Rovira, P., Lorente Acosta, J. A. (2009). "Clinical relevance associated to the analysis of circulating tumour cells in patients with solid tumours." Clin Transl Oncol **11**(10): 659-668.
- Shah, S. P., Morin, R. D., Khattra, J., Prentice, L., Pugh, T., Burleigh, A., Delaney, A., Gelmon, K., Guliany, R., Huntsman, D., Hirst, M., Marra, M. A., Aparicio, S. (2009). "Mutational evolution in a lobular breast tumour profiled at single nucleotide resolution." Nature **461**(7265): 809-813.
- Shapiro, G., Kwak, E.L., Cleary, J.M., Tolaney, S., Gandhi, L., Clark, J.W., Wolanski, A., Frame, S., Rodig, S.J., Chiao, J.H. (2012). "Phase I study of sequential sapacitabine and seliciclib in patients with advanced solid tumors." J Clin Oncol **30**(suppl; abstr 3053).
- Shayesteh, L., Lu, Y., Kuo, W. L., Baldocchi, R., Godfrey, T., Collins, C., Pinkel, D., Powell, B., Mills, G. B., Gray, J. W. (1999). "PIK3CA is implicated as an oncogene in ovarian cancer." Nat Genet **21**(1): 99-102.

- Shen, G. H., Ghazizadeh, M., Kawanami, O., Shimizu, H., Jin, E., Araki, T., Sugisaki, Y. (2000). "Prognostic significance of vascular endothelial growth factor expression in human ovarian carcinoma." Br J Cancer **83**(2): 196-203.
- Sheng, Q., Y. Zhang, R. Wang, J. Zhang, B. Chen, J. Wang, W. Zhang and X. Xin (2012). "Prognostic significance of APE1 cytoplasmic localization in human epithelial ovarian cancer." Med Oncol **29**(2): 1265-1271.
- Shepherd, T. G., Theriault, B. L., Campbell, E. J., Nachtigal, M. W. (2006). "Primary culture of ovarian surface epithelial cells and ascites-derived ovarian cancer cells from patients." Nat Protoc **1**(6): 2643-2649.
- Shih, I. M. and R. J. Kurman (2004). "Ovarian Tumorigenesis: A Proposed Model Based on Morphological and Molecular Genetic Analysis." The American Journal of Pathology **164**(5): 1511-1518.
- Shih, J. Y., A. Yuan, J. J. W. Chen and P. C. Yang (2006). "Tumor-Associated Macrophage: Its Role in Cancer Invasion and Metastasis." J. Cancer Mol **2**(3): 101-106.
- Shih, M., Kurman, R. J. (2004). "Ovarian tumorigenesis: a proposed model based on morphological and molecular genetic analysis." Am J Pathol **164**(5): 1511-1518.
- Shimizu, Y., Kamoi, S., Amada, S., Akiyama, F., Silverberg, S. G. (1998). "Toward the development of a universal grading system for ovarian epithelial carcinoma: testing of a proposed system in a series of 461 patients with uniform treatment and follow-up." Cancer **82**(5): 893-901.
- Shivji, M. K., Mukund, S. R., Rajendra, E., Chen, S., Short, J. M., Savill, J., Klenerman, D., Venkitaraman, A. R. (2009). "The BRC repeats of human BRCA2 differentially regulate RAD51 binding on single- versus double-stranded DNA to stimulate strand exchange." Proc Natl Acad Sci U S A **106**(32): 13254-13259.
- Shrivastav, M., De Haro, L. P., Nickoloff, J. A. (2008). "Regulation of DNA double-strand break repair pathway choice." Cell Res **18**(1): 134-147.
- Siddik, Z. H. (2003). "Cisplatin: mode of cytotoxic action and molecular basis of resistance." Oncogene **22**(47): 7265-7279.
- Sieuwerts, A. M., Kraan, J., Bolt, J., van der Spoel, P., Elstrodt, F., Schutte, M., Martens, J. W., Gratama, J. W., Sleijfer, S., Foekens, J. A. (2009). "Anti-epithelial cell adhesion molecule antibodies and the detection of circulating normal-like breast tumor cells." J Natl Cancer Inst **101**(1): 61-66.
- Siliciano, J. D., Canman, C. E., Taya, Y., Sakaguchi, K., Appella, E., Kastan, M. B. (1997). "DNA damage induces phosphorylation of the amino terminus of p53." Genes Dev **11**(24): 3471-3481.
- Silverberg, S. G. (2000). "Histopathologic grading of ovarian carcinoma: a review and proposal." Int J Gynecol Pathol **19**(1): 7-15.
- Singer, G., R. Oldt, 3rd, Y. Cohen, B. G. Wang, D. Sidransky, R. J. Kurman and M. Shih le (2003). "Mutations in BRAF and KRAS characterize the development of low-grade ovarian serous carcinoma." J Natl Cancer Inst **95**(6): 484-486.
- Singer, G., R. Stohr, L. Cope, R. Dehari, A. Hartmann, D. F. Cao, T. L. Wang, R. J. Kurman and M. Shih le (2005). "Patterns of p53 mutations separate ovarian serous borderline tumors and low- and high-grade carcinomas and provide support for a new

- model of ovarian carcinogenesis: a mutational analysis with immunohistochemical correlation." Am J Surg Pathol **29**(2): 218-224.
- Sinicrope, F. A., Sargent, D. J. (2012). "Molecular pathways: microsatellite instability in colorectal cancer: prognostic, predictive, and therapeutic implications." Clin Cancer Res **18**(6): 1506-1512.
- Skehan, P., Storeng, R., Scudiero, D., Monks, A., McMahon, J., Vistica, D., Warren, J. T., Bokesch, H., Kenney, S., Boyd, M. R. (1990). "New colorimetric cytotoxicity assay for anticancer-drug screening." J Natl Cancer Inst **82**(13): 1107-1112.
- Sleijfer, S., Gratama, J. W., Sieuwerts, A. M., Kraan, J., Martens, J. W., Foekens, J. A. (2007). "Circulating tumour cell detection on its way to routine diagnostic implementation?" Eur J Cancer **43**(18): 2645-2650.
- Smalley, K. S. (2003). "A pivotal role for ERK in the oncogenic behaviour of malignant melanoma?" Int J Cancer **104**(5): 527-532.
- Smith, N. D., Rubenstein, J. N., Eggener, S. E., Kozlowski, J. M. (2003). "The p53 tumor suppressor gene and nuclear protein: basic science review and relevance in the management of bladder cancer." J Urol **169**(4): 1219-1228.
- Smith, S. A., D. F. Easton, D. G. Evans and B. A. Ponder (1992). "Allele losses in the region 17q12-21 in familial breast and ovarian cancer involve the wild-type chromosome." Nat Genet **2**(2): 128-131.
- Sonmezer, M., Gungor, M., Ensari, A., Ortac, F. (2004). "Prognostic significance of tumor angiogenesis in epithelial ovarian cancer: in association with transforming growth factor beta and vascular endothelial growth factor." Int J Gynecol Cancer **14**(1): 82-88.
- Souhami, R. L., Beverley, P. C., Bobrow, L. G., Ledermann, J. A. (1991). "Antigens of lung cancer: results of the second international workshop on lung cancer antigens." J Natl Cancer Inst **83**(9): 609-612.
- Spentzos, D., Levine, D. A., Ramoni, M. F., Joseph, M., Gu, X., Boyd, J., Libermann, T. A., Cannistra, S. A. (2004). "Gene expression signature with independent prognostic significance in epithelial ovarian cancer." J Clin Oncol **22**(23): 4700-4710.
- Stakenborg, T., Liu, C., Henry, O., O'Sullivan, C. K., Fermer, C., Roeser, T., Ritzi-Lehnert, M., Hauch, S., Borgen, E., Laddach, N., Lagae, L. (2010). "Lab-on-a-chip for the isolation and characterization of circulating tumor cells." Conf Proc IEEE Eng Med Biol Soc **2010**: 292-294.
- Stany, M. P., Bonome, T., Wamunyokoli, F., Zorn, K., Ozbun, L., Park, D. C., Hao, K., Boyd, J., Sood, A. K., Gershenson, D. M., Berkowitz, R. S., Mok, S. C., Birrer, M. J. (2008). "Classification of ovarian cancer: a genomic analysis." Adv Exp Med Biol **622**: 23-33.
- STEMCELL_Technologies. "EasySep Human CD45 Depletion Kit." Retrieved 23.06.13, from <http://www.stemcell.com/en/Products/All-Products/EasySep-Human-CD45-Depletion-Kit.aspx>.
- Stott, S. L., Hsu, C. H., Tsukrov, D. I., Yu, M., Miyamoto, D. T., Waltman, B. A., Rothenberg, S. M., Shah, A. M., Smas, M. E., Korir, G. K., Floyd, F. P., Jr., Gilman, A. J., Lord, J. B., Winokur, , , Springer, S., Irimia, D., Nagrath, S., Sequist, L. V., Lee, R. J., Isselbacher, K. J., Maheswaran, S., Haber, D. A., Toner, M. (2010). "Isolation of circulating tumor cells using a microvortex-generating herringbone-chip." Proc Natl Acad Sci U S A **107**(43): 18392-18397.

- Strand, J., Hamilton, A. E., Beavers, L. S., Gamboa, G. C., Apelgren, L. D., Taber, L. D., Sportsman, J. R., Bumol, T. F., Sharp, J. D., Gadski, R. A. (1989). "Molecular cloning and characterization of a human adenocarcinoma/epithelial cell surface antigen complementary DNA." Cancer Res **49**(2): 314-317.
- Strathdee, G., MacKean, M. J., Illand, M., Brown, R. (1999). "A role for methylation of the hMLH1 promoter in loss of hMLH1 expression and drug resistance in ovarian cancer." Oncogene **18**(14): 2335-2341.
- Strauss, R., Li, Z. Y., Liu, Y., Beyer, I., Persson, J., Sova, P., Moller, T., Pesonen, S., Hemminki, A., Hamerlik, P., Drescher, C., Urban, N., Bartek, J., Lieber, A. (2011). "Analysis of epithelial and mesenchymal markers in ovarian cancer reveals phenotypic heterogeneity and plasticity." PLoS One **6**(1): e16186.
- Sueblinvong, T., Carney, M.E. (2009). "Current understanding of risk factors for ovarian cancer." Curr Treat Options Oncol. **10**(1-2): 67-81.
- Sung, P. (1994). "Catalysis of ATP-dependent homologous DNA pairing and strand exchange by yeast RAD51 protein." Science **265**(5176): 1241-1243.
- Sung, P. (1997). "Function of yeast Rad52 protein as a mediator between replication protein A and the Rad51 recombinase." J Biol Chem **272**(45): 28194-28197.
- Sung, P., Klein, H. (2006). "Mechanism of homologous recombination: mediators and helicases take on regulatory functions." Nat Rev Mol Cell Biol **7**(10): 739-750.
- Suto, M. J., Turner, W. R., Arundel-Suto, C. M., Werbel, L. M., ebolt-Leopold, J. S. (1991). "Dihydroisoquinolinones: the design and synthesis of a new series of potent inhibitors of poly(ADP-ribose) polymerase." Anticancer Drug Des **6**(2): 107-117.
- Suzuki, H., Itoh, F., Toyota, M., Kikuchi, T., Kakiuchi, H., Hinoda, Y., Imai, K. (1999). "Distinct methylation pattern and microsatellite instability in sporadic gastric cancer." Int J Cancer **83**(3): 309-313.
- Sy, S. M., Huen, M. S., Chen, J. (2009). "PALB2 is an integral component of the BRCA complex required for homologous recombination repair." Proc Natl Acad Sci U S A **106**(17): 7155-7160.
- Takata, M., Sasaki, M. S., Sonoda, E., Fukushima, T., Morrison, C., Albala, J. S., Swagemakers, S. M., Kanaar, R., Thompson, L. H., Takeda, S. (2000). "The Rad51 paralog Rad51B promotes homologous recombinational repair." Mol Cell Biol **20**(17): 6476-6482.
- Talasaz, A. H., Powell, A. A., Huber, D. E., Berbee, J. G., Roh, K. H., Yu, W., Xiao, W., Davis, M. M., Pease, R. F., Mindrinos, M. N., Jeffrey, S. S., Davis, R. W. (2009). "Isolating highly enriched populations of circulating epithelial cells and other rare cells from blood using a magnetic sweeper device." Proc Natl Acad Sci U S A **106**(10): 3970-3975.
- Talpaert-Borle, M., Liuzzi, M. (1983). "Reaction of apurinic/apyrimidinic sites with [14C]methoxyamine. A method for the quantitative assay of AP sites in DNA." Biochim Biophys Acta **740**(4): 410-416.
- Tambini, C. E., Spink, K. G., Ross, C. J., Hill, M. A., Thacker, J. (2010). "The importance of XRCC2 in RAD51-related DNA damage repair." DNA Repair (Amst) **9**(5): 517-525.

- Tan, S. J., Lakshmi, R. L., Chen, P., Lim, W. T., Yobas, L., Lim, C. T. (2010). "Versatile label free biochip for the detection of circulating tumor cells from peripheral blood in cancer patients." Biosens Bioelectron **26**(4): 1701-1705.
- Tan, T. Z., Miow, Qing Hao, Huang, Ruby Yun-Ju, Wong, Meng Kang, Ye, Jieru, Lau, Jieying Amelia, Wu, Meng Chu, Bin Abdul Hadi, Luqman Hakim, Soong, Richie, Choolani, Mahesh, Davidson, Ben, Nesland, Jahn M., Wang, Ling-Zhi, Matsumura, Noriomi, Mandai, Masaki, Konishi, Ikuo, Goh, Boon-Cher, Chang, Jeffrey T., Thiery, Jean Paul, Mori, Seiichi (2013). "Functional genomics identifies five distinct molecular subtypes with clinical relevance and pathways for growth control in epithelial ovarian cancer." EMBO Molecular Medicine **5**(7): 1051-1066.
- Tanaka, M. (1992). "Enhancement of the cytotoxicity of cytosine arabinoside by interleukin-3." Jpn J Cancer Res **83**(2): 194-199.
- Tang, J. Y., Hwang, B. J., Ford, J. M., Hanawalt, P. C., Chu, G. (2000). "Xeroderma pigmentosum p48 gene enhances global genomic repair and suppresses UV-induced mutagenesis." Mol Cell **5**(4): 737-744.
- Taniguchi, T., Tischkowitz, M., Ameziane, N., Hodgson, S. V., Mathew, C. G., Joenje, H., Mok, S. C., D'Andrea, A. D. (2003). "Disruption of the Fanconi anemia-BRCA pathway in cisplatin-sensitive ovarian tumors." Nat Med **9**(5): 568-574.
- Tapia, G., Diaz-Padilla, I. (2012). Molecular Mechanisms of Platinum Resistance in Ovarian Cancer. Ovarian Cancer - A Clinical and Translational Update. I. Diaz-Padilla.
- Tavassoli, F. A., Devilee, P., World Health Organization (2003). Pathology and Genetics of Tumours of the Breast and Female Genital Organs, International Agency for Research on Cancer Press.
- Taverna, P., Liu, L., Hwang, H. S., Hanson, A. J., Kinsella, T. J., Gerson, S. L. (2001). "Methoxyamine potentiates DNA single strand breaks and double strand breaks induced by temozolomide in colon cancer cells." Mutat Res **485**(4): 269-281.
- TCGA (2011). "Integrated genomic analyses of ovarian carcinoma." Nature **474**(7353): 609-615.
- Technologies, L. "APEX™ Alexa Fluor® 594 Antibody Labeling Kit." from <http://products.invitrogen.com/ivgn/product/A10474>.
- Tentori, L., C. Leonetti and M. Scarsella (2003). "Systemic administration of GPI 15427, a novel poly(ADPribose) polymerase-1 inhibitor, increases the antitumor activity of temozolomide against intracranial melanoma, glioma, lymphoma." Clin Cancer Res **9**(7270-5379).
- Terstappen, L. W., Rao, C., Gross, S., Weiss, A. J. (2000). "Peripheral blood tumor cell load reflects the clinical activity of the disease in patients with carcinoma of the breast." Int J Oncol **17**(3): 573-578.
- Tewes, M., Aktas, B., Welt, A., Mueller, S., Hauch, S., Kimmig, R., Kasimir-Bauer, S. (2009). "Molecular profiling and predictive value of circulating tumor cells in patients with metastatic breast cancer: an option for monitoring response to breast cancer related therapies." Breast Cancer Res Treat **115**(3): 581-590.
- Thacker, J. (2005). "The RAD51 gene family, genetic instability and cancer." Cancer Lett **219**(2): 125-135.

- Therasse, P., Arbuuck, S. G., Eisenhauer, E. A., Wanders, J., Kaplan, R. S., Rubinstein, L., Verweij, J., Van Glabbeke, M., van Oosterom, A. T., Christian, M. C., Gwyther, S. G. (2000). "New guidelines to evaluate the response to treatment in solid tumors. European Organization for Research and Treatment of Cancer, National Cancer Institute of the United States, National Cancer Institute of Canada." J Natl Cancer Inst **92**(3): 205-216.
- Thiery, J. P. (2002). "Epithelial-mesenchymal transitions in tumour progression." Nat Rev Cancer **2**(6): 442-454.
- Thigpen, J. T., Vance, R. B., Khansur, T. (1993). "Second-line chemotherapy for recurrent carcinoma of the ovary." Cancer **71**(4 Suppl): 1559-1564.
- Thompson, L. H., K. W. Brookman, L. E. Dillehay, A. V. Carrano, J. A. Mazrimas, C. L. Mooney and J. L. Minkler (1982). "A CHO-cell strain having hypersensitivity to mutagens, a defect in DNA strand-break repair, and an extraordinary baseline frequency of sister-chromatid exchange." Mutat Res **95**(2-3): 427-440.
- Thompson, L. H., K. W. Brookman, L. E. Dillehay, C. L. Mooney and A. V. Carrano (1982). "Hypersensitivity to mutation and sister-chromatid-exchange induction in CHO cell mutants defective in incising DNA containing UV lesions." Somatic Cell Genet **8**(6): 759-773.
- Thompson, L. H., S. Fong and K. Brookman (1980). "Validation of conditions for efficient detection of HPRT and APRT mutations in suspension-cultured Chinese hamster ovary cells." Mutat Res **74**(1): 21-36.
- Thompson, L. H., J. S. Rubin, J. E. Cleaver, G. F. Whitmore and K. Brookman (1980). "A screening method for isolating DNA repair-deficient mutants of CHO cells." Somatic Cell Genet **6**(3): 391-405.
- Thorslund, T., West, S. C. (2007). "BRCA2: a universal recombinase regulator." Oncogene **26**(56): 7720-7730.
- Tibbe, A. G., de Grooth, B. G., Greve, J., Liberti, P. A., Dolan, G. J., Terstappen, L. W. (1999). "Optical tracking and detection of immunomagnetically selected and aligned cells." Nat Biotechnol **17**(12): 1210-1213.
- Toker, A., Cantley, L. C. (1997). "Signalling through the lipid products of phosphoinositide-3-OH kinase." Nature **387**(6634): 673-676.
- Tol, J., Koopman, M., Miller, M. C., Tibbe, A., Cats, A., Creemers, G. J., Vos, A. H., Nagtegaal, I. D., Terstappen, L. W., Punt, C. J. (2010). "Circulating tumour cells early predict progression-free and overall survival in advanced colorectal cancer patients treated with chemotherapy and targeted agents." Ann Oncol **21**(5): 1006-1012.
- Tornaletti, S., Hanawalt, P. C. (1999). "Effect of DNA lesions on transcription elongation." Biochimie **81**(1-2): 139-146.
- Tothill, R. W., Tinker, Anna V., George, Joshy, Brown, Robert, Fox, Stephen B., Lade, Stephen, Johnson, Daryl S., Trivett, Melanie K., Etemadmoghadam, Dariush, Locandro, Bianca, Traficante, Nadia, Fereday, Sian, Hung, Jillian A., Chiew, Yoke-Eng, Haviv, Izhak, Australian Ovarian Cancer Study, Group, Gertig, Dorota, deFazio, Anna, Bowtell, David D. L. (2008). "Novel Molecular Subtypes of Serous and Endometrioid Ovarian Cancer Linked to Clinical Outcome." Clinical Cancer Research **14**(16): 5198-5208.
- Turner, N., Tutt, A., Ashworth, A. (2004). "Hallmarks of 'BRCAness' in sporadic cancers." Nat Rev Cancer **4**(10): 814-819.

- Turner, N. C., Ashworth, A. (2011). "Biomarkers of PARP inhibitor sensitivity." Breast Cancer Res Treat **127**(1): 283-286.
- Tutt, A., Robson, M., Garber, J. E., Domchek, S. M., Audeh, M. W., Weitzel, J. N., Friedlander, M., Arun, B., Loman, N., Schmutzler, R. K., Wardley, A., Mitchell, G., Earl, H., Wickens, M., Carmichael, J. (2010). "Oral poly(ADP-ribose) polymerase inhibitor olaparib in patients with BRCA1 or BRCA2 mutations and advanced breast cancer: a proof-of-concept trial." Lancet **376**(9737): 235-244.
- Umachandran, M., Ioannides, C. (2006). "Stability of cytochromes P450 and phase II conjugation systems in precision-cut rat lung slices cultured up to 72 h." Toxicology **224**(1-2): 14-21.
- Vaira, V., Fedele, G., Pyne, S., Fasoli, E., Zadra, G., Bailey, D., Snyder, E., Favarsani, A., Coggi, G., Flavin, R., Bosari, S., Loda, M. (2010). "Preclinical model of organotypic culture for pharmacodynamic profiling of human tumors." Proc Natl Acad Sci U S A **107**(18): 8352-8356.
- Vaisman, A., Varchenko, M., Umar, A., Kunkel, T. A., Risinger, J. I., Barrett, J. C., Hamilton, T. C., Chaney, S. G. (1998). "The role of hMLH1, hMSH3, and hMSH6 defects in cisplatin and oxaliplatin resistance: Correlation with replicative bypass of platinum-DNA adducts." Cancer Research **58**(16): 3579-3585.
- Valerie, K., Povirk, L. F. (2003). "Regulation and mechanisms of mammalian double-strand break repair." Oncogene **22**(37): 5792-5812.
- Van de Stolpe, A., Pantel, K., Sleijfer, S., Terstappen, L. W., den Toonder, J. M. (2011). "Circulating tumor cell isolation and diagnostics: toward routine clinical use." Cancer Res **71**(18): 5955-5960.
- Van Dyck, E., Stasiak, A. Z., Stasiak, A., West, S. C. (1999). "Binding of double-strand breaks in DNA by human Rad52 protein." Nature **398**(6729): 728-731.
- Van Gent, D. C., van der Burg, M. (2007). "Non-homologous end-joining, a sticky affair." Oncogene **26**(56): 7731-7740.
- Van Loon, B., Markkanen, E., Hubscher, U. (2010). "Oxygen as a friend and enemy: How to combat the mutational potential of 8-oxo-guanine." DNA Repair (Amst) **9**(6): 604-616.
- Vang, R., Shih Ie, M., Kurman, R. J. (2009). "Ovarian low-grade and high-grade serous carcinoma: pathogenesis, clinicopathologic and molecular biologic features, and diagnostic problems." Adv Anat Pathol **16**(5): 267-282.
- Vanhaesebroeck, B., Waterfield, M. D. (1999). "Signaling by distinct classes of phosphoinositide 3-kinases." Exp Cell Res **253**(1): 239-254.
- Velcheti, V., Viswanathan, A., Govindan, R. (2006). "The proportion of patients with metastatic non-small cell lung cancer potentially eligible for treatment with bevacizumab: a single institutional survey." J Thorac Oncol **1**(5): 501.
- Venkitaraman, A. R. (2004). "Tracing the network connecting BRCA and Fanconi anaemia proteins." Nat Rev Cancer **4**(4): 266-276.
- Vergote, I., Trope, C. G., Amant, F., Kristensen, G. B., Ehlen, T., Johnson, N., Verheijen, R. H., van der Burg, M. E., Lacave, A. J., Panici, P. B., Kenter, G. G., Casado, A., Mendiola, C., Coens, C., Verleye, L., Stuart, G. C., Pecorelli, S., Reed, N. S. (2010). "Neoadjuvant chemotherapy or primary surgery in stage IIIC or IV ovarian cancer." N Engl J Med **363**(10): 943-953.

- Vergote, I. B., Joly, F., Katsaros, D., Coens, C., Reinthaller, A., Hall, M., Steer, C. B., Colombo, N., Lesoin, A., Casado, A., Petru, E., Green, J., Buck, M., Ray-Coquard, I. L., Ferrero, A., Favier, L., Reed, N., Curve, H., Jimeno, A., Pujade-Lauraine, E. (2012). "Randomized phase III study of erlotinib versus observation in patients with no evidence of disease progression after first-line platin-based chemotherapy for ovarian carcinoma: A GCIg and EORTC-GCG study." Journal of Clinical Oncology **30**(18).
- Veuger, S. J., Curtin, N. J., Richardson, C. J., Smith, G. C., Durkacz, B. W. (2003). "Radiosensitization and DNA repair inhibition by the combined use of novel inhibitors of DNA-dependent protein kinase and poly(ADP-ribose) polymerase-1." Cancer Res **63**(18): 6008-6015.
- Vichai, V., Kirtikara, K. (2006). "Sulforhodamine B colorimetric assay for cytotoxicity screening." Nat Protoc **1**(3): 1112-1116.
- Visvader, J. E., Lindeman, G. J. (2008). "Cancer stem cells in solid tumours: accumulating evidence and unresolved questions." Nat Rev Cancer **8**(10): 755-768.
- Von Heideman, A., Tholander, B., Grundmark, B., Cajander, S., Gerdin, E., Holm, L., Axelsson, A., Rosenberg, P., Mahteme, H., Daniel, E., Larsson, R., Nygren, P. (2014). "Chemotherapeutic drug sensitivity of primary cultures of epithelial ovarian cancer cells from patients in relation to tumour characteristics and therapeutic outcome." Acta Oncol **53**(2): 242-250.
- Vona, G., Sabile, A., Louha, M., Sitruk, V., Romana, S., Schutze, K., Capron, F., Franco, D., Pazzagli, M., Vekemans, M., Lacour, B., Brechot, C., Paterlini-Brechot, P. (2000). "Isolation by size of epithelial tumor cells : a new method for the immunomorphological and molecular characterization of circulating tumor cells." Am J Pathol **156**(1): 57-63.
- Wang, H. Q., Altomare, D. A., Skele, K. L., Poulikakos, P. I., Kuhajda, F. P., Di Cristofano, A., Testa, J. R. (2005). "Positive feedback regulation between AKT activation and fatty acid synthase expression in ovarian carcinoma cells." Oncogene **24**(22): 3574-3582.
- Wang, L. H., Pfister, T. D., Parchment, R. E., Kummar, S., Rubinstein, L., Evrard, Y. A., Gutierrez, M. E., Murgo, A. J., Tomaszewski, J. E., Doroshow, J. H., Kinders, R. J. (2010). "Monitoring drug-induced gammaH2AX as a pharmacodynamic biomarker in individual circulating tumor cells." Clin Cancer Res **16**(3): 1073-1084.
- Wang, Y., Liu, X., Matsuda, A., Plunkett, W. (2008). "Repair of 2'-C-cyano-2'-deoxy-1-beta-D-arabino-pentofuranosylcytosine-induced DNA single-strand breaks by transcription-coupled nucleotide excision repair." Cancer Res **68**(10): 3881-3889.
- Wang, Z. P., Eisenberger, M. A., Carducci, M. A., Partin, A. W., Scher, H. I., Ts'o, P. O. (2000). "Identification and characterization of circulating prostate carcinoma cells." Cancer **88**(12): 2787-2795.
- Ward, J. L., Sherali, A., Mo, Z. P., Tse, C. M. (2000). "Kinetic and pharmacological properties of cloned human equilibrative nucleoside transporters, ENT1 and ENT2, stably expressed in nucleoside transporter-deficient PK15 cells. Ent2 exhibits a low affinity for guanosine and cytidine but a high affinity for inosine." J Biol Chem **275**(12): 8375-8381.
- Watanabe, Y., Koi, M., Hemmi, H., Hoshai, H., Noda, K. (2001). "A change in microsatellite instability caused by cisplatin-based chemotherapy of ovarian cancer." Br J Cancer **85**(7): 1064-1069.

- Watkins, J. A., Irshad, S., Grigoriadis, A., Tutt, A. N. (2014). "Genomic scars as biomarkers of homologous recombination deficiency and drug response in breast and ovarian cancers." Breast Cancer Res **16**(3): 211.
- Watson, P., Lynch, H. T. (2001). "Cancer risk in mismatch repair gene mutation carriers." Fam Cancer **1**(1): 57-60.
- Weber, C. A., Kirchner, J. M., Salazar, E. P., Takayama, K. (1994). "Molecular analysis of CXPB mutations in the repair-deficient hamster mutants UV5 and UVL-13." Mutat Res **324**(4): 147-152.
- Weinstein, J. N., Lorenzi, P. L. (2013). "Cancer: Discrepancies in drug sensitivity." Nature **504**(7480): 381-383.
- Weiss, R. B. (1992). "The anthracyclines: will we ever find a better doxorubicin?" Semin Oncol **19**(6): 670-686.
- Welch, P. L. and M. C. King (2001). "BRCA1 and BRCA2 and the genetics of breast and ovarian cancer." Hum Mol Genet **10**(7): 705-713.
- Wells, G. J., Bihovsky, R., Hudkins, R. L., Ator, M. A., Husten, J. (2006). "Synthesis and structure-activity relationships of novel pyrrolocarbazole lactam analogs as potent and cell-permeable inhibitors of poly(ADP-ribose)polymerase-1 (PARP-1)." Bioorg Med Chem Lett **16**(5): 1151-1155.
- Whitmore, G. F., Varghese, A. J., Gulyas, S. (1989). "Cell-Cycle Responses of 2 X-Ray Sensitive Mutants Defective in DNA-Repair." Int J Radiat Biol **56**(5): 657-665.
- Wiegant, W. W., Overmeer, R. M., Godthelp, B. C., van Buul, P. P., Zdzienicka, M. Z. (2006). "Chinese hamster cell mutant, V-C8, a model for analysis of Brca2 function." Mutat Res **600**(1-2): 79-88.
- Willner, J., Wurzk, K., Allison, K. H., Galic, V., Garcia, R. L., Goff, B. A., Swisher, E. M. (2007). "Alternate molecular genetic pathways in ovarian carcinomas of common histological types." Hum Pathol **38**(4): 607-613.
- Wimberger, P., M. Heubner, F. Otterbach, T. Fehm, R. Kimmig and S. Kasimir-Bauer (2007). "Influence of platinum-based chemotherapy on disseminated tumor cells in blood and bone marrow of patients with ovarian cancer." Gynecol Oncol **107**(2): 331-338.
- Wimberger, P., N. Lehmann, R. Kimmig, A. Burges, W. Meier, A. Du Bois and G. Arbeitsgemeinschaft Gynaekologische Onkologie Ovarian Cancer Study (2007). "Prognostic factors for complete debulking in advanced ovarian cancer and its impact on survival. An exploratory analysis of a prospectively randomized phase III study of the Arbeitsgemeinschaft Gynaekologische Onkologie Ovarian Cancer Study Group (AGO-OVAR)." Gynecol Oncol **106**(1): 69-74.
- Wiseman, H., Halliwell, B. (1996). "Damage to DNA by reactive oxygen and nitrogen species: role in inflammatory disease and progression to cancer." Biochem J **313** (Pt 1): 17-29.
- Worley, M. J., Welch, W. R., Berkowitz, R. S., Ng, S. W. (2013). "Endometriosis-associated ovarian cancer: a review of pathogenesis." Int J Mol Sci **14**(3): 5367-5379.
- Wray, J., Liu, J., Nickoloff, J. A., Shen, Z. (2008). "Distinct RAD51 associations with RAD52 and BCCIP in response to DNA damage and replication stress." Cancer Res **68**(8): 2699-2707.

- Wu, Q., Vasquez, K. M. (2008). "Human MLH1 protein participates in genomic damage checkpoint signaling in response to DNA interstrand crosslinks, while MSH2 functions in DNA repair." PLoS Genet **4**(9): e1000189.
- Xing, J., Wu, X., Vaporciyan, A. A., Spitz, M. R., Gu, J. (2008). "Prognostic significance of ataxia-telangiectasia mutated, DNA-dependent protein kinase catalytic subunit, and Ku heterodimeric regulatory complex 86-kD subunit expression in patients with nonsmall cell lung cancer." Cancer **112**(12): 2756-2764.
- Xu, L., Yoneda, J., Herrera, C., Wood, J., Killion, J. J., Fidler, I. J. (2000). "Inhibition of malignant ascites and growth of human ovarian carcinoma by oral administration of a potent inhibitor of the vascular endothelial growth factor receptor tyrosine kinases." Int J Oncol **16**(3): 445-454.
- Yap, T. A., Sandhu, S. K., Carden, C. P., de Bono, J. S. (2011). "Poly(ADP-ribose) polymerase (PARP) inhibitors: Exploiting a synthetic lethal strategy in the clinic." CA Cancer J Clin **61**(1): 31-49.
- Yokomizo, A., Tindall, D. J., Hartmann, L., Jenkins, R. B., Smith, D. I., Liu, W. (1998). "Mutation analysis of the putative tumor suppressor PTEN/MMAC1 in human ovarian cancer." Int J Oncol **13**(1): 101-105.
- You, Z., Chahwan, C., Bailis, J., Hunter, T., Russell, P. (2005). "ATM activation and its recruitment to damaged DNA require binding to the C terminus of Nbs1." Mol Cell Biol **25**(13): 5363-5379.
- Yu, D. S., Sonoda, E., Takeda, S., Huang, C. L., Pellegrini, L., Blundell, T. L., Venkitaraman, A. R. (2003). "Dynamic control of Rad51 recombinase by self-association and interaction with BRCA2." Mol Cell **12**(4): 1029-1041.
- Zaremba, T., Ketzer, P., Cole, M., Coulthard, S., Plummer, E. R., Curtin, N. J. (2009). "Poly(ADP-ribose) polymerase-1 polymorphisms, expression and activity in selected human tumour cell lines." Br J Cancer **101**(2): 256-262.
- Zhang, F., J. Ma, J. Wu, L. Ye, H. Cai, B. Xia and X. Yu (2009). "PALB2 links BRCA1 and BRCA2 in the DNA-damage response." Curr Biol **19**(6): 524-529.
- Zhang, H., Zhang, S., Cui, J., Zhang, A., Shen, L., Yu, H. (2008). "Expression and promoter methylation status of mismatch repair gene hMLH1 and hMSH2 in epithelial ovarian cancer." Aust N Z J Obstet Gynaecol **48**(5): 505-509.
- Zhang, J., Sun, X., Smith, K. M., Visser, F., Carpenter, P., Barron, G., Peng, Y., Robins, M. J., Baldwin, S. A., Young, J. D., Cass, C. E. (2006). "Studies of nucleoside transporters using novel autofluorescent nucleoside probes." Biochemistry **45**(4): 1087-1098.
- Zhang, Y., J. Wang, D. Xiang, D. Wang and X. Xin (2009). "Alterations in the expression of the apurinic/apyrimidinic endonuclease-1/redox factor-1 (APE1/Ref-1) in human ovarian cancer and identification of the therapeutic potential of APE1/Ref-1 inhibitor." Int J Oncol **35**(5): 1069-1079.
- Zheng, S., Lin, H. K., Lu, B., Williams, A., Datar, R., Cote, R. J., Tai, Y. C. (2011). "3D microfilter device for viable circulating tumor cell (CTC) enrichment from blood." Biomed Microdevices **13**(1): 203-213.
- Zhou, B. B., Elledge, S. J. (2000). "The DNA damage response: putting checkpoints in perspective." Nature **408**(6811): 433-439.
- Znojek, P. (2011). "PhD Thesis." Newcastle University.

